EMERGING INFECTIOUS DISEASES®

CDC
Centers for Disease Control and Prevention

Pregnancy and Maternal Health

August 2019

EMERGING INFECTIOUS DISEASES®

Emerging Infectious Diseases is published monthly by the Centers for Disease Control and Prevention, 1600 Clifton Rd NE, Mailstop H16-2, Atlanta, GA 30329-4027, USA. Telephone 404-639-1960, fax 404-639-1954, email eideditor@cdc.gov.

EMERGING INFECTIOUS DISEASES®

Pregnancy and Maternal Health **August 2019**

On the Cover

Vincent van Gogh (1853–1890). *First Steps, after Millet* (1890). Oil on canvas; 28 1/2 in x 35 7/8 in/72.4 cm x 91.1 cm. Gift of George N. and Helen M. Richard, 1964. Image © The Metropolitan Museum of Art. Image source: Art Resource, NY.

About the Cover p. 1620

Synopses

Research

Historical Review

Dispatches

EMERGING INFECTIOUS DISEASES®

August 2019

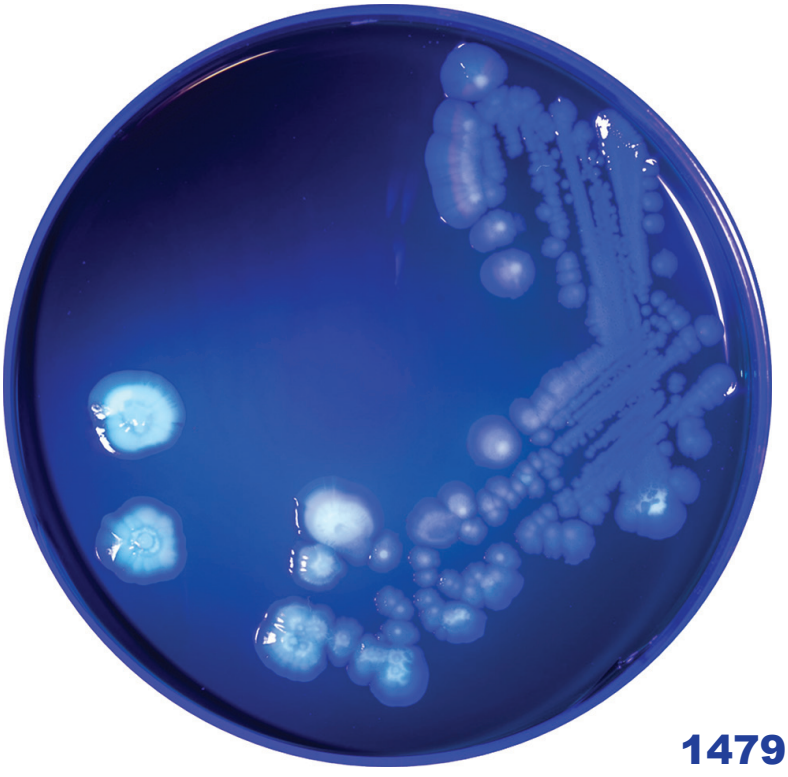

1479

Research Letters

EMERGING INFECTIOUS DISEASES®
August 2019

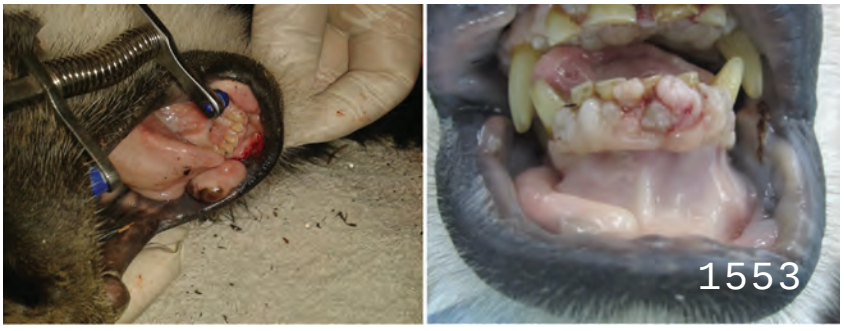

In Memoriam

About the Cover

Etymologia

Corrections

Vol. 18, No. 1 **1622**
An odds ratio and 95% CI were incorrect in Identifying Risk Factors for Shiga Toxin–producing *Escherichia coli* by Payment Information (H. Wilking et al.). The correct data for salad bar purchases were odds ratio 5.83, 95% CI 1.42–23.88.

Vol. 25, No. 6 **1622**
Author Olga Ivanov should have also been listed as affiliated with Sechenov University, Moscow, Russia, in Multirecombinant Enterovirus A71 Subgenogroup C1 Isolates Associated with Neurologic Disease, France, 2016–2017 (S. Tomba Ngangas et al.).

The World Unseen:
Intersections of Art and Science
May 20–August 30, 2019

Amie Esslinger, *Collisions*, mixed media, 2016

The World Unseen: Intersections of Art and Science gathers the work of 10 international artists who draw upon microbiology, biotechnology, anatomy, and texts in their investigations of microbes and cells, DNA, history of disease and science, the body, and beauty. Through paintings, drawings, installations, and videos, these artists ponder the humanistic and scientific implications of knowing and seeing what we normally cannot see.

DAVID J. SENCER
CDC MUSEUM
History·Legacy·Innovation

The David J. Sencer CDC Museum, a Smithsonian Affiliate, uses award-winning exhibitions, dynamic educational programming, and physical and web archives to educate visitors about the value of public health, while presenting the rich heritage and vast accomplishments of CDC.

Hours

Monday–Wednesday: 9 a.m.–5 p.m.
Thursday: 9 a.m.–7 p.m.
Friday: 9 a.m.–5 p.m.
Closed weekends and federal holidays

Location

1600 Clifton Road, NE
Atlanta, GA
30329-4021
Phone (404) 639-0830

Admission and parking free
Vehicle inspection required
Government-issued photo ID required for adults over the age of 18
Passport required for non-U.S. citizens

Pseudomonas poae–Associated Fatal Septic Transfusion Reaction, Peoria, Illinois, USA, 2017

Therese S. Woodring, John J. Farrell

In the United States, fatal transfusion-transmitted infections from red blood cell units are rare. Although this pattern mostly reflects how inhospitable refrigerated red blood cell units are to contaminant growth, fatalities caused by microorganisms that can grow at storage temperature (4°C), but not in standard clinical blood cultures at 37°C, are probably underestimated. We analyzed a fatal red blood cell transfusion in Peoria, Illinois, USA, that occurred in 2017. Samples from the patient's whole blood and the red blood cell unit remained culture-negative during the investigation, despite direct visualization of gram-negative bacilli within the unit immediately after transfusion. We identified the bacteria as *Pseudomonas poae*, a nonpathogenic pseudomonad carrying multiple cold-shock domain protein genes, and confirmed its cold tolerance and inability to grow at 37°C. Our work indicates transfusion reaction workups need to include testing for psychrophilic organisms, which could explain the cause of other apparently culture-negative transfusion reactions.

Transfusion-transmitted infections (TTIs; i.e., the transmission of bacteria, viruses, parasites, or prions through blood product transfusions) are reportable events (*1*). Although >5 million patients in the United States receive red blood cell transfusions each year, fatal TTIs from contaminated red blood cell units number in the single digits annually and arise primarily from *Babesia* infection in the donor (Table 1). Bacterial colonization of the red blood cell unit is a much rarer event, and viruses and prions, which are the target of most donor history questionnaires and blood product screening tests, have not contributed to reported fatalities in the past decade. The rarity of bacterial contamination reflects vigilant collection practices for all blood products, including skin disinfection and diversion of the first few milliliters of blood from healthy donors, as well as red blood cell refrigeration, which further decreases contamination risk compared with nonrefrigerated blood products, like platelets.

Author affiliations: University of Illinois College of Medicine, Peoria, Illinois, USA (T.S. Woodring, J.J. Farrell); OSF System Laboratory, Peoria (J.J. Farrell)

DOI: https://doi.org/10.3201/eid2508.181936

Still, the rate of fatalities resulting from red blood cell contamination, particularly by bacteria, is surprisingly low, given that, unlike platelets, bacterial contamination of red blood cell units is not screened for after collection, apart from a serologic test for syphilis and visual inspection for gross contamination immediately before transfusion (*4*). Moreover, pathogen inactivation technologies used after collection for plasma and platelets are not yet available for red blood cells (*5*). This low rate of bacterial contamination might partly reflect how inhospitable the red blood cell unit becomes to contaminating organisms over its 42-day shelf life. Held at only a few degrees above freezing (4°C), the unit becomes progressively depleted of high-energy substrates, and waste products and reactive oxygen species accumulate at a pH well below the physiologic pH range for blood (*6*,*7*). Bacteria that can grow to life-threatening numbers in this environment must be capable of surviving these conditions, and the risk for contamination with these organisms within collection facilities is rare enough to pose minimal threat to the blood supply.

Organisms adapted for survival in packed red blood cell units during storage, however, could be missed during evaluations of suspected transfusion reactions in the clinical laboratory by virtue of their specialized growth limitations. For instance, bacteria best suited to survive in a refrigerated red blood cell unit might not grow at 37°C, the standard temperature for incubation of suspected TTI workups. Yet, these bacteria do not need to grow at this temperature to trigger a fatal septic reaction upon infusion if their inoculum size is large and endotoxin concentration high. The Centers for Disease Control and Prevention National Healthcare Safety Network guidelines for definite TTIs require evidence of the infectious agent in the transfused unit or recipient (Table 2) (*8*). When standard laboratory testing is used alone, these cases involving cold-tolerant bacteria could be excluded from fatality statistics for TTIs. We present a case report of a death occurring after transfusion with a contaminated red blood cell unit; the investigation required advanced techniques, such as whole-genome sequencing (WGS), to determine the colonizing agent.

Table 1. Fatalities caused by red blood cell transfusions reported to the US Food and Drug Administration, 2005–2016*

Year	No. fatalities	Organisms (no.)
2005	1	*Serratia marcescens*
2006	4	*Babesia microti* (n = 2), *Escherichia coli* (n = 1), *Yersinia enterocolitica* (n = 1)
2007	3	*B. microti*
2008	5	*B. microti*
2009	0	
2010	1	*B. microti*
2011	1	*B. microti*
2012	1	*B. microti*
2013	2	*B. microti* (n = 1), *Pseudomonas fluorescens* (n = 1)
2014	0	
2015	1	*Enterococcus faecium*
2016	3	*B. microti* (n = 2), *P. fluorescens* (n = 1)
All	22	*B. microti* (n = 16), *P. fluorescens* (n = 2), *E. coli* (n = 1), *Y. enterocolitica* (n = 1), *S. marcescens* (n = 1), *E. faecium* (n = 1)

*See (*2,3*).

Table 2. Centers for Disease Control and Prevention National Healthcare Safety Network criteria for establishing definite transfusion-transmitted infections*

Criteria
≥1 of the following: Evidence of the pathogen in 1) the transfused component, 2) the donor at the time of donation, 3) an additional component from the same donation, or 4) an additional recipient of a component of the same donation AND No other potential exposures to the pathogen be identified for the recipient AND Either evidence that the recipient was not infected with the pathogen before transfusion or evidence that the identified pathogens are related by molecular or extended phenotypic comparison testing

*See (*8*).

Clinical Case

In 2017, a 56-year-old woman with a history of diabetes mellitus, hypertension, and right femur fracture requiring open reduction and internal fixation with total knee arthroplasty (TKA) was admitted to a hospital in Peoria, Illinois, USA, with leg pain and inability to walk. Her TKA had been complicated 5 months earlier by periprosthetic femur fracture and infection with *Corynebacterium striatum* and *Pseudomonas aeruginosa*, which was treated with intravenous vancomycin and cefepime. At admission, she was noted to have purulent drainage from an open right thigh wound above a long plate in her femur (Figure 1), and blood and wound cultures were positive for methicillin-resistant *Staphylococcus aureus*. She was immediately started on intravenous vancomycin, and operative incision and drainage were performed on day 4 of hospitalization without complications. By the day the TKA prosthetic was scheduled for removal (day 6), her blood cultures were negative for bacterial growth.

On day 6, medical staff attempted explant of the TKA hardware; however, the procedure needed to be aborted because of excessive blood loss during debridement. Her preoperative hemoglobin concentration dropped from 10.3 g/dL to 5.5 g/dL within 1 hour of the procedure. She received 3 units of typed and crossed packed red blood cells without complication. Five hours after this transfusion, her hemoglobin rose to 8.4 g/dL, but a repeat hemoglobin assessment 21 hours later indicated the concentration dropped (7.0 g/dL), so another red blood cell unit was ordered for her.

Within 5 minutes of starting the final transfusion, the patient became tachypneic; tachycardia developed, and she began to report shortness of breath. According to hospital protocol, the transfusion was stopped immediately. Clerical error and a hemolytic transfusion reaction were excluded by repeat donor ABO typing, a direct antiglobulin test, and visual inspection of plasma and urine for hemolysis. The red blood cell unit had no signs of hemolysis or breached bag integrity. Despite empiric treatment for an allergic transfusion reaction, the patient continued to exhibit signs of a systemic inflammatory response (heart rate 120–140 beats/min, respiratory rate 35–40 breaths/min) and required

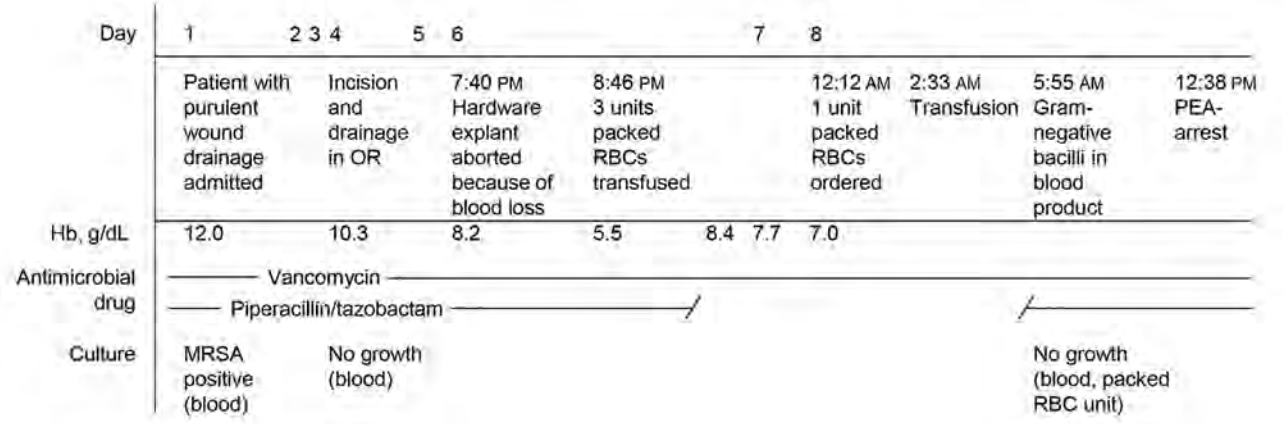

Figure 1. Timeline of patient's hospitalization for periprosthetic joint infection, followed by fatal septic transfusion reaction, Peoria, Illinois, USA, 2017. Hb, hemoglobin; MRSA, methicillin-resistant *Staphylococcus aureus*; PEA, pulseless electrical activity; RBC, red blood cell.

increasing oxygen supplementation from a nonrebreather mask and bilevel positive pressure ventilation. Three hours after the transfusion, the laboratory reported gram-negative bacteria throughout smears taken from the red blood cell unit as part of laboratory protocol for suspected transfusion reactions. The patient was started on intravenous piperacillin/tazobactam but continued to deteriorate, undergoing 4 episodes of cardiopulmonary resuscitation before she was declared dead of cardiac arrest 10 hours after the transfusion. Standard 37°C clinical blood cultures from both the patient and the red blood cell unit were negative for bacterial growth after 5 days. The transfusion reaction was reported to the Food and Drug Administration 6 days after the patient's death.

Methods

For blood culture testing, we inoculated a BACTEC Peds Plus (BD, https://www.bd.com) blood culture bottle with 1.0 mL of blood from the red blood cell unit and left the sample at ambient temperature (25°C) for 24 h. Using this culture, we streaked organisms onto a blood agar purity plate and incubated for 24 h at 25°C. We spotted 1 purified colony for matrix-assisted laser desorption/ionization time-of-flight (MALDI-TOF) mass spectrometry (VITEK MS; bioMérieux, https://www.biomerieux-diagnostics.com) and suspended another colony from the same plate in sterile saline of 0.99 McFarland turbidity standard in preparation for WGS. We extracted DNA from the suspended colony using the QIAGEN REPLI-g UltraFast Mini Kit (https://www.qiagen.com) according to manufacturer instructions and sequenced with a FLO-MIN 106 SpotON Flow Cell on a Nanopore MinION Mk1B (Oxford Nanopore Technologies, https://nanoporetech.com) using a rapid whole-genome amplification protocol (SQK-RAD004).

We analyzed reads passing the default quality score cutoff of 7 for quality in NanoPlot (*9*) and assembled de novo using Canu version 1.7.1, an assembler designed for long-read output (*10*). We evaluated the assessment of the de novo assembly quality using Bandage (*11*). We retained contigs with ≥5× coverage for further error correction using Nanopolish 0.8.5 with default settings (*12*) and annotated the final assembly with Prokka 1.13.3 (*13*). We identified the species by analyzing the 16S rRNA sequence using the Ribosomal Database Project Seqmatch tool and blastn (https://blast.ncbi.nlm.nih.gov/Blast.cgi) within the National Center for Biotechnology Information database. We performed multilocus sequence analysis with 4 conserved gene regions previously used for *Pseudomonas* taxonomy (16S-*gyrB*-*rpoB*-*rpoD*) on the isolate assembly and 20 fluorescens subgroup genomes available in GenBank (Table 3) (*14*). For multilocus sequence analysis, we aligned each gene region with MUSCLE before concatenation in Geneious 11.1.5 (*15*).

Table 3. *Pseudomonas* spp. included in multilocus sequence analysis to identify bacterial contaminant in red blood cell unit, Peoria, Illinois, USA, 2017

Species	Strain	GenBank accession no.
P. poae	RE*1–1-14	GCA_000336465.1
P. azotoformans	S4	GCA_001579805.1
P. extremorientalis	BS277	GCA_900104365.1
P. simiae	WBS417	GCA_000698265.1
P. palleroniana	MAB3	GCA_002953635.1
P. tolaasii	2192T	GCA_002072675.1
P. costantinii	LMG 22119	GCA_001870435.1
P. antarctica	PAMC 27949	GCA_001647715.1
P. fluorescens	F113	GCA_000237065.1
P. salomonii	ICMP 14252	GCA_900107155.1
P. trivialis	IHBB745	GCA_001186335.1
P. rhodesiae	BS2777	GCA_900105575.1
P. marginalis	ICMP 9505	GCA_001467265.1
P. panacis	BS2778	GCA_900104875.1
P. grimontii	BS2976	GCA_900101085.1
P. veronii	R02	GCA_002028325.1
P. cedrina	BS2981	GCA_900104915.1
P. orientalis	F9	GCA_002934065.1
P. libanensis	BS2975	GCA_900101035.1
P. synxantha	LBUM223	GCA_000968415.2
P. aeruginosa	PAO1	GCA_000006765.1

After WGS analysis, we analyzed temperature-dependent viability by incubating isolates from the original blood agar purity plate in BD BACTEC Peds Plus blood culture bottles at 4°C, 25°C, and 37°C for 5 days. We plated cultures diluted 1:100–1:10,000,000 on blood agar and counted the colonies that grew after 24 h at 25°C.

Laboratory Investigation

Initial isolate identification by MALDI-TOF mass spectrometry was split between *Pseudomonas fluorescens* (50% confidence) and *P. veronii* (50% confidence). WGS produced a total of 168,870 reads spanning 885,192,362 bp that passed the quality threshold. The median read length was 3,200 (maximum 100,184) bp. The assembly contained 2 contigs: a 7,340,165-bp contig with 23.4× coverage corresponding to the predicted chromosomal length of *Pseudomonas* spp. (GenBank accession no. CP034537) and a 150,410-bp contig with 41.6× coverage suggestive of a plasmid (GenBank accession no. CP034538).

Among the 8,602 genes annotated on the chromosome were 6 full-length 16S rRNA genes, consistent with the higher 16S gene copy numbers seen in the *P. fluorescens* and *P. putida* clusters (n = 5–7) compared with the copy number of *P. aeruginosa* clusters (n = 4) (*16*). The sequence of this gene matched with >99% similarity to that of *P. poae*, a fluorescens group pseudomonad, by both the Ribosomal Database Project Seqmatch tool and blastn (Table 4). In multilocus sequence analysis (16S-*gryrB*-*rpoB*-*rpoD*), the isolate also clustered with *P. poae*, further supporting this identification (Figure 2).

The annotated genome contained multiple copies of *capB* and *cspA*, genes for cold-shock domain proteins that enable efficient translation and long-term cold adaptation

Table 4. Identification of bacterium in red blood cell unit, Peoria, Illinois, USA, 2017, on the basis of 16S rRNA gene sequencing results, by database

Database	Identification	Metric
Ribosomal Database Project	*Pseudomonas* sp. VS05_16	1.000 similarity score
	P. poae BCHCBZ253	0.996 similarity score
GenBank	*P. poae* strain BA2776	100% coverage, 99% identity (1,530/1,532 nt)
	P. poae RE*1–1-14	100% coverage, 99% identity (1,530/1,532 nt)

in Antarctic pseudomonads (Table 5) (*17*). Correlating this genomic signature with phenotypic data, we conducted a temperature-dependent viability experiment that confirmed growth at 4°C and 25°C (Figure 3) and no growth at 37°C; >99.9% of bacteria died within 5 days of incubation at 37°C. In addition, the annotated genome included evidence of versatile iron-acquisition capacities, including 2 siderophore systems and extracellular heme scavenging (Table 5) (*18*,*19*). Fluorescent siderophores are responsible for the fluorescence that gives the fluorescens group its name. Our isolate did demonstrate fluorescence under ultraviolet light, consistent with siderophore production (Figure 4).

Discussion

WGS analysis identified the organism within the red blood cell unit from this case as *P. poae*, a cold-adapted fluorescens pseudomonad first discovered in the grass phyllosphere in 2003 and since found around the world, including the cold deserts of the Himalayas (*20*,*21*). Previous studies of this organism have focused on its potential to promote plant growth through phosphate mobilization, its production of plant-protective antifungal metabolites (*22*,*23*), and its ability to remediate contaminated ecosystems through hydrocarbon degradation (*24*). A Medline search yielded no reports of *P. poae* as a human pathogen. Considering how poorly this isolate tolerated body temperature (37°C), the lack of clinical cases might reflect a genuinely low virulence in humans.

The pathogenicity of this organism seems specific to the ecology of red blood cell storage and transfusion. On both a genomic and phenotypic level, we found evidence of cold tolerance that particularly suited *P. poae* to not just surviving but thriving in long-term refrigeration in a red blood cell unit. Because the organism grew at 25°C, any length of improper red blood cell storage at room temperature could have

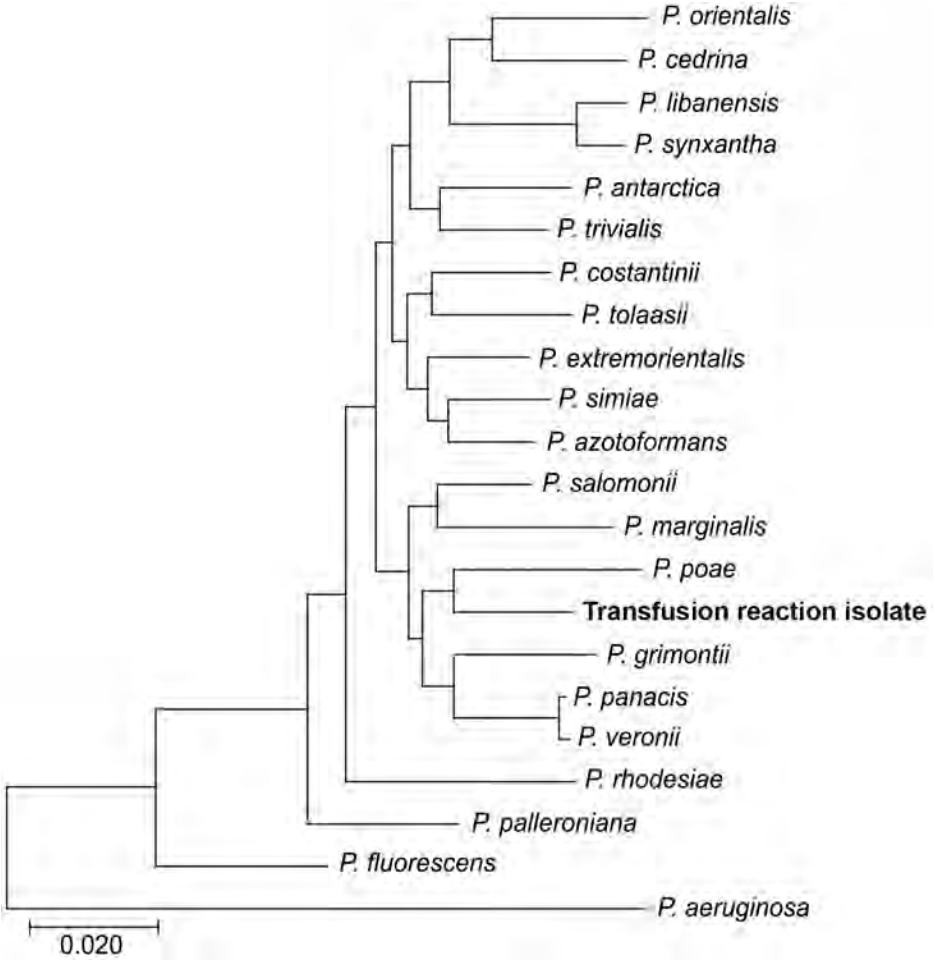

Figure 2. Neighbor-joining tree calculated by using Jukes-Cantor model for concatenated 16S-*gyrB*-*rpoB*-*rpoD* gene sequences of the *Pseudomonas* isolate from patient in Peoria, Illinois, USA, 2017 (bold), and 20 fluorescens subgroup pseudomonads. We used *P. aeruginosa* as the outlier. Scale bar indicates nucleotide substitutions per site.

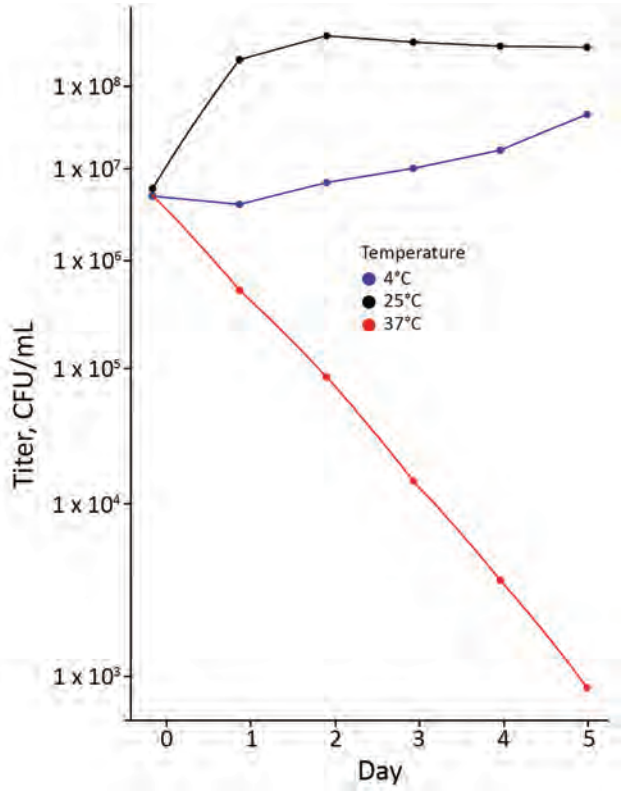

Figure 3. Titers of viable bacteria in cultures of *Pseudomonas poae* from patient in Peoria, Illinois, USA, 2017. Cultures were grown in BD BACTEC Peds Plus (https://www.bd.com) blood culture media incubated at 4°C, 25°C, and 37°C for 5 days.

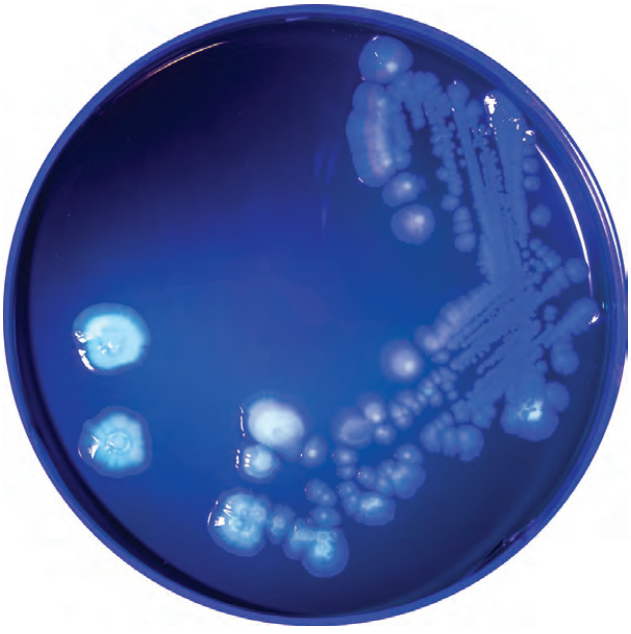

Figure 4. *Pseudomonas poae* colonies isolated from contaminated packed red blood cell unit, Peoria, Illinois, USA, 2017, fluorescing under ultraviolet light (λ = 395 nm).

provided additional opportunity for growth. The versatile iron acquisition capacities suggested by genome annotation indicate the potential for *P. poae* to exploit iron within the red blood cell unit environment (*25*). Although we cannot specify where the opportunity for colonization arose, *Pseudomonas* spp. have been traced to environmental sources, including contaminated water baths and cooling cloths in septic episodes involving blood products (*26*,*27*). *Pseudomonas* spp. are also common reagent contaminants detected in sequencing-based studies (*28*), suggesting that donor skin and the environment are not the only possible sources of contamination.

Once *P. poae* was introduced into the patient, its survival was likely not required for virulence. Given a sufficiently large inoculum, the endotoxin and other antigens from both live and dead organisms that accumulated during the unit's storage could have provided enough of an immunogenic stimulus within the bloodstream to trigger a massive dysregulated immune response, irrespective of the ability of the organism to establish a sustained infection at 37°C (*29*). Indeed, endotoxin is sufficient to activate multiple innate immune pathways that contribute to the hemodynamic, metabolic, and coagulation defects driving death due to sepsis (*30*,*31*). In the case we describe, how the history of methicillin-resistant *S. aureus* sepsis <1 week before the infection affected the patient's risk for death is unclear; systemic weakening or modification of the subsequent immune response could have been contributing factors that affected the patient's outcome. Studies of sepsis in animals with previous endotoxin exposure suggest diverging effects of this priming on the basis of the dose (*32*,*33*); in vitro, cell wall components of gram-positive bacteria (e.g., lipoteichoic acid) appear to potentiate cytokine responses at low doses of endotoxin and suppress them at high doses (*34*).

National Healthcare Safety Network criteria for a definite TTI are predicated on pathogen identification, which requires not only a Gram stain, as done in this case, but also a positive blood culture and subsequent isolation on solid media (*8*). Although standard laboratory testing alone did not meet National Healthcare Safety Network criteria for a definite TTI in this case, we believe the presence of the *P. poae* isolate in the transfused blood product was the cause of death for this patient. The patient's clinical deterioration from hemodynamic stability to death by cardiovascular collapse progressed during the 10 hours immediately after transfusion, and WGS provided postmortem evidence of *P. poae* in the red blood cell unit. Although *P. poae* is ubiquitous in soil, this patient had no other plausible systemic exposures to this otherwise nonpathogenic organism. In addition, the patient becoming infected with *P. poae* before transfusion was overwhelmingly unlikely; she had received a 6-day course of empiric piperacillin/tazobactam

covering gram-negative organisms for her periprosthetic infection within 48 hours of the transfusion, and her negative blood cultures before transfusion make any preexisting bloodstream infection with any *Pseudomonas* spp. highly improbable. Given that we believe the organism caused the patient's death without establishing infection, the more appropriate term in this case would be septic transfusion reaction rather than TTI.

Because of the rapid death of this patient, a patient-derived blood sample was not accessible for next-generation sequencing and endotoxin testing, limiting our study. Because *P. poae* is a ubiquitous plant- and soil-associated organism, we also cannot definitively exclude that the isolate we sequenced was not a contaminant from postmortem handling of the red blood cell unit. However, the absence of these gram-negative organisms (which were visible in blood smears acquired from the blood bag within 5 hours after transfusion) in the standard 37°C blood culture is consistent with the temperature intolerance observed for the gram-negative isolate later recovered from the red blood cell unit. Moreover, the growth of this isolate at 4°C coupled with the observation that most fatal bacterial TTIs are caused by cold-tolerant gram-negative organisms (e.g., *Serratia* spp., *Yersinia enterocolitica*) suggests that the isolate we recovered originated from the refrigerated red blood cell unit (Table 1) (*35*).

Our case expands the literature on microbially mediated deaths from red blood cell transfusions and represents an extraordinary human fatality from *P. poae*. This episode draws attention to the limitations of standard blood culture procedures to fulfill National Healthcare Safety Network TTI criteria, which, for all practical purposes, require that organisms be incubated under conditions that much more resemble the human body than the cold storage environment selecting for the contaminating organisms. *P. poae* is a prime example of an organism that could, by virtue of the very temperature-dependent growth that enables its survival in refrigerated red blood cell units, elude detection in a transfusion reaction investigation. Until guidelines expand to include cultures for bacteria that grow at storage temperature, the number of apparently culture-negative adverse transfusion reactions that are caused by similar organisms will remain unknown. Finally, our case demonstrates the potential for next-generation sequencing to detect, identify, and characterize organisms directly from contaminated blood products.

Acknowledgments

The authors thank the clinical laboratory scientists in the blood bank and microbiology sections of the OSF System Laboratory for their assistance, especially Angie McKeever and Valerie Gosack. We also thank Jim Carlson for photographing the isolate and Trisha Stetzler for her excellent medical care.

About the Author

Dr. Woodring is a graduate of the University of Illinois College of Medicine in Peoria, Illinois. Her primary research interests include clinical microbiology and incorporating next-generation sequencing into infectious disease diagnostics.

Dr. Farrell is Chair of Infection Control for OSF Saint Francis Medical Center, director of the Serology and Microbiology Laboratories in the OSF System Laboratory, and professor of clinical medicine in the Division of Infectious Diseases for the University of Illinois College of Medicine. His research interests include molecular diagnostics with a focus on detection of bacterial pathogens in culture-negative tissues and body fluids.

References

1. Centers for Disease Control and Prevention. Blood safety. Diseases and organisms. 2017 [cited 2018 Nov 25]. https://www.cdc.gov/bloodsafety/bbp/diseases-organisms.html
2. Food and Drug Administration. Transfusion/donation fatalities. 2018 [cited 2017 Nov 18]. https://www.fda.gov/vaccines-blood-biologics/report-problem-center-biologics-evaluation-research/transfusiondonation-fatalities
3. Haass KA, Sapiano MRP, Savinkina A, Kuehnert MJ, Basavaraju SV. Transfusion-transmitted infections reported to the National Healthcare Safety Network Hemovigilance Module. Transfus Med Rev. 2019;33:84–91. http://dx.doi.org/10.1016/j.tmrv.2019.01.001
4. Kuehnert M, Basavaraju SV. Transfusion-associated infections. In: Bennett JE, Dolin R, Blaser MJ, editors. Mandell, Douglas, and Bennett's principles and practice of infectious diseases. 8th ed. Philadelphia: Saunders; 2015. p. 3351–60.
5. Silverglied AJ. Pathogen inactivation of blood products. 2018 May 23 [cited 2018 Nov 25]. https://www.uptodate.com/contents/pathogen-inactivation-of-blood-products
6. D'Alessandro A, D'Amici GM, Vaglio S, Zolla L. Time-course investigation of SAGM-stored leukocyte-filtered red bood cell concentrates: from metabolism to proteomics. Haematologica. 2012;97:107–15. http://dx.doi.org/10.3324/haematol.2011.051789
7. D'Alessandro A, Kriebardis AG, Rinalducci S, Antonelou MH, Hansen KC, Papassideri IS, et al. An update on red blood cell storage lesions, as gleaned through biochemistry and omics technologies. Transfusion. 2015;55:205–19. http://dx.doi.org/10.1111/trf.12804
8. Centers for Disease Control and Prevention. National Healthcare Safety Network biovigilance component hemovigilance module surveillance protocol. 2018 Apr [cited 2018 Nov 25]. https://www.cdc.gov/nhsn/pdfs/biovigilance/bv-hv-protocol-current.pdf
9. De Coster W, D'Hert S, Schultz DT, Cruts M, Van Broeckhoven C. NanoPack: visualizing and processing long-read sequencing data. Bioinformatics. 2018;34:2666–9. http://dx.doi.org/10.1093/bioinformatics/bty149
10. Koren S, Walenz BP, Berlin K, Miller JR, Bergman NH, Phillippy AM. Canu: scalable and accurate long-read assembly via adaptive k-mer weighting and repeat separation. Genome Res. 2017;27:722–36. http://dx.doi.org/10.1101/gr.215087.116
11. Wick RR, Schultz MB, Zobel J, Holt KE. Bandage: interactive visualization of de novo genome assemblies. Bioinformatics. 2015; 31:3350–2. http://dx.doi.org/10.1093/bioinformatics/btv383
12. Loman NJ, Quick J, Simpson JT. A complete bacterial genome assembled de novo using only nanopore sequencing data. Nat Methods. 2015;12:733–5. http://dx.doi.org/10.1038/nmeth.3444

13. Seemann T. Prokka: rapid prokaryotic genome annotation. Bioinformatics. 2014;30:2068–9. http://dx.doi.org/10.1093/bioinformatics/btu153
14. Mulet M, Lalucat J, García-Valdés E. DNA sequence-based analysis of the *Pseudomonas* species. Environ Microbiol. 2010; 12:1513–30.
15. Kearse M, Moir R, Wilson A, Stones-Havas S, Cheung M, Sturrock S, et al. Geneious Basic: an integrated and extendable desktop software platform for the organization and analysis of sequence data. Bioinformatics. 2012;28:1647–9. http://dx.doi.org/10.1093/bioinformatics/bts199
16. Bodilis J, Nsigue-Meilo S, Besaury L, Quillet L. Variable copy number, intra-genomic heterogeneities and lateral transfers of the 16S rRNA gene in Pseudomonas. PLoS One. 2012;7:e35647. http://dx.doi.org/10.1371/journal.pone.0035647
17. Panicker G, Mojib N, Nakatsuji T, Aislabie J, Bej AK. Occurrence and distribution of capB in Antarctic microorganisms and study of its structure and regulation in the Antarctic biodegradative Pseudomonas sp. 30/3. Extremophiles. 2010;14:171–83. http://dx.doi.org/10.1007/s00792-009-0296-5
18. Cornelis P. Iron uptake and metabolism in pseudomonads. Appl Microbiol Biotechnol. 2010;86:1637–45. http://dx.doi.org/10.1007/s00253-010-2550-2
19. Blin K, Wolf T, Chevrette MG, Lu X, Schwalen CJ, Kautsar SA, et al. antiSMASH 4.0-improvements in chemistry prediction and gene cluster boundary identification. Nucleic Acids Res. 2017;45:W36–41. http://dx.doi.org/10.1093/nar/gkx319
20. Behrendt U, Ulrich A, Schumann P. Fluorescent pseudomonads associated with the phyllosphere of grasses; *Pseudomonas trivialis* sp. nov., *Pseudomonas poae* sp. nov. and *Pseudomonas congelans* sp. nov. Int J Syst Evol Microbiol. 2003;53:1461–9. http://dx.doi.org/10.1099/ijs.0.02567-0
21. Vyas P, Rahi P, Gulati A. Stress tolerance and genetic variability of phosphate-solubilizing fluorescent *Pseudomonas* from the cold deserts of the trans-Himalayas. Microb Ecol. 2009;58:425–34. http://dx.doi.org/10.1007/s00248-009-9511-2
22. Gulati A, Rahi P, Vyas P. Characterization of phosphate-solubilizing fluorescent pseudomonads from the rhizosphere of seabuckthorn growing in the cold deserts of Himalayas. Curr Microbiol. 2008;56:73–9. http://dx.doi.org/10.1007/s00284-007-9042-3
23. Cho KM, Hong SY, Lee SM, Kim YH, Kahng GG, Lim YP, et al. Endophytic bacterial communities in ginseng and their antifungal activity against pathogens. Microb Ecol. 2007;54:341–51. http://dx.doi.org/10.1007/s00248-007-9208-3
24. Khan AH, Anees M, Arshad M, Muhammad YS, Iqbal M, Yousaf S. Effects of illuminance and nutrients on bacterial photo-physiology of hydrocarbon degradation. Sci Total Environ. 2016;557–558:705–11. http://dx.doi.org/10.1016/j.scitotenv.2016.03.068
25. Collard K, White D, Copplestone A. The influence of storage age on iron status, oxidative stress and antioxidant protection in paediatric packed cell units. Blood Transfus. 2014;12:210–9.
26. Brecher ME, Hay SN. Bacterial contamination of blood components. Clin Microbiol Rev. 2005;18:195–204. http://dx.doi.org/10.1128/CMR.18.1.195-204.2005
27. Chaffin DJ, Kuehnert MJ. *Pseudomonas fluorescens*–related septic transfusion reaction resulting from contaminated cold cloths. Transfusion. 2002;42:41S.
28. de Goffau MC, Lager S, Salter SJ, Wagner J, Kronbichler A, Charnock-Jones DS, et al. Recognizing the reagent microbiome. Nat Microbiol. 2018;3:851–3. http://dx.doi.org/10.1038/s41564-018-0202-y
29. van der Poll T, van de Veerdonk FL, Scicluna BP, Netea MG. The immunopathology of sepsis and potential therapeutic targets. Nat Rev Immunol. 2017;17:407–20. http://dx.doi.org/10.1038/nri.2017.36
30. Bryant CE, Spring DR, Gangloff M, Gay NJ. The molecular basis of the host response to lipopolysaccharide. Nat Rev Microbiol. 2010;8:8–14. http://dx.doi.org/10.1038/nrmicro2266
31. Opal SM. The host response to endotoxin, antilipopolysaccharide strategies, and the management of severe sepsis. Int J Med Microbiol. 2007;297:365–77. http://dx.doi.org/10.1016/j.ijmm.2007.03.006
32. Chen K, Geng S, Yuan R, Diao N, Upchurch Z, Li L. Super-low dose endotoxin pre-conditioning exacerbates sepsis mortality. EBioMedicine. 2015;2:324–33. http://dx.doi.org/10.1016/j.ebiom.2015.03.001
33. Wheeler DS, Lahni PM, Denenberg AG, Poynter SE, Wong HR, Cook JA, et al. Induction of endotoxin tolerance enhances bacterial clearance and survival in murine polymicrobial sepsis. Shock. 2008;30:267–73.
34. Kim H, Jung BJ, Kim JY, Chung DK. Differential effects of low and high doses of lipoteichoic acid on lipopolysaccharide-induced interleukin-6 production. Inflamm Res. 2014;63:419–28. http://dx.doi.org/10.1007/s00011-014-0714-8
35. Roth VR, Arduino MJ, Nobiletti J, Holt SC, Carson LA, Wolf CF, et al. Transfusion-related sepsis due to Serratia liquefaciens in the United States. Transfusion. 2000;40:931–5. http://dx.doi.org/10.1046/j.1537-2995.2000.40080931.x

Address for correspondence: John J. Farrell, OSF St. Francis Medical Center, 1224 N Berkeley Ave, Peoria, IL 61603, USA; email: jjf@uic.edu

Zika Virus Infection in Pregnant Women, Yucatan, Mexico

Yamila Romer, Nina Valadez-Gonzalez, Silvina Contreras-Capetillo, Pablo Manrique-Saide, Gonzalo Vazquez-Prokopec, Norma Pavia-Ruz

Medscape EDUCATION ACTIVITY

In support of improving patient care, this activity has been planned and implemented by Medscape, LLC and Emerging Infectious Diseases. Medscape, LLC is jointly accredited by the Accreditation Council for Continuing Medical Education (ACCME), the Accreditation Council for Pharmacy Education (ACPE), and the American Nurses Credentialing Center (ANCC), to provide continuing education for the healthcare team.

Medscape, LLC designates this Journal-based CME activity for a maximum of 1.00 ***AMA PRA Category 1 Credit(s)™***. Physicians should claim only the credit commensurate with the extent of their participation in the activity.

Successful completion of this CME activity, which includes participation in the evaluation component, enables the participant to earn up to 1.0 MOC points in the American Board of Internal Medicine's (ABIM) Maintenance of Certification (MOC) program. Participants will earn MOC points equivalent to the amount of CME credits claimed for the activity. It is the CME activity provider's responsibility to submit participant completion information to ACCME for the purpose of granting ABIM MOC credit.

All other clinicians completing this activity will be issued a certificate of participation. To participate in this journal CME activity: (1) review the learning objectives and author disclosures; (2) study the education content; (3) take the post-test with a 75% minimum passing score and complete the evaluation at http://www.medscape.org/journal/eid; and (4) view/print certificate. For CME questions, see page 1623.

Release date: July 15, 2019; Expiration date: July 15, 2020

Learning Objectives

Upon completion of this activity, participants will be able to:

- Describe the demographic and epidemiological findings of a prospective cohort of pregnant women during the initial phase of ZIKV introduction into Yucatán, Mexico
- Explain the laboratory findings of a prospective cohort of pregnant women during the initial phase of ZIKV introduction into Yucatán, Mexico
- Identify the clinical findings of a prospective cohort of pregnant women during the initial phase of ZIKV introduction into Yucatán, Mexico

CME Editor

Thomas J. Gryczan, MS, Technical Writer/Editor, Emerging Infectious Diseases. *Disclosure: Thomas J. Gryczan, MS, has disclosed no relevant financial relationships.*

CME Author

Laurie Barclay, MD, freelance writer and reviewer, Medscape, LLC. *Disclosure: Laurie Barclay, MD, has disclosed no relevant financial relationships.*

Authors

Disclosures: ***Yamila Romer, MD; Nina Valadez-González, DSc; Silvina Noemi Contreras-Capetillo, MS; Pablo Manrique-Saide, PhD; Gonzalo Vazquez-Prokopec, PhD;*** *and* ***Norma Pavia-Ruz, MS,*** *have disclosed no relevant financial relationships.*

Author affiliations: Emory University, Atlanta, Georgia, USA (Y. Romer, G. Vazquez-Prokopec); Universidad Autónoma de Yucatan, Yucatan, Mexico (N. Valadez-Gonzalez, S. Contreras-Capetillo, P. Manrique-Saide, N. Pavia-Ruz)

DOI: https://doi.org/10.3201/eid2508.180915

We report demographic, epidemiologic, and clinical findings for a prospective cohort of pregnant women during the initial phase of Zika virus introduction into Yucatan, Mexico. We monitored 115 pregnant women for signs of active or recent Zika virus infection. The estimated cumulative incidence of Zika virus infection was 0.31 and the ratio of symptomatic to asymptomatic cases was 1.7 (range 1.3–4.0 depending on age group). Exanthema was the most sensitive clinical sign but also the least specific. Conjunctival hyperemia, joint edema, and exanthema were the combination of signs that had the highest specificity but low sensitivity. We did not find evidence of vertical transmission or fetal anomalies, likely because of the low number of pregnant women tested. We also did not find evidence of congenital disease. Our findings emphasize the limited predictive value of clinical features in areas where Zika virus cocirculates with other flaviviruses.

Zika virus, a mosquitoborne flavivirus, emerged abruptly in the Americas. It was first recognized in Brazil during 2015 in association with an outbreak of exanthematic disease, which was quickly linked to neurologic and immunological complications and congenital malformations (*1–6*). The first epidemic wave was centered in northeastern Brazil and associated with a high incidence of vertical transmission and cases of congenital disease that reached peaks of 49.9 cases/10,000 live births (*7*). The virus quickly spread to other countries and affected large sectors of Central America, South America, southern regions of North America, and the Caribbean (*8*). However, similarly high rates of congenital disease were not observed in other regions or in subsequent transmission waves in northeastern Brazil (*9,10*). The magnitude of the risk for vertical transmission and congenital syndromes, as well as possible associations that might increase or decrease these risks, remain unknown.

Multiple factors have been suggested to explain regional differences in disease incidence, including ethnic, environmental, nutritional, and virologic factors, as well as herd immunity (*11–14*). In addition, the possibility of overreporting of cases because of high public and epidemiologic awareness has been considered (*11,15*). The objectives of this study were to characterize the incidence, epidemiologic characteristics, clinical manifestations, and birth outcomes after Zika virus infection in pregnant women during the early phase of virus introduction in the state of Yucatan, Mexico.

Methods

Population

We have been evaluating integrated strategies to prevent *Aedes* mosquitoborne diseases in Yucatan State, Mexico. After health authorities confirmed the presence of Zika virus in Mexico, we designed a prospective study to quantify the incidence of disease and infection in pregnant women. The catchment area included a longitudinal cohort of 884 families (3,993 persons) residing in the cities of Merida, Ticul, and Progreso de Castro in Yucatan State (*16*). Merida and its metropolitan area, which have ≈1 million inhabitants, contain ≈50% of the Yucatan population. Progreso de Castro (population ≈37,400) and Ticul (population 32,000) are smaller urban areas. We enrolled consenting pregnant women from these areas during July 1, 2016–August 31, 2017. In addition, we independently enrolled pregnant women referred by physicians in primary care facilities or hospital facilities involved in our cohort study during the same period.

Clinical Follow-up of Pregnant Women and Newborns

Patient monitoring included a monthly visit for clinical assessment and sample collection (blood and urine), weekly doctor follow-up by text messages, and complete access to a telephone to report any clinical signs in pregnant women, their newborns, or any family contact. Fetal ultrasonography was performed at enrollment and every 3 months. At the first visit, a questionnaire was given to establish the clinical–epidemiologic profile. The pregnancy follow-up ended when the pregnancy was completed by delivery or fetal loss or the participant withdrew from the study. After initial clinical evaluation (anthropometric measurements, APGAR score [*17*], and clinical complications) and sample collection from the newborn, the postnatal follow-up included an evaluation during the first 18 months of life to detect development of any anomalies. These evaluations included cognitive and psychomotor status, neurology, ophthalmology, and genetic and audiology ≥1 time during this period. We used a definition of microcephaly based on the recommendation of the World Health Organization (*18*); cranial circumference ≥2 SDs below the mean for the age and sex of the baby.

Laboratory Testing

We detected Zika virus RNA by using real-time reverse transcription PCR (RT-PCR) for blood and urine samples as described (*19–22*). We also performed RT-PCR for Zika virus for blood of newborns and cerebrospinal fluid, as well as products of conception, including amniotic fluid, placenta, and fetal tissues, according to clinical needs (*23*). The RT-PCR studies were conducted in the Laboratory of Clinical Hematology of the Centro de Investigaciones Regionales (Merida, Mexico).

Statistical Analysis

We compared clinical and epidemiologic variables between pregnant women who were infected with Zika virus during pregnancy and women who remained Zika virus–negative by RT-PCR by calculating odds ratios and testing for their significance by using the Fisher 2-sided exact test. We evaluated differences in head circumference between groups of babies born to Zika virus–positive and –negative mothers by using the Wilcoxon signed rank test. Differences in p-values ≤0.05 were considered statistically significant. All analyses were performed by using SPSS version 24 software (IBM, https://www.ibm.com).

Results

A total of 115 pregnant women were included in the study: 66 from Merida, 45 from Ticul, and 4 from Progreso de Castro. One third were positive for Zika virus by RT-PCR of blood, urine, or both, at the initial evaluation (26 women) or during follow up (10 women). The cumulative incidence of Zika virus infection in the cohort was 0.31. The symptomatic to asymptomatic ratio among PCR-positive patients infected with Zika virus was 1.7 (range 1.3–4.0, depending on age group), and the highest proportion was in women 20–29 years of age (Table 1). Of the 26

Table 1. Symptomatic and asymptomatic Zika virus–positive pregnant women, by age group, Yucatan, Mexico*

Age group, y	Symptomatic	Asymptomatic	p value†	S:A Ratio
15–19	2	5	0.073	0.4
20–29	16	4	0.038	4
30–49	5	4	0.693	1.25
Total	23	13	<0.0001	1.7

*Patients were positive by PCR. A, asymptomatic; S, symptomatic.
†By Fisher exact test.

positive patients at baseline, 22 had blood and urine samples, 3 had only blood samples, and 1 had only a urine sample. Of 22 paired blood and urine samples, 5 were Zika virus positive for both samples, 16 were Zika virus positive only for blood samples, and 1 was Zika virus positive only for a urine sample. Three unpaired blood samples and 1 unpaired urine sample were positive for Zika virus (Table 2).

In subsequent monthly testing, 11 (42%) blood samples remained positive and 2 urine samples that were negative in the first test became positive. In the third interval, 4 (15%) blood samples remained positive, and only 1 (3%) remained positive during the fourth interval. No urine sample was positive in 2 consecutive monthly controls. No intermittent urine virus shedding was detected. Seven (50%) of 14 women with virus shedding in urine had clinical symptoms at the time of virus detection. For 5 patients, the positive urine sample occurred at the same time as the positive blood sample, and for 2 patients, urine was positive after the blood sample showed a negative result. Of the 10 patients in whom infection developed during follow-up, 7 had paired blood–urine samples; 3 of those had positive blood and urine samples, 3 had only positive blood samples, and 1 had only a positive urine sample. Two patients were positive only for the urine sample, and 1 was positive only for the blood sample. For 1 patient, a urine sample negative at the time of detecting the infection became positive in the subsequent monthly control while the blood sample became negative. One patient had a blood sample that remained positive for >1 time interval.

We obtained the distribution of the cases per epidemiologic week for Yucatan State and the national epidemiologic curve (Figure, panel A). We detected cases of Zika virus infection 3 weeks before the passive surveillance system detected any cases, and time series of case counts in the cohort matched the epidemiologic curve for the passive surveillance system in shape and temporality (Figure, panel B). Of the Zika virus–positive mothers 8 were enrolled during the first trimester, 23 during the second trimester, and 5 during the third trimester. Of the Zika virus–negative mothers, 22 were enrolled during the first trimester, 39 during the second trimester, and 18 during the third trimester. Two weeks after the date of last menstruation was considered representative of the moment of conception and was established for 100 case-patients (33 positive for Zika virus and 67 negative for Zika virus).

If one considers the probability of acquiring Zika virus infection in relation to the moment of conception, those women who conceived during 2016 during epidemiologic weeks 13–40 had a statistically significant increased risk for acquiring the infection during pregnancy than for women who conceived during epidemiologic weeks 41–52 of 2016 and 1–12 of 2017 (odds ratio 5.86; $p<0.001$). For those patients who were positive at the time of enrollment, it was not possible to identify precisely when they became infected. In patients who were detected infected during follow-up, 0 became infected in the first trimester, 5 in the second trimester, and 5 in the third trimester. The average age of pregnant women in the study was 25 years, and we found no major differences in age distribution between Zika virus–positive and Zika virus–negative mothers (Table 3). We also found no difference in Zika virus infection for women of different socioeconomic status or between women residing in urban or rural areas (Table 3).

More than half (64%) of the women had >1 sign or symptom compatible with acute infection (Table 3). We found that headache, retro-orbital pain, arthralgia, conjunctival hyperemia, joint edema, exanthema, and pruritus, each had a strong association with Zika virus infection (Table 3). If we considered separately only those objective signs that showed a strong association (conjunctival hyperemia, joint edema, and exanthema), we found that 7 Zika virus–positive had all 3 signs and that none of the Zika virus–negative patients had these 3 signs. All Zika virus–positive patients

Table 2. PCR results for pregnant women at time of first positive sample for Zika virus infection, Yucatan, Mexico

Result	No. (%)
Zika virus positive at time of enrollment, n = 26	
Blood and urine positive	5 (19)
Blood positive, urine negative	16 (61)
Blood positive without urine tested	3 (11)
Urine positive without blood tested	1 (4)
Blood negative, urine positive	1 (4)
Zika virus positive during follow-up, n = 10	
Blood and urine positive	3 (30)
Blood positive, urine negative	3 (30)
Blood positive without urine tested	1 (10)
Urine positive without blood tested	2 (20)
Blood negative, urine positive	1 (10
Total, n = 36	36 (100)
Blood and urine positive	8 (22)
Blood positive, urine negative	19 (53)
Blood positive without urine tested	4 (11)
Urine positive without blood tested	3 (8)
Blood negative, urine positive	2 (6)

who had joint edema also had exanthema and conjunctival hyperemia (Table 3). One Zika virus–negative patient had joint edema associated with exanthema but without conjunctival hyperemia.

A total of 17 Zika virus–positive patients had conjunctival injection, which was present in only 3 Zika virus–negative patients. For these 17 patients, this infection was associated with exanthema, and for 7 patients, this infection was associated with joint edema. Six patients had only exanthema. For subjective but unusual symptoms, such as retro-orbital pain (9 patients) and pruritus (11 patients), we observed that all but 1 patient with retro-orbital pain also had conjunctival hyperemia, and all had exanthema. Of patients with pruritus, all had exanthema, 10 had conjunctival hyperemia, and 6 had joint edema. The most frequent clinical findings among Zika virus–positive women were exanthema, arthralgia, and conjunctival hyperemia. Headache, retro-orbital pain, joint edema, and pruritus were the most specific signs and symptoms, but these symptoms had low sensitivity (Table 4). The proportion of symptomatic Zika virus–positive patients did not vary between cities. We did not observe hemorrhagic or systemic complications in any patient.

At the time of this study, all pregnancies were complete. Of these pregnancies, 3% were preterm, 2 for Zika virus–negative mothers and 1 for a Zika virus–positive mother (Table 5). Two fetal losses (2 in the first trimester and 1 in the third trimester) occurred among Zika virus–negative mothers. No newborns or products of conception were positive for Zika virus by virologic tests. We determined APGAR scores and percentiles of head circumference (Table 4). A Wilcoxon signed-rank test showed no significant

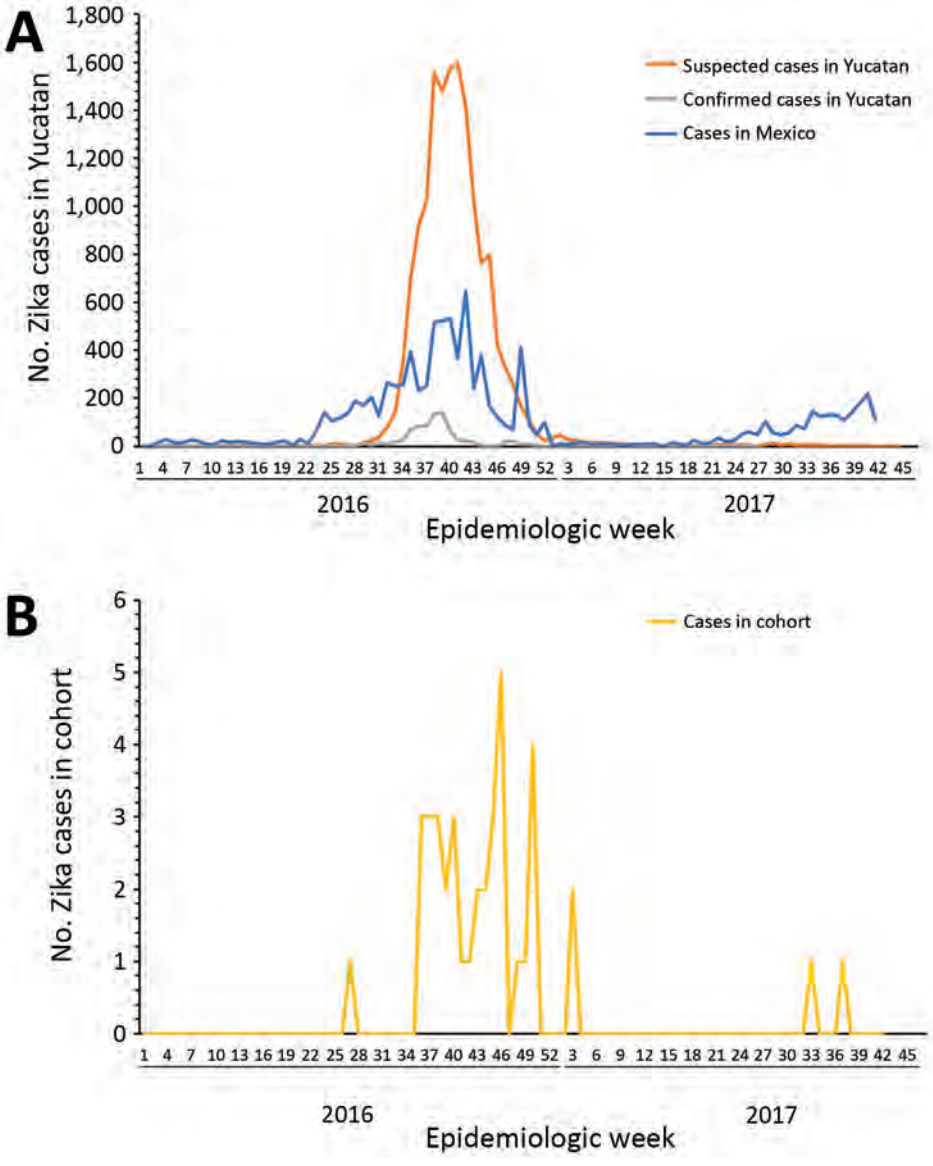

Figure. Distribution of cases of Zika virus infection, by epidemiologic week, Mexico, 2016–2017. A) Suspected and confirmed cases of Zika virus infection in Yucatan State and cases in Mexico. B) Cases of Zika virus infection among 115 pregnant women enrolled in study in 3 areas of Yucatan State.

difference between head circumference of babies from Zika virus–positive mothers and Zika virus–negative mothers (W = 213; p = 0.82). One newborn from a Zika virus–positive mother died during the first days of life because of gastroschisis. Other complications occurred among newborns but were nonspecific with regards to Zika virus infection status of the mothers (Table 4). Regarding the follow-up of the infants, although it is still in progress, no anomalies potentially related to Zika virus infection have been detected. Zika virus–positive mothers of 5 babies and Zika virus–negative mothers of 10 babies voluntarily withdrew from the study after delivery; this loss represented 13% of the cohort and was distributed proportionally between the 2 groups.

Discussion

Yucatan State in Mexico, where 84% of the population resides in urban areas, has been a hotspot for *Aedes* mosquitoborne diseases for many decades. After introduction of Zika virus, routine measures to avoid vector propagation

Table 3. PCR results for Zika virus infection of clinical samples from pregnant women who showed development of infection during follow-up*

Variable	No. (%) Zika virus–positive, n = 36	Zika virus–negative, n = 79	Total, n = 115	p value†	Odds ratio
Age group, y					
15–19	7 (19)	19 (24)	26 (23)	0.639	0.76
20–29	20 (56)	42 (53)	62 (54)	0.843	1.1
30–49	9 (25)	18 (23)	27 (23)	0.815	1.13
Socioeconomic level‡					
1	4 (11)	3 (4)	7 (6)	0.12	3
2	13 (36)	42 (53)	55 (48)	0.09	0.4
3	13 (36)	24 (30)	37 (32)	0.54	1.2
4	6 (17)	10 (13)	16 (14)	0.56	1.3
Urban residency	33 (92)	70 (90)	103 (90)	0.78	1.25
Contacts tested positive					
Family members	3 (12)	3 (5)	7§	0.3	2.7
Partner	0	2 (3)	2¶	1	1.4
Working outside home	18 (50)	19 (24)	37 (32)	0.007	3.15
GW at admission to cohort, trimester					
5–13, first	8 (22)	22 (28)	30 (26)	NA	NA
14–27, second	23 (64)	39 (49)	62 (53)	NA	NA
28–40, third	5 (14)	18 (23)	23 (20)	NA	NA
LMD/EW#					
1–12	5 (15)	22 (33)	27 (27)	0.093	0.373
13–28	15 (45)	15 (22)	30 (30)	0.021	2.9
29–40	11 (33)	11 (16)	22 (22)	0.07	2.6
41–52	2 (6)	19 (28)	21 (21)	0.017	0.166
13–40/12–41	NA	NA	NA	<0.0001	5.86
Symptomatic	23 (64)	10 (13)	33 (28)	<0.0001	12.2
Exanthema	23 (100)	10 (100)	33 (100)	<0.0001	12.2
Conjunctival hyperemia	17 (73)	3 (30)	20 (60)	<0.0001	22.6
Arthralgia	15 (65)	3 (30)	18 (55)	<0.0001	18.1
Pruritus	11 (48)	0	11 (33)	<0.0001	NA
Headache	9 (39)	2 (20)	11 (33)	<0.0001	12.8
Retro-orbital pain	9 (39)	0	9 (27)	<0.0001	NA
Joint edema	7 (30)	1 (10)	8 (24)	0.001	18.8
Myalgia	6 (26)	1 (10)	7 (21)	0.004	15.6
Fever	4 (17)	1 (10)	5 (15)	0.033	9.7
Diarrhea	3 (13)	0	3 (9)	0.029	NA
Odynophagia	2 (9)	0	2 (6)	0.096	NA
Cough	2 (9)	0	2 (6)	0.096	NA
Congested	2 (9)	0	2 (6)	0.096	NA
Nausea	2 (9)	1 (10)	3 (9)	0.230	4.5
Vomiting	1 (4)	0	1 (3)	0.313	NA
Petechia	1 (4)	0	1 (3)	0.313	NA
Gingival bleeding	1 (4)	0	1 (3)	0.313	NA

*Initial samples for all patients showed negative results. EW, epidemiologic week; GW, gestational week; LMD, last menstruation date; NA, not applicable; T, trimester.
†By Fisher exact test.
‡1, income insufficient to cover basic needs; 2, income just covers basic needs; 3, income for basic needs is met and includes certain recreational activities; 4, income is sufficient for recreational activities and luxuries.
§90 studied cases.
¶87 studied cases.
#>100 patients with LMD data.

Table 4. Statistical values of clinical variables for pregnant women infected with Zika virus, Yucatan, Mexico

Clinical variable	Positive predictive value, %	Negative predictive value, %	Diagnostic accuracy, %
Exanthema	70	84	80
Conjunctival hyperemia	85	80	80
Arthralgia	83	78	79
Itching	100	76	78
Headache	82	74	75
Retro-orbital pain	100	75	77
Joint edema	88	73	74

(e.g., ultra-low volume spraying indoors and outdoors in areas where symptomatic cases were reported, community education), as well as personal protection against mosquito bites, were implemented by the regional government. Such interventions failed to contain Zika virus propagation (*24*) and were not directed toward pregnant women. The detailed evaluation of a cohort of pregnant women who were positive for Zika virus shortly before conception or who became infected during their pregnancy provided no evidence of vertical transmission to the fetus or fetal malformations directly attributed to Zika virus. Nonetheless, our evaluation of this cohort documented useful symptomology and demographic trends of Zika virus infection in pregnant women in a poorly studied area to which dengue virus and other flaviviruses are endemic.

We showed by univariate analyses that the most sensitive clinical sign was exanthema, but it was also the least specific. Conjunctival hyperemia, joint edema, and exanthema was the combination with the highest level of specificity. Given the cocirculation of Zika virus with other arboviruses in the region with which it shares common clinical characteristics (exanthema, headache, arthralgia), it is expected that the specificity, positive predictive value, and diagnostic accuracy will decrease in relation to the differential diagnosis. The absence of fever, as well as the presence of exanthema, with or without other signs and symptoms, should alert the primary health system to suspect Zika virus infection in pregnant women at any time during the evolution of their pregnancy.

The proportion of symptomatic cases observed in our cohort can be an expression of the bias in our enrollment strategy because patients referred by physicians from primary care facilities are more likely to be positive for Zika virus infection and symptomatic. During the study period, active circulation of chikungunya virus and dengue virus was reported in the area. Because our samples were not tested for these virus infections, the chance of a co-infection cannot be ruled out. This finding represents a major limitation when we analyzed the clinical approach to orient diagnosis.

The risk for congenital disease among Zika virus–infected pregnant women has been estimated to be 1%–13% (*25*–*28*), and this rate increases when the maternal infection occurs during the first and second trimesters (*29*,*30*). Although we did not detect direct evidence of congenital

Table 5. Outcomes of pregnancy and for newborn children born to Zika virus–infected and –noninfected mothers, Yucatan, Mexico*

Outcome	Zika virus–positive mothers, n = 31	Zika virus–negative mothers, n = 69	Total, n = 100	p value†	Odds ratio
Pregnancy‡					
Live births	NA	NA	NA	NA	NA
Term	30 (97)	67 (97)	NA	0.90	0.89
Preterm	1 (3)	2 (3)	NA	0.90	1.10
Fetal loss, trimester					
First	0	2 (2)	2 (2)	NA	NA
Second	0	0	0	NA	NA
Third	0	1 (1)	1 (1)	NA	NA
Newborn					
APGAR score, 1 min, median (range)	7.9 (4–9)	8 (6–9)	NA	NA	NA
APGAR score, 5 min, median (range)	8.8 (5–9)	8.9 (8–9)	NA	NA	NA
Head circumference, median (range), cm	33.99 (29–36)	33.46 (29–35)	NA	0.82§	NA
PCR Zika virus–positive	0	0	0	NA	NA
Death or neonatal complications¶	5 (16)	3 (5)	8 (10)	0.06	4.20
Hyperbilirubinemia	1 (3)	2 (4)	3 (4)	0.90	1.10
Intrauterine growth retardation	0	2 (4)	2 (2)	0.47	NA
Syphilis	0	1 (2)	1 (1)	0.69	NA
Gastroschisis	1 (3)	0	1 (1)	0.31	NA
Erythema toxicity	2 (6)	0	2 (2)	0.09	NA
Microcephaly	0	1 (2)	1 (1)	0.69	NA
Anemia	0	1 (2)	1 (1)	0.69	NA

*Values are no. (%) unless otherwise indicated. NA, not applicable.
†By Fisher exact test.
‡Loss of follow-up for 5 Zika virus–positive mothers and for 10 Zika virus–negative mothers.
§By Wilcoxon signed-rank test.
¶Only 1 newborn death was observed and was from a Zika virus–positive mother.

transmission by testing with RT-PCR, development of abnormalities attributable to Zika virus infection could still occur during infancy (*31*). The low number of pregnant women enrolled in this study could have precluded detection of congenital infection. Alternately, the absence of overt congenital Zika virus infection in this small cohort could reflect the relative rarity of this condition, as observed in other countries (*7*,*9*,*32*,*33*). In addition, the limitations to implement serologic tests because cross-reactivity with other flavivirus (*34*–*36*) could have masked laboratory confirmation of Zika virus infection for patients after the waning of virus presence in fluids or tissues. The lack of clinical manifestations at birth does not eliminate the possibility of congenital disease, as reported (*37*,*38*).

There is recognized discordance in Zika virus detection on concurrent blood and urine samples (*39*–*41*). Urine samples are transiently positive after virus is detected in blood. Urine samples alone were insufficient in detecting 16 cases. A total of 43% of Zika virus–positive patients had a viremia for >4 weeks and 15% for >8 weeks. This prolonged viremia, which is unusual for other arboviruses, has been reported in pregnant women in other studies (*42*,*43*). The role of this prolonged viremia on pathogenesis of congenital diseases or dissemination of the infection is unclear.

Women who work outside had an increased risk for contracting the infection, potentially reflecting differential exposure to *Aedes aegypti* mosquitoes at locations other than their home (*44*,*45*); the highest incidence of pregnancies in women 20–29 years of age is consistent with results of another case series (*32*). We have not observed major differences in Zika virus infection in different age groups. We have observed that the highest proportion of Zika virus–positive women with symptomatic disease was among women 20–29 years of age, which is different from other studies that reported the highest ratio of symptomatic disease among women >30 years of age (*46*,*47*).

Although knowledge of clinical manifestations, natural history, and epidemiology of Zika virus in the Americas is incipient, the clinical–epidemiologic scenario involving severe congenital disease that was manifested initially in Brazil has not been observed at the same magnitude in other countries. Our prospective study of a cohort of pregnant women in Yucatan, Mexico, showed the value of active surveillance in early detection of infections and point to the limited predictive value of symptoms in areas where Zika virus cocirculates with other flaviviruses. In our study of 115 pregnant women with active or recent Zika virus infections, we found no evidence of congenital Zika virus disease.

This research and publication was made possible through support provided by the Office of Infectious Disease, Bureau for Global Health, US Agency for International Development, under the terms of an Interagency Agreement with CDC. The opinions expressed herein are those of the author(s) and do not necessarily reflect the views of the US Agency for International Development. The recipient of this support was the Yucatan Autonomous University and its affiliated Regional Research Center “Hideyo Nogushi.”

About the Author

Dr. Romer is an infectious disease clinician and microbiologist in the Department of Environmental Sciences at Emory University, Atlanta, GA. Her primary research interests include arthropod-borne diseases.

References

1. Cardoso CW, Paploski IA, Kikuti M, Rodrigues MS, Silva MM, Campos GS, et al. Outbreak of exanthematous illness associated with Zika, chikungunya, and dengue viruses, Salvador, Brazil. Emerg Infect Dis. 2015;21:2274–6. http://dx.doi.org/10.3201/eid2112.151167
2. Zika virus outbreaks in the Americas. Wkly Epidemiol Rec. 2015; 90:609–10.
3. Hennessey M, Fischer M, Staples JE. Zika virus spreads to new areas—region of the Americas, May 2015–January 2016. MMWR Morb Mortal Wkly Rep. 2016;65:55–8. http://dx.doi.org/10.15585/mmwr.mm6503e1
4. Pan American Health Organization/World Health Organization. Neurological syndrome, congenital malformations, and Zika virus infection. Implications for public health in the Americas. Epidemiological alert; 2015 [cited 2019 Apr 22]. https://www.paho.org/hq/dmdocuments/2015/2015-dec-1-cha-epi-alert-zika-neuro-syndrome.pdf
5. Miranda-Filho DB, Martelli CM, Ximenes RA, Araújo TV, Rocha MA, Ramos RC, et al. Initial description of the presumed congenital Zika syndrome. Am J Public Health. 2016;106:598–600. http://dx.doi.org/10.2105/AJPH.2016.303115
6. Smith DW, Mackenzie J. Zika virus and Guillain-Barré syndrome: another viral cause to add to the list. Lancet. 2016;387:1486–8. http://dx.doi.org/10.1016/S0140-6736(16)00564-X
7. de Oliveira WK, de França GV, Carmo EH, Duncan BB, de Souza Kuchenbecker R, Schmidt MI. Infection-related microcephaly after the 2015 and 2016 Zika virus outbreaks in Brazil: a surveillance-based analysis. Lancet. 2017;390:861–70. http://dx.doi.org/10.1016/S0140-6736(17)31368-5
8. World Health Organization. WHO situation report. Zika virus, microcephaly, Gillain-Barre syndrome; December 1, 2016 [cited 2017 Aug 31]. http://www.who.int/emergencies/zika-virus/situation-report
9. Cuevas EL, Tong VT, Rozo N, Valencia D, Pacheco O, Gilboa SM, et al. Preliminary report of microcephaly potentially associated with Zika virus infection during pregnancy—Colombia, January–November 2016. MMWR Morb Mortal Wkly Rep. 2016;65: 1409–13. http://dx.doi.org/10.15585/mmwr.mm6549e1
10. World Health Organization. Emergencies: the history of Zika virus; 2016 [cited 2017 Aug 31]. http://www.who.int/emergencies/zika-virus
11. Butler D. Brazil asks whether Zika acts alone to cause birth defects. Nature. 2016;535:475–6. http://dx.doi.org/10.1038/nature.2016.20309
12. Musso D, Gubler DJ. Zika virus. Clin Microbiol Rev. 2016;29: 487–524. http://dx.doi.org/10.1128/CMR.00072-15
13. Baud D, Gubler DJ, Schaub B, Lanteri MC, Musso D. An update on Zika virus infection. Lancet. 2017;390:2099–109. http://dx.doi.org/10.1016/S0140-6736(17)31450-2
14. Kuivanen S, Korhonen EM, Helisten A-A, Huhtamo E, Smura T, Vapalahti O. Differences in the growth properties of Zika virus

foetal brain isolate and related epidemic strains in vitro. J Gen Virol. 2017;98:1744–8. http://dx.doi.org/10.1099/jgv.0.000857
15. Rodrigues LC, Paixao ES. Risk of Zika-related microcephaly: stable or variable? Lancet. 2017;390:824–6. http://dx.doi.org/10.1016/S0140-6736(17)31478-2
16. Pavía-Ruz N, Salha Villanueva, Granja P, Balam-May A, Longini IM, Halloran ME, et al.; Diana Patricia Rojas. Seroprevalence of dengue antibodies in three urban settings in Yucatan, Mexico. Am J Trop Med Hyg. 2018;98:1202–8. http://dx.doi.org/10.4269/ajtmh.17-0382
17. Casey BM, McIntire DD, Leveno KJ. The continuing value of the Apgar score for the assessment of newborn infants. N Engl J Med. 2001;344:467–71. http://dx.doi.org/10.1056/NEJM200102153440701
18. World Health Organization. Screening, assessment and management of neonates and infants with complications associated with Zika virus exposure in utero: rapid advice guideline. Geneva: The Organization; 2016.
19. Lanciotti RS, Kosoy OL, Laven JJ, Velez JO, Lambert AJ, Johnson AJ, et al. Genetic and serologic properties of Zika virus associated with an epidemic, Yap State, Micronesia, 2007. Emerg Infect Dis. 2008;14:1232–9. http://dx.doi.org/10.3201/eid1408.080287
20. Bhatnagar J, Rabeneck DB, Martines RB, Reagan-Steiner S, Ermias Y, Estetter LB, et al. Zika virus RNA replication and persistence in brain and placental tissue. Emerg Infect Dis. 2017;23:405–14. http://dx.doi.org/10.3201/eid2303.161499
21. Rabe IB, Staples JE, Villanueva J, Hummel KB, Johnson JA, Rose L, et al.; MTS. Interim guidance for interpretation of Zika virus antibody test results. MMWR Morb Mortal Wkly Rep. 2016;65:543–6. http://dx.doi.org/10.15585/mmwr.mm6521e1
22. Centers for Disease Control and Prevention. Revised diagnostic testing for Zika, chikungunya, and dengue viruses in US public health laboratories [cited 2017 August 31]. https://www.cdc.gov/zika/transmission/index.htlm
23. Contreras-Capetillo SN, Valadéz-González N, Manrique-Saide P, Carcaño-Castillo RE, Pacheco-Tugores F, Barrera-Pérez HAM, et al. Birth defects associated with congenital Zika virus infection in Mexico. Clin Pediatr (Phila). 2018;57:927–36. http://dx.doi.org/10.1177/0009922817738341
24. Bisanzio D, Dzul-Manzanilla F, Gomez-Dantés H, Pavia-Ruz N, Hladish TJ, Lenhart A, et al. Spatio-temporal coherence of dengue, chikungunya and Zika outbreaks in Merida, Mexico. PLoS Negl Trop Dis. 2018;12:e0006298. http://dx.doi.org/10.1371/journal.pntd.0006298
25. Honein MA, Dawson AL, Petersen EE, Jones AM, Lee EH, Yazdy MM, et al.; US Zika Pregnancy Registry Collaboration. Birth defects among fetuses and infants of US women with evidence of possible Zika virus infection during pregnancy. JAMA. 2017;317:59–68. http://dx.doi.org/10.1001/jama.2016.19006
26. Duarte G, Moron AF, Timerman A, Fernandes CE, Mariani Neto C, Almeida Filho GL, et al. Zika virus infection in pregnant women and microcephaly. Rev Bras Ginecol Obstet. 2017;39:235–48. http://dx.doi.org/10.1055/s-0037-1603450
27. Rasmussen SA, Jamieson DJ, Honein MA, Petersen LR. Zika virus and birth defects: reviewing the evidence for causality. N Engl J Med. 2016;374:1981–7. http://dx.doi.org/10.1056/NEJMsr1604338
28. Cauchemez S, Besnard M, Bompard P, Dub T, Guillemette-Artur P, Eyrolle-Guignot D, et al. Association between Zika virus and microcephaly in French Polynesia, 2013–15: a retrospective study. Lancet. 2016;387:2125–32. http://dx.doi.org/10.1016/S0140-6736(16)00651-6
29. Noronha L, Zanluca C, Azevedo MLV, Luz KG, Santos CN. Zika virus damages the human placental barrier and presents marked fetal neurotropism. Mem Inst Oswaldo Cruz. 2016;111:287–93. http://dx.doi.org/10.1590/0074-02760160085
30. Singh RK, Dhama K, Malik YS, Ramakrishnan MA, Karthik K, Tiwari R, et al. Zika virus: emergence, evolution, pathology, diagnosis, and control: current global scenario and future perspectives—a comprehensive review. Vet Q. 2016;36:150–75. http://dx.doi.org/10.1080/01652176.2016.1188333
31. van der Linden V, Pessoa A, Dobyns W, Barkovich AJ, Júnior HV, Filho EL, et al. Description of 13 infants born during October 2015–January 2016 with congenital Zika virus infection without microcephaly at birth—Brazil. MMWR Morb Mortal Wkly Rep. 2016;65:1343–8. http://dx.doi.org/10.15585/mmwr.mm6547e2
32. Brasil P, Pereira JP Jr, Moreira ME, Ribeiro Nogueira RM, Damasceno L, Wakimoto M, et al. Zika virus infection in pregnant women in Rio de Janeiro. N Engl J Med. 2016;375:2321–34. http://dx.doi.org/10.1056/NEJMoa1602412
33. Coelho AVC, Crovella S. Microcephaly prevalence in infants born to Zika virus–infected women: a systematic review and meta-analysis. Int J Mol Sci. 2017;18:1714. http://dx.doi.org/10.3390/ijms18081714
34. Calisher CH, Karabatsos N, Dalrymple JM, Shope RE, Porterfield JS, Westaway EG, et al. Antigenic relationships between flaviviruses as determined by cross-neutralization tests with polyclonal antisera. J Gen Virol. 1989;70:37–43. http://dx.doi.org/10.1099/0022-1317-70-1-37
35. Allwinn R, Doerr HW, Emmerich P, Schmitz H, Preiser W. Cross-reactivity in flavivirus serology: new implications of an old finding? Med Microbiol Immunol (Berl). 2002;190:199–202. http://dx.doi.org/10.1007/s00430-001-0107-9
36. Mansfield KL, Horton DL, Johnson N, Li L, Barrett AD, Smith DJ, et al. Flavivirus-induced antibody cross-reactivity. J Gen Virol. 2011;92:2821–9. http://dx.doi.org/10.1099/vir.0.031641-0
37. Aragao MF, Holanda AC, Brainer-Lima AM, Petribu NC, Castillo M, van der Linden V, et al. Nonmicrocephalic infants with congenital Zika syndrome suspected only after neuroimaging evaluation compared with those with microcephaly at birth and postnatally: how large is the Zika virus "iceberg"? AJNR Am J Neuroradiol. 2017;38:1427–34. http://dx.doi.org/10.3174/ajnr.A5216
38. de Fatima Vasco Aragao M, van der Linden V, Brainer-Lima AM, Coeli RR, Rocha MA, Sobral da Silva P, et al. Clinical features and neuroimaging (CT and MRI) findings in presumed Zika virus related congenital infection and microcephaly: retrospective case series study. BMJ. 2016;353:i1901. http://dx.doi.org/10.1136/bmj.i1901
39. Sakkas H, Economou V, Papadopoulou C. Zika virus infection: Past and present of another emerging vector-borne disease. J Vector Borne Dis. 2016;53:305–11.
40. Kutsuna S, Kato Y, Takasaki T, Moi M, Kotaki A, Uemura H, et al. Two cases of Zika fever imported from French Polynesia to Japan, December 2013 to January 2014 [corrected]. Euro Surveill. 2014;19:20683. http://dx.doi.org/10.2807/1560-7917.ES2014.19.4.20683
41. Paz-Bailey G, Rosenberg ES, Doyle K, Munoz-Jordan J, Santiago GA, Klein L, et al. Persistence of Zika virus in body fluids: final report. N Engl J Med. 2017;379:1234–43. http://dx.doi.org/10.1056/NEJMoa1613108
42. Driggers RW, Ho C-Y, Korhonen EM, Kuivanen S, Jääskeläinen AJ, Smura T, et al. Zika virus infection with prolonged maternal viremia and fetal brain abnormalities. N Engl J Med. 2016;374:2142–51. http://dx.doi.org/10.1056/NEJMoa1601824
43. Meaney-Delman D, Oduyebo T, Polen KN, White JL, Bingham AM, Slavinski SA, et al.; U.S. Zika Pregnancy Registry Prolonged Viremia Working Group. Prolonged detection of Zika virus RNA in pregnant women. Obstet Gynecol. 2016;128:724–30. http://dx.doi.org/10.1097/AOG.0000000000001625
44. Stoddard ST, Forshey BM, Morrison AC, Paz-Soldan VA, Vazquez-Prokopec GM, Astete H, et al. House-to-house human

movement drives dengue virus transmission. Proc Natl Acad Sci U S A. 2013;110:994–9. http://dx.doi.org/10.1073/pnas.1213349110
45. Vazquez-Prokopec GM, Montgomery BL, Horne P, Clennon JA, Ritchie SA. Combining contact tracing with targeted indoor residual spraying significantly reduces dengue transmission. Sci Adv. 2017;3:e1602024. http://dx.doi.org/10.1126/sciadv.1602024
46. Duffy MR, Chen T-H, Hancock WT, Powers AM, Kool JL, Lanciotti RS, et al. Zika virus outbreak on Yap Island, Federated States of Micronesia. N Engl J Med. 2009;360:2536–43. http://dx.doi.org/10.1056/NEJMoa0805715
47. Flamand C, Fritzell C, Matheus S, Dueymes M, Carles G, Favre A, et al. The proportion of asymptomatic infections and spectrum of disease among pregnant women infected by Zika virus: systematic monitoring in French Guiana, 2016. Euro Surveill. 2017;22. http://dx.doi.org/10.2807/1560-7917.ES.2017.22.44.17-00102

Address for correspondence: Yamila Romer, Department of Environmental Sciences, Mathematics and Science Center, Emory University, 400 Dowman Dr, 5th Fl, Ste E523, Atlanta, GA, 30322, USA; email: yromer@emory.edu

etymologia revisited

Zika [zēkə] Virus

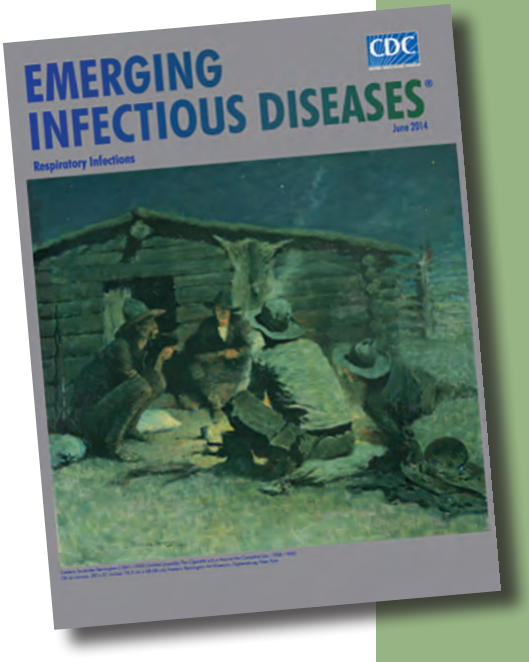

Originally published in June 2014

Zika virus is a mosquito-borne positive-sense, single-stranded RNA virus in the family *Flaviviridae*, genus *Flavivirus* that causes a mild, acute febrile illness similar to dengue. In 1947, scientists researching yellow fever placed a rhesus macaque in a cage in the Zika Forest (*zika* meaning "overgrown" in the Luganda language), near the East African Virus Research Institute in Entebbe, Uganda. A fever developed in the monkey, and researchers isolated from its serum a transmissible agent that was first described as Zika virus in 1952. It was subsequently isolated from a human in Nigeria in 1954. From its discovery until 2007, confirmed cases of Zika virus infection from Africa and Southeast Asia were rare. In 2007, however, a major epidemic occurred in Yap Island, Micronesia. More recently, epidemics have occurred in Polynesia, Easter Island, the Cook Islands, and New Caledonia.

Sources

1. Dick GW, Kitchen SF, Haddow AJ. Zika virus. I. Isolations and serological specificity. Trans R Soc Trop Med Hyg. 1952;46:509–20. http://dx.doi.org/10.1016/ 0035-9203 (52)90042-4
2. Hayes EB. Zika virus outside Africa. Emerg Infect Dis. 2009; 15: 1347–50.http://dx.doi.org/10.3201/eid1509.090442
3. MacNamara FN. Zika virus: a report on three cases of human infection during an epidemic of jaundice in Nigeria. Trans R Soc Trop Med Hyg. 1954;48:139–45. http://dx.doi.org/10.1016/0035-9203(54)90006-1
4. Murphy JD. Luganda–English dictionary. Washington (DC): The Catholic University of America Press; 1972.

https://wwwnc.cdc.gov/eid/article/20/6/et-2006_article

Multistate Outbreak of Listeriosis Associated with Packaged Leafy Green Salads, United States and Canada, 2015–2016

Julie L. Self, Amanda Conrad, Steven Stroika, Alikeh Jackson, Laura Whitlock, Kelly A. Jackson, Jennifer Beal, Allison Wellman, Marianne K. Fatica, Sally Bidol, Paula Pennell Huth, Meghan Hamel, Kristyn Franklin, Lorelee Tschetter, Christine Kopko, Penelope Kirsch, Matthew E. Wise, Colin Basler

We investigated an outbreak of listeriosis detected by whole-genome multilocus sequence typing and associated with packaged leafy green salads. Nineteen cases were identified in the United States during July 5, 2015–January 31, 2016; isolates from case-patients were closely related (median difference 3 alleles, range 0–16 alleles). Of 16 case-patients interviewed, all reported salad consumption. Of 9 case-patients who recalled brand information, all reported brands processed at a common US facility. The Public Health Agency of Canada simultaneously investigated 14 cases of listeriosis associated with this outbreak. Isolates from the processing facility, packaged leafy green salads, and 9 case-patients from Canada were closely related to US clinical isolates (median difference 3 alleles, range 0–16 alleles). This investigation led to a recall of packaged leafy green salads made at the processing facility. Additional research is needed to identify best practices and effective policies to reduce the likelihood of *Listeria monocytogenes* contamination of fresh produce.

Invasive *Listeria monocytogenes* infections (listeriosis) are the third leading cause of death from foodborne illness in the United States and cause an estimated 1,500 infections, 1,400 hospitalizations, and 250 deaths each year (*1*). Although incidence of listeriosis is lower than for many foodborne illnesses, it often results in severe illnesses, including sepsis and meningitis, and is associated with a high case-fatality rate and fetal loss in pregnant women (*2*–*4*). Populations at highest risk for invasive listeriosis include elderly persons, immunocompromised persons, and pregnant women and their newborns (*5*). Listeriosis can have a long incubation period (median 11 days, range 0–70 days) between exposure and symptom onset (*5*,*6*).

L. monocytogenes was first recognized as a foodborne pathogen after an outbreak in Canada during 1981 that was linked to cabbage in coleslaw (*7*). Outbreaks of listeriosis in the United States have historically been associated with ready-to-eat delicatessen meats and dairy products, but have more recently been associated with fresh produce, including sprouts, celery, cantaloupe, stone fruit, and caramel apples (*5*,*8*,*9*).

In October 2015, PulseNet USA (https://www.cdc.gov/pulsenet/index.html), the national molecular subtyping network for foodborne disease surveillance, identified a cluster of 8 clinical *L. monocytogenes* isolates from 6 states that were closely related genetically to one another by whole-genome multilocus sequence typing (wgMLST) (median difference 5 alleles, range 0–12 alleles); the Centers for Disease Control and Prevention (CDC; Atlanta, GA, USA) initiated a cluster investigation. During a weekly foodborne cluster investigation call on January 13, 2016, CDC informed the Public Health Agency of Canada (PHAC) of the cluster investigation, which had increased to include 13 cases of listeriosis. PHAC informed CDC of a cluster of 6 cases of listeriosis in Canada that had a pulsed-field gel electrophoresis (PFGE) pattern combination indistinguishable from that of the US cases. The United States and Canada conducted collaborative investigations to determine the source of the outbreak.

Author affiliations: Centers for Disease Control and Prevention, Atlanta, Georgia, USA (J.L. Self, A. Conrad, S. Stroika, L. Whitlock, K.A. Jackson, M.E. Wise, C. Basler); US Food and Drug Administration, College Park, Maryland, USA (A. Jackson, J. Beal, A. Wellman, M.K. Fatica); Michigan Department of Health and Human Services, Lansing, Michigan, USA (S. Bidol); New York State Department of Health, New York, New York, USA (P. Pennell Huth); Public Health Agency of Canada, Ottawa, Ontario, Canada (M. Hamel, K. Franklin, L. Tschetter); Canadian Food Inspection Agency, Ottawa (C. Kopko, P. Kirsch)

DOI: https://doi.org/10.3201/eid2507.180761

Methods

Investigation in the United States

Epidemiologic Investigation

We defined a case as laboratory-confirmed invasive listeriosis in which *L. monocytogenes* was isolated from a normally sterile site (e.g., blood or cerebrospinal fluid) or from products of conception (e.g., placental or fetal tissue). Isolates were indistinguishable from the outbreak PFGE pattern combination and closely related genetically to the outbreak clade by wgMLST (0–16 alleles) (*10*). Isolation dates were July 5, 2015–January 31, 2016.

In the United States, state and local health departments attempt to interview all patients with listeriosis (or their proxies) by using the *Listeria* Initiative (LI) questionnaire, which collects standard clinical, laboratory, and demographic information, as well as data for food exposures in the 28 days before illness onset (*11*). At the time of this investigation, the LI questionnaire included questions on 44 foods considered to have higher risk for *L. monocytogenes* contamination on the basis of previous outbreaks, case–control studies, and expert opinion (*12,13*). Questions about produce consumption were limited to melons, sprouts, fruit salad, coleslaw, and other ready-to-eat delicatessen-style salads (*11,12*). We conducted case–case comparisons by using LI questionnaire data to identify common food exposures among patients and generate hypotheses about possible outbreak food vehicles. During cluster investigations, case–case comparisons can be used in lieu of traditional but time- and resource-intensive case–control comparisons by comparing exposures reported for cluster-associated cases with those reported for non–cluster-associated (sporadic) cases (*14,15*).

After initial LI questionnaire case–case comparisons failed to identify a possible food vehicle for the outbreak, we developed a supplemental questionnaire that was implemented on October 8, 2015, to collect information about foods previously associated with the outbreak PFGE pattern, including cheeses, leafy green salads, stone fruit, and caramel apples. On December 9, 2015, we began conducting single-interviewer, semistructured, open-ended interviews by using an iterative approach to identify potential food exposures not included in the previous questionnaires and obtain more complete details on food products, purchase locations, and brands (*16,17*). During open-ended interviews, we asked about all foods consumed in the month before illness onset. When available, we reviewed grocery receipts, shopper card records, school and residential facility menus, and detailed diet logs to verify exposure details and purchase dates. Data were collected as part of the response to a public health emergency and did not meet the definition of research as provided by 45 Code of Federal Regulations 46.102(d).

Regulatory Investigation

The Ohio Department of Agriculture (ODA) routinely collects and tests retail foods for *L. monocytogenes* and other foodborne pathogens. Retail food samples can provide major clues during outbreak investigations if molecular subtyping identifies isolates as being closely related genetically to clinical isolates. US Food and Drug Administration (FDA) officials inspected and reviewed records from facilities linked to any *L. monocytogenes* isolated from food.

Laboratory Investigation

Clinical and food samples that yielded *L. monocytogenes* were subtyped by PFGE at state public health laboratories and FDA field laboratories by using *Asc*I and *Apa*I restriction endonucleases according to PulseNet standardized protocols (*18*). We performed whole-genome sequencing (WGS) for all isolates and analyzed results in BioNumerics version 7.5 (Applied Maths, http://www.applied-maths.com) by using wgMLST and the Lyve-SET pipeline (*10*). Sequence data were uploaded to the National Center for Biotechnology Information database (https://www.ncbi.nlm.nih.gov) for sequencing analysis.

Investigation in Canada

In Canada, a case was defined as illness in a resident or visitor to Canada with laboratory-confirmed listeriosis and isolates having any of 3 outbreak PFGE pattern combinations and symptom onset on or after May 1, 2015. The primary PFGE pattern combination in the outbreak in Canada was indistinguishable from that of the outbreak in the United States; 2 additional PFGE pattern combinations (patterns A and B), were included for the outbreak in Canada. Initial interviews were completed by either the national Enhanced Listeriosis Surveillance Program questionnaire or provincial listeriosis questionnaires to gather food exposures during the 4 weeks before illness onset. After leafy green salads were identified as a suspected vehicle, a coordinated, centralized interviewing approach was used to reinterview patients (or proxies) who had isolates indistinguishable from those with the primary outbreak PFGE pattern.

The Canadian Food Inspection Agency (CFIA, Ottawa, Ontario, Canada) used a targeted retail sampling plan to obtain packaged leafy green salads made at a suspected processing facility from stores in Ontario and Nova Scotia during January 18–19, 2016. The targeted sampling plan included multiple salad varieties and manufacturer's code combinations from multiple processing lines that were processed during January 3–14.

Provincial laboratories performed PFGE typing of clinical isolates, and CFIA performed PFGE typing on food isolates. PFGE patterns were uploaded to the PulseNet Canada national database (https://www.canada.ca/en/public-health/programs/pulsenet-canada.html) for

national designation by the National Microbiology Laboratory (Winnipeg, Manitoba, Canada). WGS was completed by the National Microbiology Laboratory, Public Health Ontario Laboratory (Toronto, Ontario, Canada), and CFIA on all Canadian clinical and food isolates by using single nucleotide polymorphisms (SNPs) with the SNVPhyl pipeline (*19*) and wgMLST in BioNumerics version 7.5. We compared isolates from Canada with those from the United States by using PFGE and WGS.

Results

Investigation in the United States

Epidemiologic Investigation

We identified 19 cases of listeriosis in 9 states: Connecticut (1), Indiana (1), Massachusetts (1), Michigan (4), Montana (2), New Jersey (1), New York (6), Ohio (2), and Pennsylvania (1) (Figure 1). All patient isolates were serotype 4b, indistinguishable by PFGE pattern combination, 7-gene sequence type (ST) 382, and closely related genetically to one another by wgMLST, differing by a median of 3 alleles (range 0–16 alleles) (*20*). Illness onset dates were July 5, 2015–January 31, 2016 (Figure 2). Of the 8 cases initially detected, 5 were later excluded by using this case definition because the isolates were different by ≥16 alleles and had isolation dates before July 5, 2015.

All 19 patients were hospitalized; listeriosis contributed to 1 (5%) death. Case-patients had a median age of 64 (range 3–83) years; 14 (74%) were female. One case of listeriosis in a pregnant woman resulted in a preterm live birth. Meningitis developed in 1 otherwise healthy child with listeriosis (Table 1).

No exposures on the standard LI questionnaire were commonly reported by case-patients in the cluster, and case–case comparisons did not generate any potential food items. Five case-patients completed supplemental interviews, and 12 case-patients completed iterative, open-ended interviews. One patient refused to be reinterviewed but provided a detailed dietary log for analysis. Ultimately, data on leafy green vegetable consumption was available for 16 (84%) of 19 patients; all 16 reported consuming leafy green salads, including 81% (13/16) reporting romaine lettuce and 71% (10/14) reporting spinach. Of those specifically asked, 93% (13 of 14) reported consuming packaged leafy green salads in the 28 days before illness onset. Nine case-patients recalled brand information; 2 packaged leafy green salad brands were reported that we determined came from a single processing facility in the United States (Table 2). Five case-patients were able to provide receipts or shopper card records to confirm purchase dates, locations, and brands. School or residential facility menus and invoices suggested potential exposure to leafy green salads for 2 additional case-patients who could not be interviewed.

Regulatory Investigation

On January 14, 2016, PulseNet staff analyzed sequence data from *L. monocytogenes* isolated from a packaged leafy green salad that was collected by ODA during routine retail sampling and found that it was closely related by wgMLST to clinical isolates from case-patients (median 3 alleles, range 0–16 alleles). On the basis of these laboratory results, in combination with preliminary epidemiologic data suggesting a link to leafy green salads, on January 16, 2016, FDA initiated an inspection of the facility that processed the packaged leafy green salad.

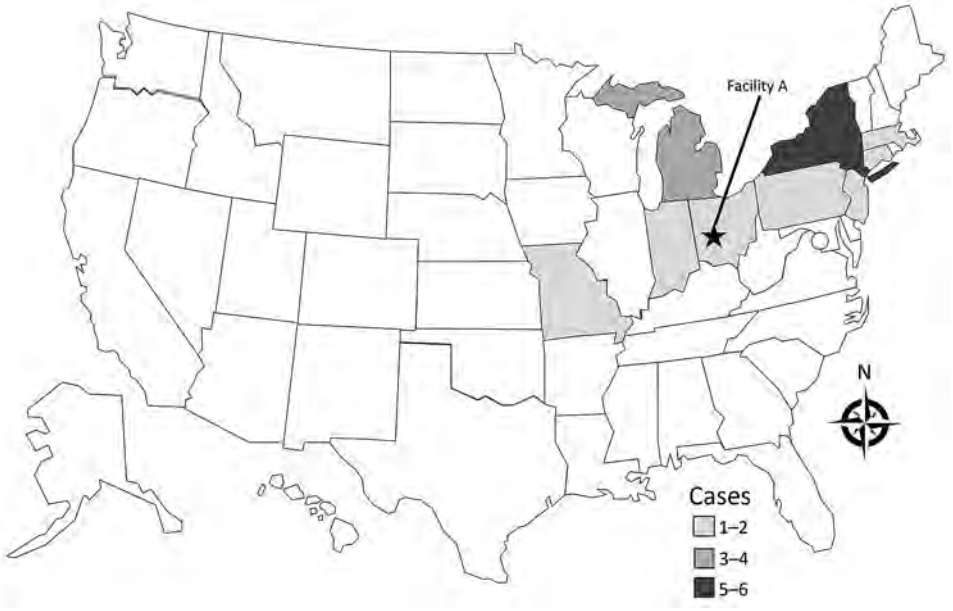

Figure 1. Outbreak-related cases of listeriosis (n = 19) in the United States by state of residence, July 5, 2015–January 31, 2016.

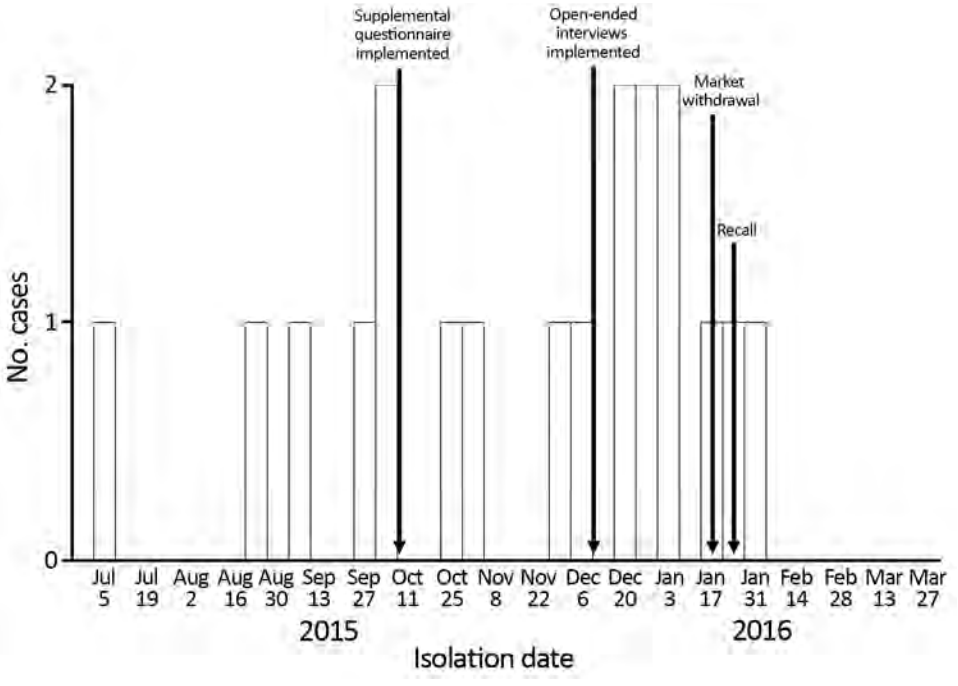

Figure 2. Timeline of *Listeria monocytogenes* isolation for 19 US patients during outbreak associated with packaged leafy green salads, July 5, 2015–January 31, 2016.

During the facility inspection, FDA investigators observed factors that might contribute to *L. monocytogenes* contamination, including failure to collect environmental samples from food contact surfaces, collection of environmental samples only before production, and failure to conduct follow-up investigations beyond the standard practices after identifying *Listeria* spp. from environmental samples over a period of 19 months (*21*). Review of records indicated that the sampling program of the facility had yielded *Listeria* spp. 11 times during July 21, 2014–January 7, 2016. Finished product, including a Caesar salad kit, and in-line samples of romaine lettuce from a production line collected by FDA from the facility on January 16, 2016, yielded *L. monocytogenes* (Table 3). Results from the Caesar salad kit were confirmed positive for *L. monocytogenes* on January 26, 2016, and those for in-line romaine lettuce were confirmed positive for *L. monocytogenes* on January 28. *L. monocytogenes* was isolated on February 9, 2016, from an open container of packaged leafy green salad collected from the home of 1 case-patient; the salad had been processed at the same facility in the United States. Five isolates identified from the processing facility and 1 leftover product from the home of a patient were closely related by wgMLST to clinical isolates and the retail isolate (median 3 alleles, range 0–16 alleles).

The inspection findings, the well-documented ability of *Listeria* species to persist in food processing/manufacturing environments, and the span of clinical cases over a period of months suggested that the source of the contamination was likely the processing/manufacturing environment, rather than a harvest site. As a result, no traceback to source farms was performed. After the FDA inspection, the processing facility implemented corrective actions.

Epidemiologic Investigation in Canada

PHAC identified 14 cases of listeriosis in 5 eastern provinces: Ontario (9), Quebec (2), New Brunswick (1), Prince Edward Island (1), and Newfoundland and Labrador (1). Illness onset dates were May 7, 2015–February 23, 2016. Ten case-patients matched the primary outbreak PFGE pattern, and 4 matched secondary PFGE pattern A. Nine (90%) of 10 isolates from patients in Canada with the primary PFGE pattern were closely related genetically to one another (0–5 SNPs) and would have met the US case definition; 1 patient from Canada with the primary PFGE pattern was not closely related to the others by WGS (>35 SNPs from outbreak cases). Isolates with secondary PFGE pattern A were not closely related genetically to one another and were genetically distinct from isolates with the primary PFGE pattern. All case-patients in Canada were hospitalized, and 3 (21%) died, but it was not determined whether listeriosis contributed to the deaths.

Detailed food exposure information was collected for all 10 case-patients who had the primary outbreak PFGE pattern. Eight (80%) reported consuming packaged leafy green salads and salad kits before illness onset. Brand information was available for 4 case-patients, and all reported or provided a purchase history that included brands made at the same US processing facility. One case-patient with secondary PFGE pattern A was interviewed by using the focused questionnaire and reported consuming coleslaw but was unable to recall the brand or product details.

Table 1. Characteristics of 19 patients with outbreak-related listeriosis associated with packaged leafy green salads, United States, July 5, 2015–January 31, 2016*

Characteristic	Value
Age, y, median (range)	64 (3–83)
Female sex	14 (74)
Pregnancy-associated cases†	1 (5)
Hospitalization	19 (100)
Death	1 (5)
Listeria monocytogenes culture site	
Blood	14 (74)
Cerebrospinal fluid	3 (16)
Placenta	1 (5)
Hip	1 (5)

*Values are no. (%) unless otherwise indicated.
†A pregnancy-associated case was defined as an illness in a pregnant woman or infant ≤28 d of age. Cases involving mother–infant pairs are counted as a single case.

Regulatory Investigation in Canada

CFIA collected and tested 137 packaged leafy green salads at the retail level, representing 45 unique product type and lot code combinations processed at the same US processing facility during January 3–14, 2016. Packaged leafy green salads from 4 unique product types and lot code combinations yielded *L. monocytogenes*; these products included 3 varieties of packaged salad (Chopped Romaine, Caesar Salad Kit, and Colorful Coleslaw), 4 production dates (January 9–14, 2016), and 3 production lines (Table 3). Three of these varieties yielded the primary PFGE pattern that was indistinguishable from the US outbreak strain. The isolate from Colorful Coleslaw, which was distributed only in Canada, had secondary PFGE pattern B, which was not closely related by wgMLST to other clinical or food isolates. WGS showed that all food isolates from Canada that had the primary outbreak PFGE pattern were closely related to one another, to the 9 closely related clinical isolates from Canada that had the primary PFGE pattern, and to the US clinical and food isolates (range 0–16 SNPs) (*20*).

Product Actions and Public Reporting

On the basis of the epidemiologic data and the ODA retail surveillance sample of packaged salad that yielded the outbreak strain of *L. monocytogenes*, on January 21, 2016, the US processing facility voluntarily stopped production of all packaged leafy green salads because of possible *L. monocytogenes* contamination. On January 22, the facility issued a market withdrawal of products manufactured at that location, including 22 varieties of packaged salad sold under 6 brands in the United States and 2 brands in Canada, both organic and nonorganic brands. These products were distributed to ≥23 states in the eastern and midwestern United States and eastern regions of Canada (*22*,*23*). CDC, FDA, PHAC, and CFIA issued communications advising the public how to identify affected products by the manufacturing code found on the package and advised consumers and retailers to discard affected products (*22*–*25*). Consumers and retailers were also advised to thoroughly wash and sanitize anything that might have come in contact with the affected products, including refrigerator drawers and shelves, reusable grocery bags, food storage containers, countertops, and food preparation tools (*22*,*24*,*26*). On January 27, after receiving notification from FDA that samples from packaged leafy green salads collected during the facility inspection were confirmed positive for *L. monocytogenes*, the firm issued a voluntary recall of all packaged salad products made at the US processing facility with information for consumers to identify the recalled products and brands (*27*).

Table 2. Consumption of leafy green salads for patients with outbreak-associated listeriosis, United States, July 5, 2015–January 31, 2016

Leafy green salads consumed	No. reported/no. responses (%)
Any leafy green salad	16/16 (100)
Romaine	13/16 (81)
Spinach	10/14 (71)
Packaged salad	13/14 (93)
Packaged salad brand processed at facility A	9/9 (100)

Discussion

The combination of epidemiology, retail food sampling, environmental investigation, and laboratory data confirmed packaged leafy green salads from a single processing facility in the United States as the source of this listeriosis outbreak. Observations from the facility inspection suggest that the environmental sampling plan at the facility might have limited the ability of the facility to identify *L. monocytogenes* contamination or harborage, which might have contributed to food contamination. Production was halted at the facility for 4 months, during which time the facility conducted testing and a root cause investigation (*28*). The recall and suspension of operations cost the firm an estimated $25.5 million (*28*).

Several unique aspects of this investigation were essential in detecting this outbreak and identifying the food vehicle, which likely prevented additional illnesses and deaths. First, wgMLST was instrumental in distinguishing the isolates in this cluster from other *L. monocytogenes* isolates with the same common PFGE pattern, which has previously been isolated from multiple foods (*29*,*30*). PFGE provided a standard typing scheme to facilitate interagency communication. However, the number of cases with this PFGE pattern was not above the baseline number of expected cases, and the cluster would not have been detected and could not be defined by PFGE alone. wgMLST offers greater specificity than PFGE subtyping methods and demonstrated that clinical and packaged leafy green salad isolates were closely related genetically.

Second, use of single-interviewer, open-ended iterative interviews was essential for identifying this novel vehicle. Previous foodborne outbreak investigations have identified outbreak food vehicles by using this approach after standard

Table 3. Food isolates yielding the outbreak strain of *Listeria monocytogenes*, United States and Canada*

Location of packaged salad sample collection	Packaged salad product	Collected by
Retail store in Ohio	Field greens	Ohio Department of Agriculture
US processing facility	Caesar	FDA
US processing facility	Romaine (in-process)	FDA
Patient's home	Romaine	Ohio Department of Health
Retail store in Canada	Chopped Romaine	CFIA
Retail store in Canada	Caesar Salad Kit	CFIA
Retail store in Canada	Caesar Salad Kit	CFIA
Retail store in Canada	Colorful Coleslaw†	CFIA

*CFIA, Canadian Food Inspection Agency; FDA, Food and Drug Administration.
†Yielded *L. monocytogenes* with secondary pulsed-field gel electrophoresis pattern B.

interview procedures were unable to identify a likely source of infection (*16*,*17*). At the time of the outbreak, the LI questionnaire did not include questions about leafy green salads, and produce questions were limited to melons, sprouts, fruit salad, coleslaw, and other ready-to-eat delicatessen-style salads. The supplemental questionnaire developed for this investigation included questions about leafy green vegetables, but data collected did not identify a specific food item or brand. In April 2016, health departments in the United States began using an updated LI questionnaire that included additional questions about produce exposures, including leafy green salads and other foods identified in recent outbreaks or recalls. In addition, institutional menus, invoices, shopper card records, and personal dietary logs can be helpful in documenting exposure details that might otherwise be unavailable and identifying new vehicles.

Third, routine retail sampling by ODA and sequencing by the state laboratory provided a molecular association between clinical isolates and a specific food product that likely would not have been made in the absence of wgMLST. Packaged leafy green salads were the leading hypothesis in the epidemiologic investigation, but the molecular relationship between the retail food isolate and clinical isolates strengthened the early epidemiologic evidence for a link to packaged leafy green salads and provided evidence needed to identify the facility and processing environment for the investigation to move forward, setting the stage for the market withdrawal and subsequent recall.

Fourth, collaboration between investigators in the United States and Canada strengthened the investigation and likely contributed to a more timely and comprehensive market withdrawal and recall. Frequent, open communication between public health and regulatory partners from both countries ensured that each party had relevant information about suspected food vehicles and laboratory findings. Extensive retail product sampling by CFIA demonstrated that the contamination of products from the implicated facility was not restricted to a single product, production line, or production day, suggesting potentially widespread contamination, and helped determine the scope of the market withdrawal and recall. WGS was also helpful in demonstrating that clinical and food isolates from Canada and the United States were closely related genetically.

Leafy green salads were one of several suspected foods identified during investigation of an outbreak of listeriosis in a hospital in Boston in 1979, and food safety research has demonstrated *L. monocytogenes* is capable of contaminating leafy green salads and ready-to-eat salads (*7*,*31*–*39*). However, outbreaks of listeriosis were rarely linked to produce items until outbreaks in the past decade linked to sprouts, celery, cantaloupe, stone fruit, and caramel apples. Reasons for the emergence of fresh produce as a vehicle for *L. monocytogenes* are unclear and might be based on increased contamination of fresh produce or improved detection. One hypothesis is that increased postharvest processing and technologies that enable increased shelf life of many products, including fresh produce, create an opportunity for proliferation of *L. monocytogenes*. Unlike many other foodborne pathogens, *L. monocytogenes* can grow at cooler temperatures (*40*). Studies with lettuce have demonstrated that although most foodborne pathogens on lettuce decrease in number under proper storage conditions, *L. monocytogenes* can multiply (*31*,*41*). Other plausible explanations for an increase in identification of *L. monocytogenes* associated with produce outbreaks include improved detection of clusters because of advanced molecular techniques, such as WGS, and improved outbreak investigation techniques, such as availability of shopper card data.

Unlike most other foodborne pathogens, *L. monocytogenes* bacteria have the potential to grow in cold processing/manufacturing environments and form biofilms. Therefore, additional steps might be necessary to reduce the risk for *L. monocytogenes* contamination (*31*,*42*,*43*). For this outbreak, several factors suggest persistent contamination at the processing/manufacturing facility: distribution of illnesses over many months, facility records indicating the presence of *Listeria* spp. throughout a 19-month period, and CFIA retail sampling results indicating contamination on multiple days and manufacturing lines. A single case of listeriosis in the United States in 2013 was linked by wgMLST to an isolate from packaged leafy green salad produced at the same facility in the United States implicated in this investigation. The isolate from 2013 was not closely related by wgMLST (difference >1,400 alleles) to the isolates from this outbreak

(*44*), but these findings suggest possible long-term, ongoing issues with *L. monocytogenes* contamination in this facility. In 2017, FDA published draft guidance for control of *L. monocytogenes* in ready-to-eat foods (*45*).

Vegetables and fruits are fundamental components of a healthy diet, and the US Department of Agriculture recommends that half of a person's diet be composed of fruits and vegetables (*46*). CDC and FDA recommend that consumers follow general food safety practices for fruits and vegetables, including leafy green salads: properly refrigerating and separating from other foods such as raw meat and seafood, discarding products that are spoiled or have been recalled, and washing thoroughly to remove surface contamination unless the packaging indicates products are prewashed or ready-to-eat (*47*,*48*). However, the effectiveness of washing produce to reduce contamination varies by produce type, prior storage temperature, and washing method (*39*,*49*,*50*). Additional research should focus on identifying best practices and effective policies to reduce the likelihood of *L. monocytogenes* contamination of fresh produce, especially as technological innovations enable increased shelf life of packaged leafy green salads and other produce.

Acknowledgments

We thank local, state, and federal partners for contributing to the *Listeria* Initiative (https://www.cdc.gov/listeria/surveillance/listeria-initiative.html) and the health, laboratory, and regulatory officials in the United States and Canada for contributing to this study.

About the Author

At the time of this study, Dr. Self was an Epidemic Intelligence Service officer in the Division of Foodborne, Waterborne, and Environmental Diseases, National Center for Emerging and Zoonotic Infectious Diseases, CDC, Atlanta, GA. She is currently an epidemiologist in the Division of Tuberculosis Elimination, National Center for HIV/AIDS, Viral Hepatitis, STD, and TB Prevention, CDC. Her primary research interest is the epidemiology of infectious diseases.

References

1. Scallan E, Hoekstra RM, Angulo FJ, Tauxe RV, Widdowson M-A, Roy SL, et al. Foodborne illness acquired in the United States—major pathogens. Emerg Infect Dis. 2011;17:7–15. http://dx.doi.org/10.3201/eid1701.P11101
2. Silk BJ, Date KA, Jackson KA, Pouillot R, Holt KG, Graves LM, et al. Invasive listeriosis in the Foodborne Diseases Active Surveillance Network (FoodNet), 2004–2009: further targeted prevention needed for higher-risk groups. Clin Infect Dis. 2012;54 (Suppl 5):S396–404. http://dx.doi.org/10.1093/cid/cis268
3. Centers for Disease Control and Prevention (CDC). Vital signs: *Listeria* illnesses, deaths, and outbreaks—United States, 2009–2011. MMWR Morb Mortal Wkly Rep. 2013;62:448–52.
4. *Listeria monocytogenes* infections (listeriosis). In: Kimberlin DW, Brady MT, Jackson MA, Long SS, editors. Red Book: 2015 Report of the Committee on Infectious Diseases. 30th ed. Elk Grove Village (IL): American Academy of Pediatrics; 2015. p. 513–6.
5. Swaminathan B, Gerner-Smidt P. The epidemiology of human listeriosis. Microbes Infect. 2007;9:1236–43. http://dx.doi.org/10.1016/j.micinf.2007.05.011
6. Angelo KM, Jackson KA, Wong KK, Hoekstra RM, Jackson BR. Assessment of the incubation period for invasive listeriosis. Clin Infect Dis. 2016;63:1487–9. http://dx.doi.org/10.1093/cid/ciw569
7. Schlech WF III, Lavigne PM, Bortolussi RA, Allen AC, Haldane EV, Wort AJ, et al. Epidemic listeriosis: evidence for transmission by food. N Engl J Med. 1983;308:203–6. http://dx.doi.org/10.1056/NEJM198301273080407
8. Garner D, Kathariou S. Fresh produce–associated listeriosis outbreaks, sources of concern, teachable moments, and insights. J Food Prot. 2016;79:337–44. http://dx.doi.org/10.4315/0362-028X.JFP-15-387
9. Gottlieb SL, Newbern EC, Griffin PM, Graves LM, Hoekstra RM, Baker NL, et al.; Listeriosis Outbreak Working Group. Multistate outbreak of listeriosis linked to turkey deli meat and subsequent changes in US regulatory policy. Clin Infect Dis. 2006;42:29–36. http://dx.doi.org/10.1086/498113
10. Katz LS, Griswold T, Williams-Newkirk AJ, Wagner D, Petkau A, Sieffert C, et al. A Comparative analysis of the Lyve-SET phylogenomics pipeline for genomic epidemiology of foodborne pathogens. Front Microbiol. 2017;8:375. http://dx.doi.org/10.3389/fmicb.2017.00375
11. Centers for Disease Control and Prevention. The *Listeria* initiative [cited 2017 Mar 24]. https://www.cdc.gov/listeria/surveillance/listeria-initiative.html
12. Cartwright EJ, Jackson KA, Johnson SD, Graves LM, Silk BJ, Mahon BE. Listeriosis outbreaks and associated food vehicles, United States, 1998–2008. Emerg Infect Dis. 2013;19:1–9, quiz 184. http://dx.doi.org/10.3201/eid1901.120393
13. Varma JK, Samuel MC, Marcus R, Hoekstra RM, Medus C, Segler S, et al. *Listeria monocytogenes* infection from foods prepared in a commercial establishment: a case–control study of potential sources of sporadic illness in the United States. Clin Infect Dis. 2007;44:521–8. http://dx.doi.org/10.1086/509920
14. Mayet A. Case–case studies: an innovative tool in the field of outbreak investigation. Swiss Med Wkly. 2015;145:w14203.
15. McCollum JT, Cronquist AB, Silk BJ, Jackson KA, O'Connor KA, Cosgrove S, et al. Multistate outbreak of listeriosis associated with cantaloupe. N Engl J Med. 2013;369:944–53. http://dx.doi.org/10.1056/NEJMoa1215837
16. Mody RK, Meyer S, Trees E, White PL, Nguyen T, Sowadsky R, et al. Outbreak of *Salmonella enterica* serotype I 4,5,12:i:- infections: the challenges of hypothesis generation and microwave cooking. Epidemiol Infect. 2014;142:1050–60. http://dx.doi.org/10.1017/S0950268813001787
17. Angelo KM, Conrad AR, Saupe A, Dragoo H, West N, Sorenson A, et al. Multistate outbreak of *Listeria monocytogenes* infections linked to whole apples used in commercially produced, prepackaged caramel apples: United States, 2014–2015. Epidemiol Infect. 2017;145:848–56. http://dx.doi.org/10.1017/S0950268816003083
18. Graves LM, Swaminathan B. PulseNet standardized protocol for subtyping *Listeria monocytogenes* by macrorestriction and pulsed-field gel electrophoresis. Int J Food Microbiol. 2001;65:55–62. http://dx.doi.org/10.1016/S0168-1605(00)00501-8
19. Petkau A, Mabon P, Sieffert C, Knox NC, Cabral J, Iskander M, et al. SNVPhyl: a single nucleotide variant phylogenomics pipeline for microbial genomic epidemiology. Microb Genom. 2017;3:e000116.
20. Self JL, Conrad A, Stroika S, Jackson A, Burnworth L, Beal J, et al. Notes from the field: outbreak of listeriosis associated with consumption of packaged salad—United States and Canada, 2015–2016. MMWR Morb Mortal Wkly Rep. 2016;65:879–81. http://dx.doi.org/10.15585/mmwr.mm6533a6
21. Food and Drug Administration. Letter to Coral Beach regarding FDA form 483. Food Safety News [cited 2018 Apr 5]. http://www.foodsafetynews.com/files/2016/04/Dole-483-04-25-16.pdf

22. Food and Drug Administration. Recalls, market withdrawals, and safety alerts. Dole Fresh Vegetables announces voluntary withdrawal for salads [cited 2017 Mar 24]. https://www.fda.gov/safety/recalls/ucm482822.htm
23. Canadian Food Inspection Agency. Food recall warning. Certain Dole brand pre-packaged chopped salads, salad blends and kits and leafy greens and certain PC Organics brand leafy greens recalled due to *Listeria monocytogenes* [cited 2017 Oct 13]. http://www.inspection.gc.ca/about-the-cfia/newsroom/food-recall-warnings/complete-listing/2016-01-22c/eng/1453522915084/1453522920123
24. Centers for Disease Control and Prevention. Recall and advice to consumers, restaurants, and retailers. Multistate outbreak of listeriosis linked to packaged salads produced at Springfield, Ohio Dole processing facility [cited 2017 Mar 24]. https://www.cdc.gov/listeria/outbreaks/bagged-salads-01-16/advice-consumers.html
25. Public Health Agency of Canada. Public health notice update: Outbreak of *Listeria* infections linked to packaged salad products produced at the Dole processing facility in Springfield, Ohio [cited 2017 Oct 13]. https://www.canada.ca/en/public-health/services/public-health-notices/2016/public-health-notice-update-outbreak-listeria-infections-linked-packaged-salad-products-produced-dole-processing-facility-springfield-ohio.html
26. Centers for Disease Control and Prevention. Multistate outbreak of listeriosis linked to packaged salads produced at Springfield, Ohio Dole processing facility [cited 2017 Mar 24]. https://www.cdc.gov/listeria/outbreaks/bagged-salads-01-16/index.html
27. Food and Drug Administration. Recalls, market withdrawals, and safety alerts: Dole statement regarding voluntary recall of salads processed at the Springfield, Ohio facility [cited 2017 Mar 24]. https://www.fda.gov/Safety/Recalls/ucm483588.htm
28. Dole Food Company, Inc. United States Securities and Exchange Commission form S-1: registration statement, 2017 [cited 2017 May 17]. https://www.sec.gov/Archives/edgar/data/18169/000119312517134852/d374342ds1.htm
29. Burall LS, Grim CJ, Datta AR. A clade of *Listeria monocytogenes* serotype 4b variant strains linked to recent listeriosis outbreaks associated with produce from a defined geographic region in the US. PLoS One. 2017;12:e0176912. http://dx.doi.org/10.1371/journal.pone.0176912
30. Chen Y, Luo Y, Pettengill J, Timme R, Melka D, Doyle M, et al. Singleton ST382, an emerging clonal group of *Listeria monocytogenes* associated with three multistate outbreaks linked to contaminated stone fruit, caramel apples and leafy green salad. J Clin Microbiol. 2017;55:931–41. http://dx.doi.org/10.1128/JCM.02140-16
31. Beuchat LR, Brackett RE. Survival and growth of *Listeria monocytogenes* on lettuce as influenced by shredding, chlorine treatment, modified atmosphere packaging and temperature. J Food Sci. 1990;55:755–8. http://dx.doi.org/10.1111/j.1365-2621.1990.tb05222.x
32. Beuchat LR, Adler BB, Lang MM. Efficacy of chlorine and a peroxyacetic acid sanitizer in killing *Listeria monocytogenes* on iceberg and Romaine lettuce using simulated commercial processing conditions. J Food Prot. 2004;67:1238–42. http://dx.doi.org/10.4315/0362-028X-67.6.1238
33. Lokerse RF, Maslowska-Corker KA, van de Wardt LC, Wijtzes T. Growth capacity of *Listeria monocytogenes* in ingredients of ready-to-eat salads. Food Control. 2016;60:338–45. http://dx.doi.org/10.1016/j.foodcont.2015.07.041
34. Delaquis S, Stewart S, Cazaux S, Toivonen P. Survival and growth of *Listeria monocytogenes* and *Escherichia coli* O157:H7 in ready-to-eat iceberg lettuce washed in warm chlorinated water. J Food Prot. 2002;65:459–64. http://dx.doi.org/10.4315/0362-028X-65.3.459
35. Carrasco E, Pérez-Rodríguez F, Valero A, Garcı'a-Gimeno RM, Zurera G. Growth of *Listeria monocytogenes* on shredded, ready-to-eat iceberg lettuce. Food Control. 2008;19:487–94. http://dx.doi.org/10.1016/j.foodcont.2007.05.014
36. Hanning IB, Johnson MG, Ricke SC. Precut prepackaged lettuce: a risk for listeriosis? Foodborne Pathog Dis. 2008;5:731–46. http://dx.doi.org/10.1089/fpd.2008.0142
37. Crépet A, Stahl V, Carlin F. Development of a hierarchical Bayesian model to estimate the growth parameters of *Listeria monocytogenes* in minimally processed fresh leafy salads. Int J Food Microbiol. 2009;131:112–9. http://dx.doi.org/10.1016/j.ijfoodmicro.2009.01.028
38. Sant'Ana AS, Landgraf M, Destro MT, Franco BD. Growth potential of *Salmonella* and *Listeria monocytogenes* in ready-to-eat lettuce and collard greens packaged under modified atmosphere and in perforated film. J Food Prot. 2013;76:888–91. http://dx.doi.org/10.4315/0362-028X.JFP-12-479
39. Nastou A, Rhoades J, Smirniotis P, Makri I, Kontominas M, Likotrafiti E. Efficacy of household washing treatments for the control of *Listeria monocytogenes* on salad vegetables. Int J Food Microbiol. 2012;159:247–53. http://dx.doi.org/10.1016/j.ijfoodmicro.2012.09.003
40. Kornacki JL, Gurtler JB. Incidence and control of *Listeria* in food processing facilities. In: Ryser ET, Marth EH, editors. Listeria, listeriosis, and food safety. 3rd ed. Boca Raton (FL): CRC Press; 2007. p. 681–766 [cited 2019 May 7]. http://www.crcnetbase.com/doi/abs/10.1201/9781420015188.ch17
41. Harris LJ, Farber JN, Beuchat LR, Parish ME, Suslow TV, Garrett EH, et al. Outbreaks associated with fresh produce: incidence, growth, and survival of pathogens in fresh and fresh-cut produce. Compr Rev Food Sci Food Saf. 2003;2(s1):78–141. http://dx.doi.org/10.1111/j.1541-4337.2003.tb00031.x
42. Walker SJ, Archer P, Banks JG. Growth of *Listeria monocytogenes* at refrigeration temperatures. J Appl Bacteriol. 1990;68:157–62. http://dx.doi.org/10.1111/j.1365-2672.1990.tb02561.x
43. Carpentier B, Cerf O. Review: persistence of *Listeria monocytogenes* in food industry equipment and premises. Int J Food Microbiol. 2011;145:1–8. http://dx.doi.org/10.1016/j.ijfoodmicro.2011.01.005
44. Jackson KA, Stroika S, Katz LS, Beal J, Brandt E, Nadon C, et al. Use of whole genome sequencing and patient interviews to link a case of sporadic listeriosis to consumption of prepackaged lettuce. J Food Prot. 2016;79:806–9. http://dx.doi.org/10.4315/0362-028X.JFP-15-384
45. Food and Drug Administration. Draft guidance: control of *Listeria monocytogenes* in ready-to-eat foods: guidance for industry [cited 2018 Mar 30]. https://www.fda.gov/downloads/Food/GuidanceRegulation/GuidanceDocumentsRegulatoryInformation/CM535981.pdf
46. United States Department of Agriculture. Choose my plate [cited 2017 Mar 15]. https://www.choosemyplate.gov/MyPlate
47. Centers for Disease Control and Prevention. Fruit and vegetable safety [cited 2017 May 1]. https://www.cdc.gov/features/foodsafetyquiz/index.html
48. United States Food and Drug Administration. Produce: selecting and serving it safely [cited 2017 May 1]. https://www.fda.gov/food/resourcesforyou/consumers/ucm114299
49. Doménech E, Botella S, Ferrús MA, Escriche I. The role of the consumer in the reduction of *Listeria monocytogenes* in lettuces by washing at home. Food Control. 2013;29:98–102. http://dx.doi.org/10.1016/j.foodcont.2012.05.074
50. Baur S, Klaiber R, Wei H, Hammes WP, Carle R. Effect of temperature and chlorination of pre-washing water on shelf-life and physiological properties of ready-to-use iceberg lettuce. Innov Food Sci Emerg Technol. 2005;6:171–82. http://dx.doi.org/10.1016/j.ifset.2005.02.002

Address for correspondence: Julie L. Self, Centers for Disease Control and Prevention, 1600 Clifton Rd NE, Mailstop US12-4, Atlanta, GA 30329-4027, USA; email: yxj9@cdc.gov

Congenital Syphilis as a Measure of Maternal and Child Healthcare, Brazil

Maria Lusia de Morais Belo Bezerra, Flávia Emília Cavalcante Valença Fernandes, João Paulo de Oliveira Nunes, Solma Lúcia Souto Maior de Araújo Baltar, Karina Perrelli Randau

Syphilis is a sexually transmitted infection that has direct adverse effects on maternal and infant health through vertical *Treponema pallidum* transmission during early pregnancy. We evaluated congenital syphilis as a predictor of the quality of basic maternal and child healthcare in Brazil during 2010–2015. We investigated case rates and correlations with epidemiologic and socioeconomic indicators. We observed rising congenital syphilis incidence rates and increasing syphilis-associated perinatal and infant mortality rates in all regions. Case rates were highest in the Northeast, Southeast, and South, and congenital syphilis infant mortality rates were highest in the Northeast and Southeast. We observed correlations between congenital syphilis rates and infant death, spontaneous abortion (miscarriage), and stillbirth rates. We also noted correlations between rates of stillbirth caused by syphilis and inadequate prenatal care. Our study suggests gaps in basic healthcare for pregnant women and indicates the urgent need for measures to increase early diagnosis and appropriate treatment.

In 2012, ≈5.6 million new syphilis cases occurred worldwide (*1*). Syphilis is a sexually transmitted disease caused by the bacterium *Treponema pallidum* subspecies *pallidum*, which belongs to the family *Treponemataceae*. Syphilis can lead to chronic and systemic infectious disease affecting several organs, including skin and mucous membranes. Contact with genital syphilitic lesions is responsible for 95% of syphilis cases. Congenital syphilis is vertically transmitted from mother to fetus via the placental route and can cause fetal loss after the first trimester and death of the fetus or neonate. A mother can transmit the disease vertically to her newborn during delivery if she has primary syphilis lesions on her genitalia (*2*,*3*). The pathogenic potential of the bacterium is responsible for a wide range of sequelae caused by congenital syphilis (*4*).

Author affiliations: Universidade Federal de Pernambuco, Recife, Brazil (M.L.M.B. Bezerra, F.E.C.V. Fernandes, S.L.S.M.A. Baltar, K.P. Randau); Universidade Federal de Alagoas, Arapiraca, Brazil (J.P.O. Nunes).

DOI: https://doi.org/10.3201/eid2508.180298

Global epidemiologic data show *T. pallidum* caused ≈930,000 maternal infections in 2012, which led to 350,000 adverse pregnancy outcomes, including 143,000 early fetal deaths and stillbirths, 62,000 neonatal deaths, 44,000 preterm or low birthweight neonates, and 102,000 infections in infants worldwide (*5*). Progress toward elimination of maternal and congenital syphilis was observed during 2008–2012. Despite improvements, syphilis continues to affect a high number of pregnant women, causing high rates of perinatal illness and death (*5*). Elimination efforts are hindered further by a global shortage of benzathine penicillin G, a drug indicated for congenital syphilis prevention (*6*).

Countries in the Americas have experienced high rates of syphilis and congenital syphilis. Latin America and the Caribbean have demonstrated high syphilis prevalence among pregnant women (*7*), which contributes to substantial stillbirth rates (*8*). Recent data indicate that congenital syphilis rates in South America, excluding Brazil, have been stable since 2009, but Brazil has seen increasing case rates (up to 1.7/1,000 live births) that have raised the congenital syphilis rates for the continent. However, each country uses its own case definition for congenital syphilis surveillance, sometimes excluding stillbirths caused by syphilis (syphilitic stillbirths), which makes it difficult to monitor congenital syphilis case rates in the Americas (*9*).

In Brazil, Ordinance No. 542 made congenital syphilis a mandatory notifiable disease as of December 22, 1986 (*10*). Maternal syphilis, however, was not included in the national compulsory notification list until July 14, 2005, through Ordinance No. 33 (*11*). Epidemiologic surveillance demonstrates increased rates of reported congenital syphilis and deaths; infant mortality rates from syphilis increased from 2.4/100,000 live births in 2005 to 7.4/100,000 live births in 2015 (*12*). The Brazilian Ministry of Health attributes higher maternal syphilis rates to improved epidemiologic surveillance methods and expanded distribution of rapid syphilis tests. Ordinance No. 1,459 established the health policy known as the Stork Network in 2011. The Stork Network promotes improved prenatal care, increased availability of rapid syphilis tests, and fiscal subsidies to control both the maternal and congenital forms of the

disease (*12*–*14*). Rapid tests use digital puncture sampling to detect the presence of treponemal antibodies and enable screening and treatment during a clinical visit. Widespread prenatal syphilis testing improved maternal treatment by reducing difficulties in patient follow-up (*15*) but simultaneously revealed the high syphilis rates in Brazil. However, a study by Cooper et al. demonstrated that this epidemic has not only become established but worsened in the country (*16*).

Implementation and expansion of the Family Health Strategy (FHS) also was intended to improve maternal and child healthcare. According to 2013 data from the National Health Survey, 53.4% of households were registered in family health units in Brazil; greatest coverage was seen in the Northeast (64.7%) and South (56.2%) and lowest coverage in the Southeast (46.0%). Expansion of the FHS for quality primary healthcare is essential for syphilis control and elimination (*17*,*18*). However, one study demonstrated inequality in healthcare access in municipalities of Brazil, low effectiveness of prenatal coverage by FHS, and no association with congenital syphilis control (*19*).

In this context, we evaluated congenital syphilis as a predictor for the quality of basic maternal and child healthcare in Brazil during 2010–2015. We assessed case rates by region and their correlation with epidemiologic and socioeconomic indicators.

Methods

Study Characteristics

We used a quantitative approach to conduct an ecologic study of aggregated epidemiologic data on syphilis in pregnant women and children. We collected data from the official website of the Department of Sexually Transmissible Diseases, AIDS and Viral Hepatitis of the Secretariat of Health Surveillance of the Ministry of Health in Brazil (http://indicadoressifilis.aids.gov.br). During August–November 2017, we obtained basic syphilis indicators for 6 years, 2010–2015, from the public domain database and assessed annual syphilis rates for 5 regions of Brazil: North, Northeast, Southeast, South, and Midwest. Data for 2016 were not available during the period we collected indicators for this study.

We collected data on all syphilis cases in pregnant women and those in children <1 year of age (considered congenital syphilis) that were reported to national surveillance. In Brazil, health professionals from private and public healthcare settings must complete an official epidemiologic reporting and investigation form for case notification and enter the data into the Notification of Injury Information System database of the Unified Health System. For surveillance, Brazil considers a congenital syphilis case in the following situations: live birth of any fetal age, spontaneous abortion (miscarriage) of a fetus, or stillbirth of an infant born to a woman with clinical or serologic evidence of syphilis who was not treated or received inadequate treatment, including lack of partner treatment; a person <13 years of age with increasing nontreponemal titers over time, a reactive nontreponemal titer after 6 months of age, reactive treponemal tests after 18 months of age, or a reactive nontreponemal titer higher than those of the mother; an infant or child with clinical, cerebrospinal fluid, or radiologic evidence of syphilis; or microbiologic evidence of *T. pallidum* in the placenta or umbilical cord, sample lesion, biopsy, or necropsy of a child, spontaneously aborted fetus, or stillborn infant (*12*,*20*), as outlined by the Pan American Health Organization (*9*). We considered spontaneous abortion due to syphilis as gestational loss at <22 weeks' gestation or a fetus that weighed <500 g from a woman with syphilis who did not receive treatment or received inadequate treatment. We considered syphilitic stillbirth as death of a fetus ≥22 weeks' gestation or fetus that weighed ≥500 g from a woman with syphilis who did not receive treatment or received inadequate treatment (*12*,*21*).

Epidemiologic Variables

We assessed congenital syphilis by using the following variables: syphilis detection rates in pregnant women/1,000 live births; maternal schooling level; congenital syphilis cases in the absence of prenatal care; congenital syphilis cases from mothers with inadequate maternal treatment; congenital syphilis cases whose maternal partner did not receive treatment and the number of rapid syphilis tests conducted on pregnant women; congenital syphilis detection rates in children <1 year of age/1,000 live births; infant death, excluding stillbirths and fetal deaths, due to congenital syphilis in children <1 year of age/100,000 live births; spontaneous abortion due to congenital syphilis/100,000 live births; and syphilitic stillbirths/100,000 live births. We considered child death as death between birth and 12 months of age in a live-born child from a mother with syphilis, excluding spontaneous and stillbirth. We excluded data for any given variable if it was ignored or not included on the official notification form.

Because compulsory notification for congenital syphilis has been in effect since 1986, the available database is more established (*12*). We estimated congenital syphilis incidence rates by considering the number of new cases in children <1 year of age by year in a region multiplied by 1,000 and divided by the number of live births to mothers residing in the same region during that year. We used the same formula to calculate detection of maternal syphilis rates. We calculated infant mortality rates, stillbirths, and spontaneous abortions from congenital syphilis by considering the ratio of the number of cases in the region in a given

year multiplied by 100,000 and the number of live births to mothers residing in that region during the same year.

Socioeconomic Variables

We correlated congenital syphilis cases with the following socioeconomic variables from 2010, the year of the country's last population census: illiteracy rate, considered for persons ≥15 of age who cannot read or write; Human Development Index (HDI), which is a measurement calculated on the basis of income parameters (Gross Domestic Product), education (years of schooling), and health (life expectancy); Gini Index for family income per capita, which points out differences between the poorest and the richest incomes; and the Social Vulnerability Index (SVI), which is anchored in 3 dimensions: urban infrastructure, human capital, and income and work (*14*,*22*,*23*).

Data Analyses

We considered annual congenital syphilis rates and rate increases per region, calculated by the difference between the rates recorded in 2010 and 2015, to evaluate the temporal evolution of incidence rates. We applied the Shapiro Wilk test to verify data normality, with data adherence to the normal distribution. We applied a 1-way analysis of variance followed by a Tukey test to calculate the difference between rates, considering year and geographic region, to identify differences in pairs. We conducted a bivariate analysis by using Pearson's correlation test to verify correlations between variables. We considered a 95% CI and significance level of 5% for all analyses. We organized the data on an Excel 2007 worksheet (Microsoft, https://www.microsoft.com) and conducted analyses by using Stata 14.0 (StataCorp., LLC, https://www.stata.com) and GraphPad Prism 5.0 (GraphPad Software, Inc., https://www.graphpad.com).

Results

Evolution of Congenital Syphilis Rates

We observed a continuous increase in congenital syphilis case rates in the 5 regions of Brazil during 2010–2015. Case rates doubled and, in some cases, tripled (Figure). For each year, the Northeast and Southeast had the highest congenital syphilis case rates at 2.7–6.9/1,000 live births. In 2015, case rates in the South were consistent with those in the Northeast and Southeast at 6.9/1,000 live births.

We saw a statistically significant increase ($p<0.001$) in mean congenital syphilis rates per year, with the highest mean rate recorded in 2015 (5.92/1,000 live births). Congenital syphilis incidence rates increased in every triennium. Mean rates between regions were not statistically significant. We saw the highest congenital syphilis case rates in the Northeast (4.9/1,000 live births) and Southeast (4.85/1,000 live births) (Table 1).

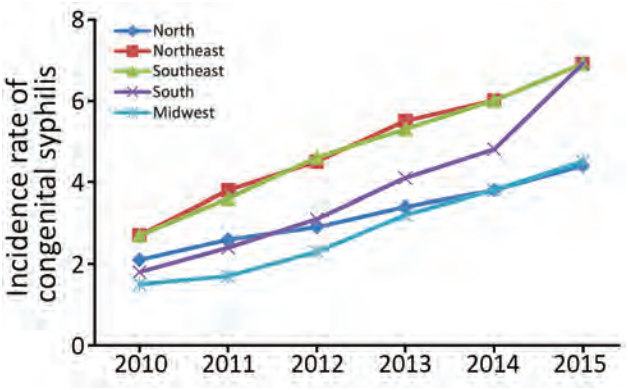

Figure. Incidence rates of congenital syphilis in children <1 year of age per 1,000 live births, by year and region, Brazil, 2010–2015.

The mean rates for infant death, spontaneous abortion, and stillbirths per year and region increased during the period we evaluated. We detected statistically significant differences in infant death from congenital syphilis ($p = 0.005$) compared to the mean mortality rate for children <1 year of age. We observed a single 3-year range, 2010–2012, without statistically significant increases in infant mortality rates. We also observed statistically significant differences by region ($p = 0.041$); the highest mean congenital syphilis infant mortality rates were in the North (6.27/100,000 live births), Southeast (5.50/100,000), and Northeast (5.28/100,000). We did not observe statistically significant differences between death rates for the North and Midwest (Table 2).

We did not see statistically significant changes in rates of spontaneous abortion or stillbirth, but we did observe differences by region in the mean spontaneous abortion rates ($p = 0.002$) and syphilitic stillbirth rates ($p<0.001$). The Southeast (20.32/100,000 live births), Northeast (18.03/100,000), and South (15.02/100,000) had the highest mean spontaneous abortion rates. We also observed the highest stillbirth rates in these regions, with 24.18/100,000 live births in the Northeast, 19.63/100,000 live births in the Southeast, and 12.15/100,000 live births in the South. We observed differences in stillbirth rates between the Northeast and the South, and between the Northeast and the Midwest (Table 3). We saw increases and statistically significant differences ($p = 0.046$) in mortality rates associated with congenital syphilis, including death of children <1 year of age, spontaneous abortion, and stillbirth. We observed high and discrepant ($p = 0.0007$) rates among regions (Table 4).

Variables Correlated with Congenital Syphilis

We observed positive correlations between incidence of congenital syphilis and maternal syphilis screening ($r = 0.688$; $p<0.001$), infant death due to syphilis ($r = 0.679$; $p<0.001$), spontaneous abortion due to syphilis ($r = 0.859$; $p<0.001$), stillbirths due to syphilis ($r = 0.829$; $p<0.001$),

Table 1. Mean congenital syphilis case rates in children <1 year of age reported to national surveillance, by year and region of Brazil, 2010–2015*

Category	No. cases, n = 77,414	Mean rate (95% CI†)	p value‡
Year			
2010	6,944	2.16[a,b,c] (1.67–2.65)	<0.001
2011	9,484	2.82[d,e] (2.02–3.62)	
2012	11,630	3.48[f] (2.55–4.41)	
2013	13,967	4.30[a] (3.33–5.27)	
2014	16,161	4.88[b,d] (3.87–5.89)	
2015	19,228	5.92[c,e,f] (4.69–7.15)	
Region			
North	6,055	3.20 (2.50–3.90)	0.063
Northeast	24,597	4.90 (3.62–6.18)	
Southeast	33,699	4.85 (3.56–6.14)	
South	8,974	3.85 (2.30–5.40)	
Midwest	4,089	2.83 (1.83–3.83)	

*Per 1,000 live births. Values with superscript letters indicate significant differences between the pairs calculated by using the Tukey test.
†Assuming Poisson distribution.
‡1-way analysis of variance; p<0.05 indicates statistical significance.

Table 2. Mean infant mortality rates for congenital syphilis in children <1 year of age reported to national surveillance, by year and region of Brazil, 2010–2015*

Category	No. cases, n = 906	Mean rate (95% CI†)	p value‡
Year			
2010	90	2.74[a,b] (1.86–3.62)	
2011	111	3.44[c] (2.55–4.33)	
2012	147	4.22 (2.68–5.76)	0.005
2013	161	5.12 (3.37–6.87)	
2014	176	6.38[a] (4.36–8.40)	
2015	221	6.94[b,c] (4.94–8.94)	
Region			
North	119	6.27[d] (3.77–8.77)	
Northeast	265	5.28 (4.16–6.41)	
Southeast	384	5.50 (4.00–7.00)	0.041
South	99	4.25 (2.82–5.68)	
Midwest	39	2.73[d] (1.51–3.96)	

*Excluding stillbirths and fetal deaths; mean rates/100,000 live births. Values with superscript letters indicate significant differences between the pairs calculated by using the Tukey test.
†Assuming Poisson distribution
‡1-way analysis of variance; p<0.05 indicates statistical significance.

maternal schooling >8 years (r = 0.824; p<0.001), and the number of rapid syphilis tests performed in pregnant women (r = 0.519; p = 0.003). We did not observe any correlations in the other variables we investigated (inadequate maternal treatment, untreated maternal partner, no prenatal care), including socioeconomic indicators (illiteracy rate, HDI, Gini index, SVI).

We saw positive correlations between infant mortality, spontaneous abortion, and syphilitic stillbirth rates and maternal schooling >8 years and with the number of rapid syphilis test performed in pregnant women. Syphilitic stillbirth rates were the only area in which we saw correlation with lack of prenatal care (r = 0.613; p<0.001), and we did not detect any correlation between these events and socioeconomic indicators (Table 5).

Discussion

Our study showed continuous increases in congenital syphilis incidence rates in children <1 year of age and infant death from syphilis during 2010–2015. We also observed increased rates of infant mortality, spontaneous abortion, and syphilitic stillbirth in several regions of Brazil, even with FHS expansion and a greater availability of rapid tests for the early detection of maternal disease.

Rates of primary and secondary syphilis in women are high in Brazil but are not increasing greatly over time (*21*), suggesting that the high and rising rates of congenital syphilis are due to better detection. New ordinances promoting rapid syphilis testing in pregnancy and better documentation of syphilis in pregnancy and in live and stillborn infants seem to have increased capacity to identify previously unidentified and new cases in Brazil.

Our data indicate that the congenital syphilis incidence rate in 2015 was >12 times the reduction target of <0.5 cases/1,000 live births for that year, a commitment Brazil assumed along with the Pan American Health Organization and the World Health Organization (*9*,*24*). Cooper et al.

Table 3. Mean case rates for spontaneous abortion and stillbirth from congenital syphilis reported to national surveillance, by year and region of Brazil, 2010–2015*

Category	Mean spontaneous abortion rate, n = 2,877 cases (95% CI†)	p value‡	Mean stillbirth rate, n = 3,130 cases (95% CI†)	p value‡
Year				
2010	6.72 (1.74–11.70)	0.105	7.38 (2.30–12.46)	0.154
2011	9.48 (3.54–15.42)		10.50 (2.24–18.76)	
2012	11.72 (4.74–18.70)		15.44 (7.03–23.85)	
2013	11.88 (4.20–19.56)		15.60 (6.99–24.21)	
2014	17.18 (8.54–25.82)		17.56 (11.75–23.37)	
2015	21.24 (11.34–31.14)		19.80 (14.73–24.87)	
Region				
North	5.37[a,b] (3.19–7.54)	0.002	7.42[c,d] (2.74–12.09)	<0.001
Northeast	18.03[a] (14.68–21.39)		24.18[c,e,f] (18.98–29.38)	
Southeast	20.32[b,g] (16.82–23.81)		19.63[d,h] (16.73–22.53)	
South	15.02 (3.65–26.38)		12.15[e] (7.17–17.13)	
Midwest	6.45[g] (2.81–10.08)		8.52[f,h] (4.80–12.23)	

*Per 100,000 live births. Values with superscript letters indicate significant differences between the pairs calculated by using the Tukey test.
†Assuming a Poisson distribution.
‡1-way analysis of variance; p<0.05 indicates statistical significance.

Table 4. Mean rates of death associated with congenital syphilis reported to national surveillance, by year and region of Brazil, 2010–2015*

Category	Mean death rate, n = 6,913 cases (95% CI†)	p value‡
Year		
2010	16.84[a] (2.42–31.26)	
2011	23.42 (3.44–43.40)	
2012	31.38 (9.36–53.40)	0.046
2013	32.60 (10.06–55.14)	
2014	41.12 (24.12–58.12)	
2015	47.9[a] (29.99–65.97)	
Region		
North	19.05[b,c] (7.94–30.15)	
Northeast	47.50[b,d] (35.52–59.48)	
Southeast	45.45[c,e] (36.31–54.59)	0.0007
South	30.08 (7.35–52.81)	
Midwest	17.70[d,e] (8.03–27.37)	

*Death rates include death in children <1 year of age, stillbirth, and spontaneous abortion. Values with superscript letters indicate significant differences between the pairs calculated by using the Tukey test.
†Assuming a Poisson distribution.
‡1-way analysis of variance; p<0.05 indicates statistical significance.

also highlighted this aspect by affirming that Brazil, despite its progress in detecting the disease, has lost its focus toward eliminating congenital syphilis (*16*).

We saw no correlation between congenital syphilis incidence rates and socioeconomic variables, including illiteracy rate, HDI, Gini index, and SVI, which counters the hypothesis that these factors contribute to the persistence of this disease. A study by Nonato et al. also showed no correlation between congenital syphilis and SVI (*25*). Data indicate social vulnerability varies between regions of Brazil (*23*), but we noted that increases in congenital syphilis rates were independent from lower or higher social vulnerability. Low social vulnerability regions, such as the Southeast and South, had high mean congenital syphilis, spontaneous abortion, and stillbirth rates. However, we also noted high mean rates in high social vulnerability regions. For instance, the North had high infant mortality rates and the Northeast had high mean rates of fetal loss after the first trimester and high mean rates of stillbirth from congenital syphilis.

Congenital syphilis is considered a sentinel event of the quality of prenatal care (*26*). We saw a correlation between a lack of prenatal care and stillbirth rates due to congenital syphilis. We also saw a correlation between congenital syphilis rates and rates of infant death, spontaneous abortion, and stillbirth. These correlations reinforce the hypothesis that congenital syphilis is a predictor of the quality of prenatal care and reveal the precarious conditions of maternal and child healthcare in Brazil. Adverse outcomes might be related to failure to diagnose or inadequately treat syphilis in pregnant women, which in turn demonstrates fragilities in basic healthcare for mothers and children.

Nonato et al. conducted a study of 353 pregnant women in the state capital of Minas Gerais, in Southeast Brazil, and found a correlation between congenital syphilis and late prenatal care, <6 prenatal consultations, and failure to diagnose the disease during the first trimester (*25*). Our results are further corroborated in a meta-analysis by Qin et al. that found that pregnant women whose syphilis diagnosis and treatment occurred in the first trimester experienced no higher adverse outcomes than women without syphilis (*27*). In addition, that analysis showed that women whose syphilis was diagnosed and treated in the third trimester had similar adverse pregnancy outcomes to those who did not receive treatment (*27*).

Increasing access to testing will not reduce congenital syphilis incidence if tests are conducted late in the pregnancy. Even when testing is performed early, adequate treatment is needed to produce a noticeable effect on

Table 5. Correlation between congenital syphilis case rates, death, epidemiologic, and socioeconomic variables, Brazil, 2010–2015*

Variable	Congenital syphilis,† n = 77,414		Infant death,‡ n = 906		Fetal death,§ n = 2,877		Stillbirth,¶ n = 3,130	
	r value#	p value	r value#	p value	r value#	p value	r value#	p value
Maternal syphilis	0.688	**<0.001**	0.535	**0.002**	0.563	**0.001**	0.301	0.106
Infant death	0.679	**<0.001**	–	–	0.439	**0.015**	0.523	**0.003**
Fetal death	0.859	**<0.001**	0.439	**0.015**	–	–	0.814	**<0.001**
Stillbirth	0.829	**<0.001**	0.523	**0.003**	0.814	**<0.001**	–	–
Maternal schooling >8 y	0.824	**<0.001**	0.505	**0.004**	0.748	**<0.001**	0.737	**<0.001**
No prenatal care	0.305	0.101	0.132	0.486	0.360	0.051	0.613	**<0.001**
Inadequate maternal treatment	0.066	0.728	0.160	0.399	0.129	0.498	0.014	0.941
Untreated maternal partner	0.066	0.728	0.342	0.064	0.012	0.950	0.040	0.833
Rapid syphilis test of pregnant women	0.519	**0.003**	0.419	**0.020**	0.511	**0.003**	0.727	**<0.001**
Illiteracy rates**	0.476	0.418	0.430	0.470	0.251	0.684	0.348	0.566
Human Development Index**	0.355	0.557	0.456	0.441	0.013	0.984	0.040	0.949
Gini Index**	0.323	0.596	0.604	0.281	0.096	0.878	0.103	0.870
Social Vulnerability Index**	0.467	0.426	0.627	0.256	0.172	0.781	0.193	0.754

*Bold text indicates statistically significant values (p<0.05).
†Congenital syphilis rates include spontaneous abortion and stillbirth rates.
‡Death in live-born infants from birth through 12 months of age.
§Fetal death at <22 weeks gestation in mothers with positive syphilis seroreactive test results.
¶Stillborn infants of ≥22 weeks gestation born to mothers with positive syphilis seroreactive test results.
#Calculated using Pearson correlation coefficient.
**Values from 2010, during the country's last population census.

congenital syphilis incidence. The high and increasing congenital syphilis rates we recorded might be explained by the inclusion of partner treatment in the congenital syphilis case definition, but it does not explain the higher deaths we noted.

Brazil's Ministry of Health points out that, among mothers of children diagnosed with congenital syphilis in 2015, a total of 78.4% sought prenatal care, and 51.4% of cases were diagnosed. However, more than half of mothers (56.5%) received inadequate treatment, and 27.3% did not have access to treatment (*12*). Penicillin shortages and resistance of professional health workers to prescribe penicillin during pregnancy likely contributed to the problem. In 2015, only 55% of the basic health units in Brazil prescribed penicillin to treat syphilis in pregnant mothers. The risk for congenital syphilis increases 5-fold when maternal partners are infected (*28*), and 62.3% of maternal partners did not receive treatment in 2015 (*12*). Late identification, inadequate management, lack of partner treatment, and incomplete treatment in identified cases are important factors involved in congenital syphilis persistence (*26*).

According to de la Calle et al., adequate treatment is essential for controlling congenital syphilis (*29*). The most effective syphilis treatment is benzathine penicillin G (*6*,*30*,*31*), but despite the medication's efficacy and affordability, syphilis continues to be a public health problem (*2*). Benzathine penicillin G shortages have compromised treatment for diagnosed syphilis cases in several countries (*32*), including Brazil (*6*), which in turn has seen increasing congenital syphilis cases. Countries seeking to expand and improve prenatal care, reduce adverse pregnancy outcomes, and achieve congenital syphilis elimination goals should have access to a steady supply of benzathine penicillin G (*33*).

Of note, Brazil experienced increases in congenital syphilis rates before penicillin shortages. We must consider other factors that could be causing these increases, including the quality of prenatal care, resistance or difficulty of pregnant women and their sexual partners to adhere to treatment, and underreporting of the condition (*26*,*34*). Cooper et al. (*16*), as well as several others, indicate that the elimination of maternal and child syphilis transmission can only become a reality in the Americas with implementation and maintenance of clinical excellence in public health services. To reach its goal for eliminating congenital syphilis, Brazil must prioritize congenital syphilis; increase resource allocation to public health; improve syphilis screening in hard-to-reach populations; and invest in organizing health services, professional training, and review of prenatal care procedures, especially for pregnant adolescents (*2*,*35*–*38*).

Our study has some limitations. The data represent aggregated secondary data and, because we analyzed cases together and not individually, we cannot generalize the results. However, a national study demonstrated that estimates for congenital syphilis incidences at birth (3.5/1,000 live births) during 2011–2012 did not differ significantly from those registered by Brazil's Information System for Notifiable Diseases (3.3/1,000 live births) in 2011 (*39*). Despite this finding, underreporting is a problem in Brazil (*34*,*40*). We did not exclude regional variations in case reporting because the quality of the data provided depends on technical and operational conditions of the epidemiologic surveillance system in each region. More worrisome, if underreporting exists, congenital syphilis rates could be even greater than we report.

Our study results indicate that congenital syphilis rates increased in all regions of Brazil during 2010–2015, progressing rapidly and moving the country farther from its target of <0.5 cases/1,000 live births. In addition, high rates of fetal loss after the first trimester and stillbirth rates due to congenital syphilis accentuate the seriousness of this problem. Brazil should prioritize investments in public health, especially for improving prenatal care, with a focus on the early diagnosis of maternal syphilis and strengthening management of benzathine penicillin G treatment to prevent congenital syphilis.

M.L.M.B.B. received financial support from a doctoral scholarship provided by the Federal University of Alagoas Program of Personnel Development, Maceió, Alagoas, Brazil.

About the Author

Dr. Bezerra is a biologist and professor at the Federal University of Alagoas, Arapiraca, and a PhD student in the Postgraduate Program in Therapeutic Innovation at the Federal University of Pernambuco, Recife, under the advisement of K.P.R. Her research focus is on the epidemiology of sexually transmitted infections and the study of educational strategies for health promotion.

References

1. Newman L, Rowley J, Vander Hoorn S, Wijesooriya NS, Unemo M, Low N, et al. Global estimates of the prevalence and incidence of four curable sexually transmitted infections in 2012 based on systematic review and global reporting. PLoS One. 2015;10:e0143304. http://dx.doi.org/10.1371/journal.pone.0143304
2. Avelleira JCR, Bottino G. Syphilis: diagnosis, treatment and control [in Portuguese]. An Bras Dermatol. 2006;81:111–26. http://dx.doi.org/10.1590/S0365-05962006000200002
3. Dorado JS, Arellano ER, Pichardo AR, Ezcurra MM. Treponemal infections. Syphilis [in Portuguese]. Medicine-Programa de Formación Médica Continuada Acreditado. 2014;51:2993–3002. https://doi.org/10.1016/S0304-5412(14)70729-2
4. Lago EG, Vaccari A, Fiori RM. Clinical features and follow-up of congenital syphilis. Sex Transm Dis. 2013;40:85–94. http://dx.doi.org/10.1097/OLQ.0b013e31827bd688
5. Wijesooriya NS, Rochat RW, Kamb ML, Turlapati P, Temmerman M, Broutet N, et al. Global burden of maternal and congenital syphilis in 2008 and 2012: a health systems

modelling study. Lancet Glob Health. 2016;4:e525–33. http://dx.doi.org/10.1016/S2214-109X(16)30135-8
6. Nurse-Findlay S, Taylor MM, Savage M, Mello MB, Saliyou S, Lavayen M, et al. Shortages of benzathine penicillin for prevention of mother-to-child transmission of syphilis: An evaluation from multi-country surveys and stakeholder interviews. PLoS Med. 2017;14:e1002473. http://dx.doi.org/10.1371/journal.pmed.1002473
7. Schmid GP, Stoner BP, Hawkes S, Broutet N. The need and plan for global elimination of congenital syphilis. Sex Transm Dis. 2007;34(Suppl):S5–10. http://dx.doi.org/10.1097/01.olq.0000261456.09797.1b
8. Arnesen L, Martínez G, Mainero L, Serruya S, Durán P. Gestational syphilis and stillbirth in Latin America and the Caribbean. Int J Gynaecol Obstet. 2015;128:241–5. http://dx.doi.org/10.1016/j.ijgo.2014.09.017
9. Pan American Health Organization. Elimination of mother-to-child transmission of HIV and syphilis in the Americas. Update 2016. Washington: The Organization; 2017 [cited 2017 Oct 20]. http://iris.paho.org/xmlui/bitstream/handle/123456789/34072/9789275119556-eng.pdf
10. Ordinance no. 542/1986, sect. 1 [in Portuguese]. Official Gazette of the Federative Republic of Brazil. 1986 Dec 24 [cited 2017 Dec 18]. http://www3.crt.saude.sp.gov.br/arquivos/arquivos_biblioteca_crt/Portarian542de22dez86.pdf
11. Ordinance MS/SVS no. 33, of July 14, 2005, National list of compulsory notification aggravations [in Portuguese]. Official Gazette of the Federative Republic of Brazil. 2005 Jul 15 [cited 2017 Dec 18]. http://bvsms.saude.gov.br/bvs/saudelegis/svs/2005/prt0033_14_07_2005.html
12. Brazil Ministry of Health, Secretary of Health Care. Epidemiologic bulletin of syphilis—2016 [in Portuguese]. 2016 [cited 2017 Dec 18]. http://www.aids.gov.br/pt-br/pub/2016/boletim-epidemiologico-de-sifilis-2016
13. Brazil Ministry of Health. Ministerial Order No. 1,459 of June 24, 2011, establishing within the scope of the Unified Health System, the Stork Network, sect. 1 [in Portuguese]. 2011 [cited 2017 Dec 18]. http://bvsms.saude.gov.br/bvs/saudelegis/gm/2011/prt1459_24_06_2011.html
14. Institute of Research and Applied Economics. Development in macroregions, Brazil: 2016 [in Portuguese]. Brasília, Brazil: The Institute; 2016 [cited 2017 Nov 9]. http://www.br.undp.org/content/brazil/pt/home/library/idh/Atlas/macro-regioes-brasileiras.html
15. Benzaken AS, Galbán García E, Sardinha JC, Dutra Junior JC, Peeling R. Rapid tests for diagnosing syphilis: validation in an STD clinic in the Amazon Region, Brazil [in Portuguese]. Cad Saude Publica. 2007;23(Suppl 3):S456–64. http://dx.doi.org/10.1590/S0102-311X2007001500013
16. Cooper JM, Michelow IC, Wozniak PS, Sánchez PJ. In time: the persistence of congenital syphilis in Brazil—more progress needed! [in Portuguese]. Rev Paul Pediatr. 2016;34:251–3. http://dx.doi.org/10.1016/j.rpped.2016.06.001
17. Malta DC, Santos MAS, Stopa SR, Vieira JEB, Melo EA, Reis C, et al. Family Health Strategy Coverage in Brazil, according to the National Health Survey, 2013 [in Portuguese]. Rev Ciência & Saúde Coletiva. 2016;2:327–8. http://dx.doi.org/10.1590/1413-81232015212.23602015
18. Saraceni V, Miranda AE. Coverage by the Family Health Strategy and diagnosis of syphilis in pregnancy and congenital syphilis [in Portuguese]. Cad Saude Publica. 2012;28:490–6. http://dx.doi.org/10.1590/S0102-311X2012000300009
19. Araújo CL, Shimizu HE, Sousa AI, Hamann EM. Incidence of congenital syphilis in Brasil and its relationship with the Family Health Strategy [in Portuguese]. Rev Saude Publica. 2012;46 479–86. http://dx.doi.org/10.1590/S0034-89102012000300010
20. Paz LC, Pereira GF, Pinto VM, Medeiros MG, Matida LH, Saraceni V, et al. New case definition of congenital syphilis for epidemiologic surveillance purposes in Brazil, 2004 [in Portuguese]. Rev Bras Enferm. 2005;58:486–7. http://dx.doi.org/10.1590/S0034-71672005000400021
21. Brazil Ministry of Health, Secretary of Health Surveillance, National STD and AIDS Program. Guidelines for the control of congenital syphilis, manual series, 62 [in Portuguese]. 2005 [cited 2017 Dec 19]. http://bvsms.saude.gov.br/bvs/publicacoes/diretrizes_controle_sifilis_congenita.pdf
22. Brazilian Institute of Geography and Statistics. 2010 Census [in Portuguese] [cited 2017 Nov 7]. https://censo2010.ibge.gov.br
23. Costa MA, Marguti BO, editors. Atlas of social vulnerability in Brazilian municipalities [in Portuguese]. Brasília, Brazil: Institute of Economic and Applied Research; 2015 [cited 2017 Nov 09]. http://ivs.ipea.gov.br/images/publicacoes/Ivs/publicacao_atlas_ivs.pdf
24. Ministry of Health, Department of Health Surveillance. Guide to surveillance in health [in Portuguese]. 2014 [cited 2018 Jan 17]. http://www.saude.campinas.sp.gov.br/doencas/Guia_VE.pdf
25. Nonato SM, Melo APS, Guimarães MDC. Syphilis in pregnancy and factors associated with congenital syphilis in Belo Horizonte-MG, Brazil, 2010–2013 [in Portuguese]. Epidemiol Serv Saude. 2015;24:681–94. http://dx.doi.org/10.5123/S1679-49742015000400010
26. Domingues RMSM, Saracen V, Hartz ZMDA, Leal MDC. Congenital syphilis: a sentinel event in antenatal care quality [in Portuguese]. Rev Saude Publica. 2013;47:147–57. http://dx.doi.org/10.1590/S0034-89102013000100019
27. Qin J, Yang T, Xiao S, Tan H, Feng T, Fu H. Reported estimates of adverse pregnancy outcomes among women with and without syphilis: a systematic review and meta-analysis. PLoS One. 2014;9:e102203. http://dx.doi.org/10.1371/journal.pone.0102203
28. Qin JB, Feng TJ, Yang TB, Hong FC, Lan LN, Zhang CL. Maternal and paternal factors associated with congenital syphilis in Shenzhen, China: a prospective cohort study. Eur J Clin Microbiol Infect Dis. 2014;33:221–32. http://dx.doi.org/10.1007/s10096-013-1948-z
29. de la Calle M, Cruceyra M, de Haro M, Magdaleno F, Montero MD, Aracil J, et al. Syphilis and pregnancy: study of 94 cases [in Spanish]. Med Clin (Barc). 2013;141:141–4. http://dx.doi.org/10.1016/j.medcli.2012.11.033
30. Rodríguez-Cerdeira C, Silami-Lopes VG. Congenital syphilis in the 21st century [in Spanish]. Actas Dermosifiliogr. 2012;103:679–93. http://dx.doi.org/10.1016/j.adengl.2012.09.003
31. Walker GJA, Walker DG. Congenital syphilis: a continuing but neglected problem. Semin Fetal Neonatal Med. 2007;12:198–206. https://doi.org/10.1016/j.siny.2007.01.019
32. US Centers for Disease Control and Prevention. Bicillin-L-A (benzathine penicillin G) shortage. Atlanta: The Centers; 2016 [cited 2017 Dec 18].
33. Taylor MM, Zhang X, Nurse-Findlay S, Hedman L, Kiarie J. The amount of penicillin needed to prevent mother-to-child transmission of syphilis. Bull World Health Org Suppl. 2016;94:559-A. http://dx.doi.org/10.2471/BLT.16.173310
34. Lafetá KR, Martelli Júnior H, Silveira MF, Paranaíba LM. Maternal and congenital syphilis, underreported and difficult to control [in Portuguese]. Rev Bras Epidemiol. 2016;19:63–74. http://dx.doi.org/10.1590/1980-5497201600010006
35. Gomez GB, Kamb ML, Newman LM, Mark J, Broutet N, Hawkes SJ. Untreated maternal syphilis and adverse outcomes of pregnancy: a systematic review and meta-analysis. Bull World Health Org Suppl. 2013;91:217–26. http://dx.doi.og10.2471/BLT.12.107623
36. Sabidó M, Benzaken AS, de-Andrade-Rodrigues EJ, Mayaud P. Rapid point-of-care diagnostic test for syphilis in high-risk

populations, Manaus, Brazil. Emerg Infect Dis. 2009;15:647–9. http://dx.doi.org/10.3201/eid1504.081293
37. Saraceni V, Pereira GFM, da Silveira MF, Araujo MAL, Miranda AE. Epidemiological surveillance of vertical transmission of syphilis: data from six federal units in Brazil [in Portuguese]. Rev Panam Salud Publica. 2017;41:e44.
38. Vilarinho LM, Nogueira LT, Nagahama EE. Evaluation of quality of health care for adolescents in the prenatal and puerperium [in Portuguese]. Escola Anna Nery Revista de Enfermagem. 2012; 16:312–9.http://dx.doi.org/10.1590/S1414-81452012000200015
39. Domingues RM, Leal MD. Incidence of congenital syphilis and factors associated with vertical transmission: data from the Birth in Brazil study [in Portuguese]. Cad Saude Publica. 2016;32. http://dx.doi.org/10.1590/0102-311X00082415
40. Carvalho ID, Brito RS. Congenital syphilis in the state of Rio Grande do Norte: a descriptive study in the period 2007–2010 [in Portuguese]. Epidemiol Serv Saude. 2014;23:287–94. http://dx.doi.org/10.5123/S1679-49742014000200010

Address for correspondence: Karina Perrelli Randau, Universidade Federal de Pernambuco, Departamento de Ciências Farmacêuticas, Av Prof Arthur de Sá S/N CDU, Recife-PE CEP:50740-521, Brazil; email: krandau@hotmail.com

Natural Vertical Transmission of Zika Virus in Larval *Aedes aegypti* Populations, Morelos, Mexico

Mónica Izquierdo-Suzán, Selene Zárate, Jesús Torres-Flores, Fabián Correa-Morales, Cassandra González-Acosta, Edgar E. Sevilla-Reyes, Rosalia Lira, Sofía L. Alcaraz-Estrada, Martha Yocupicio-Monroy

We characterized natural vertical transmission of Zika virus in pools of *Aedes aegypti* larvae hatched from eggs collected in Jojutla, Morelos, Mexico. Of the 151 pools analyzed, 17 tested positive for Zika virus RNA; infectious Zika virus was successfully isolated from 1 of the larvae pools (31N) in C6/36 cells. Real-time quantitative PCR and indirect immunofluorescence assays confirmed the identity of the isolate, named Zika virus isolate 31N; plaque assays in Vero cells demonstrated the isolate's infectivity in a mammalian cell line. We obtained the complete genome of Zika virus isolate 31N by next-generation sequencing and identified 3 single-nucleotide variants specific to Zika virus isolate 31N using the meta-CATS tool. These results demonstrate the occurrence of natural vertical transmission of Zika virus in wild *Ae. aegypti* mosquitoes and suggest that this transmission mode could aid in the spread and maintenance of Zika virus in nature.

Zika virus is an enveloped, positive-sense, single-stranded sRNA, arthropod-borne virus (arbovirus) that is classified in the genus *Flavivirus*, family *Flaviviridae*. Zika virus is closely related to other viruses of medical importance, such as dengue, West Nile, and yellow fever viruses (*1*). Zika virus was discovered in Uganda in 1947, but it has attracted the attention of specialists in the past few years because of its rapid spread through the Pacific and into the Americas in 2015, as well as the severe neurologic manifestations associated with Zika virus infections, such as neonatal microcephaly and Guillain-Barré syndrome (*2*).

Several studies carried out under laboratory conditions have demonstrated that Zika virus can infect many different *Aedes* mosquito species (*3*); still, the key species for the transmission of Zika virus to humans are *Ae. aegypti* and *Ae. albopictus* (*4*–*6*). In this study, we focused on the species *Ae. aegypti*, which has an urban behavior and is usually in close contact with humans (*7*). To date, 2 different mechanisms by which *Ae. aegypti* mosquitoes can become infected with flaviviruses have been described: horizontal transmission and vertical transmission (*8*).

Horizontal transmission is considered the most common mode of transmission of arboviruses between mosquitoes and their vertebrate hosts and is responsible for the maintenance of arboviruses in nature, particularly during disease outbreaks. In contrast, the environmental maintenance of dengue virus (DENV) during interepidemic periods is thought to be caused by vertical transmission of the virus from the infected adult mosquitoes to their offspring for ≥7 successive generations (*9*–*11*). Both mechanisms together are thought to be essential for the survival of viral pathogens in their habitats, preventing their extinction during harsh environmental conditions or in populations in which the presence of susceptible mammal hosts is low.

Vertical transmission of Zika virus in *Ae. aegypti* mosquitoes has been evaluated under laboratory conditions by searching for the presence of Zika virus RNA in several organs from the offspring of infected mosquitoes, demonstrating the presence of viral RNA in the guts and salivary glands of the offspring (*12*). Additional studies have also demonstrated the presence of infectious Zika virus in the offspring of artificially infected *Ae. aegypti* and *Ae. albopictus* mosquitoes, suggesting that vertical transmission can occur in laboratory-bred mosquitoes (*13*). However, evidence is insufficient to confirm that vertical transmission is a principal maintenance mechanism for Zika virus in wild *Aedes* mosquitoes.

Author affiliations: Universidad Autónoma de la Ciudad de Mexico, Mexico City, Mexico (M. Izquierdo-Suzán, S. Zárate, M. Yocupicio-Monroy); Instituto Politécnico Nacional, Mexico City (J. Torres-Flores); Centro Nacional de Programas Preventivos y Control de Enfermedades, Mexico City (F. Correa-Morales, C. González-Acosta); Instituto Nacional de Enfermedades Respiratorias, Mexico City (E.E. Sevilla-Reyes); Instituto Mexicano del Seguro Social, Mexico City (R. Lira); Instituto de Seguridad y Servicios Sociales de los Trabajadores del Estado, Mexico City (S.L. Alcaraz-Estrada)

DOI: https://doi.org/10.3201/eid2508.181533

In this study, we sought to demonstrate natural vertical transmission in *Ae. aegypti* mosquitoes by detecting viral RNA and isolating infectious Zika virus from larvae hatched from field-collected eggs. We also assessed the infectivity of the isolate in a mammalian cell line and obtained the complete genome of the virus by next-generation sequencing (NGS).

Materials and Methods

Study Site

We collected mosquito egg samples in the municipality of Jojutla, located in the southern region of the state of Morelos, Mexico (18°36′N, 99°10′W). Arboviral infections are common in this municipality, which is usually hot and dry during October–April and warm and humid during May–September. During 2016, the incidence of Zika virus infections increased in Morelos; 269 cases were reported by the end of the year, of which 69 cases were from Jojutla. The reported cases in Jojutla were recorded as follows: 1 in August, 17 in September, 20 in October, 25 in November, and 6 in December (*14*).

Egg Collection and Hatching

We collected *Ae. aegypti* eggs in collaboration with the National Center of Preventive Programs and Disease Control (CENAPRECE), following regulations for entomological surveillance with ovitraps (NOM-032-SSA2–2014). In 2016, 180 ovitraps were placed and maintained throughout the year in different locations in Jojutla (Figure 1). We determined the locations of the ovitraps on the basis of the incidence of human arbovirus infections. We collected the eggs using filter paper, which we then air dried for 2 days and stored in paper bags for further use.

We placed the egg papers in water containers and incubated them at 37°C for 1 wk under 24-h light/dark cycles. After the incubation period, we collected larvae in stages 2–3 and separated them into pools of 20–30 larvae. We macerated each of the pools in viral transport media (5% BSA, 100 U/mL penicillin, 100 μg/mL streptomycin, 2.5 μg/mL fungizone, and $NaHCO_3$ in Hank's solution) using a pestle mixer (Thomas Scientific, https://www.thomassci.com) and stored pools at –80°C for further analysis.

Detection of Zika Virus in Larvae of *Aedes aegypti*

We incubated the macerated larvae pools with Trizol (Invitrogen, https://www.thermofisher.com) for 10 min, extracted total RNA from the lysates using Zymo-Spin RNA extraction columns (Zymo Research, https://www.zymoresearch.com), and quantified the RNA with a Nano Drop 2000 (Thermo Scientific, https://www.thermofisher.com). We detected the presence of Zika virus RNA by quantitative reverse transcription PCR (qRT-PCR) using the TaqMan system (https://www.thermofisher.com) with primers

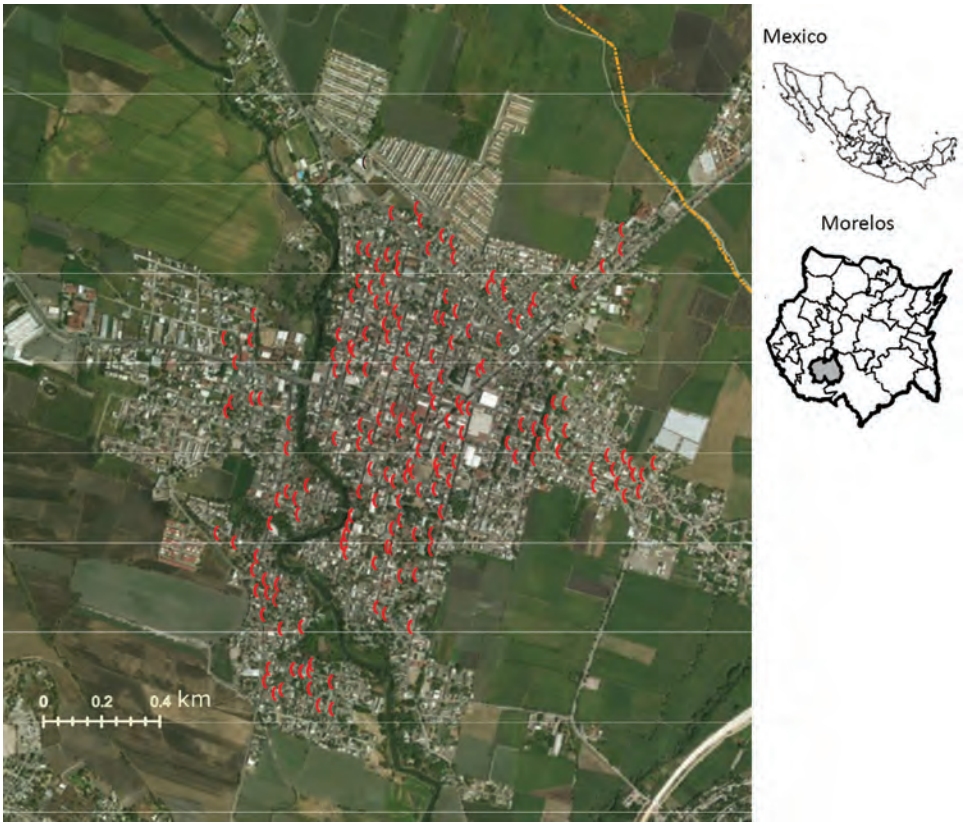

Figure 1. Location of ovitraps in the municipality of Jojutla, Morelos, Mexico (red). The ovitraps were set according to the guidelines of the Vector Transmitted Diseases Program of the National Center of Preventive Programs and Disease Control (CENAPRECE; http://www.cenaprece.salud.gob.mx/programas/interior/portada_vectores.html). Insets show location of Morelos in Mexico (top) and Jojutla in Morelos (bottom).

Zikv 1086 Fw 5′-CCGCTGCCCAACACAAG-3′ and Zikv 1162c Rv 5′-CCACTAACGTTCTTTTGCAGACAT-3′; and probe Zikv 1107-FAM probe 5′-AGCCTACCTTGACAAGCAGTCAGACACTCAA-3′, as previously described by Lanciotti et al. (*15*). We calculated the minimum infection rate (MIR) of the larvae pools by dividing the number of positive larvae pools by the total number of larvae tested and multiplying by 1,000.

Viral Isolation and Identification

We selected the larvae pools that tested positive for Zika virus RNA and displayed the lowest quantitation cycle (Cq) values (range 22.3–33.4) for viral isolation. In brief, we diluted macerated larvae pools in maintenance medium (EMEM medium with 1% FBS, 100 U/mL penicillin, and 100 μg/mL streptomycin) and filtered them through 0.22 μm membranes (Millex, http://www.emdmillipore.com). Twenty-four hours before infection, we seeded C6/36 cells in 24-well plates at 80% of confluence in growth medium (EMEM medium supplemented with 10% FBS, 100 U/mL penicillin, and 100 μg/mL streptomycin) and incubated them at 28°C in a 5% CO_2 atmosphere. Cells were adsorbed with the clarified larvae macerates for 2 h at 28°C. After the incubation period, we added fresh maintenance medium to the cells and left the infection to proceed for 7 d at 28°C and a 5% CO_2 atmosphere until a cytopathic effect was observable. We tested the supernatants of the infected cells for the presence of Zika virus RNA by qRT-PCR, as described earlier in this section. We performed 4 passages of each isolate in C6/36 cells to increase viral titers for NGS.

Indirect Immunofluorescence Assay

For the indirect immunofluorescence assays, we grew Vero cells over glass coverslips and then infected them with the Zika virus isolate. At 48 hours postinfection, we fixed cells with 4% paraformaldehyde and then incubated them with ice-cold methanol for 10 min. We blocked the cells using 10% FBS in phosphate-buffered saline (PBS) for 1 h and then incubated them overnight at 4°C with a 1:500 dilution of the monoclonal antibody 4G2. After the incubation period, we washed the cells twice with PBS and then incubated them with an Alexa Fluor 488-conjugated goat antimouse IgG antibody (Jackson Immunoresearch, https://www.jacksonimmuno.com) for 1 h. We washed the cells twice with PBS and then mounted them with VECTASHIELD medium with DAPI (Vector Laboratories, https://vectorlabs.com) for confocal microscopy (Nikon, https://www.nikon.com).

Plaque Assays

For the plaque assays, we seeded Vero cells in 24-well plates until they reached a confluence of 80%. We used 10-fold serial dilutions of the Zika virus isolate to infect the cell monolayers and left them to adsorb for 1 h. After the adsorption period, we removed the virus and overlaid cell monolayers with 1 mL of DMEM (Invitrogen) supplemented with 2% carboxymethyl-cellulose (Sigma-Aldrich, https://www.sigmaaldrich.com), 2% FBS, 100 U/mL penicillin, 100 μg/mL streptomycin, and 2 mM L-glutamine (Gibco, https://www.thermofisher.com) and incubated at 37°C for 4 d. We fixed the cells with 4% paraformaldehyde in PBS and counterstained them with crystal violet-formaldehyde (Sigma-Aldrich).

Full Genome Sequencing and Assembly

For the complete genome sequencing of the Zika virus isolate, we depleted 200 ng of total RNA extracted from the supernatants of infected Vero cell monolayers of rRNA using the NEBNext rRNA Depletion Kit (human/mouse/rat) following the manufacturer's instructions (New England Biolabs, https://www.neb.com). We constructed RNaseq Illumina shotgun libraries at the Unidad Universitaria de Secuenciación Masiva y Bioinformática-Instituto de Biotecnología and sequenced them using paired-end sequencing with a MySeq system (Illumina, https://www.illumina.com). We assessed the quality of reads using FASTQC (http://www.bioinformatics.babraham.ac.uk/projects/fastqc); low-quality positions and reads were eliminated using in-house scripts. We assembled the valid reads without reference using the program Trinity 2.8 (*16*) and evaluated the assembly using Qualimap (*17*). Finally, we verified the identity of the contig using blastn (http://blast.ncbi.nlm.nih.gov/Blast.cgi).

Phylogenetic Reconstruction

To determine the phylogenetic relatedness of the Zika virus isolate, we retrieved relevant Zika virus open reading frame (ORF) RNA sequences from the Virus Pathogen Resource (ViPR) database (*18*) (http://www.viprbrc.org). We removed identical sequences and those with undetermined bases from alignment. We applied near-identity clustering (0.999) to the remaining sequences in Cd-hit-test (*19*) and used 98 sequences for phylogenetic inference by maximum likelihood in RAxML (*20*) under a general time-reversible plus gamma substitution model. We reconstructed the tree with 200 bootstrap replicas. We normalized branch lengths and condensed nodes with bootstrap values <50% to emphasize tree topology.

Variant Analysis

To determine the presence of variants in the larva-derived sequence, we used the alignment to identify positions that had mutations unique to our sequence or that were primarily shared with other mosquito-derived sequences and that were absent or rare in the human-derived genomes. To this end, we examined the alignment

with the tool meta-CATS (*21*), which performs a χ^2 test to find positions with different polymorphism distribution between groups.

Results

Zika Virus Isolation and Identification in *Ae. aegypti* Larvae

During the study period, we analyzed 151 larvae pools by qRT-PCR in search of Zika virus RNA. Only 17 (10.8%) of the pools tested positive: 9 (5.7%) from the larvae raised from the eggs collected in June and 8 (5.1%) from larvae raised from the eggs collected in November. To determine the proportion of infected larvae in the population, we calculated MIRs for the 2 collection periods (June and November 2016) and found an increase in the MIR observed from the larvae raised from the eggs collected in June (2.5) to the MIR from the eggs collected in November (6.9) (Table 1).

To confirm the presence of infectious Zika virus in the larvae pools, we used 11 of the 17 pools that tested positive for Zika virus RNA that displayed the lowest Cq values to attempt viral isolation. We were able to isolate infectious Zika virus from only 1 of the larvae pools (31N), as determined by the presence of cytopathic effect in C6/36 cells characterized by monolayer detachment (Figure 2, panel A) and the detection of Zika virus RNA in culture supernatants by qRT-PCR with a Cq value of 23.73.

The ability of the 31N isolate to infect a mammalian cell line was confirmed by the appearance of the characteristic cytopathic effect of Zika virus in infected Vero cell cultures, characterized by cell rounding and detachment (Figure 2, panel A). Moreover, immunofluorescent detection of the viral envelope (E) protein using the monoclonal antibody 4G2 revealed perinuclear staining (Figure 2, panel B). The plaque assays carried out in Vero cells revealed that the 31N isolate has the ability to produce lytic plaques; thus, this isolate can be considered cytopathic in mammalian cell culture (Figure 2, panel C).

Complete Genome Sequencing of Zika Virus Isolate 31N

We isolated viral RNA from the supernatant of Vero cells infected with the fourth passage of Zika virus isolate 31N and processed it by RNA sequencing by the NGS MiSeq Illumina protocol. Around 40% of the total reads (6,535,816) were assembled in a single contig of 10,795 nt in length, with a mean depth of 42,000 reads. BLAST results of the assembled contig revealed that the strain ZIKV/Aedes.sp/MEX/MEX_I-7/2016, which belongs to a Zika virus isolated from *Aedes* mosquitoes obtained in the state of Chiapas, Mexico, had the highest identity (98.8%) with our isolate.

Table 1. MIR for Zika virus in *Aedes aegypti* larvae, Jojutla, Morelos, Mexico, June and November 2016*

Collection date	Positive pools/ analyzed pools	Specimens analyzed	MIR
June	9/105	3150	2.8
November	8/46	1150	6.9

*MIR, minimum infection rate.

Variant Analysis

We identified single-nucleotide variants (SNVs) in the Zika virus isolate 31N genome by aligning the sequence with other mosquito- and human-derived sequences obtained from the ViPR database and running the meta-CATS analytic tool, as described in the Materials and Methods section. To carry out this analysis, we grouped the sequences by the host of origin. We identified SNVs in positions 3176, 3286, and 5636 that were unique to the larva genome. On the other hand, the SNVs in positions 2071 and 3333 were found in human-derived sequences but were not present in other mosquito genomes. The SNV in position 2071 was shared only with a sequence from French Polynesia, likely an example of parallel evolution, whereas the polymorphism in position 3333 was common with 2 sequences from Mexico and may correspond to a local variant. Finally, we found 8 SNVs that were also present in other human and mosquito sequences but were more common in mosquitoes. Only 1 SNV was found in the E gene, whereas the rest were found in nonstructural (NS) genes: 5 in NS2A, 4 in NS3, 2 in NS5, and 1 in NS1 (Table 2).

Phylogenetic Reconstruction of Zika Virus

To characterize the evolutionary relationship between the 31N isolate and other Zika virus genomes that have been previously reported, we performed a phylogenetic analysis. The phylogenetic reconstruction of the complete genomes of 98 Zika virus sequences, including the 31N isolate, revealed that the 31N isolate belongs to the Asian-American lineage of Zika virus and clusters together with other sequences of human and mosquito origin from Mexico (Figure 3).

Discussion

Natural vertical transmission of mosquito-carried viruses has been proposed as one of the main ecologic processes involved in the maintenance of these viruses in susceptible mosquito populations, particularly during interepidemic periods and harsh climate conditions when horizontal transmission becomes difficult (*11*,*22*). In Mexico, most of the studies regarding natural vertical transmission of arboviruses in mosquitoes have been carried out using DENV as a study model (*23*–*25*), so the diversity of viruses that can be transmitted from infected adult mosquitoes to their offspring still needs to be characterized.

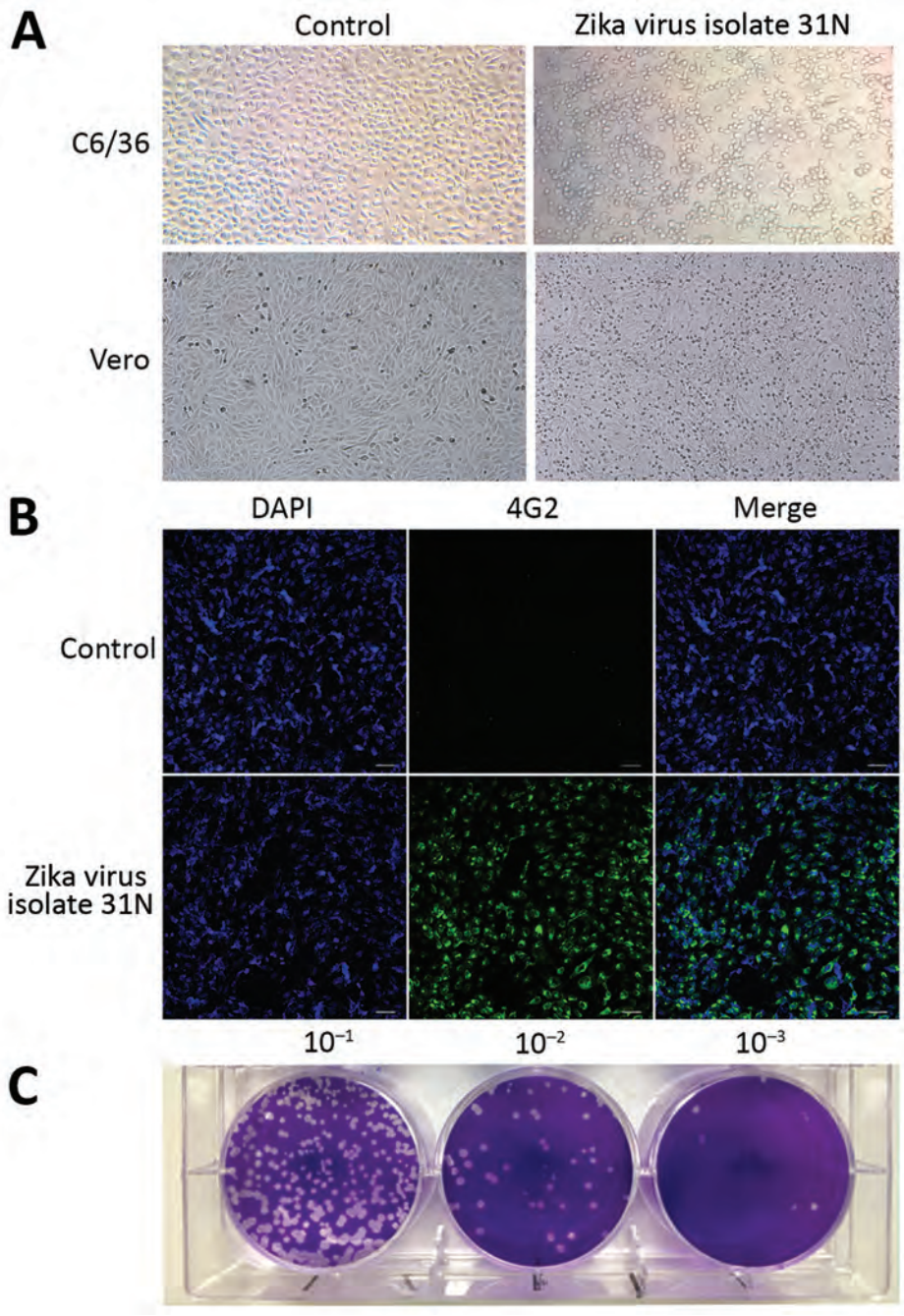

Figure 2. Phenotypic analysis of Zika virus isolate 31N from an *Aedes aegypti* larval pool, Jojutla, Morelos, Mexico. A) Cytopathic effect of the Zika virus isolate 31N in C6/36 and Vero cells. The left panel shows mock infected cells. Original magnification x 20. B) Infected Vero cells with Zika virus isolate 31N at a multiplicity of infection of 0.1 and mock infected cells. Nuclei are stained in blue (DAPI), and the envelope protein is stained in green (4G2). Original magnification x 20. C) Plaque assay of Zika virus isolate 31N in Vero cells. Serial decimal dilutions of Zika virus isolate 31N are depicted.

Only a few studies have addressed the natural vertical transmission of Zika virus in wild mosquito populations; most of these have been carried out in Brazil, where Zika virus RNA has been detected in male *Ae. aegypti* mosquitoes and in adult *Ae. albopictus* mosquitoes raised from field-collected eggs (*26*,*27*).

In this study, we demonstrated the occurrence of natural vertical transmission of Zika virus in wild mosquito populations from the municipality of Jojutla in the state of Morelos, Mexico. The RNA of Zika virus was detected in 17 larvae pools; the rates of vertical transmission of Zika virus in the wild *Ae. aegypti* populations were estimated by calculating the MIR. In Morelos, the rainy season begins in late May and extends through the end of September, after which both the precipitation and the mosquito populations start to decrease. Thus, the higher MIR (6.95) calculated from the larvae hatched from the eggs collected in November 2016, in contrast to the MIR from the larvae hatched from the eggs collected in June (2.6), might be correlated with the increased number of human Zika virus cases that

Table 2. Residue diversity between Zika virus isolate 31N from an *Aedes aegypti* larval pool and human- and mosquito-derived genomes, Jojutla, Morelos, Mexico*

Position	Genome region	Human-derived sequences		Mosquito-derived sequence		p value
		SNVs, %	Origin of minority variant	SNVs, %	Origin of minority variant	
1008	E	T→C, 3.65	Mexico, United States, Thailand	T→C, 17.64	31N, Mexico	0.000253
2071†	NS1	C→T, 0.26	French Polynesia	C→T, 2.94	31N	0.03
2871	NS2A	T→C, 4.43	Mexico, United States	T→C, 35.29	31N, Mexico, United States	<0.0001
3176‡	NS2A	CS		A→C, 2.94	31N	0.01022
3286‡	NS2A	CS		A→G, 2.94	31N	0.01022
3333†	NS2A	A→G, 0.52	Mexico	A→G, 2.94	31N	>0.05
3788	NS2A	C→T, 0.26	Brazil	C→T, 8.82	31N, Mexico	<0.0001
4500	NS2A	A→G, 3.65	Mexico, United States, Philippines, South Korea	A→G, 17.64	31N, Mexico	0.003847
4624	NS3	G→A, 3.39	United States, Mexico	G→A, 17.64	31N, Mexico	0.002194
4980	NS3	T→C, 6.00	Mexico, Puerto Rico, Colombia, United States	T→C, 17.64	31N, Mexico	0.01
5636‡	NS3	CS		C→T, 2.94	31N	0.01022
7200	NS5	T→A 0.26; T→C, 3.91§	Mexico, USA, Suriname	T→C, 17.64	31N, Mexico	0.006182
9139	NS5	C→T, 0.52	Mexico	C→T, 11.76	31N, Mexico	<0.0001

*CS, conserved site in human-derived sequences; SNV, single nucleotide variant.
†SNVs in human-derived sequences but not in other mosquito genomes.
‡SNVs unique to the larva genome.
§Two SNVs located in the same genome position.

were reported in Jojutla during November, whereas during June no human cases were reported. The absence of reported Zika virus human cases in June could be the result of asymptomatic cases, cases clinically misdiagnosed as dengue virus infections, or both.

The higher number of persons infected with Zika virus in Jojutla during November reflects an increase in the number of infected mosquitoes resulting from horizontal transmission of the virus between mosquitoes and infected humans. It is possible that vertical transmission is contributing to the number of infected mosquitoes, which are, in turn, capable of transmitting this virus to a higher number of humans. However, the relative importance of vertical transmission for the maintenance and spread of the virus cannot be elucidated with the data available so far.

The MIR is usually affected by the number of mosquitoes that make up the pool of mosquitoes (or their immature stages) tested, which usually causes an underestimation of the real number of infected mosquitoes in a population (*10*). Thus, the rate of vertical transmission in the mosquito populations from Morelos might be even higher than estimated. Previous studies performed with other flaviviruses, such as DENV, have reported MIRs as low as 0.18 (*28*) and 0.6 (*29*) or as high as 40 (*30*) in wild larvae, usually associated with the collection date and the place of sampling. Under laboratory conditions, the filial infectious rate of Zika virus in *Ae. aegypti* mosquitoes ranged from 4.9 to 24.6, depending on the strain of the virus tested (*31*), which corroborates that our results are comparable to the MIRs reported for other Zika viruses and other flaviviruses, including DENV (*32*,*33*).

In this work, we were also able to demonstrate the natural vertical transmission of Zika virus in *Ae. aegypti* mosquitoes by the successful isolation of infectious Zika virus (31N) from larvae raised from field-collected eggs. This evidence strongly suggests that infectious Zika virus can be transmitted from adult female mosquitoes to their offspring and increases the evidence of the role of natural vertical transmission in the maintenance of Zika virus in wild mosquito populations.

The isolation of infective Zika virus vertically transmitted from adult mosquitoes to their offspring suggests that this virus could be potentially transmissible between mosquitoes and their vertebrate hosts; nevertheless, this transmission still needs to be demonstrated. Moreover, we were able to detect several SNVs in the larvae-derived Zika virus isolate 31N, of which 3 were specific to this larvae-derived genome, as well as 10 others that were shared between the larvae and other mosquito and human sequences. Although it is plausible that these SNVs were acquired during virus culture, we think this is unlikely because 72 of the sequences included in the alignment corresponded to cultured viruses and none of them presented these mutations; however, the sequences from more larvae-derived viruses need to be determined to establish the significance of these SNVs. The larvae-specific SNVs were located in the coding regions for the NS2A and NS3 proteins, which are involved in the replication of the viral RNA (*34*). Nevertheless, whether the larvae-specific SNVs are associated with the maintenance and vertical transmission of infectious Zika virus from adult mosquitoes to their offspring still needs to be determined.

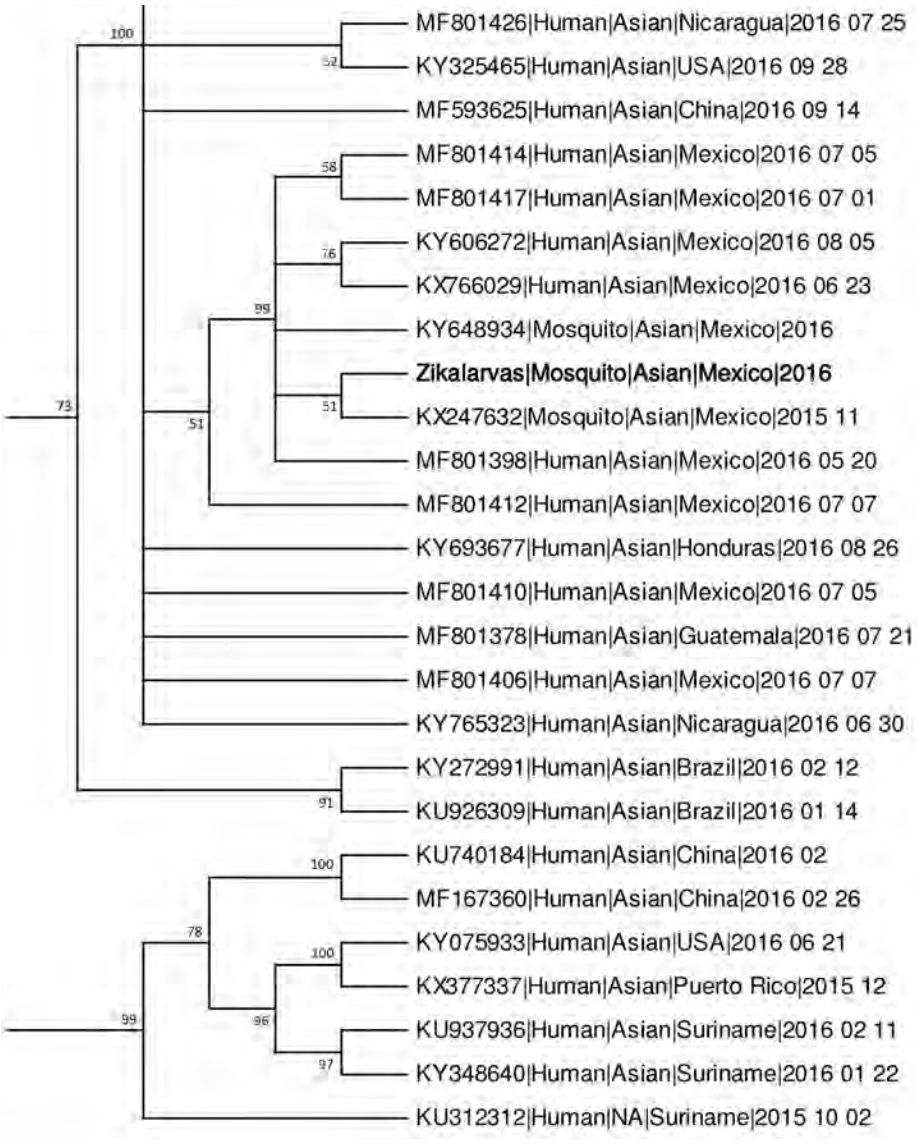

Figure 3. Condensed phylogenetic reconstruction of selected complete Zika virus genomes. This selection from the tree depicts the phylogenetic relationships between Zika virus isolate 31N from an *Aedes aegypti* larval pool, Jojutla, Morelos, Mexico (bold), and 98 complete genome sequences of Zika viruses obtained from the Virus Pathogen Resource database. GenBank accession numbers are provided. Nodes with bootstrap values support <50% were condensed and branch lengths were normalized to emphasize tree topology. The full phylogenetic tree is available online (http://wwwnc.cdc.gov/EID/article/25/8/18-1533-F1.htm).

In summary, we demonstrated natural vertical transmission of Zika virus in wild *Ae. aegypti* mosquitoes. Our results suggest that this transmission mode could aid in the spread and maintenance of Zika virus in nature, expanding the ongoing zoonotic threat from this virus to human health.

Acknowledgments

We thank Jorge Luis Peralta Rodríguez and Carlos Marx Ramírez Huicochea for their help in the mosquito collection and identification and Vadim Pérez Koldenkova for his support with the confocal microscopy at the Laboratorio Nacional de Microscopia Avanzada/Centro Medico Nacional Siglo XXI, IMSS.

This work was supported by grants CONACyT 183448, CONACyT 233977, and CONACyT 269826.

About the Author

Ms. Izquierdo-Suzán is a graduate student at Universidad Autónoma de la Ciudad de México, Mexico City, Mexico. Her primary research interests are molecular and ecological aspects of emerging infectious diseases in wildlife.

References

1. Hasan SS, Sevvana M, Kuhn RJ, Rossmann MG. Structural biology of Zika virus and other flaviviruses. Nat Struct Mol Biol. 2018;25:13–20. http://dx.doi.org/10.1038/s41594-017-0010-8
2. Russo FB, Jungmann P, Beltrão-Braga PCB. Zika infection and the development of neurological defects. Cell Microbiol. 2017;19:e12744. http://dx.doi.org/10.1111/cmi.12744
3. Main BJ, Nicholson J, Winokur OC, Steiner C, Riemersma KK, Stuart J, et al. Vector competence of *Aedes aegypti*, *Culex tarsalis*, and *Culex quinquefasciatus* from California for Zika virus. PLoS Negl Trop Dis. 2018;12:e0006524. http://dx.doi.org/10.1371/journal.pntd.0006524

4. Saiz JC, Vázquez-Calvo Á, Blázquez AB, Merino-Ramos T, Escribano-Romero E, Martín-Acebes MA. Zika virus: the latest newcomer. Front Microbiol. 2016;7:496. http://dx.doi.org/10.3389/fmicb.2016.00496
5. Vorou R. Zika virus, vectors, reservoirs, amplifying hosts, and their potential to spread worldwide: what we know and what we should investigate urgently. Int J Infect Dis. 2016;48:85–90. http://dx.doi.org/10.1016/j.ijid.2016.05.014
6. Tilak R, Ray S, Tilak VW, Mukherji S. Dengue, chikungunya … and the missing entity—Zika fever: a new emerging threat. Med J Armed Forces India. 2016;72:157–63. http://dx.doi.org/10.1016/j.mjafi.2016.02.017.
7. Kraemer MU, Sinka ME, Duda KA, Mylne A, Shearer FM, Brady OJ, et al. The global compendium of *Aedes aegypti* and *Ae. albopictus* occurrence. Sci Data. 2015;2:150035. http://dx.doi.org/10.1038/sdata.2015.35
8. da Costa CF, Dos Passos RA, Lima JBP, Roque RA, de Souza Sampaio V, Campolina TB, et al. Transovarial transmission of DENV in *Aedes aegypti* in the Amazon basin: a local model of xenomonitoring. Parasit Vectors. 2017;10:249. http://dx.doi.org/10.1186/s13071-017-2194-5
9. Adams B, Boots M. How important is vertical transmission in mosquitoes for the persistence of dengue? Insights from a mathematical model. Epidemics. 2010;2:1–10. http://dx.doi.org/10.1016/j.epidem.2010.01.001
10. Grunnill M, Boots M. How important is vertical transmission of dengue viruses by mosquitoes (Diptera: Culicidae)? J Med Entomol. 2016;53:1–19. http://dx.doi.org/10.1093/jme/tjv168
11. Lequime S, Fontaine A, Ar Gouilh M, Moltini-Conclois I, Lambrechts L. Genetic drift, purifying selection and vector genotype shape dengue virus intra-host genetic diversity in mosquitoes. PLoS Genet. 2016;12:e1006111. http://dx.doi.org/10.1371/journal.pgen.1006111
12. Li CX, Guo XX, Deng YQ, Xing D, Sun AJ, Liu QM, et al. Vector competence and transovarial transmission of two *Aedes aegypti* strains to Zika virus. Emerg Microbes Infect. 2017;6:1–7. http://dx.doi.org/10.1038/emi.2017.8
13. Thangamani S, Huang J, Hart CE, Guzman H, Tesh RB. Vertical transmission of Zika virus in Aedes aegypti mosquitoes. Am J Trop Med Hyg. 2016;95:1169–73. http://dx.doi.org/10.4269/ajtmh.16-0448
14. Dirección General de Epidemiologia SS. Boletín Epidemiológico. Sistema Nacional de Vigilancia Epidemiológica. Contract no. semana 52. 2016 [cited 2018 Sep 21]. https://www.gob.mx/cms/uploads/attachment/file/179535/sem52.pdf
15. Lanciotti RS, Kosoy OL, Laven JJ, Velez JO, Lambert AJ, Johnson AJ, et al. Genetic and serologic properties of Zika virus associated with an epidemic, Yap State, Micronesia, 2007. Emerg Infect Dis. 2008;14:1232–9. http://dx.doi.org/10.3201/eid1408.080287
16. Grabherr MG, Haas BJ, Yassour M, Levin JZ, Thompson DA, Amit I, et al. Full-length transcriptome assembly from RNA-Seq data without a reference genome. Nat Biotechnol. 2011;29:644–52. http://dx.doi.org/10.1038/nbt.1883
17. García-Alcalde F, Okonechnikov K, Carbonell J, Cruz LM, Götz S, Tarazona S, et al. Qualimap: evaluating next-generation sequencing alignment data. Bioinformatics. 2012;28:2678–9. http://dx.doi.org/10.1093/bioinformatics/bts503
18. Pickett BE, Greer DS, Zhang Y, Stewart L, Zhou L, Sun G, et al. Virus pathogen database and analysis resource (ViPR): a comprehensive bioinformatics database and analysis resource for the coronavirus research community. Viruses. 2012;4:3209–26. http://dx.doi.org/10.3390/v4113209
19. Guindon S, Gascuel O. A simple, fast, and accurate algorithm to estimate large phylogenies by maximum likelihood. Syst Biol. 2003;52:696–704. http://dx.doi.org/10.1080/10635150390235520
20. Anisimova M, Gascuel O. Approximate likelihood-ratio test for branches: A fast, accurate, and powerful alternative. Syst Biol. 2006;55:539–52. http://dx.doi.org/10.1080/10635150600755453
21. Pickett BE, Liu M, Sadat EL, Squires RB, Noronha JM, He S, et al. Metadata-driven comparative analysis tool for sequences (meta-CATS): an automated process for identifying significant sequence variations that correlate with virus attributes. Virology. 2013;447:45–51. http://dx.doi.org/10.1016/j.virol.2013.08.021
22. Coffey LL, Page BL, Greninger AL, Herring BL, Russell RC, Doggett SL, et al. Enhanced arbovirus surveillance with deep sequencing: identification of novel rhabdoviruses and bunyaviruses in Australian mosquitoes. Virology. 2014;448:146–58. http://dx.doi.org/10.1016/j.virol.2013.09.026
23. Ibáñez-Bernal S, Briseño B, Mutebi JP, Argot E, Rodríguez G, Martínez-Campos C, et al. First record in America of *Aedes albopictus* naturally infected with dengue virus during the 1995 outbreak at Reynosa, Mexico. Med Vet Entomol. 1997;11:305–9. http://dx.doi.org/10.1111/j.1365-2915.1997.tb00413.x
24. Günther J, Ramírez-Palacio LR, Pérez-Ishiwara DG, Salas-Benito JS. Distribution of dengue cases in the state of Oaxaca, Mexico, during the period 2004–2006. J Clin Virol. 2009;45:218–22. http://dx.doi.org/10.1016/j.jcv.2009.05.007
25. Martínez NE, Dzul-Manzanilla F, Gutiérrez-Castro C, Ibarra-López J, Bibiano-Marín W, López-Damián L, et al. Natural vertical transmission of dengue-1 virus in *Aedes aegypti* populations in Acapulco, Mexico. J Am Mosq Control Assoc. 2014;30:143–6. http://dx.doi.org/10.2987/14-6402.1
26. Ferreira-de-Brito A, Ribeiro IP, Miranda RM, Fernandes RS, Campos SS, Silva KA, et al. First detection of natural infection of *Aedes aegypti* with Zika virus in Brazil and throughout South America. Mem Inst Oswaldo Cruz. 2016;111:655–8. http://dx.doi.org/10.1590/0074-02760160332
27. Smartt CT, Shin D, Alto BW. Dengue serotype-specific immune response in *Aedes aegypti* and *Aedes albopictus*. Mem Inst Oswaldo Cruz. 2017;112:829–37. http://dx.doi.org/10.1590/0074-02760170182
28. Vilela AP, Figueiredo LB, dos Santos JR, Eiras AE, Bonjardim CA, Ferreira PC, et al. Dengue virus 3 genotype I in *Aedes aegypti* mosquitoes and eggs, Brazil, 2005–2006. Emerg Infect Dis. 2010;16:989–92. http://dx.doi.org/10.3201/eid1606.091000
29. Guedes DR, Cordeiro MT, Melo-Santos MA, Magalhaes T, Marques E, Regis L, et al. Patient-based dengue virus surveillance in *Aedes aegypti* from Recife, Brazil. J Vector Borne Dis. 2010;47:67–75.
30. Lee HL, Rohani A. Transovarial transmission of dengue virus in *Aedes aegypti* and *Aedes albopictus* in relation to dengue outbreak in an urban area in Malaysia. New Delhi: WHO Regional Office for South-East Asia; 2005. p. 106–11.
31. Ciota AT, Bialosuknia SM, Zink SD, Brecher M, Ehrbar DJ, Morrissette MN, et al. Effects of Zika virus strain and *Aedes* mosquito species on vector competence. Emerg Infect Dis. 2017;23:1110–7. http://dx.doi.org/10.3201/eid2307.161633
32. Edillo FE, Sarcos JR, Sayson SL. Natural vertical transmission of dengue viruses in *Aedes aegypti* in selected sites in Cebu City, Philippines. J Vector Ecol. 2015;40:282–91. http://dx.doi.org/ 10.1111/jvec.12166
33. Apodaca-Medina AI, Torres-Avendaño JI, Rendón-Maldonado JG, Torres-Montoya EH, Flores-López BA, Del Angel RM, et al. First evidence of vertical infection of dengue virus 2 in *Aedes aegypti* mosquitoes from Sinaloa, Mexico. Vector Borne Zoonotic Dis. 2018;18:231–3. http://dx.doi.org/10.1089/vbz.2017.2202
34. Barrows NJ, Campos RK, Liao KC, Prasanth KR, Soto-Acosta R, Yeh SC, et al. Biochemistry and molecular biology of flaviviruses. Chem Rev. 2018;118:4448–82. http://dx.doi.org/10.1021/acs.chemrev.7b00719

Address for correspondence: Martha Yocupicio-Monroy, Universidad Autónoma de la Ciudad de México, Posgrado en Ciencias Genómicas, San Lorenzo #290 Col Del Valle, CP 03100, Mexico City, Mexico; email: martha.ym1@gmail.com

Cross-Protection of Dengue Virus Infection against Congenital Zika Syndrome, Northeastern Brazil

Celia Pedroso,[1] Carlo Fischer,[1] Marie Feldmann,[1] Manoel Sarno, Estela Luz, Andrés Moreira-Soto, Renata Cabral, Eduardo Martins Netto, Carlos Brites, Beate M. Kümmerer, Jan Felix Drexler

The Zika virus outbreak in Latin America resulted in congenital malformations, called congenital Zika syndrome (CZS). For unknown reasons, CZS incidence was highest in northeastern Brazil; one potential explanation is that dengue virus (DENV)–mediated immune enhancement may promote CZS development. In contrast, our analyses of historical DENV genomic data refuted the hypothesis that unique genome signatures for northeastern Brazil explain the uneven dispersion of CZS cases. To confirm our findings, we performed serotype-specific DENV neutralization tests in a case–control framework in northeastern Brazil among 29 Zika virus–seropositive mothers of neonates with CZS and 108 Zika virus–seropositive control mothers. Neutralization titers did not differ significantly between groups. In contrast, DENV seroprevalence and median number of neutralized serotypes were significantly lower among the mothers of neonates with CZS. Supported by model analyses, our results suggest that multitypic DENV infection may protect from, rather than enhance, development of CZS.

The 2015–2016 Zika epidemic in Brazil was associated with congenital malformations summarized as congenital Zika syndrome (CZS) (*1*–*6*). As a consequence, abortion requests and pregnancy delays increased dramatically in Brazil and all of Latin America (*7*,*8*). For unknown reasons, CZS incidence was highest in northeastern Brazil (*1*,*4*,*9*,*10*). In Asia and Africa, where Zika virus circulated for much longer than it did in the Americas, Zika virus infections have not been consistently linked to CZS development; only sporadic cases have been reported (*11*). Thus, CZS development might be affected by ≥1 cofactor (*9*,*12*). The hypothetical list of cofactors affecting CZS development includes maternal vaccination history (*12*), exposure to larvicides (*5*), or socioeconomic factors (*1*,*13*).

Similar to the ubiquitous dengue virus (DENV), which occurs as 4 distinct serotypes, Zika virus is a flavivirus (*14*). Secondary DENV infections can be more severe than primary infections because of antibody-dependent enhancement (i.e., heterotypic subneutralizing antibodies enhancing virus entry into poorly susceptible cells) (*15*,*16*). Zika virus infection can also be enhanced by DENV antibodies in vitro (*17*,*18*) and in mice (*19*). Thus, DENV-mediated antibody-dependent enhancement may be a major cofactor of CZS development in humans (*19*–*21*). However, antibody-dependent enhancement was not observed in experimentally Zika virus–infected nonhuman primates (*22*) and during pivotal epidemiologic studies from Brazil that assessed neither individual DENV serotypes nor microcephaly cases (*5*,*9*,*23*). In addition, DENV is ubiquitous in all regions of Brazil (*20*). Therefore, to explain the accumulation of CZS cases in northeastern Brazil, a hypothetical DENV-mediated effect enhancing CZS development would require region-specific differences in past DENV exposure. To investigate the role that preexisting DENV immunity has in CZS development, we conducted serologic testing in a nested case–control framework and analyzed historical DENV genomic data from Brazil.

Materials and Methods

Study Population

We compared 29 mothers of children born with CZS (cases) and 108 mothers of children born without CZS (controls) from Salvador, northeastern Brazil. All mothers had

Author affiliations: Universidade Federal da Bahia, Salvador, Brazil (C. Pedroso, M. Sarno, E. Luz, R. Cabral, E. Martins Netto, C. Brites); Charité-Universitätsmedizin Berlin, corporate member of Freie Universität Berlin Humbolt-Universität zu Berlin and Berlin Institute of Health, Institute of Virology, Berlin, Germany (C. Fischer, A. Moreira-Soto, J.F. Drexler); University of Bonn Medical Centre, Bonn, Germany (M. Feldmann, B.M. Kümmerer); German Centre for Infection Research (B.M. Kümmerer, J.F. Drexler); Martsinovsky Institute of Medical Parasitology, Tropical and Vector-Borne Diseases, Sechenov University, Moscow, Russia (J.F. Drexler)

DOI: https://doi.org/10.3201/eid2508.190113

[1]These authors contributed equally to this article.

evidence of past Zika virus exposure, determined by use of ELISAs and plaque-reduction neutralization tests (PRNTs) as described previously (*13*). Samples were collected consecutively at the time of delivery from May 2015 through December 2016 at the University of Bahia Climério de Oliveira maternity ward (Appendix Figure, https://wwwnc.cdc.gov/EID/article/25/8/19-0113-App1.pdf). The study was approved by the Institutional Research Ethics Board under protocol no. 1.408.49, and all women delivering during that period accepted participation in the protocol. Age distributions of cases and controls did not differ significantly (median age 26 years for cases, interquartile range 22.0–33.5; median age 29 years for controls, interquartile range 23.3–34.0; p = 0.26 by *t*-test).

Diagnosis of CZS

CZS was diagnosed by attending gynecologists. Lead symptoms of CZS, as defined by Moore et al. (*24*), included microcephaly and other neurologic birth defects (e.g., intracranial calcifications, ventriculomegaly, dysgenesis of the corpus callosum, Dandy-Walker–like malformations, hydranencephaly, porencephaly, hydrocephalus, severe intracranial calcifications, and decreased brain tissue) (*13*). Microcephaly was identified when the measurement of the cephalic circumference was 2 SDs below that of neonates of the corresponding gestational age, according to intergrowth charts from the World Health Organization in addition to clinical and imaging data.

PRNTs

For the serotype-specific PRNT for DENV, we used 3 μL of heat-inactivated serum (56°C, 30 min) diluted by using Dulbecco modified Eagle medium, supplemented with 1% fetal calf serum at 1:50, 1:150, 1:450, 1:1,350, 1:4,050, and 1:12,150. We split serum dilutions into 4 equal aliquots and incubated them separately in 96-well plates with 60 PFUs of DENV serotypes 1–4 (Appendix Table 1) for 60 min at 37°C. Next, we incubated the virus/serum mixtures for 90 min at 37°C in 5% CO_2 on Vero cells grown in 24-well plates, followed by a methylcellulose/minimum essential medium overlay (2% fetal calf serum, 1.2% final methylcellulose concentration). After incubation for 4 days (DENV-1, -3, and -4) or 5 days (DENV-2), we performed formaldehyde fixation, crystal violet staining, and plaque counting. We calculated neutralizing antibody titers by using the built-in variable slope model in GraphPad Prism 6 (GraphPad Software, LLC, https://www.graphpad.com). Any titer ≥1:10 that reduced DENV PFU by ≥90% compared with control titers was considered positive. PRNT is the standard for flavivirus serology. DENV vaccine studies commonly rely on 50% plaque reduction to determine DENV serotype-specific antibody responses (*25*). To minimize the effect of potential cross-reactivity between DENV serotypes on our results, we selected a less sensitive but highly specific 90% PRNT ($PRNT_{90}$).

Phylogenetic Analyses

For phylogenetic analyses, we retrieved all DENV sequences available from GenBank as of June 15, 2018, that contained information on year and place of isolation. We constructed neighbor-joining trees in MEGA7 (*26*) by using a percentage distance method, a pairwise deletion option, and 1,000 bootstrap replicates. We analyzed either the junction of the envelope and the nonstructural protein 1 (NS1) encoding regions (polyprotein gene positions 2215–2454) or a fragment of 561 nt within the NS1 region (polyprotein gene positions 2650–3210). For clarity of presentation, we excluded sequences of <0.5% mutual nucleotide sequence distance. To show different genotypes, we included selected reference strains (Appendix Table 2). All DENV genome positions given within this article refer to a DENV prototype strain available in GenBank under accession no. KC294223.

Confirmation of DENV Strains Used for PRNT

We confirmed the designation and serotype of DENV strains applied for PRNT by Sanger sequencing of the prM-C domains using strain-specific oligonucleotide primers. These primers are available upon request.

Statistical Analyses and Visualization of PRNT Results

To plot PRNT results, we used GraphPad Prism 6. All p values result from 2-tailed tests. For power calculations, we used OpenEpi version 3 (*27*) for 2-sided 95% CIs. Regression lines were calculated by using a least squares (ordinary) fit method.

Model Testing

To compare the effects of different factors on CZS formation, we tested mathematical logistic regression models. Each model considered 1 defined variable to predict the binary outcome as CZS case or control. We included for testing binary predictor variables such as presence or absence of DENV-1 neutralization, as well as ordinal (e.g., number of neutralized DENV serotypes) or continuous predictor variables, such as DENV-1 PRNT titers. Cases were coded as 1 and controls as 0. We fitted 15 models by using the generalized linear model function of R version 3.5.2 (https://www.r-project.org). To compare different models, we calculated the Akaike information criterion (AIC), the difference between a given and the best-supported model in AIC, and the Akaike weights by using the bbmle package version 1.0.20 in R. To show which models allow significant CZS case prediction, we calculated likelihood ratio tests for each model, and to show the effect strength of the models, we calculated odds ratios.

Results

After the reinfestation of Brazil with the main DENV vector, *Aedes aegypti* mosquitoes, in 1976 (*28*), DENV-1 was introduced in 1986 (*29*), DENV-2 in 1990 (*30*), and DENV-3 in 2000 (*31*); DENV-4 reemerged in 2007 after an absence of 25 years (*32*) (Figure 1). At most, 4 years after their first detection in other regions of Brazil, all 4 DENV serotypes were found in northeastern Brazil. In the databases, we identified 992 unique DENV sequences from Brazil that we used to analyze genomic DENV signatures hypothetically segregating the northeast and other regions in Brazil. Analyses of the envelope-NS1 junction, which is frequently used for genome-based serotyping (*33*), revealed high genetic identity of DENV strains from the northeast and other regions of Brazil during 30 years (Figure 2, panel A). A single DENV-4 clade apparently was found uniquely in northeastern Brazil during 2011–2015 (Figure 2, panel A). Nonetheless, these DENV-4 strains were closely related to strains from other regions when a different, larger partial NS1 region was analyzed (Figure 2, panel B). In summary, our analyses showed no phylogenetic evidence for a unique DENV signature segregating northeastern Brazil from other regions.

Low DENV antibody titers have been shown to be a risk factor for severe disease with heterotypic DENV infection (*15*). Therefore, we analyzed the magnitude of DENV antibody titers. Overall median reciprocal $PRNT_{90}$ titers within this study were 56.5 (95% CI 42.0–79.0) for cases and 61.4 (95% CI 54.3–73.1) for controls. Serotype-specific titers were 68.7 (95% CI 51.2–83.2) for DENV-1, 102.8 (95% CI 79.6–130.6) for DENV-2, 44.8 (95% CI 35.3–55.8) for DENV-3, and 52.6 (95% CI 41.9–66.6) for DENV-4. DENV titers did not differ significantly between cases and controls or between serotypes (Figure 3, panel A). However, we have previously shown that Zika virus antibody titers are significantly higher among mothers of neonates with CZS than among mothers of neonates without evidence of CZS (*34*), hypothetically affecting DENV antibody titer estimates. In our cohorts, Zika virus titers did not correlate with DENV titers (Figure 3, panel B) or with the number of neutralized DENV serotypes ($p = 0.8459$ by analysis of variance) (Figure 3, panel C), suggesting robustness of our results irrespective of individual Zika virus PRNT titers.

Strikingly, the overall DENV seroprevalence was significantly lower among cases, at 65.5%, than among controls, at 91.7% ($p = 0.0003$ by χ^2 test; power 90.4%). For each DENV serotype, seroprevalence was also consistently higher among cases than controls (Figure 4, panel A). The relatively lower seroprevalence of DENV-3 and DENV-4 compared with DENV-1 and DENV-2 among study participants is consistent with the shorter circulation of these viruses in Brazil (Figure 1), again suggesting robustness of our data. Last, the median number of neutralized DENV serotypes was significantly lower among cases than among controls ($p<0.0004$ by Mann-Whitney U test; power 94.8%) (Figure 4, panel B). Only 27.6% of cases, compared with 50.9% of controls, had neutralizing antibodies against all 4 serotypes. Predominance of multitypic DENV exposure among controls over cases was consistently observed among participants in all age groups (Figure 4, panel C).

We conducted generalized linear model analyses to compare the effects of various factors on CZS formation. For model analysis, we considered factors that differed significantly between cases and controls in bivariate comparisons and factors that did not differ significantly. Factors included the presence and titers of neutralizing antibodies against specific DENV serotypes and the overall number of neutralized serotypes. We created 15 logistic regression models, each considering 1 factor potentially affecting CZS development (Table). With our data applied, the models considering neutralization of ≥2 DENV serotypes (AIC = 130.4) or the cumulative number of neutralized DENV serotypes showed the highest support (AIC = 130.6).

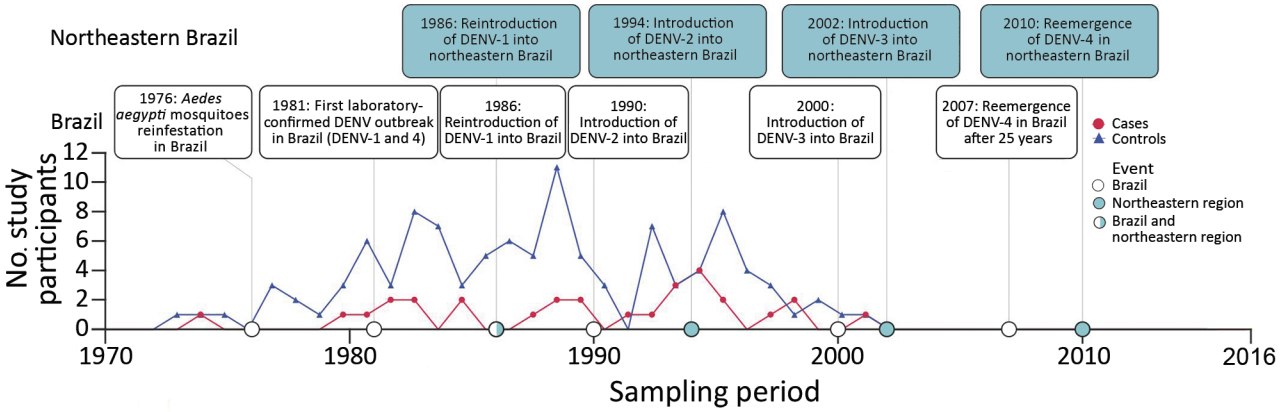

Figure 1. Timeline of dengue virus introduction in Brazil and birth years of participants in study of dengue virus cross-protection against congenital Zika syndrome, northeastern Brazil. DENV, dengue virus.

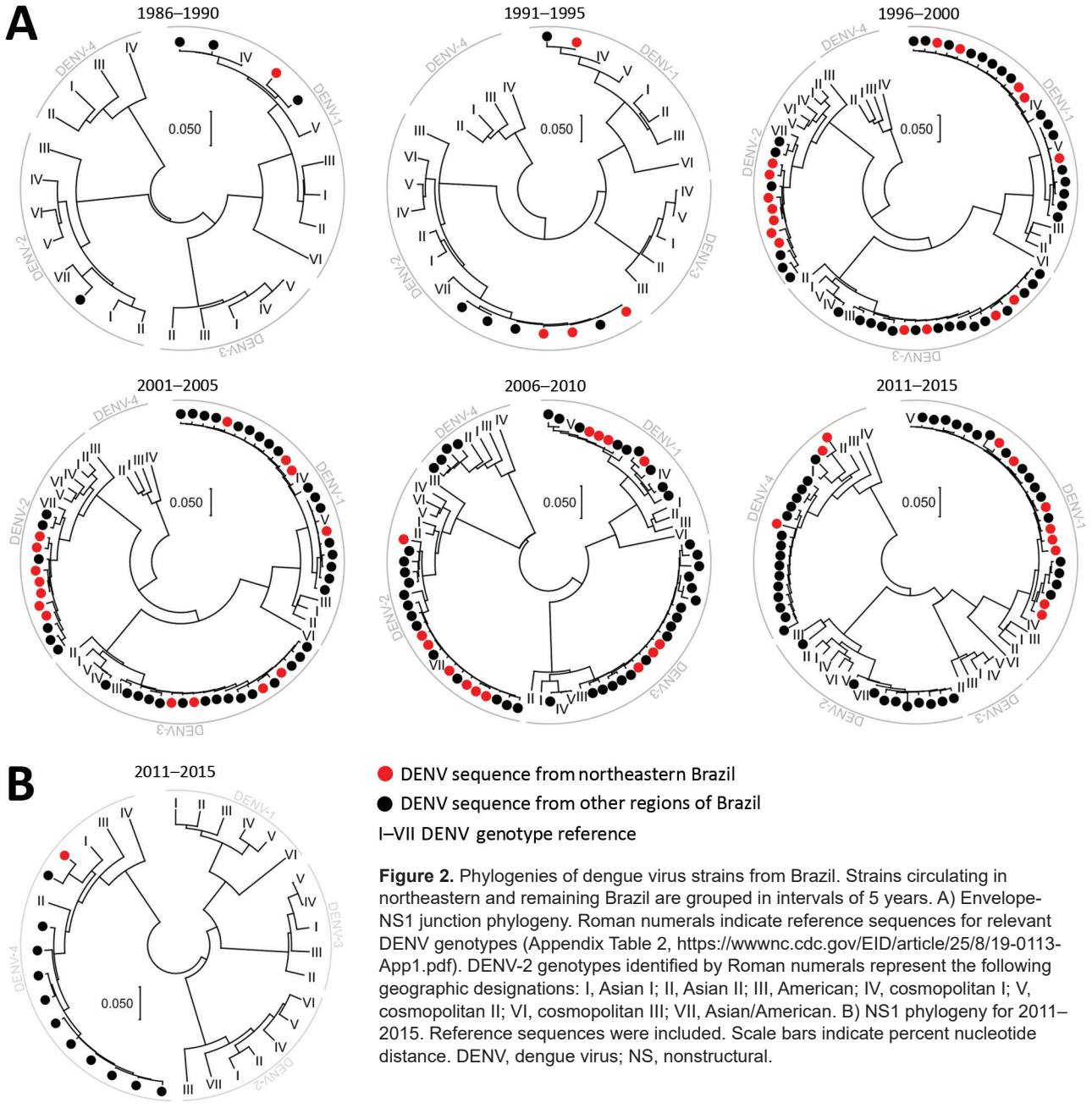

Figure 2. Phylogenies of dengue virus strains from Brazil. Strains circulating in northeastern and remaining Brazil are grouped in intervals of 5 years. A) Envelope-NS1 junction phylogeny. Roman numerals indicate reference sequences for relevant DENV genotypes (Appendix Table 2, https://wwwnc.cdc.gov/EID/article/25/8/19-0113-App1.pdf). DENV-2 genotypes identified by Roman numerals represent the following geographic designations: I, Asian I; II, Asian II; III, American; IV, cosmopolitan I; V, cosmopolitan II; VI, cosmopolitan III; VII, Asian/American. B) NS1 phylogeny for 2011–2015. Reference sequences were included. Scale bars indicate percent nucleotide distance. DENV, dengue virus; NS, nonstructural.

Regarding the presence of serotype-specific neutralizing antibodies, models considering DENV-4 (AIC = 131.4) and DENV-2 (AIC = 131.5) neutralization showed the best support. Models considering age or antibody titers showed relatively lower support with AICs >140. Of all tested models, the model considering neutralization of ≥2 DENV serotypes showed the highest reduction of CZS risk by 84.2% (95% CI 60.5%–93.8%). Of those models considering nonbinary factors, the cumulative number of neutralized DENV serotypes showed the highest reduction of CZS risk by 42.3% (95% CI 23.7%–56.8%) per increase of neutralized serotype. The model considering neutralization of 1 DENV serotype only as a risk factor was not supported statistically or by AIC.

Discussion

Contrary to a large body of in vitro data, our epidemiologic data strongly suggest cross-protection from CZS development by multitypic DENV immunity. The protective effect was observed in bivariate comparisons and in model analyses. Our interpretation is consistent with anecdotal evidence reporting near-complete lack of DENV

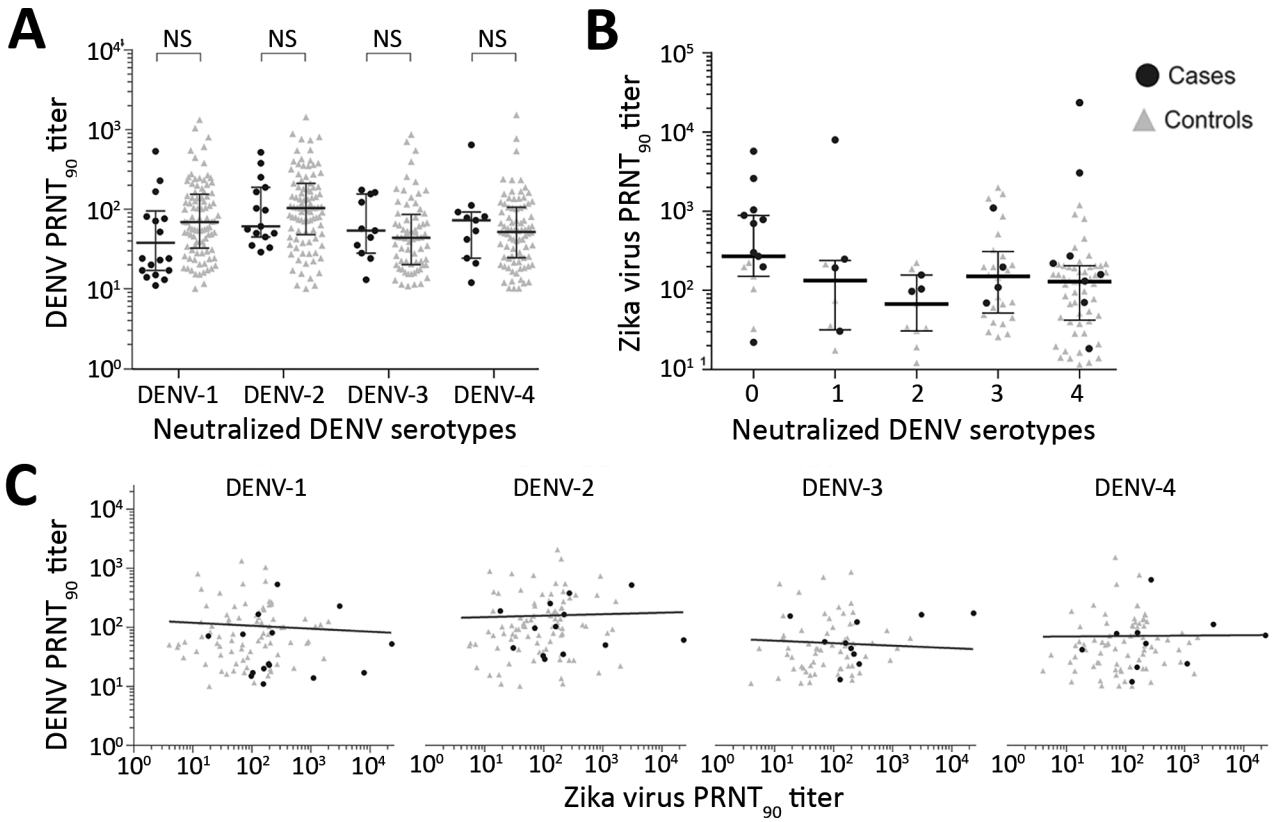

Figure 3. Serologic test results from participants in case–control study of cross-protection of dengue virus infection against congenital Zika syndrome, northeastern Brazil. A) Serotype-specific $PRNT_{90}$ titers for cases and controls. Statistical significance ($p<0.05$) was calculated by the Mann–Whitney U test; no significance was found. B) Zika virus neutralizing antibody titers as a function of the number of neutralized DENV serotypes. C) Correlation of DENV and Zika virus titers. Statistical significance ($p<0.05$) was calculated by Pearson correlation; no significance was found. DENV, dengue virus; NS, not significant; $PRNT_{90}$, 90% plaque reduction neutralization test.

activity during the Zika virus epidemic, hypothetically resulting from cross-protection induced by previous Zika virus exposure (*35*). Moreover, in experimentally infected nonhuman primates, preexisting DENV immunity caused relatively faster clearance of Zika viremia (*22*). Strong support for our interpretation is provided by 2 recently published epidemiologic studies from Brazil and Nicaragua (*36*,*37*). In both studies, preexisting DENV immunity significantly reduced the risk for symptomatic Zika virus infection. Although those studies did not examine the effect of serotype-specific antibodies, in several epidemiologic studies, multitypic DENV immunity was cross-protective for postsecondary DENV infections (*15*,*38*,*39*). In our study, the relatively stronger cross-protection by neutralization of DENV-2 and DENV-4 may suggest that recent DENV infection boosts cross-protection against CZS because both serotypes reportedly were the predominant serotypes in northeastern Brazil before the Zika virus outbreak (*40*).

Antibody protection against DENV is related to antibody titers, and low titers are a risk factor for severe dengue (*15*). In our study, putative DENV-mediated cross-protection against CZS was apparently not linked to antibody titers. Thus, cross-protection from CZS may be mediated by immune responses (*41*) other than cross-protective antibodies. In humans, preexisting DENV immunity has been shown to boost $CD4^+$ and $CD8^+$ T-cell responses during Zika virus infections (*42*–*44*). In pregnant mice, DENV cross-reactive $CD8^+$ T cells have been shown to be a key component of protection from fetal injury or demise during Zika virus infection (*45*,*46*). Of note, $CD8^+$ T cells form a part of the placental barrier that protects the fetus from vertically acquired infections. DENV-primed CD8+ T cells might provide cross-protection from CZS at the placental barrier (*45*). As T-cell–mediated DENV cross-protection wanes over time (*39*,*45*), consecutive heterotypic DENV infections might have afforded relatively stronger and prolonged cross-protection from CZS in controls.

Our study was limited by the absence of longitudinal samples, thereby preventing definite assessments of identical DENV serostatus at the time of congenital

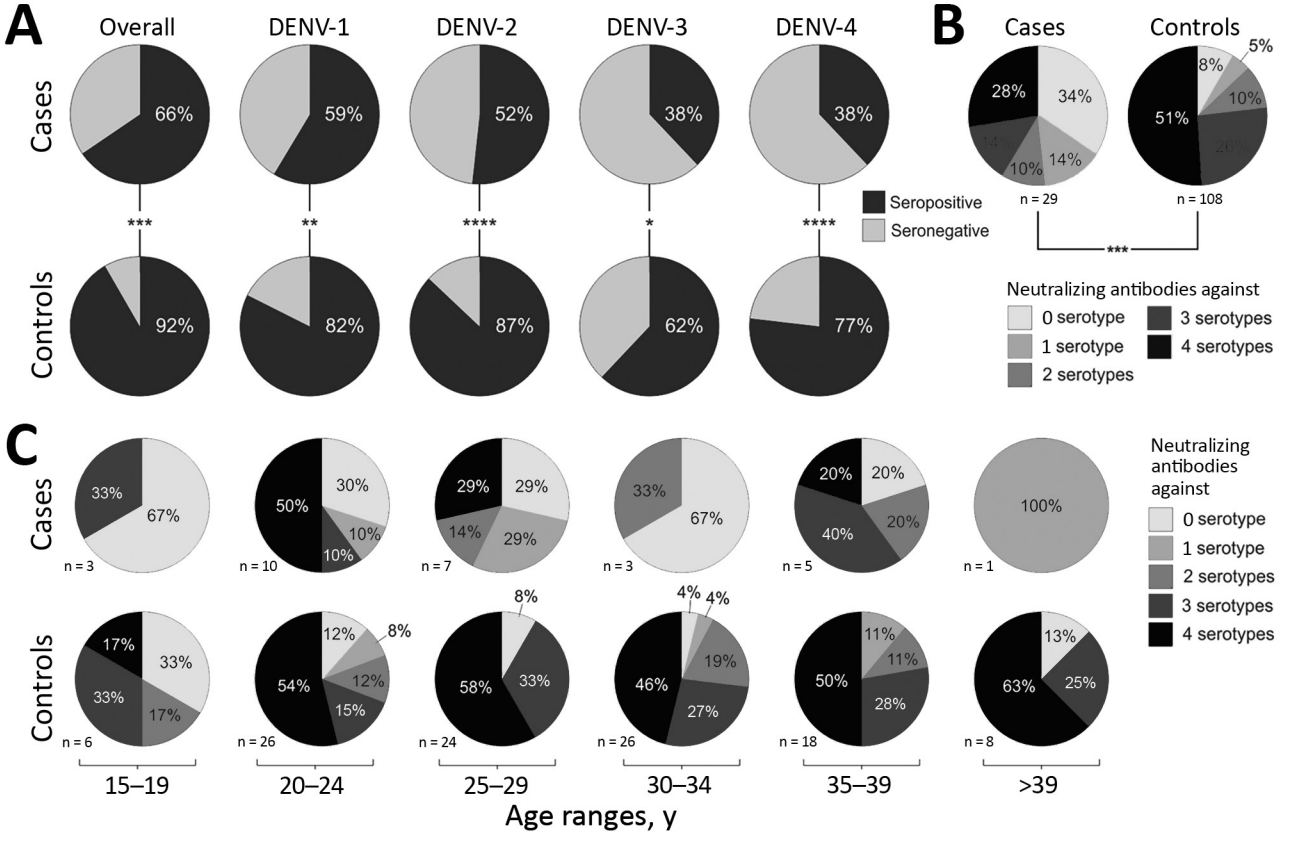

Figure 4. Dengue virus prevalence and neutralization among participants in case–control study of cross-protection of dengue virus infection against congenital Zika syndrome, northeastern Brazil. A) Serotype-specific DENV seroprevalence in cases and controls. Statistical significance was calculated by χ^2 test. *p<0.05; **p<0.01; ***p<0.001; ****p<0.0001. B) Multitypic DENV neutralization in cases and controls. Statistical significance for the numbers of neutralized DENV serotypes was calculated by using the Mann–Whitney U test. ***p = 0.0004. C) Multitypic DENV neutralization in cases and controls in different age groups. DENV, dengue virus. A color version of this figure is available online (http://wwwnc.cdc.gov/EID/article/25/8/19-0113-F4.htm).

Zika virus infection compared with the time of testing at delivery. Nonetheless, the uniformity of our results and low DENV activity during the Zika epidemic (*1*,*35*) speak against putative DENV exposure of mothers after the time of congenital Zika virus infection. Because sampling was conducted at delivery, we could not assess

Table. Comparison of models used to identify factors affecting development of congenital Zika syndrome in study of dengue virus cross-protection against congenital Zika syndrome, northeastern Brazil*

Model	Predictor scale	AIC	ΔAIC	AW	Odds ratio (95% CI)	p value
Neutralization of ≥2 DENV serotypes	Binary	130.4	0	0.2812	0.158 (0.062–0.395)	<0.0001
No. neutralized serotypes	Ordinal, 5 ranks	130.6	0.2	0.2590	0.577 (0.432–0.763)	<0.0001
DENV-4 neutralization	Binary	131.4	0.9	0.1750	0.192 (0.078–0.449)	<0.0001
DENV-2 neutralization	Binary	131.5	1.1	0.1657	0.170 (0.068–0.423)	<0.0001
Neutralization of ≥3 DENV serotypes	Binary	133.0	2.6	0.0771	0.210 (0.086–0.492)	<0.0001
Neutralization of ≥1 DENV serotypes	Binary	134.8	4.4	0.0319	0.170 (0.060–0.477)	<0.0001
DENV-1 neutralization	Binary	139.1	8.6	0.0038	0.298 (0.122–0.733)	0.009
DENV-3 neutralization	Binary	140.3	9.9	0.0020	0.368 (0.154–0.844)	0.018
Neutralization of 4 DENV serotypes	Binary	140.5	10.1	0.0018	0.361 (0.139–0.852)	0.020
Anti-DENV-2 $PRNT_{90}$ titer	Continuous	141.8	11.4	<0.001	0.998 (0.990–1.000)	0.043
Anti-DENV-1 $PRNT_{90}$ titer	Continuous	142.8	12.4	<0.001	0.997 (0.990–1.000)	0.079
Neutralization of 1 DENV serotype	Binary	143.2	12.8	<0001	3.328 (0.776–13.477)	0.101
Age of mothers when giving birth	Continuous	143.2	12.8	<0.001	0.953 (0.896–1.010)	0.136
Anti-DENV-3 $PRNT_{90}$ titer	Continuous	144.2	13.8	<0.001	0.996 (0.990–1.000)	0.195
Anti-DENV-4 $PRNT_{90}$ titer	Continuous	144.9	14.5	<0.001	0.998 (0.990–1.000)	0.326

*p values were calculated by likelihood ratio tests of the different models. Models are sorted by AIC, which is an estimator of the model's quality; models with lower AIC values are superior to models with higher AIC values. The scale of predictor variables must be considered when comparing ORs of different models. AIC, Akaike information criterion; AW, Akaike weight; DENV 1–4, dengue virus types 1–4; OR, odds ratio; $PRNT_{90}$, 90% plaque reduction neutralization test; ΔAIC, difference between a given and the best-supported model in AIC.

the time of maternal and potential congenital Zika virus infection, which affects CZS development (*2*). Because the dates of deliveries were similar among cases and controls sampled continuously within Salvador during the peak of the Zika outbreak (*1*), it seems plausible that cases and controls acquired Zika virus infection at similar stages of pregnancy (i.e., cases were probably not exclusively infected during the first trimester of pregnancy, which is most critical for CZS formation, compared with putatively later times of maternal infection in controls). Because of the small sample sizes, we could not perform PRNT for other endemic flaviviruses (e.g., yellow fever virus) that may also affect CZS development (*19*). However, northeastern Brazil has not consistently implemented yellow fever vaccination, and samples were collected before the large yellow fever outbreak that struck Brazil in the aftermath of the Zika epidemic (*47*). The comparison of historic DENV circulation in northeastern Brazil and other regions of the country is limited by incomplete genome coverage, sampling biases, and resolution of the phylogenetic trees. Nevertheless, our results match the cornerstones of DENV circulation in Brazil and the dataset is larger than other virus databases. The strengths of our study include the combination of highly specific serotype-discriminating DENV $PRNT_{90}$ for examination of preexisting DENV immunity with serologically well-characterized samples from the most relevant persons (i.e., cases and controls sampled during the same time and in the same region) (*13*,*34*), model selection analyses, and an analysis of historical DENV exposure in Brazil.

Our data do not exclude the possibility of sporadic enhancement of CZS development by monotypic DENV immunity or subneutralizing antibodies from nonrecent exposure to DENV depending on the combination (*48*) and the chronologic sequence (*49*) of previous flavivirus infection and the time since previous flavivirus infections (*50*). However, our study strongly suggests a complex interaction between Zika virus and DENV immunity and a protective effect of strong preexisting multitypic DENV immunity of the mother on CZS development in the fetus during the Zika virus outbreak in northeastern Brazil.

Acknowledgments

We thank Petra Emmerich and Jonas Schmidt-Chanasit for providing dengue viruses and Janett Wieseler for technical support.

This work was supported by the German Centre for Infection Research through the ZIKApath project, an intramural funding program at the University of Bonn, and the European Union's Horizon 2020 research and innovation program through the ZIKAlliance project (grant agreement no. 734548). The data used are part of the thesis of M.F.

About the Author

Dr. Pedroso is a researcher at the Universidade Federal de Bahia in Salvador. Her research focuses on the pathogenesis of infectious diseases.

References

1. Netto EM, Moreira-Soto A, Pedroso C, Höser C, Funk S, Kucharski AJ, et al. High Zika virus seroprevalence in Salvador, northeastern Brazil limits the potential for further outbreaks. MBio. 2017;8:e01390–17. http://dx.doi.org/10.1128/mBio.01390-17
2. Brasil P, Pereira JP Jr, Moreira ME, Ribeiro Nogueira RM, Damasceno L, Wakimoto M, et al. Zika virus infection in pregnant women in Rio de Janeiro. N Engl J Med. 2016;375:2321–34. http://dx.doi.org/10.1056/NEJMoa1602412
3. França GV, Schuler-Faccini L, Oliveira WK, Henriques CM, Carmo EH, Pedi VD, et al. Congenital Zika virus syndrome in Brazil: a case series of the first 1501 livebirths with complete investigation. Lancet. 2016;388:891–7. http://dx.doi.org/10.1016/S0140-6736(16)30902-3
4. de Oliveira WK, de França GVA, Carmo EH, Duncan BB, de Souza Kuchenbecker R, Schmidt MI. Infection-related microcephaly after the 2015 and 2016 Zika virus outbreaks in Brazil: a surveillance-based analysis. Lancet. 2017;390:861–70. http://dx.doi.org/10.1016/S0140-6736(17)31368-5
5. de Araújo TVB, Ximenes RAA, Miranda-Filho DB, Souza WV, Montarroyos UR, de Melo APL, et al.; investigators from the Microcephaly Epidemic Research Group, Brazilian Ministry of Health, Pan American Health Organization, Instituto de Medicina Integral Professor Fernando Figueira, State Health Department of Pernambuco. Association between microcephaly, Zika virus infection, and other risk factors in Brazil: final report of a case-control study. Lancet Infect Dis. 2018;18:328–36. http://dx.doi.org/10.1016/S1473-3099(17)30727-2
6. Cugola FR, Fernandes IR, Russo FB, Freitas BC, Dias JL, Guimarães KP, et al. The Brazilian Zika virus strain causes birth defects in experimental models. Nature. 2016;534:267–71. http://dx.doi.org/10.1038/nature18296
7. Aiken AR, Scott JG, Gomperts R, Trussell J, Worrell M, Aiken CE. Requests for abortion in Latin America related to concern about Zika virus exposure. N Engl J Med. 2016;375:396–8. http://dx.doi.org/10.1056/NEJMc1605389
8. Mayor S. Abortion requests increase in Latin America after Zika warning, figures show. BMJ. 2016;353:i3492. http://dx.doi.org/10.1136/bmj.i3492
9. Campos MC, Dombrowski JG, Phelan J, Marinho CRF, Hibberd M, Clark TG, et al. Zika might not be acting alone: using an ecological study approach to investigate potential co-acting risk factors for an unusual pattern of microcephaly in Brazil. PLoS One. 2018;13:e0201452. http://dx.doi.org/10.1371/journal.pone.0201452
10. Faria NR, Quick J, Claro IM, Thézé J, de Jesus JG, Giovanetti M, et al. Establishment and cryptic transmission of Zika virus in Brazil and the Americas. Nature. 2017;546:406–10. http://dx.doi.org/10.1038/nature22401
11. Pettersson JH, Bohlin J, Dupont-Rouzeyrol M, Brynildsrud OB, Alfsnes K, Cao-Lormeau VM, et al. Re-visiting the evolution, dispersal and epidemiology of Zika virus in Asia. Emerg Microbes Infect. 2018;7:79. http://dx.doi.org/10.1038/s41426-018-0082-5
12. Butler D. Brazil asks whether Zika acts alone to cause birth defects. Nature. 2016;535:475–6. http://dx.doi.org/10.1038/nature.2016.20309
13. Moreira-Soto A, Cabral R, Pedroso C, Eschbach-Bludau M, Rockstroh A, Vargas LA, et al. Exhaustive TORCH pathogen diagnostics corroborate Zika virus etiology of congenital

malformations in northeastern Brazil. mSphere. 2018; 3:pii:e00278–18. http://dx.doi.org/10.1128/mSphere.00278-18
14. Moureau G, Cook S, Lemey P, Nougairede A, Forrester NL, Khasnatinov M, et al. New insights into flavivirus evolution, taxonomy and biogeographic history, extended by analysis of canonical and alternative coding sequences. PLoS One. 2015; 10:e0117849. http://dx.doi.org/10.1371/journal.pone.0117849
15. Katzelnick LC, Gresh L, Halloran ME, Mercado JC, Kuan G, Gordon A, et al. Antibody-dependent enhancement of severe dengue disease in humans. Science. 2017;358:929–32. http://dx.doi.org/10.1126/science.aan6836
16. Halstead SB, Mahalingam S, Marovich MA, Ubol S, Mosser DM. Intrinsic antibody-dependent enhancement of microbial infection in macrophages: disease regulation by immune complexes. Lancet Infect Dis. 2010;10:712–22. http://dx.doi.org/10.1016/S1473-3099(10)70166-3
17. Li M, Zhao L, Zhang C, Wang X, Hong W, Sun J, et al. Dengue immune sera enhance Zika virus infection in human peripheral blood monocytes through Fc gamma receptors. PLoS One. 2018;13:e0200478. http://dx.doi.org/10.1371/journal.pone.0200478
18. Hermanns K, Göhner C, Kopp A, Schmidt A, Merz WM, Markert UR, et al. Zika virus infection in human placental tissue explants is enhanced in the presence of dengue virus antibodies in-vitro. Emerg Microbes Infect. 2018;7:198. http://dx.doi.org/10.1038/s41426-018-0199-6
19. Bardina SV, Bunduc P, Tripathi S, Duehr J, Frere JJ, Brown JA, et al. Enhancement of Zika virus pathogenesis by preexisting antiflavivirus immunity. Science. 2017;356:175–80. http://dx.doi.org/10.1126/science.aal4365
20. Castanha PMS, Nascimento EJM, Braga C, Cordeiro MT, de Carvalho OV, de Mendonça LR, et al. Dengue virus-specific antibodies enhance Brazilian Zika virus infection. J Infect Dis. 2017;215:781–5.
21. Priyamvada L, Hudson W, Ahmed R, Wrammert J. Humoral cross-reactivity between Zika and dengue viruses: implications for protection and pathology. Emerg Microbes Infect. 2017;6:e33. http://dx.doi.org/10.1038/emi.2017.42
22. Pantoja P, Pérez-Guzmán EX, Rodríguez IV, White LJ, González O, Serrano C, et al. Zika virus pathogenesis in rhesus macaques is unaffected by pre-existing immunity to dengue virus. Nat Commun. 2017;8:15674. http://dx.doi.org/10.1038/ncomms15674
23. Terzian ACB, Schanoski AS, Mota MTO, da Silva RA, Estofolete CF, Colombo TE, et al. Viral load and cytokine response profile does not support antibody-dependent enhancement in dengue-primed Zika virus-infected patients. Clin Infect Dis. 2017;65:1260–5. http://dx.doi.org/10.1093/cid/cix558
24. Moore CA, Staples JE, Dobyns WB, Pessoa A, Ventura CV, Fonseca EB, et al. Characterizing the pattern of anomalies in congenital Zika syndrome for pediatric clinicians. JAMA Pediatr. 2017;171:288–95. http://dx.doi.org/10.1001/jamapediatrics.2016.3982
25. Kirkpatrick BD, Whitehead SS, Pierce KK, Tibery CM, Grier PL, Hynes NA, et al. The live attenuated dengue vaccine TV003 elicits complete protection against dengue in a human challenge model. Sci Transl Med. 2016;8:330ra36. http://dx.doi.org/10.1126/scitranslmed.aaf1517
26. Kumar S, Stecher G, Tamura K. MEGA7: Molecular Evolutionary Genetics Analysis version 7.0 for bigger datasets. Mol Biol Evol. 2016;33:1870–4. http://dx.doi.org/10.1093/molbev/msw054
27. Sullivan KM, Dean A, Soe MM. OpenEpi: a web-based epidemiologic and statistical calculator for public health. Public Health Rep. 2009;124:471–4. http://dx.doi.org/10.1177/003335490912400320
28. Pan American Health Organization. The feasibility of eradicating *Aedes aegypti* in the Americas. Rev Panam Salud Publica. 1997; 1:68–72. http://dx.doi.org/10.1590/S1020-49891997000100023
29. Schatzmayr HG, Nogueira RM, Travassos da Rosa AP. An outbreak of dengue virus at Rio de Janeiro—1986. Mem Inst Oswaldo Cruz. 1986;81:245–6. http://dx.doi.org/10.1590/S0074-02761986000200019
30. Nogueira RM, Miagostovich MP, Lampe E, Souza RW, Zagne SM, Schatzmayr HG. Dengue epidemic in the stage of Rio de Janeiro, Brazil, 1990-1: co-circulation of dengue 1 and dengue 2 serotypes. Epidemiol Infect. 1993;111:163–70. http://dx.doi.org/10.1017/S0950268800056788
31. Nogueira RM, Miagostovich MP, de Filippis AM, Pereira MA, Schatzmayr HG. Dengue virus type 3 in Rio de Janeiro, Brazil. Mem Inst Oswaldo Cruz. 2001;96:925–6. http://dx.doi.org/10.1590/S0074-02762001000700007
32. Figueiredo RM, Naveca FG, Bastos MS, Melo MN, Viana SS, Mourão MP, et al. Dengue virus type 4, Manaus, Brazil. Emerg Infect Dis. 2008;14:667–9. http://dx.doi.org/10.3201/eid1404.071185
33. Kurolt IC, Betica-Radić L, Daković-Rode O, Franco L, Zelená H, Tenorio A, et al. Molecular characterization of dengue virus 1 from autochthonous dengue fever cases in Croatia. Clin Microbiol Infect. 2013;19:E163–5. http://dx.doi.org/10.1111/1469-0691.12104
34. Moreira-Soto A, Sarno M, Pedroso C, Netto EM, Rockstroh A, Luz E, et al. Evidence for congenital Zika virus infection from neutralizing antibody titers in maternal sera, northeastern Brazil. J Infect Dis. 2017;216:1501–4. http://dx.doi.org/10.1093/infdis/jix539
35. Ribeiro GS, Kikuti M, Tauro LB, Nascimento LCJ, Cardoso CW, Campos GS, et al.; Salvador Arboviral Research Group. Does immunity after Zika virus infection cross-protect against dengue? Lancet Glob Health. 2018;6:e140–1. http://dx.doi.org/10.1016/S2214-109X(17)30496-5
36. Rodriguez-Barraquer I, Costa F, Nascimento EJM, Nery N, Castanha PMS, Sacramento GA, et al. Impact of preexisting dengue immunity on Zika virus emergence in a dengue endemic region. Science. 2019;363:607–10. http://dx.doi.org/10.1126/science.aav6618
37. Gordon A, Gresh L, Ojeda S, Katzelnick LC, Sanchez N, Mercado JC, et al. Prior dengue virus infection and risk of Zika: a pediatric cohort in Nicaragua. PLoS Med. 2019;16:e1002726. http://dx.doi.org/10.1371/journal.pmed.1002726
38. Olkowski S, Forshey BM, Morrison AC, Rocha C, Vilcarromero S, Halsey ES, et al. Reduced risk of disease during postsecondary dengue virus infections. J Infect Dis. 2013;208:1026–33. http://dx.doi.org/10.1093/infdis/jit273
39. Uno N, Ross TM. Dengue virus and the host innate immune response. Emerg Microbes Infect. 2018;7:167. http://dx.doi.org/10.1038/s41426-018-0168-0
40. Salles TS, da Encarnação Sá-Guimarães T, de Alvarenga ESL, Guimarães-Ribeiro V, de Meneses MDF, de Castro-Salles PF, et al. History, epidemiology and diagnostics of dengue in the American and Brazilian contexts: a review. Parasit Vectors. 2018;11:264. http://dx.doi.org/10.1186/s13071-018-2830-8
41. Collins M, de Silva A. Host response: cross-fit T cells battle Zika virus. Nat Microbiol. 2017;2:17082. http://dx.doi.org/10.1038/nmicrobiol.2017.82
42. Grifoni A, Pham J, Sidney J, O'Rourke PH, Paul S, Peters B, et al. Prior dengue virus exposure shapes T cell immunity to Zika virus in humans. J Virol. 2017;91:e01469-17. http://dx.doi.org/10.1128/JVI.01469-17
43. Delgado FG, Torres KI, Castellanos JE, Romero-Sánchez C, Simon-Lorière E, Sakuntabhai A, et al. Improved immune responses against Zika virus after sequential dengue and Zika virus

infection in humans. Viruses. 2018;10:E480. http://dx.doi.org/10.3390/v10090480
44. Saron WAA, Rathore APS, Ting L, Ooi EE, Low J, Abraham SN, et al. Flavivirus serocomplex cross-reactive immunity is protective by activating heterologous memory CD4 T cells. Sci Adv. 2018;4:eaar4297.
45. Regla-Nava JA, Elong Ngono A, Viramontes KM, Huynh AT, Wang YT, Nguyen AT, et al. Cross-reactive dengue virus-specific $CD8^+$ T cells protect against Zika virus during pregnancy. Nat Commun. 2018;9:3042. http://dx.doi.org/10.1038/s41467-018-05458-0
46. Wen J, Tang WW, Sheets N, Ellison J, Sette A, Kim K, et al. Identification of Zika virus epitopes reveals immunodominant and protective roles for dengue virus cross-reactive $CD8^+$ T cells. Nat Microbiol. 2017;2:17036. http://dx.doi.org/10.1038/nmicrobiol.2017.36
47. Moreira-Soto A, Torres MC, Lima de Mendonca MC, Mares-Guia MA, Dos Santos Rodrigues CD, Fabri AA, et al. Evidence for multiple sylvatic transmission cycles during the 2016–2017 yellow fever virus outbreak, Brazil. Clin Microbiol Infect. 2018;24:1019.e1–4. http://dx.doi.org/10.1016/j.cmi.2018.01.026
48. Guzman MG, Alvarez A, Vazquez S, Alvarez M, Rosario D, Pelaez O, et al. Epidemiological studies on dengue virus type 3 in Playa municipality, Havana, Cuba, 2001–2002. Int J Infect Dis. 2012;16:e198–203. http://dx.doi.org/10.1016/j.ijid.2011.09.026
49. Katzelnick LC, Harris E; participants in the Summit on Dengue Immune Correlates of Protection. Immune correlates of protection for dengue: state of the art and research agenda. Vaccine. 2017; 35:4659–69. http://dx.doi.org/10.1016/j.vaccine.2017.07.045
50. OhAinle M. Balmaseda A, Macalalad AR, Tellez Y, Zody MC, Saborío S, et al. Dynamics of dengue disease severity determined by the interplay between viral genetics and serotype-specific immunity. Sci Transl Med. 2011;3:114ra128. http://dx.doi.org/10.1126/scitranslmed.3003084

Address for correspondence: Jan Felix Drexler, Charité-Universitätsmedizin Berlin, Institute of Virology, Helmut-Ruska-Haus Charitéplatz 1, 10098 Berlin, Germany; email: felix.drexler@charite.de

Retrospective Cohort Study of Lassa Fever in Pregnancy, Southern Nigeria

Sylvanus Okogbenin, Joseph Okoeguale, George Akpede, Andres Colubri, Kayla G. Barnes, Samar Mehta, Reuben Eifediyi, Felix Okogbo, Joseph Eigbefoh, Mojeed Momoh, Mojeed Rafiu, Donatus Adomeh, Ikponmwosa Odia, Chris Aire, Rebecca Atafo, Martha Okonofua, Meike Pahlman, Beate Becker-Ziaja, Danny Asogun, Peter Okokhere, Christian Happi, Stephan Günther, Pardis C. Sabeti, Ephraim Ogbaini-Emovon

Medscape EDUCATION ACTIVITY

In support of improving patient care, this activity has been planned and implemented by Medscape, LLC and Emerging Infectious Diseases. Medscape, LLC is jointly accredited by the Accreditation Council for Continuing Medical Education (ACCME), the Accreditation Council for Pharmacy Education (ACPE), and the American Nurses Credentialing Center (ANCC), to provide continuing education for the healthcare team.

Medscape, LLC designates this Journal-based CME activity for a maximum of 1.00 ***AMA PRA Category 1 Credit(s)™***. Physicians should claim only the credit commensurate with the extent of their participation in the activity.

Successful completion of this CME activity, which includes participation in the evaluation component, enables the participant to earn up to 1.0 MOC points in the American Board of Internal Medicine's (ABIM) Maintenance of Certification (MOC) program. Participants will earn MOC points equivalent to the amount of CME credits claimed for the activity. It is the CME activity provider's responsibility to submit participant completion information to ACCME for the purpose of granting ABIM MOC credit.

All other clinicians completing this activity will be issued a certificate of participation. To participate in this journal CME activity: (1) review the learning objectives and author disclosures; (2) study the education content; (3) take the post-test with a 75% minimum passing score and complete the evaluation at http://www.medscape.org/journal/eid; and (4) view/print certificate. For CME questions, see page 1624.

Release date: July 16, 2019; Expiration date: July 16, 2020

Learning Objectives

Upon completion of this activity, participants will be able to:

- Compare maternal and fetal outcomes for 2 broad patterns of clinical presentation in 30 pregnant patients with LF: patients with complications vs patients with milder, nonspecific symptoms, according to a retrospective study of cases seen at ISTH n Nigeria between January 2009 and March 2018
- Describe predictors of maternal and fetal outcomes in 30 pregnant patients with LF treated with early ribavirin and a conservative obstetric approach at ISTH in Edo State, Nigeria, between January 2009 and March 2018, according to a retrospective study
- Identify clinical implications of maternal and fetal outcomes in 30 pregnant patients with LF treated with early ribavirin and a conservative obstetric approach at ISTH in Edo State, Nigeria, between January 2009 and March 2018, according to a retrospective study.

CME Editor

Jude Rutledge, BA, Technical Writer/Editor, Emerging Infectious Diseases. *Disclosure: Jude Rutledge has disclosed no relevant financial relationships.*

CME Author

Laurie Barclay, MD, freelance writer and reviewer, Medscape, LLC. *Disclosure: Laurie Barclay, MD, has disclosed no relevant financial relationships.*

Authors

Disclosures: ***Sylvanus Okogbenin, MBBS, FWACS; Joseph Okoeguale, MBBS, MSc, FWACS; George O. Akpede, FWACP, FMC Ped; Andres Colubri, PhD, MFA,; Kayla Barnes, PhD; Samar Mehta, MD, PhD; Reuben Eifediyi, MBBS, FMCOG, FWACS; Felix Okogbo, MBBS, FWACS, FICS; Joseph Eigbefoh, MBBS, FMCOG, FWACS, FICS; Mojeed Momoh, MBBS, FWACS, FICS; Mojeed Olaitan Rafiu, MBBS, FMCP; Donatus Adomeh, PhD, MSc, AMLSCN, FMLSCN; Ikponmwosa Odia, MSc; Chris Okafi Aire, FMLSCN, BMLS; Rebecca O. Atafo, BScH/FeI, BSc Nursing, HMD PUB/H; Martha Okonofua, RN, RM, LLM, LLB; Meike Pahlman, PhD; Beate Becker-Ziaja; Danny Asogun, MBBS, MHPM, MD; Peter Okokhere, MBBS, FWACP; Christian Happi, PhD; Stephan Günther, MD;*** *and* ***Ephraim Ogbaini-Emovon, MBBS, MPH, FMCPath,*** *have disclosed no relevant financial relationships.* ***Pardis Sabeti, MD, DPhil, MSc,*** *has disclosed the following relevant financial relationships: served as an advisor or consultant for NextGen Jane, Sherlock Biosciences; owns stocks, stock options, or bonds from NextGen Jane, Sherlock Biosciences, TruGenomix, Inc.*

Lassa fever in pregnancy causes high rates of maternal and fetal death, but limited data are available to guide clinicians. We retrospectively studied 30 pregnant Lassa fever patients treated with early ribavirin therapy and a conservative obstetric approach at a teaching hospital in southern Nigeria during January 2009–March 2018. Eleven (36.7%) of 30 women died, and 20/31 (64.5%) pregnancies ended in fetal or perinatal loss. On initial evaluation, 17/30 (56.6%) women had a dead fetus; 10/17 (58.8%) of these patients died, compared with 1/13 (7.7%) of women with a live fetus. Extravaginal bleeding, convulsions, and oliguria each were independently associated with maternal and fetal or perinatal death, whereas seeking care in the third trimester was not. For women with a live fetus at initial evaluation, the positive outcomes observed contrast with previous reports, and they support a conservative approach to obstetric management of Lassa fever in pregnancy in Nigeria.

Lassa fever (LF), a viral hemorrhagic fever endemic to West Africa (*1*–*3*), was first reported in 1969 from northern Nigeria (*4*,*5*). Since that time, LF has been documented in several countries in West Africa, including Sierra Leone, Liberia, Guinea, Mali, and, more recently, Benin and Togo (*6*–*9*). Historical reports of LF in pregnancy have described poor maternal and fetal outcomes; an early direct comparison in Sierra Leone reported a 50% mortality rate in pregnant women (n = 30), compared with 16% among nonpregnant women (n = 234) (*10*). A subsequent study conducted in Sierra Leone in 1988 observed a smaller disparity of a 21% mortality rate in pregnant women (n = 68) versus 13% among nonpregnant women (n = 79) but found a worse mortality rate (30%, n = 40) for mothers in the third trimester and an overall fetal and neonatal mortality rate of 87% (*11*). Although the Sierra Leone study demonstrated the considerable contribution of LF to overall maternal mortality rates at a single hospital, since then, large studies of pregnant patients with LF have been lacking, leading to difficulty in estimating the actual regional burden on maternal health. This problem is exacerbated by the large variability in Lassa virus across regions (*12*) and the often nonspecific early signs and symptoms of the disease, including overlap with other common infectious diseases in the region, such as malaria, influenza, and bacterial sepsis (*2*,*13*).

Pathophysiologically, the poor outcome of LF in pregnancy has been attributed to the higher viral loads often observed in pregnant compared with nonpregnant patients, possibly because of the poorly understood immunologic changes in pregnancy or the affinity of the virus for the highly vascularized placenta (*14*,*15*). Also, the overlap of symptoms such as nausea, headache, and abdominal pain with complicated or even uncomplicated pregnancy might further delay identification or diagnosis and result in worse outcomes when the infection is severe (*16*).

The management of LF in pregnancy requires making difficult decisions with sparse data for guidance. The antiviral drug ribavirin represents the only established pharmacologic therapy for LF and is believed to substantially reduce overall mortality rates (*17*,*18*), although the mechanism of action is not clear and data on safety of the drug in pregnancy are limited (*19*). The 1988 Sierra Leone study, which has been the largest LF case series in the literature to date, found that delivery, spontaneous abortion (miscarriage), and evacuation of the uterus all improve maternal outcome (*11*); the study recommended active obstetric management, particularly because the authors observed high fetal mortality rate irrespective of the modality of management (*2*). However, patients in the study did not receive ribavirin before delivery because of published evidence of teratogenicity in animal studies (*19*). To improve maternal and fetal outcomes and explore their relationship to clinical signs and symptoms, we retrospectively analyzed >9 years of records at a hospital in Nigeria that treated a substantial number of LF cases and applied both a more conservative approach to obstetric management and more liberal antepartum use of ribavirin.

Methods

Irrua Specialist Teaching Hospital (ISTH) is a tertiary-care federal hospital that served as the LF national referral center for the duration of our study. Providers at ISTH and outside facilities in >30 states refer specimens for Lassa virus (LASV) testing by reverse-transcription PCR (RT-PCR) for patients who fit our previously described case definition (*20*); outside patients who test positive by RT-PCR are often referred to ISTH for management. Two authors (S.O.

Author affiliations: Institute of Lassa Fever Research and Control, Irrua Specialist Teaching Hospital, Irrua, Nigeria (S.A. Okogbenin, J. Okoeguale, G. Akpede, R. Eifediyi, F. Okogbo, J. Eigbefoh, M. Momoh, M. Rafiu, D. Adomeh, I. Odia, C. Aire, R. Atafo, M. Okonofua, D. Asogun, P. Okokhere, E. Ogbaini-Emovon); Ambrose Alli University Faculty of Clinical Science, Ekpoma, Nigeria (S.A. Okogbenin, G. Akpede, D. Asogun, P. Okokhere), Broad Institute of MIT and Harvard, Cambridge, Massachusetts, USA (A. Colubri, K.G. Barnes, S. Mehta, P.C. Sabeti); Harvard University, Cambridge (A. Colubri, P.C. Sabeti); Beth Israel Deaconess Medical Center, Boston, Massachusetts (S. Mehta); Bernhard Nocht Institute for Tropical Medicine and German Centre for Infection Research, Partner Site, Hamburg, Germany (M. Pahlman, B. Becker-Ziaja, S. Günther); Department of Biological Sciences and African Center of Excellence for Genomics of Infectious Diseases, Redeemer's University, Ede, Nigeria (C. Happi); Harvard School of Public Health, Boston (P.C. Sabeti)

DOI: https://doi.org/10.3201/eid2508.181299

and J.O.) reviewed and abstracted from hospital medical records clinical data for every laboratory-confirmed case of LF in a pregnant woman eventually admitted to ISTH during January 2009–March 2018. During this period, 44 pregnant women were managed for LF. On initial review of these patient records, we found 30 patients for whom documentation of signs and symptoms at admission and during hospitalization were sufficiently complete for inclusion in this study. Comparison data for facility maternal mortality rates over the same period was based on summaries maintained by the ISTH Department of Obstetrics and Gynaecology.

During the study period, pregnant women with confirmed LF received the same supportive care as nonpregnant LF patients, including intravenous fluids (either normal saline or lactated Ringer solution) to improve organ perfusion. All patients had antimicrobial prophylaxis with broad-spectrum antibiotics (ceftriaxone in most cases) and antimalarial drugs (typically oral artemether/lumefantrine; when required, parenteral treatment was quinine before 2014 and artemether after 2014). Fifteen of the 30 pregnant women in our series received blood transfusions for anemia (defined as packed red cell volume ≤25%), and 2 women required renal dialysis (they were referred for nephrologic evaluation when urine output was <0.5 mL/kg/h, although final decision to dialyze was clinical).

All patients were treated with intravenous ribavirin, except 2 patients who died shortly after arrival. Intravenous ribavirin treatment was started with a 100 mg/kg loading dose (two thirds dose on admission, one third 8 hours later), then 16 mg/kg every 6 hours for 4 days, followed by 8 mg/kg every 8 hours for 6 days. All pregnant women had an ultrasound scan on arrival to confirm fetal cardiac activity. After admission, fetal well-being was monitored at least 2 times each week by using either Doppler velocimetry, a nonstress test, or a biophysical profile, as appropriate for gestational age. We used a conservative obstetric management strategy throughout, only inducing labor in cases of fetal compromise and only performing uterine evacuation in women with fetal death. When uterine evacuation was required, we initiated vaginal misoprostol, dosed as appropriate for gestational age and consistent with International Federation of Gynecology and Obstetrics guidelines (*21*,*22*), followed by manual vacuum aspiration and curettage when required.

Before 2014, women who cleared viremia on the basis of RT-PCR results were discharged home and had outpatient weekly follow-up, including a nonstress test or biophysical profile. After 2014, in response to a case of late intrauterine fetal death after discharge, women were kept as inpatients for close monitoring until delivery. In all cases, patients had postpartum follow-up at 2 and 6 weeks after delivery. Newborns were not discharged until ≥1 week after delivery, in accordance with hospital protocol for LASV-exposed infants.

For our study, we defined the first trimester as <14 weeks from the first day of the last menstrual period (LMP), the second trimester as 14 weeks to <28 weeks from LMP, and the third trimester as ≥28 weeks from LMP. We defined stillbirth as delivery after 28 weeks' gestation of a baby without signs of life (i.e., absent cardiac and respiratory activity). Perinatal mortality rate attributable to LF was defined as the proportion of all pregnancies with laboratory-confirmed maternal diagnosis of LF that ended in either intrauterine fetal death after 28 weeks, stillbirth, or neonatal death in the first week of life. Overall maternal mortality rate was defined as the proportion of women who died while pregnant or within 42 days of the end of pregnancy, irrespective of the duration or site of the pregnancy, from causes related to or aggravated by pregnancy or its management, but not from accidental or incidental causes (*23*). When discussing maternal mortality rates related to LF in the context of this study, we refer to the proportion of women in whom LF was diagnosed during pregnancy and who did not survive that pregnancy.

For statistical analysis, we calculated the mean ± SD for quantitative variables, whereas we used prevalence to characterize qualitative variables. We calculated the univariate correlation between clinical features (signs and symptoms) with maternal and fetal death and then ranked these features by the p value of their association with maternal outcome (either death or survival) by using a χ^2 test with Yates correction. Tests of statistical significance (defined as $p \leq 0.05$) were based on a 95% CI.

Results

Forty-four cases of LF in pregnancy were managed at ISTH during the study period, out of a total of 5,048 pregnant women admitted to ISTH during that period. The 30 women for whom we were able to recover complete records were 16–39 years of age (mean ± SD 28.1 ± 5.1 years). These 30 women were admitted at gestational ages of 5–39 weeks (mean 21.6 ± 10.6 weeks) (Table 1). Parity ranged from 0–6 (mean 3.0 ± 1.6). One woman had a twin pregnancy.

We divided clinical signs and symptoms into 2 broad patterns. First, 16 women had complications, defined as either coma, convulsions, irrational behavior, extravaginal bleeding, or oliguria. All of these 16 women were also found to have intrauterine fetal death or an abortive process. Maternal death ensued within 24–48 hours in 10/16 (58.8%) of these cases and, in most cases, uterine evacuation was not completed before death. The second clinical pattern was observed in 14 women who had with milder, nonspecific symptoms, including fever, malaise, cough, and sore throat. Thirteen of these 14 women had a live fetus on ultrasound, and only 1 (7.1%) of the 14 women died.

Table 1. Demographic characteristics and outcomes observed in a retrospective cohort study of Lassa fever in pregnancy conducted at Irrua Specialist Teaching Hospital, Irrua, Edo State, Nigeria, January 2009–March 2018*

Year of diagnosis	Maternal age, y	Fetal gestational age, wks	Maternal clinical status†	Fetal status	Maternal outcome	Perinatal outcome
2009	24	10	Severe	Dead	Died	NA
2009	35	6	Severe	Dead	Died	NA
2009	28	12	Severe	Dead	Survived	NA
2009	29	7	Severe	Dead	Survived	NA
2009	31	22	Severe	Dead	Died	NA
2010	16	33	Mild†	Alive	Survived	Survived
2010	26	32	Severe	Dead	Died	NA
2010	37	11	Severe	Dead	Died	NA
2010	30	31	Severe	Dead	Survived	NA
2011	26	24	Severe	Dead	Died	NA
2011	26	9	Severe	Dead	Died	NA
2011	32	36	Mild	Alive	Survived	Survived
2011	27	11	Severe	Dead	Survived	NA
2012	39	35	Mild	Alive	Survived	Died 3 d after birth
2012	26	33	Mild	Alive	Survived	Survived
2013	25	8	Severe	Dead	Died	NA
2013	30	31	Mild	Alive	Survived	Survived
2013	31	29	Mild	Alive	Died	Died at 38 wks
2013	32	10	Severe	Dead	Survived	NA
2014	18	33	Mild	Dead	Survived	NA
2014	28	12	Severe	Dead	Survived	NA
2015	26	28	Mild	Alive	Survived	Survived
2016	33	27	Mild	Alive	Survived	Survived
2017	35	34	Mild	Alive	Survived	Survived
2017	32	29	Mild	Alive	Survived	Twins; 1 died at 37 wks, 1 survived
2017	23	32	Severe	Dead	Died	NA
2017	24	31	Mild	Alive	Survived	Survived
2017	36	25	Severe	Dead	Died	NA
2018	33	29	Mild	Alive	Survived	Survived
2018	32	33	Severe	Alive	Survived	Survived

*NA, not applicable.
†Severe maternal outcome defined as any of the following: convulsions, irrational behavior, coma, extravaginal bleeding, or oliguria (<0.5 mL/kg/h for ≥6 h). Mild maternal presentation defined as the absence of all of these features.

Irrespective of initial signs and symptoms, in all cases of intrauterine fetal death, uterine evacuation was initiated using misoprostol vaginal tablets as we described. Four of these patients died before complete evacuation, and 5 women required manual vacuum aspiration for evacuation of retained products of conception.

All 30 women had fever. Overall, 19 women survived and 11 died, resulting in an overall LF-related maternal mortality rate of 36.7% in this cohort. Seven of the 11 deaths occurred within 24 hours of admission, and 4 occurred within 24–48 hours of admission. Fetal death in utero, retrosternal chest pain, vomiting, and cough were the most frequent clinical features apart from fever, whereas deafness was the least frequent (Table 2). Extravaginal bleeding, convulsions, oliguria, fetal death in utero, and cough were each significantly associated with maternal death. In contrast, admission with a live fetus and breast pain or engorgement were each significantly associated with survival.

The mean ± SD duration of symptoms before admission was 6 ± 3.1 days among the survivors and 10 ± 3.5 days among those who died. When divided by trimester of pregnancy, maternal mortality rate was 50.0% (5/10) in the first, 75.0% (3/4) in the second, and 18.7% (3/16) in the third trimester. We noted a trend toward a lower maternal mortality rate in the third trimester, but this difference did not reach statistical significance ($p = 0.06$). Overall, deaths attributed to LF accounted for 13.1% (11/84, out of 5,048 total admissions of pregnant women) of maternal deaths at ISTH during the study period, second only to postpartum hemorrhage (28.5%) and eclampsia (22.6%).

Overall, 17/31 (56.7%) of fetuses had died by the time of admission. Of the 13 women with viable pregnancies at admission, 1 had a twin gestation and subsequently delivered 1 live baby (Apgar score 4 at 1 minute, 8 by 5 minutes) without apparent abnormality and 1 stillbirth at term. Another patient returned with delayed intrauterine fetal death at 38 weeks' gestation, despite having cleared her viremia after initial examination 9 weeks earlier, and died shortly after the return admission; a repeat LASV RT-PCR test was not performed. Five of the women with viable pregnancies at discharge had full-term deliveries, 5 had preterm deliveries at 33–36 weeks' gestation, and 1 had early neonatal death on the third day of life. The rate of perinatal death or spontaneous abortion in women who were admitted with a live fetus was 21.4% (3/14), compared with an overall rate of fetal and perinatal loss of 64.5% (20/31).

Table 2. Relationship between clinical manifestations and maternal death observed in a retrospective cohort study of Lassa fever in pregnancy conducted at Irrua Specialist Teaching Hospital, Irrua, Edo State, Nigeria, January 2009–March 2018*

	No. (%)				
Sign or symptom	All women, N = 30	Women who survived, n = 19	Women who died, n = 11	p value	OR (95% CI)
Retrosternal pain	19 (63)	13 (68)	6 (54)	0.7	0.55 (0.12–2.6)
Vomiting	18 (60)	12 (63)	6 (54)	0.7	0.7 (0.15–3.2)
Headache	16 (53)	13 (68)	3 (27)	0.06	0.17 (0.03–0.89)
Fetal death	17 (56)	7 (36)	10 (90)	**0.007**	**17 (1.8–>100)**
Vaginal bleeding	14 (46)	6 (31)	8 (72)	0.06	5.8 (1.1–30)
Breast pain or engorgement	13 (43)	12 (63)	1 (9)	**0.007**	**0.06 (0.01–0.56)**
Difficulty swallowing	12 (40)	6 (31)	6 (54)	0.3	2.6 (0.56–12)
Sore throat	11 (36)	6 (31)	5 (45)	0.7	1.8 (0.39–8.3)
Abdominal pain	10 (33)	6 (31)	4 (36)	1	1.2 (0.26–5.9)
Cough	10 (33)	3 (15)	7 (63)	**0.01**	**9.3 (1.6–53)**
Extravaginal bleeding	9 (30)	0 (0)	9 (81)	**<0.0001**	**>100 (0–>100)**
Renal angle tenderness	9 (30)	6 (31)	3 (27)	1	0.81 (0.16–4.2)
Convulsions	8 (26)	1 (5)	7 (63)	**0.001**	**31 (3–>100)**
Oliguria†	8 (26)	1 (5)	7 (63)	**0.001**	**32 (3–>100)**
Preterm contractions	8 (26)	7 (36)	1 (9)	0.2	0.17 (0.02–1.6)
Jaundice	7 (23)	2 (10)	5 (45)	0.07	7.1 (1.1–47)
Deafness	5 (16)	3 (15)	2 (18)	1	1.2 (0.17–8.5)

*Boldface indicates a statistically significant correlation between a sign or symptom and death ($p<0.05$ by χ^2 or Fisher exact test for maternal death among women with a stated sign or symptom compared with women without that sign or symptom). OR, odds ratio.
†Defined as <0.5 mL/kg/h for ≥6 h.

In relation to the fetus, the mortality rate was significantly lower when the mother was admitted to the hospital in the third trimester; the rate was 31.2% (6/17) for the third trimester compared with 92.9% (13/14) for the first and second trimesters combined ($p<0.001$). Maternal signs and symptoms that included extravaginal bleeding, convulsions, oliguria, or vaginal bleeding were each associated with fetal death ($p<0.01$) (Table 2).

Finally, we noted that 17 (56.7%) of the 30 women had been to other health facilities before admission, whereas the remaining 13 (43.3%) patients sought care at our hospital as their first point of call. Among the 17 women from other facilities, LF was suspected in 8 cases; differential diagnoses included eclampsia, malaria, pyelonephritis, miscarriage, puerperal sepsis, and placenta previa.

Discussion

LF is endemic to several states in Nigeria, and the number of women at risk for LASV infection during pregnancy is high. Our study highlights the contribution of LF to maternal mortality rates at a teaching hospital in Nigeria, where LF was diagnosed in 44/5,048 (0.87%) of all admitted pregnant women but accounted for 11/84 (13.1%) of maternal deaths at the facility during the study period. The 36.7% LF-related maternal mortality rate we report is roughly in the range of a case series described in Sierra Leone in 1988 (21%) (*11*) and of limited data from Liberia (where the LF-related mortality rate reported before 1973 was 33%–75%) (*24*), although detailed comparison is difficult given the sample sizes involved, decades of separation, and different geographic and genetic contexts.

Most of the deaths in our case series occurred during 2009–2013 (9/19, 47.4%); the mortality rate decreased by more than half for 2014–2018 (2/11, 18.2%). Despite the relatively small numbers in our study, a few key changes occurred in Nigeria, and specifically at ISTH, that are consistent with dropping mortality rates. First, testing of LF and other viral hemorrhagic fevers increased after the 2013–2016 Ebola virus disease outbreak. Second, ISTH has dramatically increased resources devoted to LF research and clinical care. Third, public health activities at ISTH and throughout Edo State increased, including a series of community campaigns and seminars for healthcare workers, with the goal of raising awareness of LF and improving management strategies.

Ongoing public health efforts presume the importance of timely referrals and quick diagnosis of LF, given that poor health-seeking behaviors resulting from lack of awareness are believed to delay medical care and worsen outcomes (*17*,*25*). Furthermore, in our study, 64% of maternal deaths occurred within 24 hours of admission and 100% within 48 hours of admission, suggesting that the disease was often advanced before referrals were made, a finding consistent with previously described delays in care for other obstetric complications (*26*). This observation further emphasizes the need for continuous community engagement, healthcare worker sensitization, an increased index of suspicion in LF-endemic areas, and ready availability of rapid diagnostic tools. The actual contribution of LF to maternal mortality rates is likely underreported in Nigeria, and we suspect LF constitutes a hidden cause of maternal deaths in several LF-endemic communities in a country that already has one of the highest maternal mortality rates in the world (*27*,*28*).

Extravaginal bleeding, convulsions, and oliguria have been found to be associated with poor outcomes in

nonpregnant adults (*16*), and we have found similar associations in maternal and fetal prognosis. In addition, we report the concerning finding that more than half of mothers who were admitted to our hospital with a deceased fetus eventually died themselves. This finding is consistent with the experience reported from Sierra Leone in 1988 (*11*), although the causal relationship between intrauterine death and severe LF disease is unknown. The number of cases in our retrospective series was insufficient to compare strategies of evacuation alone, evacuation and ribavirin, or ribavirin alone; further studies are needed to determine the best approach to obstetric care.

Although in Sierra Leone a major correlate of poor outcome was the diagnosis of LF in the third trimester (*11*), we did not observe the same correlation. Many factors might have contributed to this difference; however, we note that the Sierra Leone study endorsed active uterine evacuation in the third trimester and deferred ribavirin (*11*), whereas ISTH uses ribavirin as early therapy in all cases. Because ribavirin has been reported to be teratogenic in animal studies and data on its safety in pregnant women are insufficient (*19*), our decision to use this treatment was not taken lightly. However, although high-quality efficacy trials are lacking and safety data are pending, ribavirin is one of few therapeutic modalities available to us in this situation. The results in terms of maternal and fetal outcomes have been positive in our experience.

The favorable maternal outcome associated with admission with a live fetus suggests the importance of early detection, and we believe the results acquired through our conservative management of these patients challenge the view that active uterine evacuation is required, at least in our setting. Although we did find a significant risk of fetal death overall, we are encouraged because 12 of the 13 women admitted with live fetuses survived the illness, and 11 live births resulted. Our single experience with late uterine death of unexplained cause did increase our surveillance of pregnant survivors of LF, and we now admit such women for more frequent fetal monitoring (biometric and biophysical surveillance) and the option to induce labor in case of fetal compromise.

The generalizability of our findings is limited by a relatively small sample size at a single tertiary-care hospital and the exclusion of several cases because of incomplete records. We further recognize that we lack clinical laboratory data, quantitative RT-PCR assays needed to assess viral load, and pathologic confirmation of cause of death. Although availability of these data points has improved over time at our hospital, we note that they are not always routinely available in our resource-limited setting. We have instead highlighted key clinical findings associated with poor prognosis, including extravaginal bleeding, convulsions, oliguria, and fetal death, that do not require infrastructure for laboratory or pathologic confirmation. In our hospital, women with any of these signs or symptoms receive emergent and aggressive supportive care, including ribavirin therapy.

In conclusion, LF in pregnancy has a high case-fatality rate and is an important and likely underreported cause of maternal death in LF-endemic areas of Nigeria and in other West African countries. Admission to care with a live fetus is predictive of improved maternal outcome, and conservative obstetric management with early ribavirin (instead of evacuation) is producing good outcomes in our hands. Further studies are needed to confirm these conclusions and to provide an updated, data-driven algorithm for clinical management of pregnant women with LF.

About the Author

Dr. Okogbenin is a professor of fetal–maternal medicine and infectious diseases expert at Ambrose Alli University Ekpoma as well as a consultant obstetrician and gynecologist at ISTH. He is the chief medical director of ISTH.

References

1. Knobloch J, McCormick JB, Webb PA, Dietrich M, Schumacher HH, Dennis E. Clinical observations in 42 patients with Lassa fever. Tropenmed Parasitol. 1980;31:389–98.
2. Richmond JK, Baglole DJ. Lassa fever: epidemiology, clinical features, and social consequences. BMJ. 2003;327:1271–5. http://dx.doi.org/10.1136/bmj.327.7426.1271
3. Houlihan C, Behrens R. Lassa fever. BMJ. 2017;358:j2986. http://dx.doi.org/10.1136/bmj.j2986
4. Frame JD, Baldwin JM Jr, Gocke DJ, Troup JM. Lassa fever, a new virus disease of man from West Africa. I. Clinical description and pathological findings. Am J Trop Med Hyg. 1970;19:670–6. http://dx.doi.org/10.4269/ajtmh.1970.19.670
5. Buckley SM, Casals J. Lassa fever, a new virus disease of man from West Africa. 3. Isolation and characterization of the virus. Am J Trop Med Hyg. 1970;19:680–91. http://dx.doi.org/10.4269/ajtmh.1970.19.680
6. Jahrling PB, Frame JD, Smith SB, Monson MH. Endemic Lassa fever in Liberia. III. Characterization of Lassa virus isolates. Trans R Soc Trop Med Hyg. 1985;79:374–9. http://dx.doi.org/10.1016/0035-9203(85)90386-4
7. Fraser DW, Campbell CC, Monath TP, Goff PA, Gregg MB. Lassa fever in the Eastern Province of Sierra Leone, 1970–1972. I. Epidemiologic studies. Am J Trop Med Hyg. 1974;23:1131–9. http://dx.doi.org/10.4269/ajtmh.1974.23.1131
8. Frame JD. Surveillance of Lassa fever in missionaries stationed in West Africa. Bull World Health Organ. 1975;52:593–8.
9. Ogbu O, Ajuluchukwu E, Uneke CJ. Lassa fever in West African sub-region: an overview. J Vector Borne Dis. 2007;44:1–11.
10. Keane E, Gilles HM. Lassa fever in Panguma Hospital, Sierra Leone, 1973–6. BMJ. 1977;1:1399–402. http://dx.doi.org/10.1136/bmj.1.6073.1399
11. Price ME, Fisher-Hoch SP, Craven RB, McCormick JB. A prospective study of maternal and fetal outcome in acute Lassa fever infection during pregnancy. BMJ. 1988;297:584–7. http://dx.doi.org/10.1136/bmj.297.6648.584
12. Andersen KG, Shapiro BJ, Matranga CB, Sealfon R, Lin AE, Moses LM, et al.; Viral Hemorrhagic Fever Consortium. Clinical sequencing uncovers origins and evolution of Lassa virus. Cell. 2015;162:738–50. http://dx.doi.org/10.1016/j.cell.2015.07.020

13. McCormick JB, King IJ, Webb PA, Johnson KM, O'Sullivan R, Smith ES, et al. A case-control study of the clinical diagnosis and course of Lassa fever. J Infect Dis. 1987;155:445–55. http://dx.doi.org/10.1093/infdis/155.3.445
14. Walker DH, McCormick JB, Johnson KM, Webb PA, Komba-Kono G, Elliott LH, et al. Pathologic and virologic study of fatal Lassa fever in man. Am J Pathol. 1982;107:349–56.
15. Mor G, Cardenas I. The immune system in pregnancy: a unique complexity. Am J Reprod Immunol. 2010;63:425–33. http://dx.doi.org/10.1111/j.1600-0897.2010.00836.x
16. Okokhere P, Colubri A, Azubike C, Iruolagbe C, Osazuwa O, Tabrizi S, et al. Clinical and laboratory predictors of Lassa fever outcome in a dedicated treatment facility in Nigeria: a retrospective, observational cohort study. Lancet Infect Dis. 2018;18:684–95. http://dx.doi.org/10.1016/S1473-3099(18)30121-X
17. McCormick JB, King IJ, Webb PA, Scribner CL, Craven RB, Johnson KM, et al. Lassa fever. Effective therapy with ribavirin. N Engl J Med. 1986;314:20–6. http://dx.doi.org/10.1056/NEJM198601023140104
18. Bausch DG, Hadi CM, Khan SH, Lertora JJL. Review of the literature and proposed guidelines for the use of oral ribavirin as postexposure prophylaxis for Lassa fever. Clin Infect Dis. 2010;51:1435–41. http://dx.doi.org/10.1086/657315
19. Sinclair SM, Jones JK, Miller RK, Greene MF, Kwo PY, Maddrey WC. The Ribavirin Pregnancy Registry: an interim analysis of potential teratogenicity at the mid-point of enrollment. Drug Saf. 2017;40:1205–18. http://dx.doi.org/10.1007/s40264-017-0566-6
20. Asogun DA, Adomeh DI, Ehimuan J, Odia I, Hass M, Gabriel M, et al. Molecular diagnostics for Lassa fever at Irrua Specialist Teaching Hospital, Nigeria: lessons learnt from two years of laboratory operation. PLoS Negl Trop Dis. 2012;6:e1839. http://dx.doi.org/10.1371/journal.pntd.0001839
21. Gómez Ponce de León R, Wing D, Fiala C. Misoprostol for intrauterine fetal death. Int J Gynaecol Obstet. 2007;99(Suppl 2):S190–3. http://dx.doi.org/10.1016/j.ijgo.2007.09.010
22. International Federation of Gynecology and Obstetrics. Prevention of post-partum haemorrhage with misoprostol [cited 2019 Feb 21]. https://www.figo.org/sites/default/files/uploads/project-publications/Miso/PPH%20prevention/Prevention%20of%20PPH%20with%20Misoprostol_In%20Brief_2012_English.pdf
23. World Health Organization. The WHO application of ICD-10 to deaths during pregnancy, childbirth and puerperium: ICD MM [cited 2019 Feb 21]. https://apps.who.int/iris/bitstream/handle/10665/70929/9789241548458_eng.pdf
24. Monath TP, Mertens PE, Patton R, Moser CR, Baum JJ, Pinneo L, et al. A hospital epidemic of Lassa fever in Zorzor, Liberia, March–April 1972. Am J Trop Med Hyg. 1973;22:773–9. http://dx.doi.org/10.4269/ajtmh.1973.22.773
25. Faith I, O AA, Samuel MK, Ifeanyi O, Ekundare FO, Danny A, et al. An assessment of onset-to-intervention time and outcome of Lassa fever during an outbreak in Edo State, Nigeria. International Journal of Prevention and Treatment. 2018;7:1–5.
26. Adamu YM, Salihu HM, Sathiakumar N, Alexander GR. Maternal mortality in Northern Nigeria: a population-based study. Eur J Obstet Gynecol Reprod Biol. 2003;109:153–9. http://dx.doi.org/10.1016/S0301-2115(03)00009-5
27. Okonofua FE, Abejide A, Makanjuola RA. Maternal mortality in Ile-Ife, Nigeria: a study of risk factors. Stud Fam Plann. 1992;23:319–24. http://dx.doi.org/10.2307/1966529
28. Harrison KA. Maternal mortality in Nigeria: the real issues. Afr J Reprod Health. 1997;1:7–13. http://dx.doi.org/10.2307/3583270

Address for correspondence: Sylvanus Okogbenin, Irrua Specialist Teaching Hospital, KM 87, Benin Auchi Rd, PMB 08, Irrua, Edo State, Nigeria; email: okogbenins@yahoo.com

Direct Medical Costs of 3 Reportable Travel-Related Infections in Ontario, Canada, 2012–2014

Rachel D. Savage, Laura C. Rosella, Natasha S. Crowcroft, Maureen Horn, Kamran Khan, Laura Holder, Monali Varia

Immigrants traveling to their birth countries to visit friends or relatives are disproportionately affected by travel-related infections, in part because most preventive travel health services are not publicly funded. To help identify cost-effective policies to reduce this disparity, we measured the medical costs (in 2015 Canadian dollars) of 3 reportable travel-related infectious diseases (hepatitis A, malaria, and enteric fever) that accrued during a 3-year period (2012–2014) in an ethnoculturally diverse region of Canada (Peel, Ontario) by linking reportable disease surveillance and health administrative data. In total, 318 case-patients were included, each matched with 2 controls. Most spending accrued in inpatient settings. Direct healthcare spending totaled $2,058,196; the mean attributable cost per case was $6,098 (95% CI $5,328–$6,868) but varied by disease (range $4,558–$7,852). Costs were greatest for enteric fever. Policies that address financial barriers to preventive health services for high-risk groups should be evaluated.

Because of the rapid growth of air travel and immigration, more travelers worldwide are exposed to nonendemic infectious diseases (e.g., Zika, measles, malaria) than ever before (*1*–*3*). In Ontario, Canada, >3,000 travel-related infections are reported to public health annually (*4*); this number is an underestimate because not all sick persons seek healthcare treatment, especially while traveling, and not all conditions are diagnosed and reported. Immigrant travelers who return to their birth countries to visit friends or relatives are a substantial risk group (*5*). In Canada and elsewhere, regions with high proportions of immigrant travelers to South Asia and Africa have the highest rates of imported cases of hepatitis A, malaria, and enteric fever (*4*,*6*–*8*). The disproportionate burden of travel-related infections in immigrants has been attributed to their traveling to riskier destinations (*9*) and prolonged travel stays (*10*,*11*) but also to their poor uptake of pretravel health services (*10*,*12*–*14*).

Pretravel health consultations provide an opportunity to intervene and reduce travel-related infections (*14*). The Committee to Advise on Tropical Medicine and Travel recommends that nonimmune travelers going to developing countries receive the hepatitis A vaccine (*15*), travelers going to South Asia receive the typhoid vaccine (*16*), and travelers going to regions where malaria is endemic receive chemoprophylaxis (*17*) before traveling. Despite these recommendations, pretravel health services are generally not covered by provincial universal insurance plans, with few exceptions (*18*). Private health insurance can fill these gaps by providing partial or complete coverage for these services; however, many travelers, including those visiting friends or relatives (VFR), who are at greater risk for infection, often do not have private insurance. The cost of pretravel health services has been described by VFR travelers as a barrier (*9*,*19*–*22*). As a result, public health officials have advocated for universal coverage of pretravel health services to reduce the substantial public health resources required for the management of these imported cases (*6*,*23*).

The direct medical costs of reportable travel-related infections to healthcare systems has not been measured. The existing estimates were determined primarily by using inpatient settings or are considered outdated (*24*–*26*). As outbound travel and annual immigration targets continue to increase, evidence is needed to determine if policies are meeting the healthcare needs of an increasingly diverse population. Furthermore, mathematic and economic models require this information as inputs, so the lack of cost estimates has limited the development of these models. In this report, we sought to measure healthcare utilization and attributable medical costs of 3 key reportable travel-related

Author affiliations: Women's College Hospital, Toronto, Ontario, Canada (R.D. Savage); University of Toronto, Toronto (R.D. Savage, L.C. Rosella, N.S. Crowcroft, K. Khan); ICES, Toronto (R.D. Savage, L.C. Rosella, L. Holder); Public Health Ontario, Toronto (N.S. Crowcroft); Peel Public Health, Mississauga, Ontario, Canada (M. Horn, M. Varia); St. Michael's Hospital, Toronto (K. Khan)

DOI: https://doi.org/10.3201/eid2508.190222

infections in an ethnoculturally diverse region of Canada by linking public health reportable disease surveillance data with health administrative data.

Materials and Methods

Design and Setting

We received ethics approval (no. 31366) for this study from the University of Toronto Research Ethics Board (Toronto, Canada). We used a population-based, matched-cohort design to estimate attributable medical costs of incident cases of hepatitis A, malaria, and enteric fever from a healthcare payer perspective. This study was conducted in the Peel region of Ontario, one of Canada's largest and most ethnoculturally diverse municipalities, which has ≈1.4 million residents, ≈50% of whom are foreign-born (*27*). South Asians are the largest visible minority in both the Peel region and Canada (*28*). For the purposes of our study, we needed to link reportable disease surveillance data with the health administrative data collected as part of Ontario's government-funded, universal healthcare. Each data source independently would have been insufficient to achieve the study objective, and thus, the linkage represents a valuable feature of this study.

Case-Patients

During the study period, reporting hepatitis A, malaria, and enteric fever (i.e., typhoid fever and paratyphoid fever) to public health authorities in Ontario was required by the Health Protection and Promotion Act (*29*). We identified the laboratory-confirmed hepatitis A, malaria, and enteric fever case-patients reported to Peel Public Health during January 1, 2012–December 31, 2014, using the integrated Public Health Information System (iPHIS). We excluded case-patients who were unable to be linked to the Ontario Registered Persons Database, which contains the demographic information of all persons issued an Ontario health card, and we compared linked and unlinked case-patients to identify potential sources of bias (*30*). Because reporting is known to be incomplete, we additionally identified Peel region residents with information in the health administrative datasets who were hospitalized with the following diagnostic codes from the International Classification of Diseases, 10th Revision, with Canadian Enhancements: hepatitis A (B15), malaria (B50–54), or typhoid and paratyphoid fever (A01). If hospitalizations were recurrent, we counted the series once (i.e., we considered all hospitalizations to be a part of the same case). We excluded case-patients identified in the health administrative datasets if their healthcare record indicated uncertainty of the diagnosis (*31*). Index dates were based on the iPHIS episode accurate date (i.e., the symptom onset date for 95% of case-patients and specimen collection date for the remainder) or the case-patient's hospital admission date. Index dates for iPHIS case-patients were December 20, 2011–December 17, 2014. To account for delays between symptom onset and healthcare seeking, we included case-patients from hospitalization records if they were admitted during December 20, 2011–January 4, 2015. We chose to add this ≈3-week extension to the end of the accrual window because iPHIS case-patients had, on average, an 18-day delay between symptom onset and healthcare presentation.

Controls

For each disease, we matched 2 controls per case-patient from a pool of eligible controls in the health administrative datasets. We used controls to determine the baseline medical costs so that we could calculate the costs attributable to travel. Controls were eligible if they were registrants of the Ontario Health Insurance Program, had contact with the healthcare system within the 3 years before their assigned index date, and resided in the Peel region (according to their postal code) during the period of study (Figure 1). We excluded persons from the pool of eligible controls if they had a travel-related diagnostic code during the study period (Table 1). We randomly assigned index dates to eligible controls according to the index date distribution of case-patients and then excluded controls who did not reside in the Peel region or had died as of their assigned index date.

Matching and Covariates

For each disease, we matched controls to case-patients by index date (±60 days), age (±3 years), sex, neighborhood income quintile, foreign-born status, years in Canada if foreign-born (0–4, 5–9, or ≥10), and concurrent medical conditions. We estimated neighborhood income quintile by linking case-patients' postal codes to existing average household income data for their neighborhoods and stratifying neighborhoods by quintile to generate neighborhood-specific income quintiles (*32*). We enhanced the study cohort by linking to the Ontario portion of the Immigration, Refugees, and Citizenship Canada Permanent Resident (IRCC-PR) database (1985–2012) (*33*). We defined case-patients as foreign-born if they had a country of birth outside of Canada recorded in iPHIS or if they had a record present in the IRCC-PR database. We designated controls as foreign-born solely using IRCC-PR data. To calculate years in Canada, we used the immigration date in the IRCC-PR database. For immigrants not yet captured in the IRCC-PR database (i.e., immigrants who landed in Ontario after 2012), we assigned their immigration date as the date 3 months before their first healthcare contact because new Ontario residents have a 3-month waiting period before they become eligible for the Ontario Health Insurance Program (*34*). For a small number of case-patients (n<6), we set their years in Canada to 0 because their index date

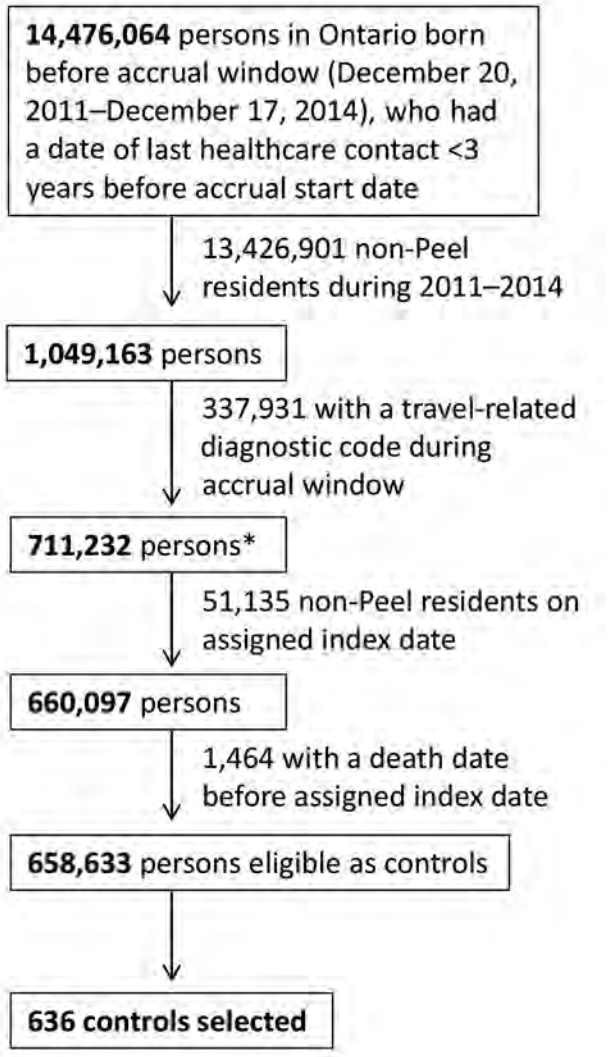

Figure 1. Flowchart of control selection in study of direct costs of hepatitis A, malaria, and enteric fever, Peel region, Ontario, Canada, 2011–2014. *Index date randomly assigned on the basis of the index date distribution of case-patients.

preceded their first contact with healthcare. We determined the concurrent medical conditions of case-patients and controls during the 2 years before their index date by using the Johns Hopkins ACG System collapsed Aggregated Diagnostic Groups validated for use in Ontario (*35*,*36*). We further collapsed categories of like duration and severity of condition (i.e., unstable chronic conditions requiring medical [category 5] or specialty care [category 9], stable chronic conditions requiring medical [category 6] or specialty care [category 7]).

Healthcare Utilization and Costs

We measured healthcare utilization and the medical costs that occurred up to 90 days after and including the index date; we chose this period on the basis of published estimates of illness duration (*37*). We probabilistically linked case-patients present in iPHIS to their health administrative data with unique identifiers and used a validated person-centered costing method developed for analyzing Ontario health administrative data to estimate direct medical costs (*38*). Those datasets were linked using unique encoded identifiers and analyzed at ICES (Toronto, Canada). The costing method used captured all relevant costs covered by the Ontario single-payer health insurance plan, including inpatient hospitalizations, emergency department (ED) visits, same-day surgery, dialysis, oncology clinic visits, fee-for-service physician and nonphysician services, non–fee-for-service physicians, prescription medications, laboratory services, rehabilitation, complex continuing care, long-term care, mental health inpatient stays, and home care services. We adjusted costs for inflation by using health sector–specific consumer price indices and reported all costs in 2015 Canadian dollars (Can).

Table 1. Diagnostic codes used to identify and exclude noneligible controls in study of direct costs of hepatitis A, malaria, and enteric fever, Peel region, Ontario, Canada, 2012–2014*

Disease	ICD-10-CA	OHIP
Hepatitis A	B15, B19, A09, A08.3–A08.5	070, 009, 079, 136, 787
Malaria	B50–B54, P37.3–P37.4, B64	062, 136, 781, 784, 787
Enteric fever	A01, A02.9, A02.1, A04.9, A05.9, A09, A49.9	002, 009, 003, 005, 136, 784, 787

*ICD-10-CA, International Classification of Diseases, 10th Revision, Canadian Enhancement; OHIP, Ontario Health Insurance Plan claims database.

Analysis

We assessed the quality of matching by comparing case-patients and controls using the standardized difference (*d*); we used a *d* value of >0.10 to identify significant imbalances (*39*,*40*). We estimated attributable, 90-day per-person costs as the mean of the differences in costs among case-patient–control pairs (*41*). To account for the clustered nature of the data (i.e., 2 controls per case-patient), we used generalized estimating equations with an exchangeable correlation matrix to estimate 95% CIs (*41*). We stratified all attributable cost estimates by disease and setting and, for malaria, by infecting species. We categorized inpatient settings as inpatient hospitalizations, inpatient mental health hospitalizations, rehabilitation services, and complex continuing care; ED settings as ED visits and shadow billings to ED physicians; and the remainder of settings as outpatient settings. We performed analyses using SAS version 9.3 (https://www.sas.com).

Sensitivity Analyses

To examine the effect of healthcare database selection and the time window on estimated costs, we repeated our analysis in 2 ways. In the first sensitivity analysis, we included

only the cost calculations for expenditures considered most relevant to diagnosing and treating acute infections (i.e., inpatient hospitalizations, ED visits, same-day surgery, fee-for-service physician and nonphysician services, non–fee-for-service physicians, prescription medications, laboratory services). In the second, we limited the measurement of costs to a 60-day follow-up period.

Results

During 2012–2014, a total of 289 cases of hepatitis A, malaria, or enteric fever were reported to Peel Public Health in case-patients linkable to the health administrative data, a linkage ratio of 90% (289/321). No deaths were identified among the case-patients. Unlinked case-patients (n = 32) were more likely than linked case-patients (n = 289) to be recent immigrants (i.e., immigrants who arrived in Ontario during the incubation period of their disease) or visitors (53.3% unlinked vs. 8.7% linked; p<0.001), but otherwise the linked and unlinked case-patients were similar in terms of sex, age, disease distribution, and foreign-born status. We identified an additional 29 case-patients in hospital records for a total case-patient cohort size of 318.

Compared with all (unmatched) eligible controls, case-patients were younger and a higher proportion were male (Table 2). Case-patients were also more likely than unmatched controls to be foreign-born, have acute or stable chronic medical conditions, and live in neighborhoods of lower income quintiles. Case-patients and matched controls were similar in terms of all matching variables, with the exception of missing neighborhood income quintile (Tables 2, 3).

Table 2. Characteristics of case-patients in study of direct costs of hepatitis A, malaria, and enteric fever and pools of unmatched and matched eligible controls, Peel region, Ontario, Canada, 2012–2014*

Variable	Case-patients, n = 318	Prematching		Postmatching	
		Controls, n = 658,633	*d*	Controls, n = 636	*d*
Age, y					
Mean ± SD	31 ± 21	37 ± 22	0.273	31 ± 21	0.001
Median (IQR)	30 (12–47)	36 (20–53)	0.268	30 (12–47)	0.001
<1	0	9,694 (1.5)	0.173	0	0
1–4	21 (6.6)	27,381 (4.2)	0.109	42 (6.6)	0
5–9	36 (11.3)	40,692 (6.2)	0.183	75 (11.8)	0.015
10–14	33 (10.4)	41,235 (6.3)	0.149	63 (9.9)	0.016
15–24	43 (13.5)	93,870 (14.3)	0.021	85 (13.4)	0.005
25–49	120 (37.7)	245,090 (37.2)	0.011	240 (37.7)	0
50–74	57 (17.9)	167,999 (25.5)	0.185	115 (18.1)	0.004
≥75	8 (2.5)	32,672 (5.0)	0.129	16 (2.5)	0
Sex					
F	123 (38.7)	321,510 (48.8)	0.205	252 (39.6)	0.019
M	195 (61.3)	337,123 (51.2)	0.205	384 (60.4)	0.019
Neighborhood income quintile					
1, lowest	70 (22.0)	103,751 (15.8)	0.160	133 (20.9)	0.027
2	88 (27.7)	109,728 (16.7)	0.268	169 (26.6)	0.025
3	94 (29.6)	121,601 (18.5)	0.262	203 (31.9)	0.051
4 or 5, highest	60–70 (S)	159,348 (24.2)	0.231	131 (20.6)	0.027
Missing	<6 (S)	356 (0.1)	0.150	0	0.160
Foreign-born, database					
IRCC-PR†	183 (57.5)	73,564 (11.2)	1.119	449 (70.6)	0.275
iPHIS or IRCC-PR‡	227 (71.4)	73,564 (11.2)	1.546	449 (70.6)	0.017
Years in Canada, no./total (%)					
0–4	58/227 (25.6)	13,535/73,564 (18.4)	0.170	113/449 (25.2)	0.009
5–9	56/227 (24.7)	15,868/73,564 (21.6)	0.070	114/449 (25.4)	0.017
≥10	113/227 (49.8)	44,161/73,564 (60.0)	0.210	222/449 (49.4)	0.007
Concurrent medical condition§					
1	240 (75.5)	351,379 (53.3)	0.475	475 (74.7)	0.018
2	210 (66.0)	313,777 (47.6)	0.378	420 (66.0)	0
3	178 (56.0)	286,375 (43.5)	0.252	359 (56.4)	0.010
4	28 (8.8)	33,259 (5.0)	0.148	59 (9.3)	0.016
5 and 9	44 (13.8)	90,116 (13.7)	0.004	118 (18.6)	0.008
6 and 7	107 (33.6)	164,535 (25.0)	0.191	222 (34.9)	0.007
8	12 (3.8)	39,357 (6.0)	0.102	23 (3.6)	0.008
10	63 (19.8)	135,170 (20.5)	0.018	127 (20.0)	0.004
11	119 (37.4)	216,829 (32.9)	0.094	216 (34.0)	0.072
12	12 (3.8)	15,640 (2.4)	0.081	24 (3.8)	0

*Values are no. (%) except as indicated. *d*, standardized difference; iPHIS, integrated Public Health Information System; IQR, interquartile range; IRCC-PR, Immigration, Refugee and Citizenship Canada Permanent Resident; S, suppressed per ICES reidentification risk assessment policy.
†Case-patients and controls were designated as foreign-born if they had a record in the IRCC-PR database.
‡Case-patients were designated as foreign-born if country of birth was listed as outside of Canada in iPHIS, or they had a record in the IRCC-PR database; controls were designated as foreign-born if they had a record in the IRCC-PR database.
§Listed by John Hopkins collapsed Aggregated Diagnostic Group: 1 (acute minor), 2 (acute major), 3 (likely to recur), 4 (asthma), 5 and 9 (chronic unstable), 6 and 7 (chronic stable), 8 (eye and dental), 10 (psychosocial), 11 (preventive and administrative), and 12 (pregnancy).

Most (>90%) case-patients had travel-associated illnesses (Table 4); of these case-patients, most (50%) traveled to India, and more than half (63%) reported traveling to visit friends or relatives. A similar proportion of children <16 years of age (57% [43/76]) also reported traveling to visit friends or relatives, although this proportion varied by disease (47% [8/17] for hepatitis A, 40% [6/15] for malaria, 66% [29/44] for enteric fever). Most of the case-patients identified as recent immigrants received malaria diagnoses, and of these, 65% (13/20) were caused by *Plasmodium vivax*, probably representing relapsed malaria rather than primary disease acquired by travel. Case-patients with *P. falciparum* malaria primarily traveled to West Africa (83%, 40/48), and all case-patients with *P. vivax* malaria had traveled to India (58%, 15/26) or Pakistan (42%, 11/26). Few case-patients reported having a pretravel health consultation.

Of the 318 case-patients, 197 (61.9%) were hospitalized, 232 (73.0%) visited the ED, and 298 (93.7%) visited a physician (i.e., family or general practice physician or specialist) for their illness. However, a total of 225 hospitalizations, 429 ED visits, and 4,831 unique physician visits occurred (Table 5); more than half of these encounters were for enteric fever diagnoses or treatment.

The overall cost of the 318 travel-related infections that occurred during the 3-year study period in Peel was $2,058,196 (Table 6). Extrapolating the estimated mean cost of these infections per case-patient for the Peel region to the Ontario case counts (*42*) amounted to a total of $7,870,341 in direct healthcare spending. More than one

Table 3. Characteristics of case-patients and matched controls in study of direct costs of hepatitis A, malaria, and enteric fever, by disease, Peel region, Ontario, Canada, 2012–2014*

	Hepatitis A			Malaria			Enteric fever		
Variable	Case-patients, n = 55	Controls, n = 110	*d*	Case-patients, n = 122	Controls, n = 244	*d*	Case-patients, n = 141	Controls, n = 282	*d*
Age, y									
Median ± IQR	24 ± 21	24 ± 21	0	40 ± 19	40 ± 19	0.001	26 ± 19	26 ± 19	0.002
Mean (SD)	19 (10–32)	19 (10–32)	0.003	43 (27–55)	43 (27–55)	0.002	25 (10–40)	25 (9–40)	0.001
0–9	13 (23.6)	23 (23.6)	0	10 (8.2)	20 (8.2)	0	34 (24.1)	71 (25.1)	0.025
10–14	7 (12.7)	14 (12.7)	0	7 (5.7)	14 (5.7)	0	19 (13.5)	35 (12.4)	0.032
15–24	17 (30.9)	34 (30.9)	0	10 (8.2)	20 (8.2)	0	16 (11.3)	31 (11.0)	0.011
25–49	12 (21.8)	24 (21.8)	0	54 (44.3)	107 (43.9)	0.008	54 (38.3)	109 (38.7)	0.007
≥50	6 (11.0)	12 (11.0)	0	41 (33.6)	83 (34.0)	0.008	18 (12.8)	36 (12.8)	0
Sex									
F	27 (49.1)	54 (49.1)	0	37 (30.3)	78 (32.0)	0.035	59 (41.8)	120 (42.6)	0.014
M	28 (50.9)	56 (50.9)	0	85 (69.7)	166 (68.0)	0.035	82 (58.2)	162 (57.4)	0.014
Income quintile									
1, lowest	9 (16.4)	15 (13.6)	0.076	36 (29.5)	68 (27.9)	0.036	25 (17.7)	50 (17.7)	0
2	6 (10.9)	10 (9.1)	0.061	39 (32.0)	77 (31.6)	0.009	43 (30.5)	82 (29.1)	0.031
3	17 (30.9)	36 (32.7)	0.039	20–25 (S)	56 (23.0)	0.060	52 (36.9)	111 (39.4)	0.051
4 and 5, highest	23 (41.8)	49 (44.5)	0.055	20–25 (S)	43 (17.6)	0.033	15–20 (S)	39 (13.8)	0.010
Missing	0	0	0	<6 (S)	0	0.183	<6 (S)	0	0.170
Foreign-born	30 (54.5)	58 (52.7)	0.036	101 (82.8)	200 (82.0)	0.022	96 (68.1)	191 (67.7)	0.008
Years in Canada, no./total (%)									
0–4	6/30 (20.0)	10/58 (17.2)	0.071	29/101 (28.7)	63/200 (31.5)	0.061	23/96 (24.0)	40/191 (20.9)	0.072
5–9	10/30 (33.3)	20/58 (34.5)	0.024	21/101 (20.8)	40/200 (20.0)	0.020	25/96 (26.0)	54/191 (28.3)	0.050
≥10	14/30 (46.7)	28/58 (48.3)	0.032	51/101 (50.5)	97/200 (48.5)	0.040	48/96 (50.0)	97/191 (50.8)	0.016
Concurrent medical conditions†									
1	43 (78.2)	84 (76.4)	0.043	84 (68.9)	166 (68.0)	0.018	113 (80.1)	225 (79.8)	0.009
2	37 (67.3)	75 (68.2)	0.019	78 (63.9)	161 (66.0)	0.043	95 (67.4)	184 (65.2)	0.045
3	32 (58.2)	68 (61.8)	0.074	59 (48.4)	118 (48.4)	0	87 (61.7)	173 (61.3)	0.007
4	<6 (S)	6 (5.5)	0	7 (5.7)	17 (7.0)	0.050	18 (12.8)	36 (12.8)	0
5 and 9	11 (20.0)	19 (17.3)	0.070	25 (20.5)	56 (23.0)	0.060	24 (17.0)	43 (15.2)	0.048
6 and 7	13 (23.6)	25 (22.7)	0.022	49 (40.2)	98 (40.2)	0	50 (35.5)	99 (35.1)	0.007
8	<6 (S)	<6 (S)	0	<6 (S)	9 (3.7)	0.022	7 (5.0)	12 (4.3)	0.034
10	12 (21.8)	26 (23.6)	0.043	24 (19.7)	44 (18.0)	0.042	27 (19.1)	57 (20.2)	0.027
11	23 (41.8)	42 (38.2)	0.074	37 (30.3)	69 (28.3)	0.045	59 (41.8)	105 (37.2)	0.094
12	<6 (S)	<6 (S)	0	<6 (S)	12 (4.9)	0.040	<6 (S)	8 (2.8)	0.040

*Values are no. (%) except as indicated. *d*, standardized difference; IQR, interquartile range; S, suppressed per ICES reidentification risk assessment policy.
†Listed by John Hopkins collapsed Aggregated Diagnostic Group: 1 (acute minor), 2 (acute major), 3 (likely to recur), 4 (asthma), 5 and 9 (chronic unstable), 6 and 7 (chronic stable), 8 (eye and dental), 10 (psychosocial), 11 (preventive and administrative), and 12 (pregnancy).

Table 4. Travel-related characteristics of case-patients with hepatitis A, malaria, or enteric fever reported to public health, Peel region, Ontario, Canada, 2012–2014*

Characteristic	No. (%) case-patients			
	Hepatitis A	Malaria	Enteric fever	Overall
Travel associated†				
Yes	39 (79.6)	103 (91.2)	120 (94.5)	262 (90.7)
No or unknown	10 (20.4)	10 (8.8)	7 (5.5)	27 (9.3)
Region of birth†				
South Asia	10 (20.4)	38 (33.6)	78 (61.4)	126 (43.6)
North America	14 (28.6)	6 (5.3)	35 (27.6)	55 (19.0)
West Africa	0	29 (25.7)	0	29 (10.0)
Other or missing	25 (51.0)	40 (35.4)	14 (11.0)	79 (27.3)
Primary travel country‡				
India	11 (29.0)	16 (19.5)	92 (78.6)	119 (50.2)
Pakistan	14 (36.8)	11 (13.4)	19 (16.2)	44 (18.6)
Nigeria	0	20 (24.4)	0	20 (8.4)
Ghana	0	19 (23.2)	0	19 (8.0)
Other or missing	13 (34.2)	16 (19.5)	6 (5.1)	35 (14.8)
Purpose of travel‡§				
Visiting friends or relatives	18 (47.4)	45 (54.9)	87 (74.4)	150 (63.3)
Leisure, business, or other	<6 (S)	13 (15.9)	11 (9.4)	25–29 (S)
Missing	17 (44.7)	27 (32.9)	24 (20.5)	68 (28.7)
Pretravel health consultation‡				
Yes	<6 (S)	14 (17.1)	10 (8.5)	25–29 (S)
No or unknown	33–38 (S)	68 (82.9)	107 (91.5)	208–213 (S)

*S, suppressed per ICES reidentification risk assessment policy.
†Includes recent immigrants (i.e., immigrants who arrived in Ontario during the incubation period of their disease) and visitors: hepatitis A (n = 49), malaria (n = 113), enteric fever (n = 127), and overall (n = 289).
‡Does not include recent immigrants and visitors: hepatitis A (n = 38), malaria (n = 82), enteric fever (n = 117), and overall (n = 237).
§Not mutually exclusive.

quarter (26.2%) of the healthcare costs of hepatitis A, malaria, and enteric fever in Ontario were accrued in the Peel region, despite this region comprising only 10.3% of the Ontario population (*28*).

The average healthcare spending per case-patient ($6,472) was >17 times the cost per control ($375), for an attributable additional cost of $6,098 (95% CI $5,328–$6,868) per case-patient (Table 6). Costs varied by disease and were greatest for enteric fever. Attributable healthcare costs were primarily accrued in inpatient settings, which accounted for 57%–70% of costs across infections (Figure 2), followed by outpatient (22%–36%) and ED settings (8%).

Attributable costs were robust across sensitivity analyses. When restricted to the most relevant healthcare costs, costs were ≈$1,000 less for hepatitis A but remained similar for the other infectious diseases (Table 6). A shorter follow-up period of 60 days similarly did not substantially change cost estimates ($5,859, 95% CI $5,126 $6,592). To examine how costs were affected by our decision to include the small number of case-patients with locally acquired hepatitis A and those for which travel exposure was unknown (n = 10), we conducted a post hoc sensitivity analysis excluding these case-patients. The overall attributable cost remained relatively unchanged at $5,942 (95% CI $5,247 $6,637) per case-patient, and the mean hepatitis A–specific attributable cost was reduced to $3,710 (95% CI 95% CI $2,044–$5,376) per case-patient.

Table 5. Healthcare utilization by type of healthcare visit among case-patients with travel-related hepatitis A, malaria, or enteric fever, stratified by foreign-born status, Peel region, Ontario, Canada, 2012–2014

Population	No. hospitalizations	Length of hospital stay, d			No. emergency department visits	No. physician visits	No. outpatients
		Mean	Median	Range			
All, n = 318	225	4	3	0–42	429	4,831	1,317
Hepatitis A	31	4	3	0–14	61	742	208
Malaria	75	3	2	0–42	118	1,488	427
Enteric fever	119	5	4	0–34	250	2,601	682
Canada-born, n = 91							
All	71	4	3	0–14	126	1,318	369
Hepatitis A	15	3	2	0–6	27	276	78
Malaria	16	2	2	0–8	30	293	85
Enteric fever	40	6	5	1–14	69	749	206
Foreign-born, n = 227							
All	154	4	3	0–42	303	3,513	948
Hepatitis A	16	5	4	0–14	34	466	130
Malaria	59	3	2	0–42	88	1,195	342
Enteric fever	79	5	4	0–34	181	1,852	476

Table 6. Total direct and attributable medical costs of hepatitis A, malaria, and enteric fever, Peel region, Ontario, Canada, 2012–2014*

	Peel region					Ontario	
Category	No. case-patients	Total direct costs, $	Cost per case-patient, $, mean (range)	Cost per control, $, mean (range)	Attributable cost (95% CI), $	No. case-patients	Total direct costs, $†
Overall 90-d cost	318	2,058,196	6,472 (0–59,358)	375 (0–42,213)	6,098 (5,328–6,868)	1,216	7,870,341
By disease							
Hepatitis A	55	306,707	5,576 (0–59,358)	560 (0–42,213)	5,016 (2,414–7,619)	300	1,672,944
Malaria	122	613,488	5,029 (0–38,556)	471 (0–26,598)	4,558 (3,557–5,558)	612	3,077,497
Plasmodium vivax	43	230,487	ND	ND	4,812 (2,675–6,949)	ND	ND
P. falciparum	59	297,106	ND	ND	4,743 (3,588–5,898)	ND	ND
Other	20	85,895	ND	ND	3,463 (1,397–5,528)	ND	ND
Enteric fever	141	1,138,002	8,071 (0–33,563)	219 (0–13,824)	7,852 (6,812–8,893)	304	2,453,566
Restricted to most relevant costs							
Hepatitis A	55	233,771	4,250 (0–23,048)	266 (0–10,163)	3,984 (2,823–5,145)	300	1,275,117
Malaria	122	611,030	5,008 (0–37,335)	361 (0–17,626)	4,647 (3,593–5,701)	612	3,065,171
Enteric fever	141	1,029,311	7,300 (0–33,563)	211 (0–13,824)	7,089 (6,097–8,081)	304	2,219,224

*Cost given in 2015 Canadian dollars. Attributable cost indicates the additional cost for each case-patient. ND, not determined.
†Extrapolated by multiplying the number of cases in the province reported to Public Health Ontario for the same period by the mean cost per case-patient estimated by using Peel region data.

Discussion

By linking reportable disease surveillance data with health administrative data, this study provides comprehensive, population-based estimates of the medical costs of 3 reportable travel-related infections. Total medical costs were >$2 million in the Peel region of Ontario during our 3-year study period; scaled up to the provincial level, we estimated close to $8 million in healthcare spending for the 1,216 reported cases in Ontario that occurred over the same period. Attributable 90-day medical costs ranged from $4,558 for malaria to $7,852 for enteric fever; these estimates are in line with total per capita health expenditures in Ontario of $6,584 in 2018 (*43*), highlighting the substantial resources required for diagnosis and treatment of these infections. Costs were primarily driven by care provided in inpatient settings and represent mostly avoidable healthcare spending, considering that safe and effective medical interventions (e.g., pretravel health consultations, immunization, chemoprophylaxis) are available to prevent infection and clinical disease.

To the best of our knowledge, the comprehensive medical costs of hepatitis A, malaria, and enteric fever have not been estimated elsewhere. In London, England, where rates of reportable travel-related infections are high and reflective of an ethnically diverse population, inpatient costs have been estimated at £1,375 (≈2015 Can $2,300) per admission for malaria and £1,976 (≈2015 Can $3,300) per admission for typhoid (*25*,*26*). These values are comparable, albeit slightly lower than the costs reported in our study, probably because of their restriction to the inpatient setting and lower healthcare costs in the United Kingdom (*38*,*44*). In both settings, costs of enteric fever were greater than those of malaria. This difference might be attributable to the poor sensitivity of available microbiological tests for the detection of *Salmonella enterica* serovars Typhi and Paratyphi, which can lead to repeated testing and delays in receiving appropriate treatment (*45*). Emerging antimicrobial resistance also contributes to costs. In a retrospective chart review of a large, tertiary care pediatric center in Toronto, only 40% of isolates were found to be fully susceptible to the drugs typically used to treat enteric fever, and 64% of patients needed to be recalled to the hospital after positive blood cultures (*46*). Improving diagnostics for enteric fever is critical to reducing hospitalizations and associated healthcare spending.

Although public health costs related to case and contact management are substantial, they are often excluded because they are not routinely or systematically tracked. Omission of these expenditures can lead to underestimates of disease burden, particularly for infections with hepatitis A virus and *S. enterica* serovars Typhi and Paratyphi, which require follow-up and resource-intensive postexposure prophylaxis (in cases of hepatitis A) to prevent secondary transmission (*47*). In 2014, Peel Public Health tracked staff hours spent to manage reported travel-related cases and estimated personnel costs of Can $3,500 per case for hepatitis A, Can $3,300 per case for enteric fever, and Can $40 per case for malaria (M. Varia, unpub. data). These estimates are in line with reports from the United States (US $3,221 per hepatitis A case) (*48*). However, costs can be >US $40,000 when including the cost of immunoglobulin and vaccines (*49*).

Overall, >70% of the case-patients in our study were foreign-born, suggesting that more needs to be done to ensure equitable access to these interventions for those who are at greatest risk. Although public funding of pretravel health services for VFR travelers might eliminate cost-related barriers, other factors need to be considered and addressed to effectively reduce disease burden in this population. Qualitative studies have found that social contexts and relationships are mediators of the choices and behaviors of

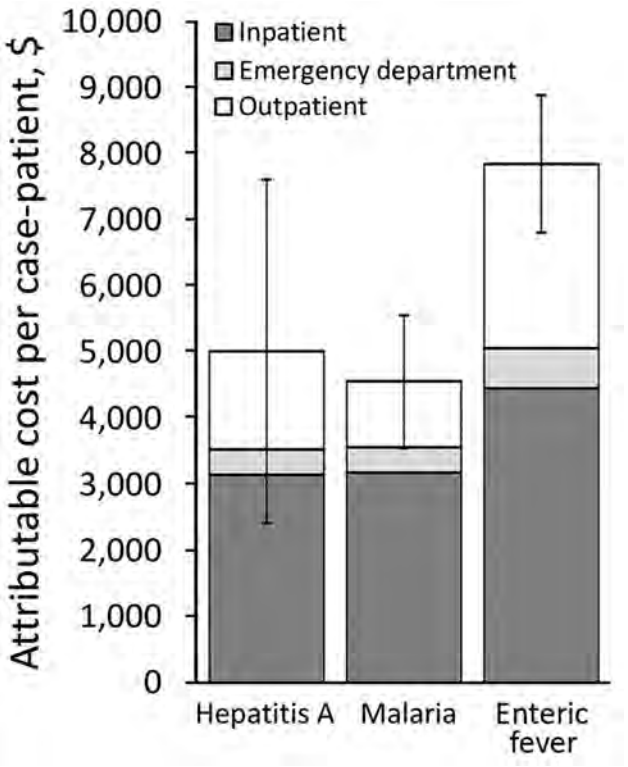

Figure 2. Attributable 90-day healthcare costs in study of direct costs of hepatitis A, malaria, and enteric fever, by disease and healthcare sector, Peel region, Ontario, Canada, 2012–2014. Cost is given in 2015 Canadian dollars. Error bars indicate 95% CIs.

VFR travelers (*20*,*22*). Unlike business or leisure travelers, VFR travelers often stay with family members when visiting and are part of collectivist cultures that place a strong emphasis on acting in the best interest of the family rather than an individual member. These cultural value systems might influence VFR travelers to make decisions to maintain family harmony at the expense of personal health and to go against medical or public health advice to be able to fully participate in cultural activities or rituals that are of value to them (*20*). They also might need to travel in rushed circumstances to attend to a sick or dying relative. To be effective, public health interventions need to consider the complex social environment in which VFR travelers make decisions. Interventions could include leveraging family in peer-education programs, providing culturally appropriate strategies for making safe food and drink choices that are respectful of hosts and enable travelers to participate in valued rituals, and developing streamlined planning resources for rushed travelers.

Because we took the perspective of the healthcare payer, we were unable to estimate costs incurred by new immigrants not yet eligible for publicly funded healthcare. The financial burden, emotional hardship, and negative health impact of the 3-month waiting period policy have been highlighted in a qualitative study (*50*). Whether and how new immigrants access care for reportable travel-related infections and subsequent risks for secondary transmission merits further investigation.

Total costs could have also been underestimated if relevant healthcare encounters of case-patients preceded the index date. The costing method we used, though comprehensive, did not include medical costs incurred by community health centers. Because these centers provide care to a small proportion (1%) of Ontario's population, their exclusion was not anticipated to appreciably change our results. Our analysis also does not consider costs related to secondary cases or outbreaks, although no locally identifiable outbreaks of hepatitis A or enteric fever occurred in the Peel region during the study period.

For pragmatic reasons, our analysis focused on 3 reportable travel-related infections. The true burden of preventable travel-related infections on the healthcare system is expected to be much larger. Likewise, this analysis does not include healthcare costs for other adverse health events associated with travel, such as events related to concurrent medical conditions, incubating disease events, trauma, and heat- and smog-related illnesses that likely also substantially affect travelers. Although case-patients and controls were comparable by key confounding variables available in the health administrative datasets, they might have differed by other factors that were not measurable with the existing data (e.g., factors that influence healthcare-seeking behaviors and costs), which could have led to an overestimation or underestimation of the attributable cost. Last, we estimated the costs of reportable travel-related infections in a VFR traveler population that was primarily foreign-born and traveling to India and Pakistan. Findings might not be generalizable to other settings with different traveler types and travel patterns.

In conclusion, we found that the attributable medical costs of 3 key reportable travel-related infections were substantial and concentrated in the Peel region of Ontario among immigrants who traveled to visit friends or relatives. Our results could be used to parameterize economic evaluations aimed at determining whether subsidizing or eliminating costs of pretravel health services for high-risk travelers or other policies might be cost-effective. As more and more citizens travel and have links to developing countries through birth or parentage, policy makers must consider equitable strategies that are responsive to the evolving health needs of their populations.

Acknowledgment

The authors thank Alex Kopp for methodologic support and the staff of Immigration, Refugees, and Citizenship Canada for providing data to ICES, where the analyses were conducted.

This study was supported by ICES, which is funded by an annual grant from the Ontario Ministry of Health and Long-Term Care. Parts of this material are based on data and/or information compiled and provided by the Canadian Institute for Health Information. However, the analyses, conclusions, opinions, and statements expressed in the material are those of the authors, and not necessarily those of the Canadian Institute for Health Information.

About the Author

Dr. Savage is an epidemiologist and postdoctoral fellow at Women's College Hospital, Toronto, Ontario, Canada. Her interests are in conducting collaborative, applied public health research focused on improving the health of vulnerable populations, including immigrants, older adults, and women.

References

1. Boggild AK, Geduld J, Libman M, Yansouni CP, McCarthy AE, Hajek J, et al. Surveillance report of Zika virus among Canadian travellers returning from the Americas. CMAJ. 2017;189:E334–40. http://dx.doi.org/10.1503/cmaj.161241
2. De Serres G, Markowski F, Toth E, Landry M, Auger D, Mercier M, et al. Largest measles epidemic in North America in a decade—Quebec, Canada, 2011: contribution of susceptibility, serendipity, and superspreading events. J Infect Dis. 2013;207: 990–8. http://dx.doi.org/10.1093/infdis/jis923
3. Boggild AK, Geduld J, Libman M, Ward BJ, McCarthy AE, Doyle PW, et al. Travel-acquired infections and illnesses in Canadians: surveillance report from CanTravNet surveillance data, 2009–2011. Open Med. 2014;8:e20–32.
4. Public Health Ontario. Reportable disease trends in Ontario, 2014 technical report. 2016 Apr [cited 2019 Feb 12]. https://www.publichealthontario.ca/-/media/documents/rdto-2014.pdf?la=en
5. Brophy J, Bui Y, Crockett M, Greenaway C, McCarthy A, Ellia L, et al.; Committee to Advise on Tropical Medicine and Travel. Statement on international travellers who intend to visit friends and relatives. An advisory committee statement (ACS). 2015 Apr [cited 2019 Feb 12]. https://www.canada.ca/content/dam/phac-aspc/migration/phac-aspc/tmp-pmv/catmat-ccmtmv/assets/pdfs/friends-amis-eng.pdf
6. Zimmer R. A forgotten vulnerable group: Canadian children visiting relatives in the developing world. CMAJ. 2018;190:E1023. http://dx.doi.org/10.1503/cmaj.70191
7. Lee CS, Gregson DB, Church D, Laupland KB, Eckhardt R, Ross T, et al. Population-based laboratory surveillance of imported malaria in metropolitan Calgary, 2000–2011. PLoS One. 2013;8:e60751. http://dx.doi.org/10.1371/journal.pone.0060751
8. Horn M, Ratansi A, Varia M. Encouraging travellers to take preventive measures against travel-related communicable diseases: a rapid review of the literature. 2013 Jul 12 [cited 2019 Feb 12]. http://www.peelregion.ca/health/library/pdf/travellers-preventive-measures.pdf
9. Bacaner N, Stauffer B, Boulware DR, Walker PF, Keystone JS. Travel medicine considerations for North American immigrants visiting friends and relatives. JAMA. 2004;291:2856–64. http://dx.doi.org/10.1001/jama.291.23.2856
10. Ericsson CD, Hatz C, Leder K, Tong S, Weld L, Kain KC, et al.; GeoSentinel Surveillance Network. Illness in travelers visiting friends and relatives: a review of the GeoSentinel Surveillance Network. Clin Infect Dis. 2006;43:1185–93. http://dx.doi.org/10.1086/507893
11. Bui YG, Trépanier S, Milord F, Blackburn M, Provost S, Gagnon S. Cases of malaria, hepatitis A, and typhoid fever among VFRs, Quebec (Canada). J Travel Med. 2011;18:373–8. http://dx.doi.org/10.1111/j.1708-8305.2011.00556.x
12. Baggett HC, Graham S, Kozarsky PE, Gallagher N, Blumensaadt S, Bateman J, et al. Pretravel health preparation among US residents traveling to India to VFRs: importance of ethnicity in defining VFRs. J Travel Med. 2009;16:112–8. http://dx.doi.org/10.1111/j.1708-8305.2008.00284.x
13. Van Herck K, Castelli F, Zuckerman J, Nothdurft H, Van Damme P, Dahlgren AL, et al. Knowledge, attitudes and practices in travel-related infectious diseases: the European airport survey. J Travel Med. 2004;11:3–8. http://dx.doi.org/10.2310/7060.2004.13609
14. Schlagenhauf P, Weld L, Goorhuis A, Gautret P, Weber R, von Sonnenburg F, et al.; EuroTravNet. Travel-associated infection presenting in Europe (2008–12): an analysis of EuroTravNet longitudinal, surveillance data, and evaluation of the effect of the pre-travel consultation. Lancet Infect Dis. 2015; 15:55–64. http://dx.doi.org/10.1016/S1473-3099(14)71000-X
15. Committee to Advise on Tropical Medicine and Travel. Statement on hepatitis vaccines for travellers. An advisory committee statement (ACS). Can Commun Dis Rep. 2008;34(ACS-2):1–24.
16. Greenaway C, Schofield S, Henteleff A, Plourde P, Geduld J, Abdel-Motagally M, et al. Summary of the statement on international travellers and typhoid by the Committee to Advise on Tropical Medicine and Travel (CATMAT). Can Commun Dis Rep. 2014;40:60–70. http://dx.doi.org/10.14745/ccdr.v40i04a01
17. Boggild A, Brophy J, Charlebois P, Crockett M, Geduld J, Ghesquiere W, et al.; Committee to Advise on Tropical Medicine and Travel. Canadian recommendations for the prevention and treatment of malaria: an advisory committee statement (ACS). 2014 May [cited 2019 Feb 12]. http://publications.gc.ca/pub?id=9.699136&sl=0
18. Ontario Ministry of Health and Long-Term Care. Fact sheet: travel medicine services. Ontario health insurance plan. 1998 [cited 2019 Feb 12]. http://www.health.gov.on.ca/en/pro/programs/ohip/bulletins/4317/bul4317b.aspx
19. Seale H, Kaur R, Mahimbo A, MacIntyre CR, Zwar N, Smith M, et al. Improving the uptake of pre-travel health advice amongst migrant Australians: exploring the attitudes of primary care providers and migrant community groups. BMC Infect Dis. 2016;16:213. http://dx.doi.org/10.1186/s12879-016-1479-1
20. Savage RD, Rosella LC, Crowcroft NS, Arneja J, de Villa E, Horn M, et al. How can we keep immigrant travelers healthy? Health challenges experienced by Canadian South Asian travelers visiting friends and relatives. Qual Health Res. 2018;28:610–23. http://dx.doi.org/10.1177/1049732317746381
21. Angell SY, Cetron MS. Health disparities among travelers visiting friends and relatives abroad. Ann Intern Med. 2005;142:67–72. http://dx.doi.org/10.7326/0003-4819-142-1-200501040-00013
22. Neave PE, Behrens RH, Jones CO. "You're losing your Ghanaianess": understanding malaria decision-making among Africans visiting friends and relatives in the UK. Malar J. 2014;13:287. http://dx.doi.org/10.1186/1475-2875-13-287
23. Dario Balca. Travel vaccines should be covered by OHIP: Toronto Public Health. CTV News Toronto. 2015 Jul 1 [cited 2019 Feb 12]. https://toronto.ctvnews.ca/travel-vaccines-should-be-covered-by-ohip-toronto-public-health-1.2449553
24. Harling R, Crook P, Lewthwaite P, Evans M, Schmid ML, Beeching NJ. Burden and cost of imported infections admitted to infectious diseases units in England and Wales in 1998 and 1999. J Infect. 2004;48:139–44. http://dx.doi.org/10.1016/S0163-4453(03)00080-X
25. Reddy S, Rangaiah J, Addiman S, Wareham D, Wilson P, Sefton A. Epidemiology, antibiotic resistance trends and the cost of

enteric fever in East London, 2005–2010. Travel Med Infect Dis. 2011;9:206–12. http://dx.doi.org/10.1016/j.tmaid.2011.03.003
26. Rees E, Saavedra-Campos M, Usdin M, Anderson C, Freedman J, de Burgh J, et al. Trend analysis of imported malaria in London; observational study 2000 to 2014. Travel Med Infect Dis. 2017;17:35–42. http://dx.doi.org/10.1016/j.tmaid.2017.04.004
27. Peel Data Centre, Region of Peel. 2011 NHS bulletin: immigration and citizenship. 2013 May [cited 2019 Feb 12]. http://www.peelregion.ca/planning/pdc/pdf/Immigration_Citizenship_Bulletin.pdf
28. Statistics Canada. Census profiles, 2016 Census. 2018 May 30 [cited 2019 Feb 12]. http://www12.statcan.gc.ca/census-recensement/2016/dp-pd/prof/index.cfm?Lang=E
29. Government of Ontario. Health Protection and Promotion Act, R.S.O. 1990, c. H.7. 2011.
30. Harron KL, Doidge JC, Knight HE, Gilbert RE, Goldstein H, Cromwell DA, et al. A guide to evaluating linkage quality for the analysis of linked data. Int J Epidemiol. 2017;46:1699–710. http://dx.doi.org/10.1093/ije/dyx177
31. Canadian Institute for Health Information. DAD abstracting manual, 2015–2016 Edition. Ottawa, Canada: The Institute; 2015.
32. Wilkins R. PCCF+ Version 4D User's Guide (Geocodes/PCCF). Automated geographic coding based on the Statistics Canada postal code conversion files, including postal codes to December 2003. Ottawa (Canada): Statistics Canada; 2004.
33. Chiu M, Lebenbaum M, Lam K, Chong N, Azimaee M, Iron K, et al. Describing the linkages of the Immigration, Refugees and Citizenship Canada Permanent Resident data and Vital Statistics Death Registry to Ontario's administrative health database. BMC Med Inform Decis Mak. 2016;16:135. http://dx.doi.org/10.1186/s12911-016-0375-3
34. Goel R, Beder M. Welcome to Canada ... but don't get sick. CMAJ. 2012;184:E103. http://dx.doi.org/10.1503/cmaj.111095
35. The Johns Hopkins University Bloomberg School of Public Health. The Johns Hopkins ACG® System: excerpt from technical reference guide version 9.0. 2009 Dec [cited 2019 Feb 12]. https://www.healthpartners.com/ucm/groups/public/@hp/@public/documents/documents/dev_057914.pdf
36. Austin PC, Walraven C. The mortality risk score and the ADG score: two points-based scoring systems for the Johns Hopkins Aggregated Diagnosis Groups to predict mortality in a general adult population cohort in Ontario, Canada. Med Care. 2011;49:940–7. http://dx.doi.org/10.1097/MLR.0b013e318229360e
37. Heymann D. Control of communicable diseases manual. 19th edition. Washington, DC: American Public Health Association; 2008.
38. Wodchis WP, Bushmeneva K, Nikitovic M, McKillop I. Guidelines on person-level costing using administrative databases in Ontario. 2013 May [cited 2019 Feb 12]. http://www.hsprn.ca/uploads/files/Guidelines_on_PersonLevel_Costing_May_2013.pdf
39. Normand ST, Landrum MB, Guadagnoli E, Ayanian JZ, Ryan TJ, Cleary PD, et al. Validating recommendations for coronary angiography following acute myocardial infarction in the elderly: a matched analysis using propensity scores. J Clin Epidemiol. 2001;54:387–98. http://dx.doi.org/10.1016/S0895-4356(00)00321-8
40. Austin PC. An introduction to propensity score methods for reducing the effects of confounding in observational studies. Multivariate Behav Res. 2011;46:399–424. http://dx.doi.org/10.1080/00273171.2011.568786
41. Rosella LC, Lebenbaum M, Fitzpatrick T, O'Reilly D, Wang J, Booth GL, et al. Impact of diabetes on healthcare costs in a population-based cohort: a cost analysis. Diabet Med. 2016;33:395–403. http://dx.doi.org/10.1111/dme.12858
42. Public Health Ontario. Monthly infectious disease surveillance reports. Data reports 2017 Nov 9 [cited 2019 Feb 12]. https://www.publichealthontario.ca/en/data-and-analysis/infectious-disease/infectious-diseases-monthly
43. Canadian Institute for Health Information. National health expenditure trends, 1975 to 2018. 2018 Nov [cited 2019 Feb 12]. https://www.cihi.ca/sites/default/files/document/nhex-trends-narrative-report-2018-en-web.pdf
44. National Health Service England. National tariff payment system 2014/15. 2013 Dec 17 [cited 2019 Feb 12]. https://www.gov.uk/government/publications/national-tariff-payment-system-2014-to-2015
45. Parry CM, Hien TT, Dougan G, White NJ, Farrar JJ. Typhoid fever. N Engl J Med. 2002;347:1770–82. http://dx.doi.org/10.1056/NEJMra020201
46. Zhou K, Sauve LJ, Richardson SE, Ford-Jones EL, Morris SK. Enteric fever in a multicultural Canadian tertiary care pediatric setting: a 28-year review. J Pediatric Infect Dis Soc. 2017;6:98–101.
47. Ontario Ministry of Health and Long-Term Care. Infectious diseases protocol, 2016. Ontario Public Health Standards. Toronto: The Ministry; 2016.
48. Epson EE, Cronquist A, Lamba K, Kimura AC, Hassan R, Selvage D, et al. Risk factors for hospitalisation and associated costs among patients with hepatitis A associated with imported pomegranate arils, United States, 2013. Public Health. 2016;136:144–51. http://dx.doi.org/10.1016/j.puhe.2016.03.027
49. Morey RJ, Collier MG, Nelson NP. The financial burden of public health responses to hepatitis A cases among food handlers, 2012-2014. Public Health Rep. 2017;132:443–7. http://dx.doi.org/10.1177/0033354917710947
50. Goel R, Bloch G, Caulford P. Waiting for care: effects of Ontario's 3-month waiting period for OHIP on landed immigrants. Can Fam Physician. 2013;59:e269–75.

Address for correspondence: Rachel D. Savage, Women's College Hospital, 76 Grenville St, Toronto, ON M5S 1B2, Canada; email: rachel.savage@wchospital.ca

17DD Yellow Fever Revaccination and Heightened Long-Term Immunity in Populations of Disease-Endemic Areas, Brazil

Ana Carolina Campi-Azevedo, Vanessa Peruhype-Magalhães, Jordana Grazziela Coelho-dos-Reis, Lis Ribeiro Antonelli, Christiane Costa-Pereira, Elaine Speziali, Laise Rodrigues Reis, Jandira Aparecida Lemos, José Geraldo Leite Ribeiro, Luiz Antônio Bastos Camacho, Maria de Lourdes de Sousa Maia, Sheila Maria Barbosa de Lima, Marisol Simões, Reinaldo de Menezes Martins, Akira Homma, Luiz Cosme Cota Malaquias, Pedro Luiz Tauil, Pedro Fernando Costa Vasconcelos, Alessandro Pecego Martins Romano, Carla Magda Domingues, Andréa Teixeira-Carvalho, Olindo Assis Martins-Filho; Collaborative Group for Studies of Yellow Fever Vaccine

We evaluated the duration of neutralizing antibodies and the status of 17DD vaccine–specific T- and B-cell memory following primary and revaccination regimens for yellow fever (YF) in Brazil. We observed progressive decline of plaque-reduction neutralization test (PRNT) seropositivity and of the levels of effector memory CD4+ and CD8+ T cells, as well as interferon-γ+CD8+ T cells, 10 years after primary vaccination. Revaccination restored PRNT seropositivity as well as the levels of effector memory CD4+, CD8+, and interferon-γ+CD8+ T cells. Moreover, secondary or multiple vaccinations guarantee long-term persistence of PRNT positivity and cell-mediated memory 10 years after booster vaccination. These findings support the relevance of booster doses to heighten the 17DD-YF–specific immune response to guarantee the long-term persistence of memory components. Secondary or multiple vaccinations improved the correlates of protection triggered by 17DD-YF primary vaccination, indicating that booster regimens are needed to achieve efficient immunity in areas with high risk for virus transmission.

Author affiliations: Instituto René Rachou of Fundação Oswaldo Cruz (FIOCRUZ-Minas), Belo Horizonte, Brazil (A.C. Campi-Azevedo, V. Peruhype-Magalhães, J.G. Coelho-dos-Reis, L.R. Antonelli, C. Costa-Pereira, E. Speziali, L.R. Reis, A. Teixeira-Carvalho, O.A. Martins-Filho); Universidade Federal de Minas Gerais, Belo Horizonte (J.G. Coelho-dos-Reis); Secretaria Municipal de Saúde, Belo Horizonte (J.A. Lemos); Secretaria do Estado de Saúde de Minas Gerais, Belo Horizonte (J.G.L. Ribeiro); Escola Nacional de Saúde Pública (FIOCRUZ-Rio), Rio de Janeiro, Brazil (L.A.B. Camacho); Instituto de Tecnologia em Imunobiológicos Bio-Manguinhos (FIOCRUZ-Rio), Rio de Janeiro (M. de Lourdes de Sousa Maia, S.M. Barbosa de Lima, M. Simões, R. de Menezes Martins, A. Homma); Universidade Federal de Alfenas, Alfenas, Brazil (L.C.C. Malaquias); Universidade de Brasília, Brasília, Brazil (P.L. Tauil); Instituto Evandro Chagas, Ananindeua, Brazil (P.F.C. Vasconcelos); Secretaria de Vigilância em Saúde—Ministério da Saúde, Brasília (A.P.M. Romano, C.M. Domingues)

DOI: https://doi.org/10.3201/eid2508.181432

Yellow fever (YF) vaccination is recommended for persons living in YF-endemic areas as the most effective strategy to reduce the risk for infection (*1*). The 17D and 17DD live attenuated vaccines are considered similarly safe and immunogenic, regardless of the minor differences in their nucleotide sequences (*1*). The progressive expansion of areas with YF viral circulation in YF-endemic countries has required extensive vaccination campaigns that reduced the international vaccine stockpile and brought to light the discussion about the need for booster doses to guarantee long-term cell memory in populations living in YF-endemic countries. Outbreaks of YF occur occasionally in areas of Africa and South America (*2*–*7*).

In 2013, the World Health Organization (WHO) stated that a single dose of YF vaccine sufficed to provide lifelong protection and that no booster dose was required to guarantee protection against the disease (*1*,*8*). However, time-dependent loss of protective immunity has been reported (*9*–*11*). The levels of YF-neutralizing antibodies decrease significantly 10 years after vaccination; ≈25%–30% of primary vaccinees lack protective antibodies (*10*,*11*). In addition, the polyfunctional cellular immune responses elicited by YF vaccination that contribute to protection also

displayed a time-dependent decline following primary vaccination (*11*,*12*). In light of this information, the single-dose regimen for YF vaccine has been questioned, especially in YF-endemic countries where the proportion of persons exposed to potential risks should be considered against the primary-vaccine failure rate and time-dependent decline of protective immunity.

The goal of this study was to evaluate the proxies of protection elicited by primary, secondary, and multiple vaccinations and verify the duration of neutralizing antibodies and 17DD-specific T- and B-cell memory following these distinct vaccination regimens. We sought to clarify the importance of 17DD-YF booster vaccination to heighten the immune response of those primary vaccinees living in endemic areas whose immunity declines to nonprotective levels.

Materials and Methods

Study Population

We conducted this investigation during May 12, 2014–December 16, 2016, simultaneously sampling from Rio de Janeiro and 2 municipalities of Minas Gerais state (Alfenas and Ribeirão das Neves), Brazil. We assigned participants to groups on the basis of official vaccination records. The study included 421 samples collected from 326 healthy adults 18–77 years of age, initially categorized into 3 arms: primary vaccination, secondary vaccination, and multiple vaccination (Figure 1). We designed the primary vaccination and secondary vaccination arms as 2 complementary independent approaches, each including a longitudinal (95 paired samples) and a cross-sectional investigation (231 unpaired samples). Study groups were coded to indicate participants' vaccination status (NV for nonvaccinated persons, PV for those who had had primary YF vaccination only, RV for those who had been revaccinated) and time since last vaccination, given in days or years (e.g, d0 for day zero).

Samples and Tests

We collected whole blood samples from each participant. We used samples of 5 mL without anticoagulant for plaque-reduction neutralization test (PRNT) and samples of 20 mL in heparin for 17DD-YF phenotypic and functional analyses.

PRNT

We used serum samples to quantify the PRNT levels to the 17DD-YF virus by the micro-PRNT50 test, as described previously by Simões et al. (*13*). We performed assays at Laboratório de Tecnologia Virológica (LATEV), Bio-Manguinhos, and expressed results from replicates as the reciprocal of sample dilution, considering seropositivity of PRNT titers >1:50 serum dilution.

Dengue IgG Indirect ELISA

We performed serologic tests for dengue virus (DENV) IgG using a Panbio dengue IgG indirect ELISA kit (https://www.alere.com). Tests were performed at Laboratório de Flavivírus, Instituto Osvaldo Cruz, as previously reported (*14*).

Phenotypic and Functional Memory Biomarkers

We performed in vitro 17DD-YF–specific peripheral blood lymph proliferative assay as previously reported by Costa-Pereira et al. (*12*). In brief, we incubated replicates of PBMC suspension (1.0×10^6/well) for 144 hours at 37°C in 5% CO_2. We harvested cells from control (CC) and 17DD-YF antigen–stimulated (17DD-YF Ag) cultures, labeled them with live/dead dye (Life Technologies, https://www.thermofisher.com), and used a cocktail of monoclonal antibodies (mAbs) to quantify the phenotypic memory status of T cells and B cells. For T cells we used anti-CD4/(RPA-T4)/FITC, anti-CD8/(SK1)/PerCP-Cy5.5, anti-CD27/(M-T271)/PE, anti-CD45RO/(UCHL1)/PE-Cy7, and anti-CD3/

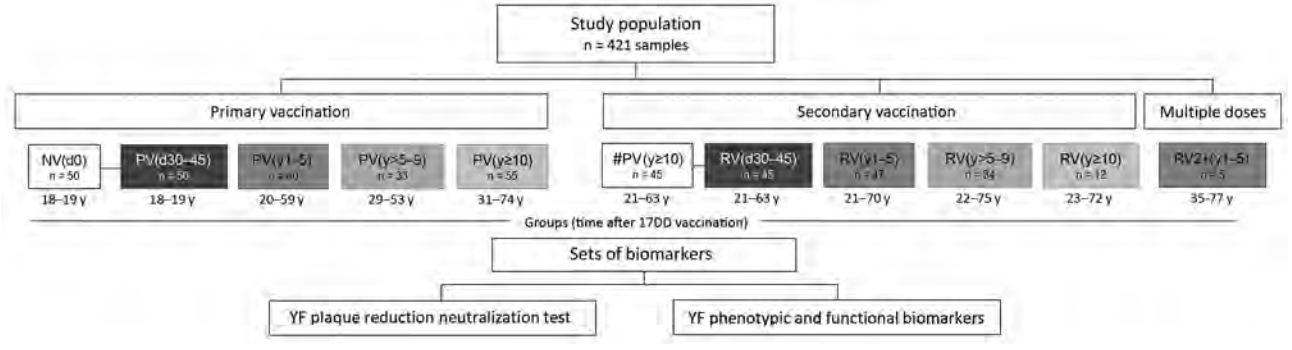

Figure 1. Study population and methods for analyzing 17DD vaccine–specific neutralizing antibodies and phenotypic/functional cell memory in YF. The primary vaccination arm (reference group) includes participants who have never been vaccinated or have had 1 YF vaccination; secondary vaccination arm includes participants who have received 1 or 2 vaccinations; and multiple doses arm includes participants who have received ≥2 revaccinations. Participant subgroups indicate number of days or years since vaccination (in parentheses; d0 for those never vaccinated). Participant age ranges are given below subgroup boxes. #PV, had primary vaccination ≥10 years previously; NV, not vaccinated; PV, had primary vaccination only; RV, revaccinated; YF, yellow fever.

(SK7)/APC-Cy7; for B cells, we used anti-CD19/(HIB19)/PerCP, anti-CD27/(M-T271)/PE, and anti-IgD/(IA6–2)/FITC. We obtained all mAbs from BD Pharmingen (https://bdbiosciences.com).

In parallel, we stained cultured PBMC aliquots with live/dead dye and a mix of mAbs to quantify the functional memory status of T and B cells: anti-CD3/(UCHT1)/Qdot605 (Invitrogen, https://www.thermofisher.com); anti-CD4/(GK1.5)/APCe-Fluor780 (eBioscience, https://www.thermofisher.com); anti-CD8/(SK1)/PerCP (BD Biosciences, https://bdbiosciences.com); and anti-CD19/(HIB19)/Alexa-Fluor700 (eBioscience). After a fix/permeabilize procedure, we incubated cells with a mAbs cocktail of anti-TNF-α/(clone MAb11)/PE-Cy7, anti-interferon (IFN)-γ/(clone B27)/Alexa-Fluor488), anti-interleukin (IL)-5/(JES1–39D10)/PE, and anti-IL-10/(JES3–19F1)/APC, all from BD Biosciences. We fixed the stained cells and stored them at 4°C for ≤24 hours before acquisition on a BD LSR Fortessa Flow Cytometer (BD Biosciences).

We acquired a total of 100,000 lymphocytes from each sample. We used FlowJo version 9.3.2 software (Tree Star, https://www.flowjo.com) to quantify the memory T-cell and B-cell subsets, as well as the percentage of cytokine-producing T and B cells. We expressed the results as 17DD-YF Ag/CC Index, calculated as the ratio of cells observed in the 17DD-YF Ag cultures divided by the respective control culture.

Data Analysis

This study was composed of 2 independent but complementary approaches: a longitudinal investigation and a cross-sectional investigation. We performed statistical analyses for the longitudinal investigation using paired t-test to compare NV(d0) versus PV(d30–45) groups for primary vaccination, as well as #PV(y≥10) (primary vaccination >10 years ago) versus RV(d30–45) for secondary vaccination. For the cross-sectional design, we made the transversal comparisons among groups using analysis of variance adjusted to multiple comparisons and set statistical significance at $p<0.05$. (We did not highlight nonsignificant differences in the figures.) We used the χ^2 test to compare seropositivity rates between NV and PV groups and also between #PV and RV groups.

We performed biomarker signature analysis as described previously by Luiza-Silva et al. (*15*). In brief, we calculated the global median value of 17DD-YF Ag/CC Index for each phenotypic and functional biomarker and used that value as the cutoff to identify each biomarker as low index (below global median) or high index (above global median). We considered only biomarkers observed in >50% of study participants for comparative analysis among groups.

We conducted Venn diagram analysis (http://bioinformatics.psb.ugent.be/webtools/Venn) to select common biomarkers among subgroups. We overlaid biomarker signatures for comparative analysis of time-dependent changes of biomarker sets observed after vaccination.

Results

Booster Vaccination and PRNT

Data analysis demonstrated that primary vaccination triggered significant levels of 17DD-YF–specific neutralizing antibodies ($p<0.0001$), reaching a seropositivity rate of 96% (Figure 2). Of note, we observed progressive decrease in PRNT levels ($p<0.0001$) and in the PRNT seropositivity rates along the time compared with PV(d30–45). The seropositivity rate declined to ≈71% by 10 years after

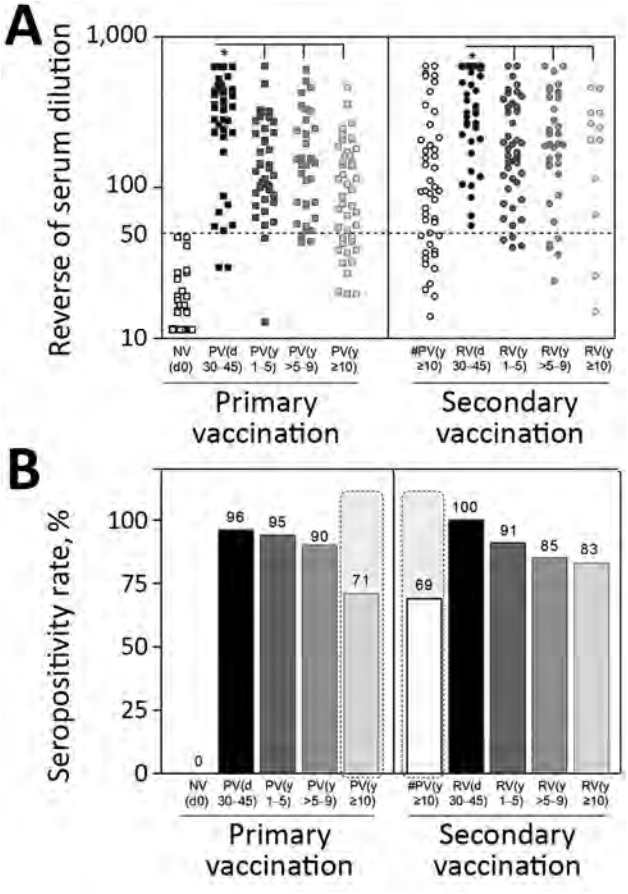

Figure 2. Neutralizing antibody levels and seropositivity rates before and after primary and secondary 17DD vaccination for YF. We detected 17DD-specific neutralizing antibodies by micro plaque-reducing neutralization test (micro-PRNT50) and determined seropositivity rates by considering serum dilution >1:50 as the cutoff criterion for PRNT positivity. A) Scatter graph of PRNT titers, expressed as reverse of serum dilution. B) Percentage of PRNT seropositivity (serum dilution >1:50). Gray dashed lines indicate critical seropositivity rates <80%. Participant subgroups indicate number of days or years since vaccination (in parentheses; d0 for those never vaccinated). #PV, had primary vaccination ≥10 years previously; NV, not vaccinated; PV, had primary vaccination only; RV, revaccinated; YF, yellow fever.

primary vaccination (Figure 2, panel B). Booster vaccination significantly increased the PRNT levels ($p<0.0001$) and raised the seropositivity rate from 69% to 100% (Figure 2, panels A, B). The secondary vaccination was accompanied by higher seropositivity rate after 10 years upon booster dose, regardless of the decrease in PRNT levels ($p<0.0001$) observed over time compared with #PV(d30–45) (Figure 2, panel B).

Secondary Booster Vaccination and YF-specific Cell-Mediated Memory

Comparative analysis of NV(d0) versus PV(d30–45) after 1 or 2 doses of 17DD-YF vaccine demonstrated that primary vaccination is followed by an increase of memory T cells, including eEfCD4 ($p<0.05$), EMCD4 ($p<0.05$), and EMCD8 ($p = 0.0006$), and all B-cell subsets evaluated, NCD19 ($p = 0.01$), nCMCD19 ($p = 0.001$), and CMCD19 ($p = 0.001$). We also observed a decrease of NCD8 ($p = 0.02$), eEfCD8 ($p = 0.02$), and CMCD8 ($p = 0.001$). The results showed that cellular immunity, eEfCD4 ($p = 0.01$), EMCD4 ($p = 0.01$), and EMCD8 ($p = 0.009$); and all B-cell subsets, NCD19 ($p = 0.003$), nCMCD19 ($p = 0.02$), and CMCD19 ($p = 0.0002$), clearly wane over 10 years, compared with 30–45 days after primary vaccination (Figure 3, https://wwwnc.cdc.gov/EID/article/25/8/18-1432-F3.htm).

Secondary vaccination with 17DD-YF was able not only to increase the level of memory T-cell subsets, eEfCD4 ($p<0.05$), EMCD4 ($p<0.05$), and EMCD8 ($p = 0.04$) at 30–45 days after the second dose but also to sustain the maintenance of eEfCD4 and EMCD8 levels even after ≥10 years upon booster vaccination compared with 30–45 days after secondary vaccination. We observed no substantial changes in memory B-cell subsets upon secondary vaccination (Figure 3).

Revaccination and IFN-γ–Mediated T-Cell Memory

Data analysis for in vitro 17DD-YF antigen recall revealed that primary vaccination induced significant increases of functional memory biomarkers in CD4+ (tumor necrosis factor [TNF]–α/$p = 0.04$, IFN-γ/$p = 0.04$ and IL-5/$p = 0.0001$) and CD8+ T cells (TNF-α/$p = 0.0003$, IFN-γ/$p = 0.008$ and IL-5/$p = 0.0002$) as well as in B cells (TNF-α/$p<0.05$ and IL-5/$p = 0.016$) (Figure 4). We observed a decrease of IL-10+CD4+ T cells ($p = 0.04$) at 30–45 days after primary vaccination and a clear decrease of TNF-α, IFN-γ, and IL-5 produced by CD4+ and CD8+ T cells. We also saw a decrease in TNF-α and IL-5 from B cells over time, particularly at >10 years, compared with 30–45 days after primary vaccination ($p<0.05$ in all cases). Conversely, we detected an increase of IL-10+ B cells over time after primary vaccination (Figure 4).

Secondary vaccination was able to restore T-cell functional memory mediated by IFN-γ and B-cell functional memory by TNF-α. We observed sustained production of IFN-γ by CD8+ T cells even ≥10 years after booster vaccination (Figure 4).

Booster Vaccination and Long-lasting Persistence of Effector Memory

We constructed overlays of biomarker signatures of NV(d0) versus PV(d30–45) in the primary-vaccination arm of the study as well as #PV(y≥10) versus RV(d30–45) in the secondary-vaccination arm to select those attributes eligible as universal memory-related biomarkers (Appendix Figure 1, https://wwwnc.cdc.gov/EID/article/25/8/18-1432-App1.pdf). Venn diagram analysis revealed 3 common attributes (EMCD4, EMCD8, and IFNCD8) that we tagged for follow-up analysis after primary, secondary, or multiple 17DD-YF vaccination (Appendix Figure 1).

After we selected the universal set of follow-up attributes, we compared biomarker signatures over time after 17DD-YF primary or secondary vaccination (Figure 5). Data analysis demonstrated that all 3 biomarkers were observed in PV(d30–45) and PV(y1–5). EMCD8 was maintained in PV(y>5–9) but not in PV(y≥10). Comparative analysis between #PV(y≥10) and RV(d30–45) demonstrated restoration of universal memory-related biomarkers (EMCD4, EMCD8, and IFNCD8) upon revaccination. Moreover, we identified EMCD8 in a high proportion of secondary vaccinees across the time periods after booster dose (Figure 5).

Comparison of 17DD-YF Primary and Booster Vaccination Effects on Cell-Mediated Memory

We used individual PRNT and EMCD8 profiles to assemble a memory matrix and calculated the resultant YF-specific memory. We classified each volunteer by positive results above the cutoff threshold as EMCD8, PRNT, none, or both (Figure 6). Data analysis demonstrated that primary vaccination leads to a resultant memory in 97% of volunteers, with 3% of failure in the PV(d30–45) group. However, an increase in the proportion of primary vaccinees with "none" positive attributes, neither PRNT nor EMCD8 biomarkers, was observed, reaching a critical value of 30% at ≥10 years after primary vaccination (Figure 6, panel A).

The comparison between #PV(y≥10) and RV(d30–45) demonstrated that secondary vaccination restored the resultant memory in 100% of the volunteers, which was different from primary vaccination results. All secondary vaccines evaluated simultaneously for PRNT and EMCD8 profile presented a preserved resultant memory. In particular, at ≥10 years after secondary vaccination, 100% of vaccinees had 1 or both biomarkers detectable (Figure 6, panel B).

Multiple Vaccination and the Overall Profile of Protection

We analyzed 17DD-YF memory status triggered by multiple vaccinations (Figure 7). The results demonstrated that

all vaccinees who received multiple shots had PRNT levels above the cutoff limit (Figure 7, panel A). The proportion of vaccinees with EMCD8 above the cutoff limit was higher for RV(y1–5) and RV2+(y1–5) than for PV(y1–5) (Figure 7, panel B). Likewise, the overall resultant memory for RV(y1–5) and RV2+(y1–5) was higher than that for PV(y1–5) – (Figure 7, panel C).

PRNT Seronegativity before Revaccination and Cell-Mediated Memory Response

The volunteers from the #PV(y≥10) group were further categorized into subgroups, PRNT– and PRNT+, according to their PRNT results before revaccination. The levels of humoral and cellular biomarkers, as well as the magnitude of baseline fold changes in neutralizing antibodies, were higher in PRNT– than in PRNT+ vaccines (Figures 8, 9). An increase in PRNT titer by a factor >4 at follow-up further demonstrated the relevance of booster doses to restore the immunological memory of these subjects (Figure 8). Furthermore, the booster dose had higher impact on cellular immunity and biomarker signature of PRNT– than PRNT+ primary vaccinees, and both groups restored the EMCD8 biomarker compared with the #PV(y≥10) group (Figure 9).

Dengue Virus Seropositivity

We analyzed the results to determine whether DENV seropositivity influences the humoral and cellular memory after secondary vaccination (Appendix Figures 2, 3). We found DENV seropositivity in 28% of volunteers in the secondary vaccination arm. The results demonstrated that DENV seropositivity did not influence PRNT seropositivity

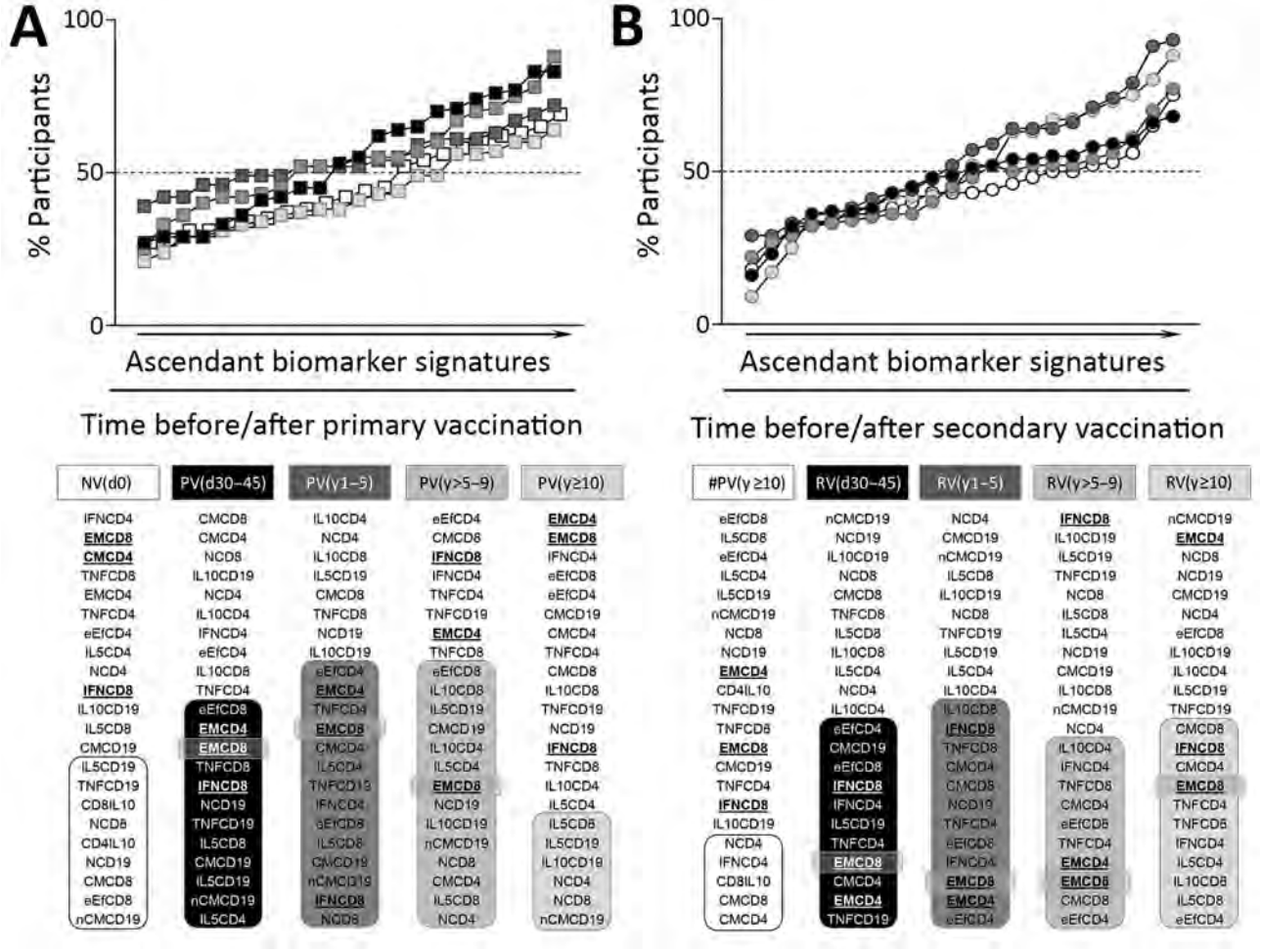

Figure 5. Ascendant biomarker signatures before and after primary and secondary 17DD vaccination for YF. Overlaid biomarker signatures were assembled to identify changes in the 17DD-specific phenotypic and functional features observed over time in primary vaccination arm (A) and secondary vaccination arm (B). Shading indicates time point before and after primary or secondary vaccination for each biomarker; dashed line indicates the global median >50th percentile. Boldface text indicates the 3 biomarkers considered relevant universal attributes to monitor 17DD-YF–specific memory (EMCD4, EMCD8, IFNCD8). Participant subgroups indicate number of days or years since vaccination (in parentheses; d0 for those never vaccinated). IFN, interferon; IL, interleukin; TNF, tumor necrosis factor; YF, yellow fever.

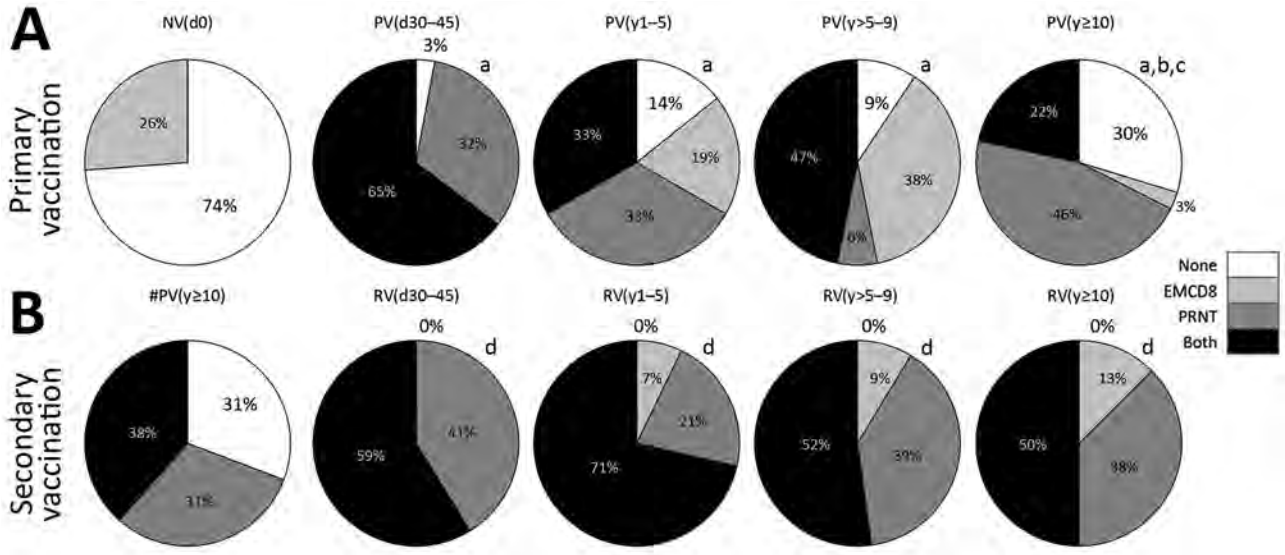

Figure 6. Overall proportion of participants with resultant memory before and after primary or secondary 17DD vaccination for YF as assessed by PRNT and EMCD8 measurement at participant level. Graphs show the proportion of participants above the cutoff threshold; that is, PRNT positivity at serum dilution >1:50 and EMCD8 index above the global median value. We then determined the resultant memory for each subgroup in the primary vaccination arm (A) and secondary vaccination (B) of the study. Participant subgroups indicate number of days or years since vaccination (in parentheses; d0 for those never vaccinated). Lowercase letters indicate significant differences ($p<0.05$ by χ^2 test) of resultant memory status among study groups: a for comparisons with NV(d0) participants; b for comparisons with PV(d30–45) participants; c for comparison with PV(y1–5) participants; and d for comparison with #PV(y≥10) participants. #PV, had primary vaccination ≥10 years previously; NV, not vaccinated; PRNT, plaque-reducing neutralization test; PV, had primary vaccination only; RV, revaccinated; YF, yellow fever.

over time after secondary vaccination (Appendix Figure 2). Moreover, DENV seropositivity did not affect cellular immunity (EMCD8), which remained above the cutoff limit in all subgroups of secondary vaccinees (Appendix Figure 3).

Discussion

YF vaccination induces an efficient immunity and represents one of the most effective strategies to reduce the risk for infection in YF-endemic countries. The vaccine is highly immunogenic, eliciting a strong antibody response together with a broad and complex innate (*16–22*) and adaptive immunity (*23–28*). Although the YF vaccine has been considered a benchmark among vaccines because of its ability to induce long-lasting immune response, the duration of humoral and cellular immunity following YF vaccination is still controversial. Some studies demonstrate that neutralizing antibodies and YF-specific CD8+ T cells after primary vaccination are suggestive imprints compatible with long-lived memory (*8*,*26*,*29–31*); other studies emphasize that the immunity to YF vaccine wanes over time, suggesting the need for booster doses to guarantee long-lasting, efficient immunity memory (*9–12*,*32–36*).

We could not assess protective immunity to YF in humans by challenge with live wild-type YF virus. Therefore, the protective or nonprotective immunity status to YF virus in humans is based on laboratory methods, known as correlates of protection; PRNT level has been considered the standard for measuring postvaccination immunity to YF. Pinpointing cellular immunity biomarkers is relevant in studies that pose the question of whether PRNT seronegativity necessarily means absence of protective immunity (*34*). Our investigation proposes that, in addition to PRNT seropositivity, YF-specific cellular immunity may be a useful tool for monitoring the duration of YF vaccine-induced memory over time. However, upon closer examination, our findings indicate the decline of YF-specific immune response over time, emphasizing that the YF-specific immunity wanes shortly after primary vaccination and that a substantial proportion of primary vaccines (14%–30%) do not present sufficient levels of neutralizing antibodies or CD8+ T-cell memory within 5–10 years after primary vaccination.

Some studies have investigated the relevance of booster doses to heighten the YF-specific immune response in primary vaccinees whose immunity has declined to nonprotective levels. Weiten et al. (*31*) postulated that booster vaccination did not increase the titers of YF-specific antibodies nor induce or alter the phenotypes of CD8+ T cells. Conversely, Kongsgaard et al. (*37*) have demonstrated that, although most vaccinees responded to a booster vaccination, the antibody titers and the cellular immune responses observed following revaccination were lower than for primary vaccination responses. In this study, we have demonstrated that the booster dose was able to upregulate the

levels of neutralizing antibodies and heighten the cellular immunity signature and restore the proportion of vaccinated participants with high levels of effector memory CD8+ T cells. We strongly believe that the differences we observed among the published studies could be attributed to differences in the populations under scrutiny.

The magnitude of increase in the neutralizing antibody titers and YF-specific CD8+ T-cell response achieved with a booster dose may be closely related to the baseline immune activation, suggesting that an activated immune microenvironment before revaccination impairs the response to the YF vaccine. Muyanja et al. (*38*) showed that 17D-204 vaccinees in Africa displayed decreased levels of YF-specific immunity compared with vaccinees in Europe. It is possible that the immune microenvironment affects the quantitative and qualitative response, as well as the vaccine efficacy. Whereas vaccinees in Europe displayed persistent PRNT levels even at 10 years after vaccination, those in Africa exhibited reduced persistence of YF immunological memory. Constant exposure to infectious diseases, as well as diet and gut microbiota, may lead to a state of immune hyperactivation and exhaustion that can contribute to reduced magnitude of cellular and humoral responses and impair the YF

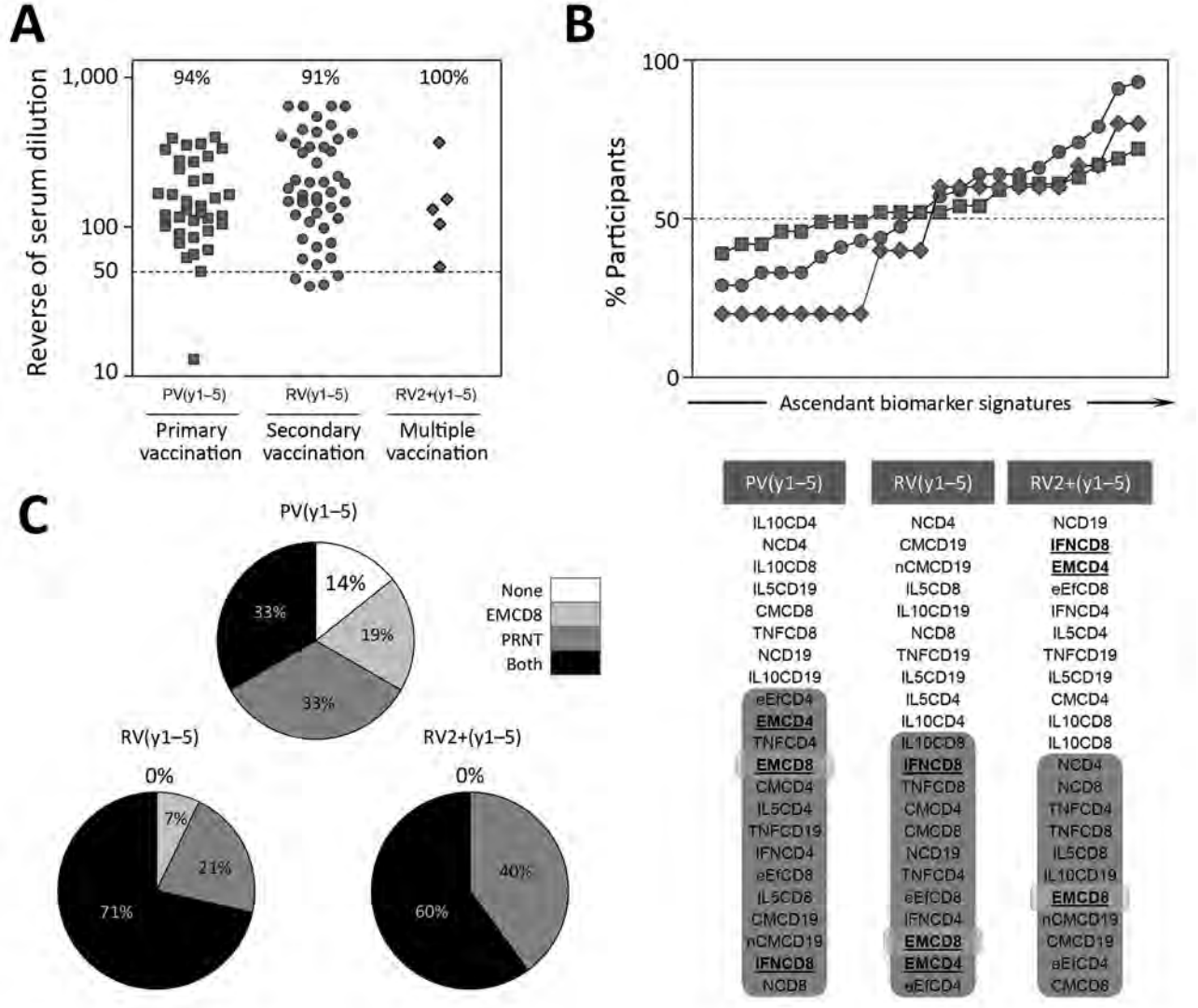

Figure 7. Overall profile of immune response after primary, secondary, or multiple 17DD vaccination for YF. A) Levels of 17DD-YF–specific neutralizing antibodies; B) 17DD-YF–specific phenotypic and functional biomarkers; and C) resultant memory status PRNT and EMCD8 measurement (PRNT and EMCD8) for individual participants. Results are expressed in reverse of serum dilution, percentage of participants with overlaid biomarker signatures, and resultant memory status at 1–5 years after primary (gray circle), secondary (gray square), or multiple (gray diamond) vaccination. Participant subgroups indicate number of days or years since vaccination (in parentheses; d0 for those never vaccinated). #PV, had primary vaccination ≥10 years previously; IFN, interferon; IL, interleukin; NV, not vaccinated; PRNT, plaque-reducing neutralization test; PV, had primary vaccination only; RV, revaccinated; TNF, tumor necrosis factor; YF, yellow fever.

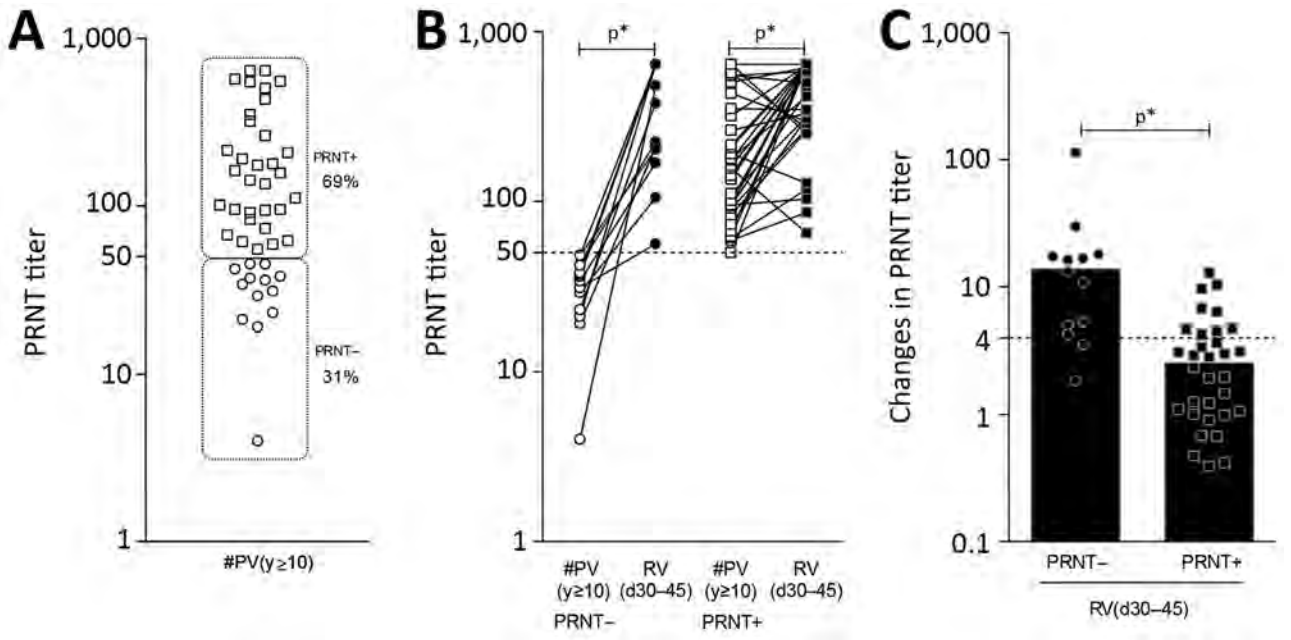

Figure 8. Baseline PRNT reactivity before revaccination (A) and impact on PRNT levels triggered by secondary 17DD vaccination for YF (B, C). Subgroups PRNT– (circles) and PRNT+ (squares) were defined considering the cutoff criterion for PRNT positivity at serum dilution >1:50. The ability of secondary vaccination to increase the levels of neutralizing antibodies as well as the magnitude of changes in PRNT titers (baseline fold changes) are indicated for PRNT– (filled circles) and PRNT+ (filled squares) vaccinees. Increases in PRNT titer by a factor of ≥4 at follow-up were considered as classical criteria to evaluate booster response. Bars indicate significant differences ($p<0.05$) between subgroups. Participant subgroups indicate number of days or years since vaccination (in parentheses). #PV, had primary vaccination ≥10 years previously; PRNT, plaque-reducing neutralization test; RV, revaccinated; YF, yellow fever.

vaccine memory. Of note, the impaired YF vaccine-induced memory was boosted by a second vaccination (*38*). Our results corroborate this hypothesis, showing the relevance of a booster dose to improve the immune response among primary vaccinees. This recommendation should be considered to restore the YF protective immunity in those primary vaccinees whose correlates of protection fade over time, reaching nonprotective levels.

The loss of immunity in a subpopulation of vaccine recipients should be taken into consideration, and a booster dose should be administered. Previous studies have demonstrated that, on average, approximately 1 in 5 persons from non–YF-endemic areas and 3 in 10 persons living in YF-endemic areas may lose measurable antibody responses within 10 years after primary vaccination. In this sense, it is true that the 17DD-YF vaccination elicits long-lasting immunity; however, lifelong immunity is not observed in every vaccinated individual. Although PRNT is the standard assay to monitor YF protective immunity, it is not a feasible method available in local laboratories to identify participants who should receive a booster vaccination.

The expansion of risk areas for YF worldwide has contributed to the depletion of YF vaccine stockpile and the need for new strategies to reverse the imminent shortage of vaccine. WHO has considered measures to improve YF vaccine supply, including a dose-sparing strategy as a short-term measure. However, the dose sparing is not proposed for routine immunization. WHO also considered advising a single lifetime dose of YF vaccine. In YF outbreaks or periods of limited vaccine production and reduced stockpiles, the YF primary vaccination should be the priority, as recommended by the Strategic Advisory Group of Experts on Immunization. However, once the YF vaccine supply has normalized and no outbreaks are reported, revaccination should be suggested. On the basis of our findings, ≥1 booster dose at 10 years after primary vaccination is suggested for travelers entering higher-risk areas and required for residents of YF-endemic countries who are at risk for infection (*34*,*39*).

Altogether, our findings emphasize the relevance of booster doses to heighten the 17DD-YF specific immune response to achieve efficient immunity. Secondary vaccination improved the correlates of protection that had waned over time after 17DD-YF primary vaccination and lowered the loss of protection over time. However, multiple vaccination seems to better support long-lasting protection in all vaccinees, which suggests that ≥3 booster doses at 10-year intervals should be recommended, especially in areas with high risk for YF transmission. Whether the waning of immune markers observed over time is associated with loss of YF vaccine effectiveness

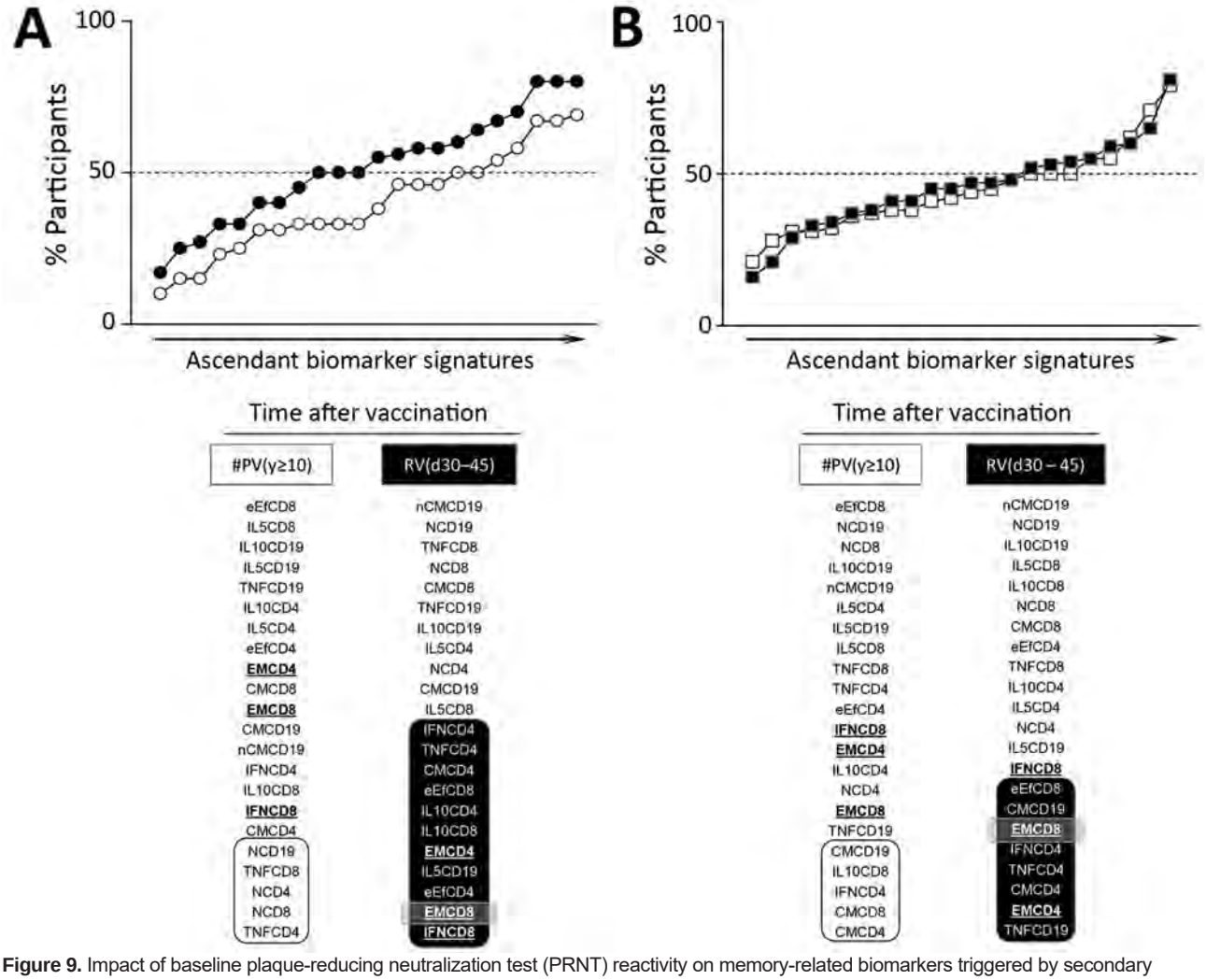

Figure 9. Impact of baseline plaque-reducing neutralization test (PRNT) reactivity on memory-related biomarkers triggered by secondary 17DD vaccination for YF. We assessed the impact of secondary vaccination on phenotypic and functional biomarkers in participants with negative (A) and positive (B) PRNT results. Shading indicates time point after primary vaccination for each biomarker: white for participants who were vaccinated ≥10 years previously, and black for those who were revaccinated in the previous 30–45 days. The dashed line shows the global median >50th percentile. Boldface text indicates the 3 biomarkers considered relevant universal attributes to monitor 17DD-YF–specific memory (EMCD4, EMCD8, IFNCD8). Participant subgroups indicate number of days or years since vaccination (in parentheses). #PV, had primary vaccination ≥10 years previously; IFN, interferon; IL, interleukin; RV, revaccinated; TNF, tumor necrosis factor; YF, yellow fever.

and increased risk for breakthrough YF infection remains to be seen.

In summary, we evaluated the evidence for benefits and risks associated with YF vaccine booster doses using the Grading of Recommendations, Assessment, Development, and Evaluation framework (*40*). A primary dose of YF vaccine is well known to be highly safe and effective, with few vaccine failures. However, a critical wane of correlates of protection has been documented by our group and others, particularly at ≥10 years postvaccination. Few reports of serious adverse events have been observed following booster doses of the vaccine. We recommend the booster dose to prevent this serious disease that has no treatment and substantial mortality rates.

Acknowledgments

We thank the Program for Technological Development in Tools for Health-RPT-FIOCRUZ for the use of the flow cytometry facility.

This study was supported by Fundação de Amparo à Pesquisa do Estado de Minas Gerais, Coordenação de Aperfeiçoamento de Pessoal de Nível Superior, Bio-Manguinhos/FIOCRUZ, PROEP/CPqRR/FIOCRUZ, Conselho Nacional de Desenvolvimento Científico e Tecnológico–CNPq (grant nos. 444417/2014-1 and 458134/2014-7), and Programa Nacional de Imunizações, Secretaria de Vigilância em Saúde–Ministério da Saúde, Brazil (grant no. TC 277/2013). O.A.M.-F., A.T.-C., and L.R.A. received research fellowships from CNPq.

Author contributions: study design, A.C.C.-A., L.A.B.C., M.L.S.M., R.M.M., A.H., P.L.T., P.F.C.V., A.P.M.R., C.M.D., A.T.-C., O.A.M.-F.; funding acquisition, L.A.B.C., O.A.M.-F., A.P.M.R., C.M.D.; experiments: A.C.C.-A., V.P.-M., J.G.C.-R., L.R.A., C.C.-P., E.S., L.R.R., S.M.B.L., M.S., A.T.-C., O.A.M.-F.; field study: J.A.L., J.G.L.R., L.A.B.C., L.C.C.M.; data acquisition: A.C.C.-A., V.P.-M., J.G.C.-R., L.R.A., C.C.-P., E.S., S.M.B.L., M.S.; data analysis: A.C.C.-A., A.T.-C., O.A.M.-F.; validation: P.L.T., P.F.C.V.; advisory committee: R.M.M., A.H., P.L.T., P.F.C.V.; manuscript: A.C.C.-A., J.G.C.-R., C.C.-P., L.R.R., A.T.-C., O.A.M.-F.

About the Author

Dr. Campi-Azevedo is a cellular and molecular immunologist working in the Biomarker Research Group at the René Rachou Institute, Oswaldo Cruz Foundation (FIOCRUZ-Minas), Belo Horizonte, Brazil. Her primary research interests include vaccine immunity; diagnosis and management of infectious/parasitic diseases and biomarkers for posttherapeutic follow-up; bioprospection in experimental therapeutics; and biomarkers in oncology.

References

1. World Health Organization. Vaccines and vaccination against yellow fever. WHO position paper—June 2013. Wkly Epidemiol Rec. 2013;88:269–83.
2. World Health Organization. Yellow fever in Disease Outbreak News [cited 2019 Jun 20]. https://www.who.int/csr/don/archive/disease/yellow_fever
3. The Lancet. Yellow fever: a major threat to public health. Lancet. 2018;391:402. http://dx.doi.org/10.1016/S0140-6736(18)30152-1
4. de Almeida MA, Dos Santos E, da Cruz Cardoso J, da Fonseca DF, Noll CA, Silveira VR, et al. Yellow fever outbreak affecting *Alouatta* populations in southern Brazil (Rio Grande do Sul State), 2008–2009. Am J Primatol. 2012;74:68–76. http://dx.doi.org/10.1002/ajp.21010
5. Romano APM, Costa ZGA, Ramos DG, Andrade MA, Jayme VdS, Almeida MA, et al. Yellow fever outbreaks in unvaccinated populations, Brazil, 2008–2009. PLoS Negl Trop Dis. 2014;8:e2740.
6. Secretaria de Vigilância em Saúde—Ministério da Saúde. Reemergence of wild yellow fever in Brazil, 2014–2015: epidemiological situation and the importance of preventive vaccination and intensified surveillance in the seasonal period [in Portuguese]. Boletim Epidemiológico. 2015;46:29 [cited 2019 May 29]. http://portalarquivos2.saude.gov.br/images/pdf/2015/outubro/19/2015-032---FA-ok.pdf
7. Secretaria de Vigilância em Saúde—Ministério da Saúde. Epidemiological emergence of yellow fever in Brazil, December 2016–July 2017 [in Portuguese]. Boletim Epidemiológico. 2017; 48:28 [cited 2019 May 29]. http://portalarquivos2.saude.gov.br/images/pdf/2017/setembro/06/2017_027.pdf
8. World Health Organization. Background paper on yellow fever vaccine. In: Vaccine position papers. Geneva: SAGE Working Group; 2013.
9. Collaborative group for studies on yellow fever vaccines. Duration of post-vaccination immunity against yellow fever in adults. Vaccine. 2014;32:4977–84. http://dx.doi.org/10.1016/j.vaccine.2014.07.021
10. Niedrig M, Lademann M, Emmerich P, Lafrenz M. Assessment of IgG antibodies against yellow fever virus after vaccination with 17D by different assays: neutralization test, haemagglutination inhibition test, immunofluorescence assay and ELISA. Trop Med Int Health. 1999;4:867–71. http://dx.doi.org/10.1046/j.1365-3156.1999.00496.x
11. Campi-Azevedo AC, Costa-Pereira C, Antonelli LR, Fonseca CT, Teixeira-Carvalho A, Villela-Rezende G, et al. Booster dose after 10 years is recommended following 17DD-YF primary vaccination. Hum Vaccin Immunother. 2016;12:491–502. http://dx.doi.org/10.1080/21645515.2015.1082693
12. Costa-Pereira C, Campi-Azevedo AC, Coelho-dos-Reis JG, Peruhype-Magalhães V, Araújo MSS, do Vale Antonelli LR, et al. Multi-parameter approach to evaluate the timing of memory status after 17DD-YF primary vaccination. PLoS Negl Trop Dis. 2018;12:e0006462. http://dx.doi.org/10.1371/journal.pntd.0006462
13. Simões M, Camacho LAB, Yamamura AMY, Miranda EH, Cajaraville ACRA, da Silva Freire M. Evaluation of accuracy and reliability of the plaque reduction neutralization test (micro-PRNT) in detection of yellow fever virus antibodies. Biologicals. 2012;40:399–404. http://dx.doi.org/10.1016/j.biologicals.2012.09.005
14. Nogueira RMR. Diagnóstico Laboratorial Específico e Diagnóstico Imunológico da Dengue [Specific laboratory diagnosis and immunodiagnosis of dengue]. Dengue Diagnóstico, Tratamento e Prevenção [Dengue diagnosis, treatment and prevention]. 2nd ed. Rio de Janeiro (Brazil): Editora Rubio Ltda.; 2008. p. 97–108.
15. Luiza-Silva M, Campi-Azevedo AC, Batista MA, Martins MA, Avelar RS, da Silveira Lemos D, et al. Cytokine signatures of innate and adaptive immunity in 17DD yellow fever vaccinated children and its association with the level of neutralizing antibody. J Infect Dis. 2011;204:873–83. http://dx.doi.org/10.1093/infdis/jir439
16. Querec T, Bennouna S, Alkan S, Laouar Y, Gorden K, Flavell R, et al. Yellow fever vaccine YF-17D activates multiple dendritic cell subsets via TLR2, 7, 8, and 9 to stimulate polyvalent immunity. J Exp Med. 2006;203:413–24. http://dx.doi.org/10.1084/jem.20051720
17. Querec TD, Akondy RS, Lee EK, Cao W, Nakaya HI, Teuwen D, et al. Systems biology approach predicts immunogenicity of the yellow fever vaccine in humans. Nat Immunol. 2009;10:116–25. http://dx.doi.org/10.1038/ni.1688
18. Martins MA, Silva ML, Marciano APV, Peruhype-Magalhães V, Eloi-Santos SM, Ribeiro JGL, et al. Activation/modulation of adaptive immunity emerges simultaneously after 17DD yellow fever first-time vaccination: is this the key to prevent severe adverse reactions following immunization? Clin Exp Immunol. 2007;148:90–100. http://dx.doi.org/10.1111/j.1365-2249.2006.03317.x
19. Martins MA, Silva ML, Elói-Santos SM, Ribeiro JG, Peruhype-Magalhães V, Marciano AP, et al. Innate immunity phenotypic features point toward simultaneous raise of activation and modulation events following 17DD live attenuated yellow fever first-time vaccination. Vaccine. 2008;26:1173–84. http://dx.doi.org/10.1016/j.vaccine.2007.12.035
20. Pulendran B. Learning immunology from the yellow fever vaccine: innate immunity to systems vaccinology. Nat Rev Immunol. 2009;9:741–7. http://dx.doi.org/10.1038/nri2629
21. Silva ML, Martins MA, Espírito-Santo LR, Campi-Azevedo AC, Silveira-Lemos D, Ribeiro JG, et al. Characterization of main cytokine sources from the innate and adaptive immune responses following primary 17DD yellow fever vaccination in adults. Vaccine. 2011;29:583–92. http://dx.doi.org/10.1016/j.vaccine.2010.08.046
22. Kohler S, Bethke N, Böthe M, Sommerick S, Frentsch M, Romagnani C, et al. The early cellular signatures of protective

immunity induced by live viral vaccination. Eur J Immunol. 2012;42:2363–73. http://dx.doi.org/10.1002/eji.201142306
23. Miller JD, van der Most RG, Akondy RS, Glidewell JT, Albott S, Masopust D, et al. Human effector and memory CD8+ T cell responses to smallpox and yellow fever vaccines. Immunity. 2008;28:710–22. http://dx.doi.org/10.1016/j.immuni.2008.02.020
24. Akondy RS, Monson ND, Miller JD, Edupuganti S, Teuwen D, Wu H, et al. The yellow fever virus vaccine induces a broad and polyfunctional human memory CD8+ T cell response. J Immunol. 2009;183:7919–30. http://dx.doi.org/10.4049/jimmunol.0803903
25. James EA, LaFond RE, Gates TJ, Mai DT, Malhotra U, Kwok WW. Yellow fever vaccination elicits broad functional CD4+ T-cell responses that recognize structural and nonstructural proteins. J Virol. 2013;87:12794–804. http://dx.doi.org/10.1128/JVI.01160-13
26. Reinhardt B, Jaspert R, Niedrig M, Kostner C, L'age-Stehr J. Development of viremia and humoral and cellular parameters of immune activation after vaccination with yellow fever virus strain 17D: a model of human flavivirus infection. J Med Virol. 1998;56:159–67. http://dx.doi.org/10.1002/(SICI)1096-9071(199810)56:2<159::AID-JMV10>3.0.CO;2-B
27. Akondy RS, Fitch M, Edupuganti S, Yang S, Kissick HT, Li KW, et al. Origin and differentiation of human memory CD8 T cells after vaccination. Nature. 2017;552:362–7. http://dx.doi.org/10.1038/nature24633
28. Blom K, Braun M, Ivarsson MA, Gonzalez VD, Falconer K, Moll M, et al. Temporal dynamics of the primary human T-cell response to yellow fever virus 17D as it matures from an effector- to a memory-type response. J Immunol. 2013;190:2150–8. http://dx.doi.org/10.4049/jimmunol.1202234
29. Poland JD, Calisher CH, Monath TP, Downs WG, Murphy K. Persistence of neutralizing antibody 30–35 years after immunization with 17D yellow fever vaccine. Bull World Health Organ. 1981;59:895–900.
30. Gotuzzo E, Yactayo S, Córdova E. Efficacy and duration of immunity after yellow fever vaccination: systematic review on the need for a booster every 10 years. Am J Trop Med Hyg. 2013;89:434–44. http://dx.doi.org/10.4269/ajtmh.13-0264
31. Wieten RW, Jonker EF, van Leeuwen EM, Remmerswaal EB, Ten Berge IJ, de Visser AW, et al. A single 17D yellow fever vaccination provides lifelong immunity; characterization of yellow-fever-specific neutralizing antibody and T-cell responses after vaccination. PLoS One. 2016;11:e0149871.
32. Patel D, Simons H. Yellow fever vaccination: is one dose always enough? Travel Med Infect Dis. 2013;11:266–73. http://dx.doi.org/10.1016/j.tmaid.2013.08.007
33. Grobusch MP, Goorhuis A, Wieten RW, Verberk JD, Jonker EF, van Genderen PJ, et al. Yellow fever revaccination guidelines change—a decision too feverish? Clin Microbiol Infect. 2013;19:885–6. http://dx.doi.org/10.1111/1469-0691.12332
34. Amanna IJ, Slifka MK. Questions regarding the safety and duration of immunity following live yellow fever vaccination. Expert Rev Vaccines. 2016;15:1519–33. http://dx.doi.org/10.1080/14760584.2016.1198259
35. Vasconcelos PF. Single shot of 17D vaccine may not confer life-long protection against yellow fever. Mem Inst Oswaldo Cruz. 2018;113:135–7. http://dx.doi.org/10.1590/0074-02760170347
36. Estofolete CF, Nogueira ML. Is a dose of 17D vaccine in the current context of yellow fever enough? Braz J Microbiol. 2018;S1517–8382(18)30196–5.
37. Kongsgaard M, Bassi MR, Rasmussen M, Skjødt K, Thybo S, Gabriel M, et al. Adaptive immune responses to booster vaccination against yellow fever virus are much reduced compared to those after primary vaccination. Sci Rep. 2017;7:662. http://dx.doi.org/10.1038/s41598-017-00798-1
38. Muyanja E, Ssemaganda A, Ngauv P, Cubas R, Perrin H, Srinivasan D, et al. Immune activation alters cellular and humoral responses to yellow fever 17D vaccine. J Clin Invest. 2014;124:3147–58. http://dx.doi.org/10.1172/JCI75429
39. Staples JE, Bocchini JA Jr, Rubin L, Fischer M; Centers for Disease Control and Prevention (CDC). Yellow fever vaccine booster doses: recommendations of the Advisory Committee on Immunization Practices, 2015. MMWR Morb Mortal Wkly Rep. 2015;64:647–50.
40. Centers for Disease Control and Prevention (CDC). GRADE evidence tables. 2015 [cited 2019 May 24]. http://www.cdc.gov/vaccines/acip/recs/GRADE/table-refs.html

Address for correspondence: Olindo Assis Martins-Filho or Ana Carolina Campi-Azevedo, Grupo Integrado de Pesquisas em Biomarcadores—Instituto René Rachou, FIOCRUZ-Minas, Avenida Augusto de Lima, 1715, Barro Preto, Belo Horizonte, Minas Gerais, 30.190-002, Brazil; email: oamfilho@minas.fiocruz.br or accampi@minas.fiocruz.br

Lessons Learned from Dengue Surveillance and Research, Puerto Rico, 1899–2013

Tyler M. Sharp, Kyle R. Ryff, Gilberto A. Santiago, Harold S. Margolis, Stephen H. Waterman

Dengue was first reported in Puerto Rico in 1899 and sporadically thereafter. Following outbreaks in 1963 and 1969, the Centers for Disease Control and Prevention has worked closely with the Puerto Rico Department of Health to monitor and reduce the public health burden of dengue. During that time, evolving epidemiologic scenarios have provided opportunities to establish, improve, and expand disease surveillance and interventional research projects. These initiatives have enriched the tools available to the global public health community to understand and combat dengue, including diagnostic tests, methods for disease and vector surveillance, and vector control techniques. Our review serves as a guide to organizations seeking to establish dengue surveillance and research programs by highlighting accomplishments, challenges, and lessons learned during more than a century of dengue surveillance and research conducted in Puerto Rico.

In 1916, Walter W. King (Figure 1), a surgeon in the US Public Health Service stationed at the San Juan (Puerto Rico) Quarantine Station, presented to the American Society of Tropical Medicine a firsthand account of his experiences during the 1915 dengue outbreak in Puerto Rico (*1*). Health Commissioner William Lippitt had invited Henry Rose Carter and William Gorgas to work with King, then a captain in the US Army Medical Corps, to determine whether yellow fever virus or dengue virus caused the outbreak. After Carter, who had survived a bout with yellow fever years earlier and thus was immune, fell ill soon after examining patients in a mosquito-infested hospital, the team concluded that dengue caused the outbreak (*2*). King credited Arthur H. Glennan, his predecessor at the San Juan Quarantine Station, as the first to have reported local dengue cases in Puerto Rico in 1899 (*3*). King also cited local physicians who reported having seen dengue cases nearly every year since and an apparent outbreak in 1905 (*1*). King noted that younger persons and residents of San Juan were affected more often than elderly persons and persons from rural areas and that the epidemic was associated with a "superabundance" of *Aedes* mosquitoes. In addition, dengue cases frequently appeared in the same household ≈2 weeks after the first household member fell ill, which suggested to King that infections might occur around the household. These observations collectively led King to suspect that dengue already was endemic in Puerto Rico by 1915.

Many of King's prescient observations remain true. Yet, despite extensive resources expended to understand and combat dengue, rates of illness and death caused by dengue continue to increase worldwide (*4*). We describe lessons learned during >100 years of dengue surveillance and research in Puerto Rico. (Because the names of some entities have changed since 1899, we have used their contemporary names to maintain consistency.)

Early Epidemiologic Investigations

Only 1 report of dengue in Puerto Rico was published in the nearly 50 years after King's report (*5*). In 1963, the Puerto Rico Department of Health (PRDH) requested assistance from the Centers for Disease Control and Prevention (CDC) to respond to a dengue outbreak in which ≈27,000 suspected cases were ultimately reported to PRDH by telegram from across the island (Table 1) (*6*,*15*). A team was sent from CDC headquarters to help PRDH respond to the outbreak, along with colleagues from CDC's Puerto Rico Field Station, which had been established in 1951 to research and control schistosomiasis and investigate rabies, histoplasmosis, and leptospirosis. Later known as the San Juan Laboratories, the Field Station had grown out of the Office of Malaria Control in War Areas, which became CDC in 1946.

Through observation of 2,777 persons during the 1963 outbreak, dengue was described as an acute febrile illness lasting 4–7 days with infrequent minor hemorrhagic manifestations (*6*). Two thirds of persons with serologic evidence of infection reported a recent illness consistent with dengue (*6*). Distinct from King's observations from 1915,

Author affiliations: Centers for Disease Control and Prevention, San Juan, Puerto Rico, USA (T.M. Sharp, K.R. Ryff, G.A. Santiago, H.S. Margolis, S.H. Waterman); US Public Health Service, Rockville, Maryland, USA (T.M. Sharp, S.H. Waterman)

DOI: https://doi.org/10.3201/eid2508.190089

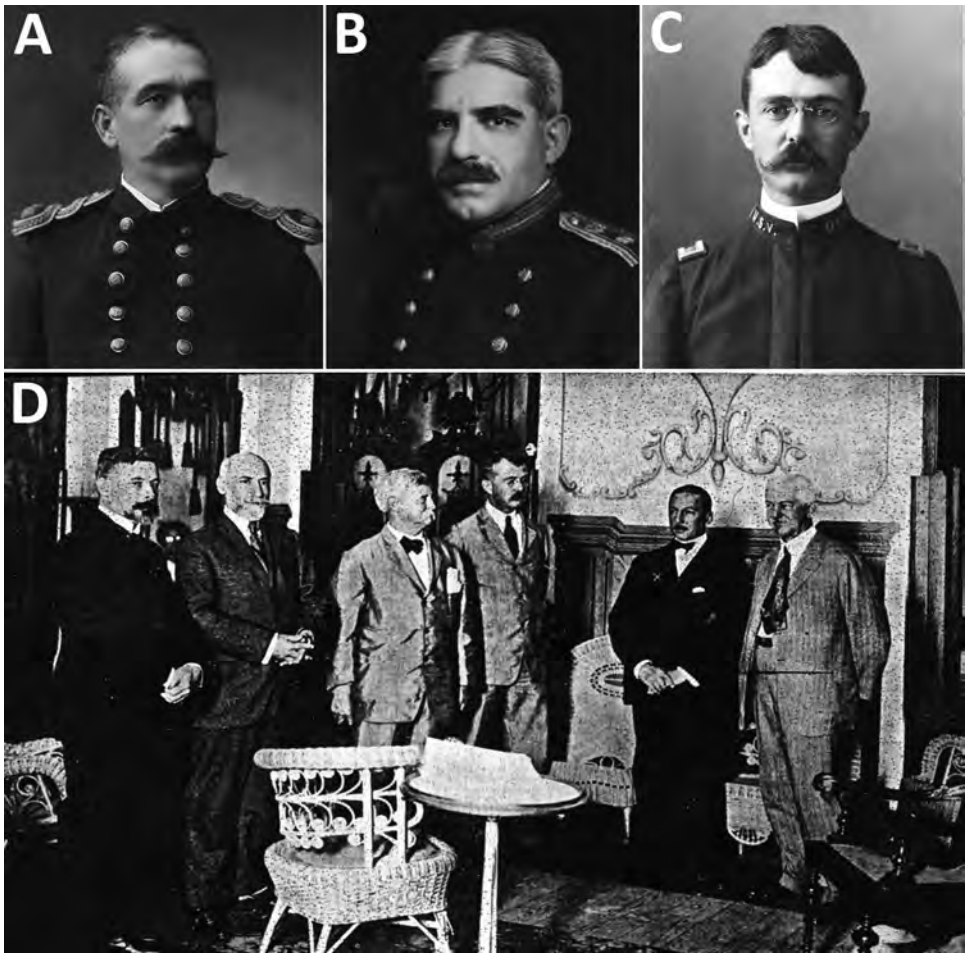

Figure 1. Prominent public health figures in Puerto Rico during the early 1900s. A) Assistant Surgeon General Arthur H. Glennan, pictured circa 1895. B) Walter W. King, Chief Quarantine Officer of the US Quarantine Station, San Juan, Puerto Rico, pictured in 1915. C) San Juan Health Commissioner William F. Lippitt, pictured in 1899. D) From left to right: Puerto Rican tropical medicine physicians Isaac González Martínez and Pedro Gutiérrez Igaravídez met with yellow fever expert Henry Rose Carter, San Juan Commissioner of Health William Lippitt, Mariano Lebredo from Cuba, William Gorgas, and (not pictured) Bailey K. Ashford and Walter W. King to determine the etiology of an outbreak in 1915 that was ultimately attributed to dengue. Images were obtained from the National Library of Medicine (A–C) or were originally published in Puerto Rico Ilustrado (https://en.wikipedia.org/wiki/Puerto_Rico_Ilustrado) (D).

in 1963 all age groups were equally affected by both illness and infection, suggesting the outbreak was caused by a virus type that had not previously circulated in Puerto Rico. Further analysis revealed that only persons >25 years of age had serologic evidence of prior exposure to any of the 4 dengue virus types (DENV-1–4), suggesting that a dengue outbreak might have occurred during the late 1930s or early 1940s, consistent with reports of a dengue-like illness of "minor epidemic proportions" in 1945 (*5*).

PRDH again requested assistance from CDC during an outbreak of DENV-2 in 1969 (*8*). Serosurveys in 4 neighborhoods in northern Puerto Rico demonstrated that 47% of participants had been infected with a DENV and that 43% of infections were asymptomatic (*8*). Moreover, investigators found no evidence of protective immunity in persons who reported having been ill during the 1963 epidemic, again demonstrating type-specific immunity. Aerial spraying of malathion was used to combat the epidemic in 1969, but malathion was observed to not efficiently enter households, where most *Aedes* mosquitoes are present, and a natural decline in cases precluded analysis of its effectiveness in reducing transmission (*16*).

Evolution and Improvement of Case Surveillance

An islandwide case reporting system (later named the Passive Dengue Surveillance System [PDSS]) was established in 1969 to collect basic demographic and clinical data from patients with suspected dengue. By 1970, PDSS enabled detection of dengue cases in southwestern Puerto Rico during the dry season, providing further evidence that dengue was endemic (*17*); however, later reports questioned this finding (*18*). In 1973, CDC's mission in Puerto Rico included studying dengue, assisting PRDH to operate PDSS, and identifying approaches to combat dengue.

Surveillance in subsequent years demonstrated that detection of cases based solely on clinical signs and symptoms (i.e., syndromic surveillance) was insufficient to monitor dengue because clinicians were often unable to distinguish dengue from influenza, leptospirosis, rubella, and other common causes of acute febrile illness (*9*,*18*). In response, laboratory-based surveillance for dengue was initiated in 1974. Cross-island expressways opened in the mid-1970s, resulting in increased detection of dengue cases from throughout the island because of more rapid dissemination of infections and improved case detection. In 1975,

Table 1. Dengue outbreaks and epidemics, Puerto Rico, 1899–2013*

Year(s)	DENV(s)†	No. reported suspected cases (cases/1,000 pop)	Most affected age group(s), y†	No. reported DHF cases (DHF cases/1,000 dengue cases)	Reported dengue-related deaths (deaths/1,000 dengue cases)	Reference
1899	Unknown	"Some"	NA	NA	NA	(*3*)
1915	Unknown	Hundreds or thousands (≈20)	<10	NA	0 (0)	(*1*)
1963	3	≈27,000 (NA)	20–29, 30–39, 10–19	0	NA	(*6*,*7*)
1969	2	16,665 (NA)	30–49	0	0	(*8*)
1977	2, 3, 1	12,733 (3.75)	15–19, 20–29, 10–14	0	0	(*9*)
1978–1979	1, 2, 3	12,314 (3.63)	15–19, 20–29, 10–14	0	0	‡
1981–1982	1, 4	≈17,160 (NA)	NA	NA	5 (≈0.3)	‡
1986	4, 1, 2	10,659 (NA)	6–15, 31–45, <1	29§ (27§)	3§ (0.3)	(*10*)
1994–1995	2, 4, 1	24,700 (7.0)	15–19, 10–14, 20–24	152 (6.2)	40 (1.6)	(*11*)
1998	4, 1, 2, 3	17,000 (4.8)	10–19, <1	174 (10.2)	56 (3.3)	(*12*)
2007	3, 2, 1, 4	10,508 (2.7)	10–14, 15–19, <1	227 (21.6)	40 (3.8)	(*13*)
2010	1, 4, 2, 3	26,766 (7.2)	10–14, 15–19, 5–9	448 (16.7)	128 (4.8)	(*14*)
2012–2013	1, 4, 2, 3	30,921 (8.6)	10–14, 15–19, <1	11 (0.4)	199 (6.4)	‡

*DENV, dengue virus; DHF, dengue hemorrhagic fever; NA, data not available; pop, population.
†In order of relative frequency.
‡Centers for Disease Control and Prevention and Puerto Rico Department of Health, unpub. data.
§Laboratory-positive cases; number of suspected cases not available.

the importance of improving surveillance in small outpatient clinics was identified as a priority to quantify the incidence of dengue in rural communities. After epidemics in 1977 and 1978, in 1981 CDC's mission in Puerto Rico was officially changed to focus primarily on dengue (Table 2).

In 1982, a new surveillance system that included active surveillance sites to augment passive reporting was implemented; this system emphasized monitoring virus transmission in 31 sites across the island (*19*). Approximately 100 acute serum specimens were processed for virus isolation and serology each week using new diagnostic methods (*19*). Test results were reported to surveillance sites, and close communication was maintained with clinicians. Prompt communication of test results provided a sensitive spatial and early warning system of increased DENV transmission around the island. A monthly surveillance summary was published and sent to stakeholders in Puerto Rico and elsewhere, and in 1987 a computerized system was implemented to track and manage data. Although this surveillance system provided early epidemic warnings, the control program was still reactive instead of proactive, and ultimately response efforts did not appreciably affect epidemic trends.

In 1994, the government-funded healthcare system was privatized with the aim of increasing efficiency, streamlining bureaucracy, and decreasing government expenditures. A consequence was that public health nurses and vector control staff, whose regional offices had been in government-operated hospitals that managed ≈60% of all patients, became disconnected from clinicians. This change resulted

Table 2. Nomenclature and chiefs of the Centers for Disease Control and Prevention* research station located in San Juan, Puerto Rico, 1951–present

Year	Name	Chief	Location
1951–1954	Communicable Disease Center,	David Pimentel	La Puntilla, Arsenal, Viejo San Juan (1951–1972)
1954–1955	Ecologic Investigations Program,	Charles S. Gerhardt	
1955–1970	Puerto Rico Field Station	Frederick "Fred" Ferguson	
1970–1976	Center for Disease Control, San Juan	Barnett "Barney" Cline	Rio Piedras (1972–2000)
1976–1980	(Tropical Disease) Laboratories	John "Jack" Woodall	
1980–1981		Ernest Ruiz Tibén (interim), Roslyn Q. Robinson	
1981–1989	Centers for Disease Control	Duane J. Gubler	
1989–2006	(and Prevention), Dengue Branch†	Gary G. Clark	Puerto Nuevo (2000–present)
2006–2008		Wellington Sun	
2008–2010		Kay M. Tomashek (interim)	
2010–2015		Harold "Hal" S. Margolis	
2015–present		Stephen "Steve" H. Waterman	

*Current name.
†Currently in the Division of Vector-Borne Diseases, National Center for Emerging and Zoonotic Infectious Diseases.

in a decreased capacity to report suspected dengue cases and disproportionate case reporting from outpatient clinics. In the early 1990s, ≈42% of hospitalized dengue patients were reported (*20*,*21*); after the change in the structure of the healthcare system, this proportion decreased to ≈16% (*22*). As a result, comparing epidemiologic trends from before and after the mid-1990s is difficult (Figure 2).

During the large dengue epidemic of 1994 (*11*), the volume of case report forms and specimens overwhelmed the available capacity for data management and diagnostic testing, resulting in substantial delays in real-time analysis of case data. In part because of this delay, local authorities disputed that an epidemic was in fact occurring (*23*). In response, a standardized method was needed to determine when dengue epidemics were occurring. Epidemiologists at CDC and PRDH developed a method wherein weekly dengue surveillance data were tabulated along with deviation bar charts, which were used to compare data from the municipalities experiencing epidemics with historic averages (*24*). This method enabled a rigorous method to define epidemics, which in turn enabled PRDH to initiate early intervention strategies. Following this approach, the islandwide incidence of dengue cases has been summarized in weekly reports since the early 2000s. When 2 consecutive weeks of above-threshold cases are reported with a concomitant increase in laboratory-positive dengue cases, an epidemic was to be declared and response activities initiated.

Changes in Disease Severity that Necessitated Innovations in Case Surveillance

After increasing reports of dengue hemorrhagic fever (DHF) in Southeast Asia during the 1970s, increased effort was dedicated to monitoring the clinical severity of dengue in Puerto Rico. The first DHF cases were retrospectively detected from 1975 (*25*), and the first confirmed dengue-related death was identified in 1982 (*26*). DHF cases were again detected in 1985, and increased numbers of DHF and fatal cases were detected during the 1986 epidemic (*10*) and continued into 1987.

Starting in the early 1980s, collaborations were established with regional infectious disease physicians and neurologists to monitor fatal dengue-like illness, and the Demographic Registry of Puerto Rico consulted physicians who had listed dengue on a patient's death certificate. Because of the time-consuming nature of this process and media claims of unreported fatal dengue cases, PRDH and CDC implemented new approaches to better understand and quantify the incidence of fatal dengue.

First, medical examiners were identified as an ideal resource to detect dengue-related deaths (*27*). CDC, PRDH, and the Puerto Rico Institute of Forensic Sciences also collaborated to collect tissue specimens during autopsy of persons who died after an acute febrile illness. In addition, diagnostic testing using immunohistochemical analysis and PCR enabled the diagnosis of dengue cases that would have been missed by only testing serum (*28*). Last, increasing recognition of DENV as a cause of severe neurologic illness led to enhanced surveillance for neuropathies associated with DENV infection in 2003 and subsequent estimation that dengue with neurologic manifestations was an outcome with comparatively low incidence (*29*).

Community and Clinician Education Campaigns

During the 1963 epidemic and for years thereafter, outbreak response activities focused on space spraying with insecticides, community cleanup campaigns, and educational activities to inspire community-based vector control campaigns. A major community-based control program supported by Rotary International in collaboration with CDC and PRDH included outreach through school education programs, church and community organizations, and clinicians. A medical anthropologist was hired in 1986 to help CDC, PRDH, and local media companies develop professional community outreach and education programs to promote control of *Aedes* mosquitoes (*30*). These efforts were associated with higher levels of awareness of control methods and some behavior changes but limited decreases in larval indices (*31*). Rotary International subsequently expanded the program to Colombia, the Philippines, Indonesia, and

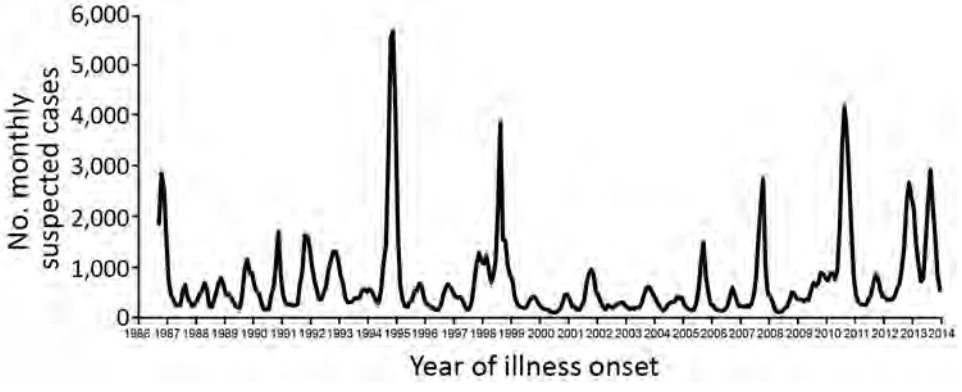

Figure 2. Suspected dengue cases reported to the Puerto Rico Department of Health, by month, 1986–2013. The healthcare system of Puerto Rico changed from public to semiprivate in 1994.

other countries; the program was the basis for the World Health Organization (WHO) COMBI (communication for behavioral impact) program that is now part of the WHO global strategy for controlling dengue.

During the 1977 epidemic, 76% of municipalities in Puerto Rico instituted public education and cleanup campaigns to reduce mosquito production sites (*9*). Public notification of the epidemic and dengue prevention strategies were conducted through radio and television ads, dissemination of printed materials at public schools, and clinician education; however, the effectiveness of behavioral messaging again could not be evaluated because the epidemic peaked before control measures began (*9*). Evaluation of sustained community education and outreach campaigns conducted during endemic and epidemic DENV transmission during the 1980s and early 1990s demonstrated reasonable success in improving residents' dengue-related knowledge and reducing mosquito-infested water containers in homes (*31*).

Dengue patient management seminars were frequently offered to clinicians during dengue epidemics starting during the 1970s and focused on case diagnosis and differentiation from other causes of acute febrile illness. As clinical management of dengue patients gradually came into focus as the mainstay secondary method to prevent deaths, in-person clinical training events emphasized the importance of early and appropriate patient management strategies as recommended by WHO (*32*). At the First International Conference on Dengue Hemorrhagic Fever in the Americas hosted by CDC and PRDH in San Juan in 1985, DHF experts from Asia gave plenary lectures at the conference and around the island on all aspects of the disease. A peer education program for physicians and nurses funded by a local pharmaceutical company followed the conference.

As the frequency of clinical trainings waned after the aforementioned changes to the healthcare system in the mid-1990s, case-fatality rates began to rise concurrent with the increasing incidence of dengue and improvements in fatal case detection. Investigation of fatal dengue cases during the 2007 epidemic and a survey of physicians' practices revealed common missteps in dengue patient management (*33*,*34*). Because similar issues had been observed in Southeast Asia and Central America, the 2009 WHO guidelines for clinical care of dengue patients were incorporated into a 4-hour dengue clinical management course (*35*).

During a large epidemic in 2010, the Puerto Rico Secretary of Health redirected public health resources from vector control campaigns, which had repeatedly been shown to be ineffective, and instead used them to conduct islandwide clinical trainings. To ensure participation, the Secretary made it mandatory for most practicing physicians to complete the course or face a penalty of losing their medical license (*35*). As a result, ≈8,000 clinicians were trained in <6 months, mostly during a 6-week period around the peak of the epidemic. Comparison of physician practices before and after the training demonstrated improvement in several key aspects of dengue clinical case management (*35*). A critical component of the success of these training programs was explaining in detail the rationale behind recommended practices to a cadre of local, well-respected physicians, and having them, not CDC personnel, train their peers throughout the island, as had been done during the 1980s. After the success of the 2010 classroom-based dengue clinical training course, an online training course was also developed (https://www.cdc.gov/dengue/training).

Advances in Laboratory Diagnostic Testing

The first laboratory diagnostic tool used to detect increased antibody titers in serum specimens collected from persons enrolled in the serosurvey during the 1963 outbreak was hemagglutination inhibition (HI), confirmed with complement fixation (CF) (*6*) (Figure 3). CF also was used during the 1969 serosurvey, and cell culture was used to isolate virus and identify the cause of the 1963 outbreak as DENV-3 (*7*). CF, HI, virus isolation, and plaque-reduction neutralization test (PRNT) were used to test specimens throughout the 1970s (*9*). The first insectary was built in Puerto Rico not to study the mosquito vectors of DENV but to use them as a diagnostic tool. A technique had been developed in Hawaii wherein the serum from suspected dengue patients was intrathoracically injected into *Aedes* or *Toxorhynchites* mosquitoes followed by immunofluorescent detection of DENV antigen (*36*). As case reporting improved during the 1970s, capacity to test all received specimens overwhelmed the system so that only a portion of specimens could be tested.

HI and virus isolation were the most common diagnostic techniques used in the early 1980s to mid-1980s. Use of cultured mosquito cells to isolate virus and immunofluorescence with monoclonal antibodies to identify viruses enabled observation of dissemination of DENV-1 and DENV-4 across Puerto Rico during the 1981–82 epidemic (*19*), as well as the first reported detection of coinfection with 2 DENVs (*37*). During the 1986 epidemic, the IgM antibody capture (MAC) ELISA was adapted to diagnose suspected dengue cases (*38*). MAC-ELISA replaced HI as the standard serologic diagnostic method, enabling simpler diagnosis of patients with suspected dengue. During the first years of the new millennium, CDC participated as a WHO Collaborating Center to evaluate dengue serologic diagnostic tests (*39*) and adapted PRNT for higher throughput by development of the microneutralization assay (*40*). In 2011, the Food and Drug Administration approved a serologic diagnostic test akin to the

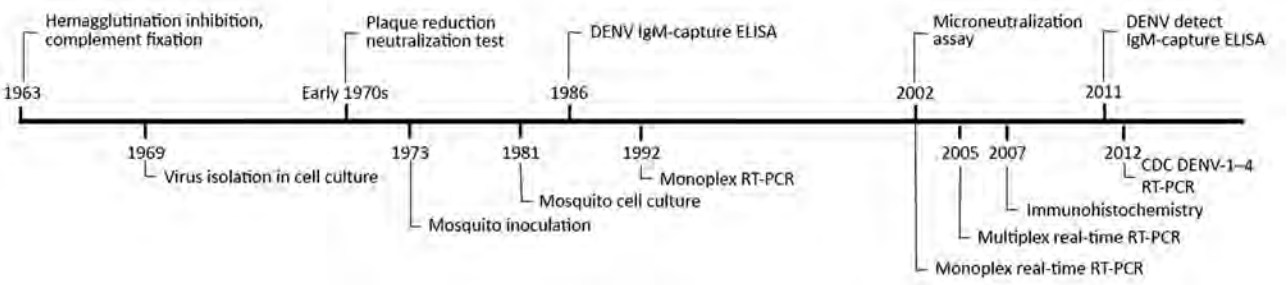

Figure 3. Timeline of incorporation of laboratory techniques used to diagnose suspected dengue reported through the islandwide Passive Dengue Surveillance System in Puerto Rico, 1963–2013. CDC, Centers for Disease Control and Prevention; DENV, dengue virus; RT-PCR, reverse transcription PCR.

MAC-ELISA (*41*), and this test is now routinely used in Puerto Rico and elsewhere.

In the early 1990s, CDC developed a reverse transcription PCR (RT-PCR) protocol to detect DENV nucleic acid in serum specimens (*42*). Subsequent RT-PCRs were adapted for real time (rRT-PCR) to assess the magnitude of viremia and for multiplex rRT-PCR to detect all 4 DENVs in the same reaction (*43*,*44*). Automation of RNA extraction began in 2006, and high-throughput RNA amplification was implemented in 2010. Following primer specification to detect a wider variety of modern DENVs, the Food and Drug Administration approved the CDC multiplex rRT-PCR in 2012 (*45*).

rRT-PCR coupled with anti-DENV IgM ELISA became the standard diagnostic tools for diagnosing acute DENV infection, such that the combination of these 2 assays enabled diagnosis of >90% of dengue cases from a single serum specimen (*46*). After improvements to increase laboratory capacity, reported dengue attack rates increased during epidemics during the early 2000s (Figure 4). Diagnosis of fatal dengue cases improved during the 2007 epidemic, when RT-PCR and immunohistochemical analysis were systematically performed on tissue specimens from patients with fatal acute febrile illness (*28*). Contemporary efforts seek to improve the timeliness and utility of dengue diagnostic testing by evaluating point-of-care rapid diagnostic tests (*47*) and modification of molecular assays to simultaneously detect the 4 DENVs, as well as chikungunya and Zika viruses (*48*).

Development of Tools for Vector Surveillance and Control

Entomologic studies conducted by CDC in Puerto Rico during the early 1960s demonstrated the presence of *Ae. aegypti* mosquitoes in more than half of the homes in neighborhoods affected by dengue (*6*) and these mosquitoes' susceptibility to various adulticides (*49*). Malathion was used during outbreak responses and during an ultimately unsuccessful *Ae. aegypti* elimination campaign during 1965–1969 (*50*), after which resistance to malathion was identified (reference *51* in Appendix, https://wwwnc.cdc.gov/EID/article/25/8/19-0089-App1.pdf). To attempt to control the 1977 epidemic, space spraying of malathion from trucks and airplanes in San Juan transiently decreased adult mosquito populations, but the number of reported dengue cases did not differ between treated and untreated areas (*9*). Additional studies during the 1970s investigated the environmental determinants of *Aedes* mosquito abundance to show a direct relationship with rainfall and identified discarded tires and animal water pans as common breeding sites (references *52*,*53* in Appendix).

Extensive research was conducted during the 1980s on use of insecticides to control adult *Ae. aegypti* densities; use of larvicides (e.g., temephos, *Bacillus thuringiensis*), biocontrol (i.e., copepods), and source reduction to control larvae; and studies of vector competence and transmission dynamics. The efficacy of ultralow volume space spraying with malathion and pyrethroids was evaluated in 1987, as was aerial application of naled using C-130 aircraft. Unfortunately, such efforts had no effect on epidemic trends and variable levels of success in reducing DENV transmission (*31*).

After having been standardized as a vector surveillance tool during the *Ae. aegypti* eradication program during the 1960s (*50*), the ovitrap was modernized at the CDC Dengue Branch during the 1980s (reference *54* in Appendix). Around the same time, the backpack mosquito aspirator was adapted for adult mosquito collection in households (reference *55* in Appendix), enabling direct quantitation of the absolute number of mosquitoes in a household. These methods were also used in place of bioassays to evaluate the efficacy of space spraying.

After observations that adult mosquito populations do not correlate well with larval densities, in the early 2000s pupal populations were reported to have a nonlinear relationship with density of adults (reference *56* in Appendix). As had been done at the US Department of Agriculture, vector surveys were simplified to focus on pupae as a predictor of vector abundance (reference *57* in Appendix). The focus on pupae for vector surveys in turn confirmed that if mosquito

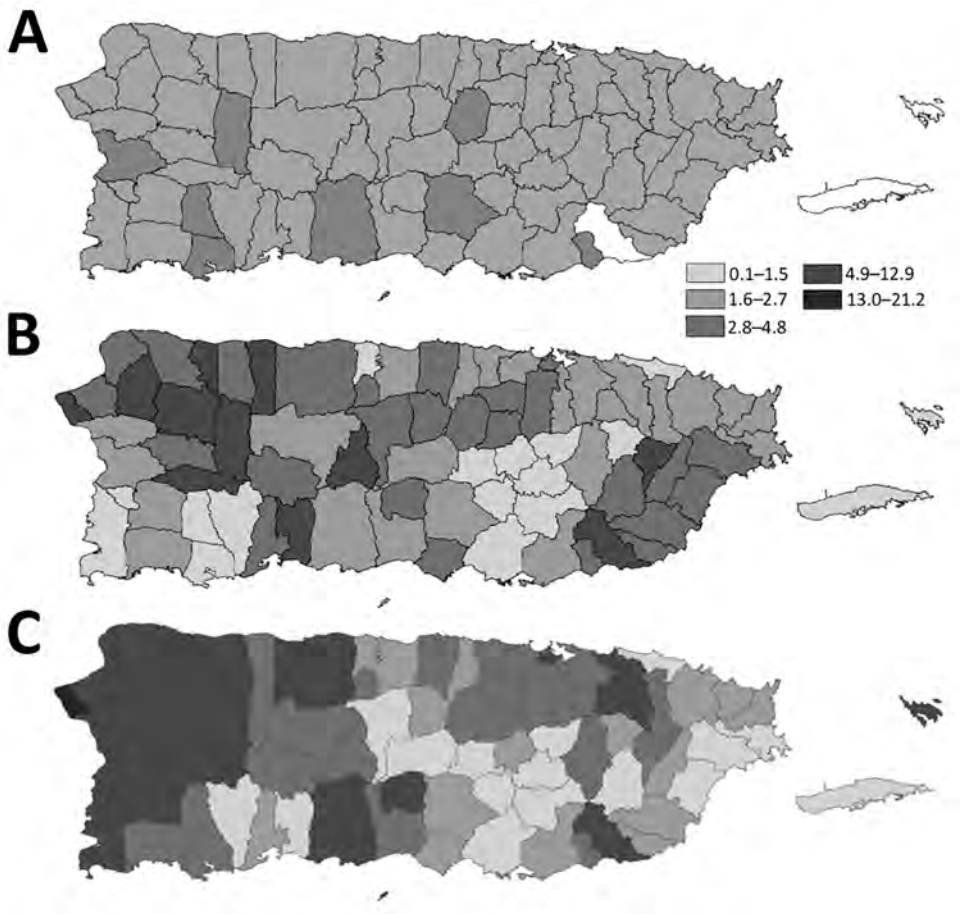

Figure 4. Number of laboratory-positive dengue cases per 1,000 residence reported to Puerto Rico Department of Health by municipality during epidemics in 2007 (A), 2010 (B), and 2012–2013 (C).

surveillance monitors only immature mosquitoes, no effect on adult populations is detected after vector control interventions, as had been observed by others. Later efforts demonstrated an association between household densities of adult female *Ae. aegypti* mosquitoes and risk for DENV infection (reference *58* in Appendix), and cryptic breeding sites (e.g., septic tanks) were identified as major producers of adult mosquitoes (reference *59* in Appendix). Contemporary efforts have focused on the design of autocidal gravid ovitraps that can be used for simultaneous mosquito surveillance and control and are associated with sustainable decreases in vector abundance (reference *60* in Appendix) and reduced risk for infection from pathogens transmitted by *Ae. aegypti* mosquitoes (reference *61* in Appendix). Evaluations of autocidal gravid ovitraps on a larger scale are under way.

Conclusions

Dengue remains a major public health concern throughout the tropics and subtropics. In Puerto Rico, close alliance of CDC with PRDH has proven to be integral not only in detecting and responding to epidemics but also in furthering the collective understanding of the molecular, diagnostic, epidemiologic, and entomologic characteristics of dengue. Dengue surveillance and research have therefore demonstrated a mutually beneficial and interdependent relationship to combat dengue. Dengue surveillance also has promoted the recognition and study of nondengue acute febrile illnesses, an attribute further shown during the recent emergence in Puerto Rico of chikungunya virus in 2014 and Zika virus in 2015 (references *62*,*63* in Appendix).

The demonstrated limitations in chemical approaches to dengue control have inspired several alternative interventions (reference *64* in Appendix). As dengue vaccines and vector control interventions continue to be developed and evaluated, the need for surveillance and research to design, implement, and evaluate these tools will continue. Academic, public, and private organizations play both complementary and overlapping roles in various aspects of dengue surveillance and research; thus, close partnerships will continue to be integral components of successful public health initiatives to combat dengue. Because of decades of experience and baseline surveillance data, Puerto Rico is expected to continue to be a site that leads evaluation of interventions designed to control dengue. Collaborations such as that of CDC, the Pan American Health Organization, WHO, and PRDH will be instrumental in such efforts, as will implementation of lessons learned from Puerto Rico and other areas.

Acknowledgments

We gratefully acknowledge Roberto Barrera, Paul Blake, Barnett Cline, Vance Dietz, Duane J. Gubler, Goro Kuno, Chester Moore, Elizabeth Hunsperger, Jorge L. Muñoz-Jordan, David M. Morens, José Rigau-Pérez, and Kay M. Tomashek for their useful insights and manuscript review. We regret any omissions of relevant publications that were not included in this review because of constraints on manuscript length.

About the Author

Dr. Sharp joined the CDC in 2010 as an Epidemic Intelligence Service officer and is stationed at the Dengue Branch, Division of Vector-Borne Diseases, National Center for Emerging and Zoonotic Infectious Diseases, where he works as a health scientist. His public health and research interests are the epidemiology and pathophysiology of emerging tropical infectious diseases.

References

1. King W. The epidemic of dengue in Porto Rico: 1915. In: Annual Meeting of the American Society of Tropical Medicine, 1916. Washington: American Society of Tropical Medicine; 1916. p. 564–71.
2. Lippitt WF. Supuestos cases de fiebre amarilla en la isla de Puerto Rico. Bol Asoc Med P R. 1916;13:50–5, 172–7.
3. Glennan AH. Monthly report from San Juan. Public Health Rep. 1899;14:1362–4.
4. Stanaway JD, Shepard DS, Undurraga EA, Halasa YA, Coffeng LE, Brady OJ, et al. The global burden of dengue: an analysis from the Global Burden of Disease Study 2013. Lancet Infect Dis. 2016;16:712–23. http://dx.doi.org/10.1016/S1473-3099(16)00026-8
5. Diaz-Rivera RS. A bizarre type of seven day fever clinically indistinguishable from dengue. Bol Asoc Med P R. 1946;38:75–80.
6. Neff JM, Morris L, Gonzalez-Alcover R, Coleman PH, Lyss SB, Negron H. Dengue fever in a Puerto Rican community. Am J Epidemiol. 1967;86:162–84. http://dx.doi.org/10.1093/oxfordjournals.aje.a120722
7. Russell PK, Buescher EL, McCown JM, Ordõnez J. Recovery of dengue viruses from patients during epidemics in Puerto Rico and East Pakistan. Am J Trop Med Hyg. 1966;15:573–9. http://dx.doi.org/10.4269/ajtmh.1966.15.573
8. Likosky WH, Calisher CH, Michelson AL, Correa-Coronas R, Henderson BE, Feldman RA. An epidermiologic study of dengue type 2 in Puerto Rico, 1969. Am J Epidemiol. 1973;97:264–75. http://dx.doi.org/10.1093/oxfordjournals.aje.a121508
9. Morens DM, Rigau-Pérez JG, López-Correa RH, Moore CG, Ruiz-Tibén EE, Sather GE, et al. Dengue in Puerto Rico, 1977: public health response to characterize and control an epidemic of multiple serotypes. Am J Trop Med Hyg. 1986;35:197–211. http://dx.doi.org/10.4269/ajtmh.1986.35.197
10. Dietz V, Gubler DJ, Ortiz S, Kuno G, Casta-Vélez A, Sather GE, et al. The 1986 dengue and dengue hemorrhagic fever epidemic in Puerto Rico: epidemiologic and clinical observations. P R Health Sci J. 1996;15:201–10.
11. Rigau-Pérez JG, Vorndam AV, Clark GG. The dengue and dengue hemorrhagic fever epidemic in Puerto Rico, 1994-1995. Am J Trop Med Hyg. 2001;64:67–74. http://dx.doi.org/10.4269/ajtmh.2001.64.67
12. Rigau-Pérez JG, Ayala-López A, García-Rivera EJ, Hudson SM, Vorndam V, Reiter P, et al. The reappearance of dengue-3 and a subsequent dengue-4 and dengue-1 epidemic in Puerto Rico in 1998. Am J Trop Med Hyg. 2002;67:355–62. http://dx.doi.org/10.4269/ajtmh.2002.67.355
13. Tomashek KM, Rivera A, Muñoz-Jordan JL, Hunsperger E, Santiago L, Padro O, et al. Description of a large island-wide outbreak of dengue in Puerto Rico, 2007. Am J Trop Med Hyg. 2009;81:467–74. http://dx.doi.org/10.4269/ajtmh.2009.81.467
14. Sharp TM, Hunsperger E, Santiago GA, Muñoz-Jordan JL, Santiago LM, Rivera A, et al. Virus-specific differences in rates of disease during the 2010 Dengue epidemic in Puerto Rico. PLoS Negl Trop Dis. 2013;7:e2159. http://dx.doi.org/10.1371/journal.pntd.0002159
15. Center for Disease Control. Dengue fever—Puerto Rico. MMWR Morb Mortal Wkly Rep. 1963;12:286–7.
16. Center for Disease Control. Dengue follow-up—Puerto Rico. MMWR Morb Mortal Wkly Rep. 1969;18:1.
17. Center for Disease Control Dengue—Puerto Rico. 1970. MMWR Morb Mortal Wkly Rep. 1971;20:74–5.
18. Rymzo WT Jr, Cline BL, Kemp GE, Sather GE, Craven PC. Dengue outbreaks in Guánica-Ensenada and Villalba, Puerto Rico, 1972-1973. Am J Trop Med Hyg. 1976;25:136–45. http://dx.doi.org/10.4269/ajtmh.1976.25.136
19. Gubler DJ, Kuno G, Sather GE, Velez M, Oliver A. Mosquito cell cultures and specific monoclonal antibodies in surveillance for dengue viruses. Am J Trop Med Hyg. 1984;33:158–65. http://dx.doi.org/10.4269/ajtmh.1984.33.158
20. Dechant EJ, Rigau-Pérez JG; The Puerto Rico Association of Epidemiologists. Hospitalizations for suspected dengue in Puerto Rico, 1991–1995: estimation by capture-recapture methods. Am J Trop Med Hyg. 1999;61:574–8. http://dx.doi.org/10.4269/ajtmh.1999.61.574
21. Meltzer MI, Rigau-Pérez JG, Clark GG, Reiter P, Gubler DJ. Using disability-adjusted life years to assess the economic impact of dengue in Puerto Rico: 1984–1994. Am J Trop Med Hyg. 1998;59:265–71. http://dx.doi.org/10.4269/ajtmh.1998.59.265
22. Shankar MB, Rodríguez-Acosta RL, Sharp TM, Tomashek KM, Margolis HS, Meltzer MI. Estimating dengue under-reporting in Puerto Rico using a multiplier model. PLoS Negl Trop Dis. 2018;12:e0006650. http://dx.doi.org/10.1371/journal.pntd.0006650
23. Rigau-Perez JG, Clark GG. How to respond to a dengue epidemic: overview and experience in Puerto Rico [in Spanish]. Am J Public Health. 2005;17:282–93.
24. Rigau-Pérez JG, Millard PS, Walker DR, Deseda CC, Casta-Vélez A. A deviation bar chart for detecting dengue outbreaks in Puerto Rico. Am J Public Health. 1999;89:374–8. http://dx.doi.org/10.2105/AJPH.89.3.374
25. López-Correa RH, Cline BL, Ramirez-Ronda C, Bermudez R, Sather GE, Kuno G. Dengue fever with hemorrhagic manifestations: a report of three cases from Puerto Rico. Am J Trop Med Hyg. 1978;27:1216–24. http://dx.doi.org/10.4269/ajtmh.1978.27.1216
26. Gubler DJ. Dengue in the United States, 1982. MMWR Surveill Summ. 1984;33:9SS–13SS.
27. Rigau-Pérez JG, Torres JV, Mosely Hayes J, Vorndam V, Clark GG. Medical examiner samples: a source for dengue surveillance. P R Health Sci J. 2006;25:67–9.
28. Tomashek KM, Rivera A, Torres-Velasquez B, Hunsperger EA, Munoz-Jordan JL, Sharp TM, et al. Enhanced surveillance for fatal dengue-like acute febrile illness in Puerto Rico, 2010–2012. PLoS Negl Trop Dis. 2016;10:e0005025. http://dx.doi.org/10.1371/journal.pntd.0005025
29. García-Rivera EJ, Vorndam V, Rigau-Pérez JG. Use of an enhanced surveillance system for encephalitis and aseptic meningitis for the detection of neurologic manifestations of dengue in Puerto Rico, 2003. P R Health Sci J. 2009;28:114–20.
30. Gubler DJ, Clark GG. Community involvement in the control of *Aedes aegypti*. Acta Trop. 1996;61:169–79. http://dx.doi.org/10.1016/0001-706X(95)00103-L

31. Winch PJ, Leontsini E, Rigau-Pérez JG, Ruiz-Pérez M, Clark GG, Gubler DJ. Community-based dengue prevention programs in Puerto Rico: impact on knowledge, behavior, and residential mosquito infestation. Am J Trop Med Hyg. 2002;67:363–70. http://dx.doi.org/10.4269/ajtmh.2002.67.363
32. Rigau-Pérez JG, Laufer MK. Dengue-related deaths in Puerto Rico, 1992–1996: diagnosis and clinical alarm signals. Clin Infect Dis. 2006;42:1241–6. http://dx.doi.org/10.1086/501355
33. Tomashek KM, Biggerstaff BJ, Ramos MM, Pérez-Guerra CL, Garcia Rivera EJ, Sun W. Physician survey to determine how dengue is diagnosed, treated and reported in Puerto Rico. PLoS Negl Trop Dis. 2014;8:e3192. http://dx.doi.org/10.1371/journal.pntd.0003192
34. Tomashek KM, Gregory CJ, Rivera Sánchez A, Bartek MA, Garcia Rivera EJ, Hunsperger E, et al. Dengue deaths in Puerto Rico: lessons learned from the 2007 epidemic. PLoS Negl Trop Dis. 2012;6:e1614. http://dx.doi.org/10.1371/journal.pntd.0001614
35. Han GS, Gregory CJ, Biggerstaff BJ, Horiuchi K, Perez-Guerra C, Soto-Gomez E, et al. Effect of a dengue clinical case management course on physician practices in Puerto Rico. Clin Infect Dis. 2016;63:1297–303. http://dx.doi.org/10.1093/cid/ciw511
36. Rosen L, Gubler D. The use of mosquitoes to detect and propagate dengue viruses. Am J Trop Med Hyg. 1974;23:1153–60. http://dx.doi.org/10.4269/ajtmh.1974.23.1153
37. Gubler DJ, Kuno G, Sather GE, Waterman SH. A case of natural concurrent human infection with two dengue viruses. Am J Trop Med Hyg. 1985;34:170–3. http://dx.doi.org/10.4269/ajtmh.1985.34.170
38. Kuno G, Gómez I, Gubler DJ. An ELISA procedure for the diagnosis of dengue infections. J Virol Methods. 1991;33:101–13. http://dx.doi.org/10.1016/0166-0934(91)90011-N
39. Peeling RW, Artsob H, Pelegrino JL, Buchy P, Cardosa MJ, Devi S, et al. Evaluation of diagnostic tests: dengue. Nat Rev Microbiol. 2010;8(Suppl):S30–8. http://dx.doi.org/10.1038/nrmicro2459
40. Vorndam V, Beltran M. Enzyme-linked immunosorbent assay-format microneutralization test for dengue viruses. Am J Trop Med Hyg. 2002;66:208–12. http://dx.doi.org/10.4269/ajtmh.2002.66.208
41. Namekar M, Ellis EM, O'Connell M, Elm J, Gurary A, Park SY, et al. Evaluation of a new commercially available immunoglobulin M capture enzyme-linked immunosorbent assay for diagnosis of dengue virus infection. J Clin Microbiol. 2013;51:3102–6. http://dx.doi.org/10.1128/JCM.00351-13
42. Lanciotti RS, Calisher CH, Gubler DJ, Chang GJ, Vorndam AV. Rapid detection and typing of dengue viruses from clinical samples by using reverse transcriptase-polymerase chain reaction. J Clin Microbiol. 1992;30:545–51.
43. Chien LJ, Liao TL, Shu PY, Huang JH, Gubler DJ, Chang GJ. Development of real-time reverse transcriptase PCR assays to detect and serotype dengue viruses. J Clin Microbiol. 2006;44:1295–304. http://dx.doi.org/10.1128/JCM.44.4.1295-1304.2006
44. Johnson BW, Russell BJ, Lanciotti RS. Serotype-specific detection of dengue viruses in a fourplex real-time reverse transcriptase PCR assay. J Clin Microbiol. 2005;43:4977–83. http://dx.doi.org/10.1128/JCM.43.10.4977-4983.2005
45. Santiago GA, Vergne E, Quiles Y, Cosme J, Vazquez J, Medina JF, et al. Analytical and clinical performance of the CDC real time RT-PCR assay for detection and typing of dengue virus. [Erratum in: PLoS Negl Trop Dis. 2013;7]. PLoS Negl Trop Dis. 2013;7:e2311. http://dx.doi.org/10.1371/journal.pntd.0002311
46. Hunsperger EA, Muñoz-Jordán J, Beltran M, Colón C, Carrión J, Vazquez J, et al. Performance of dengue diagnostic tests in a single-specimen diagnostic algorithm. J Infect Dis. 2016;214:836–44. http://dx.doi.org/10.1093/infdis/jiw103
47. Hunsperger EA, Sharp TM, Lalita P, Tikomaidraubuta K, Cardoso YR, Naivalu T, et al. Use of a rapid test for diagnosis of dengue during suspected dengue outbreaks in resource-limited regions. J Clin Microbiol. 2016;54:2090–5. http://dx.doi.org/10.1128/JCM.00521-16
48. Santiago GA, Vázquez J, Courtney S, Matías KY, Andersen LE, Colón C, et al. Performance of the Trioplex real-time RT-PCR assay for detection of Zika, dengue, and chikungunya viruses. Nat Commun. 2018;9:1391. http://dx.doi.org/10.1038/s41467-018-03772-1
49. Flynn ADSH, Morlan HB, Porter JE. Susceptibility of seventeen strains of *Aedes aegypti* (L.) from Puerto Rico and the Virgin Islands to DDT, dieldrin, and malathion. Mosq News. 1964;24:118–23.
50. Fontaine RE, Mulrennan JA, Schliessmann DJ. 1964 progress report of the *Aedes aegypti* eradication program. Am J Trop Med Hyg. 1965;14:900–3. http://dx.doi.org/10.4269/ajtmh.1965.14.900

Address for correspondence: Tyler M. Sharp, Centers for Disease Control and Prevention, 1324 Calle Cañada, San Juan, PR 00920, USA; email: tsharp@cdc.gov

Case Series Study of Melioidosis, Colombia

José Y. Rodríguez, Soraya E. Morales-López, Gerson J. Rodríguez, Carlos A. Álvarez-Moreno, Kelin Esquea, Heidy Pinzon, Luis R. Ramirez, Lilian Moreno, Walter Ocampo, Martha L. Cepeda

We report 7 cases of melioidosis in Colombia and comparision of 4 commercial systems for identifying *Burkholderia pseudomallei*. Phoenix systems were not a definitive method for identifying *B. pseudomallei*. For accurate identification, we recommend including this bacterium in the library databases of matrix-assisted laser desorption/ionization mass spectrometry systems in Latin America.

Melioidosis is an infectious disease caused by *Burkholderia pseudomallei*, a saprophytic soil bacterium (*1*). Recently, an increase in cases outside the Asia–Pacific region, including the Americas, has been reported. It is not clear whether this increased number of cases reflects an increase in incidence of this disease or improvements in its identification by microbiological laboratories and research facilities (*2*).

The Study

We describe 7 cases of melioidosis in the Caribbean coast region of Colombia among patients who sought emergency services or were referred to 3 hospitals in the city of Valledupar (Figure). None of the patients reported travel abroad. Four patients were admitted during 2015 and 2016; we analyzed the corresponding isolates using 4 commercial methods and a molecular identification method. For the other 3 cases, which were diagnosed in 2014, we reviewed patient medical records and microbiological results. These isolates were not available. The study was approved by the ethics committees of Clinica Laura Daniela, Clínica Médicos, and Instituto Cardiovascular del Cesar.

Of the 7 patients, 6 (86%) were men; 2 patients were admitted to the intensive care unit (Table 1). The most common clinical presentation was bacteremic pneumonia (in 4 patients); 5 patients had a history of diabetes.

The 4 strains isolated in 2015 and 2016 were identified as *B. pseudomallei* by Vitek Compact 2 (bioMérieux, https://www.biomerieux.com) and Microscan (Walkaway Beckman Coulter, https://www.beckmancíoulter.com) but as *B. cepacia* by Phoenix (Becton Dickinson, http://www.bd.com) and as *B. thailandesis* by MALDI Biotyper v3.1 matrix-assisted laser desorption/ionization time-of-flight (MALDI-TOF) mass spectrometry (Bruker Daltonics, https://www.bruker.com). Internal transcribed spacer (ITS) DNA sequencing identified all the isolates as *B. pseudomallei*. Sequences of these 4 isolates were submitted to GenBank (accession nos. KX898558, KY659330, KY996759, and KY659331). According to patient medical records, the 3 isolates from 2014 were identified as *B. pseudomallei* using the Vitek or Microscan system or both (Table 2).

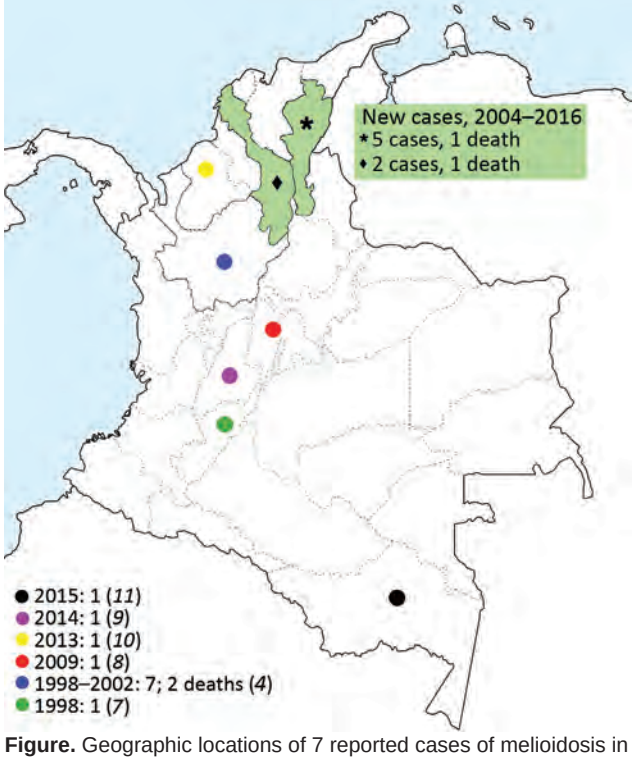

Figure. Geographic locations of 7 reported cases of melioidosis in Colombia.

Author affiliations: Hospital Rosario Pumarejo de López, Valledupar, Colombia (J.Y. Rodríguez); Centro de Investigaciones Microbiológicas del Cesar (CIMCE), Valledupar (J.Y. Rodríguez, G.J. Rodríguez); Clínica Laura Daniela, Valledupar (J.Y. Rodríguez, K. Esquea); Clínica Médicos LTDA, Valledupar (J.Y. Rodríguez, H. Pinzon); Laboratorios Nancy Flórez García S.A.S., Valledupar (S.E. Moralez-López); Universidad Popular del Cesar, Valledupar (S.E. Moralez-López); Universidad Nacional de Colombia, Bogotá, Colombia (C.A. Álvarez-Moreno); Clínica Universitaria Colombia, Clínicas Colsanitas, Bogotá (C.A. Álvarez-Moreno); Grupo de Investigaciones Microbiológicas del Cesar, Valledupar (L.R. Ramirez, L. Moreno); Corporación CorpoGen, Bogotá (W. Ocampo, M.L. Cepeda)

DOI: https://doi.org/10.3201/eid2508.170786

Table 1. Epidemiologic and demographic characteristics, underlying conditions, clinical manifestations, and outcomes of patients with melioidosis in the Caribbean coast region of Colombia*

Patient no.	Patient age, y/ sex	Medical history and risk factors	Clinical manifestation	Type of sample	Empirical treatment	Appropriate treatment (duration)	ICU	Outcome	Relapse
1	72/M	Diabetes, arterial hypertension	Bacteremic pneumonia	Blood culture, urine culture, endotracheal aspirate	TZP + CLR	IP: MER + TMP/SMX (14 d); EP: NA	Yes	Died	NA
2	60/F	Diabetes, arterial hypertension, minor head injury with open scalp wound	Bacteremic SSTI	Wound secretion, blood culture	CFZ + CLI	IP: MER (10 d); EP: TMP/SMX (3 mo)	No	Alive	No
3	49/M	Diabetes, leprosy, erythema nodosum leprosum, chronic use of steroids	Bacteremic pneumonia	Blood culture, urine culture, sputum culture	TZP + CLR	IP: MER (10 d); EP: TMP/SMX (6 mo)	No	Alive	No
4	71/M	Arterial hypertension, multiple myeloma, bone marrow transplant, chronic use of steroids and thalidomide	Bacteremic pneumonia	Blood culture	TZP + DOX	IP: MER (14 d); EP: TMP/SMX (3 mo)	No	Alive	No
5	66/M	Diabetes, arterial hypertension	Bacteremic pneumonia	Blood culture, endotracheal aspirate	TZP	NA	Yes	Died	NA
6	56/M	Diabetes, chronic renal failure	UTI	Urine culture	TZP	IP: MER (10 d); EP: TMP/SMX (3 mo)	No	Alive	At 6 mo: bacteremia, UTI, SSTI
7	54/M	Tibia and fibula open fracture	SSTI	Wound secretion, blood culture	CFZ + CLI	IP: MER (10 d); EP: TMP/SMX (6 mo)	No	Alive	No

*CFZ, cefazolin; CLI, clindamycin; CLR, clarithromycin; DOX, doxycycline; EP, eradication phase; IP, intensive phase; MER, meropenem; NA, not available; SSTI, skin and soft tissue infection; TMP/SMX, trimethoprim/sulfamethoxazole; TZP, piperacillin/tazobactam; UTI, urinary tract infection.

MIC testing was performed using the system available in the institution where the patient was being treated: Microscan Walkaway (isolates 1, 2, 3, 5) and Phoenix systems (isolates 4, 6, 7). According to published cutoff points for *B. pseudomallei* (Clinical and Laboratory Standards Institute, https://clsi.org/standards/products/microbiology/documents/m45), all isolates were susceptible to trimethoprim/sulfamethoxazole and meropenem, and 2 isolates (isolates 2 and 7) were resistant to ceftazidime (MIC >16 μg/mL); however, isolate 7 was tested 2 more times using Microscan, resulting in a value of <2 μg/mL. Isolate 2 was not available for further analysis.

Within the genus *Burkholderia*, *B. pseudomallei*, *B. mallei*, and the *B. cepacia* complex are the species usually associated with human infection (*3*,*4*). Historically, melioidosis is recognized as a major cause of fatal pneumonia and sepsis in Southeast Asia, South Asia, and northern Australia. It is believed that movements of both humans and cargo have contributed to the dissemination. A phylogenetic reconstruction study determined the African origin of the American isolates and the overlapping of the introduction of *B. pseudomallei* into the New World with the height of the slave trade from Africa to the Americas (*5*).

In Colombia, melioidosis is not a disease of public health interest and thus could be underreported. However, Colombia is second to Brazil with the highest number of cases reported in South America (*1*). The actual number of cases is unknown, probably because of the lack of awareness and suspicion of the disease by health professionals, together with the absence of technology for proper diagnosis and the underreporting of diagnosed cases. At least 10 reported cases of melioidosis have been acquired in the Andean region of Colombia. Severiche published a report in 1998 about a patient with pneumonia (*6*). Montúfar et al. described a series of 7 patients during 1998–2012, of whom 5 had bacteremic pneumonia (*7*). Since then, other cases of bacteremic pneumonia have been reported (*8*,*9*), as well as 1 case of chronic lung melioidosis in a patient on Colombia's west Caribbean coast (*10*). Guzmán-Gómez et al. described a case of osteoarticular melioidosis acquired in the Colombian rainforest in 2015 (*11*), the only case confirmed by sequencing (ITS-16S rRNA gene). The areas in Colombia where melioidosis cases have been reported, including these new cases from the Caribbean coast, are consistent with the previously proposed model (*2*) (Figure 1).

The isolation of *B. pseudomallei* from clinical specimens is the standard for a diagnosis of melioidosis. However, the microorganism is not often recovered and may not be correctly identified even when isolated. *B. pseudomallei*

Table 2. Isolate identification results by commercial systems, 16S rRNA sequencing analysis, and antimicrobial drug susceptibility of isolates of *Burkholderia pseudomallei* obtained from clinical specimens in the Caribbean coast region of Colombia*

Isolate no.	Commercial bacterial identification systems				ITS sequencing segments	GenBank accession no.	MIC, μg/mL		
	Vitek (% probability)	Walkaway/ Microscan (% probability)	Phoenix (% probability)	MALDI-TOF MS (score)			CAZ	MER	TMP/ SMX
1	ND	*B. pseudomallei* (93%)	ND	ND	ND	ND	2	≤1	≤2/38
2	*B. pseudomallei* (99%)	*B. pseudomallei* (99.5%)	ND	ND	ND	ND	>16	≤1	≤2/38
3	*B. pseudomallei* (94%)	*B. pseudomallei* (99.8%)	ND	ND	ND	ND	2	≤1	≤1/19
4	*B. pseudomallei* (94%)	*B. pseudomallei* (99.9%)	*B. cepacia* (99%)	*B. thailandensis* (1,899)	*B. pseudomallei*	KX898558	4	1	2/38
5	*B. pseudomallei* (94%)	*B. pseudomallei* (99.5%)	*B. cepacia* (99%)	*B. thailandensis* (1,898)	*B. pseudomallei*	KY659330	4	2	1/19
6	*B. pseudomallei* (95%)	*B. pseudomallei* (99.9%)	*B. cepacia* (99%)	*B. thailandensis* (1,898)	*B. pseudomallei*	KY996759	4	1	1/19
7	*B. pseudomallei* (94%)	*B. pseudomallei* (93%)	*B. cepacia* (99%)	*B. thailandensis* (1,898)	*B. pseudomallei*	KY659331	<2	2	1/19

*CAZ, ceftazidime; ITS, internal transcribed spacer; MALDI-TOF MS, matrix-assisted laser desorption/ionization time-of-flight mass spectrometry; MER, meropenem; ND, no data; TMP/SMX, trimethoprim/sulfamethoxazole.

can be identified using commercial identification systems. However, these tests may fail to distinguish *B. pseudomallei* from *B. thailandensis* and other members of the *B. cepacia* complex (*12*,*13*). MALDI-TOF mass spectrometry is an accurate and rapid procedure for the identification of *B. pseudomallei* if the appropriate database is used (*14*). However, genotyping methods based on rRNA sequencing should be used for a more accurate diagnosis. We compared different phenotyping methods (Vitek, MicroScan Walkaway, Phoenix, and MALDI-TOF mass spectrometry) using 4 isolates from this report. Sequencing of the ITS region confirmed the identification of *B. pseudomallei* and matched the identifications obtained by the Vitek and Walkaway systems. However, the Phoenix system erroneously identified isolates as *B. cepacia*, and MALDI-TOF mass spectrometry incorrectly identified isolates as *B. thailandensis*. Although *B. pseudomallei* was included in the Phoenix database, we strongly recommend not using Phoenix as a single or final method to identify possible isolates of *B. pseudomallei* (for example, gram-negative, oxidase-positive, and positive-arginine bacilli). MALDI-TOF mass spectrometry is currently being introduced in Colombia, and we recommend the inclusion of *B. pseudomallei* in the database.

The treatment of melioidosis is prolonged and includes 2 phases: intensive treatment with intravenous antimicrobial therapy for 10–14 days using ceftazidime, imipenem, or meropenem; and an eradication phase with oral antimicrobial therapy for 3–6 months with trimethoprim/sulfamethoxazole alone or in combination with doxycycline (*15*). In the cases we report, treatment with meropenem was started, because it is easier to prescribe this antimicrobial drug in Colombia, given the high rate of extended-spectrum β-lactamase–producing *Enterobacteriaceae*; the use of ceftazidime is restricted for the same reason. Because of the severity of illness and the high rate of death from this disease, along with the required prolonged antimicrobial drug therapy and the small number of drugs available for its treatment, it is necessary not only to strengthen the public health surveillance and clinical suspicion of melioidosis but also to acquire tools that permit an adequate diagnosis, especially in potentially endemic areas, which, in the case of Colombia, could be an extensive geographic area.

Conclusions

With the presence of *B. pseudomallei* on Colombia's Caribbean coast confirmed, clinicians should suspect melioidosis in patients with risk factors, suggestive clinical symptoms, and microbiological isolates from clinical specimens of *B. pseudomallei* or other members of the *Burkholderia* genus. In this case, >1 microbiological identification method should be used, especially if the outdated Phoenix or MALDI-TOF mass spectrometry databases are used.

Finally, it is necessary to include melioidosis in a passive surveillance system, especially in those regions of Latin America where the environmental conditions create high probabilities for the presence of the disease. Currently, Colombia has a public health surveillance and control system under the supervision of the National Institute of Health, to which all health institutions must notify diseases of public health interest. To determine the true magnitude of melioidosis in Colombia, it must be included as a notifiable disease and measures established to enable its early diagnosis and treatment.

About the Author

Dr. Rodríguez is chief of the Division of Infectious Diseases at the Instituto Cardiovascular del Cesar, Medicos Clinic, and Laura Daniela Clinic, Valledupar, Colombia. He is director and founder of Centro de Investigaciones Microbiológicas del Cesar, Valledupar, Colombia. His main research interest is nosocomial infections.

References

1. Benoit TJ, Blaney DD, Doker TJ, Gee JE, Elrod MG, Rolim DB, et al. A review of melioidosis cases in the Americas. Am J Trop Med Hyg. 2015;93:1134–9. http://dx.doi.org/10.4269/ajtmh.15-0405
2. Limmathurotsakul D, Golding N, Dance DAB, Messina JP, Pigott DM, Moyes CL, et al. Predicted global distribution of *Burkholderia pseudomallei* and burden of melioidosis. Nat Microbiol. 2016;1:15008. http://dx.doi.org/10.1038/nmicrobiol.2015.8
3. Eberl L, Vandamme P. Members of the genus Burkholderia: good and bad guys. F1000 Res. 2016;5:1007. http://dx.doi.org/10.12688/f1000research.8221.1
4. Depoorter E, Bull MJ, Peeters C, Coenye T, Vandamme P, Mahenthiralingam E. Burkholderia: an update on taxonomy and biotechnological potential as antibiotic producers. Appl Microbiol Biotechnol. 2016;100:5215–29. http://dx.doi.org/10.1007/s00253-016-7520-x
5. Chewapreecha C, Holden MTG, Vehkala M, Välimäki N, Yang Z, Harris SR, et al. Global and regional dissemination and evolution of *Burkholderia pseudomallei.* Nat Microbiol. 2017;2:16263. http://dx.doi.org/10.1038/nmicrobiol.2016.263
6. Severiche D. *Pseudomonas pseudomallei* community acquired pneumonia. Rev Colomb Neumol. 1998;10:188–92.
7. Montúfar FE, Ochoa JE, Ortega H, Franco L, Montúfar MC, Monsalve A, et al. Melioidosis in Antioquia, Colombia: an emerging or endemic disease? A case series. Int J Infect Dis. 2015;37:50–7. http://dx.doi.org/10.1016/j.ijid.2015.05.023
8. Gonzalez G, Mantilla W, Rada R. Pneumonia and osteomyelitis by *Burkholderia pseudomallei*: report of a clinical case. Rev Med. 2009;17:146–9.
9. Osorio Carmona HE, Duran LF. Melioidosis: reporte de un caso en el departamento del Huila—Colombia. RFS Rev Fac Salud. 2014;6:56–9. http://dx.doi.org/10.25054/rfs.v6i2.166
10. Rosero CH, Gómez G, Gutiérrez OI. Tos y disnea de seis años de evolución en un adulto joven con melioidosis pulmonar crónica. Reporte de caso. Med Lab. 2013;19:465–72.
11. Guzmán-Gómez L, Agudo Bilbao M, Peiro-Callizo E, Salas C. Melioidosis importada desde Colombia a España. Enferm Infecc Microbiol Clin. 2015;33:214–6. http://dx.doi.org/10.1016/j.eimc.2014.06.003
12. Lau SKP, Sridhar S, Ho C-C, Chow W-N, Lee K-C, Lam C-W, et al. Laboratory diagnosis of melioidosis: past, present and future. Exp Biol Med (Maywood). 2015;240:742–51. http://dx.doi.org/10.1177/1535370215583801
13. Kiratisin P, Santanirand P, Chantratita N, Kaewdaeng S. Accuracy of commercial systems for identification of *Burkholderia pseudomallei* versus *Burkholderia cepacia*. Diagn Microbiol Infect Dis. 2007;59:277–81. http://dx.doi.org/10.1016/j.diagmicrobio.2007.06.013
14. Wang H, Chen Y-L, Teng S-H, Xu Z-P, Xu Y-C, Hsueh P-R. Evaluation of the Bruker Biotyper matrix-assisted laser desorption/ionization time-of-flight mass spectrometry system for identification of clinical and environmental isolates of *Burkholderia pseudomallei.* Front Microbiol. 2016;7:415.
15. Kingsley PV, Arunkumar G, Tipre M, Leader M, Sathiakumar N. Pitfalls and optimal approaches to diagnose melioidosis. Asian Pac J Trop Med. 2016;9:515–24. http://dx.doi.org/10.1016/j.apjtm.2016.04.003

Address for correspondence: José Y. Rodríguez, Centro de Investigaciones Microbiológicas del Cesar (CIMCE), Calle 16c no 19d-14 Barrio Dangond, Valledupar, Colombia; email: jyrodriguezq@gmail.com

Sustained Low-Level Transmission of Zika and Chikungunya Viruses after Emergence in the Fiji Islands

Mike Kama,[1] Maite Aubry,[1] Taina Naivalu, Jessica Vanhomwegen, Teheipuaura Mariteragi-Helle, Anita Teissier, Tuterarii Paoaafaite, Stéphane Hué, Martin L. Hibberd, Jean-Claude Manuguerra, Ketan Christi, Conall H. Watson, Eric J. Nilles, John Aaskov, Colleen L. Lau, Didier Musso, Adam J. Kucharski,[1] Van-Mai Cao-Lormeau[1]

Zika and chikungunya viruses were first detected in Fiji in 2015. Examining surveillance and phylogenetic and serologic data, we found evidence of low-level transmission of Zika and chikungunya viruses during 2013–2017, in contrast to the major outbreaks caused by closely related virus strains in other Pacific Island countries.

Zika virus and chikungunya virus (CHIKV) have caused outbreaks in several tropical regions, including the Pacific (*1*). The first known Zika virus outbreak occurred in Yap Island (Federated States of Micronesia) in 2007 (*2*), followed by an explosive outbreak in French Polynesia in 2013–2014 (*3*), then other Pacific islands (*4*) and Latin America (*5*). CHIKV first appeared in the Pacific in 2011 (*6*), causing multiple outbreaks from 2013 onward (*4*).

Author affiliations: Fiji Centre for Communicable Disease Control, Suva, Fiji (M. Kama); The University of the South Pacific, Suva (M. Kama, T. Naivalu, K. Christi); Institut Louis Malardé, Papeete, Tahiti (M. Aubry, T. Mariteragi-Helle, A. Teissier, T. Paoaafaite, D. Musso, V.-M. Cao-Lormeau); Fiji National University, Suva (T. Naivalu); Institut Pasteur, Paris, France (J. Vanhomwegen, J.-C. Manuguerra); London School of Hygiene and Tropical Medicine, London, UK (S. Hué, M.L. Hibberd, C.H. Watson, A.J. Kucharski); World Health Organization, Suva (E.J. Nilles); Harvard Medical School and Brigham and Women's Hospital, Boston, Massachusetts, USA (E.J. Nilles); Harvard Humanitarian Initiative, Cambridge, Massachusetts, USA (E.J. Nilles); Queensland University of Technology, Brisbane, Queensland, Australia (J. Aaskov); Australian National University, Canberra, Australian Capital Territory, Australia (C.L. Lau); Aix Marseille University, Marseille, France (D. Musso)

DOI: https://doi.org/10.3201/eid2508.180524

In Fiji, the first confirmed Zika virus infections were detected in July 2015; these were locally acquired. By March 2016, a total of 13 confirmed infections had been reported (*7*). The first recorded CHIKV infection was an imported case detected in March 2015 (*8*); 24 autochthonous infections were identified by June 2016 (*9*). CHIKV and Zika virus were subsequently detected in travelers returning from Fiji (*10*,*11*). Outbreaks of dengue virus (DENV) have been recorded in Fiji (*4*,*12*), and evidence from other settings indicates that DENV and Zika virus can exhibit similar transmission characteristics in the same location (*13*). Despite enhanced surveillance, no large outbreaks of Zika or chikungunya were identified in Fiji, unlike in other settings (*3*,*4*). We describe the introduction, epidemiology, and transmission of Zika virus and CHIKV in Fiji during 2013–2017, in a context of concurrent circulation of DENV (*4*,*12*).

The Study

We retrieved surveillance data for patients with prolonged fever (PF), defined as any fever lasting ≥3 days, and acute fever and rash (AFR) in Fiji (Figure), as well as data on suspected and confirmed Zika virus, CHIKV, and DENV infections (Appendix Table 1, https://wwwnc.cdc.gov/EID/article/25/8/18-0524-App1.pdf). We reconstructed phylogenetic trees of Zika virus and CHIKV sequences by using Bayesian inference (Appendix Tables 2, 3). We recruited 778 participants in Fiji during September–November 2013 as part of a community-based serologic survey (Appendix Figure 1). We collected follow-up samples from the same participants in the Central Division (N = 333) during October–November 2015. We tested serum samples by using a recombinant antigen-based microsphere immunoassay to detect Zika virus, CHIKV, and DENV-1–4 IgG (Appendix). Analysis of neutralizing antibodies against Zika virus and DENV in a subset of 69 paired serum samples showed good concordance with the microsphere immunoassay for Zika virus ($\kappa = 0.71$) and DENV ($\kappa = 0.80$) (Appendix Table 4).

Surveillance data recorded during 2013–2017 indicated cyclical increases in AFR and PF each year, concurrent

[1]These authors contributed equally to this article.

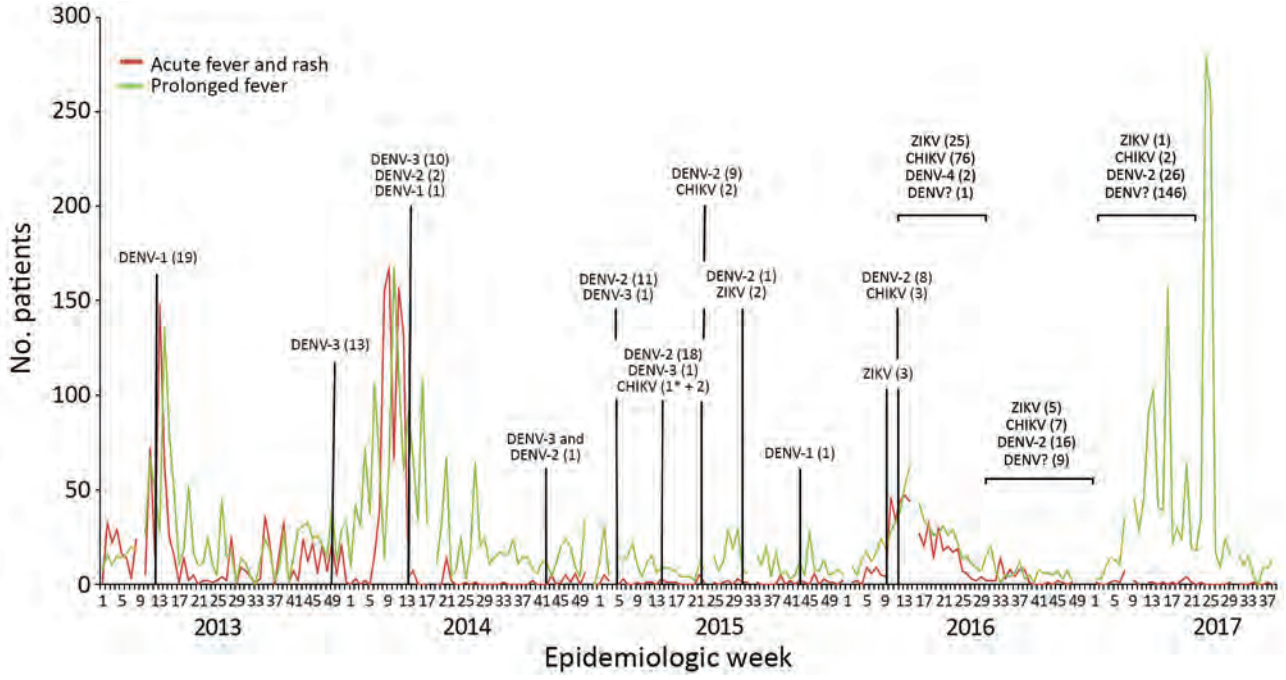

Figure. Reports of patients with acute fever and rash, prolonged fever, and infections with dengue, Zika, or chikungunya viruses confirmed by reverse transcription PCR in Fiji, 2013–2017. Number of dengue, Zika, or chikungunya virus infections were confirmed by reverse transcription PCR. Asterisks (*) indicate imported chikungunya virus infections. CHIKV, chikungunya virus; DENV-1, dengue virus serotype 1; DENV-2, dengue virus serotype 2; DENV-3, dengue virus serotype 3; DENV-4, dengue virus serotype 4; DENV?, information on dengue virus serotype not available; ZIKV, Zika virus.

with the hot and rainy season occurring in December–April (Figure). Molecular testing of blood samples from symptomatic patients suggested outbreaks of DENV-1 in 2013, DENV-3 in 2014, and DENV-2 in 2017. In 2015, Zika virus and CHIKV apparently were co-circulating at low levels alongside DENV-1, DENV-2, and DENV-3. In 2016, an increase in proportional positivity for Zika virus and CHIKV was detected among 804 AFR and PF patients, suggesting higher transmission of these viruses but not widespread circulation (Zika virus, 32/804 [4%]; CHIKV, 86/804 [11%]; DENV-2, 10/804 [1%]; DENV-4, 2/804 [<1%]). Additional CHIKV (n = 2) and Zika virus (n = 1) infections were detected during the first half of 2017.

We aligned the envelope (E) gene sequences of Zika virus strains collected in Fiji during 2015–2016 (Appendix Table 2) with sequences from other countries. All Zika virus strains belonged to the Asia lineage and segregated into 2 separate clades (posterior probability >0.99) (Appendix Figure 2, panel A). The Fiji Zika virus strains belonged to the Asia and Oceania clade; 2 strains collected in 2016 grouped with viruses isolated in Japan in 2016 (posterior probability >0.99), including 1 from a traveler returning from Fiji. The estimated time of most recent common ancestor of this cluster was September 2013 (95% higher probability density [HPD] interval September 2011–August 2015). The remaining Fiji strains formed a distinct cluster with strains from Southeast Asia and other Pacific Islands. We dated the origin of this second cluster to November 2013 (95% HPD interval March 2013–July 2015).

We aligned the E1 gene sequences of Fiji CHIKV strains collected during 2015–2016 (Appendix Table 2) with sequences from other countries. All strains belonged to the Asia genotype; Fiji strains formed a monophyletic group with strains from Tonga sampled in 2014 (posterior probability 1.00) (Appendix Figure 2, panel B). This grouping suggested a single introduction of CHIKV into Fiji in February 2014 (95% HPD interval December 2013–August 2014) and subsequent persistence in the population.

Zika virus seroprevalence in 2013 was 7.8% (95% CI 6.1%–10%); we observed no significant differences between age groups, sexes, residential divisions, or areas (Table). In 2015, seroprevalence was 21.9% (95% CI 17.6%–26.8%), and the only significant difference observed was between rural (14.2% [95% CI 8.3%–22%]) and urban (26.6% [95% CI 19.5%–34.6%]) areas (p = 0.0202). Compared with 2013, Zika virus seroprevalence in 2015 was significantly higher overall (p<0.0001). However, no change was observed in the CHIKV seroprevalence between 2013 (0.8% [95% CI 0.3%–1.7%]) and 2015 (0.9% [95% CI 0.2%–2.6%]), and no significant differences were observed in the demographic variables described for Zika virus. The seroprevalence of DENV in 2013 was 73% (95% CI 69.7%–76.1%) and was lower among

Table. Prevalence of Zika, chikungunya, and dengue virus antibodies in a representative subset of the population sampled during September–November 2013 and October–November 2015, Fiji Islands*

	No. seropositive/no. tested (% [95% CI])					
	Zika virus		Chikungunya virus		Dengue viruses†	
Variable	2013	2015	2013	2015	2013	2015
Total	61/778‡ (7.8 [6.1–10])	73/333 (21.9 [17.6–26.8])	6/778 (0.8 [0.3–1.7])	3/333 (0.9 [0.2–2.6])	568/778 (73 [69.7–76.1])	276/333 (82.9 [78.4–86.8])
Age range (median), y	2–85 (28)	4–80 (29)	2–85 (28)	4–80 (29)	2–78 (28)	4–80 (29)
Age group, y						
0–19	29/282 (10.3 [7–14.4])	29/115 (25.2 [17.6–34.2])	4/282 (1.4 [0.4–3.6])	1/115 (0.9 [0–4.7])	141/282 (50 [44–56])	78/115 (67.8 [58.5–76.2])
20–39	15/239 (6.3 [3.6–10.1])	18/103 (17.5 [10.7–26.2])	1/239 (0.4 [0–2.3])	1/103 (1 [0–5.3])	201/239 (84.1 [78.8–88.5])	93/103 (90.3 [82.9–95.2])
40–59	11/179 (6.1 [3.1–10.7])	13/73 (17.8 [9.8–28.5])	1/179 (0.6 [0–3.1])	1/73 (1.4 [0–7.4])	161/179 (89.9 [84.6–93.9])	68/73 (93.2 [84.7–97.7])
≥60	6/77 (7.8 [2.9–16.2])	13/42 (31 [17.6–47.1])	0/77 (0 [0–4.7])	0/42 (0 [0–8.4])	64/77 (83.1 [72.9–90.7])	37/42 (88.1 [74.4–96])
Sex						
F	28/423 (6.6 [4.4–9.4])	41/190 (21.6 [16–28.1])	4/423 (0.9 [0.3–2.4])	2/190 (1.1 [0.1–3.8])	312/423 (73.8 [69.3–77.9])	165/190 (86.8 [81.2–91.3])
M	33/354 (9.3 [6.5–12.8])	32/143 (22.4 [15.8–30.1])	2/354 (0.6 [0.1–2])	1/143 (0.7 [0–3.8])	255/354 (72 [67–76.6])	111/143 (77.6 [69.9–84.2])
Division						
Central	30/451 (6.7 [4.5–9.4])	73/333 (21.9 [17.6–26.8])	5/451 (1.1 [0.4–2.6])	3/333 (0.9 [0.2–2.6])	331/451 (73.4 [69.1–77.4])	276/333 (82.9 [78.4–86.8])
Northern	7/59 (11.9 [4.9–22.9])	ND	0/59 (0 [0–6.1])	ND	51/59 (86.4 [75–94])	ND
Western	24/268 (9 [5.8–13])	ND	1/268 (0.4 [0–2.1])	ND	186/268 (69.4 [63.5–74.9])	ND
Area						
Periurban	10/135 (7.4 [3.6–13.2])	19/77 (24.7 [15.6–35.8])	2/135 (1.5 [0.2–5.2])	0/77 (0 [0–4.7])	104/135 (77 [69–83.8])	66/77 (85.7 [75.9–92.6])
Rural	24/344 (7 [4.5–10.2])	16/113 (14.2 [8.3–22])	2/344 (0.6 [0.1–2.1])	0/113 (0 [0–3.2])	234/344 (68 [62.8–72.9])	84/113 (74.3 [65.3–82.1])
Urban	27/298 (9.1 [6.1–12.9])	38/143 (26.6 [19.5–34.6])	2/298 (0.7 [0.1–2.4])	3/143 (2.1 [0.4–6])	229/298 (76.8 [71.6–81.5])	126/143 (88.1 [81.6–92.9])

*No participants were recruited in the Northern and Western divisions in 2015. ND, no data.
†Seropositivity for ≥1 serotypes of dengue virus.
‡For 1 participant, demographic data were not available except for the administrative division of residence.

persons in the 0–19 years age group compared with other age groups ($p<0.0001$) (Table). We observed no significant difference by sex. DENV seropositivity was higher in the Northern than in the Central and Western divisions ($p\leq0.0368$) and higher in urban than in rural areas ($p = 0.0136$). During 2013–2015, we observed a significant increase in DENV seroprevalence (82.9% [95% CI 78.4%–86.8%]; $p = 0.0004$) among persons 0–19 years of age ($p = 0.0013$), women and girls ($p = 0.0002$), and participants living in the Central Division ($p = 0.0018$) and urban areas ($p = 0.0048$). Seroprevalence in 2015 remained lower in persons 0–19 years of age than in other age groups ($p\leq0.0137$) but was significantly higher in women and girls compared with men and boys ($p = 0.039$) and in urban compared with rural areas ($p = 0.0053$).

Analysis of paired samples collected in 2013 and 2015 from the same participants supported previous serologic findings on all samples collected (Appendix Table 5). Among these participants, 55/311 (17.7% [95% CI 13.6%–22.4%]) seroconverted to Zika virus, 40/311 (12.9% [95% CI 9.3%–17.1%]) seroconverted to DENV, and 1/311 (0.3% [95% CI 0.008%–1.8%]) seroconverted to CHIKV (Appendix Table 6).

Conclusions

We found evidence of low-level transmission of Zika virus and CHIKV in Fiji for multiple years after their initial introduction into a population that probably was immunologically naive, despite an ecologic environment subject to large and recurrent DENV outbreaks. Similar evidence of low-level Zika virus circulation has been observed in other settings (*14*). Our findings indicate that Zika virus circulated before the first confirmed cases in 2015 and that multiple introductions from other Pacific islands might have occurred, which suggests the possible role of Zika virus in a cluster of Guillain-Barré syndrome cases of unknown etiology in Fiji during February–May 2014 (*15*). However, there was no epidemiologic or serologic evidence that CHIKV circulated in Fiji before it was first reported in 2015. High DENV seroprevalence in 2013 and 2015 suggests that DENV is endemic in Fiji, with seroprevalence increasing with age. Our data also suggest that DENV and Zika virus transmission occurs mostly in urban areas where peridomestic mosquitoes, notably *Aedes aegypti* and *Ae. albopictus*, are abundant.

Our study highlights the difficulties in detecting and anticipating outbreaks of Zika virus and CHIKV and the value of having multiple data sources available. Stronger clinical and laboratory surveillance capacities are needed to ensure the early detection of these and future infectious disease threats.

This work was part of ISID-Pacific and R-ZERO Pacific programs funded by the French Ministry for Europe and Foreign Affairs (Pacific Fund nos. 06314-09/04/14, 12115-02/09/15, 03016-20/05/16, and 04917-19/07/17). The study also received support from the Embassy of France in the Republic of the Fiji Islands. The study was supported by the French Government's "Investissement d'Avenir" Program (Labex IBEID no. ANR-10-LABX-62-IBEID). C.L.L. was supported by an Australia National Health and Medical Research Council Fellowship (grant no. 1109035). A.J.K. was supported by a Wellcome Trust/Royal Society Sir Henry Dale Fellowship (grant no. 206250/Z/17/Z). The seroprevalence study was part of MSc research work by M.K. performed at the University of the South Pacific.

About the Author

Dr. Kama is a medical doctor with the Fiji Ministry of Health. Since 2008, he has worked in communicable disease control in Fiji. His area of interest is public health surveillance and response to communicable disease emergencies.

References

1. Cao-Lormeau V-M. Tropical islands as new hubs for emerging arboviruses. Emerg Infect Dis. 2016;22:913–5. http://dx.doi.org/10.3201/eid2205.150547
2. Duffy MR, Chen T-H, Hancock WT, Powers AM, Kool JL, Lanciotti RS, et al. Zika virus outbreak on Yap Island, Federated States of Micronesia. N Engl J Med. 2009;360:2536–43 http://dx.doi.org/10.1056/NEJMoa0805715
3. Cao-Lormeau V-M, Roche C, Teissier A, Robin E, Berry A-L, Mallet H-P, et al. Zika virus, French Polynesia, South Pacific, 2013. Emerg Infect Dis. 2014;20:1085–6. http://dx.doi.org/10.3201/eid2011.141380
4. Cao-Lormeau V-M, Musso D. Emerging arboviruses in the Pacific. Lancet. 2014;384:1571–2. http://dx.doi.org/10.1016/S0140-6736(14)61977-2
5. Ikejezie J, Shapiro CN, Kim J, Chiu M, Almiron M, Ugarte C, et al. Zika virus transmission—Region of the Americas, May 15, 2015–December 15, 2016. MMWR Morb Mortal Wkly Rep. 2017;66:329–34. http://dx.doi.org/10.15585/mmwr.mm6612a4
6. Dupont-Rouzeyrol M, Caro V, Guillaumot L, Vazeille M, D'Ortenzio E, Thiberge J-M, et al. Chikungunya virus and the mosquito vector *Aedes aegypti* in New Caledonia (South Pacific Region). Vector Borne Zoonotic Dis. 2012;12:1036–41. http://dx.doi.org/10.1089/vbz.2011.0937
7. Fiji Ministry of Health and Medical Services. Fiji Ministry of Health and Medical Services travel advice [cited 2018 Jan 31]. http://www.health.gov.fj/wp-content/uploads/2016/02/Fiji-Ministry-of-Health-Travel-Advice.pdf
8. Fiji Ministry of Health and Medical Services. Chikungunya alert [cited 2018 Jan 31]. http://www.health.gov.fj/?p=4366
9. Fiji Ministry of Health and Medical Services. People continue to support Fight the Bite—Clean Up Fiji campaign [cited 2018 Jan 31]. http://www.health.gov.fj/?p=5751
10. Institute of Environmental Science and Research Limited. Zika virus infection weekly report, 27 February 2017 [cited 2018 Jan 31]. https://surv.esr.cri.nz/PDF_surveillance/ZikaWeekly/2017/20170227Zikaweekly.pdf
11. Australian Government Department of Health. Summary information about overseas-acquired vectorborne disease notifications in Australia [cited 2018 Jan 31]. http://www.health.gov.au/internet/main/publishing.nsf/Content/F4E393746A4B690FCA2580D4007DB251/$File/13-Jan-18-overseas-notifications.pdf
12. Kucharski AJ, Kama M, Watson CH, Aubry M, Funk S, Henderson AD, et al. Using paired serology and surveillance data to quantify dengue transmission and control during a large outbreak in Fiji. eLife. 2018;7:e34848. http://dx.doi.org/10.7554/eLife.34848
13. Funk S, Kucharski AJ, Camacho A, Eggo RM, Yakob L, Murray LM, et al. Comparative analysis of dengue and Zika outbreaks reveals differences by setting and virus. PLoS Negl Trop Dis. 2016;10:e0005173. http://dx.doi.org/10.1371/journal.pntd.0005173
14. Ruchusatsawat K, Wongjaroen P, Posanacharoen A, Rodriguez-Barraquer I, Sangkitporn S, Cummings DAT, et al. Long-term circulation of Zika virus in Thailand: an observational study. Lancet Infect Dis. 2019;19:439–46. http://dx.doi.org/10.1016/S1473-3099(18)30718-7
15. Pastula DM, Khan AS, Sharp TM, Biaukula VL, Naivalu TK, Rafai E, et al. Investigation of a Guillain-Barré syndrome cluster in the Republic of Fiji. J Neurol Sci. 2017;372:350–5. http://dx.doi.org/10.1016/j.jns.2016.08.064

Address for correspondence: Van-Mai Cao-Lormeau, Institut Louis Malardé, PO Box 30, 98713 Papeete, Tahiti; email: mlormeau@ilm.pf

Lethal Encephalitis in Seals with Japanese Encephalitis Virus Infection, China, 2017

Xiangdong Li,[1] Mingming Qiao,[1] Xiaoyu Deng, Xi Chen, Shengyong Sun, Qian Zhang, Wenjie Zhang, Feifei Tan, Zhe Sun, Xizhao Chen, Ming Sun,[2] Kegong Tian[2]

We isolated Japanese encephalitis virus (JEV) from brain samples of 2 seals with lethal encephalitis at Weihai Aquarium, Weihai, China, in 2017. We confirmed our findings by immunohistochemical staining and electron microscopy. Phylogenetic analysis showed this virus was genotype I. Our findings suggest that JEV might disseminate though infected zoo animals.

Japanese encephalitis is a mosquitoborne zoonotic viral disease caused by Japanese encephalitis virus (JEV; family *Flaviviridae*, genus *Flavivirus*). The virus genome contains a 5′ untranslated region (UTR), followed by a 10,296-nt coding region and a 3′ UTR. The polyprotein consists of 3 structural proteins designated capsid, membrane, and envelope (E) and 7 nonstructural proteins (NS1, NS2A, NS2B, NS3, NS4A, NS4B, and NS5) (*1*). JEVs are classified into 5 genotypes (I–V) on the basis of the E gene sequence. Of these 5 genotypes, genotype I is the main type circulating in Asia (*2*).

JEV is transmitted primarily through *Culex* spp. mosquitoes and infects birds and some livestock species (*3*). Humans can also become infected but are dead-end hosts for JEV. Viral encephalitis can develop after JEV infection in humans and has a 30% mortality rate. Survivors have permanent neurologic sequelae, making JEV a clinically significant pathogen for viral encephalitis in Asia (*4*). Pigs are the reservoir hosts of JEV and play a role in transmitting this virus to humans. Pigs infected with JEV show pyrexia and anorexia, and pregnant pigs infected with JEV have an increased risk for stillborn offspring and offspring with congenital deformities (*5*). Horses and cattle can also become infected with JEV and occasionally show neurologic signs (*6*,*7*). Besides humans and the previously mentioned animals, JEV has rarely been reported in other mammals. In this study, we investigate the causative agent of lethal viral encephalitis in 2 aquatic mammalian seals.

The Study

In 2017, 2 speckled seals (*Phoca hispida*), a 1-year-old male seal and 1.5-year-old female seal, kept in Weihai Aquarium (Weihai, Shandong Province, China) were found displaying neurologic signs (backward head). The rest of the seals (3 male, 9 female, 2–8 years of age) in this aquarium did not display any clinical signs of illness. All seals were raised in the same pools and fed a diet of frozen smashed fish. The 2 sick seals were found dead the next day; immediately afterward, we performed necropsies. We observed hemorrhages in the brain (Figure 1, panel A) but found no lesions in other organs or tissues.

We collected tissue samples to test for seal parvovirus, phocine distemper virus, influenza A virus, coronavirus, canine distemper virus, canine adenovirus, pseudorabies virus, rabies virus, and JEV using commercial real-time PCR kits (Beijing Anheal Laboratories Co. Ltd., http://www.anheal.com). PCR results were negative for all tested pathogens except JEV, indicating this virus might have infected these seals.

We collected brain samples and fixed them in 10% buffered formalin for histopathologic analysis. We embedded samples in paraffin, sectioned them, and stained them with hematoxylin and eosin according to standard protocols. We used anti-JEV polyclonal mouse serum (kindly provided by the Department of Viral Encephalitis, National Institute for Viral Disease Control and Prevention, Beijing, China) to detect viral antigen in brain samples and performed immunohistochemical staining as previously described (*8*). Histopathologic analysis of seal brain samples showed lymphocyte infiltration around small blood vessels and typical nonsuppurative encephalitis (Figure 1, panels B, C). Immunohistochemical staining with anti-JEV polyclonal mouse serum indicated JEV antigen in seal brain samples (Figure 1, panel D), confirming infection with JEV.

We passaged supernatants of brain homogenates from infected seals on baby hamster kidney cell line BHK-21. We cultured cells in Dulbecco-modified Eagle medium

Author affiliations: National Research Center for Veterinary Medicine, Luoyang, China (X. Li, F. Tan, Z. Sun, K. Tian); Beijing Anheal Laboratories Co. Ltd., Beijing, China (M. Qiao, X. Deng, Xi Chen, S. Sun, Q. Zhang, W. Zhang, Xizhao Chen, M. Sun); Henan Agricultural University, Zhengzhou, China (K. Tian)

DOI: https://doi.org/10.3201/eid2508.181663

[1]These authors contributed equally to this article.

[2]These senior authors contributed equally to this article.

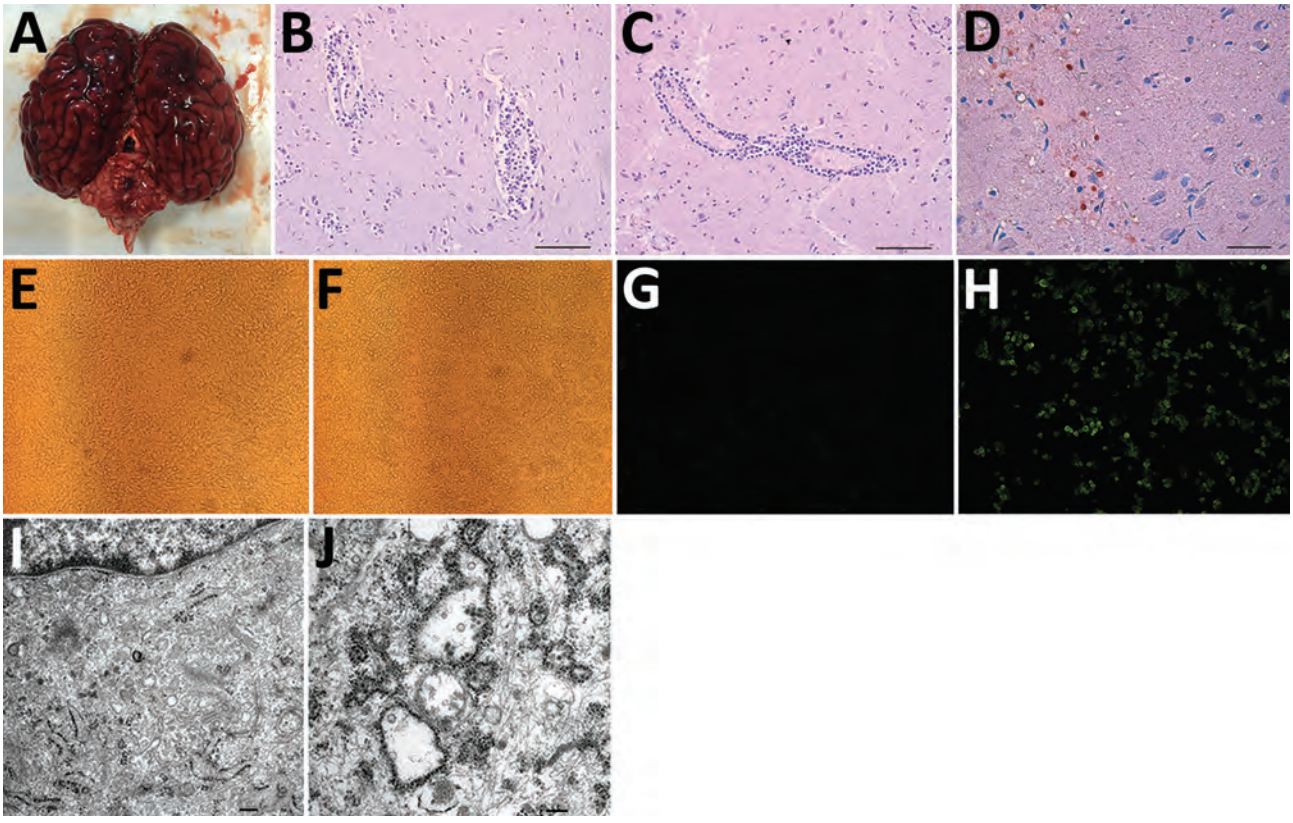

Figure 1. Pathologic examination and virus culturing of brain tissue samples from 2 seals with lethal encephalitis infected with Japanese encephalitis virus (JEV), China, 2017. A) Hemorrhaging seal brain. B) Histochemical staining of a glial nodule in the cerebrum showing lymphocyte infiltration around small blood vessels. Scale bar represents 50 μm. C) Histochemical staining of tissue showing coalescing nonsuppurative encephalitis with neuronal degeneration and perivascular cuffing. Scale bar represents 50 μm. D) Immunohistochemical staining of tissue with anti-JEV polyclonal mouse serum showing JEV antigen. Scale bar represents 20 μm. E–H) Baby hamster kidney cell line BHK-21 incubated with (F, H) and without (E, G) JEV Seal-Anheal-2017 (i.e., brain homogenate supernatant from infected seals passaged through BHK-21 cells 4 times) fluorescently stained by using anti-JEV polyclonal mouse serum (G, H). Cells incubated with the fourth passage of brain homogenate demonstrated cytopathic effect (F) and fluorescence (H), indicating the presence of JEV antigen. Original magnification ×200. I, J) Electron microscopic images of BHK-21 cells not infected (I) and infected (J) with Seal-Anheal-2017. Many mature virions and proliferative vesicles were observed in the endoplasmic reticulum of JEV-infected cells (J). Scale bars represent 0.2 μm.

supplemented with 10% (vol/vol) calf serum, 100 U/mL penicillin, and 100 mg/mL streptomycin at 37°C in 5% CO_2. We observed cytopathic effects (cell swelling and detachment, intercellular space dilatation) with the fourth passage of brain homogenate supernatant (Figure 1, panels E, F). Immunofluorescent staining of these cells with anti-JEV polyclonal mouse serum revealed JEV antigen (Figure 1, panels G, H).

We subjected this fourth passage of virus to negative-staining electron microscopy (EM) analysis. We ultracentrifuged cell supernatant at 82,000 × *g* for 30 min, pelleted virus onto 3-mm grids, and then stained grids with 2% sodium phosphotungstate for 1.5 min. We used the Tecnai G2 BioTWIN Transmission Electron Microscope (FEI Company, https://www.fei.com) operating at 85 kV to visualize virus particles. We observed round-shaped virions morphologically similar to those of the *Flavivirus* genus (data not shown). Compared with uninfected cells, many mature virions were found in the endoplasmic reticulum of infected cells by transmission EM (Figure 1, panels I, J). We also observed the ultrastructural pathologic change of proliferative vesicles in the endoplasmic reticulum, which were likely induced by JEV infection.

We extracted total RNA from the supernatant of this fourth passage of virus, which we designated Seal-Anheal-2017, using the NucleoSpin RNA Midi kit (TaKaRa Bio Inc., http://www.takara-bio.com), reverse transcribed RNA to cDNA, and amplified the cDNA by PCR using 15 different primer pairs (Table). We obtained the 5′ and 3′ UTR sequences using the 5′ RACE and 3′ RACE Systems for Rapid Amplification of cDNA Ends kits (Invitrogen, https://www.thermofisher.com). Sequence analysis indicated that the complete genome sequence of JEV Seal-Anheal-2017 (GenBank accession no. MH165313) was 10,965 nt in length, encoding a 10,299-nt single open reading frame flanked by a 96-nt 5′ UTR and 570-nt 3′ UTR.

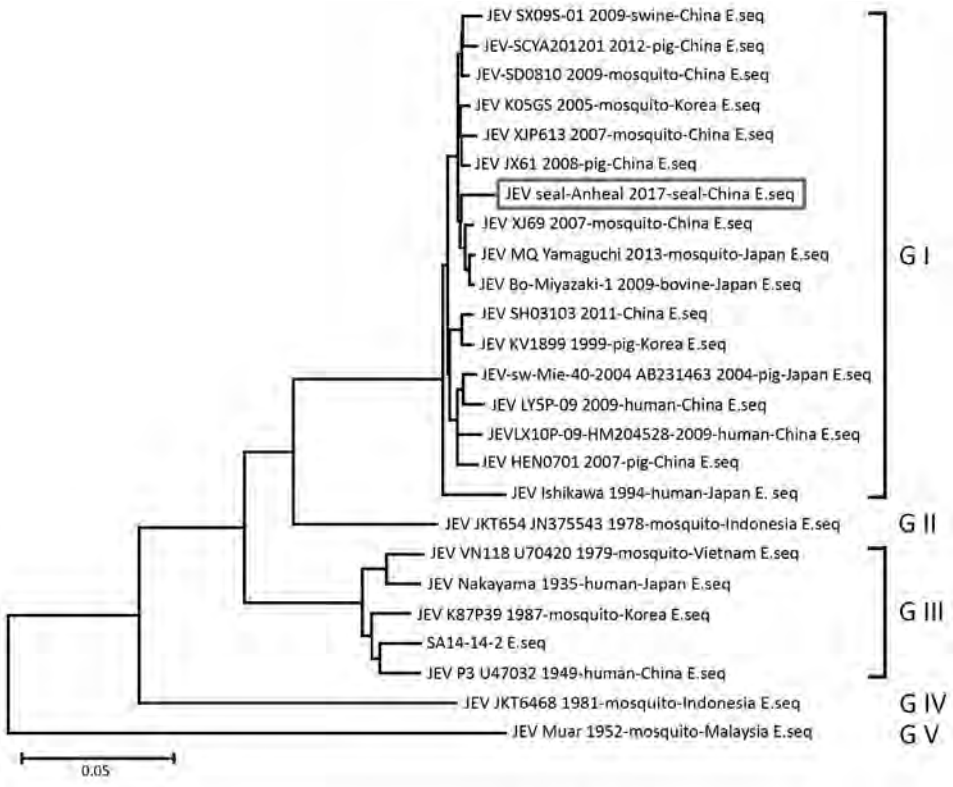

Figure 2. Phylogenetic analysis of JEV E gene of Seal-Anheal-2017 isolate from a seal with lethal encephalitis, China, 2017, compared with 24 JEV strains of different genotypes and species origins. We constructed the tree using the neighbor-joining method and MEGA5.05 (https://www.megasoftware.net). Reliability of the branching orders was evaluated by the bootstrap test (n = 1,000). E, envelope; G, genotype; JEV, Japanese encephalitis virus; seq, sequence. Scale bar indicates nucleotide substitutions per site.

We performed a phylogenetic analysis of the E gene sequence of Seal-Anheal-2017 with those of 24 JEV strains of different genotypes. Results showed that Seal-Anheal-2017 grouped with genotype I, sharing the highest nucleotide sequence homology (99.09%) with XJ69, a mosquito-origin JEV isolated in Xianju County of Zhengjiang Province, China (Figure 2) (*9*). XJ69 and Seal-Anheal-2017 differ by 11 aa: R77Q in membrane; R111G in E; D175N in NS1; Y127S in NS2A; S14L, K26M, and L586M in NS3; I2V in NS4A; K20R in NS4B; and S429G and I721V in NS5. In contrast, SA14-14-2, an attenuated JEV vaccine strain used in humans and pigs in China, differs from Seal-Anheal-2017 at 79 aa (data not shown).

The JEV E protein is a major structural protein contributing to viral virulence, host tropism, and antigenicity (*10*,*11*); in this protein, there are 13 aa substitutions between Seal-Anheal-2017 and SA14-14-2 and 1 between Seal-Anheal-2017 and XJ69. The 8 key amino acid residues that determine virulence did not differ between Seal-Anheal-2017 and XJ69 (data not shown), indicating that Seal-Anheal-2017 might possess typical characteristics of virulent JEV.

Conclusions

Our data indicate that the causative agent of these 2 seal deaths was JEV. Why and how disease developed is unclear. In humans, young children are susceptible to JEV infection and often have fatal outcomes. Because the 2 seals that died were in their adolescence and the others with no clinical signs were older, age might have contributed to the fatal outcomes seen with these seals.

Culex tritaeniorhynchus mosquitoes were found in the aquarium, and seal keepers reported that they had often been bitten by mosquitoes. No human cases of Japanese encephalitis were reported in the vicinity of the aquarium; however, most of the population received compulsory JEV vaccination. *C. tritaeniorhynchus* mosquitoes also feed on livestock and birds, which act as bridging vectors leading to infections in other animals (*12*). A number of pig farms are located several miles away from the aquarium, but wild pigs had never been reported in the area of the aquarium. Therefore, the virus might have been transmitted through the bite of mosquitoes infected with JEV. In summary, we confirmed JEV genotype I as the causative agent of 2 cases of lethal viral encephalitis in seals, on the basis of results from pathologic examinations, virus isolation, immunostaining, and EM.

JEV might cause neurologic disease in more organisms than previously thought. Zoo staff should determine the causative agents in animals displaying neurologic disease, so they can better protect their animals from pathogens. Seals might need to be screened for JEV before they are transported to non–JEV-endemic areas.

This work is supported by the National Key R&D Program of China (no. 2016YFD0501006), Ten-thousand Talents Program (to X.L.), and Luoyang Heluo Talent Plan (to K.T.).

Table. Primers used to amplify the full-length genome of JEV isolate Seal-Anheal-2017 obtained from a seal with lethal encephalitis, China, 2017*

Primer pair no.	Primer name	Primer binding site	Length of fragment amplified, bp
1	JEV-1F	1–26	879
	JEV-1R	878–855	
2	JEV-2F	805–823	833
	JEV-2R	1,637–1,615	
3	JEV-3F	1,559–1,580	703
	JEV-3R	2,261–2,242	
4	JEV-4F	2,151–2,170	827
	JEV-4R	2,977–2,959	
5	JEV-5F	2,898–2,917	779
	JEV-5R	3,676–3,658	
6	JEV-6F	3,582–3,599	740
	JEV-6R	4,321–4,300	
7	JEV-7F	4,204–4,224	919
	JEV-7R	5,122–5,104	
8	JEV-8F	5,005–5,024	934
	JEV-8R	5,938–5,918	
9	JEV-9F	5,841–5,858	939
	JEV-9R	6,779–6,757	
10	JEV-10F	6,676–6,697	880
	JEV-10R	7,555–7,537	
11	JEV-11F	7,431–7,451	817
	JEV-11R	8,247–8,228	
12	JEV-12F	8,121–8,139	875
	JEV-12R	8,995–8,974	
13	JEV-13F	8,924–8,946	866
	JEV-13R	9,789–9,771	
14	JEV-14F	9,653–9,675	827
	JEV-14R	10,479–10,460	
15	JEV-15F	10,217–10,236	769

*JEV, Japanese encephalitis virus.

About the Author

Dr. Li is a veterinary virologist at the National Research Center for Veterinary Medicine, Luoyang, China. His research interests include epidemiology and the pathogenesis of new and emerging infectious diseases.

References

1. Mackenzie JS, Gubler DJ, Petersen LR. Emerging flaviviruses: the spread and resurgence of Japanese encephalitis, West Nile, and dengue viruses. Nat Med. 2004;10(Suppl):S98–109. http://dx.doi.org/10.1038/nm1144
2. Pan XL, Liu H, Wang HY, Fu SH, Liu HZ, Zhang HL, et al. Emergence of genotype I of Japanese encephalitis virus as the dominant genotype in Asia. J Virol. 2011;85:9847–53. http://dx.doi.org/10.1128/JVI.00825-11
3. Weaver SC, Reisen WK. Present and future arboviral threats. Antiviral Res. 2010;85:328–45. http://dx.doi.org/10.1016/j.antiviral.2009.10.008
4. Zhang JS, Zhao QM, Guo XF, Zuo SQ, Cheng JX, Jia N, et al. Isolation and genetic characteristics of human genotype 1 Japanese encephalitis virus, China, 2009. PLoS One. 2011;6:e16418. http://dx.doi.org/10.1371/journal.pone.0016418
5. Yuan L, Wu R, Liu H, Wen X, Huang X, Wen Y, et al. Tissue tropism and molecular characterization of a Japanese encephalitis virus strain isolated from pigs in southwest China. Virus Res. 2016;215:55–64. http://dx.doi.org/10.1016/j.virusres.2016.02.001
6. Katayama T, Saito S, Horiuchi S, Maruta T, Kato T, Yanase T, et al. Nonsuppurative encephalomyelitis in a calf in Japan and isolation of Japanese encephalitis virus genotype 1 from the affected calf. J Clin Microbiol. 2013;51:3448–53. http://dx.doi.org/10.1128/JCM.00737-13
7. Mansfield KL, Hernández-Triana LM, Banyard AC, Fooks AR, Johnson N. Japanese encephalitis virus infection, diagnosis and control in domestic animals. Vet Microbiol. 2017;201:85–92. http://dx.doi.org/10.1016/j.vetmic.2017.01.014
8. Tian K, Yu X, Zhao T, Feng Y, Cao Z, Wang C, et al. Emergence of fatal PRRSV variants: unparalleled outbreaks of atypical PRRS in China and molecular dissection of the unique hallmark. PLoS One. 2007;2:e526. http://dx.doi.org/10.1371/journal.pone.0000526
9. Xie RH, Fu SH, Cheng YK, Xu F, Yao PP, Weng JQ, et al. Isolation and identification of Japanese encephalitis virus from mosquitoes in Zhejiang Province [in Chinese]. Zhonghua Liu Xing Bing Xue Za Zhi. 2008;29:712–5.
10. Nam JH, Chung YJ, Ban SJ, Kim EJ, Park YK, Cho HW. Envelope gene sequence variation among Japanese encephalitis viruses isolated in Korea. Acta Virol. 1996;40:303–9.
11. Fan JM, Luo J, Zhang GP, Chen L, Teng M, Yang MF, et al. Identification and characterization of Japanese encephalitis virus envelope protein gene from swine. Lett Appl Microbiol. 2010;51:11–7.
12. Pearce JC, Learoyd TP, Langendorf BJ, Logan JG. Japanese encephalitis: the vectors, ecology and potential for expansion. J Travel Med. 2018;25(suppl_1):S16–26.

Address for correspondence: Ming Sun, Beijing Anheal Laboratories Co. Ltd., 68 Beiqing Rd, Haidian District, Beijing, 100094, China; email: sunming@anheal.net; Kegong Tian, Henan Agricultural University, 3 Cuiwei Rd, High-Tech District, Zhengzhou, 471003, China; email: tiankg@263.net

Emergent Invasive Group A *Streptococcus dysgalactiae* subsp. *equisimilis*, United States, 2015–2018

Sopio Chochua, Joy Rivers, Saundra Mathis, Zhongya Li, Srinivasan Velusamy, Lesley McGee, Chris Van Beneden, Yuan Li, Benjamin J. Metcalf, Bernard Beall

The term group A *Streptococcus* is considered synonymous for the species *Streptococcus pyogenes*. We describe an emergent invasive *S. dysgalactiae* subspecies *equisimilis* lineage that obtained the group A antigen through a single ancestral recombination event between a group C *S. dysgalactiae* subsp. *equisimilis* strain and a group A *S. pyogenes* strain.

The Centers for Disease Control and Prevention's Active Bacterial Core surveillance (ABCs) performs population-based surveillance of invasive group A *Streptococcus* (GAS) infections. Isolates collected from a population of ≈34 million persons are subjected to whole-genome sequence (WGS)–based characterization. We recently detected group A carbohydrate-positive *S. dysgalactiae* subsp. *equisimilis* (SE) isolates employing the *gacI* (*1*) sequence query within our bioinformatics pipeline (*2*). GAS is considered synonymous with *S. pyogenes*, rare occurrences of group A SE have been noted (*3*,*4*).

The Study

During January 1, 2015–November 1, 2018, a total of 5,480 ABCs GAS isolates were subjected to WGS. We identified 35 atypical *gacI*-positive isolates; each yielded 1 of the M protein gene (*emm*) subtypes *stG245.0*, *stG485.0*, or *stG652.0* commonly associated with SE (*4*–*6*). These 35 isolates lacked multilocus sequence types (MLSTs) inclusive of known *S. pyogenes* allelic designations. Lancefield grouping (*7*) and MLST (https://pubmlst.org/sdysgalactiae) (*6*) revealed the 35 isolates were serologically group A and MLST sequence type (ST) 128 (GAS/ST128/SE). We received 13 additional SE isolates recovered through ABCs GAS surveillance during this period that were found to be non–group A isolates (9 group G, 2 group C, and 2 group L) with MLSTs unrelated to ST128 (Figure 1). According to our normal protocol, these 13 non–group A SE isolates and 2 group G *S. canis* isolates that we also received were removed from the ABCs GAS database.

The Lancefield group A carbohydrate consists of a polyrhamnose chain with an immunodominant *N*-acetylglucosamine side chain (*9*) that functions in GAS pathogenesis (*1*). The group C carbohydrate also has a polyrhamnose backbone; however, its immunodominant side chain is the dissaccharide *N*-acetylglucosaminosyl-*N*-acetylglucosamine (*9*). Genomic comparison of the 12 gene group A carbohydrate synthetic cluster *gacA-L* (*1*) from *S. pyogenes* with the corresponding regions of the 35 GAS/ST128/SE revealed an upstream crossover point within the *S. pyogenes gacE* ABC transporter gene and a downstream crossover point within *ebsA* (Figure 2). The ancestral recipient SE strain was implicated as group C *S. equisimilis* (GCS/SE) by virtue of the near-identical sequence of the 1,363-bp sequence within GAS/ST128/SE encompassing sections of *gacD* and *gacE* homologs (designated as *gccD* and *gccE*) (Figure 2) with GCS and the marked divergence of this 1,363-bp sequence from group G SE (data not shown). This sequence is immediately adjacent to the upstream crossover point shown between *S. pyogenes* and GCS/SE (SP-5005 and SE-7136; Figure 2). We also found these same crossover points within the group carbohydrate gene cluster of the available genomic sequence from the previously described invasive GAS/SE strain AC-2713 recovered in 1999 (*3*). Subsequent genomic analysis revealed AC-2713 to be ST128 and *emm* type *stG485.0*. Phylogenetic analysis revealed that AC-2713 differed by 126 single-nucleotide polymorphisms from a pair of genetically indistinguishable GAS/ST128/SE recovered within the East Bay area of San Francisco, California, USA (Figure 1). These 2 isolates were from recurrent invasive GAS infections within the same patient that occurred 1.5 months apart.

Comparison of the *S. pyogenes gacA-L* cluster with the corresponding *gcc* loci from group C SE strains (SE-7136; Figure 2) revealed that GCS/SE genes shared homology with all 12 *gacA-L* genes (56%–89% sequence identity). The weakest conservation was observed between the *gac/gccIJK* genes (56%–69% identity), consistent with the requirement of *gacIJK* for the group A immunodominant

Author affiliation: Centers for Disease Control and Prevention, Atlanta, Georgia, USA

DOI: https://doi.org/10.3201/eid2508.181758

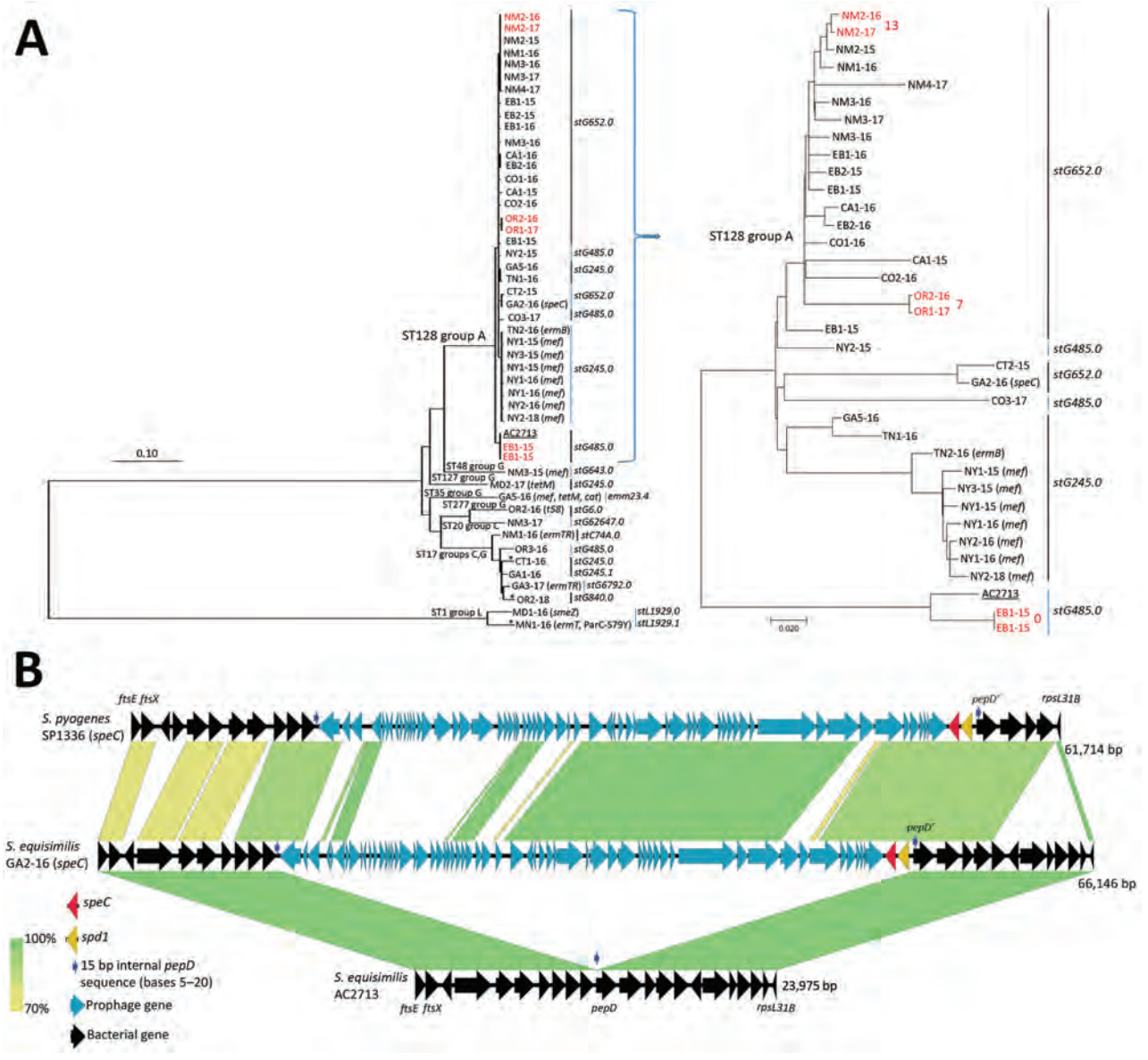

Figure 1. Analyses of invasive group A *Streptococcus dysgalactiae* subspecies *equisimilis* and conserved genomic *pepD* gene insertion site of highly related exotoxin *speC* gene–containing prophages found within group A ST128 *S. equisimilis* strain and *S. pyogenes* strain SP1336. Methods are described in the Appendix (https://wwwnc.cdc.gov/EID/article/25/8/18-1758-App1.pdf). A) Phylogenetic tree of 35 invasive group A *S. dysgalactiae* subsp. *equisimilis* (GAS/SE/MLST128 [ST128] complex) isolates and 13 unrelated group C, G, and L SE isolates recovered through the Centers for Disease Control and Prevention's Active Bacterial Core surveillance during January 1, 2015–November 1, 2018. Trees are drawn to scale; branch lengths indicate number of substitutions per site. Surveillance areas (https://www.cdc.gov/abcs/reports-findings/surv-reports.html) are indicated: EB, East Bay San Francisco area, California; NY, New York; NM, New Mexico; CA, San Francisco Bay area, California; OR, Oregon; CO, Colorado; GA, Georgia; CT, Connecticut. Different counties and years of isolation are indicated (e.g., EB1–15 indicates county 1 in East Bay area and year 2015). The left tree depicts all 49 isolates and the right includes only the subset of the 36 GAS/ST128/SE (also including GAS/ST128/SE described by Brandt et al. [*3*] and assigned GenBank accession no. HE858529). Three pairs of isolates differing by 13 or fewer single-nucleotide polymorphisms are shown in red. Single-locus variants of the indicated multilocus sequence types are indicated with asterisks. B) Conserved genomic *pepD* gene insertion site of highly related exotoxin *speC* gene–containing prophages found within group A ST128 *S. equisimilis* strain (middle) and *S. pyogenes* strain SP1336 (GenBank accession no. CP031738). The nonfunctional *pepD* structural genes lacking bases 1–4 are depicted in the 2 prophage-containing strains. Nucleotide sequence identity is scaled from 70% (yellow) to 100% (green). The *S. equisimilis* prophage also contained the virulence-associated DNase gene *spd1* as shown and previously described for the depicted SP1336 phage shown (*8*). Within both species, the *pepD* insertion site lies within a region between the conserved bacterial cell division genes *ftsE/ftsX* and the small ribosomal protein gene *rpsL31b* (GenBank accession no. for *S. equisimilis* AC2713 is HE858529).

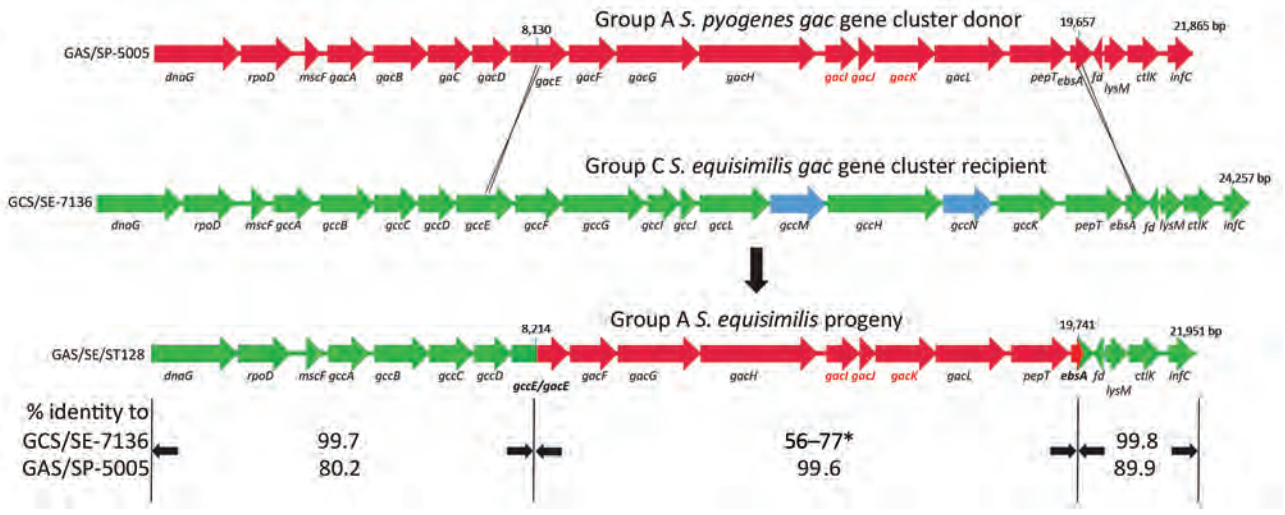

Figure 2. Ancestral recombination event depicting *Streptococcus pyogenes* group A carbohydrate gene donor (GAS/SP-5005; GenBank accession no. NC007297), group C *S. dysgalactiae* subsp. *equisimilis* recipient (GCS/SE7136; GenBank accession no. NCTC7136), and progeny group A *S. dysgalactiae* subsp. *equisimilis* progeny (GAS/SE/ST128) described in study of emergent invasive group A *Streptococcus dysgalactiae* subspecies *equisimilis*, United States, 2015–2018. The deduced crossover points between the group A gene cluster (red) donor and group C (green) recipient strains are shown. The 3 genes required for inclusion of the immunodominant *N*-acetylglucosamine side chain within the group A carbohydrate (*gacI, gacJ*, and *gacK*) are shown in red. The coordinates of the fragment transferred that is highly conserved between the donor and the progeny are indicated. The length of the 3 genomic regions are indicated. The *gacE/gccE* and *ebsA* genes are shown as green/red hybrids. The extra *gcc* cluster genes not conserved within the *gac* cluster are shown in blue. The relative sequence identities of the 3 different regions of progeny (bottom) *gac* cluster genes with the group A *S. pyogenes* donor (top) and group C *S. equisimilis* recipient (middle) are indicated. The middle segment (asterisk) indicates a range of 56%–77% sequence identity beween each of the 8 structural genes (*gacF–pepT*) that were received intact from the *S. pyogenes* donor. The *gac* cluster genes are described in more detail in van Sorge et al. (*1*). Gene assignments are as follows: *dnaG*, DNA primase; *rpoD*, major RNA polymerase sigma factor; *mscF*, metal sulfur complex assembly factor; *gacA-L*, group A carbohydrate biosynthetic genes (putative functions described in van Sorge et al. [*1*]); *gccA-N*, group C carbohydrate biosynthetic genes. *gccA-L* are functional homologs of *gacA-L*. *gccM* and *gccN* putatively encode an additional glycosyl transferase and UDP-monosaccharide 4-epimerase, respectively; *ebsA*, pore-forming protein; *fd*, ferredoxin (complement strand); *ctlK*, cytidylate kinase; *infC*, translation initiation factor IF-3.

N-acetylglucosamine side chain but not for synthesis of the polyrhamnose core (*1*). Two additional genes, designated *gccM* (glycotransferase gene) and *gccN* (UDP-monosaccharide epimerase gene), were evident within the *gcc* gene cluster. In the ancestral recombination event, an 11,527-bp GAS (*S. pyogenes*) chromosomal segment composed of the *gacE* 3′ portion, along with the *gacF-L* genes and a 5J portion of *ebsA*, replaced the corresponding 13,813 bp of a GCS/ST128/SE strain, resulting in the recombinant GAS/ST128/SE lineage (Figure 2). This fragment encompasses the intact 7-gene *gacF–gacL* segment; each gene shared 99.4%–99.7% sequence identity with counterparts in *S. pyogenes*. The evident functionality of the hybrid *gac/gcc* cluster within the GAS/ST128/SE progeny lineage is consistent with identical roles of the first 3 genes of the cluster (*gac/gccA–C*) in the biosynthesis of the polyrhamnose core (*1*) that is present within the groups A, C, and G carbohydrates (*9*). Each of these 3 genes are also required for *S. pyogenes* viability (*1*).

The occurrence of multiple *emm* types within the same MLST is common in SE (*5*,*6*) and differs from *emm*/MLST associations within *S. pyogenes*, where an MLST is nearly always definitive of a single *emm* type (*2*,*10*). The presence of 3 different *emm* types and 8 macrolide-resistant isolates within GAS/ST128/SE (Figure 1) is indicative of a long-standing successful lineage. A single isolate of this lineage was positive for the exotoxin gene *speC* (Figure 1) that was carried on a prophage highly similar to a previously described *speC*-positive *S. pyogenes* strain (*8*). The relative genomic positions of the prophages are exactly conserved between the 2 species, inserted within the *pepD* gene in the genomic region that lies between the bacterial cell division genes *ftsE/ftsX* and the ribosomal protein gene *rpsL31B* (Figure 1). The number of single-nucleotide polymorphism differences between individual GAS/ST128/SE core genomes ranged from 0 to 613 (Figure 1). The GAS/ST128/SE strain AC-2713 recovered 20 years ago (*3*) is also indicative of a long-established lineage.

The 34 GAS/ST128/SE isolates for which information was available (32 from blood, 1 from a joint, and 1 from a surgical wound) recovered in ABCs since January 1, 2015, were recovered from older adults (age range 22–93

years; mean age 63 years) from 8 ABCs sites; most (85%) patients were men. Most patients had underlying medical conditions (data not shown), including 16 with diabetes, 15 with cellulitis (including 1 who had necrotizing fasciitis), 8 with pneumonia, and 6 with septic shock. One patient with bacteremia died.

Conclusions

ABCs identifies invasive infections caused by GAS without identification of isolates to the species level. Since 2015, when we implemented WGS as our primary platform for GAS characterization, we have identified rarely occurring non–*S. pyogenes* isolates through our bioinformatics pipeline automated MLST function rather than previously employed phenotypic testing. Of ≈16,000 GAS isolates recovered from ABCs during 1994–2014, only 11 had *emm* types characteristic of SE. All 11 were collected during 2011–2014 and were of the 3 *emm* types found among the 35 GAS/ST128/SE isolates from this study. Genomic analysis verified the GAS/ST128/SE lineage of these 11 older isolates (data not shown). Finding 35 additional invasive isolates of this lineage recovered during January 1, 2015–November 1, 2018, through ABCs suggests a level of expansion attributable to strain adaptation and fitness or to a more susceptible population. Attempts to identify circulating ST128/SE strains of the original group C have been unsuccessful, including an examination of a population-based sampling of SE (*5*).

Because group A SE is suspected to be rare, these findings raise the question of whether invasive disease attributable to SE of groups C, G, and L is also increasing. A 2-year population-based study of β-hemolytic streptococcal disease attributable to Lancefield groups other than A and B within 2 ABCs sites during 2002–2004 revealed that 80% of such isolates were SE (*11*), with clinical manifestations and targeted susceptible populations similar to *S. pyogenes*. Incidence of invasive disease attributable to non–group A SE during this period was estimated at 2.5 cases/100,000 population, similar to the incidence of GAS infections (2.89 cases/100,000 population) in these same 2 sites. The incidence of overall invasive GAS disease in the United States has also markedly increased during recent years, from 3.4 cases/100,000 population in 2012 to 7.2 cases/100,000 population in 2017 (https://www.cdc.gov/abcs/reports-findings/survreports/gas17.html).

Acknowledgments

We are indebted to all of the hospitals and laboratories participating in the ABCs component of the Emerging Infections Programs network, a collaboration of the CDC, state health departments, and universities. We thank the following persons from the following programs and institutions for their contributions to the establishment and maintenance of the ABCs system: California Emerging Infections Program, J. Watt, A. Reingold, G. Rothrock, and M. Apostol; Colorado Emerging Infections Program, R. Herlihy, N. Alden, and H. Maguire; Connecticut Emerging Infections Program, S. Petit, M. Cartter, C. Marquez, and D. Noel; Georgia Emerging Infections Program, M. Farley, S. Thomas, A. Tunali, and D. Goodenough; Maryland Emerging Infections Program, L. Harrison, T. Carter, R. Hollick, K. Holmes, and R. Myers; Minnesota Emerging Infections Program, R. Lynfield, K. Como-Sabetti, R. Danila, and P. Vangnone; New Mexico Emerging Infections Program, C. Smelser, S. Torres, S. Khanlian, R. Mansmann, and K. Angeles; New York Emerging Infections Program, N. Bennett, A. Muse, L. Dufort, G. Dumyati, S. McGuire, and N. Spina; Oregon Emerging Infections Program, P. Cieslak, A. Thomas, and T. Poissant; Tennessee Emerging Infections Program, W. Schaffner, B. Barnes, K. Leib, and A. Elie; CDC, M. Arvay, J. Onukwube, O.M. Almendares, and H.R. Pham.

This study used the *S. dysgalactiae* subsp. *equisimilis* MLST website (http://pubmlst.org/sdysgalactiae) at the University of Oxford. The development of this site has been funded by the Wellcome Trust.

Major funding for this work was provided through support from CDC's Emerging Infection Program and the CDC Advanced Molecular Detection initiative.

About the Author

Dr. Chochua is a researcher in the Streptococcus Laboratory, National Center for Immunization and Respiratory Diseases, Centers for Disease Control and Prevention, Atlanta, Georgia, USA. Her research interests are next-generation sequencing, characterization of clinical streptococcal isolates, antimicrobial resistance, genetic adaptations, and outbreak responses.

References

1. van Sorge NM, Cole JN, Kuipers K, Henningham A, Aziz RK, Kasirer-Friede A, et al. The classical Lancefield antigen of group A *Streptococcus* is a virulence determinant with implications for vaccine design. Cell Host Microbe. 2014;15:729–40. http://dx.doi.org/10.1016/j.chom.2014.05.009
2. Chochua S, Metcalf BJ, Li Z, Rivers J, Mathis S, Jackson D, et al. Population and whole genome sequence based characterization of invasive group A streptococci recovered in the United States during 2015. MBio. 2017;8:e01422–17. http://dx.doi.org/10.1128/mBio.01422-17
3. Brandt CM, Haase G, Schnitzler N, Zbinden R, Lütticken R. Characterization of blood culture isolates of *Streptococcus dysgalactiae* subsp. *equisimilis* possessing Lancefield's group A antigen. J Clin Microbiol. 1999;37:4194–7.
4. Tanaka D, Isobe J, Watahiki M, Nagai Y, Katsukawa C, Kawahara R, et al.; Working Group for Group A Streptococci in Japan. Genetic features of clinical isolates of *Streptococcus dysgalactiae* subsp. *equisimilis* possessing Lancefield's group A antigen. J Clin Microbiol. 2008;46:1526–9. http://dx.doi.org/10.1128/JCM.02188-07

5. Ahmad Y, Gertz RE Jr, Li Z, Sakota V, Broyles LN, Van Beneden C, et al. Genetic relationships deduced from *emm* and multilocus sequence typing of invasive *Streptococcus dysgalactiae* subsp. *equisimilis* and *S. canis* recovered from isolates collected in the United States. J Clin Microbiol. 2009; 47:2046–54. http://dx.doi.org/10.1128/JCM.00246-09
6. McMillan DJ, Bessen DE, Pinho M, Ford C, Hall GS, Melo-Cristino J, et al. Population genetics of *Streptococcus dysgalactiae* subspecies *equisimilis* reveals widely dispersed clones and extensive recombination. PLoS One. 2010;5:e11741. http://dx.doi.org/10.1371/journal.pone.0011741
7. Lancefield RC. The antigenic complex of *Streptococcus haemolyticus*: I. Demonstration of a type-specific substance in extracts of *Streptococcus haemolyticus.* J Exp Med. 1928; 47:91–103. http://dx.doi.org/10.1084/jem.47.1.91
8. Walker MJ, Brouwer S, Forde BM, Worthing KA, McIntyre L, Sundac L, et al. Detection of epidemic scarlet fever group A Streptococcus in Australia. Clin Infect Dis. 2019; Epub ahead of print. http://dx.doi.org/10.1093/cid/ciz099
9. Coligan JE, Kindt TJ, Krause RM. Structure of the streptococcal groups A, A-variant and C carbohydrates. Immunochemistry. 1978;15:755–60. http://dx.doi.org/10.1016/0161-5890(78)90105-0
10. Enright MC, Spratt BG, Kalia A, Cross JH, Bessen DE. Multilocus sequence typing of *Streptococcus pyogenes* and the relationships between *emm* type and clone. Infect Immun. 2001;69:2416–27. http://dx.doi.org/10.1128/IAI.69.4.2416-2427.2001
11. Broyles LN, Van Beneden C, Beall B, Facklam R, Shewmaker PL, Malpiedi P, et al. Population-based study of invasive disease due to beta-hemolytic streptococci of groups other than A a nd B. Clin Infect Dis. 2009;48:706–12. http://dx.doi.org/10.1086/597035

Address for correspondence: Bernard Beall, Centers for Disease Control and Prevention, 1600 Clifton Rd NE, Mailstop C02, Atlanta, GA 30329-4027, USA; email: bbeall@cdc.gov

Novel Virus Related to Kaposi's Sarcoma–Associated Herpesvirus from Colobus Monkey

Akshay Dhingra, Tina Ganzenmueller, Elias Hage, Nicolás M. Suárez, Kerstin Mätz-Rensing, Dimitri Widmer, Stefan Pöhlmann, Andrew J. Davison,[1] Thomas F. Schulz,[1] Artur Kaul[1]

We determined the complete genome sequence of a virus isolated from a mantled guereza that died of primary effusion lymphoma. The virus is closely related to Kaposi's sarcoma–associated herpesvirus (KSHV) but lacks some genes implicated in KSHV pathogenesis. This finding may help determine how KSHV causes primary effusion lymphoma in humans.

Kaposi's sarcoma–associated herpesvirus (KSHV) causes Kaposi sarcoma, primary effusion lymphoma, and the plasma cell variant of multicentric Castleman disease in humans (*1*). KSHV-related viruses (also known as rhadinoviruses) naturally infect New and Old World primates (*2*–*5*). Old World primate rhadinoviruses fall into 2 lineages, rhadinovirus 1 (RV1) and rhadinovirus 2 (RV2) (*2*,*6*). The RV1 lineage contains KSHV; the retroperitoneal fibromatosis–associated herpesviruses (RFHVs) identified in *Macaca nemestrina*, *M. fascicularis*, and *M. mulatta* macaques; and closely related viruses of other Old World primates (*2*,*5*). The RV2 lineage contains macaque viruses more distantly related to KSHV, such as rhesus macaque rhadinovirus, *M. nemestrina* RV2, *M. fascicularis* RV2, and Japanese macaque rhadinovirus (*2*,*7*). Complete genome sequences of the RV1 lineage viruses KSHV and RFHV of *M. nemestrina* macaques (RFHVMn), as well as of the RV2 lineage viruses rhesus macaque rhadinovirus, Japanese macaque rhadinovirus, and *M. nemestrina* RV2, have been generated from cultured viruses or directly from clinical material by conventional or high-throughput sequencing (*7*–*11*).

Apart from KSHV, all fully sequenced Old World primate rhadinoviruses have been found in primates of the genus *Macaca*, subfamily Cercopithecinae (*7*–*9*,*12*–*14*). We describe a novel rhadinovirus of the Old World primate genus *Colobus* (*14*), subfamily Colobinae, which was detected in a mantled guereza (*Colobus guereza kikuyensis*) that died of primary effusion lymphoma. The virus belongs to the RV1 lineage, together with KSHV and RFHVMn.

The Study

In 2014, a 3-year-old male mantled guereza at a zoo in Germany died suddenly after developing severe anemia (<5 g/dL hemoglobin), subcutaneous edema, and leukocytosis. A necropsy conducted at the German Primate Centre, Göttingen, Germany, led to a diagnosis of primary effusion lymphoma. Large numbers of abnormal leukocytes were found in the vascular system of several organs. The pleura pulmonalis and the pleural space were severely infiltrated with pleomorphic round cells (Figure 1, panel A) identified as CD20-positive B lymphocytes (Figure 1, panel B) with high expression of the proliferation marker Ki67 (Figure 1, panel C). Many neoplastic cells also showed typical nuclear staining with antibodies against the KSHV latent nuclear-associated antigen, suggesting infection with a related herpesvirus (Figure 1, panel D). We detected viral genomes in several organs by using PCR with a panherpesvirus primer set, a primer set specific for the virus detected in this study (colobine gammaherpesvirus 1 [CbGHV1]), or both, for the viral DNA polymerase gene. Sanger sequencing of the panherpes PCR products followed by BLAST (https://blast.ncbi.nlm.nih.gov) analysis revealed the best match to be RFHVMn. Using a commercial microarray (Simian Panel E Kit; Intuitive Biosciences, http://intuitivebio.com), we detected antibodies to lymphocryptovirus but not to simian immunodeficiency virus, simian retrovirus, herpes B virus, simian T-cell leukemia virus, measles virus, rhesus

Author affiliations: Hannover Medical School Institute of Virology, Hannover, Germany (A. Dhingra, T. Ganzenmueller, E. Hage, T.F. Schulz); German Centre for Infection Research, Hannover-Braunschweig Site, Germany (A. Dhingra, T. Ganzenmueller, E. Hage, T.F. Schulz); University Hospital Tübingen, Tübingen, Germany (T. Ganzenmueller); MRC–University of Glasgow Centre for Virus Research, Glasgow, Scotland, UK (N.M. Suárez, A.J. Davison); German Primate Center–Leibniz Institute for Primate Research, Göttingen, Germany (K. Mätz-Rensing, S. Pöhlmann, A. Kaul); Zoo Dresden GmbH, Dresden, Germany (D. Widmer); University Göttingen, Göttingen (S. Pöhlmann)

DOI: https://doi.org/10.3201/eid2508.181802

[1]These authors contributed equally to this article.

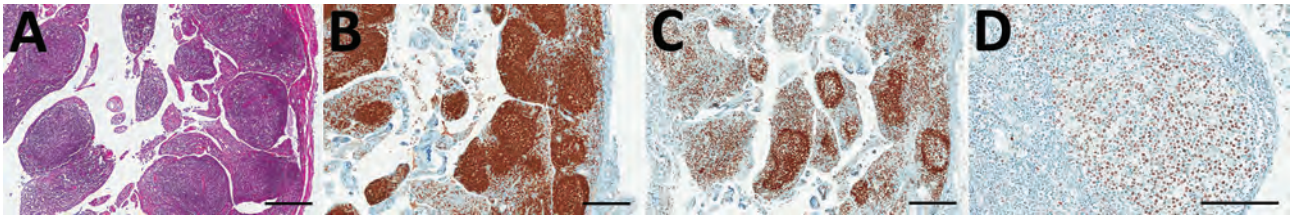

Figure 1. Identification of primary effusion lymphoma and immunohistochemical staining of primary effusion lymphoma cells with Kaposi's sarcoma–associated herpesvirus latent nuclear-associated antigen (LANA)–specific antibody. A) Diffuse infiltration of the pleura pulmonalis and pleural space with pleomorphic round cells resembling primary effusion lymphoma. Hematoxylin and eosin stain; scale bar indicates 400 μm. B) The neoplastic cells are lymphocytic cells of B cell origin. CD20 immunohistochemistry; scale bar indicates 400 μm. C) Numerous neoplastic cells express the proliferation marker Ki67. Ki67 immunohistochemistry; scale bar indicates 400 μm. D) Typical nuclear expression of a protein related to Kaposi's sarcoma–associated herpesvirus LANA in neoplastic cells. LANA immunohistochemistry; scale bar indicates 200 μm.

macaque rhadinovirus, human cytomegalovirus, or simian foamy virus (data not shown).

DNA extracted from a spleen necropsy specimen was sequenced by using an Illumina MiSeq (https://www.illumina.com). The 22,978,561 trimmed reads were depleted of host sequences by screening against the human genome sequence. The remaining 3,082,106 reads were assembled de novo into contigs, the largest of which was 126,024 bp. Assemblies of the initial trimmed reads with this sequence, followed by manual extension and incorporation of smaller contigs, resulted in a final, complete viral sequence of 133,999 bp. This essentially circular sequence consists of a unique region (U; 132,514 bp; 52% G+C) followed by a copy of a terminal repeat unit (TR; 758 bp; 84% G+C) and then by a partial copy of TR (727 bp). A total of 84,532 (0.4%) of the initial trimmed reads aligned with this sequence at an average depth of 170 reads per nucleotide. Inspection of the read alignment indicated that most genomes (85%) lack a 7,045-bp region toward the right end of U. In addition, a telomere-like tandem repeat was noted near the left end of U. A similar feature is present in the genome of RFHVMn but not KSHV.

The viral genome sequence is 51% identical to that of KSHV (137,969 bp) and 59% identical to that of RFHVMn (127,320 bp). Phylogenetic analysis of these 3 sequences with those of viruses in the RV2 lineage, using Epstein-Barr virus (a lymphocryptovirus) as the outgroup, confirmed that the novel virus clusters in the RV1 lineage with RFHVMn and KSHV (Figure 2). The novel virus was thus

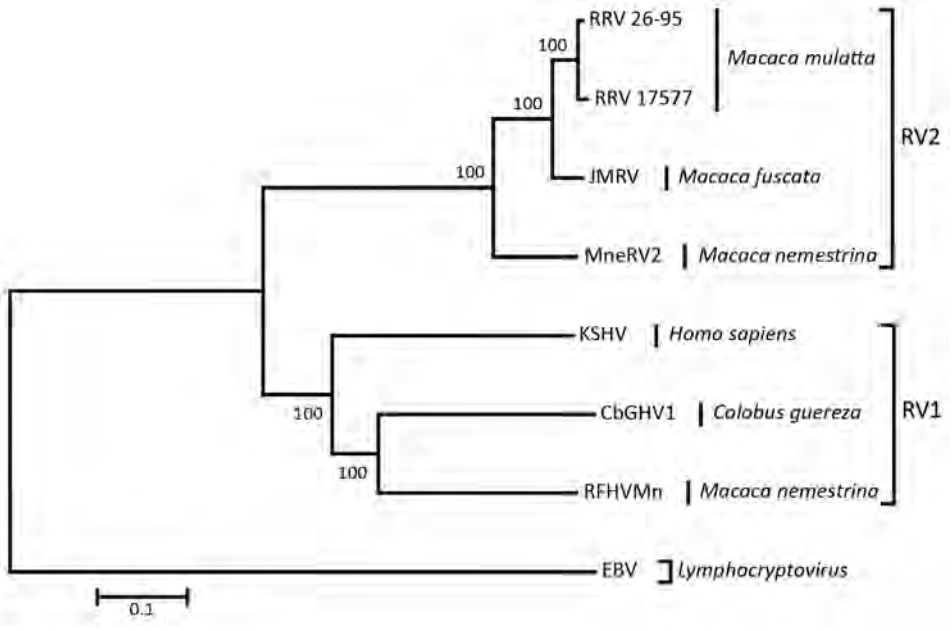

Figure 2. Nucleotide sequence–based phylogenetic analysis of the genomes of CbGHV1 and other gammaherpesviruses. The genus *Lymphocryptovirus* is represented by Epstein-Barr virus as outgroup, and the genus *Rhadinovirus* is represented by the RV1 and RV2 lineages, with host species indicated. Sequences are based on the complete U region, bootstrap values are shown as percentages, and the scale bar represents nucleotide substitutions per site. CbGHV1, colobine gammaherpesvirus 1 (KHSV-like virus isolated from a mantled guereza); EBV, Epstein-Barr virus; JMRV, Japanese macaque rhadinovirus; KSHV, Kaposi's sarcoma–associated herpesvirus; MneRV2, *Macaca nemestrina*; RV2; RFHVMn, retroperitoneal fibromatosis–associated herpesviruses of *Macaca nemestrina* macaques; RRV, rhesus macaque RV; RV, *Rhadinovirus*.

distinguished from other rhadinoviruses, and we named it colobine gammaherpesvirus 1 (CbGHV1).

We named the 78 protein-coding genes annotated in the CbGHV1 genome according to the KSHV nomenclature (Appendix Figure 1, https://wwwnc.cdc.gov/EID/article/25/8/18-1802-App1.pdf). All are located in U and have orthologs in both KSHV and RFHVMn (Appendix Table). Reanalysis of genome sequences confirmed that RFHVMn contains 82 genes, whereas KSHV contains 86 genes. Several genes first described in KSHV lack orthologs in CbGHV1 (K2, K4.2, K5, K6, K7, and K12) and RFHVMn (K5, K6, and K12). In addition, CbGHV1 lacks open reading frame (ORF) 11 (as does RFHVMn) and ORF49, and ORF2 is truncated. In comparison with RFHVMn, CbGHV1 lacks K2, K4.2, K7, and ORF49. The deletion present in most CbGHV1 genomes affects part of ORF68, all of ORF69, and part of ORF71. Values for percentage amino acid sequence identity between CbGHV1 genes and their counterparts in KSHV and RFHVMn are listed in the Appendix Table. An alignment of the KSHV, RFHVMn, and CbGHV1 latent nuclear-associated antigen (ORF73) sequences showed that all 3 contain the typical extended internal repeat region (Appendix Figure 2).

Conclusions

We identified and sequenced the complete genome of a novel KSHV-like virus (CbGHV1) from a mantled guereza. The animal died of primary effusion lymphoma, which we assume was caused by CbGHV1. CbGHV1 and its close relatives KSHV and RFHVMn cluster in the RV1 lineage. The presence of a telomere-like tandem repeat near the left end of U in the CbGHV1 and RFHVMn genomes suggests that an ancestral virus may have been integrated into the host genome, and its persistence suggests that these viruses may retain the ability to integrate.

The CbGHV1 genome contains all genes that are conserved in all members of the family *Herpesviridae*. Orthologs of 8 KSHV genes (ORF11, K2, K4.2, K5, K6, K7, ORF49, and K12) are absent from CbGHV1. In KSHV, some of these genes, such as K2 and K12, encode proteins (vIL6 and kaposin, respectively) that have been linked to viral pathogenesis. Their absence from CbGHV1 suggests that they may not be needed for the development of primary effusion lymphoma. Because ORF10 and ORF11 are related and may have arisen by duplication from an ancestral deoxyuridine triphosphatase gene (*15*), their functions may overlap. ORF49 is a cofactor of the KSHV lytic cycle activator Rta (ORF50) and may not be required for the function of CbGHV1 Rta. It is likely that the viral subpopulation lacking all or part of ORF68, ORF69, and ORF71, which encode essential proteins involved in packaging of viral DNA into capsids, egress of capsids from the nucleus, and inhibition of apoptosis, represents a replication-defective deletion mutant generated in the animal investigated. Of note, CbGHV1 has also been identified by PCR in an older female sibling guereza with Kaposi sarcoma–like disease (*16*). The latest offspring of this female guereza were also positive for CbGHV1 but did not show clinical signs. Discovery of CbGHV1 in multiple animals and the determination of its genome sequence may inform future studies of the pathogenesis of primary effusion lymphoma and Kaposi sarcoma, including how KSHV causes primary effusion lymphoma in humans.

This work was supported by the Deutsche Forschungsgemeinschaft Collaborative Research Centre 900 (grant no. 158989968–SFB900 core project Z1) and the UK Medical Research Council (grant no. MC_UU_12014/3). Akshay Dhingra was supported by the Infection Biology graduate program of Hannover Biomedical Research School.

About the Author

Mr. Dhingra is a PhD candidate at the Institute of Virology, Hannover Medical School. His research interest is the diversity and evolution of DNA viruses in vivo.

References

1. Cesarman E. Gammaherpesvirus and lymphoproliferative disorders in immunocompromised patients. Cancer Lett. 2011; 305:163–74. http://dx.doi.org/10.1016/j.canlet.2011.03.003
2. Bruce AG, Bielefeldt-Ohmann H, Barcy S, Bakke AM, Lewis P, Tsai CC, et al. Macaque homologs of EBV and KSHV show uniquely different associations with simian AIDS-related lymphomas. PLoS Pathog. 2012;8:e1002962. http://dx.doi.org/10.1371/journal.ppat.1002962
3. Albrecht JC, Nicholas J, Biller D, Cameron KR, Biesinger B, Newman C, et al. Primary structure of the herpesvirus saimiri genome. J Virol. 1992;66:5047–58.
4. Rose TM, Strand KB, Schultz ER, Schaefer G, Rankin GW Jr, Thouless ME, et al. Identification of two homologs of the Kaposi's sarcoma-associated herpesvirus (human herpesvirus 8) in retroperitoneal fibromatosis of different macaque species. J Virol. 1997;71:4138–44.
5. Greensill J, Sheldon JA, Renwick NM, Beer BE, Norley S, Goudsmit J, et al. Two distinct gamma-2 herpesviruses in African green monkeys: a second gamma-2 herpesvirus lineage among Old World primates? J Virol. 2000;74:1572–7. http://dx.doi.org/10.1128/JVI.74.3.1572-1577.2000
6. Schultz ER, Rankin GW Jr, Blanc MP, Raden BW, Tsai CC, Rose TM. Characterization of two divergent lineages of macaque rhadinoviruses related to Kaposi's sarcoma-associated herpesvirus. J Virol. 2000;74:4919–28. http://dx.doi.org/10.1128/JVI.74.10.4919-4928.2000
7. Estep RD, Hansen SG, Rogers KS, Axthelm MK, Wong SW. Genomic characterization of Japanese macaque rhadinovirus, a novel herpesvirus isolated from a nonhuman primate with a spontaneous inflammatory demyelinating disease. J Virol. 2013;87:512–23. http://dx.doi.org/10.1128/JVI.02194-12
8. Bruce AG, Ryan JT, Thomas MJ, Peng X, Grundhoff A, Tsai CC, et al. Next-generation sequence analysis of the genome of RFHVMn, the macaque homolog of Kaposi's sarcoma

(KS)-associated herpesvirus, from a KS-like tumor of a pig-tailed macaque. J Virol. 2013;87:13676–93. http://dx.doi.org/10.1128/JVI.02331-13
9. Bruce AG, Thouless ME, Haines AS, Pallen MJ, Grundhoff A, Rose TM. Complete genome sequence of pig-tailed macaque rhadinovirus 2 and its evolutionary relationship with rhesus macaque rhadinovirus and human herpesvirus 8/Kaposi's sarcoma-associated herpesvirus. J Virol. 2015;89:3888–909. http://dx.doi.org/10.1128/JVI.03597-14
10. Olp LN, Jeanniard A, Marimo C, West JT, Wood C. Whole-genome sequencing of Kaposi's sarcoma-associated herpesvirus from Zambian Kaposi's sarcoma biopsy specimens reveals unique viral diversity. J Virol. 2015;89:12299–308. http://dx.doi.org/10.1128/JVI.01712-15
11. Russo JJ, Bohenzky RA, Chien MC, Chen J, Yan M, Maddalena D, et al. Nucleotide sequence of the Kaposi sarcoma-associated herpesvirus (HHV8). Proc Natl Acad Sci U S A. 1996;93:14862–7. http://dx.doi.org/10.1073/pnas.93.25.14862
12. Searles RP, Bergquam EP, Axthelm MK, Wong SW. Sequence and genomic analysis of a Rhesus macaque rhadinovirus with similarity to Kaposi's sarcoma-associated herpesvirus/human herpesvirus 8. J Virol. 1999;73:3040–53.
13. Alexander L, Denekamp L, Knapp A, Auerbach MR, Damania B, Desrosiers RC. The primary sequence of rhesus monkey rhadinovirus isolate 26-95: sequence similarities to Kaposi's sarcoma-associated herpesvirus and rhesus monkey rhadinovirus isolate 17577. J Virol. 2000;74:3388–98. http://dx.doi.org/10.1128/JVI.74.7.3388-3398.2000
14. Groves CP, Wilson DE, Reeder DM. Mammal species of the world: a taxonomic and geographic reference. 3rd ed. Baltimore (MD): Johns Hopkins University Press; 2005. p. 161–72.
15. Davison AJ, Stow ND. New genes from old: redeployment of dUTPase by herpesviruses. J Virol. 2005;79:12880–92. http://dx.doi.org/10.1128/JVI.79.20.12880-12892.2005
16. Grewer A, Bleyer M, Mätz-Rensing K, Hahn A, Rüggeberg T, Babaryka G, et al. Kaposi sarcoma in mantled guereza. Emerg Infect Dis. 2019;25:1552–5.

Address for correspondence: Thomas F. Schulz, Hannover Medical School, Institute of Virology, Carl-Neuberg-Str. 1, 30625 Hannover, Lower Saxony, Germany; email: schulz.thomas@mh-hannover.de; Andrew J. Davison, MRC–University of Glasgow Centre for Virus Research, Sir Michael Stoker Bldg, 464 Bearsden Rd, Glasgow, Scotland G61 1QH, UK; email: andrew.davison@glasgow.ac.uk

Kaposi Sarcoma in Mantled Guereza

Anna Grewer, Martina Bleyer, Kerstin Mätz-Rensing, Alexander S. Hahn, Tim Rüggeberg, Gregor Babaryka, Andre Zimmermann, Stefan Pöhlmann, Artur Kaul

We identified a novel Kaposi's sarcoma herpesvirus–related rhadinovirus (Colobine gammaherpesvirus 1) in a mantled guereza (*Colobus guereza kikuyensis*). The animal had multiple oral tumors characterized by proliferation of latent nuclear antigen 1–positive spindle cells and was not co-infected with immunosuppressive simian viruses, suggesting that it had Kaposi sarcoma caused by this novel rhadinovirus.

Kaposi's sarcoma herpesvirus (KSHV), a member of the genus *Rhadinovirus*, is the causative agent of Kaposi sarcoma (*1*), an endothelial neoplasm of the dermis, oral cavity, and intestinal organs. The tumors are highly vascularized and characterized by proliferation of spindle cells that contain KSHV DNA and antigen (*2*,*3*). Predisposing factors for Kaposi sarcoma include immunodeficiency, especially infection with HIV (*4*). Nevertheless, a major portion of Kaposi sarcoma cases in Africa occurs in HIV-negative persons (*5*).

Clinically, Kaposi sarcoma is divided into 4 forms: classical Kaposi sarcoma, African endemic Kaposi sarcoma, Kaposi sarcoma caused by iatrogenic immunosuppression, and HIV-associated Kaposi sarcoma (*6*,*7*). Lesions of classical Kaposi sarcoma initially occur on the lower extremities, progress slowly, and affect visceral organs at a late stage (*6*,*7*). In contrast, the remaining Kaposi sarcoma forms affect lymph nodes, mucosa, and visceral organs at early stages, progress rapidly, and encompass symptoms in the hard palate and oral mucosa (*6*,*7*).

Rhadinoviruses with high similarity to KSHV have been detected in Old World monkeys, including chimpanzees (*8*), macaques (*9*–*11*), and African green monkeys (*12*). The rhadinoviruses have split into 2 lineages, RV1 and RV2, and many Old World monkeys harbor viruses of both lineages. In contrast, humans harbor only KSHV, which belongs to the RV1 lineage. Kaposi sarcoma–like disease has been observed in rhadinovirus-infected nonhuman primates (NHP), but only in the presence of immunodeficiency, induced, for instance, by co-infection with simian immunodeficiency virus (*13*,*14*).

We report Kaposi sarcoma in a simian immunodeficiency virus– and simian retrovirus–negative mantled guereza (*Colobus guereza kikuyensis*) that was infected with a novel rhadinovirus that had high homology to KSHV. This new virus is called Colobine gammaherpesvirus 1 (CbGHV1).

The Study

A 13-year-old female mantled guereza who was born in a zoological garden in Germany showed development of swelling on the inner aspects of the lower lips; several circumscribed masses were found on the inner upper and lower labial mucosa. The masses were pink to light red and had a smooth and shiny surface, coarse consistence, and a diameter of 1–2 cm (Figure 1, panel A). After incision of 1 mass, the surface of the cut appeared to be cavernous and highly vascularized.

The mucosal masses were removed by surgery. Subsequently, bilateral cataract, progressive weight loss, and recurrence of the mucosal masses developed in the animal, and it had to be euthanized (Appendix, https://wwwnc.cdc.gov/EID/article/25/8/18-1804-App1.pdf). Necropsy showed several flattened and smooth tumorous lesions on the inner aspects of the upper and lower lips, as well as multiple small, partly ulcerated nodules at the gingival margin of the upper and lower jaw (Figure 1, panel B).

Histologically, masses and nodules consisted of a collagen-rich fibrous stroma with multifocal areas of increased cellularity represented by spindle cell proliferations with moderate lymphoplasmacellular infiltrates (Figure 1, panel C). The tonsils and mandibular and axillary lymph nodes showed similar foci of fibrovascular tissue. In the perinodal adipose tissue of 1 mandibular lymph node, we found distinct formation of caverns lined by endothelial cells, filled with erythrocytes, and surrounded by spindle cells (Figure 1, panel D).

Immunohistochemical examination showed distinct immunoreaction of most spindle cells with endothelial cell markers CD31 and von Willebrand factor. We found variable expression of Ki67 in ≤20% of spindle cells (Figure 1, panel E), and ≈50%–60% of spindle cells reacted with

Author affiliations: Zoo Krefeld GmbH, Krefeld, Germany (A. Grewer); German Primate Center–Leibniz Institute for Primate Research, Göttingen, Germany (M. Bleyer, K. Mätz-Rensing, A.S. Hahn, S. Pöhlmann, A. Kaul); Heinrich-Heine-University Düsseldorf, Düsseldorf, Germany (T. Rüggeberg, G. Babaryka, A. Zimmermann); Joint Practice for Oral and Maxillofacial Surgery, Neuss, Germany (A. Zimmermann); University of Göttingen, Göttingen (S. Pöhlmann)

DOI: https://doi.org/10.3201/eid2508.181804

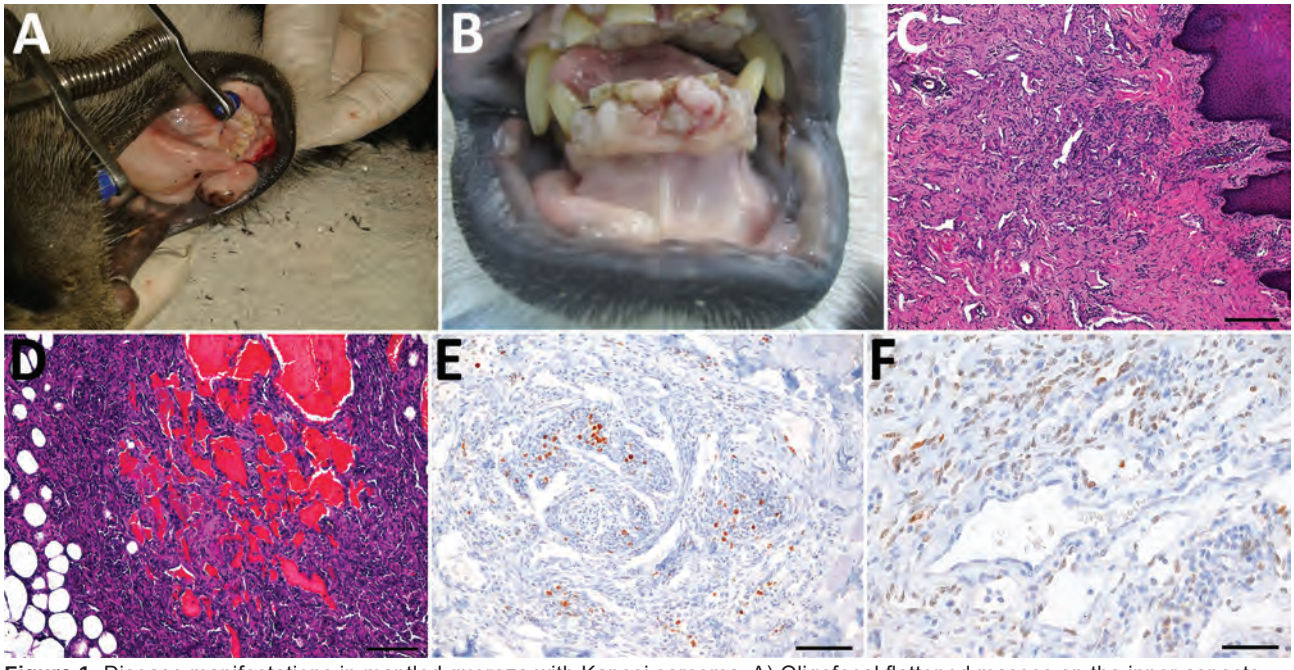

Figure 1. Disease manifestations in mantled guereza with Kaposi sarcoma. A) Oligofocal flattened masses on the inner aspects of the lower lip. B) Multinodular fissured masses at the gingival margin. C) Fibrovascular stroma in the subepithelial propria of the lower lip with spindle cell proliferations delineating narrow vascular clefts and containing lymphoplasmacytic inflammatory cell infiltrates, hematoxylin and eosin stained; scale bar indicates 200 μm. D) Spindle cell proliferation with cavern formation in the perinodal adipose tissue of the mandibular lymph node; hematoxylin and eosin stained; scale bar indicates 100 μm. E) Immunohistochemical staining showing variable Ki67 expression in ≤20% of spindle cells, streptavidin-biotin complex method–diaminobenzidine tetrahydrochloride; scale bar indicates 100 μm. F) Immunohistochemical staining showing nuclear expression of latent nuclear antigen 1 in ≈50%–60% of spindle cells, streptavidin-biotin complex method–diaminobenzidine tetrahydrochloride; scale bar indicates 50 μm.

antibodies against KSHV latent nuclear antigen (Figure 1, panel F). These findings were compatible with Kaposi sarcoma. A pan herpesvirus PCR amplified DNA fragments in all tested samples (blood, swabs, pathologic tissues of upper and lower lips) that contained identical sequences of a novel herpesvirus (CbGHV1). This virus is most closely related to retroperitoneal fibromatosis herpesvirus from *Macaca nemestrina* (the pig-tailed macaque) (Figure 2, panel A) and was also identified in a sibling of the animal we studied (*15*).

We found high viral loads in the tumorous masses of the oral cavity, in swabs from cut surfaces of mucosal masses, and in tumorous lesions on the inner upper and lower lips, as well as in nodules at the gingival margin (Table 1). A lower viral load was detected in blood and was identical to that measured in the blood of a healthy offspring of the animal (Table 1). Viral load in all remaining organs was in the range of that measured for blood, potentially because of circulation of positive blood cells through these organs. Moreover, mucosal, anal, and fluid swab samples were clearly positive for viral genomes and the high viral load in the mucosa of the eye and in the lacrimal glands might be explained by Kaposi sarcoma in unusual locations (*16*). Finally, CbGHV1-negative samples were not available for calibration by PCR; their inclusion might have altered overall, but not relative, CbGHV1 genome copies measured.

Serologic analysis showed that the guereza had antibodies against lymphocryptovirus, cytomegalovirus, and simian foamy virus but, somewhat counter intuitively, not against rhesus rhadinovirus (RRV) (Table 2). In contrast, serum from the animal was reactive against KSHV antigen in an ELISA (Figure 2, panel B) and an immunofluorescence-based assay (data not shown). Finally, we did not detect antibodies reactive against KSHV in a CbGHV1-positive healthy offspring, potentially because CbGHV1 antibody levels were higher in diseased compared with healthy animals.

Conclusions

The animal we studied had several characteristic features of Kaposi sarcoma, including tumorous lesions in the buccal mucosa and proliferation of spindle cells, which harbored viral antigen. Although the disease symptoms did not fully match those of Kaposi sarcoma in humans (*3*,*4*), in part because of absence of initial symptoms in the lower extremities, an animal model based on CbGHV1 might still provide major insights into Kaposi sarcoma/KSHV infection of humans.

Table 1. Viral loads of CbGHV1 genomes in various organs of mantled guereza with Kaposi sarcoma*

Category	Copies of CbGHV1 DNA/μg total DNA ± SD
Sampling during anesthesia	
Blood	$4 \times 10^4 \pm 8 \times 10^3$
Blood	$7 \times 10^4 \pm 2 \times 10^4$†
Mucosal masses	
Swab specimen from cut surface	$6 \times 10^7 \pm 3 \times 10^7$
Buccal	$9 \times 10^6 \pm 1 \times 10^6$
Upper labial	$3 \times 10^7 \pm 6 \times 10^6$
Lower labial	$2 \times 10^7 \pm 3 \times 10^6$
Sampling during necropsy	
Mucosal masses	
Gingiva	$9 \times 10^5 \pm 1 \times 10^5$
Upper labial	$6 \times 10^6 \pm 1 \times 10^6$
Lower labial	$1 \times 10^7 \pm 5 \times 10^6$
Oral swab specimen	$5 \times 10^3 \pm 2 \times 10^3$‡
	$5 \times 10^4 \pm 2 \times 10^4$‡
Genital swab specimen	$6 \times 10^4 \pm 1 \times 10^4$
Anal swab specimen	$3 \times 10^5 \pm 5 \times 10^4$
Lacrimal fluid swab specimen	$3 \times 10^6 \pm 6 \times 10^5$
Spleen	$5 \times 10^5 \pm 9 \times 10^4$
Kidney	$6 \times 10^3 \pm 3 \times 10^3$‡
Kidney	$2 \times 10^5 \pm 2 \times 10^4$‡
Liver	$3 \times 10^3 \pm 2 \times 10^3$
Lung	$1 \times 10^4 \pm 6 \times 10^3$
Heart	$9 \times 10^3 \pm 3 \times 10^3$
Brain	$1 \times 10^4 \pm 5 \times 10^3$

*Values are mean ± SD for 3 independent quantitative PCRs. CbGHV1, Colobine gammaherpesvirus 1.
†Results for healthy offspring.
‡Two samples were obtained during necropsy.

Table 2. Antibodies against selected viral antigens in mantled guereza with Kaposi sarcoma*

Antigen source	Test result	
	Monkey with Kaposi sarcoma	Healthy offspring
Herpes simplex viruses	–	–
Simian immunodeficiency virus	–	–
Simian retrovirus	–	–
Simian T-cell leukemia virus	–	–
Measles virus	–	–
Rhesus rhabdovirus	–	–
Lymphocryptovirus	+	+
Cytomegalovirus	+	+
Simian foamy virus	+	–

*–, negative; +, positive.

CbGHV1 exhibited a higher similarity to KSHV and retroperitoneal fibromatosis herpesvirus from *M. nemestrina*, which are RV1 rhadinoviruses, when compared with RRV, a RV2 rhadinovirus. Consistent with these findings, serum from the guereza cross-reacted with KSHV but not RRV. However, we cannot exclude that assay specificity was moderate and confirmation with independent tests is pending. Apart from the animal having Kaposi sarcoma, 4 genetically related animals were also PCR-positive for CbGHV1, raising questions regarding the route of transmission. We detected high copy numbers of the viral genome in swab specimens of the oral cavity and the anogenital mucosa, suggesting that transmission might occur by close contact, including sex, the route of KSHV transmission between humans (*3*,*4*).

CbGHV1 was most likely involved in tumorigenesis because high numbers of the viral genome were found within tumorous tissues. Moreover, viral antigen was detected in spindle cells. However, it was unclear that infection by CbGHV1 was sufficient to induce Kaposi sarcoma. A link between immunosuppression and Kaposi sarcoma has been established for human patients and cannot be excluded for

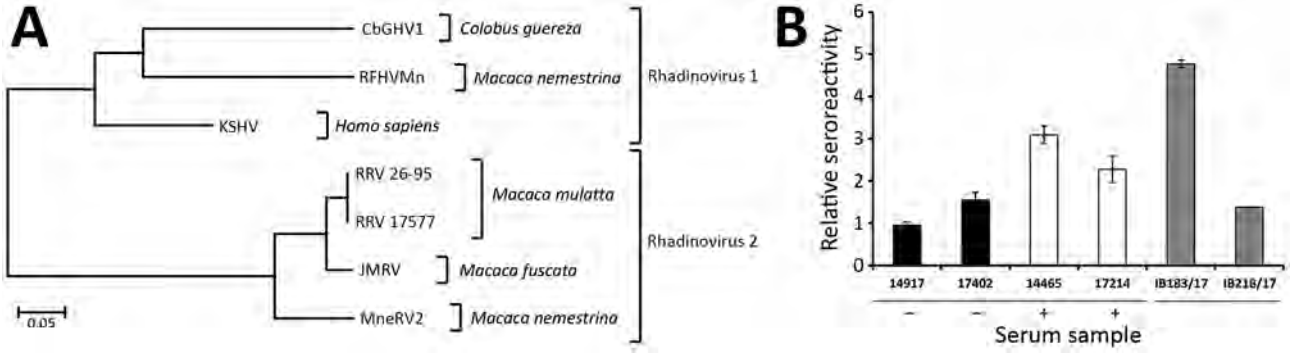

Figure 2. Analysis of CbGHV1 and seroreactivity in mantled guereza with Kaposi sarcoma. A) Phylogenetic analysis of partial sequences of the polymerase gene. Analysis was performed by using the neighbor-joining method. The distance between CbGHV1 and selected viruses was analyzed by using the maximum composite–likelihood method and MEGA6 (https://www.megasoftware.net). The PCR sequence of CbGHV1 was compared with KSHV (GenBank accession no. NC_009333.1); RFHVMn (KF703446.1); RRV 26–95 (AF210726.1); RRV 17577 (NC_003401.1); JMRV (AY528864.1); and MneRV2 (KP265674.2). Scale bar indicates nucleotide substitutions per site. B) Antibodies from mantled guereza with Kaposi sarcoma showing cross-reactivity against KSHV. Reactivities of KSHV antibody–positive human serum samples (14465 and 17214), KSHV antibody–negative human serum samples (14917 and 17402), and serum sample from the Kaposi sarcoma–affected mantled guereza (IB183/17) and its healthy offspring (IB218/17) were analyzed by ELISA. Relative reactivities of serum samples with KSHV-positive and KSHV-negative cell lysates are shown. The sum of relative errors is used as an error estimate for the ratio and is indicated by error bars (mean ± half error). Reactivity of human serum samples against KSHV is indicated. CbGHV1, Colobine gammaherpesvirus 1; JMRV, Japanese macaque rhadinovirus; KSHV, Kaposi's sarcoma herpesvirus; MneRV2, *Macaca nemestrina* rhadinovirus 2; RFHVMn, retroperitoneal fibromatosis–associated herpesvirus *M. nemestrina*; RRV, rhesus rhadinovirus; –, negative; +, positive.

CbGHV1/NHP (*3*,*4*). A younger male sibling of the guereza analyzed in this study was PCR positive for CbGHV1 and showed development of primary effusion lymphoma, another disease caused by KSHV, without evidence for immunosuppression (*15*). Thus, a genetic component might contribute to disease development. Finally, 1 offspring of the animal infected with Kaposi sarcoma and 2 genetically related animals were also CbGHV1-positive but healthy; it remains to be examined whether they will show development of disease in the future.

We report a case of spontaneous Kaposi sarcoma in an NHP. Our findings might aid the development of an NHP model for KSHV/Kaposi sarcoma in humans. For development of this model, it is critical to isolate CbGHV1; those efforts are under way.

Acknowledgments

We thank Klaus Korn for providing serum samples from KSHV+ and KSHV– patients and Bastian-Felix Danitz, Sarah Schlagowski, Nadine Schminke, and Larissa Hummel for providing excellent technical assistance.

About the Author

Dr. Grewer is a veterinarian at the Zoo Krefeld, Krefeld, Germany. Her primary research interest is infectious diseases in zoo animals.

References

1. Moore PS, Chang Y. Detection of herpesvirus-like DNA sequences in Kaposi's sarcoma in patients with and those without HIV infection. N Engl J Med. 1995;332:1181–5. https://doi.org/10.1056/NEJM199505043321801
2. Boshoff C, Schulz TF, Kennedy MM, Graham AK, Fisher C, Thomas A, et al. Kaposi's sarcoma-associated herpesvirus infects endothelial and spindle cells. Nat Med. 1995;1:1274–8. https://doi.org/10.1038/nm1295-1274
3. Mariggiò G, Koch S, Schulz TF. Kaposi sarcoma herpesvirus pathogenesis. Philos Trans R Soc Lond B Biol Sci. 2017; 372:20160275. https://doi.org/10.1098/rstb.2016.0275
4. Yarchoan R, Uldrick TS. HIV-associated cancers and related diseases. N Engl J Med. 2018;378:1029–41. https://doi.org/10.1056/NEJMra1615896
5. Host KM, Horner MJ, van der Gronde T, Moses A, Phiri S, Dittmer DP, et al. Kaposi's sarcoma in Malawi: a continued problem for HIV-positive and HIV-negative individuals. AIDS. 2017;31:318–9. https://doi.org/10.1097/QAD.0000000000001341
6. Antman K, Chang Y. Kaposi's sarcoma. N Engl J Med. 2000; 342:1027–38. https://doi.org/10.1056/NEJM200004063421407
7. Friedman-Kien AE, Saltzman BR. Clinical manifestations of classical, endemic African, and epidemic AIDS-associated Kaposi's sarcoma. J Am Acad Dermatol. 1990;22:1237–50. https://doi.org/10.1016/0190-9622(90)70169-I
8. Greensill J, Sheldon JA, Murthy KK, Bessonette JS, Beer BE, Schulz TF. A chimpanzee rhadinovirus sequence related to Kaposi's sarcoma-associated herpesvirus/human herpesvirus 8: increased detection after HIV-1 infection in the absence of disease. AIDS. 2000;14:F129–35. https://doi.org/10.1097/00002030-200012010-00001
9. Desrosiers RC, Sasseville VG, Czajak SC, Zhang X, Mansfield KG, Kaur A, et al. A herpesvirus of rhesus monkeys related to the human Kaposi's sarcoma-associated herpesvirus. J Virol. 1997;71:9764–9.
10. Rose TM, Strand KB, Schultz ER, Schaefer G, Rankin GW Jr, Thouless ME, et al. Identification of two homologs of the Kaposi's sarcoma-associated herpesvirus (human herpesvirus 8) in retroperitoneal fibromatosis of different macaque species. J Virol. 1997;71:4138–44.
11. Strand K, Harper E, Thormahlen S, Thouless ME, Tsai C, Rose T, et al. Two distinct lineages of macaque gamma herpesviruses related to the Kaposi's sarcoma associated herpesvirus. J Clin Virol. 2000;16:253–69. https://doi.org/10.1016/S1386-6532(99)00080-3
12. Greensill J, Sheldon JA, Renwick NM, Beer BE, Norley S, Goudsmit J, et al. Two distinct gamma-2 herpesviruses in African green monkeys: a second gamma-2 herpesvirus lineage among old world primates? J Virol. 2000;74:1572–7. https://doi.org/10.1128/JVI.74.3.1572-1577.2000
13. Orzechowska BU, Powers MF, Sprague J, Li H, Yen B, Searles RP, et al. Rhesus macaque rhadinovirus-associated non-Hodgkin lymphoma: animal model for KSHV-associated malignancies. Blood. 2008;112:4227–34. https://doi.org/10.1182/blood-2008-04-151498
14. Wong SW, Bergquam EP, Swanson RM, Lee FW, Shiigi SM, Avery NA, et al. Induction of B cell hyperplasia in simian immunodeficiency virus-infected rhesus macaques with the simian homologue of Kaposi's sarcoma-associated herpesvirus. J Exp Med. 1999;190:827–40. https://doi.org/10.1084/jem.190.6.827
15. Dhingra A, Ganzenmueller T, Hage E, Suárez NM, Mätz-Rensing K, Widmer D, et al. Novel virus related to Kaposi sarcoma–associated herpesvirus from *Colobus* monkey. Emerg Infect Dis. 2019;25:1548–51.
16. Pantanowitz L, Dezube BJ. Kaposi sarcoma in unusual locations. BMC Cancer. 2008;8:190. https://doi.org/10.1186/1471-2407-8-190

Address for correspondence: Anna Grewer, Zoo Krefeld GmbH, Uerdinger Strasse 377, Krefeld 47800, Germany; email: anna.grewer@zookrefeld.de

Emergence of a Novel Recombinant Norovirus GII.P16-GII.12 Strain Causing Gastroenteritis, Alberta, Canada

Kanti Pabbaraju, Anita A. Wong, Graham A. Tipples, Xiaoli-Li Pang

We identified a novel recombinant GII.P16-GII.12 norovirus associated with epidemic and endemic gastroenteritis during March 1, 2018–February 12, 2019, in Alberta, Canada. GII.12 viruses have not been detected in Alberta since 2000. Comparing the full genome of this strain to previously published sequences revealed this virus to be a novel recombinant strain.

Norovirus is the leading cause of epidemic and endemic acute gastroenteritis (AGE) worldwide. Norovirus can evade the host immune response by accumulating mutations that have a biological advantage by antigenic drift (*1*). In addition, recombination at the junction of open reading frame (ORF) 1 and 2 can result in the circulation of a novel strain.

In the past 2 decades, emerging genetic clusters of norovirus GII.4 were associated with epidemics in Alberta, Canada. Multiple GII.4 viruses were associated with epidemics during the 2000s. Since 2010, a single variant, GII.4 Sydney, has been the predominant virus (*2*–*5*). A recombinant GII.P16-GII.4 Sydney strain emerged in July 2015 and caused 72% of the outbreaks in the winter of 2017–18 (*2*). A small wave of activity with the Kawasaki GII.17 and GII.P16-GII.2 strains was seen during 2016–2017, but they did not predominate.

The Alberta Molecular Surveillance Program includes genotyping of 1 norovirus-positive stool sample from each outbreak for the early detection of novel strains. During March 1, 2018–February 12, 2019, we report the detection of a novel recombinant GII.P16-GII.12 that was identified in May 2018 and caused AGE outbreaks and sporadic cases in children <6 years of age.

The Study

Public health officials and the Public Health Laboratory (ProvLab) in the province of Alberta use established protocols to investigate all suspected AGE outbreaks. Stool samples are tested for norovirus genogroups I and II using a real-time reverse transcription PCR (*4*). An outbreak includes ≥2 epidemiologically linked AGE cases with ≥1 norovirus-positive sample. ProvLab genotyped 1 norovirus-positive sample from each outbreak and those from children with sporadic AGE by using the dual polymerase-capsid genotyping protocol (*6*). In our study, 72/108 (67%) AGE outbreaks had test results positive for norovirus, of which 5 (7%) were identified as norovirus GI, 66 (92%) as GII, and 1 (1%) as GI and GII (Table 1). During the same period, 94/755 (12%) AGE cases in children had test results positive for norovirus, 6 as GI and 88 as GII.

We genotyped 64/72 (89%) outbreaks and 74/94 (79%) sporadic cases and detected diverse genotypes and different monthly trends (Table 2; Figure 1). GII.P16-GII.4 Sydney 2012 was the predominant strain followed by GII.P16-GII.12 in both outbreaks and sporadic AGE, but distribution of other genotypes was different, most notably GII.P16-GII.2 and GII.P12-GII.3 strains were detected in the sporadic cases but not in outbreaks (Table 2).

The GII.P16-GII.2 strain emerged in 2016 and caused a large norovirus epidemic in Asia (*7*,*8*), followed by a small wave in Alberta in winter 2016–17 (*2*), but this strain was not detected in outbreaks during our study. Of note, the emerging GII.P16-GII.12 strain became the second most predominant strain with increasing cases, especially in sporadic AGE, after November 2018 (Figure 1, panel B). This strain caused 80% (8/10) of outbreaks in long-term care facilities and 2 in hospital acute-care units. Of the 17 sporadic cases associated with this strain, we retrieved patient information for 14 cases; 12 were hospitalized, 1 was seen in the emergency department, and 1 was an outpatient. The number of hospitalized patients probably indicates more severe disease associated with this strain. However, because the number of cases was small, further study and caution in interpretation of disease severity is warranted.

We sequenced the near-complete genome of the novel GII.P16-GII.12 strain from 2 different outbreaks by Sanger sequencing using primers designed in-house (available upon request). We performed contig assembly with Seqscape v2.7 (Advanced Biosystems, https://seqscape.software.informer.com/2.7) and sequence alignments with

Author affiliations: Public Health Laboratory (ProvLab), Alberta Public Laboratories, Edmonton, Alberta, Canada (K. Pabbaraju, A.A. Wong, G.A. Tipples, X.-L. Pang); University of Alberta, Edmonton, Alberta, Canada (G.A. Tipples, X.-L. Pang)

DOI: https://doi.org/10.3201/eid2508.190059

Table 1. Investigation of outbreaks of acute gastroenteritis, March 1, 2018–February 12, 2019, Alberta, Canada

Month	Outbreaks	Norovirus-positive, no. (%)	GI	GII	GI and GII
Mar	16	11 (69)	1	10	0
Apr	9	8 (89)	1	7	0
May	4	2 (50)	1	1	0
Jun	2	0 (0)	0	0	0
Jul	3	1 (33)	0	1	0
Aug	3	1 (33)	0	0	1
Sep	3	1 (33)	0	1	0
Oct	4	3 (75)	0	3	0
Nov	12	8 (67)	0	8	0
Dec	26	17 (65)	0	17	0
Jan	21	15 (71)	2	13	0
Feb	5	5 (100)	0	5	0
Total	108	72 (67)	5	66	1

Table 2. Genotyping results for outbreak and sporadic cases of acute gastroenteritis, March 1, 2018–February 12, 2019, Alberta, Canada

Characteristics	Outbreak	Sporadic	Total
No. cases	72	94	166
No. (%) genotyped	64 (89)	74 (79)	138 (83)
GI genotypes, no. cases			
GI.P2-GI.2	0	1	1
GI.P3-GI.3	3	2	5
GI.Pb-GI.6	1	0	1
GI.P6-GI.6*	1	0	1
GI.P7-GI.7	0	1	1
GI.PUnknown-GI.7	1	0	1
GII genotypes, no. cases			
GII.P4-GII.4	1	1	2
GII.P7-GII.6	1	0	1
GII.P7-GII.14*	1	0	1
GII.P12-GII.3	0	4	4
GII.P16-GII.2	0	2	2
GII.P16-GII.4	46	44	90
GII.16-GII.12	10	17	27
GII.P-unknown_GII.12	0	2	2

*Co-infection with genogroups GI and GII.

ClustalW (http://www.clustal.org/clustal2). For phylogenetic analysis, we inferred evolutionary history by using the neighbor-joining method. We computed evolutionary distance by using the maximum composite likelihood model for nucleotide sequences and the Poisson model for amino acid sequences. We performed a bootstrap test by using 1,000 replicates in MEGA6 (http://www.megasoftware.net) (*9*). We obtained 7,406 bp and submitted the sequences to GenBank (accession nos. MK355712–3).

We compared the ORF1 sequence to the RIVM (http://www.rivm.nl/mpf/norovirus/typingtool) and National Center for Biotechnology Information (http://www.ncbi.nlm.nih.gov) databases. The closest sequence match was from GII.P16-GII.4 Sydney 2012 (accession no. LC175468), the current predominant genotype worldwide (*6*,*10*). At the nucleotide level, ORF1 of MK355712 shared 96.92% identity with the Sydney 2012 strain and MK355713 shared 96.98% identity. At the amino acid level, ORF1 of MK355712 shared 98.56% identity and MK355713 shared 98.65% identity with the Sydney 2012 strain. We constructed a phylogenetic tree comparing the near full-length ORF1 of the strains we report with the GII.P16 sequence associated with the viral protein (VP) 1 capsid region from different genotypes (Figure 2). The ORF1 clustered with the ORF1 from contemporary strains including GII.4 Sydney, GII.2, and the recently described GII.3 and GII.1 sequences (accession nos. KY887597 and MG572182), but our sequences lie on an independent branch.

GII.P16 sequences from this study clustered with GII.P16 sequences that form a previously reported distinct monophyletic clade with a common ancestor from 2013 (*10*) but lie on an independent branch (data not shown). Others have described the GII.P16 sequences belonging to this clade as containing nonsynonymous substitutions in ORF1 along the branch leading to the common ancestor of the GII.P16-GII.4 Sydney 2012/GII.3 clade, several of which occur close to positions known to affect polymerase function and transmission (*10*). We saw amino acid changes in our sequences that were also noted in the GII.Pe and GII.P16 polymerase of GII.4 Sydney viruses, including D173E, G163A, L337M, and S502N, but we did not see the K1646R unique to GII.P16 associated with GII.4 Sydney. We noted some of the point mutations in our sequences that have been described on the polymerase surface of novel GII.P16 strains, including

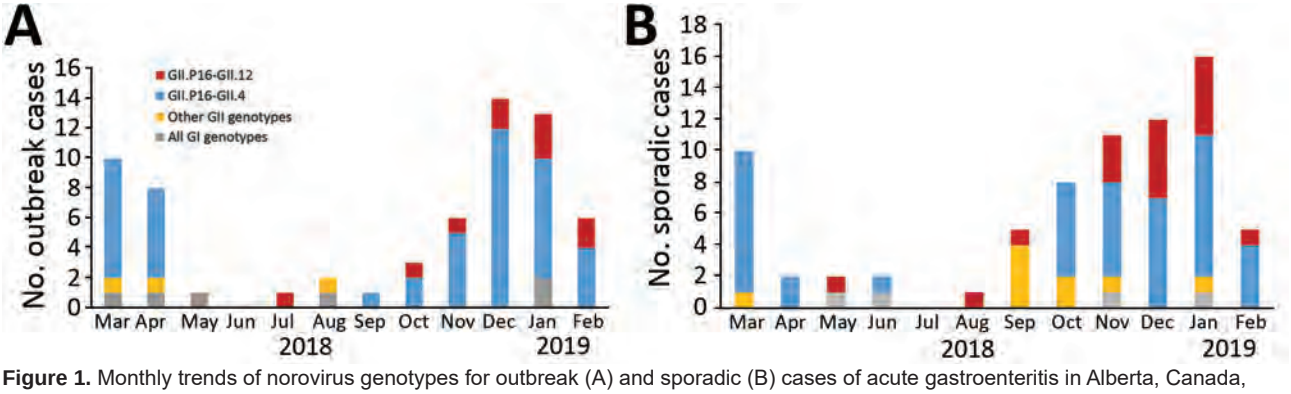

Figure 1. Monthly trends of norovirus genotypes for outbreak (A) and sporadic (B) cases of acute gastroenteritis in Alberta, Canada, during March 2018–February 2019. Genotypes included under other are listed in Table 2.

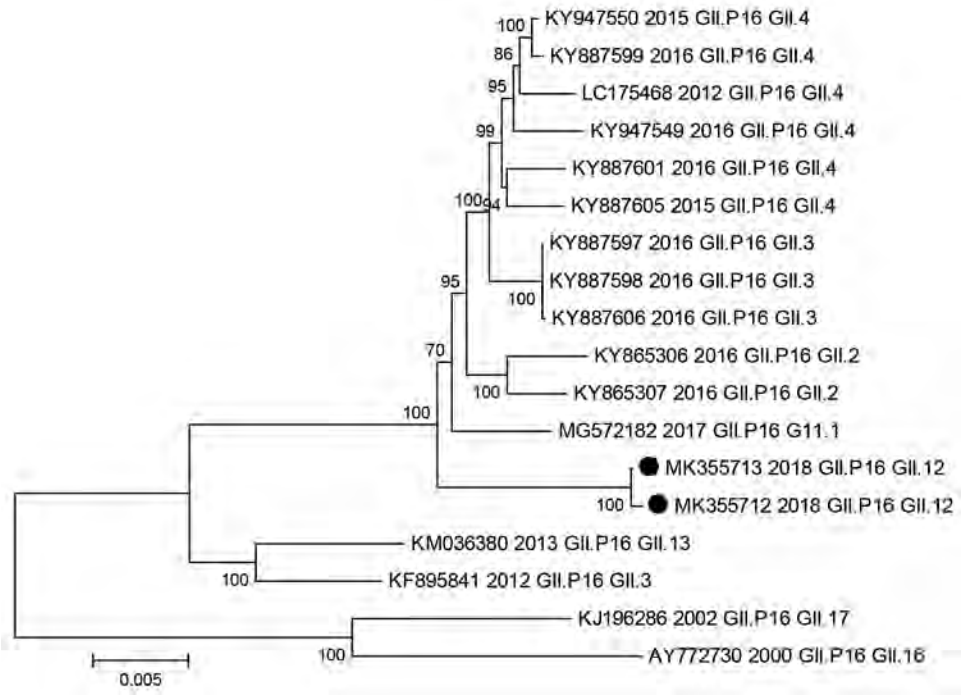

Figure 2. Phylogenetic tree of open reading frame 1 for norovirus GII.P16 strains. Black dots indicate nucleotide sequences of novel GII.P16-GII.12 strains identified in Alberta, Canada, during March 2018–February 2019. GenBank accession numbers and year identified are provided. Scale bar indicates nucleotide substitutions per site.

K357Q, T360A, and V332I (*6*,*7*,*10*,*11*), which caused re-emergence of a new cluster. Because we did not see all the known mutations, effects of these amino acid changes will require further investigation.

We compared ORF2 and ORF3 to the GenBank database using BLAST (https://blast.ncbi.nlm.nih.gov/Blast.cgi) and found the closest sequence matches are contemporary strains described in Taiwan (*12*), Australia (*13*), and the United States (*14*,*15*). Identity with these sequences were 93%–94% at the nucleotide level and 98%–99% at the amino acid level in ORF2 and 84%–85% at the nucleotide level and 86%–87% at the amino acid level in ORF3. Identity with the prototype Wortley strain (accession no. AJ277618) was lower. Our sequences demonstrated amino acid changes reported in the contemporary GII.12 strains, including A22V, I47V, and S465T, but we did not see the N392S described in all sequences of the GII.12 strain cluster in our sequence (*15*). The P2 region of VP1 has the antigenic and histoblood group antigen attachment sites, and 3 unique amino acid substitutions, including N350D, A352T, and I361V were seen in this region. Studies to explore whether these mutations play a role in binding profiles and immunity will help us understand if this virus is under selective pressure, which can give rise to novel variants.

Conclusions

We describe a novel recombinant GII.P16-GII.12 norovirus strain identified in Alberta, Canada. Although the GII.P16-GII.4 strain is still predominant, this novel strain seems to be playing a role in both outbreaks and sporadic cases in young children. Continued surveillance and prompt genotyping are critical to monitor the emergence and prevalence of novel norovirus strains.

Acknowledgments

We thank Chen Liu for managing the samples for this study. We also thank the staff of the Public Health Laboratory (ProvLab), especially the virology and molecular departments, for performing norovirus testing; the collaborative teams participating in outbreak investigations in Alberta, Northwest Territories, Yukon, and Nunavut; and the members of the ProvLab Outbreak Investigation Committee.

This work was supported by the Public Health Laboratory (ProvLab), Alberta, Canada, and Alberta Health, Canada.

About the Author

Dr. Pabbaraju is a laboratory scientist at the Public Health Laboratory (ProvLab), Alberta, Canada. Her research focuses on the development of diagnostic tests for viral and bacterial pathogens and studies on the epidemiology of viruses.

References

1. Siebenga JJ, Vennema H, Renckens B, de Bruin E, van der Veer B, Siezen RJ, et al. Epochal evolution of GGII.4 norovirus capsid proteins from 1995 to 2006. J Virol. 2007;81:9932–41. http://dx.doi.org/10.1128/JVI.00674-07
2. Hasing ME, Lee BE, Qiu Y, Xia M, Pabbaraju K, Wong A, et al. Changes in norovirus genotype diversity in gastroenteritis outbreaks in Alberta, Canada: 2012-2018. BMC Infect Dis. 2019;19:177. http://dx.doi.org/10.1186/s12879-019-3792-y

3. Hasing ME, Lee BE, Preiksaitis JK, Tellier R, Honish L, Senthilselvan A, et al. Emergence of a new norovirus GII.4 variant and changes in the historical biennial pattern of norovirus outbreak activity in Alberta, Canada, from 2008 to 2013. J Clin Microbiol. 2013;51:2204–11. http://dx.doi.org/10.1128/JCM.00663-13
4. Pang XL, Preiksaitis JK, Wong S, Li V, Lee BE. Influence of novel norovirus GII.4 variants on gastroenteritis outbreak dynamics in Alberta and the Northern Territories, Canada between 2000 and 2008. PLoS One. 2010;5:e11599. http://dx.doi.org/10.1371/journal.pone.0011599
5. Siebenga JJ, Vennema H, Zheng DP, Vinjé J, Lee BE, Pang XL, et al. Norovirus illness is a global problem: emergence and spread of norovirus GII.4 variants, 2001–2007. J Infect Dis. 2009;200:802–12. http://dx.doi.org/10.1086/605127
6. Cannon JL, Barclay L, Collins NR, Wikswo ME, Castro CJ, Magaña LC, et al. Genetic and Epidemiologic Trends of Norovirus Outbreaks in the United States from 2013 to 2016 Demonstrated Emergence of Novel GII.4 Recombinant Viruses. J Clin Microbiol. 2017;55:2208–21. http://dx.doi.org/10.1128/JCM.00455-17
7. Ao Y, Wang J, Ling H, He Y, Dong X, Wang X, et al. Norovirus GII.P16/GII.2-associated gastroenteritis, China, 2016. Emerg Infect Dis. 2017;23:1172–5. http://dx.doi.org/10.3201/eid2307.170034
8. Liu LT, Kuo TY, Wu CY, Liao WT, Hall AJ, Wu FT. Recombinant GII.P16-GII.2 norovirus, Taiwan, 2016. Emerg Infect Dis. 2017;23:1180–3. http://dx.doi.org/10.3201/eid2307.170212
9. Tamura K, Stecher G, Peterson D, Filipski A, Kumar S. MEGA6: Molecular Evolutionary Genetics Analysis version 6.0. Mol Biol Evol. 2013;30:2725–9. http://dx.doi.org/10.1093/molbev/mst197
10. Ruis C, Roy S, Brown JR, Allen DJ, Goldstein RA, Breuer J. The emerging GII.P16-GII.4 Sydney 2012 norovirus lineage is circulating worldwide, arose by late-2014 and contains polymerase changes that may increase virus transmission. PLoS One. 2017;12:e0179572. http://dx.doi.org/10.1371/journal.pone.0179572
11. Tohma K, Lepore CJ, Ford-Siltz LA, Parra GI. Phylogenetic analyses suggest that factors other than the capsid protein play a role in the epidemic potential of GII.2 norovirus. mSphere. 2017;2:e00187-17. PubMed http://dx.doi.org/10.1128/mSphereDirect.00187-17
12. Tsai CN, Lin CY, Lin CW, Shih KC, Chiu CH, Chen SY. Clinical relevance and genotypes of circulating noroviruses in northern Taiwan, 2006-2011. J Med Virol. 2014;86:335–46. http://dx.doi.org/10.1002/jmv.23728
13. Eden JS, Bull RA, Tu E, McIver CJ, Lyon MJ, Marshall JA, et al. Norovirus GII.4 variant 2006b caused epidemics of acute gastroenteritis in Australia during 2007 and 2008. J Clin Virol. 2010;49:265–71. http://dx.doi.org/10.1016/j.jcv.2010.09.001
14. Takanashi S, Wang Q, Chen N, Shen Q, Jung K, Zhang Z, et al. Characterization of emerging GII.g/GII.12 noroviruses from a gastroenteritis outbreak in the United States in 2010. J Clin Microbiol. 2011;49:3234–44. http://dx.doi.org/10.1128/JCM.00305-11
15. Vega E, Vinjé J. Novel GII.12 norovirus strain, United States, 2009–2010. Emerg Infect Dis. 2011;17:1516–8. http://dx.doi.org/10.3201/eid1708.110025

Address for correspondence: Xiao-Li Pang, Public Health Laboratory (ProvLab), Alberta Public Laboratories, University of Alberta Hospital, WMC 2B4.58, 8440-112 Street, Edmonton, AB T6G 2J2, Canada; email: xiao-li.pang@albertapubliclabs.ca

Underreporting of Fatal Congenital Zika Syndrome, Mexico, 2016–2017

Victor M. Cardenas, Angel Jose Paternina-Caicedo, Ernesto Benito Salvatierra

To determine completeness of fatal congenital Zika syndrome reporting in Mexico, we examined data from the Mexican National Institute of Statistics and Geography. We found that an estimated 50% more infants died from microcephaly attributable to congenital Zika syndrome during 2016–2017 than were reported by the existing surveillance system.

Congenital Zika syndrome (CZS), described in Brazil in 2015, consists of a set of congenital malformations (saliently microcephaly) and an increased risk for stillbirth and early childhood death (*1*–*3*). Epidemiologic studies have demonstrated that Zika virus causes CZS (*4*) and that Zika virus–associated birth defects developed in ≈5% of fetuses and newborns of infected pregnant women (*3*,*5*–*7*).

Rates of reported CZS cases in the Americas vary widely. Most (79%) of the 3,720 confirmed cases of CZS reported in the Americas as of January 2018 were reported in Brazil (*8*). The higher reported rates in Brazil could result from the preexisting birth defects registration in Brazil, enhanced by the occurrence of embriopathy associated with use of thalidomide to treat leprosy (*9*). If the 5% prevalence of CZS among neonates of infected pregnant women found in population studies (*3*,*5*–*7*) were applied to the 7,113 pregnant women reported in Mexico as being Zika virus infected (*10*), one would expect ≈355 CZS cases, not the 51 reported as of November 2018 (*11*).

To improve the public health surveillance and research of CZS, we assessed the effects of the Zika virus epidemic on rates of infant death from microcephaly and estimated the completeness of reporting of fatal CZS cases in Mexico. This study was exempt from institutional review board oversight.

The Study

We accessed tabulated data on infant deaths and births available from the Mexican National Institute of Statistics and Geography for 1998–2017 (*12*,*13*). Using the International Classification of Diseases, 10th Revision, we selected records for infants whose underlying cause of death was coded as microcephaly (Q02X). We used the most recent published report of CZS available from the Mexico Ministry of Health Division of Epidemiology (*13*).

We estimated infant mortality rates by using the number of registered live births per year for the entire country (i.e., cause-specific infant death rates, expressed per 100,000 live births). Because the Zika virus epidemic in Mexico started in November 2015 (*14*), our exposure period of interest was 2016–2017. We identified the baseline period by using joinpoint trend analysis (*15*), a statistical method used to decompose temporal trends (annual percent change [APC]) into meaningful segments. We used the permutation test to identify the most parsimonious results (*15*). We then compared the baseline rate with that of the epidemic period by using the rate ratio and estimating its 95% CI. Infant deaths possibly resulting from the Zika virus epidemic were estimated by using the attributable risk and compared with the number of fatal CZS cases reported by the existing CZS surveillance system. We tested statistical significance by using normal approximation and set the threshold at $p = 0.05$.

From 1998 through 2017, a total of 467 infants died of microcephaly in Mexico (Table 1). Joinpoint regression identified an overall significant decrease of 6.80% APC (95% CI –11.9% to –1.4%) for 2007–2015 and a statistically significant increase of 27.25% APC for 2016–2017 (95% CI 3.0% to 57.2%) (Figure). On the basis of the results of the trend analysis and the documentation of the first Zika virus outbreak in Mexico during November 2015, we selected the period 2007–2015 as baseline (Table 2).

During the epidemic period (2016–2017), the rate of infant deaths from microcephaly was 1.17 deaths/100,000 live births; during the preceding 4 years (2007–2015), the rate was 0.80 deaths/100,000 live births. Thus, the rate ratio was 1.5 (95% CI 1.1–2.0). The attributable risk was 31.7%.

From January 1, 2016, through November 26, 2018, a total of 51 cases of CZS were reported in Mexico; of these, 11 deaths were reported during 2016–2017. Applying the attributable risk of 31.7% to the 53 reported infant deaths from microcephaly during 2016–2017, we estimated that ≈17 infant deaths from microcephaly were attributable to the Zika virus epidemic. Compared with the 11 reported

Author affiliations: University of Arkansas for Medical Sciences, Little Rock, Arkansas, USA (V.M. Cardenas); Universidad Nacional de Colombia, Bogota, Colombia (A.J. Paternina-Caicedo); Unidad San Cristóbal, Chiapas, Mexico (E.B. Salvatierra)

DOI: https://doi.org/10.3201/eid2508.190106

Table 1. Infant deaths from microcephaly and death rates per 100,000 live births, by year, Mexico, 1998–2018

Year	No. infant deaths from microcephaly*	Live births	Rate of infant deaths from microcephaly/100,000 live births
1998	26	2,668,428	0.97
1999	24	2,769,089	0.87
2000	21	2,798,339	0.75
2001	27	2,767,610	0.98
2002	23	2,699,084	0.85
2003	23	2,655,894	0.87
2004	27	2,625,056	1.03
2005	31	2,567,906	1.21
2006	29	2,505,939	1.16
2007	26	2,655,083	0.98
2008	22	2,636,110	0.83
2009	22	2,577,214	0.85
2010	21	2,643,908	0.79
2011	27	2,586,287	1.04
2012	17	2,498,880	0.68
2013	18	2,478,889	0.73
2014	13	2,463,420	0.53
2015	17	2,353,596	0.72
2016	26	2,293,708	1.13
2017	27	2,234,039	1.21

*International Classification of Diseases, 10th Revision, code Q02x.

fatal cases, this estimate resulted in a ratio of 1.5 (95% CI 0.9–2.4), indicating that 50% more infants died of microcephaly caused by CZS than were reported.

Conclusions

We found evidence that the Zika virus epidemic reversed the declining trend of infant deaths from microcephaly in Mexico and that the number of deaths from microcephaly associated with Zika virus was 50% higher than that reported by the existing CZS surveillance system. In addition, on the basis of the case-fatality rate of 22% for reported CZS, at least 79 cases of CZS would have occurred in 2016–2017. We also observed an increase in the rates of fetal deaths coded as caused by microcephaly in 2016–2017, but we focused our report on infant deaths because the CZS case definition includes only live births.

Our assessment is not without limitations. First, it was limited to fatal CZS and relies on International Classification of Diseases coding. Increased awareness prompted by the Zika epidemic is another potential source of error. Other sources of data such as morbidity (e.g., hospital discharge and other medical records) still need to be evaluated for changes in temporal trends of microcephaly and other manifestations of CZS, such as arthrogryposis, blindness, and deafness. In addition, the accuracy of microcephaly as the underlying cause of death is unknown; microcephaly could have been present among other conditions mentioned in death records but not selected as the underlying cause of death. We believe that death records are prone to underregistration, and yet we found a significant increase in deaths from CZS in the 2 years of the Zika epidemic in Mexico.

Several factors may lead to incomplete reporting of the Zika virus epidemic and CZS. Had primary infection with Zika virus during pregnancy not resulted in CZS, Zika virus would have gone mostly unnoticed, as do many other arboviral infections (e.g., dengue, chikungunya). For instance, the short duration of viremia (3–5 days) complicates confirmatory testing. Although obtaining and testing paired serum specimens would provide more certainty, doing so is logistically harder to achieve. Furthermore, the fact that CZS can occur as a result of Zika virus subclinical infection precludes suspicions and testing.

Reporting of communicable diseases in Mexico, as in other countries, is far from complete. In 1981, we found 2 cases of poliomyelitis for every reported case, and in 1989, we found 1 recorded neonate death from tetanus for every 50 such deaths. However, a good surveillance system does not need to achieve complete reporting to be useful; rather, it should accurately depict the patterns of occurrence of the events or conditions of interest that can lead to their control, presuming existence of effective prevention and control methods.

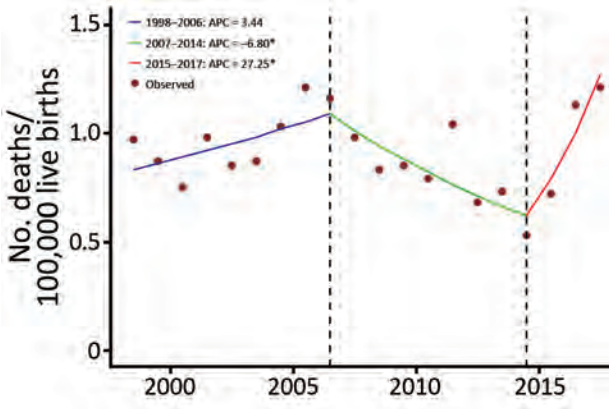

Figure. Infant deaths from microcephaly in Mexico, 1998–2017. APC, annual percent change. *p<0.05.

Table 2. Infant deaths from microcephaly in Mexico during 2007–2015 and 2016–2017

Period	No. infant deaths from microcephaly*	No. live births	Rate of infant deaths from microcephaly/100,000 live births	Rate ratio (95% CI)
2016–2017	53	4,527,747	1.17	1.5 (1.1–2.0)
2007–2015	183	22,893,387	0.80	Referent

*International Classification of Diseases, 10th Revision, code Q02x.

To improve Zika virus and CZS surveillance in Mexico, resources could be more efficiently used. Zika-endemic areas could be targeted, using active surveillance to monitor the occurrence of microcephaly at birth and flagging neonates born with gestational age and gender-specific head circumference <2 SDs of the reference. The surveillance system could use sentinel sites selected according to the existing risk stratification strategies used for dengue, which could enable extrapolation of the data to the rest of the country. These data would be particularly helpful in *Aedes aegypti* mosquito surveillance and control, which represents an enormous public health challenge.

Acknowledgments

We thank Irma Cardenas for her critical review of the manuscript and Cuitláhuac Ruiz Matus for his enthusiastic support.

About the Author

Dr. Cardenas is an associate professor of epidemiology at the University of Arkansas for Medical Sciences. He is currently conducting research on the role of environmental factors such as Zika virus and electronic cigarettes on pregnancy outcomes.

References

1. Schuler-Faccini L, Ribeiro EM, Feitosa IM, Horovitz DD, Cavalcanti DP, Pessoa A, et al.; Brazilian Medical Genetics Society–Zika Embryopathy Task Force. Possible association between Zika virus infection and microcephaly—Brazil, 2015. MMWR Morb Mortal Wkly Rep. 2016;65:59–62. http://dx.doi.org/10.15585/mmwr.mm6503e2
2. Miranda-Filho DB, Martelli CM, Ximenes RA, Araújo TV, Rocha MA, Ramos RC, et al. Initial description of the presumed congenital Zika syndrome. Am J Public Health. 2016;106:598–600. http://dx.doi.org/10.2105/AJPH.2016.303115
3. Brasil P, Pereira JP Jr, Moreira ME, Ribeiro Nogueira RM, Damasceno L, Wakimoto M, et al. Zika virus infection in pregnant women in Rio de Janeiro. N Engl J Med. 2016;375:2321–34. http://dx.doi.org/10.1056/NEJMoa1602412
4. de Araújo TVB, Ximenes RAA, Miranda-Filho DB, Souza WV, Montarroyos UR, de Melo APL, et al.; investigators from the Microcephaly Epidemic Research Group; Brazilian Ministry of Health; Pan American Health Organization; Instituto de Medicina Integral Professor Fernando Figueira; State Health Department of Pernambuco. Association between microcephaly, Zika virus infection, and other risk factors in Brazil: final report of a case-control study. Lancet Infect Dis. 2018;18:328–36. http://dx.doi.org/10.1016/S1473-3099(17)30727-2
5. Shapiro-Mendoza CK, Rice ME, Galang RR, Fulton AC, VanMaldeghem K, Prado MV, et al.; Zika Pregnancy and Infant Registries Working Group. Pregnancy outcomes after maternal Zika virus infection during pregnancy—U.S. Territories, January 1, 2016–April 25, 2017. MMWR Morb Mortal Wkly Rep. 2017;66:615–21. http://dx.doi.org/10.15585/mmwr.mm6623e1
6. Honein MA, Dawson AL, Petersen EE, Jones AM, Lee EH, Yazdy MM, et al. Birth defects among fetuses and infants of US women with evidence of possible Zika virus infection during pregnancy. JAMA. 2017;317:59–68. http://dx.doi.org/10.1001/jama.2016.19006
7. Hoen B, Schaub B, Funk AL, Ardillon V, Boullard M, Cabié A, et al. Pregnancy outcomes after ZIKV infection in French territories in the Americas. N Engl J Med. 2018;378:985–94. http://dx.doi.org/10.1056/NEJMoa1709481
8. Pan American Health Organization. Zika cumulative cases [cited 2019 Jan 15]. https://www.paho.org/hq/index.php?option=com_content&view=article&id=12390:zika-cumulative-cases&Itemid=42090&lang=en
9. Castilla EE, Ashton-Prolla P, Barreda-Mejia E, Brunoni D, Cavalcanti DP, Correa-Neto J, et al. Thalidomide, a current teratogen in South America. Teratology. 1996;54:273–7. http://dx.doi.org/10.1002/(SICI)1096-9926(199612)54:6<273::AID-TERA1>3.0.CO;2-#
10. Dirección General de Epidemiología. Casos confirmados autóctonos de enfermedad por virus Zika en mujeres embarazadas, por entidad de infección, México 2015–2018 [cited 2019 Jan 3]. https://www.gob.mx/cms/uploads/attachment/file/424933/Cuadro_Casos_ZIKA_y_Emb_sem_51_2018.pdf
11. Instituto Nacional de Estadística y Geografía. Defunciones generals [cited 2019 Jan 3]. https://www.inegi.org.mx/sistemas/olap/proyectos/bd/continuas/mortalidad/mortalidadgeneral.asp?s=est&c=11144&proy=mortgral_mg
12. Instituto Nacional de Estadística y Geografía. Nacimientos [cited 2019 Jan 3]. https://www.inegi.org.mx/temas/natalidad/
13. Secretaría de Salud. Casos confirmados de síndrome congénito asociado a Zika, México 2016–2018 [cited 2019 Jan 3]. https://www.gob.mx/cms/uploads/attachment/file/415187/Cuadro_Sx_Cong_nito_asociado_a_Zika_26112018.pdf
14. Guerbois M, Fernandez-Salas I, Azar SR, Danis-Lozano R, Alpuche-Aranda CM, Leal G, et al. Outbreak of Zika virus infection, Chiapas State, Mexico, 2015, and first confirmed transmission by *Aedes aegypti* mosquitoes in the Americas. J Infect Dis. 2016;214:1349–56. http://dx.doi.org/10.1093/infdis/jiw302
15. Kim HJ, Fay MP, Feuer EJ, Midthune DN. Permutation tests for joinpoint regression with applications to cancer rates. Stat Med. 2000;19:335–51. http://dx.doi.org/10.1002/(SICI)1097-0258(20000215)19:3<335::AID-SIM336>3.0.CO;2-Z

Address for correspondence: Victor M. Cardenas, University of Arkansas for Medical Sciences, Department of Epidemiology, Fay W. Boozman College of Public Health, 4301 West Markham, #820, Little Rock, AR 72205, USA; email: vmcardenas@uams.edu

Evaluating Temperature Sensitivity of Vesicular Stomatitis Virus–Based Vaccines

Derek R. Stein, Patrycja Sroga, Bryce M. Warner, Yvon Deschambault, Guillaume Poliquin, David Safronetz

Use of the vesicular stomatitis virus (VSV)–based Ebola virus vaccine during outbreaks and the potential use of a similar VSV-based Lassa virus vaccine has raised questions about the vaccines' stability should the cold chain fail. We demonstrated that current cold chain conditions might tolerate significant variances without affecting efficacy.

Ebola virus (EBOV; family *Filoviridae*, genus *Ebolavirus*) and Lassa virus (LASV; family *Arenaviridae*, genus *Mammarenavirus*) are prominent etiologic agents of viral hemorrhagic fever diseases in humans that have variable but typically high death rates (*1*,*2*). At least 20 major EBOV outbreaks have occurred in sub-Saharan Africa, including 2 during 2018–2019. During 2013–2016, the largest documented EBOV outbreak caused ≈28,000 cases and ≈11,000 deaths in several countries in West Africa (*1*). In response to the extent of the outbreak, the development of experimental vaccines was accelerated, culminating in a ring vaccination trial of the live-attenuated vesicular stomatitis virus–based EBOV vaccine (VSVΔG/EBOVGPC) (*3*). Based on the success of the trial, a similar strategy is being used in the 2018–2019 outbreak in the Democratic Republic of the Congo; preliminary results from the World Health Organization have identified the vaccine as >97% effective (*4*).

LASV, a rodentborne virus, is endemic to most of West Africa. Annually, ≈300,000–500,000 LASV infections occur. Most are acquired after direct contact with infected rodents or their contaminated excreta or secreta (*5*). Several large LASV outbreaks have occurred, most recently in Nigeria. During 2015–2018, prolonged and severe Lassa fever outbreaks were documented across most of the country (*6*).

VSVΔG/EBOVGPC and a similar VSV-based LASV vaccine, VSVΔG/LASVGPC, are leading candidates to help reduce illnesses and death from EBOV and LASV infections (*7*). Under manufacturer recommendations, these products are intended to be maintained at –80°C. Given the often remote locations where EBOV and LASV emerge, concern exists about maintaining such a rigorous cold chain to deliver the vaccines to areas where they are most needed. We evaluated the temperature sensitivity of VSVΔG/EBOVGPC and VSVΔG/LASVGPC in vitro and their ability to provide protection against lethal LASV infection.

Author affiliations: Public Health Agency of Canada, Winnipeg, Manitoba, Canada (D.R. Stein, Y. Deschambault, G. Poliquin, D. Safronetz); University of Manitoba, Winnipeg (P. Sroga, B.M. Warner, G. Poliquin, D. Safronetz)

DOI: https://doi.org/10.3201/eid2508.190281

The Study

To evaluate the effects of prolonged and multiple breaks in the cold chain on titer and protective efficacy of VSVΔG/EBOVGPC and VSVΔG/LASVGPC, we thawed cryopreserved stock vials of experimental-grade VSVΔG/EBOVGPC and VSVΔG/LASVGPC and maintained them for 7 d at 4°C, room temperature (≈21°C), or 32°C. In addition, we freeze–thawed (–80°C to room temperature) a vial of each stock 3 times over 7 days (3× freeze–thaw group). After incubation, we diluted the test vaccines according to the original stock titer and vaccinated groups of 9 outbred female Hartley guinea pigs (350–400 g) by the intraperitoneal route. A control group (9 animals per vaccine) comprising vaccination with 1×10^6 PFU of stock unmanipulated VSVΔG/EBOVGPC or VSVΔG/LASVGPC was included with each condition. A mock vaccination control group (9 animals per vaccine) received the equivalent dose of an irrelevant VSV-based Andes virus vaccine (VSVΔG/ANDVGPC). For each group of vaccinated animals, we randomly selected 6 for monitoring survival and 3 for timed necropsy and analysis when control animals demonstrated advanced signs of disease. All animal work was approved by the Canadian Science Centre for Human and Animal Health's Institutional Animal Care and Use Committee and was conducted according the guidelines of the Canadian Council on Animal Care. All work with infectious materials was conducted in the National Microbiology Laboratory's Biosafety Level 4 laboratory. After vaccination, the test and control vaccines were titered on Vero E6 cells using 10-fold serial dilutions and standard plaque assay methods.

Twenty-eight days after vaccination, we challenged the guinea pigs with 1,000 times the median lethal dose (LD_{50}; equivalent to 22 PFU) of guinea pig–adapted (GPA)

Table. Comparison of in vitro titers after 7 days of suboptimal storage of vesicular stomatitis–based vaccines*

Vaccine	Condition	Actual dose, PFU	Fold change	% Survival
VSVΔG/EBOVGPC	Stock vaccine	4.69×10^6	†	100
	3× freeze–thaw	1.97×10^6	2.38	100
	4°C for 7 d	4.28×10^6	1.10	100
	Room temperature for 7 d	9.11×10^5	5.15	100
	32°C for 7 d	2.31×10^4	203.00	100
VSVΔG/LASVGPC	Stock vaccine	1.29×10^6	†	83
	3× freeze–thaw	7.43×10^5	1.74	100
	4°C for 7 d	1.05×10^6	1.23	83
	Room temperature for 7 d	2.86×10^5	4.51	83
	32°C for 7 d	3.75×10^4	34.40	66

*VSVΔG/EBOVGPC, vesicular stomatitis virus–based Ebola virus vaccine; VSVΔG/LASVGPC, vesicular stomatitis virus–based Lassa virus vaccine. †Stock vaccine was not subject to any treatments and thus had no -fold change. The fold change for all other treatment groups was calculated on the basis of the original dose of stock vaccine.

EBOV, or 10 × LD_{50} (equivalent to 1×10^4 50% tissue culture infectious dose [$TCID_{50}$]) of GPA-LASV. After challenge, we monitored animals daily, recording body weights and monitoring temperatures using previously implanted IPTT-300 temperature transponders using a DAS 6002 hand-held scanner (Bio Medic Data Systems, https://www.bmds.com).

The in vitro titer resulting from vaccination with VSVΔG/EBOVGPC was relatively stable across all conditions; only the 32°C test group showed a significant decrease (Table). This finding did not affect vaccine-derived protection from a GPA-EBOV challenge; we observed 100% survival across all conditions (Figure 1, panel A). After challenge, all vaccinated animals demonstrated no weight loss or increased body temperature (Figure 1, panels B, C). In contrast, sham-vaccinated animals (VSVΔG/ANDVGPC) demonstrated increased temperatures and decreases in body weights before reaching the study humane endpoints. Once the control animals achieved the humane endpoint, 3 animals per test group were euthanized to compare viremia and tissue titers. Vaccinated animals demonstrated significantly lower, and in many cases no, detectable infectious EBOV in tissue and blood samples (Figure 1, panel D).

VSVΔG/LASVGPC was similarly stable across all experimental groups but to a lesser degree in the 32°C group than in VSVΔG/EBOVGPC (Table). Despite the relative stability, deaths occurred in most groups, including the positive control vaccinated animals (Figure 2, panel A). The exception was in the 3× freeze–thaw group, which maintained 100% survival. Consistent with these findings, we noted weight loss and increased body temperatures in all but the 3× freeze–thaw groups (Figure 2, panels B, C). Sham-vaccinated animals progressed as previously described after challenge, and infection was uniformly lethal within 18 days after challenge. Similarly, we noted infectious virus at varying levels in some or all samples tested in all groups (Figure 2, panel D).

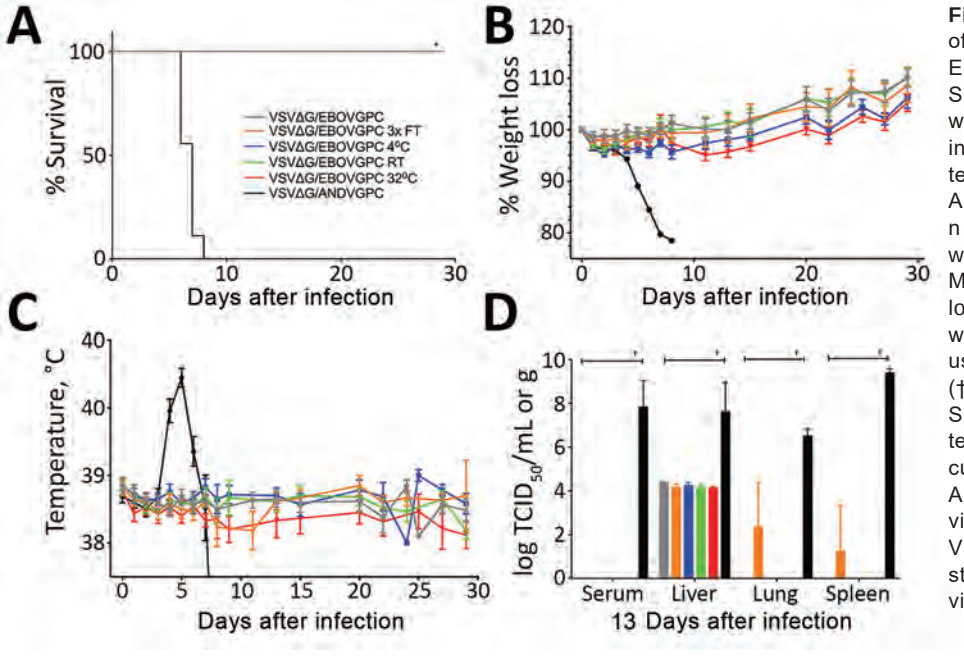

Figure 1. Evaluation of the effects of suboptimal storage of VSVΔG/EBOVGPC in guinea pigs. A) Survival rates. B) Percentage weight loss. Values >100% indicate weight gain. C) Body temperatures. D) Viral titers. In A, B, and C, n = 6 animals; in D, n = 3 animals. Survival analysis was conducted using a log-rank Mantel-Cox test (*p<0.0001). Viral loads in tissues were compared with VSVΔG/ANDVGPC controls using a 2-way analysis of variance (†p<0.0001). Error bars indicate SEM. FT, freeze–thaw; RT, room temperature; $TCID_{50}$, 50% tissue culture infectious dose; VSVΔG/ANDVGPC, vesicular stomatitis virus–based Andes virus vaccine; VSVΔG/EBOVGPC, vesicular stomatitis virus–based Ebola virus vaccine.

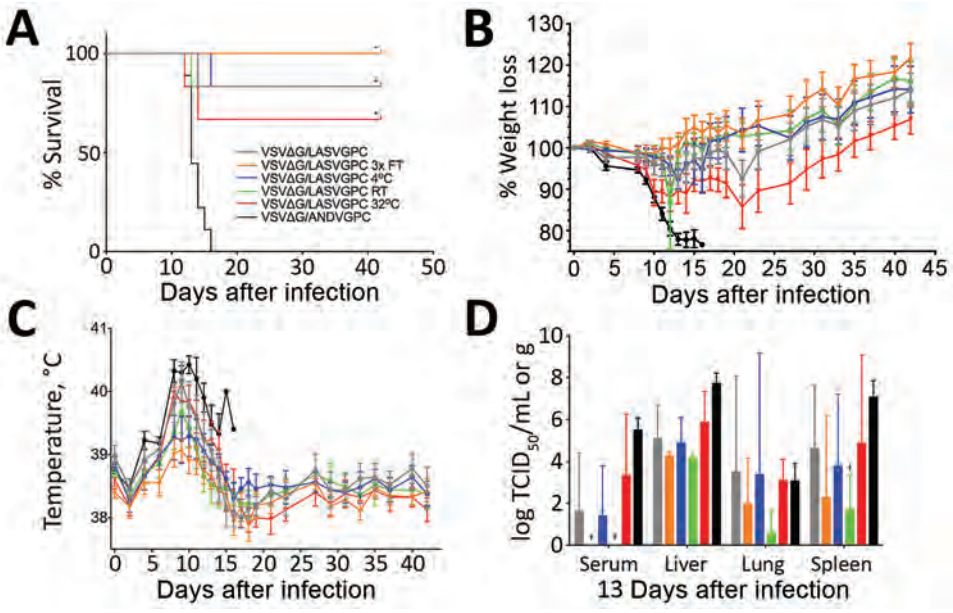

Figure 2. Evaluation of the effects of suboptimal storage of VSVΔG/LASVGPC in guinea pigs. A) Survival rates. B) Percentage weight loss. Values >100% indicate weight gain. C) Body temperatures. D) Viral titers. For A, B, and C, n = 6; for D, n = 3. Survival analysis was conducted using a log-rank Mantel-Cox test. Viral loads in tissues were compared with VSVΔG/ANDVGPC controls using a 2-way analysis of variance. *p<0.0001; †p = 0.002. Error bars indicate SEM. FT, freeze–thaw; RT, room temperature; $TCID_{50}$, 50% tissue culture infectious dose; VSVΔG/ANDVGPC, vesicular stomatitis virus–based Andes virus vaccine; VSVΔG/LASVGPC, vesicular stomatitis virus–based Lassa virus vaccine.

Conclusions

VSVΔG/EBOVGPC was surprisingly durable despite 7 days of suboptimal storage with no obvious clinical signs of disease and no deaths among animals across the treatment groups. We detected low-level viral titers in liver samples collected when the control animals were experiencing terminal disease. The 3× freeze–thaw condition resulted in detectable virus in both lung and spleen, although 100% of animals still survived. Curiously, VSVΔG/LASVGPC demonstrated improved performance under the same condition; however, a small sample size precludes any definitive conclusion.

The other temperature conditions had little effect on VSVΔG/LASVGPC in vitro titers. However, in most animals we noted clinical signs of disease, including lethargy, inappetence, moderate to severe increases in body temperature, and mild to moderate decreases in body weight. Consistent with these findings, experimental animals sampled when control animals were perimortem had infectious viral titers that were not significantly different from those of the control animals. Nevertheless, statistically significant increases in survival rates occurred in all experimental groups. Although 32°C proved more deleterious than other temperature conditions, the efficacy was similar to the control vaccination group. The GPA-LASV model is relatively new and has been adapted for maximum lethality in Hartley guinea pigs. VSVΔG/LASVGPC has proved to be extremely effective in both nonhuman primates and strain 13 guinea pigs when tested against several genetically and geographically distinct wild-type LASVs (*8*). This slight reduction in efficacy has been noted previously and might speak to the aggressiveness of the outbred guinea pig Lassa fever model (*9*). Follow-up studies in the inbred strain 13 guinea pig model, which is better characterized, could be considered (*10*).

Every effort needs to be made to ensure optimal storage and dosages of medical countermeasures to treat and prevent human disease. However, in remote and often tropical areas, maintaining these standards can be challenging, particularly if, in addition to climatic conditions, civil conflict is ongoing. Vaccine shortages are problematic, particularly during outbreaks, as demonstrated by the recent yellow fever vaccine shortage (*11*). Enhanced knowledge of vaccine stability under suboptimal storage conditions can help mitigate shortage issues by ensuring breaks in the cold chain do not necessarily translate into unusable vaccine lots. Our data demonstrate that the current –80°C cold chain condition might tolerate significant variances without affecting efficacy, at least in animals.

Acknowledgments

We thank the National Microbiology Laboratory's veterinary technical services for animal care and clinical support.

This work was funded by the Public Health Agency of Canada.

About the Author

Dr. Stein is a senior research fellow working at the Public Health Agency of Canada. His research involves the rapid development of vaccine and therapeutic antibody modalities for emerging pathogens. His research also involves the characterization of animal models of pathogenesis and transmission for high containment pathogens.

References

1. Holmes EC, Dudas G, Rambaut A, Andersen KG. The evolution of Ebola virus: insights from the 2013–2016 epidemic. Nature. 2016;538:193–200. http://dx.doi.org/10.1038/nature19790
2. Frame JD, Baldwin JM Jr, Gocke DJ, Troup JM. Lassa fever, a new virus disease of man from West Africa. I. Clinical description and pathological findings. Am J Trop Med Hyg. 1970;19:670–6. http://dx.doi.org/10.4269/ajtmh.1970.19.670
3. Henao-Restrepo AM, Longini IM, Egger M, Dean NE, Edmunds WJ, Camacho A, et al. Efficacy and effectiveness of an rVSV-vectored vaccine expressing Ebola surface glycoprotein: interim results from the Guinea ring vaccination cluster-randomised trial. Lancet. 2015;386:857–66. http://dx.doi.org/10.1016/S0140-6736(15)61117-5
4. World Health Organization. Preliminary results on the efficacy of rVSV-ZEBOV-GP Ebola vaccine using the ring vaccination strategy in the control of an Ebola outbreak in the Democratic Republic of the Congo: an example of integration of research into epidemic response. Geneva: The Organization; 2019.
5. Monath TP, Newhouse VF, Kemp GE, Setzer HW, Cacciapuoti A. Lassa virus isolation from *Mastomys natalensis* rodents during an epidemic in Sierra Leone. Science. 1974;185:263–5. http://dx.doi.org/10.1126/science.185.4147.263
6. Roberts L. Nigeria hit by unprecedented Lassa fever outbreak. Science. 2018;359:1201–2. http://dx.doi.org/10.1126/science.359.6381.1201
7. Warner BM, Safronetz D, Stein DR. Current research for a vaccine against Lassa hemorrhagic fever virus. Drug Des Devel Ther. 2018;12:2519–27. http://dx.doi.org/10.2147/DDDT.S147276
8. Safronetz D, Mire C, Rosenke K, Feldmann F, Haddock E, Geisbert T, et al. A recombinant vesicular stomatitis virus-based Lassa fever vaccine protects guinea pigs and macaques against challenge with geographically and genetically distinct Lassa viruses. PLoS Negl Trop Dis. 2015;9:e0003736. http://dx.doi.org/10.1371/journal.pntd.0003736
9. Stein DR, Warner BM, Soule G, Tierney K, Frost KL, Booth S, et al. A recombinant vesicular stomatitis-based Lassa fever vaccine elicits rapid and long-term protection from lethal Lassa virus infection in guinea pigs. NPJ Vaccines. 2019;4:8. http://dx.doi.org/10.1038/s41541-019-0104-x
10. Safronetz D, Strong JE, Feldmann F, Haddock E, Sogoba N, Brining D, et al. A recently isolated Lassa virus from Mali demonstrates atypical clinical disease manifestations and decreased virulence in cynomolgus macaques. J Infect Dis. 2013;207:1316–27. http://dx.doi.org/10.1093/infdis/jit004
11. Wu JT, Peak CM, Leung GM, Lipsitch M. Fractional dosing of yellow fever vaccine to extend supply: a modelling study. Lancet. 2016;388:2904–11. http://dx.doi.org/10.1016/S0140-6736(16)31838-4

Address for correspondence: David Safronetz, National Microbiology Laboratory, Public Health Agency of Canada, Zoonotic Diseases and Special Pathogens, 1015 Arlington St, Winnipeg, MB R3E 3R2, Canada; email: david.safronetz@canada.ca

Wild-Type Yellow Fever Virus RNA in Cerebrospinal Fluid of Child

Paula E.S. Marinho,[1] Pedro P.M. Alvarenga,[1] Ana P.C. Crispim, Talitah M.S. Candiani, Alice M. Alvarenga, Isabela M. Bechler, Pedro A. Alves, Fabio P. Dornas, Danilo B. de Oliveira, Aline A. Bentes, Paulo P. Christo, Erna G. Kroon

We report a 3-year-old child who was hospitalized because of severe manifestations of the central nervous system. The child died after 6 days of hospitalization. Analysis of postmortem cerebrospinal fluid showed the presence of yellow fever virus RNA. Nucleotide sequencing confirmed that the virus was wild-type yellow fever virus.

Yellow fever virus (family *Flaviviridae*, genus *Flavivirus*) is spread by bites of infected mosquitoes of the genera *Aedes*, *Haemagogus*, and *Sabethes* (*1*). During 2017, an epidemic of yellow fever in Brazil resulted in 1,266 confirmed human cases and 415 deaths; 532 confirmed cases and 181 deaths occurred in Minas Gerais State (*2*). We report wild-type yellow fever virus RNA in the cerebrospinal fluid of a child who died during this outbreak.

The Study

In May 2017, a 3-year-old girl born on February 13, 2014, and who lived in Belo Horizonte, Minas Gerais, Brazil, was hospitalized because of influenza-like signs and symptoms that started 2 days earlier. Signs and symptoms included nasal congestion and discharge, sneezing, and fever. The medical history included no seizures or epilepsy, family history of neurologic diseases, or allergies. Immunizations for the patient were current and included 1 dose of yellow fever vaccine (vaccine lot 136VFA022Z, expiration date June 30, 2015), given at 10 months of age on December 18, 2014, following the vaccination schedule of the Ministry of Health of Brazil.

During hospitalization, the patient showed a loss of consciousness and several episodes of seizures. She was given intravenous midazolam and phenobarbital for status epilepticus. During one of the seizures, the patient had cardiac arrest; she was given cardiac resuscitation for 12 min and transferred to an intensive care unit because of hemodynamic instability. Only brain stem reflexes were detected. Ceftriaxone and acyclovir were given as empiric treatment for possible meningoencephalitis. No lumbar puncture or computed tomography of the brain were performed because the patient was clinically unstable.

On day 1 after admission, we performed liver biochemical function tests. These tests showed the following levels: alanine aminotransferase 67 U/L, aspartate aminotransferase 109 U/L, direct bilirubin 0.49 mg/dL, indirect bilirubin 0.34 mg/dL, alkaline phosphatase 125 U/L, γ-glutamyl transpeptidase 26 U/L, and albumin 2.1 mg/dL.

On day 2 of hospitalization, the patient still had a severe hemodynamically unstable condition that required constant adjustments in amine doses (noraderenalin 2 μg/kg/min and dobutamin 8 μg/kg/min), but she showed spontaneous opening of the eyes and nonspecific thoracic movements. No major metabolic or hydroelectrolytic disturbances were detected in the time since her hospitalization. No signs of hemorrhage and hemostatic disorders were detected.

Despite the therapeutic measures, on the third day of hospitalization, the child showed a severe worsening of her condition, which included fixed mydriasis, absence of corneopalpebral and oculocephalic reflexes, and no reflex of coughing during aspiration of the orotracheal tube. The Glasgow Coma Scale score was 3. The child had deep hypotonia and areflexia and no clonus during her examination. Funduscopic examination showed bilateral papilledema. Congruent with these findings, computed tomography of the brain showed diffuse cerebral edema with erasure of basement cisterns and imminent signs of herniation.

Even after institution of neuroprotection measures (3% saline solution and mannitol), the patient showed a worsening of her condition, which included multiple organ dysfunction, refractory shock to the use of vasoactive drugs, diabetes

Author affiliations: Universidade Federal de Minas Gerais, Belo Horizonte, Brazil (P.E.S. Marinho, A.P.C. Crispim, A.A. Bentes, E.G. Kroon); Hospital Infantil João Paulo II, Belo Horizonte (P.P.M. Alvarenga, T.M.S. Candiani, A.M. Alvarenga, I.M. Bechler, A.A. Bentes); Instituto René Rachou, Belo Horizonte (P.A. Alves); Universidade Federal dos Vales do Jequitinhonha e Mucuri, Diamantina, Brazil (F.P. Dornas, D.B. de Oliveira); Instituto de Ensino e Pesquisa Santa Casa de Belo Horizonte, Belo Horizonte (P.P. Christo)

DOI: https://doi.org/10.3201/eid2508/181479

[1]These authors contributed equally to this article.

insipidus, and deterioration of glycemic control. The patient died 6 days after her hospitalization. After obtaining permission of her parents, we collected a postmortem CSF sample immediately after her death (Figure 1, panel A).

Postmortem CSF biochemical analyses showed glucose 117 mg/dL, protein 434 mg/dL, lactate 6.8 mmol/L, and leukocyte count 18 cells/mm^3 (61% lymphocytes, 4% neutrophils, and 24% monocytes). We tested the CSF by using a quantitative PCR for DNA and RNA viruses commonly associated with central nervous system (CNS) infections, such as herpesvirus, enteroviruses, flaviviruses (dengue virus, Zika virus, St. Louis encephalitis virus, West Nile virus, and yellow fever virus), and chikungunya virus. The CSF showed negative results for other potential neurotropic viruses and meningococcus, *Haemophilus* spp., and pneumococcus when tested by a reference laboratory in Minas Gerais. However, the CSF was positive for yellow fever virus RNA according to the protocol reported by Domingo et al. (*3*). Results were negative for the other virus tested by a quantitative PCR. We performed a quantitative PCR specific for flavivirus nonstructural protein 5 gene (*4*) and obtained a DNA fragment that we used directly for nucleotide sequencing.

We aligned the sequence and used it to construct a phylogenetic tree by using the maximum-likelihood method (Figure 1, panel B). Phylogenetic analysis showed that sequence grouped with other wild-type yellow fever virus sequences from Brazil in a clade separate from vaccine virus samples, and the alignment confirmed a sequence difference of 25 nt (Figure 2). We performed a plaque reduction neutralization test with CSF and obtained a negative result.

Conclusions

We detected wild-type yellow fever virus RNA by reverse transcription PCR in the CSF of a previously healthy child who died during a yellow fever outbreak in Brazil. Virus RNA was detected 2 days after manifestation of mild influenza-like signs and symptoms, sensory impairment, and recurrent epileptic seizures. We detected no hemorrhagic,

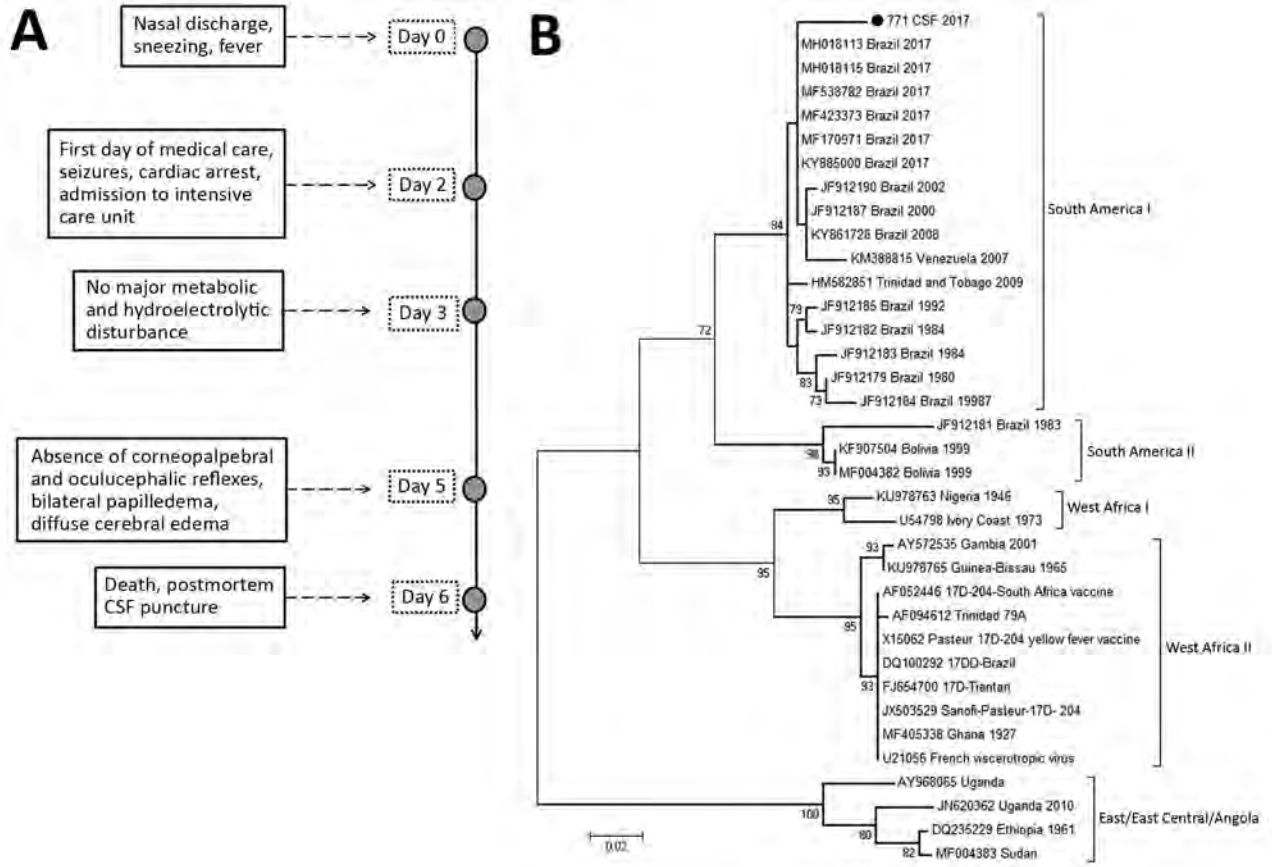

Figure 1. Illness timeline and phylogenetic testing in case of child with wild-type yellow fever virus RNA in CSF, Brazil, 2017. A) Timeline of symptoms, ambulatory procedures, and laboratory results. B) Phylogenetic tree of yellow fever viruses. The tree was constructed by using the maximum-likelihood method and the Tamura-Nei model in MEGA 7.0 software (https://www.megasoftware.net). Numbers to the left of nodes are bootstrap values (1,000 replicates). Sequences were compared with sequences in GenBank; black dot indicates sequence isolated in this study. This sequence was deposited in GenBank (accession no. 771_2017_CSF_NS5 MK450540). Scale bar indicates nucleotide substitutions per site. CSF, cerebrospinal fluid.

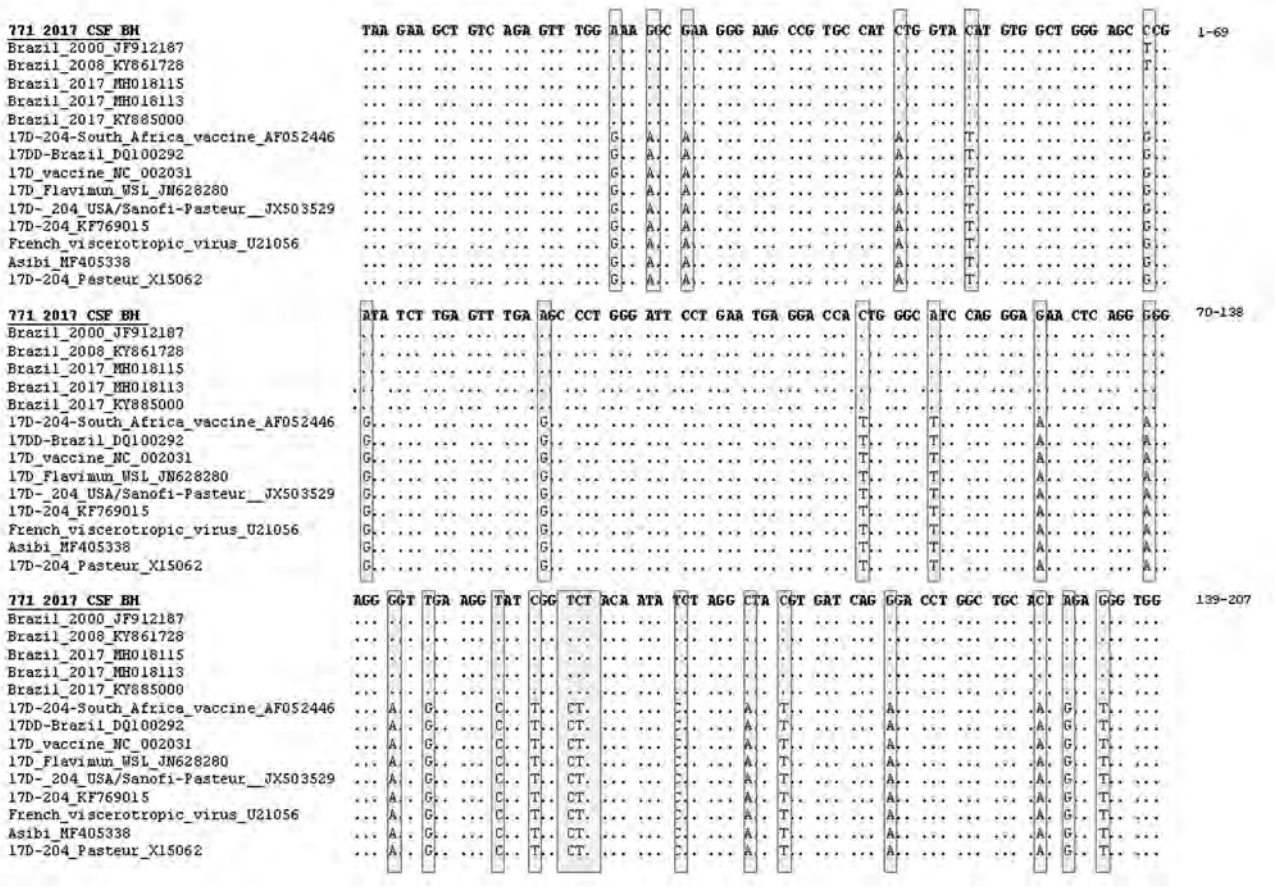

Figure 2. Alignment of a fragment of yellow fever virus 771_2017_CSF_ NS5 sequence (207 bp) from child with wild-type yellow fever virus in CSF, Brazil, 2017, with other yellow fever virus sequences. Sequences were obtained from GenBank and aligned by using standard parameters of ClustalW (http://www.clustal.org). Shaded boxes indicate major variations among wild-type virus sequences and vaccine virus sequences. Dots indicate sequence identity. BH, Belo Horizonte; CSF, cerebrospinal fluid.

metabolic, or hydroelectrolytic changes in this patient, and test results for other pathogens, such as bacteria and neurotropic viruses, were negative.

Neurologic involvement in wild-type yellow fever virus infection was described in a study conducted in Nigeria during a 1969 epidemic in which 103 patients were given a diagnosis of yellow fever, including 14 children and adolescents ≤19 years of age (*5*). In that study, signs and symptoms of CNS involvement were reported in 26 (25%) patients, 8 of whom had generalized seizures. CNS involvement was also reported in Nigeria during 1990 (*6*), and altered mental state was described in >61% of the patients in a yellow fever outbreak in Uganda during 2016 (*7*).

In a study in Darfur, Sudan, during a 2012 yellow fever epidemic, 844 cases of suspected yellow fever were reported (*8*). Children ≤15 years of age accounted for 21.4% of these case-patients, and 15.6% of them had seizures. In the same study, ≈8% of case-patients were reported to have been vaccinated, suggesting that the immunity caused by the vaccine might be affected by other factors that influence the effectiveness and duration of the vaccine (*8*).

Meningoencephalitis caused by yellow fever virus vaccine–associated neurotropic disease has been frequently reported in infants and adults (*1*,*9*,*10*). However, in our case report, the child had received 1 dose of 17D yellow fever vaccine at 10 months of age, which was 29 months before onset of signs and symptoms of encephalitis. The reported seroconversion rate of the 17D vaccine in this age group is only 72% (*11*). It is possible that this child was within the small percentage of vaccine failures because she had no history of previous hospitalizations or concurrent conditions that indicated immunosuppression.

Our patient had no classical signs or symptoms of yellow fever. Neurologic manifestations after infections with other flaviviruses are also often not accompanied by classic signs or symptoms of infection (*12*,*13*). Because signs and symptoms of encephalitis preceded cardiac arrest in our patient, it is unlikely that the virus infection occurred because of hemodynamic instability and cardiac arrest, which might

increase the permeability of the blood–brain barrier and enable passage of the virus into the CNS. Despite scarce description of neurologic diseases in humans caused by wild-type yellow fever virus, a study with animal models confirmed that yellow fever virus is neurotropic and leads to fatal encephalitis (*14*).

The nucleotide sequence of the virus from the patient in our study was also identical to that of the virus that circulated during an outbreak of yellow fever in Belo Horizonte, Brazil (*15*). Although yellow fever encephalitis is rare, it was the primary neurologic manifestation in our patient.

Acknowledgments

We thank our colleagues at the Laboratório de Vírus, Universidade Federal de Minas Gerais, for providing excellent technical support.

The study was supported by the Conselho Nacional de Desenvolvimento Científico e Tecnológico, the Departamento de Ciência e Tecnologia do Ministério da Saúde do Brasil, the Coordenação de Aperfeiçoamento de Pessoal de Nível Superior (finance code 001), and Fundação de Amparo à Pesquisa do Estado de Minas Gerais. E.G.K. is a fellow of Conselho Nacional de Desenvolvimento Científico e Tecnológico and Fundação de Amparo à Pesquisa do Estado de Minas Gerais.

About the Author

Ms. Marinho is a PhD student at the Laboratório de Vírus, Departamento de Microbiologia, Instituto de Ciências Biológicas, Universidade Federal de Minas Gerais, Belo Horizonte, Brazil. Her primary research interest is detection of flavivirus in CSF.

References

1. Barnett ED. Yellow fever: epidemiology and prevention. Clin Infect Dis. 2007;44:850–6. http://dx.doi.org/10.1086/511869
2. Secretariat of Health Surveillance, Ministry of Health. Monitoring the seasonal period of yellow fever, Brazil, 2017/2018. Report no. 26, 2017/2018 [in Portuguese] [cited 2019 Apr 27]. http://portalarquivos2.saude.gov.br/images/pdf/2018/maio/18/Informe-FA-26.pdf
3. Domingo C, Patel P, Yillah J, Weidmann M, Méndez JA, Nakouné ER, et al. Advanced yellow fever virus genome detection in point-of-care facilities and reference laboratories. J Clin Microbiol. 2012;50:4054–60. http://dx.doi.org/10.1128/JCM.01799-12
4. Patel P, Landt O, Kaiser M, Faye O, Koppe T, Lass U, et al. Development of one-step quantitative reverse transcription PCR for the rapid detection of flaviviruses. Virol J. 2013;10:58. http://dx.doi.org/10.1186/1743-422X-10-58
5. Jones EM, Wilson DC. Clinical features of yellow fever cases at Vom Christian Hospital during the 1969 epidemic on the Jos Plateau, Nigeria. Bull World Health Organ. 1972;46:653–7.
6. Ekenna O, Chikwem JO, Mohammed I, Durojaiye SO. Epidemic yellow fever in Borno State of Nigeria: characterization of hospitalized patients. West Afr J Med. 2010;29:91–7.
7. Kwagonza L, Masiira B, Kyobe-Bosa H, Kadobera D, Atuheire EB, Lubwama B, et al. Outbreak of yellow fever in central and southwestern Uganda, February–May 2016. BMC Infect Dis. 2018;18:548. http://dx.doi.org/10.1186/s12879-018-3440-y
8. Alhakimi HA, Mohamed OG, Khogaly HS, Arafa KA, Ahmed WA. Epidemiological, clinical and entomological characteristics of yellow fever outbreak in Darfur 2012. AIMS Public Health. 2015;2:132–41. http://dx.doi.org/10.3934/publichealth.2015.1.132
9. Gerin M, Wroblewski I, Bost-Bru C, N'guyen MA, Debillon T. YEL-AND meningoencephalitis in a 4-year-old boy consecutive to a yellow-fever vaccine [in French]. Arch Pediatr. 2014;21:384–7. http://dx.doi.org/10.1016/j.arcped.2014.01.014
10. Fatal viral encephalitis following 17D yellow fever vaccine inoculation. Report of a case in a 3-year-old child. JAMA. 1966;198:671–2. http://dx.doi.org/10.1001/jama.1966.03110190153047
11. Collaborative group for studies on yellow fever vaccines. Duration of post-vaccination immunity against yellow fever in adults. Vaccine. 2014;32:4977–84. https://doi.org/10.1016/j.vaccine.2014.07.021
12. Horwood PF, Duong V, Laurent D, Mey C, Sothy H, Santy K, et al. Aetiology of acute meningoencephalitis in Cambodian children, 2010-2013. Emerg Microbes Infect. 2017;6:e35. https://doi.org/10.1038/emi.2017.15
13. de Oliveira DB, Candiani TM, Franco-Luiz AP, Almeida GMF, Abrahão JS, Rios M, et al. Etiological agents of viral meningitis in children from a dengue-endemic area, Southeast region of Brazil. J Neurol Sci. 2017;375:390–4. https://doi.org/10.1016/j.jns.2017.02.025
14. Mims CA. The invasion of the brain by yellow fever virus present in the blood of mice. Br J Exp Pathol. 1957;38:329–38.
15. Faria NR, Kraemer MU, Hill SC, Goes de Jesus J, Aguiar RS, Iani FC, et al. Genomic and epidemiological monitoring of yellow fever virus transmission potential. Science. 2018;361:894–9. https://doi.org/10.1126/science.aat7115

Address for correspondence: Erna G. Kroon, Laboratório de Vírus, Departamento de Microbiologia, Instituto de Ciências Biológicas, Universidade Federal de Minas Gerais, Av. Antônio Carlos 6627 Caixa Postal 486, 31270-901 Belo Horizonte, Minais Gerais, Brazil; email: ernagkroon@gmail.com

Artyfechinostomum sufrartyfex Trematode Infections in Children, Bihar, India

Yugal K. Prasad,[1] Suman Dahal,[1] Barsha Saikia, Bobita Bordoloi, Veena Tandon, Sudeep Ghatani

Eating raw or insufficiently cooked mollusks is a known risk factor for human echinostomiasis. We confirmed identification of *Artyfechinostomum sufrartyfex* trematodes as the causative agent of disease among 170 children in northern Bihar, India. We also identified the snail *Pila globosa* as a potential source of infections in the study area.

Foodborne intestinal trematodiasis, especially that caused by members of the family *Echinostomatidae*, is an emerging yet neglected public health disease. Approximately 24 echinostome species cause human echinostomiasis and are highly endemic to Southeast Asia and the Far East; major foci are located in China, India, Indonesia, South Korea, Malaysia, the Philippines, and Thailand (*1*).

Previously, only 2 deaths attributed to the echinostomid fluke *Artyfechinostomum sufrartyfex* were reported from the states of Assam and Tamil Nadu in India (*2*,*3*). During 2004–2017, several cases of echinostome infection were reported in children at Shri Shubh Lal Hospital and Research Centre in Bihar, India.

The Study

This study was approved by the Institutional Ethics Committee of Sikkim University (SU/IEC/2017/04), Gangtok, India. A total of 170 cases of *A. sufrartyfex* trematode infection occurred in northern Bihar, India, mostly in children ≤12 years of age. The children lived in the districts of Sitamarhi and Sheohar in the state of Bihar. Signs and symptoms were diarrhea (persistent/chronic and acute) with watery or mucus-bound stool, vomiting, loss of appetite, weakness, passage of red worms in stool or vomit, swelling of the feet and the entire body, fever, cough, breathlessness, night blindness, and urticarial rashes (Table 1).

Physical examination showed that most patients were anemic. Clinical laboratory investigations showed leukocytosis and eosinophilia. However, systemic examination showed no adverse effects of the cardiovascular, abdominal, and central nervous systems (Table 2). Levels of serum alanine aminotransferase, bilirubin, blood urea, creatinine, electrolytes, sodium, potassium, and chloride were within reference limits.

These children were immediately hospitalized and kept under careful observation with routine monitoring of stool and vomit for worms. Once worms were observed in samples, the patients were given praziquantel (75 mg/kg in 3 divided doses orally for 2 days) and monitored. At administration of the drug, patients started passing more worms in stool. We recovered >50 worms but ≤300 worms from each child patient. The infection subsided after the standard dose of praziquantel, and most patients recovered from the infection.

However, we observed 11 deaths: 2 patients each during 2004, 2007, 2008, 2012, and 2013 and 1 patient during 2009. Severe acute malnutrition with or without edema and large numbers of worms were major clinical conditions observed for these deaths. Nine children had persistent diarrhea with severe dehydration and shock, and 2 of them had acute diarrhea, severe dehydration, and shock.

The infected patients frequently consumed raw snails. The most prevalent snail species in the study areas was *Pila globosa*, which the children collected from the banks of ponds/ditches and waterlogged paddy fields grossly contaminated with human and animal excreta (168/170 cases, 99%). Therefore, we surveyed as many as 8 sites in 2 districts (Sitamarhi and Sheohar) for snail samples from their natural habitats (Figure 1).

We screened the snails by using a digestion technique with a 0.5% pepsin/0.1% HCl solution and found that the snails were heavily infected with metacercariae, which are the encysted infective stage of the trematode. The prevalence of metacercariae in the snails ranged from 16.12% in Hanumannagar to ≤48.19% in Punaura (Appendix, https://wwwnc.cdc.gov/EID/article/25/8/18-1427-App1.pdf).

To establish the source of infection, we attempted to identify the clinical parasite samples and the metacercariae. We morphologically identified representative parasite samples isolated from the patients (*2*,*4*,*5*). However, we could not identify metacercaria by only morphologic characteristics

Author affiliations: Shri Shubh Lal Hospital and Research Centre, Sitamarhi, India (Y.K. Prasad); Sikkim University, Gangtok, India (S. Dahal, B. Saikia, B. Bordoloi, S. Ghatani); Biotech Park, Lucknow, India (V. Tandon)

DOI: https://doi.org/10.3201/eid2508.181427

[1]These authors contributed equally to this article.

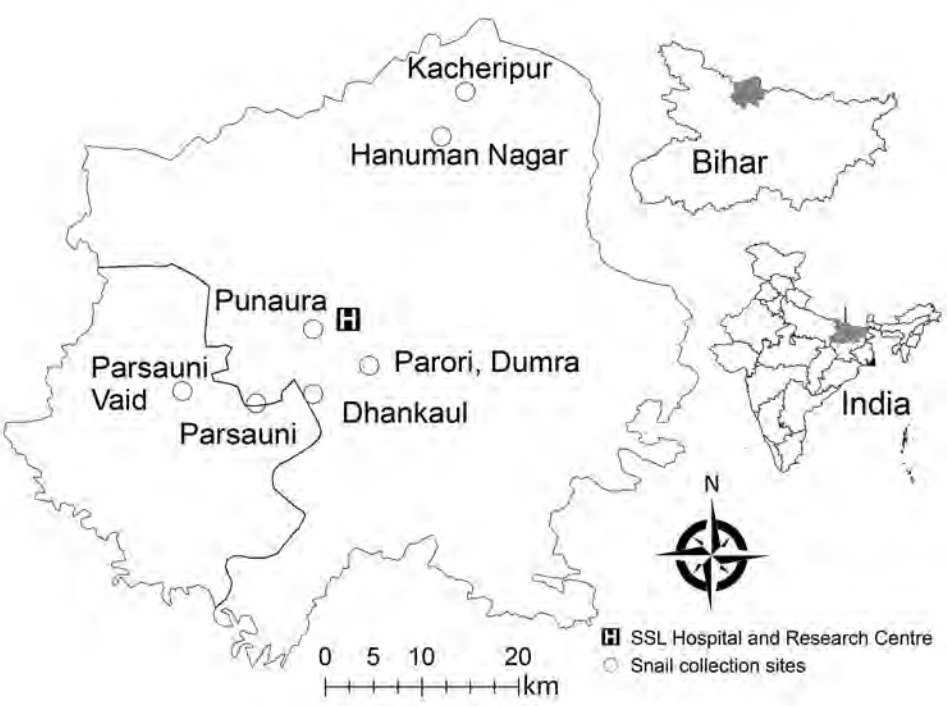

Figure 1. Collection sites of clinical samples from patients infected with *Artyfechinostomum sufrartyfex* trematodes at SSL Hospital and Research Center, Sitamarhi, Bihar, India. Black border indicates district boundary. Insets show location of Sitamarhi in Bihar and location of Bihar in India. SSL, Shri Shubh Lal.

(Figure 2). Therefore, we used a molecular approach to confirm the identity of the life cycle stages.

We isolated total genomic DNA from individual adult trematodes (*6*). For metacercariae, we isolated genomic DNA from ≈200 cysts/isolation by using a DNA Isolation Kit (Macherey-Nagel, https://www.mn-net.com) according to the manufacturer's protocol. We then amplified and sequenced nuclear 28S rRNA and internal transcribed spacer (ITS) 2 genes and the mitochondrial cytochrome c oxidase (COI) gene for both stages by using universal trematode primers (*7*–*9*). Individual gene regions tested were 1,042 bp for the 28S rRNA gene, 433 bp for ITS2 gene, and 343 bp for the mitochondrial COI gene. We deposited sequences in GenBank (accession nos. MH236132–3, MH237730–1, and MH253673–4).

For specific identification of the parasites, we performed a blastn search (https://blast.ncbi.nlm.nih.gov/Blast.cgi). The 28S rRNA and mitochondrial COI gene regions showed maximum sequence identity with GenBank accession no. KF781303.1 for *A. sufrartyfex* (99%) and accession no. NC037150.1 for *A. sufrartyfex* from Shillong, India (100%). For the ITS2 gene region, we observed maximum sequence identity with GenBank accession no. JF412727 *Echinostoma malayanum* from Khon Kaen, Thailand (99%), and with accession no. EF027100.1 *A. sufrartyfex* from Meghalaya, India (96%). On the basis of these findings, we concluded that clinical specimens and metacercariae isolated from *P. globosa* snails were the same species (*A. sufrartyfex*).

Furthermore, we generated barcode sequences by using trematode-specific primers (*10*) and deposited them in the BOLD database (BOLDSYSTEMS version, http://www.boldsystems.org). We obtained unique barcodes for both life cycle stages (identification no. BIN URI-BOLD:ADM2711). The barcode sequence had a length of 777 bp. To check for its specificity, we performed a similarity search across the BOLD database by using the BOLD Identification System. This search showed that our sequences were highly species specific; the closest match with other species was with *Nephrostomum limai* worms (83.24% identity).

Conclusions

Our findings conclusively establish that these children were infected with *A. sufrartyfex* trematodes. We identified the causal agent and its infective metacercarial stage as *A. sufrartyfex* trematodes by using morphologic and molecular approaches. For ease of accurate identification in the future, we also provide unique DNA barcodes for the species.

Overall, we detected 170 infected case-patients and 11 deaths from these infections. Because of lack of proper diagnostic tools available to medical practitioners in the affected parts, several other infection cases might have remained undefined. This trematode species poses a serious threat to public health in this part of India and, if not contained early, might spread to other and nonendemic areas of the region.

We also report the prevalence of trematode metacercariae in *P. globosa* snails from foci of infections in Bihar, thus implicating this snail species as the potential source of infection. At the same time, we found

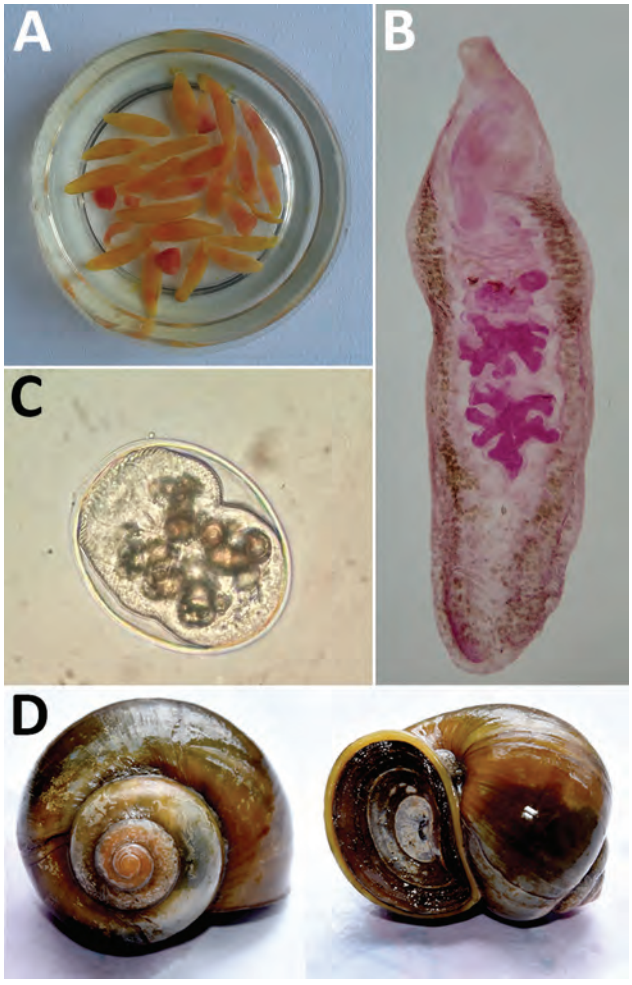

Figure 2. *Artyfechinostomum sufrartyfex* trematodes isolated from infected patients in Bihar, India. A) Trematodes in physiologic saline collected from stool samples. B) Whole mount of an adult trematode (acetocarmine stain). C) Metacercaria isolated from *Pila globosa* snails. Original magnification ×400. D*) Pila globosa* snails, the second intermediate host of the trematode.

metacercaria prevalence to be quite high, which is indicative of greater transmission risk to the inhabitants who are eating raw snails.

We found the DNA barcodes generated for life cycle stages to be unique in the entire BOLD database. Therefore, we expect these barcodes to act as references for easy and accurate diagnosis of the disease in the future.

We observed that some high-risk practices, such as open defecation in the infected areas, are still rampant, which is a cause of concern because this practice helps maintain the parasite cycle in the environment. However, a cleanliness program, such as the Swachh Bharat Mission started by the Government of India (http://sbm.gov.in/sbmreport/home.aspx), and installing toilets in every household in rural areas might immensely help to contain the parasite infection.

Acknowledgments

We thank the hospital staff at Shri Shubh Lal Hospital and Research Centre for providing help with sample collection and Sailendra Dewan for designing Figure 1.

This study was supported by the Science and Engineering Research Board, Department of Science and Technology, Government of India, through the Young Scientist Scheme (Sanction no. SB/YS/LS-195/2014 dated October 26, 2015) to S.G.

About the Authors

Dr. Prasad is director, consultant pediatrician, and neonatologist at Shri Shubh Lal Hospital and Research Centre, Sitamarhi, Bihar, India. His primary research interest is helminth parasite infections in children. Mr. Dahal is a PhD student in the Department of Zoology, School of Life Sciences, Sikkim University, Gangtok, Sikkim, India. His research interests include helminth parasitology and transcriptomic studies of human parasitic infections with a focus on identifying diagnostic markers and drug targets.

References

1. Toledo R, Esteban JG. An update on human echinostomiasis. Trans R Soc Trop Med Hyg. 2016;110:37–45. http://dx.doi.org/10.1093/trstmh/trv099
2. Lane C. *Artyfechinostomum sufrartyfex*. A new parasitic echinostome of man. J Med Res. 1915;2:977–83.
3. Reddy DG, Varmah K. *Paryphostomum sufrartyfex* (intestinal fluke) infection in man. Ind Med Gaz. 1950;85:546–7.
4. Skrjabin KI, Baschkirova EI. Trematodes of animals and man. Osnovy Trematodologii. 1956;12:53–930.
5. Kostadinova A. Family *Echinostomatidae*. In: Jones A, Bray RA, Gibson D, editors. Keys to the Trematoda. Vol. 2. Wallingford (UK): CABI Publishing and the Natural History Museum; 2005. p. 9–64.
6. Sambrook J, Russell DW. Purification of nucleic acids by extraction with phenol:chloroform. CSH Protoc. 2006;2006:pdb.prot4455. http://dx.doi.org/10.1101/pdb.prot4455
7. Tkach V, Pawlowski J, Mariaux J. Phylogenetic analysis of the suborder Plagiorchiata (Platyhelminthes, Digenea) based on partial lsrDNA sequences. Int J Parasitol. 2000;30:83–93. http://dx.doi.org/10.1016/S0020-7519(99)00163-0
8. Bowles J, Blair D, McManus DP. A molecular phylogeny of the human schistosomes. Mol Phylogenet Evol. 1995;4:103–9. http://dx.doi.org/10.1006/mpev.1995.1011
9. Blair D, Agatsuma T, Watanobe T, Okamoto M, Ito A. Geographical genetic structure within the human lung fluke, *Paragonimus westermani*, detected from DNA sequences. Parasitology. 1997;115:411–7. http://dx.doi.org/10.1017/S0031182097001534
10. Moszczynska A, Locke SA, McLaughlin JD, Marcogliese DJ, Crease TJ. Development of primers for the mitochondrial cytochrome c oxidase I gene in digenetic trematodes (Platyhelminthes) illustrates the challenge of barcoding parasitic helminths. Mol Ecol Resour. 2009;9(Suppl s1):75–82. http://dx.doi.org/10.1111/j.1755-0998.2009.02634.x

Address for correspondence: Sudeep Ghatani, Department of Zoology, School of Life Sciences, Sikkim University, Gangtok, Sikkim, India; email: sghatani@cus.ac.in

Efficacy of High-Dose Albendazole with Ivermectin for Treating Imported Loiasis, Italy

Federico Gobbi, Dora Buonfrate, Francesca Tamarozzi, Monica Degani, Andrea Angheben, Zeno Bisoffi

We describe the outcomes of 16 cases of imported loiasis in Italy. Patients had microfilaremia <20,000/mL and were treated with high-dose albendazole for 28 days and a single dose of ivermectin. This combination might be an effective treatment option in nonendemic areas, when diethylcarbamazine, the drug of choice, is not available.

Loa loa is a filarial nematode transmitted by tabanid flies of the genus *Chrysops*, which inhabits forested areas of West and Central Africa (*1*). It is estimated that >10 million people are infected with this parasite (*2*). Adult worms move under the skin or in the intermuscular fascia and can produce microfilariae. Loiasis can cause a wide range of symptoms, most frequently migrant edemas (Calabar swellings). Severe neurologic complications have also been reported (*2*). A retrospective study showed increased mortality rates in patients with high microfilaremia (*3*), indicating that this infection is not a benign condition, as previously thought.

Three drugs are currently used to treat loiasis: diethylcarbamazine, ivermectin, and albendazole (*4*). Diethylcarbamazine is preferred but is usually unavailable outside of specific World Health Organization mass drug administration programs. In addition, multiple courses of diethylcarbamazine are often required to achieve a clinical and parasitological cure (*5*), and the drug should not be used in patients with high microfilaremia levels because of the risk of encephalopathy (*4*). Trials in loiasis-endemic countries showed that short courses of albendazole had little effect on *L. loa* infection (*6*,*7*), but longer treatments (200 mg 2×/d for 21 d) resulted in decreased microfilaremia, blood eosinophil levels, and antifilarial antibodies (*8*). In 2018, a patient with high microfilaremia was reported to be clear of infection after four 21-day courses of albendazole at a dose of 400 mg daily, followed by a single 150 μg/kg dose of ivermectin (*9*). We describe the outcomes of 16 cases of imported loiasis in Italy with high-dose albendazole for 28 days and a single dose of ivermectin.

Author affiliations: IRCCS Sacro Cuore Don Calabria Hospital, Negrar di Valpolicella, Italy (F. Gobbi, D. Buonfrate, F. Tamarozzi, M. Degani, A. Angheben, Z. Bisoffi); ISS (Istituto Superiore Sanità), Rome, Italy (F. Tamarozzi); Università degli Studi di Verona, Verona, Italy (Z. Bisoffi)

DOI: https://doi.org/10.3201/eid2508.190011

The Study

The reference Ethics Committee (Comitato Etico per la Sperimentazione Clinica delle Province di Verona e Rovigo) approved this study in July 2016 (study protocol no. 33908). We reviewed the medical records of patients with loiasis admitted to IRCCS Sacro Cuore Don Calabria Hospital (Negrar di Valpolicella, Italy) during 1993–2016 who had been treated with albendazole (400 mg 2×/d for 28 days), followed by ivermectin (200 μg/kg, in single or multiple doses). For study purposes, we defined a case of loiasis by having previously stayed in an endemic country plus meeting ≥1 of 3 criteria: 1) eyeworm observed in the eye conjunctiva within the previous 2 months; 2) detection of *L. loa* microfilariae in the peripheral blood, determined by the leukoconcentration method (processing 13 mL of venous blood, with density assessed by examining Giemsa-stained thick smears, prepared with 100 μL of blood); or 3) Calabar swellings associated with eosinophilia (>500 eosinophils/μL) within the previous 2 months. In addition, only patients with ≥12 months of follow-up were included.

A total of 23 patients were considered eligible for inclusion. We excluded 7 of them because they had <12 months of follow-up. We included the remaining 16 patients (6 migrants and 10 expatriates) in the analysis (Table). Eleven patients had *L. loa* microfilariae in their blood; 5 had Calabar swellings and eosinophilia; none had an observed eyeworm. Of note, all 6 migrants had eosinophil counts of 500–1,500/μL, whereas all expatriates had eosinophil counts >1,500/μL, in line with previous observations (*10*).

A commercial ELISA test, based on *Acanthocheilonema vitae* as source of antigens (Bordier Affinity Products, http://www.bordier.ch), returned positive results for all patients. We also evaluated serologic results retrospectively for patients diagnosed before 2014. Liver function (alanine transaminase and aspartate transaminase levels) had been checked after ≈2 weeks from the onset of treatment with albendazole; no changes were observed in any patient. We recommended that blood tests be repeated every 2 months until patients were free of microfilaremia

Table 1. Clinical and laboratory characteristics of 16 patients with imported loiasis treated with albendazole and ivermectin, Italy, 1993–2016*

Pt no.	Age, y/sex	Status	Place of infection	Year of diagnosis	Calabar swelling	EOS/μL	Antifilarial antibodies, OD*	MFF/ mL	Co-infections	Other treatments	Follow-up period
1	64/M	E	CAR	2005	Yes	4,650	5.06	Neg	Giardiasis, strongyloidiasis	Tinidazole	12 y
2	28/F	E	Gabon	2008	Yes	3,300	4.79	Neg	None	None	10 y
3	56/M	E	Chad	2008	No	4,500	4.22	270	Amebiasis	Tinidazole, paromomycin	4 y
4	28/F	M	Angola	2010	No	790	None	263	None	None	14 mo
5	58/M	E	CAR	2010	Yes	9,320	1.74	Neg	None	None	8 y
6	52/M	E	Cameroon	2010	Yes	2,940	5.10	1	None	None	8 y
7	55/M	E	DRC	2011	Yes	2,040	5.21	9	None	None	7 y
8	49/M	E	Congo	2014	Yes	4,930	4.31	Neg	None	None	4 y
9	67/F	E	Nigeria	2014	Yes	13,100	4.05	Neg	Schistosomiasis, strongyloidiasis	Praziquantel	4 y
10	69/M	E	Cameroon	2015	Yes	1,620	2.19	152	None	None	3 y
11†	24/M	M	Nigeria	2015	No	1,300	2.16	160	Hookworm, latent tuberculosis	DEC	26 mo
12‡	27/M	M	Cameroon	2015	No	700	1.53	491	Hookworm, schistosomiasis	Praziquantel	26 mo
13	75/M	E	Cameroon	2015	Yes	4,100	2.85	Neg	None	None	18 mo
14	29/M	M	Cameroon	2016	No	590	2.85	990	Hookworm, schistosomiasis, HMS	Praziquantel, atovaquone/ proguanile	19 mo
15	22/M	M	Cameroon	2016	No	500	1.39	9,800	Schistosomiasis, *Mansonellosis perstans*, chronic HBV	Praziquantel, mebendazole	18 mo
16	18/M	M	Nigeria	2016	No	1,200	2.52	477	Hookworm	None	16 mo

*CAR, Central African Republic; DEC, diethylcarbamazine; DRC, Democratic Republic of the Congo; E, expatriate; EOS, eosinophils; HBV, hepatitis B virus; HMS, hyperreactive malarial splenomegaly; M, migrant; MFF, microfilariae; Neg, negative; OD, optical density; Pos, positive; Pt, patient.
*OD test is positive at ≥1 s.
†Patient with failure of albendazole and ivermectin treatment.
‡Received 1 additional course of ivermectin.

and that patients make annual follow-up visits for 4–5 years. However, these recommendations were seldom followed, and follow-up visits had to be tailored to each patient's characteristics and needs. One patient received a further course of ivermectin due to the persistence of low-level microfilaremia 4 months after treatment; testing at subsequent follow-up visits showed no microfilaremia. No severe adverse events were reported, although 2 patients reported itching.

Posttreatment follow-up periods ranged from 14 months to 12 years. Within 6 months after the end of the treatment, 15 (93.8%) of 16 patients had recovered completely, as demonstrated by disappearance of symptoms, normalization of eosinophil counts, and negative microfilaremia. The remaining patient reported presence of Calabar swelling and microfilaremia 1 month after treatment, so he received a single course of diethylcarbamazine, after which symptoms disappeared within 2 months.

Conclusions

Our retrospective study indicates that using the combination of albendazole and ivermectin resulted in a high rate of recovery (15/16, 93.8%) in patients with loiasis with microfilaremia <20,000/mL. By comparison, a study by Klion et al. found that only 38% of 32 patients treated with diethylcarbamazine were cured after 1 course of therapy, and some patients continued to be symptomatic despite >4 courses of treatment (*5*). Three of these symptomatic patients, unresponsive to diethylcarbamazine, were administered albendazole (200 mg 2×/d for 21 d) and then recovered (*8*). Moreover, Klion et al. performed a double-blind, placebo-controlled trial to assess the filaricidal activity and clinical safety of albendazole at the 200 mg dosage (*11*). Within 6 months, albendazole treatment reduced microfilaremia substantially, although not completely. After 6 months, microfilarial density was at 20% of pretreatment level in the albendazole treatment group compared with 84.8% in the

placebo group. Ivermectin has been administered alone only to substantially reduce microfilaremia levels, not as a cure, because macrofilaricidal action was not demonstrated (*12*,*13*). It was on the basis of these earlier reports, and because of the unavailability of diethylcarbamazine in Italy, that in 2004 we decided to treat our loiasis patients with a regimen of albendazole at a higher dosage (400 mg 2×/d) for a longer period (28 d), followed by a single dose of ivermectin (200 μg/kg) (*14*).

The main limitations of this study are the retrospective design and the low number of patients included. Moreover, only 1 patient had a microfilaremia level of ≈10,000/mL; however, this level was still lower than the threshold of 20,000/mL established by Kamgno et al. to avoid severe adverse events (*15*). Hence, in our patients, ivermectin could have been administered safely before albendazole. However, we cannot recommend this treatment schedule for patients with microfilaremia >20,000/mL.

Because data are scant, additional information about the treatment and outcome of loiasis imported into nonendemic countries is useful for clinicians. A previous study pointed out wide heterogeneity of treatment strategies for imported loiasis (*16*), highlighting the need for guidelines for treating loiasis in nonendemic areas, where there is no risk of reinfection.

In conclusion, a combination of high-dose albendazole (400 mg 2×/d for 28 d) plus a single 200 μg/kg dose of ivermectin might be recommended for loiasis patients with microfilaremia <20,000/mL as an alternative to diethylcarbamazine, which is the treatment of choice for loiasis but is often unavailable. In case of clinical cure (absence of symptoms) but persistence of low levels of microfilaremia, an option might be a second course of ivermectin to achieve clearance of microfilariae (*9*).

Funding for this work was provided by the Italian Ministry of Health “Fondi Ricerca Corrente - Linea 3, progetto 8” to IRCCS Sacro Cuore Don Calabria Hospital.

About the Author

Dr. Gobbi is a specialist in infectious diseases at the Centre for Tropical Diseases of Negrar, Verona, Italy. His main research interests focus on schistosomiasis, loiasis, mansonellosis, malaria, and arbovirosis surveillance.

References

1. Boussinesq M. Loiasis. Ann Trop Med Parasitol. 2006;100:715–31. http://dx.doi.org/10.1179/136485906X112194
2. Metzger WG, Mordmuller B. *Loa loa*—does it deserve to be neglected? Lancet Infect Dis. 2014;14:353–7.
3. Chesnais CB, Takougang I, Paguélé M, Pion SD, Boussinesq M. Excess mortality associated with loiasis: a retrospective population-based cohort study. Lancet Infect Dis. 2017;17:108–16. http://dx.doi.org/10.1016/S1473-3099(16)30405-4
4. Boussinesq M. Loiasis: new epidemiologic insights and proposed treatment strategy. J Travel Med. 2012;19:140–3. http://dx.doi.org/10.1111/j.1708-8305.2012.00605.x
5. Klion AD, Ottesen EA, Nutman TB. Effectiveness of diethylcarbamazine in treating loiasis acquired by expatriate visitors to endemic regions: long-term follow-up. J Infect Dis. 1994;169:604–10. http://dx.doi.org/10.1093/infdis/169.3.604
6. Kamgno J, Nguipdop-Djomo P, Gounoue R, Téjiokem M, Kuesel AC. Effect of two or six doses 800 mg of albendazole every two months on *Loa loa* microfilaraemia: a double blind, randomized, placebo-controlled trial. PLoS Negl Trop Dis. 2016;10:e0004492. http://dx.doi.org/10.1371/journal.pntd.0004492
7. Tabi TE, Befidi-Mengue R, Nutman TB, Horton J, Folefack A, Pensia E, et al. Human loiasis in a Cameroonian village: a double-blind, placebo-controlled, crossover clinical trial of a three-day albendazole regimen. Am J Trop Med Hyg. 2004;71:211–5. http://dx.doi.org/10.4269/ajtmh.2004.71.211
8. Klion AD, Horton J, Nutman TB. Albendazole therapy for loiasis refractory to diethylcarbamazine treatment. Clin Infect Dis. 1999;29:680–2. http://dx.doi.org/10.1086/598654
9. Arrey-Agbor DB, Nana-Djeunga HC, Mogoung-Wafo AE, Mafo M, Danwe C, Kamgno J. Case report: probable case of spontaneous encephalopathy due to loiasis and dramatic reduction of *Loa loa* microfilariaemia with prolonged repeated courses of albendazole. Am J Trop Med Hyg. 2018;99:112–5. http://dx.doi.org/10.4269/ajtmh.17-0664
10. Antinori S, Schifanella L, Million M, Galimberti L, Ferraris L, Mandia L, et al. Imported *Loa loa* filariasis: three cases and a review of cases reported in non-endemic countries in the past 25 years. Int J Infect Dis. 2012;16:e649–62.
11. Klion AD, Massougbodji A, Horton J, Ekoué S, Lanmasso T, Ahouissou NL, et al. Albendazole in human loiasis: results of a double-blind, placebo-controlled trial. J Infect Dis. 1993;168:202–6. http://dx.doi.org/10.1093/infdis/168.1.202
12. Martin-Prevel Y, Cosnefroy JY, Tshipamba P, Ngari P, Chodakewitz JA, Pinder M. Tolerance and efficacy of single high-dose ivermectin for the treatment of loiasis. Am J Trop Med Hyg. 1993;48:186–92. http://dx.doi.org/10.4269/ajtmh.1993.48.186
13. Pion SD, Tchatchueng-Mbougua JB, Chesnais CB, Kamgno J, Gardon J, Chippaux JP, et al. Effect of a single standard dose (150–200 μg/kg) of ivermectin on *Loa loa* microfilaremia: systematic review and meta-analysis. Open Forum Infect Dis. 2019;6:ofz019. http://dx.doi.org/10.1093/ofid/ofz019
14. Gobbi F, Postiglione C, Angheben A, Marocco S, Monteiro G, Buonfrate D, et al. Imported loiasis in Italy: an analysis of 100 cases. Travel Med Infect Dis. 2014;12(6 Pt B):713–7. http://dx.doi.org/10.1016/j.tmaid.2014.07.004
15. Kamgno J, Pion SD, Chesnais CB, Bakalar MH, D’Ambrosio MV, Mackenzie CD, et al. A test-and-not-treat strategy for onchocerciasis in *Loa loa*–endemic areas. N Engl J Med. 2017;377:2044–52. http://dx.doi.org/10.1056/NEJMoa1705026
16. Gobbi F, Bottieau E, Bouchaud O, Buonfrate D, Salvador F, Rojo-Marcos G, et al. Comparison of different drug regimens for the treatment of loiasis—a TropNet retrospective study. PLoS Negl Trop Dis. 2018;12:e0006917. http://dx.doi.org/10.1371/journal.pntd.0006917

Address for correspondence: Federico Gobbi, IRCCS Sacro Cuore Don Calabria Hospital, Department of Infectious-Tropical Diseases and Microbiology (DITM), Via Sempreboni 5, 37024 Negrar (Verona), Italy; email: federico.gobbi@sacrocuore.it

Marburgvirus in Egyptian Fruit Bats, Zambia

Masahiro Kajihara, Bernard M. Hang'ombe, Katendi Changula, Hayato Harima, Mao Isono, Kosuke Okuya, Reiko Yoshida, Akina Mori-Kajihara, Yoshiki Eto, Yasuko Orba, Hirohito Ogawa, Yongjin Qiu, Hirofumi Sawa, Edgar Simulundu, Daniel Mwizabi, Musso Munyeme, David Squarre, Victor Mukonka, Aaron Mweene, Ayato Takada

We detected Marburg virus genome in Egyptian fruit bats (*Rousettus aegyptiacus*) captured in Zambia in September 2018. The virus was closely related phylogenetically to the viruses that previously caused Marburg outbreaks in the Democratic Republic of the Congo. This finding demonstrates that Zambia is at risk for Marburg virus disease.

The genus *Marburgvirus*, like *Ebolavirus*, belongs to the family *Filoviridae* and consists of virus species that cause severe hemorrhagic fever in humans and nonhuman primates. *Marburgvirus* contains 1 species, *Marburg Marburgvirus*, and 2 viruses, Marburg virus (MARV) and Ravn virus (RAVV) (hereafter referred to as Marburgviruses) (*1*). Marburg virus disease (MVD) has occurred most frequently in central Africa countries such as Uganda and the Democratic Republic of the Congo (DRC) (*2*). Sporadic outbreaks including imported cases have also been reported in Angola, Kenya, and South Africa (*2*).

Epidemiologic evidence strongly suggests that Egyptian fruit bats (*Rousettus aegyptiacus*) are the primary natural reservoir of Marburgviruses. Entry into caves and mines inhabited by Egyptian fruit bats has frequently been linked to MVD outbreaks (*3*). Cave-dwelling Egyptian fruit bats in Uganda have been shown to maintain genetically diverse Marburgviruses for at least several years (*4*–*6*). However, key findings on Marburgvirus ecology have been obtained mainly through epidemiologic studies in endemic countries such as Uganda and the DRC. Although Egyptian fruit bats are widely distributed from Africa to the Middle East, northern India, and Pakistan (*7*), it remains elusive whether these bats outside endemic areas also harbor Marburgviruses.

Because a traveler who had visited Zimbabwe developed MVD in South Africa in 1975 (*3*), it has been suggested that countries in southern Africa are also at risk for MVD. Indeed, Angola has had the largest MVD outbreak, in 2004–2005 (*2*). To estimate the risk of MVD in Zambia, which has had no recognized human cases, we conducted an epidemiologic study of infection of Egyptian fruit bats with Marburgviruses in this country since 2014. Previously, we reported a high seroprevalence of Marburgvirus infection (43.8%) in the Egyptian fruit bat population in Zambia (*8*). Peaks of seroprevalence were repeatedly observed in November to December of each year, strongly suggesting the seasonality of infection in the Egyptian fruit bat colony in Zambia. However, neither infectious Marburgvirus nor its RNA genome had been detected in Egyptian fruit bats as of September 2018 (*8*).

In 2018, we captured 71 cave-dwelling Egyptian fruit bats in Lusaka Province, Zambia, as part of the research project Molecular and Serological Surveillance of Viral Zoonoses in Zambia (DNPW8/27/1), approved by the Department of National Parks and Wildlife, Ministry of Tourism and Arts of the Republic of Zambia (act no. 14 of 2015). We sampled lung, liver, kidney, spleen, and colon tissues from 22 bats in February and 25 bats in September (Table 1). In November, we collected oral and rectal swab samples from 24 bats. We extracted total RNA from pooled tissue homogenates (lung, liver, kidney, and spleen), colon homogenates, and pooled swab samples, as described previously (*8*). Subsequently, we tested RNA samples by reverse transcription PCR with panfilovirus nucleoprotein (NP) (*9*), Marburgvirus NP, viral protein (VP) 35 (*6*), and RNA-dependent RNA polymerase (L) gene primer sets (*10*).

We obtained all the expected PCR products from the RNA samples of an Egyptian fruit bat (ZB18-36) captured in September (Table 2). By Sanger sequencing of the PCR products and subsequent BLAST searches (https://blast.ncbi.nlm.nih.gov/Blast.cgi), we confirmed detection of Marburgvirus NP, VP35, and L genes (GenBank accession nos. LC465155–7). We also detected the NP gene in the pooled tissue RNA of another bat (ZB18-55) (GenBank

Author affiliations: Hokkaido University, Sapporo, Japan (M. Kajihara, H. Harima, M. Isono, K. Okuya, R. Yoshida, A. Mori-Kajihara, Y. Eto, Y. Orba, Y. Qiu, H. Sawa, A. Takada); University of Zambia, Lusaka, Zambia (B.M. Hang'ombe, K. Changula, H. Sawa, E. Simulundu, M. Munyeme, A. Mweene, A. Takada); Okayama University, Okayama, Japan (H. Ogawa); Department of National Parks and Wildlife, Lusaka (D. Mwizabi, D. Squarre); Zambia National Public Health Institute, Lusaka (V. Mukonka)

DOI: https://doi.org/10.3201/eid2508.190268

Table 1. Summary of Egyptian fruit bats (*Rousettus aegyptiacus*) captured in 2018 in Zambia and genetic screening results

Sampling month	No. tested bats (sex)	RNA source	No. (%) positive
Feb	22 (10 M, 12 F)	Tissue pool,* colon	0 (0)
Sep	25 (13 M, 12 F)	Tissue pool,* colon	2 (8.0)
Nov	24 (1 M, 23 F)	Swab pool†	0 (0)

*Liver, lung, kidney, and spleen were pooled for each bat.
†Oral and rectal swabs were pooled for each bat.

accession no. LC465158) (Table 2). Nucleotide sequences of these genes were highly similar to those of the viruses that caused outbreaks in DRC during 1998–2000. Pairwise comparison of partial NP (560-nt), VP35 (344-nt), and L (292-nt) gene sequences showed 99.1%, 96.8%, and 99.7% identities, respectively, to the respective genes of strain MARV/H.sapiens-tc/COD/2000/25 DRC (GenBank accession no. JX458849). We excluded the possibility of laboratory contamination because the detected sequences were distinct from those of viral RNA or plasmids containing Marburg virus genes used in our laboratory.

Subsequently, we phylogenetically compared the NP, VP35, and L genes with representative Marburgvirus sequences available in GenBank. We aligned nucleotide sequences by MUSCLE (https://www.ebi.ac.uk/Tools/msa/muscle) and constructed phylogenetic trees by the maximum-likelihood method with 1,000 bootstrap replicates in MEGA7 (*11*). The NP, VP35, and L-based trees showed similar topology and clearly demonstrated that the virus in Zambia belonged to the MARV, not the RAVV, lineage (Figure). The virus was closely related to Marburgviruses detected in Egyptian fruit bats in Uganda (*5*,*6*), as well as to those that caused human cases in the DRC, but were phylogenetically distinct from the viruses that caused MVD in Angola.

Recently, the Marburgvirus genome was detected in cave-dwelling Egyptian fruit bats in South Africa (*10*), suggesting that this virus might be maintained by bats in southern Africa, including previously nonendemic countries. Our previous serologic data also indicate that Marburgviruses may actively circulate in the Egyptian fruit bat population in this region, including Zambia, rather than being introduced occasionally from endemic areas in 2018, as the seroprevalence of Marburgvirus infection among Egyptian fruit bats was repeatedly increased in November–December (*8*). Furthermore, the viruses detected in Zambia, Uganda, the DRC, and South Africa belong to the same cluster phylogenetically. Taken together, these findings suggest that Marburgviruses may be maintained by the larger metapopulation of Egyptian fruit bats distributed in sub-Saharan Africa. Egyptian fruit bats are known to migrate several hundred kilometers (*7*), and the Marburgvirus genome has also been detected in *Miniopterus inflatus* and *Rhinolophus eloquens* bats, as well as Egyptian fruit bats in Gabon (*4*). Frequent contacts among multiple species of bats via long-distance movement may facilitate the maintenance of genetically diverse Marburgviruses in African bats.

Experimental infection of Egyptian fruit bats with MARV demonstrated that induced virus-specific IgG rapidly declined by 3 months postinfection (*12*). Considering the serologic peaks in November to December in the Egyptian fruit bat population in Zambia (*8*), it is reasonable that the virus was detected in September in this study. The prevalence of Marburgvirus infection in the bat colony has probably decreased to an undetectable level as the seroprevalence in the bats increases. Previous studies have suggested that biannual reproduction of Egyptian fruit bats in Uganda provides appropriate conditions for Marburgvirus perpetuation relying on the increased population of susceptible juvenile bats associated with the decline of maternal antibodies (*6*,*13*). However, this transmission manner may not be the case for Egyptian fruit bats in southern Africa, as they give birth once a year (*7*,*8*,*10*). Recently, Schuh et al. demonstrated that Marburgvirus was horizontally transmitted from inoculated to contact Egyptian fruit bats even at 7 months postinfection (*12*), suggesting that the viruses could establish persistent infection in this bat species. Even in humans, long-term viral persistence in immune-privileged sites such as the testes and eyes has occasionally been reported (*14*). Because 42% of the female bats captured in September (5 of 12 bats) were pregnant, it could still be assumed that seasonal biologic events such as breeding might be a possible trigger for recurrence of Marburgvirus infection in the bat colonies.

We report a potential risk for MVD in Zambia. It is important to clarify whether unrecognized human cases of MVD, including asymptomatic Marburgvirus infection, are present

Table 2. Summary of Egyptian fruit bats (*Rousettus aegyptiacus*) positive for Marburgviruses by reverse transcription PCR, Zambia, 2018*

Bat ID	Sex	Body weight, g	Sample	Reverse transcription PCR primer set			
				Filo NP	Marburg NP	Marburg VP35	Marburg L
ZB18-36	F	80	Tissue pool†	–	+	–	+
			Colon	+	+	+	+
ZB18-55	M	100	Tissue pool†	–	+	–	–
			Colon	–	–	–	–

*L, RNA-dependent RNA polymerase; NP, nucleoprotein; VP35, viral protein 35; –, negative; +, positive.
†Liver, lung, kidney, and spleen were pooled.

in Zambia. Moreover, further research is needed to elucidate the ecology of Marburgviruses in the entire African region and to estimate potential risks of MVD outbreaks in previously nonendemic countries. In particular, more extensive information is needed on Marburgviruses in the Egyptian fruit bat population, including the genetic diversity of the viruses, the distribution and migratory behavior of the bats, and the seasonal pattern of virus infection prevalence.

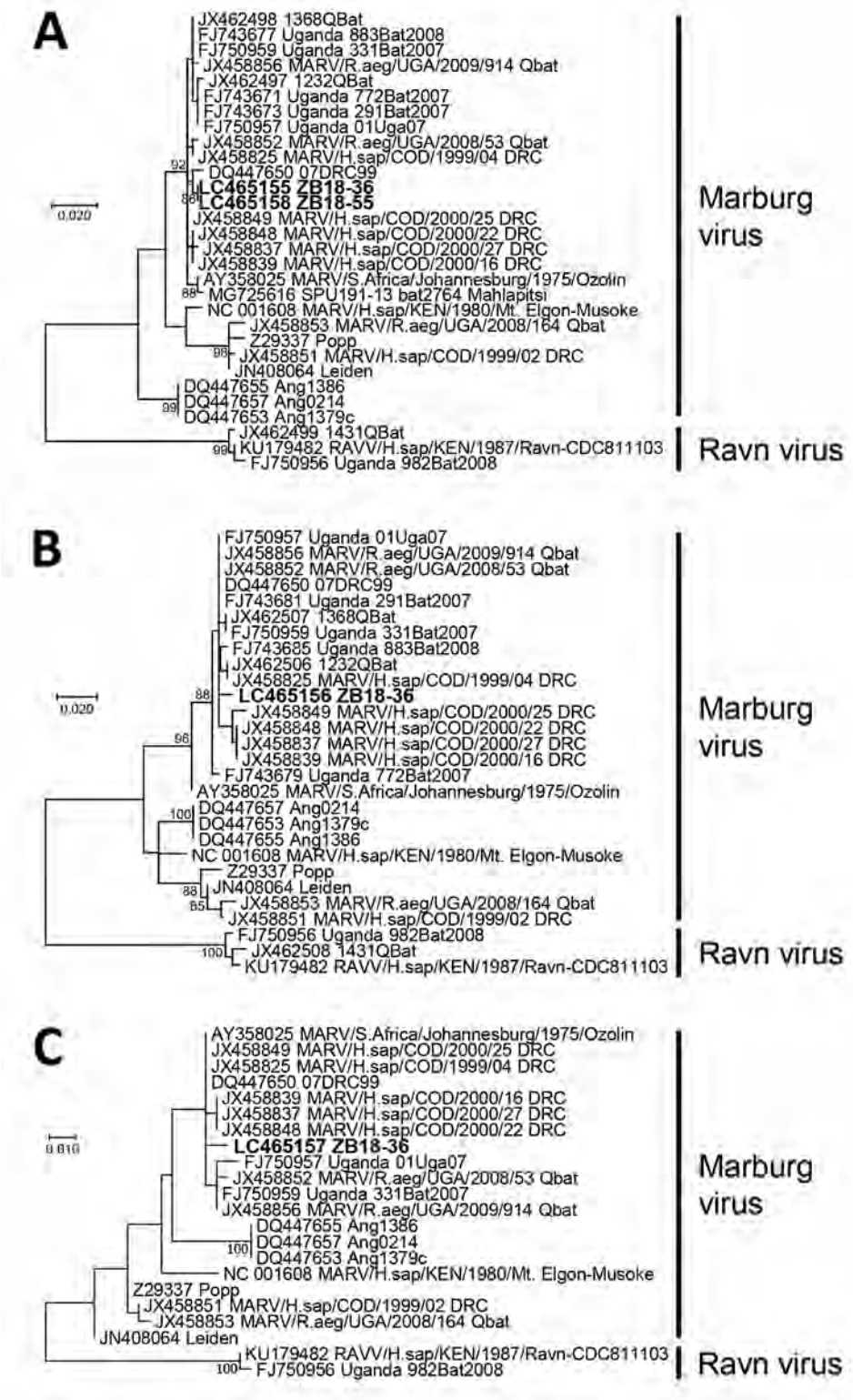

Figure. Phylogenetic trees showing evolutionary relationships of Marburgviruses from Egyptian fruit bats (*Rousettus aegyptiacus*), Zambia, 2018 (boldface), and reference viruses. The trees were constructed based on nucleotide sequences of 440 nt for the nucleoprotein gene (A), 296 nt for the viral protein 35 gene (B), and 238 nt for the RNA-dependent RNA polymerase gene (C) by using the maximum-likelihood method in MEGA7 (*11*). Nucleotide sequences of representative Marburgvirus strains were obtained from GenBank; accession numbers are shown with strain names. Bootstrap values >80 are shown near the branch nodes. Scale bars indicate nucleotide substitutions per site.

Acknowledgments

We thank staffs of the Department of National Parks and Wildlife, Ministry of Tourism and Arts, Zambia, and technicians in the School of Veterinary Medicine, the University of Zambia, for assistance in capturing the animals. We also thank K. Barrymore for editing the manuscript.

This work was supported by the Agency for Medical Research and Development and Japan International Cooperation Agency within the framework of the Science and Technology Research Partnership for Sustainable Development (grant no. JP18jm0110019) and the Japan Initiative for Global Research Network on Infectious Diseases (grant no. JP18fm0108008). Funding was provided in part by the Japan Society for the Promotion of Science (KAKENHI) (grant nos. JP16H02627, JP15K18778, JP18K15163).

About the Author

Dr. Kajihara is a postdoctoral research associate at the Hokkaido University Research Center for Zoonosis Control. He studies known and uncharacterized viruses in Africa to understand their ecology and pathogenic potential for humans and animals; he is interested primarily in batborne viruses, including filoviruses and paramyxoviruses.

References

1. Amarasinghe GK, Aréchiga Ceballos NG, Banyard AC, Basler CF, Bavari S, Bennett AJ, et al. Taxonomy of the order Mononegavirales: update 2018. Arch Virol. 2018;163:2283–94. http://dx.doi.org/10.1007/s00705-018-3814-x
2. Centers for Disease Control and Prevention. Outbreaks chronology: Marburg hemorrhagic fever. 2019 [cited 2019 Jan 29]. https://www.cdc.gov/vhf/marburg/outbreaks/chronology.html
3. Changula K, Kajihara M, Mweene AS, Takada A. Ebola and Marburg virus diseases in Africa: increased risk of outbreaks in previously unaffected areas? Microbiol Immunol. 2014;58:483–91. http://dx.doi.org/10.1111/1348-0421.12181
4. Swanepoel R, Smit SB, Rollin PE, Formenty P, Leman PA, Kemp A, et al.; International Scientific and Technical Committee for Marburg Hemorrhagic Fever Control in the Democratic Republic of Congo. Studies of reservoir hosts for Marburg virus. Emerg Infect Dis. 2007;13:1847–51. http://dx.doi.org/10.3201/eid1312.071115
5. Towner JS, Amman BR, Sealy TK, Carroll SA, Comer JA, Kemp A, et al. Isolation of genetically diverse Marburg viruses from Egyptian fruit bats. PLoS Pathog. 2009;5:e1000536. http://dx.doi.org/10.1371/journal.ppat.1000536
6. Amman BR, Carroll SA, Reed ZD, Sealy TK, Balinandi S, Swanepoel R, et al. Seasonal pulses of Marburg virus circulation in juvenile Rousettus aegyptiacus bats coincide with periods of increased risk of human infection. PLoS Pathog. 2012;8:e1002877. PubMed http://dx.doi.org/10.1371/journal.ppat.1002877
7. AfricanBats NPC, African Chiroptera Project. African Chiroptera Report 2018. Pretoria (South Africa): AfricanBats NPC; 2018.
8. Changula K, Kajihara M, Mori-Kajihara A, Eto Y, Miyamoto H, Yoshida R, et al. Seroprevalence of filovirus infection of Rousettus aegyptiacus bats in Zambia. J Infect Dis. 2018;218(suppl5):S312–7. http://dx.doi.org/10.1093/infdis/jiy266
9. Ogawa H, Miyamoto H, Ebihara H, Ito K, Morikawa S, Feldmann H, et al. Detection of all known filovirus species by reverse transcription-polymerase chain reaction using a primer set specific for the viral nucleoprotein gene. J Virol Methods. 2011;171:310–3. http://dx.doi.org/10.1016/j.jviromet.2010.11.010
10. Pawęska JT, Jansen van Vuren P, Kemp A, Storm N, Grobbelaar AA, Wiley MR, et al. Marburg virus infection in Egyptian rousette bats, South Africa, 2013–2014. Emerg Infect Dis. 2018;24:1134–7. http://dx.doi.org/10.3201/eid2406.172165
11. Kumar S, Stecher G, Tamura K. MEGA7: Molecular Evolutionary Genetics Analysis version 7.0 for bigger datasets. Mol Biol Evol. 2016;33:1870–4. http://dx.doi.org/ 10.1093/molbev/msw054
12. Schuh AJ, Amman BR, Jones ME, Sealy TK, Uebelhoer LS, Spengler JR, et al. Modelling filovirus maintenance in nature by experimental transmission of Marburg virus between Egyptian rousette bats. Nat Commun. 2017;8:14446. http://dx.doi.org/10.1038/ncomms14446
13. Hayman DTS. Biannual birth pulses allow filoviruses to persist in bat populations. Proc Biol Sci. 2015;282:20142591. http://dx.doi.org/10.1098/rspb.2014.2591
14. Schindell BG, Webb AL, Kindrachuk J. Persistence and sexual transmission of filoviruses. Viruses. 2018;10:E683. http://dx.doi.org/10.3390/v10120683

Address for correspondence: Ayato Takada, Hokkaido University Center for Global Epidemiology, Division of Global Epidemiology Research, Kita 20 Nishi 10, Kita-ku, Sapporo, Japan; email: atakada@czc.hokudai.ac.jp

Bejel, a Nonvenereal Treponematosis, among Men Who Have Sex with Men, Japan

Takuya Kawahata, Yoko Kojima, Keiichi Furubayashi, Koh Shinohara, Tsunehiro Shimizu, Jun Komano, Haruyo Mori, Kazushi Motomura

Author affiliations: Osaka Institute of Public Health, Osaka, Japan (T. Kawahata, Y. Kojima, H. Mori, K. Motomura); Sonezaki Furubayashi Clinic, Osaka (K. Furubayashi); Kyoto City Hospital, Kyoto, Japan (K. Shinohara, T. Shimizu); Nagoya Medical Center, Nagoya, Japan (J. Komano); Osaka University of Pharmaceutical Sciences, Takatsuki, Japan (J. Komano)

DOI: https://doi.org/10.3201/eid2508.181690

Bejel, an endemic treponematosis caused by infection with *Treponema pallidum* subspecies *endemicum*, has not been reported in eastern Asia and the Pacific region. We report local spread of bejel among men who have sex with men in Japan. Spread was complicated by venereal syphilis.

Treponema pallidum subspecies *pallidum* is the causative agent of venereal syphilis. Globally, syphilis remains a disease of heterosexual persons in low-to-middle-income countries. Epidemics of syphilis among men who have sex with men (MSM) occur in high-income settings (*1*). Other *Treponema* species cause nonvenereal endemic treponematosis (also called bejel, nonvenereal syphilis, or endemic syphilis, caused by *T. pallidum* subsp. *endemicum*), yaws (*T. pallidum* subsp. *pertenue*), and pinta (*T. carateum*). These pathogens are morphologically and serologically indistinguishable (*2*). Clinically, there is little need to differentiate them. However, it is useful to differentiate them from a public health standpoint because their infection routes vary. For this purpose, a nucleic acid test is useful (*3*).

Bejel was eradicated in Europe in the 20th century but was prevalent there in the 16th century (*4*). Bejel is still prevalent in dry and hot areas, such as the Sahel region in western Africa, part of Botswana, Zimbabwe, and the Arabian Peninsula (*5*). The main route of transmission is direct skin-to-skin contact. Bejel can be transmitted sexually, but this route has not been studied because bejel affects mainly children. Only a few case reports of bejel have been reported in non-endemic areas since 1999, including France (*3*), Canada (*6*), and Cuba (*7*). Bejel in France was attributed to an imported case from Pakistan, and in Canada to an imported case from Senegal, whereas transmission in Cuba was regionalized. No patient with nonvenereal treponematosis has been reported in Japan.

In Japan, syphilis has been reemerging since 2010 (*8*). However, little attention has been paid to nonvenereal treponematosis. We thus conducted a molecular epidemiologic study to characterize the genotypes of *T. pallidum* subsp. *pallidum* among patients with venereal syphilis after 2011 (*9*).

The study protocol was approved by the Ethical Review Board of Osaka Institute of Public Health. We tested specimens from patients suspected of having or given a diagnosis of syphilis by using nucleic acid amplification tests for *T. pallidum* subsp. *pallidum* specific for the TpN47 and *pol*A gene regions. We performed molecular genotyping of *T. pallidum* subsp. *pallidum* strains based on the nucleic acid sequences of the tp0548 and tp0856 gene regions (*3*,*10*).

Phylogenetic analysis showed that, of 58 isolates from nucleic acid test–positive specimens, 5 isolates (8.6%) were *T. pallidum* subsp. *endemicum* and different from *T. pallidum* subsp. *pallidum* and *T. pallidum* subsp. *pertenue*. We concluded that the 5 patients from whom these strains were isolated had bejel (Figure).

All 5 bejel patients were men from Japan 20–40 years of age; all were MSM. One patient was identified in 2014, another 3 in 2017, and 1 patient in 2018. Two of the patients identified in 2017 were in the secondary stage of the disease; the other 3 were in the primary stage. Clinical manifestations of the 3 patients in the primary stage were penile erosion or ulcer. The 2 patients in the secondary stage had systemic rashes and lymphadenopathy, in addition to pubic and perineal symptoms.

For serologic tests at admission, the 3 primary-stage patients showed negative results for the rapid plasma reagin test (<1.0 unit). Of these patients, 2 showed negative results of the *T. pallidum* latex agglutination test (<10 units) and 1 had a titer of 35.7 units. The 2 secondary-stage patients had positive results for the rapid plasma reagin test, and their *T. pallidum* latex agglutination test values were 2.4×10^3 and 20.8×10^3 units.

The first patient lived in Yamaguchi Prefecture. The other 4 patients lived in the Kansai area, including Osaka, Kyoto, and Hyogo Prefectures. Although the residential geographic areas were remote, the suspected locale of treponemal infection was the Kansai area, namely the city centers of Osaka and Kyoto. The 2018 patient was HIV positive. None of the patients had a history of overseas travel for a long period. All 5 isolates had a mutation conferring azithromycin resistance. The 3 patients who were followed up responded well to standard therapy with penicillin.

These data strongly suggest that *T. pallidum* subsp. *endemicum* is transmitted domestically in Japan by MSM. Our findings provide molecular epidemiologic evidence for a local spread of *T. pallidum* subsp. *endemicum* in eastern Asia and the Pacific region.

Clinical manifestations of venereal syphilis and bejel are similar, especially in the early stage for adults, which

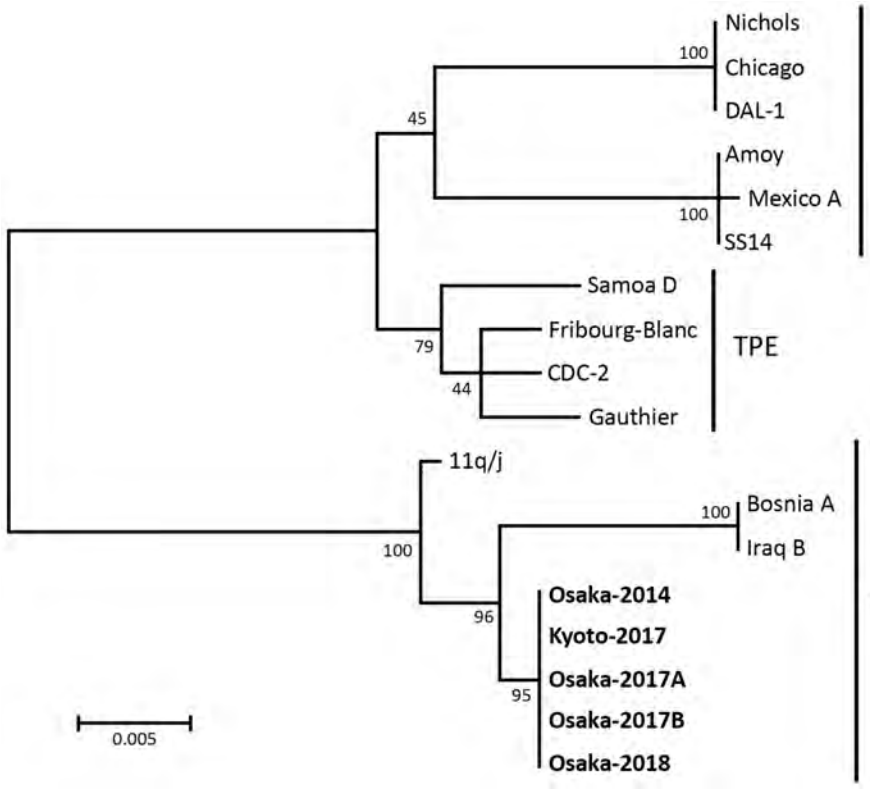

Figure. Phylogenetic tree for tp0548–tp0856 gene regions (1173–1233 bp) of clinical isolates of *Treponema pallidum* from Japan (bold) and reference isolates. The tree was constructed by using MEGA6 (https://www.megasoftware.net) with the bootstrapping maximum-likelihood algorithm and the Tamura–Nei model. Numbers along branches indicate bootstrap values. Scale bar indicates nucleotide substitutions per site. Strains from this study were submitted to GenBank under the following accession numbers: Osaka-2014, LC383799 (tp0548) and LC430604 (tp0856); Kyoto-2017, LC430601 (tp0548) and LC430606 (tp0856); Osaka-2017A, LC383801 (tp0548) and LC430605 (tp0856); Osaka-2017B, LC430602 (tp0548) and LC430607 (tp0856); and Oskaka-2018, LC430603 (tp0548) and LC430608 (tp0856). TEN, *Treponema pallidum* subspecies *endemicum*; TPA, *T. pallidum* subsp. *pallidum*; TPE, *T. pallidum* subsp. *pertenue*.

makes diagnosis difficult (*7*). Infectious diseases that have been historically not considered to be sexually transmitted infections (STIs), such as amebiasis, hepatitis A, and shigellosis, often show manifestations of STIs. Likewise, bejel might be changing from an endemic tropical disease to a global STI.

Treatment for venereal syphilis is also effective for bejel. For the 5 patients we report, laboratory test results showed a strong correspondence to the stage of bejel disease progression. Clinicians should be aware of the spread of nonvenereal treponematosis worldwide, especially in low-prevalence areas. Nucleic acid tests that can differentiate *T. pallidum* strains might be helpful (*3*,*10*). Molecular epidemiology might help determine which populations are affected and provide an effective means to prevent the further spread of treponematosis.

This study was partially supported by grants-in-aid for research on HIV/AIDS from the Ministry of Health, Labour and Welfare of Japan (grants H26-AIDS-006 and H29-AIDS-007) to T.K. and a grant from the Daido Life Welfare Foundation for Regional Health and Welfare Research in 2017 to Y.K.

About the Author

Dr. Kawahata is a principal research scientist at the Osaka Institute of Public Health, Osaka, Japan. His primary research interests are HIV infections, sexually transmitted infections, and syphilis.

References

1. Fenton KA, Breban R, Vardavas R, Okano JT, Martin T, Aral S, et al. Infectious syphilis in high-income settings in the 21st century. Lancet Infect Dis. 2008;8:244–53. https://doi.org/10.1016/S1473-3099(08)70065-3
2. Mitjà O, Šmajs D, Bassat Q. Advances in the diagnosis of endemic treponematoses: yaws, bejel, and pinta. PLoS Negl Trop Dis. 2013;7:e2283. https://doi.org/10.1371/journal.pntd.0002283
3. Mikalová L, Strouhal M, Oppelt J, Grange PA, Janier M, Benhaddou N, et al. Human *Treponema pallidum* 11q/j isolate belongs to subsp. *endemicum* but contains two loci with a sequence in TP0548 and TP0488 similar to subsp. *pertenue* and subsp. *pallidum*, respectively. PLoS Negl Trop Dis. 2017;11:e0005434. https://doi.org/10.1371/journal.pntd.0005434
4. Lipozenčić J, Marinović B, Gruber F. Endemic syphilis in Europe. Clin Dermatol. 2014;32:219–26. https://doi.org/10.1016/j.clindermatol.2013.08.006
5. Giacani L, Lukehart SA. The endemic treponematoses. Clin Microbiol Rev. 2014;27:89–115. https://doi.org/10.1128/CMR.00070-13
6. Fanella S, Kadkhoda K, Shuel M, Tsang R. Local transmission of imported endemic syphilis, Canada, 2011. Emerg Infect Dis. 2012;18:1002–4. https://doi.org/10.3201/eid1806.111421
7. Noda AA, Grillová L, Lienhard R, Blanco O, Rodríguez I, Šmajs D. Bejel in Cuba: molecular identification of *Treponema pallidum* subsp. *endemicum* in patients diagnosed with venereal syphilis. Clin Microbiol Infect. 2018;24:1210.e1–5. https://doi.org/10.1016/j.cmi.2018.02.006
8. Takahashi T, Arima Y, Yamagishi T, Nishiki S, Kanai M, Ishikane M, et al. Rapid increase in reports of syphilis associated with men who have sex with women and women who have sex with men, Japan, 2012 to 2016. Sex Transm Dis. 2018;45:139–43. https://doi.org/10.1097/OLQ.0000000000000768

9. Kojima Y, Furubayashi K, Kawahata T, Mori H, Komano J. Circulation of distinct *Treponema pallidum* strains in individuals with heterosexual orientation and men who have sex with men. J Clin Microbiol. 2019;57:e01148-18. https://doi.org/10.1128/JCM.01148-18
10. Staudová B, Strouhal M, Zobaníková M, Cejková D, Fulton LL, Chen L, et al. Whole genome sequence of the *Treponema pallidum* subsp. *endemicum* strain Bosnia A: the genome is related to yaws treponemes but contains few loci similar to syphilis treponemes. PLoS Negl Trop Dis. 2014;8:e3261. https://doi.org/10.1371/journal.pntd.0003261

Address for correspondence: Takuya Kawahata, Osaka Institute of Public Health, 1-3-69 Nakamichi, Higashinari-ku, Osaka 537-0025, Japan; email: kawahata@iph.osaka.jp

Multidrug-Resistant *Klebsiella pneumoniae* ST307 in Traveler Returning from Puerto Rico to Dominican Republic

Rita Rojas, Nenad Macesic, Gilda Tolari, Anel Guzman, Anne-Catrin Uhlemann

Author affiliations: Hospital General Plaza de la Salud, Santo Domingo, Dominican Republic (R. Rojas, G. Tolari, A. Guzman); Monash University, Melbourne, Victoria, Australia (N. Macesic); Columbia University Medical Center, New York, New York, USA (N. Macesic, A.-C. Uhlemann)

DOI: https://doi.org/10.3201/eid2508.171730

We report *bla*$_{KPC-2}$–harboring carbapenem-resistant *Klebsiella pneumoniae* in an emerging sequence type 307 lineage in a traveler returning from Puerto Rico to the Dominican Republic. Phylogenetic analyses indicate regional dissemination of this highly drug-resistant clone across the Americas, underscoring the need for adequate surveillance and infection control efforts to prevent further spread.

Carbapenemase-resistant *Enterobacteriaceae* (CRE), in particular carbapenem-resistant *Klebsiella pneumoniae* (CRKp), represent a serious threat to public health (*1*). CRKp infections have been associated with high mortality rates, up to 50% in some studies (*2*). In resource-limited regions, such as the Dominican Republic, multiple challenges hinder efforts to contain CRE infections, including lack of novel antimicrobial drugs, inability to monitor drug levels of potentially toxic treatment regimens, and absence of molecular tools to investigate outbreaks and potential spread.

In fall 2015, a 66-year-old woman with diabetes mellitus, hepatitis C virus infection, and end-stage renal disease on hemodialysis was admitted to a hospital in the Dominican Republic for fever, anorexia, chills, and myalgia. On day 3, her blood culture tested positive for *K. pneumoniae*. She had been admitted to a hospital in Puerto Rico a few months before and had been treated for a multidrug-resistant bacterial infection.

The *K. pneumoniae* isolate from the patient was nonsusceptible to all tested antimicrobial drugs except polymyxins (Appendix Table 1, http://wwwnc.cdc.gov/EID/article/25/8/17-1730-App1.pdf). We began combination therapy with a loading dose of colistin, then 100 mg postdialysis, plus ertapenem (150 mg postdialysis) and fosfomycin (2 g 3×/d). We implemented infection control measures by placing the patient in a single room and using gloves, gowns, masks, and a dedicated stethoscope. Despite initial improvement, the patient died on day 25 after admission.

Whole-genome sequencing revealed that the patient isolate, NR6025, was of the emerging sequence type 307 (ST307) (*3*) and closely related (≤185 SNPs) to several international ST307 isolates of similar phenotype (Figure). Of note, this isolate was most closely related, within 36 SNPs, to an isolate recovered from a patient in New York, NY, USA, who also had been hospitalized in Puerto Rico in 2016 (*4*). This finding raises the possibility that both patients acquired CRE in Puerto Rico and their infections subsequently developed in their home countries.

In silico resistance gene detection demonstrated that *bla*$_{KPC-2}$, on Tn*4401e*, was likely the mechanism of carbapenem resistance for this isolate. Moreover, the meropenem MIC was >32 μg/mL, consistent with high carbapenem MICs observed in the ST307 Tn*4401e* isolates (*4*) from New York, suggesting association with a strong promoter. In addition, the isolate harbored a large repertoire of acquired-resistance genes, including additional β-lactamase genes CTX-M-15, SHV-100, OXA-1, and TEM-1D (Appendix Table 1). The isolate contained IncFIBK, ColRNA1, and IncA/C2 plasmid replicons; IncA/C plasmid encodes for *bla*$_{KPC-2}$, *bla*$_{TEM}$, *sulI*, *aadB*, *aac6*, and *qacE*, which has been implicated in chlorhexidine resistance.

A case of CRKp was described from Medellin, Colombia, in 2005, and subsequent CRKp infections have been reported in Mexico, in South America in Brazil, Argentina, and Venezuela, and in the Caribbean in Cuba, Puerto Rico, and Trinidad and Tobago (*5*–*7*). In many of these studies, CRKp isolates were mainly accounted for

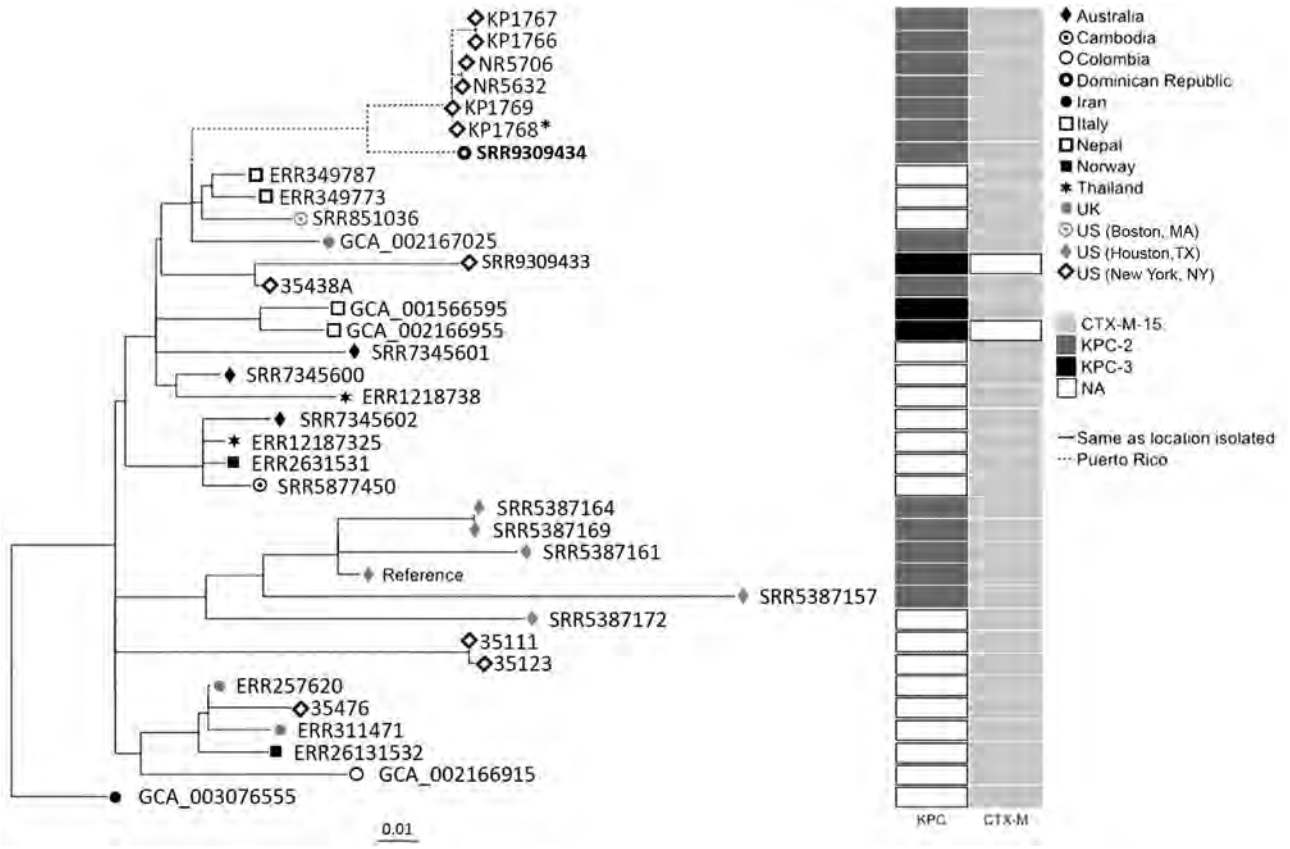

Figure. Maximum-likelihood phylogenetic tree of geographically diverse *Klebsiella pneumoniae* sequence type 307 isolates based on 860 concatenated single-nucleotide polymorphisms, extracted from an alignment length of 5,248,133 bp. Bold indicates isolate from a traveler from Puerto Rico to the Dominican Republic (this study). Asterisk (*) indicates an isolate recovered from a patient admitted to a hospital in Puerto Rico during the same year as the case-patient in this study (*4*). *bla* gene types (KPC, CTX-M) are indicated. Scale bar indicates nucleotide substitutions per site. NA, not applicable.

by ST258 and ST512. The SENTRY Antimicrobial Surveillance Program showed that bla_{KPC-2}-harboring CRE accounted for most CRE infections in Latin America and that the incidence rate has been rising sharply (*8*). These organisms also are prevalent in Puerto Rico, where a 6-month, PCR-based, islandwide hospital surveillance study conducted in 2011 found that 333/2,805 (11.9%) *K. pneumoniae* isolates harbored bla_{KPC} (*9*). However, little is known about CRKp genotypes in Puerto Rico.

Our case highlights the many challenges for controlling CRE infections in resource-limited countries like the Dominican Republic and accentuates the potential for international spread of CRKp through travel, particularly between resource-limited regions. Rapid molecular diagnostic tests for CRKp are not widely available, which can delay treatment. Optimal treatment regimens for CRKp remain controversial, but combination therapy could reduce risk for death compared with monotherapy (*10*). Our facility lacked the resources needed to monitor colistin drug levels, a major concern in particular in patients with underlying renal dysfunction.

Risk factors for acquisition of CRE in resource-limited settings are not well defined, potentially delaying diagnosis and implementation of infection control strategies. In our case, recent travel, healthcare contact, and unspecified exposure to antimicrobial drugs might have played a role in the patient's CRE infection. We did not observe additional CRKp infections at our institution during a 6-month follow-up period after this case. However, we were unable to institute an active molecular surveillance program. We cannot rule out silent transmission and colonization of other hospitalized patients or contacts. Even though 2 cases have now been linked to travel to Puerto Rico, no molecular epidemiologic data are available from that island. Future studies should target active surveillance for CRKp in the Caribbean.

Of note, although ST258 has been the dominant genotype of the CRE epidemic globally, the ST307 clone could be expanding disproportionately in some locations. For example, in Houston, Texas, USA, ST307 now accounts for more *K. pneumoniae* infections than ST258 (*3*). Moreover, ST307 Tn*4401e* bla_{KPC-2} isolates showed high carbapenem

MICs. Taken together, our data suggest that ST307 is highly drug resistant and harbors an extended repertoire of antimicrobial resistance genes, which might have accelerated its recent emergence and wide dissemination.

This work was supported by grants from the National Institutes of Health, National Institute of Allergy and Infectious Diseases R01 AI116939 (A.-C.U.). The funders had no role in study design, data collection, interpretation, or the decision to submit the work for publication. A.-C.U. has received research funding from Merck, unrelated to the current study. All other authors declare no conflict of interest.

About the Author

Dr. Rojas is medical director of Centro Medico Luperon and the hospital epidemiologist at Hospital General de la Plaza de la Salud in Santo Domingo, Dominican Republic. Her research interests include healthcare-associated infections and detection and control of carbapenemase-producing *Enterobacteriaceae*.

References

1. US Centers for Disease Control and Prevention. Antibiotic resistance threats in the United States, 2013. 2013 Apr [cited 2017 Oct 10]. http://www.cdc.gov/drugresistance/threat-report-2013/index.html
2. Zarkotou O, Pournaras S, Tselioti P, Dragoumanos V, Pitiriga V, Ranellou K, et al. Predictors of mortality in patients with bloodstream infections caused by KPC-producing *Klebsiella pneumoniae* and impact of appropriate antimicrobial treatment. Clin Microbiol Infect. 2011;17:1798–803. https://doi.org/10.1111/j.1469-0691.2011.03514.x
3. Long SW, Olsen RJ, Eagar TN, Beres SB, Zhao P, Davis JJ, et al. Population genomic analysis of 1,777 extended-spectrum beta-lactamase-producing *Klebsiella pneumoniae* isolates, Houston, Texas: unexpected abundance of clonal group 307. MBio. 2017;8:e00489–17. https://doi.org/10.1128/mBio.00489-17
4. Giddins MJ, Macesic N, Annavajhala MK, Stump S, Khan S, McConville TH, et al. Successive emergence of ceftazidime-avibactam resistance through distinct genomic adaptations in bla_{KPC-2}-harboring *Klebsiella pneumoniae* sequence type 307 isolates. Antimicrob Agents Chemother. 2018;62:e02101–17.
5. Escandón-Vargas K, Reyes S, Gutiérrez S, Villegas MV. The epidemiology of carbapenemases in Latin America and the Caribbean. Expert Rev Anti Infect Ther. 2017;15:277–97. https://doi.org/10.1080/14787210.2017.1268918
6. Pasteran FG, Otaegui L, Guerriero L, Radice G, Maggiora R, Rapoport M, et al. *Klebsiella pneumoniae* carbapenemase-2, Buenos Aires, Argentina. Emerg Infect Dis. 2008;14:1178–80. https://doi.org/10.3201/eid1407.070826
7. Falco A, Ramos Y, Franco E, Guzmán A, Takiff H. A cluster of KPC-2 and VIM-2-producing *Klebsiella pneumoniae* ST833 isolates from the pediatric service of a Venezuelan Hospital. BMC Infect Dis. 2016;16:595. https://doi.org/10.1186/s12879-016-1927-y
8. Castanheira M, Costello AJ, Deshpande LM, Jones RN. Expansion of clonal complex 258 KPC-2-producing *Klebsiella pneumoniae* in Latin American hospitals: report of the SENTRY Antimicrobial Surveillance Program. Antimicrob Agents Chemother. 2012; 56:1668–9, author reply 1670–1. https://doi.org/10.1128/AAC.05942-11
9. Robledo IE, Aquino EE, Vázquez GJ. Detection of the KPC gene in *Escherichia coli, Klebsiella pneumoniae, Pseudomonas aeruginosa*, and *Acinetobacter baumannii* during a PCR-based nosocomial surveillance study in Puerto Rico. Antimicrob Agents Chemother. 2011;55:2968–70. https://doi.org/10.1128/AAC.01633-10
10. Morrill HJ, Pogue JM, Kaye KS, LaPlante KL. Treatment options for carbapenem-resistant *Enterobacteriaceae* infections. Open Forum Infect Dis. 2015;2:ofv050. https://doi.org/10.1093/ofid/ofv050

Address for correspondence: Anne-Catrin Uhlemann, Columbia University, Department of Medicine, Division of Infectious Diseases, 630 W 168th St, New York, NY 10032, USA; email: au2110@columbia.edu

Feast of Sacrifice and Orf, Milan, Italy, 2015–2018

Stefano Veraldi, Luigi Esposito, Paolo Pontini, Fabrizio Vaira, Gianluca Nazzaro

Author affiliation: Università degli Studi di Milano, Milan, Italy

DOI: https://doi.org/10.3201/eid2508.181063

Orf (ecthyma contagiosum) is an infection of the skin caused by a DNA virus belonging to the genus *Parapoxvirus*. We recently observed 7 cases of orf in Muslim men living in the metropolitan area of Milan, Italy, who acquired the infection after the Feast of Sacrifice.

Orf (ecthyma contagiosum) is an infection of the skin caused by a DNA virus of the genus *Parapoxvirus*, family *Poxviridae*. Skin lesions (e.g., vesicles, blisters, pustules, erosions, ulcers, papules, nodules) occur at sites of inoculation of the virus 3–15 days after infection. Hands are usually affected (*1*). The differential diagnosis for orf includes milker's nodule, anthrax, tularemia, fish tank granuloma, cutaneous leishmaniasis, pyogenic granuloma, and keratoacanthoma (*1*). The disease spontaneously heals within 6 weeks, although pain, bacterial superinfections, and regional lymphadenitis are possible (*1*). Treatment is based on topical antiseptics (*1*).

Orf virus usually infects sheep and goats. Humans are infected by handling infected meat from these animals; orf is considered an occupational disease in shepherds, shearers, veterinarians, butchers, and cooks (*1*).

Table. Characteristics of orf in Muslim men after Feast of Sacrifice, Milan, Italy, 2015–2018

Patient no.	Age, y	Location	Characteristic
1	34	Left hand	Erythematous, ulcerated nodule
2	42	Back of right hand	Erythematous pustule
3	44	Back of right hand	Erythematous pustule
4	18	Back of second right finger	Ulcerated nodule
5	21	Palm of right hand	3 Erythematous pustules
6	44	Back of second left finger	Erythematous pustule
7	61	Third right finger	Ulcerated nodule

In the last few years, orf has occurred after the Muslim Feast of Sacrifice (Eid al-Adha) (*1*–*10*). In 2014, we reported a case of orf that appeared after sheep slaughtering for this feast (*1*). During 2015–2018, we observed 7 additional cases in Muslim men 18–61 years of age who were of Moroccan, Tunisian, or Egyptian origin. They had been infected 2–3 weeks after lamb slaughtering for the feast (Table). One patient was a butcher. In all patients, 1 hand and/or fingers were involved. In 4 patients, orf presented with erythematous pustules; 3 of these patients had ulcerated nodules. In all patients, clinical diagnosis was confirmed by histopathologic examinations.

Orf acquired during the Feast of Sacrifice was reported in 1982 in Turkey (*2*). Other cases were subsequently reported in France (*3*,*10*), Belgium (*4*,*5*), Italy (*1*), Turkey (*6*,*7*,*9*), and the United States (*8*). Epidemics also were reported: in Belgium, 23 cases in 2000 and 44 cases in 2001 (*4*,*5*), and in Turkey, 9 cases in 2005 and 29 cases in 2009 (*6*,*7*).

In most reported cases, orf appeared days or weeks after the Feast of Sacrifice. This feast is celebrated 2 months and 10 days after the end of Ramadan; the exact date varies (*4*). During the feast, many Muslim families kill a lamb, which has to be bled alive (*4*). Only men may kill the lamb. Orf occurs more often in men; however, it occurs also in women, who often handle the infected meat with bare hands during preparation and cooking.

In conclusion, in the metropolitan area of Milan, where ≈250,000 Muslims reside, we recently observed 7 patients with orf acquired during the Feast of Sacrifice. Prevention measures are difficult. For example, most of the Muslims living in the metropolitan area of Milan are Moroccans, who travel to Italy by car, carrying the infected meat; thus, no prevention measures have been taken.

About the Author

Dr. Veraldi is a dermatologist and venereologist at the Dermatology Unit and head of the Postgraduate School of Dermatology and Venereology at the University of Milan. His primary research interests are infectious and parasitic diseases of the skin.

References

1. Veraldi S, Nazzaro G, Vaira F, Çuka E. Presentation of orf (ecthyma contagiosum) after sheep slaughtering for religious feasts. Infection. 2014;42:767–9. http://dx.doi.org/10.1007/s15010-014-0591-7
2. Günes AT, Gezen C, Kapdağhi H, Marschall HJ. Ecthyma contagiosum epidemics in Turkey [in German]. Hautarzt. 1982;33:384–7.
3. Guibal F, Cosnes A, Wechsler J, Miseri E, Revuz J, Chosidow O. Religious ritual practices as a contamination mode of human orf. Eur J Dermatol. 1996;6:41–2.
4. Ghislain PD, Dinet Y, Delescluse J. Orf contamination may occur during religious events. J Am Acad Dermatol. 2000;42:848. http://dx.doi.org/10.1067/mjd.2000.103271
5. Ghislain PD, Dinet Y, Delescluse J. Orf in urban surroundings and religious practices: a study over a 3-year period [in French]. Ann Dermatol Venereol. 2001;128:889–92.
6. Uzel M, Sasmaz S, Bakaris S, Cetinus E, Bilgic E, Karaoguz A, et al. A viral infection of the hand commonly seen after the Feast of Sacrifice: human orf (orf of the hand). Epidemiol Infect. 2005;133:653–7. http://dx.doi.org/10.1017/S0950268805003778
7. Gündüz K, Inanir I, Sacar T. Orf and religious practices. J Dermatol. 2005;32:306–8. http://dx.doi.org/10.1111/j.1346-8138.2005.tb00769.x
8. Malik M, Bharier M, Tahan S, Robinson-Bostom L. Orf acquired during religious observance. Arch Dermatol. 2009;145:606–8. http://dx.doi.org/10.1001/archdermatol.2009.69
9. Sasmaz S, Uzel M, Sener S, Ucmak H. Rare presentation of human orf as multiple lesions. J Dermatol. 2011;38:825–6. http://dx.doi.org/10.1111/j.1346-8138.2010.01082.x
10. Nougairede A, Fossati C, Salez N, Cohen-Bacrie S, Ninove L, Michel F, et al. Sheep-to-human transmission of orf virus during Eid al-Adha religious practices, France. Emerg Infect Dis. 2013;19:102–5. http://dx.doi.org/10.3201/eid1901.120421

Address for correspondence: Stefano Veraldi, University of Milan, Dermatology Unit, Via Pace 9, 20122 Milan, Italy; email: stefano.veraldi@unimi.it

Erwinia billingiae as Unusual Cause of Septic Arthritis, France, 2017

Isabelle Bonnet, Baptiste Bozzi, Eric Fourniols, Stéphane Mitrovic, Olivia Soulier-Escrihuela, Florence Brossier,[1] Wladimir Sougakoff, Jérôme Robert, Stéphane Jauréguiberry, Alexandra Aubry, on behalf of the Pitié-Salpêtrière Infection Ostéo-articulaire group[2]

Author affiliations: Assistance Publique–Hôpitaux de Paris, Hôpitaux Universitaires Pitié Salpêtrière–Charles Foix, Paris, France (I. Bonnet, B. Bozzi, E. Fourniols, S. Mitrovic, O. Soulier-Escrihuela, F. Brossier, W. Sougakoff, J. Robert, S. Jauréguiberry, A. Aubry); Sorbonne Université, Cimi-Paris, U1135, Paris (I. Bonnet, F. Brossier, W. Sougakoff, J. Robert, A. Aubry)

DOI: https://doi.org/10.3201/eid2508.181073

In 2017 in France, we treated a patient with knee septic arthritis caused by *Erwinia billingiae* after trauma involving a palm tree. This rare pathogen could only be identified through 16S rRNA gene sequencing. For bacterial infections after injuries with plants, 16S rRNA gene sequencing might be required for species identification.

The prevalence of acute septic arthritis in Western Europe is ≈4–10 cases/100,000 inhabitants (*1*). We report a case of posttraumatic knee septic arthritis in an immunocompetent patient in France that was caused by *Erwinia billingiae*, a gram-negative environmental bacterium of the family *Enterobacteriaceae*. We also review the characteristics of *Erwinia* species and infections.

On April 9, 2017, a 65-year-old man with an unremarkable medical history was admitted to an emergency unit in Nice, southern France, for painful right knee swelling that occurred a few hours after a Phoenix palm tree needle pierced the area. The foreign body was partly removed, and the wound was sutured. The patient was discharged without any knee pain and given a prescription for amoxicillin/clavulanic acid (1 g 3×/d for 6 d).

On April 22, the patient was admitted to the emergency unit of our hospital in Paris because of sudden right knee pain and fever. Synovial fluid collected by knee puncture the day of his admission to the orthopedic unit (April 23) contained 118 × 10^9 leukocytes/L, consisting of 64% polymorphonuclear cells, 33% lymphocytes, and 3% other leukocytes; no microorganism could be identified after Gram staining and cultures. A second knee puncture was performed 3 days after admission, and gram-negative rods grew within 2 days solely within the anaerobic blood culture vial (BacT/ALERT SN; bioMérieux, https://www.biomerieux.com). Subcultures of the blood culture vial were positive after 24 hours of incubation at 37°C on blood agar (Trypticase Soy agar + 5% horse blood and Mueller Hinton 2 agar + 5% sheep blood; bioMérieux) and Drigalski agar (BD, https://www.bd.com) under aerobic conditions and chocolate agar (BD) under microaerobic conditions.

Matrix-assisted laser desorption/ionization time-of-flight (MALDI-TOF) mass spectrometry (Bruker Daltonik, https://www.bruker.com) was performed on colonies and failed to correctly identify the species. Therefore, we performed species identification by 16S rRNA amplification and sequencing with primers RNA-S (16S, 5′-AGAGTTTGATCCTGGYTCAG-3′) and RNA-AS (16AS, 5′-CTTTACGCCCARTAAWTCCG-3′) at a hybridization temperature of 52°C. We amplified a 521-bp sequence that matched the *E. billingiae* genome of 2 isolates with 99.4% similarity (GenBank accession nos. JQ929658 and JN175337). Other closely related species displayed lower similarities: *Pantoea rwandensis* (99.0%), *Erwinia persicina* (98.9%), *Pantoea coffeiphila* (98.7%), *Erwinia tasmaniensis* (98.5%), and *Erwinia aphidicola* (98.3%). Following guidelines of the Antibiogram Committee of the French Society for Microbiology (https://www.sfm-microbiologie.org/2019/01/07/casfm-eucast-2019), we tested the *E. billingiae* isolate with the antimicrobial drugs recommended for *Enterobacteriaceae*; the isolate was susceptible to all these drugs, including ampicillin.

Because of the lack of clinical improvement, the joint was washed on day 6 after admission. After this intervention, an empiric antimicrobial drug treatment was started with amoxicillin/clavulanic acid (2 g 3×/d intravenously). Once results of drug susceptibility testing became available (i.e., 10 days after admission), his treatment was switched to cefotaxime (2 g 3×/d intravenously) and ciprofloxacin (500 mg 2×/d orally for 8 d), followed by ciprofloxacin (500 mg 2×/d alone for 38 additional days). Total duration of treatment was 45 days. The clinical evolution of this patient was favorable; he fully recovered and had no relapses up to 1 year after treatment completion.

In the past, some members of the *Erwinia* genus were reassigned to the genera *Enterobacter* or *Pantoea*. *Erwinia* spp. are ubiquitous in the environment, especially in water ecosystems and soils. Plant-associated *Erwinia* species comprise epiphytic nonpathogenic (i.e., *E. billingiae* and *E. tasmaniensis*) and pathogenic (i.e., *E. amylovora* and *E. pyrifoliae*) species. The MALDI-TOF mass spectrometry system failed to identify the bacterium, even though *E. billingiae* is contained in the database for either method used (direct deposit or on-plate formic acid treatment). Future expansion of the database with more spectra will likely improve the performance of the MALDI-TOF mass

[1]Deceased.

[2]Group members are listed at the end of this article.

Table. Case reports from the literature of infection caused by *Erwinia* spp.*

Patient age, y/sex	Type of infection	Inoculated	Published (actual) species name	Identification method†	Antimicrobial drug; treatment duration	Surgery	Clinical evolution	Ref
65/F	SSTI	Yes	*Erwinia* sp.	Biochemical	Penicillin, then penicillin and sulfisoxazole; NA	Yes	Recovered	(*2*)
Adult/F	Peritoneal dialysis fluid infection	No	*Erwinia* strains of the lathyri-herbicola group	Biochemical	NA; NA	No	NA	(*3*)
Adult/F	SSTI	Yes	*Erwinia* strains of the lathyri-herbicola group	Biochemical	Chloramphenicol; NA	No	Recovered	(*3*)
Adult/M	SSTI	Yes	*Erwinia* strains of the lathyri-herbicola group	Biochemical	Ampicillin; NA	No	Recovered	(*3*)
Adult/M	SSTI	Yes	*Erwinia* strains of the lathyri-herbicola group	Biochemical	Penicillin; NA	No	Recovered	(*3*)
Adult/M	Brain abscess	No	*Erwinia* strains of the lathyri-herbicola group	Biochemical	NA; NA	Yes	NA	(*3*)
17/F	Bacteremia	Yes	*Erwinia herbicola*; (*Pantoea agglomerans*)	Biochemical	Streptomycin and penicillin; NA	No	Recovered	(*4*)
17/M	Bacteremia	Yes	*E. herbicola* (*P. agglomerans*)	Biochemical	Cephalothin; NA	No	Recovered	(*4*)
28/M	Bacteremia	Yes	*Erwinia* sp.	Biochemical	Ampicillin then ampicillin and kanamycin; NA	No	Recovered	(*4*)
57/M	Brain abscess	No	*Erwinia* sp.	Biochemical	Penicillin and streptomycin, then ampicillin, then chloramphenicol, then gentamicin; NA	Yes	Recovered	(*5*)
70/M	Endophtalmitis	Yes	*E. herbicola* (*P. gglomerans*)	Biochemical	Cefazolin and gentamicin; 37 d until surgery (NA after surgery)	Yes	Recovered	(*6*)
66/F	UTI	No	*E. herbicola* (*P. agglomerans*)	Biochemical	NA; NA	No	Died	(*7*)
69/F	UTI	No	*E. herbicola* (*P. agglomerans*)	Biochemical	NA; NA	No	Recovered	(*7*)
62/F	UTI	No	*E. herbicola* (*P. agglomerans*)	Biochemical	NA; NA	No	Recovered	(*7*)
46/M	Endocarditis	No	*E. herbicola* (*P. agglomerans*)	Biochemical	Cefotaxime and netilmicin; 6 weeks	No	Recovered	(*8*)
79/F	Cervical lymphadenitis	No	*Erwinia tasmaniensis* (*E. tasmaniensis*	16S rRNA‡	Ciprofloxacin; 2 weeks	Yes	Recovered	(*9*)
40/M	Dermohypodermitis	Yes	*Erwinia billingiae* (*E. billingiae*)	NA	Ciprofloxacin; 14 d	No	Recovered	(*10*)

*NA, not available; ref, reference; SSTI, skin and soft tissue infection; UTI, urinary tract infection.
†Biochemical testing included Kligler iron agar (assess slant, butt, H_2S production), tests for carbohydrate fermentation (adonitol, fructose, galactose, glucose, inositol, lactose, maltose, mannitol, mannose, raffinose, rhamnose, salicin, sorbitol, sucrose, xylose), ONPG (ortho-nitrophenyl-galactosidez) test, gluconate test, gelatin hydrolysis test, tests for nitrate reduction and N_2 production, indole test, methyl red test, Voges–Proskauer test, casein hydrolysis test, citrate utilization test, urease test, catalase test, oxidase test, arginine dihydrolase test, lysine decarboxylase test, ornithine decarboxylase test, lipase test, amylase test, pectinase test, deoxyribonuclease test, lecithinase test, salinity tests (2.5% NaCl, 10.0% NaCl [pH 5.6]), Tetrazolium-Formazan test (TTC [triphenyl tetrazolium chloride]), cetrimide selection agar, tyrosinase test, and tests for carbohydrate assimilation (glucose, acetate, lactate, succinate).
‡*E. tasmaniensis* (98.9%), *E. toletana* (98.8%), and *E. billingiae* (98.1%) (EzTaxon Database, https://everipedia.org/wiki/lang_en/EzTaxon_Database).

spectrometry system for *E. billingiae* identification. Indeed, the database contains fewer spectra of *E. billingiae* (n = 4) than those of frequently encountered species in medical microbiological laboratories, such as *Escherichia coli* (n = 14) and *Staphylococcus aureus* (n = 10).

To further investigate *Erwinia* infections in humans, we reviewed reports available in PubMed published during 1967–2017 written in English by using the keywords "*Erwinia*" and "infection" (Table). Among the 17 cases reported, the sites of infection were diverse, and most (53%, 9/17) cases occurred after a direct inoculation during an injury with a plant (Table). We found no reports of osteoarticular infections with *Erwinia*; the only other *E. billingiae* case reported was a dermohypodermitis

(Table). In that case, as in the case we report here, an injury with a plant was reported.

This case report illustrates the importance of the methods used for bacterial identification to correctly diagnose such infections. Biochemical methods (*2*–*8*) and MALDI-TOF mass spectrometry (as done in our investigation) could result in misidentification. This report highlights the usefulness of analyzing MALDI-TOF mass spectrometry scores before assigning a species identity and sequencing the 16S RNA gene for bacteria not identifiable by conventional methods.

Members of the Pitié-Salpêtrière Infection Ostéo-articulaire Group: Barut Nicolas, Calin Ruxandra, Clarençon Frédéric, Daas Georges, Fautrel Bruno, Fustier Anne, Gandjbakhch Frédérique, Haddad Elie, Khiami Frédéric, Lazennec Jean-Yves, Marchand Maxime, Mercy Guillaume, Metz Carole, Miu Mihaela, Monsel Gentiane, Monzani Quentin, Reubrecht Vanessa, and Zahr Noël.

About the Author

Dr. Bonnet is a clinical microbiologist in the Bacteriology Laboratory, Pitié Salpêtrière–Charles Foix University Hospital, in Paris, France. She is also part of research team 2 (Bacteriology), Centre d'Immunologie et des Maladies Infectieuses, Cimi-Paris, INSERM, U1135, Sorbonne Université, Paris, France. Her research interests relate to microbiology, especially antimicrobial drug resistance, mycobacteria, and infectious disease.

References

1. Mathews CJ, Weston VC, Jones A, Field M, Coakley G. Bacterial septic arthritis in adults. Lancet. 2010;375:846–55. http://dx.doi.org/10.1016/S0140-6736(09)61595-6
2. Slotnick IJ, Tulman L. A human infection caused by an *Erwinia* species. Am J Med. 1967;43:147–50. http://dx.doi.org/10.1016/0002-9343(67)90157-X
3. Gilardi GL, Bottone E, Birnbaum M. Unusual fermentative, gram-negative bacilli isolated from clinical specimens. I. Characterization of *Erwinia* strains of the "lathyri-herbicola group". Appl Microbiol. 1970;20:151–5.
4. von Graevenitz A. *Erwinia* infection from environmental sources. JAMA. 1971;216:1485. http://dx.doi.org/10.1001/jama.1971.03180350061029
5. Wechsler A, Bottone E, Lasser R, Korenman G. Brain abscess caused by an *Erwinia* species: report of a case and review of the literature. Am J Med. 1971;51:680–4. http://dx.doi.org/10.1016/0002-9343(71)90294-4
6. Mason GI, Bottone EJ, Podos SM. Traumatic endophthalmitis caused by an *Erwinia* species. Am J Ophthalmol. 1976;82:709–13. http://dx.doi.org/10.1016/0002-9394(76)90007-6
7. Umenai T, Saitoh Y, Takano S, Shoji E, Tanaka K, Ishida N. Significance of *Erwinia* in the vagina as causative agents of urinary tract infections. Tohoku J Exp Med. 1979;129:103–4. http://dx.doi.org/10.1620/tjem.129.103
8. Williams AJK, Scott RJD, Lightfoot NF. *Erwinia herbicola* as a cause of bacterial endocarditis. J Infect. 1986;12:71–3. http://dx.doi.org/10.1016/S0163-4453(86)94978-9
9. Shin SY, Lee MY, Song J-H, Ko KS. New *Erwinia*-like organism causing cervical lymphadenitis. J Clin Microbiol. 2008;46:3156–8. http://dx.doi.org/10.1128/JCM.00716-08
10. Prod'homme M, Micol LA, Weitsch S, Gassend JL, Martinet O, Bellini C. Cutaneous infection and bactaeremia caused by *Erwinia billingiae*: a case report. New Microbes New Infect. 2017;19:134–6. http://dx.doi.org/10.1016/j.nmni.2017.07.006

Address for correspondence: Alexandra Aubry, AP-HP, Hôpitaux Universitaires Pitié Salpêtrière–Charles Foix, Bactériologie-Hygiène, 47-83 Boulevard de l'Hôpital, Paris 75013, France; email: alexandra.aubry@sorbonne-universite.fr

Chikungunya Fever Outbreak, Zhejiang Province, China, 2017

Junhang Pan,[1] Chunfu Fang,[1] Juying Yan, Hao Yan, Bingdong Zhan, Yi Sun, Ying Liu, Haiyan Mao, Guoping Cao, Lei Lv, Yanjun Zhang, Enfu Chen

Author affiliations: Zhejiang Provincial Center for Disease Control and Prevention, Hangzhou, China (J. Pan, J. Yan, H. Yan, Y. Sun, Y. Liu, H. Mao, Y. Zhang, E. Chen); Quzhou Center for Disease Control and Prevention, Quzhou, China (C. Fang, B. Zhan, G. Cao, L. Lv)

DOI: https://doi.org/10.3201/eid2508.181212

We report a disease outbreak caused by chikungunya virus in Zhejiang Province, China, in August 2017. Phylogenic analysis indicated that this virus belonged to the Indian Ocean clade of the East/Central/South African genotype and was imported by a traveler returning from Bangladesh.

Chikungunya fever is an arboviral disease transmitted between humans and through the bites of infected *Aedes* mosquitoes, specifically the species *Ae. aegypti* and *Ae. albopictus* (*1*). High fever, myalgia, polyarthralgia, and maculopapular rash are typical clinical symptoms of chikungunya fever. However, some chikungunya virus (CHIKV) infections have led to severe clinical symptoms, such as neurologic signs or fulminant hepatitis, which have had a serious effect on human health (*2*).

[1]These authors contributed equally to this article.

CHIKV was isolated in 1952 during a dengue outbreak in Tanzania; a CHIKV outbreak in Asia was reported in Thailand in 1960. Since 2004, CHIKV has caused unexpected large outbreaks in Africa, Asia, and the Americas, becoming a major public health concern throughout the world (*3*). A nonindigenous case of CHIKV infection in mainland China was reported in 1986; no outbreaks resulting from local transmission were reported until the chikungunya outbreaks in Dongguan and Yangjiang regions in Guangdong Province, in southern China, in 2010 (*4*). Three imported cases of CHIKV infection were confirmed in travelers returning from Southeast Asia in Zhejiang Province, eastern China: 2 cases in 2008 and 1 in 2012.

Zhejiang Province is located in eastern China (27°01′–31°10′N, 118°01′–123°08′E) and has a humid subtropical monsoon climate. Its average annual temperature is 15°C–18°C, and it has abundant rainfall, an average of 1,100–2,200 mm annually. The mosquito vector *Ae. aegypti* has not been found in Zhejiang Province, whereas the range of *Ae. albopictus* mosquitoes was distributed around this region (*5*).

Zhejiang Province does not belong to the endemic area of chikungunya; however, we report an outbreak of chikungunya caused by a traveler returning from Bangladesh in August 2017 in Quzhou, Zhejiang Province. The patient with the imported case was living in Huangdun village; another 3 CHIKV infections were confirmed in the same village (Appendix Figure, http://wwwnc.cdc.gov/EID/article/25/8/18-1212-App1.pdf). After the confirmation of these infections, the Quzhou government quickly organized mosquito control measures: granules of fenthion were used to control the mosquito larvae, and the wettable powders of cyfluthrin and cyhalothrin were used to control the adult mosquito. The Breteau index (number of positive containers per 100 houses inspected) in Huangdun village decreased from 114 on August 23 to <20 in 2 days. No

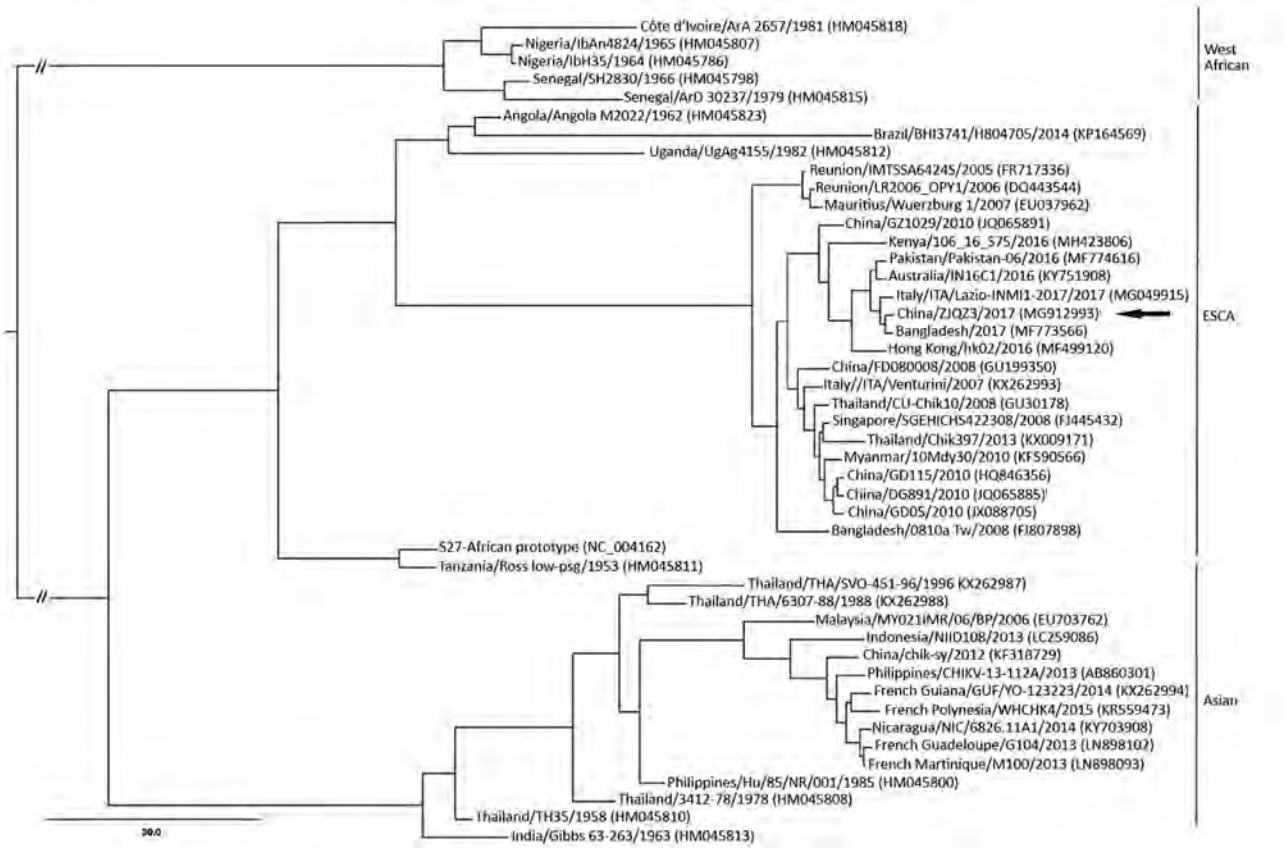

Figure. Phylogenetic analysis of the complete CHIKV genome sequences of isolate ZJQZ3 from Quzhou, Zhejiang Province, China (arrow), and reference sequences. Dataset-specific models that were selected using the Akaike Information Criterion in Modeltest 3.7 (http://darwin.uvigo.es/our-software) were analyzed. Maximum-likelihood (ML) analysis was processed in RAxML v7.2.8 (http://sco.h-its.org/exelixis/software.html). The optimal ML tree and bootstrap percentages (BP) were estimated in the same run. The ML BP values were obtained from 1,000 bootstrap replicates using the rapid bootstrap algorithm. BEAST 1.6 (http://beast.community/programs) was employed to construct a Bayesian maximum clade credibility tree based on an uncorrelated exponential distributed relaxed-clock model for our sample. The genotypes of CHIKV were divided into West African, ECSA, and Asian. Virus lineages are shown at right. GenBank accession numbers are given in parentheses. Scale bar indicates nucleotide substitutions per site. CHIKV, chikungunya virus; ECSA, East/Central/South African.

similar case was reported during the continuous monitoring in hospitals in Quzhou, and serum samples collected from the inhabitants of this village were negative for CHIKV RNA, IgM, and IgG.

We inoculated serum samples of these 4 cases on C6/36 cell lines to isolate CHIKV, and we observed complete cytopathic effects on all incubations. CHIKV RNA was confirmed in these samples; we named these strains ZJQZ3, ZJQZ4, ZJQZ5, and ZJQZ6. Sequence analysis of the CHIKV envelope (E) 1 gene showed that 4 sequences were 100% identical with one another, which indicated that the infected traveler who returned from a disease-endemic area led to this local transmission and outbreak. We sequenced the complete genome sequence of CHIKV ZJQZ3 (11,765 bp; GenBank accession no. MG912993) using Ion Torrent PGM (https://www.thermofisher.com) and performed phylogenetic analysis with 45 worldwide CHIKV strain sequences from GenBank. Results showed that the genome sequence of CHIKV ZJQZ3 was highly similar to the strain (GenBank accession no. MF773566) isolated from a patient in Australia who returned from Bangladesh in 2017 and belongs to the Indian Ocean clade of the East/Central/South African genotype (Figure). However, a large outbreak of chikungunya fever was observed in Dhaka, Bangladesh, during May–August 2017 (*6*). With an increase in global travel, the risk for spreading CHIKV to the regions in which the virus is not endemic has increased.

We observed mutations in E1-M269V, E1-D284E, and nonstructural (ns) gene P3-D372E in CHIKV ZJQZ3 but found no *Ae. albopictus*–adaptive mutations in E1-A226V, E2-L210Q, E2-K252Q, E2-K233E, and E2/E3-R198Q/S18F (*7*–*9*). However, the mutations in E1-A226V, E2-K252Q, E2-L210Q, and E2-V264A were reported previously in some imported cases in China (*10*). The growing genetic diversities observed in each strain suggested that CHIKV will be a major public health threat with the potential for further emergence and spread.

This outbreak indicates that CHIKV can be transmitted by *Ae. albopictus* mosquitoes in Zhejiang Province and may have the potential for further emergence and spread in northern China. Clinicians should be educated about the diagnosis of this disease, and public health organizations should work to overcome the diagnostic challenges of multiple arboviruses, carefully monitor imported cases, strengthen vector control, and conduct surveillance for CHIKV-infected vectors in high-risk areas to prevent local establishment of this new emerging virus.

Acknowledgments

We thank the Qujiang District Center for Disease Control and Prevention for confirming the diagnosis of chikungunya virus infections in this study.

This study was supported by the Key Disciplinary of Health and Family Planning Commission of Zhejiang Province (grant no. CX-9), the Monitor Technology Platform of Infectious Diseases of the State Major Science and Technology Special Projects during the 13th 5-year plan of China (grant no. 2017ZX10103008-002), and the Zhejiang Provincial Program for the Cultivation of High-Level Innovative Health Talents.

About the Author

Dr. Pan is a research scientist at Zhejiang Provincial Center for Disease Control and Prevention, Hangzhou, China, whose research interests are detection and epidemiology of emerging infectious diseases. Dr. Fang is an epidemiologist at Quzhou Center for Disease Control and Prevention, Quzhou, Zhejiang Province, China, whose primary research interests are epidemiology and transmission of viruses associated with emerging infectious diseases.

References

1. Burt FJ, Chen W, Miner JJ, Lenschow DJ, Merits A, Schnettler E, et al. Chikungunya virus: an update on the biology and pathogenesis of this emerging pathogen. Lancet Infect Dis. 2017; 17:e107–17. http://dx.doi.org/10.1016/S1473-3099(16)30385-1
2. Rolph MS, Foo SS, Mahalingam S. Emergent chikungunya virus and arthritis in the Americas. Lancet Infect Dis. 2015;15:1007–8. http://dx.doi.org/10.1016/S1473-3099(15)00231-5
3. Burt FJ, Rolph MS, Rulli NE, Mahalingam S, Heise MT. Chikungunya: a re-emerging virus. Lancet. 2012;379:662–71. http://dx.doi.org/10.1016/S0140-6736(11)60281-X
4. Wu D, Wu J, Zhang Q, Zhong H, Ke C, Deng X, et al. Chikungunya outbreak in Guangdong Province, China, 2010. Emerg Infect Dis. 2012;18:493–5. http://dx.doi.org/10.3201/eid1803.110034
5. Yang T, Fu G. Investigation on the distribution of dengue vector *Aedes albopictus* in Zhejiang Province. Chinese Journal of Hygienic Insecticides and Equipments. 2006;12:189–91.
6. Kabir I, Dhimal M, Müller R, Banik S, Haque U. The 2017 Dhaka chikungunya outbreak. Lancet Infect Dis. 2017;17:1118. http://dx.doi.org/10.1016/S1473-3099(17)30564-9
7. Tsetsarkin KA, Vanlandingham DL, McGee CE, Higgs S. A single mutation in chikungunya virus affects vector specificity and epidemic potential. PLoS Pathog. 2007;3:e201. http://dx.doi.org/10.1371/journal.ppat.0030201
8. Tsetsarkin KA, Weaver SC. Sequential adaptive mutations enhance efficient vector switching by Chikungunya virus and its epidemic emergence. PLoS Pathog. 2011;7:e1002412. http://dx.doi.org/10.1371/journal.ppat.1002412
9. Tsetsarkin KA, Chen R, Yun R, Rossi SL, Plante KS, Guerbois M, et al. Multi-peaked adaptive landscape for chikungunya virus evolution predicts continued fitness optimization in *Aedes albopictus* mosquitoes. Nat Commun. 2014;5:4084. http://dx.doi.org/10.1038/ncomms5084
10. Zheng K, Li J, Zhang Q, Liang M, Li C, Lin M, et al. Genetic analysis of chikungunya viruses imported to mainland China in 2008. Virol J. 2010;7:8. http://dx.doi.org/10.1186/1743-422X-7-8

Address for correspondence: Yanjun Zhang or Enfu Chen, Zhejiang Provincial Center for Disease Control and Prevention, 3399# XinCheng Road, Hangzhou, China; email: yjzhang@cdc.zj.cn or enfchen@cdc.zj.cn

Early Questing by Lone Star Tick Larvae, New York and Massachusetts, USA, 2018

Sam R. Telford III, Joanna Buchthal, Paul Elias

Author affiliations: Tufts University, North Grafton, Massachusetts, USA (S.R. Telford III); Massachusetts Institute of Technology, Cambridge, Massachusetts, USA (J. Buchthal); Naushon Trust, Boston, Massachusetts, USA (P. Elias)

DOI: https://doi.org/10.3201/eid2508.181293

Subtropical lone star tick larvae typically emerge in late summer. We found clusters of host-seeking lone star tick larvae during early June 2018 in New York and Massachusetts, USA. Invasion and persistence of this tick in more northern locations may have been promoted by adaptation to an accelerated life cycle.

Lone star ticks (*Amblyomma americanum*) transmit diverse agents of zoonoses, including human monocytic ehrlichiosis, canine granulocytic ehrlichiosis, Rocky Mountain spotted fever, and tularemia. Their bites also may induce erythema migrans, for which the etiology remains elusive (*1*) and which seems to be the cause of red meat (alpha-gal [galactose-α-1,3-galactose]) allergy.

The distribution and abundance of these ticks in the United States have recently expanded; specimens have been collected from the upper Midwest and New England (*2*,*3*). However, proof of stable infestations at most of these locations remains to be published. Before the 1990s, the known northern limit for dense infestations in the eastern United States was New Jersey (*4*), although since the late 1980s, a relict stable population of lone star ticks has been present on Prudence Island, Rhode Island (*5*), and on Fire Island, eastern Long Island, New York (*6*). Unlike the ticks on Long Island, those on Prudence Island have remained confined there, with no spread to the nearby mainland. Models suggest that climate change could facilitate the introduction of this subtropical tick into more northern locations (*3*) because temperature and relative humidity are the main drivers for the developmental cycle. In the past 5 years, we have found focal persisting lone star tick infestations (documentation of larvae, nymphs, and adults each year for 3 years) on Cape Cod, the Elizabeth Islands, Martha's Vineyard, and Tuckernuck Island (all in Massachusetts), which, to our knowledge, is the northernmost established population of this tick.

Across their wide distribution south of New York, adult lone star ticks seek hosts mid-March through late June; nymphs, mid-May through late July; and larvae, July through September (*7*). Fed larvae and nymphs overwinter and molt to nymphs and adults, respectively, the following spring. Of note, female engorgement may be suppressed until mid-May, perhaps associated with a photoperiodically regulated diapause (*8*), which would enable egg masses to be deposited during optimal temperatures and humidity. Fed females oviposit soon after engorgement, and in most locations, resulting larvae seek hosts from July through September. A comprehensive simulation model based on existing reports of lone star tick phenology (*7*) suggested a threshold of 17°C for larval host seeking. On Long Island and in New Jersey, larvae were most commonly found in August (*4*,*6*). Lone star tick larvae seem to feed mainly during late summer and early fall.

During standard drag sampling for deer tick (*Ixodes dammini*) nymphs on June 7, 2018, in New Suffolk, Long Island, New York, and on June 18, 2018, on Naushon Island, Massachusetts, we identified well-defined clusters (≈6 cm diameter) of unusual host-seeking tick larvae. Three clusters were found during 10 person-hours of dragging at the New York site and 2 clusters during 6 hours of dragging at the Massachusetts site; all clusters contained >100 larvae. Lone star tick adults and nymphs accounted for >95% of all ticks collected from these sites; the rest were deer tick nymphs and American dog tick (*Dermacentor variabilis*) adults. The clusters of larvae (Figure,

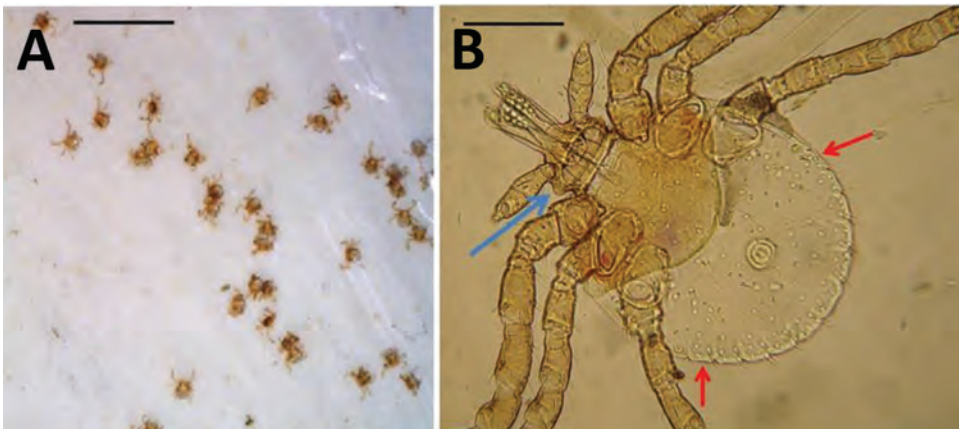

Figure. Larvae of lone star ticks collected from New York and Massachusetts, USA, in 2018. A) Portion of lint roller tape with cluster of larval lone star ticks. Scale bar indicates 10 mm. B) Rounded idiosoma, 11 festoons (short dark arrow marks festoon 1; longer dark arrow, festoon 11); rounded edge of the basis capitulum (long light arrow), and palps longer than wide. Scale bar indicates 210 microns.

panel A) were reminiscent of those of lone star ticks typically encountered during August or September on Prudence Island, but tick collection there on June 4, 2018 (9 person-hours), where these ticks have long been endemic (*5*), did not find any such clusters. Samples of larvae from New Suffolk and Naushon Island were collected on masking tape lint rollers for definitive identification. We removed larvae from the masking tape and examined them by microscopy at ×100 magnification. The presence of 11 festoons, long palpi, rounded lateral basis capitulum, and the general circular body morphology (Figure, panel B) confirmed that the samples were larval lone star ticks and not any other ticks that are common in southern New England, including deer ticks, American dog ticks (the subadults of which cannot be collected by drag sampling), winter ticks (*Dermacentor albipictus*), *Ixodes dentatus* ticks, and rabbit ticks (*Haemaphysalis leporispalustris*).

Larval lone star ticks are typically found seeking hosts only in late summer. We are aware of only 1 report of early larval activity, in which infestation of white-footed mice (*Peromyscus leucopus*, a very unusual host for this tick) was detected in March and June at a New Jersey site (*4*). The Prudence Island tick population has been studied since the early 1990s (*9*), with sampling every year during June and other months, and host-seeking lone star tick larvae have not been found before August. The recent expanded range of lone star ticks into sites previously considered too cold to allow for the developmental cycle may be partly because of a new tick lineage that may develop unusually rapidly. The biological basis for the expanding range of this invasive vector species accordingly may include selection (*10*) for a more plastic phenology and for increasingly permissive weather at the edge of its range. This fundamental change may facilitate the invasion and establishment of an aggressive human-biting disease vector, which may increase risk for diverse tickborne infections.

This study was supported by a grant from the Rainwater Foundation (Mice Against Ticks project).

About the Author

Dr. Telford is professor of Infectious Disease and Global Health and director of the New England Regional Biosafety Laboratory at the Cummings School of Veterinary Medicine, Tufts University. His research focuses on the epidemiology and ecology of tickborne infections.

References

1. Childs JE, Paddock CD. The ascendancy of *Amblyomma americanum* as a vector of pathogens affecting humans in the United States. Annu Rev Entomol. 2003;48:307–37. http://dx.doi.org/10.1146/annurev.ento.48.091801.112728
2. Keirans JE, Lacombe EH. First records of *Amblyomma americanum*, *Ixodes* (*Ixodes*) *dentatus*, and *Ixodes* (*Ceratixodes*) *uriae* (Acari: Ixodidae) from Maine. J Parasitol. 1998;84:629–31. http://dx.doi.org/10.2307/3284739
3. Springer YP, Eisen L, Beati L, James AM, Eisen RJ. Spatial distribution of counties in the continental United States with records of occurrence of *Amblyomma americanum* (Ixodida: Ixodidae). J Med Entomol. 2014;51:342–51. http://dx.doi.org/10.1603/ME13115
4. Schulze TL, Bowen GS, Lakat MF, Parkin WE, Shisler JK. Seasonal abundance and hosts of *Ixodes dammini* (Acari: Ixodidae) and other ixodid ticks from an endemic Lyme disease focus in New Jersey, USA. J Med Entomol. 1986;23:105–9. http://dx.doi.org/10.1093/jmedent/23.1.105
5. Mather TN, Mather ME. Intrinsic competence of three ixodid ticks (Acari) as vectors of the Lyme disease spirochete. J Med Entomol. 1990;27:646–50. http://dx.doi.org/10.1093/jmedent/27.4.646
6. Ginsberg HS, Ewing CP. Habitat distribution of *Ixodes dammini* (Acari: Ixodidae) and Lyme disease spirochetes on Fire Island, New York. J Med Entomol. 1989;26:183–9. http://dx.doi.org/10.1093/jmedent/26.3.183
7. Haile DG, Mount GA. Computer simulation of population dynamics of the lone star tick, *Amblyomma americanum* (Acari: Ixodidae). J Med Entomol. 1987;24:356–69. http://dx.doi.org/10.1093/jmedent/24.3.356
8. Patrick CD, Hair JA. Seasonal abundance of Lone Star ticks on white-tailed deer. Environ Entomol. 1977;6:263–9. http://dx.doi.org/10.1093/ee/6.2.263
9. Armstrong PM. Pathogen diversity at the tick-human interface [dissertation]. Boston (MA): Harvard School of Public Health; 1998.
10. Monzón JD, Atkinson EG, Henn BM, Benach JL. Population and evolutionary genomics of *Amblyomma americanum*, an expanding arthropod disease vector. Genome Biol Evol. 2016;8:1351–60. http://dx.doi.org/10.1093/gbe/evw080

Address for correspondence: Sam R. Telford III, IDGH/Tufts, 200 Westboro Rd, North Grafton, MA 01536, USA; email: sam.telford@tufts.edu

Molecular Genotyping of Hepatitis A Virus, California, USA, 2017–2018

William S. Probert, Carlos Gonzalez,[1] Alex Espinosa, Jill K. Hacker

Author affiliation: California Department of Public Health, Richmond, California, USA

DOI: https://doi.org/10.3201/eid2508.181489

We implemented subgenomic and whole-genome sequencing to support the investigation of a large hepatitis A virus outbreak among persons experiencing homelessness, users of illicit drugs, or both in California, USA, during 2017–2018. Genotyping data helped confirm case-patients, track chains of transmission, and monitor the effectiveness of public health control measures.

The United States has seen a resurgence of hepatitis A virus (HAV) infections; several states have reported outbreaks of HAV subgenotype IB, primarily among persons experiencing homelessness and users of illicit drugs (*1*). In California, during November 2016–May 2018, an outbreak of HAV IB infections resulted in 708 case-patients, 465 hospitalizations, and 21 deaths (*1*; https://www.cdph.ca.gov/Programs/CID/DCDC/CDPH%20Document%20Library/Immunization/2016-18CAOutbreakAssociatedDrugUse-Homelessness.pdf). To better respond to the surge in hepatitis A cases and facilitate vaccine acquisition and distribution, California declared a public health emergency in October 2017 (*2*). As part of this response, the California Department of Public Health implemented molecular genotyping of HAV to support epidemiologic investigation of suspect cases.

We requested serum samples for symptomatic, HAV IgM–positive case-patients from local public health jurisdictions for genotyping. We amplified a segment of the HAV viral protein 1–amino terminus of 2B (VP1–P2B) genomic region by using nested reverse-transcription PCR and performed sequencing on 160 specimens collected during August 2017–May 2018 (*3*; Appendix, https://wwwnc.cdc.gov/EID/article/25/8/18-1489-App1.pdf). HAV subgenotype classification by VP1–P2B sequence yielded 48 IA-positive, 109 IB-positive, and 3 IIIA-positive specimens (Figure, panel A). We identified 19 unique HAV IA VP1–P2B sequences with an overall average genetic distance of 0.043 nt substitutions per site. Eighteen (37.5%) HAV IA specimens yielded sequences that matched 2 sequences (VRD_521_2016 and RIVM-HAV16–090), previously associated with HAV outbreaks among men who have sex with men (MSM) (*4*,*5*). All 18 case-patients were male, and all but 1 identified as MSM.

We identified 11 unique VP1–P2B sequences with an overall average genetic distance of 0.014 nt substitutions per site among the HAV IB specimens. Phylogenetic analysis indicated 2 distinct HAV IB clusters: 1 cluster of 9 closely related sequences (CA IB cluster) identified from 107 California patients, and 1 cluster of 2 specimens matching sequences associated with a concomitant outbreak in Michigan (MI IB cluster) (*1*; Figure). Both case-patients with MI IB strains reported traveling to Michigan during the probable period of exposure. A search of GenBank and Hepatitis A Laboratory Network databases failed to reveal any exact matches to the CA and MI IB outbreak sequences (*6*; https://www.rivm.nl/en/Topics/H/HAVNET). However, Hepatitis A Laboratory Network sequence similarity analysis showed that the CA IB strains were most closely related to strains found in the Middle East and the MI IB strains to strains found in East Africa (data not shown). Three specimens with unique VP1–P2B sequences were classified as subgenotype IIIA, a genotype rarely reported in the United States (*7*). Two of these IIIA sequences (V17S07440 and V18S00013) shared 99.1% and 99.7% sequence identity, respectively, with strains from a 2018 outbreak in Denmark associated with dates imported from Iran (S. Midgley, Statens Serum Institut, Denmark, pers. comm., email, 2018 Aug 22). Neither of those case-patients had traveled internationally or had other known HAV risk factors within their exposure period. However, 1 case-patient had consumed dates from Iran, and the other reported eating dates from a local Middle Eastern grocery store.

We processed selected specimens representing the major IB VP1–P2B sequence variants for whole-genome sequencing (Appendix). Whole-genome sequencing of HAV can provide higher resolution strain typing than sequencing of short subgenomic regions (*8*). We deposited nearly complete genome sequences (7,306 nt) for strains representing the CA and MI outbreaks in GenBank (accession nos. MH577308–14). Phylogenetic comparison with other IB genome sequences in GenBank confirmed that the CA and MI IB outbreak sequences represented distinct clades (Figure, panel B). The CA IB outbreak strains shared 95.5%–95.6% nt and 99.7% aa sequence identity with the HAV IB reference strain, HM175. Similarly, the MI IB outbreak strains shared 95.8% nt and 99.6% aa sequence identity with HM175.

We rapidly implemented genotyping to help guide the public health response to a surge in reported HAV infection cases in California. Paired with epidemiologic data, genotyping information was used to confirm cases, distinguish outbreak-related cases from sporadic cases, track modes and chains of transmission, and identify populations at increased risk for infection. Our study revealed

[1]Current affiliation: Sonoma County Public Health Laboratory, Santa Rosa, California, USA.

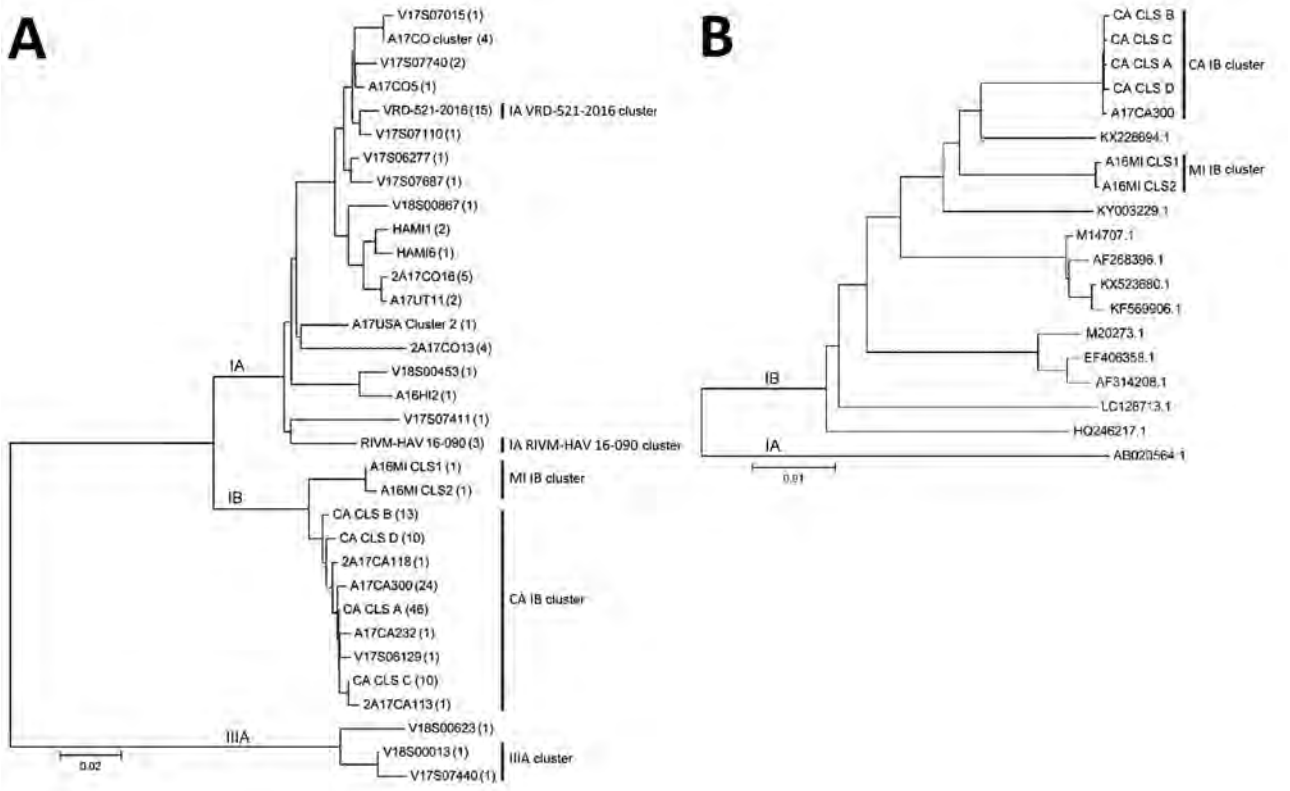

Figure. Phylogenetic analysis of HAV sequences from California, USA, and reference sequences. A) Comparison of VP1–P2B sequences obtained for 160 specimens. The number of specimens represented by each VP1–P2B sequence is indicated within parentheses. B) Comparison of nearly complete genome sequences (7,306 nt) for representative subgenotype IB cluster strains with HAV IB strain sequences found in GenBank. The genome sequence (M14707.1) represents the IB reference strain (HM175). A HAV subgenotype IA sequence (AB020564.1) was used as outlier for the analysis of the nearly complete genome sequences. Sequence alignments were performed with ClustalW (http://www.clustal.org), and the dendrograms were generated using the neighbor-joining algorithm and Kimura 2-parameter evolutionary model. Dendrogram branches corresponding to subgenotype lineage are labeled. Identified clusters of HAV are shown to the right of each dendrogram. HAV, hepatitis A virus. Scale bars indicate evolutionary distance.

several phylogenetic clusters of HAV. A large cluster of IB strains was confirmed as the primary cause of an outbreak that was chiefly transmitted person-to-person and was associated with risk factors of homelessness and illicit drug use (*1*). Genetically similar strains and risk factors have since been described for outbreaks in other states (*1*). Partly because of these outbreaks, hepatitis A vaccination was recently recommended for persons experiencing homelessness; recommendations for vaccination of users of injection and noninjection drugs were established in 1996 (*9*,*10*). By April 2018, implementation of public health control measures, including educational awareness and targeted vaccination and environmental remediation, reduced the number of reported HAV infection cases to baseline levels in California.

Limitations of our investigation were the paucity of archival genotyping data from California for strain comparisons and the lack of genotyping capabilities during early stages of the IB outbreak. Sustained public health laboratory capacity for HAV genotyping, along with diligent epidemiologic surveillance, offer the opportunity to detect outbreaks earlier and monitor the effectiveness of prevention and control efforts in California.

Acknowledgments

We gratefully acknowledge Sumathi Ramachandran and Guo-liang Xia for initially identifying the IB clusters and for their technical support in implementing VP1–P2B genotyping. We are also grateful for the epidemiological and data support provided by Monique Foster and Jennifer Zipprich, Rosie Glenn-Finer, Cynthia Yen, and Maria Salas.

About the Author

Dr. Probert is a senior microbiologist at the Viral and Rickettsial Disease Laboratory, California Department of Public Health. His research focuses on the development of molecular diagnostic tools for the detection of infectious agents.

References

1. Foster M, Ramachandran S, Myatt K, Donovan D, Bohm S, Fiedler J, et al. Hepatitis A virus outbreaks associated with drug use and homelessness—California, Kentucky, Michigan, and Utah, 2017. MMWR Morb Mortal Wkly Rep. 2018;67:1208–10. http://dx.doi.org/10.15585/mmwr.mm6743a3
2. Office of the Governor of California. Governor Brown declares state of emergency to increase supply of hepatitis A vaccines [cited 2018 Jul 23]. https://www.ca.gov/archive/gov39/2017/10/13/news20018/index.html
3. Hutin YJF, Pool V, Cramer EH, Nainan OV, Weth J, Williams IT, et al.; National Hepatitis A Investigation Team. A multistate, foodborne outbreak of hepatitis A. N Engl J Med. 1999;340:595–602. http://dx.doi.org/10.1056/NEJM199902253400802
4. Beebeejaun K, Degala S, Balogun K, Simms I, Woodhall SC, Heinsbroek E, et al. Outbreak of hepatitis A associated with men who have sex with men (MSM), England, July 2016 to January 2017. Euro Surveill. 2017;22:30454. http://dx.doi.org/10.2807/1560-7917.ES.2017.22.5.30454
5. Freidl GS, Sonder GJ, Bovée LP, Friesema IH, van Rijckevorsel GG, Ruijs WL, et al. Hepatitis A outbreak among men who have sex with men (MSM) predominantly linked with the EuroPride, the Netherlands, July 2016 to February 2017. Euro Surveill. 2017;22:30468. http://dx.doi.org/10.2807/1560-7917.ES.2017.22.8.30468
6. Clark K, Karsch-Mizrachi I, Lipman DJ, Ostell J, Sayers EW. GenBank. Nucleic Acids Res. 2016;44(D1):D67–72. http://dx.doi.org/10.1093/nar/gkv1276
7. Nainan OV, Armstrong GL, Han XH, Williams I, Bell BP, Margolis HS. Hepatitis a molecular epidemiology in the United States, 1996–1997: sources of infection and implications of vaccination policy. J Infect Dis. 2005;191:957–63. http://dx.doi.org/10.1086/427992
8. Vaughan G, Xia G, Forbi JC, Purdy MA, Rossi LMG, Spradling PR, et al. Genetic relatedness among hepatitis A virus strains associated with food-borne outbreaks. PLoS One. 2013;8:e74546. http://dx.doi.org/10.1371/journal.pone.0074546
9. Doshani M, Weng M, Moore KL, Romero JR, Nelson NP. Recommendations of the Advisory Committee on Immunization Practices for use of hepatitis A vaccine for persons experiencing homelessness. MMWR Morb Mortal Wkly Rep. 2019;68:153–6. http://dx.doi.org/10.15585/mmwr.mm6806a6
10. CDC. Prevention of hepatitis A through active or passive immunization: recommendations of the Advisory Committee on Immunization Practices (ACIP). MMWR Recomm Rep. 1996;45(No. RR-15):1–30.

Address for correspondence: William S. Probert, California Department of Public Health, Viral and Rickettsial Disease Laboratory, 850 Marina Bay Pkwy, Richmond, CA 94804, USA; email: will.probert@cdph.ca.gov

Crimean-Congo Hemorrhagic Fever, Herat Province, Afghanistan, 2017

Aziz-ur-Rahman Niazi, Mohammad Jawed Jawad, Ahmad Amirnajad, Peter A. Durr, David T. Williams

Author affiliations: Herat University, Herat, Afghanistan (A.-u.-R. Niazi, M.J. Jawad); Department of Public Health, Herat (A. Amirnajad); CSIRO, Australian Animal Health Laboratory, Geelong, Victoria, Australia (P.A. Durr, D.T. Williams)

DOI: https://doi.org/10.3201/eid2508.181491

We studied the clinical and epidemiologic features of an outbreak of Crimean-Congo hemorrhagic fever in Herat Province, Afghanistan. The study comprised 63 patients hospitalized in 2017. The overall case-fatality rate was 22.2%; fatal outcome was significantly associated with a negative IgM test result, longer prothrombin time, and nausea.

Crimean-Congo hemorrhagic fever (CCHF) is a geographically widespread tickborne disease caused by the CCHF virus (genus *Orthonairovirus*, family *Nairoviridae*). In humans, CCHF is associated with a case-fatality rate (CFR) of 5%–50% (*1*) and is considered a major public health threat (*2*).

CCHF cases were first reported in Afghanistan in 1998; no additional cases were reported until 2007 (*3*). During 2007–2016, the Afghanistan Ministry of Public Health documented 478 cases, of which Herat Province accounted for 263 (55.0%) (*4*). In 2017, an unusual increase in CCHF cases occurred in Afghanistan, mostly in Herat Province (Appendix Figures 1, 2, https://wwwnc.cdc.gov/EID/article/25/8/18-1491-App1.pdf). We analyzed the clinical and epidemiologic features of this outbreak.

A descriptive case series study at Herat Regional Hospital during January–December 2017 was undertaken. Clinical and epidemiologic features of all confirmed and probable CCHF cases were recorded. The Human Ethics Committee of Herat University approved the study protocol (approval #0317).

The first recorded case in this study occurred in a 90-year-old male farmer who visited Herat Regional Hospital on May 5. Later, more patients sought care for acute febrile syndrome matching the World Health Organization CCHF case definition (*5*). A total of 64 patients sought care for CCHF signs and symptoms over a 6-month period, of whom 1 did not consent to hospitalization and left the hospital without medical consultation.

Patients' venous blood samples were examined for levels of leukocytes, thrombocytes, aspartate aminotransferase, alanine aminotransferase, prothrombin time (PT), and activated partial thromboplastin time. Samples were also tested for CCHV IgM (VectoCrimea-CHF-IgM ELISA, Vector-Best, https://www.vector-best.ru) or viral RNA (RealStar CCHFV RT-PCR Kit, Altona Diagnostics, https://www.altona-diagnostics.com). We tested for an association among epidemiologic, clinical, and laboratory variables and clinical outcome for each patient (i.e., death or recovery) using Fisher exact test and a confirmatory multivariate logistic regression within R v3.5.0 (https://www.r-project.org).

Of the 63 patients, 32 were both IgM and PCR positive. Thirty-one patients were IgM-negative (Appendix Table 1); however, because of a positive PCR result (26 patients) or CCHF-specific clinical features (5 patients), these patients were included in this study. Thirty-eight (60.3%) patients were male (Appendix Table 2). Overall mean (± SD) age was 35.4 (± 20.0) years (range 9–90 years). Most (69.8%) patients were 11–40 years of age. The occupational groups most often affected were housewives (23 [36.5%] patients) and farmers (14 [22.2%]). Butchers accounted for 7 (11.1%) and shepherds for 3 (4.8%) cases; the remaining 16 (25.4%) patients had other occupations. Eighteen (28.6%) patients lived in the city, and 45 (71.4%) lived in rural areas. Three (4.8%) patients stated a history of tick bite, and 60 (95.2%) had prior contact with livestock or animal tissues.

Table. Laboratory findings and clinical and hemorrhagic features for patients hospitalized with Crimean-Congo hemorrhagic fever, Herat Province, Afghanistan, 2017*

Characteristic	No. (%) patients, N = 63
Laboratory	
Thrombocytopenia†	63 (100.0)
Leukopenia	62 (98.4)
AST‡	43 (68.3)
ALT§	43 (68.3)
Longer PT	29 (46.0)
Longer aPTT	23 (36.5)
Clinical features	
Fever	63 (100.0)
Headache	59 (93.7)
Myalgia	53 (84.1)
Fatigue	51 (81.0)
Abdominal pain	17 (27.0)
Nausea	15 (23.8)
Vomiting	9 (14.3)
Type of hemorrhage	
Ecchymosis	42 (66.7)
Epistaxis	36 (57.1)
Hemoptysis	12 (19.1)
Hematemesis	10 (15.9)
Melana	7 (11.1)
Petechia	4 (6.4)
Gum bleeding	3 (4.8)

*ALT, alanine aminotransferase; aPTT, activated partial thromboplastin time; AST, aspartate aminotransferase; PT, prothrombin time.
†<50 × 10^9/L (reference 150–450 × 10^9/L) (*6*).
‡>200 U/L (reference 5–40 U/L) (*7*).
§>150 U/L (reference 7–56 U/L) (*7*).

The most frequent clinical manifestations were fever, headache, and myalgia, and the most common hemorrhagic manifestations were ecchymosis, epistaxis, and hemoptysis. At admission, all patients had thrombocytopenia, and 62 (98.4%) had leukopenia. Aspartate aminotransferase and alanine aminotransferase levels were elevated in 43 (68.3%) patients. PT time was longer than normal in 29 (46.0%) and activated partial thromboplastin in 23 (36.5%) patients (Table).

All cases occurred during May–October; cases peaked during June–September (Appendix Figure 2). The average time (± SD) between onset of clinical manifestations and patients' referral to hospital was 4.9 (± 1.6) days; (range 0–9 days). The overall CFR was 22.2% (14/63 patients); the CFR for men was 18.4% (7/38) and for women, 28.0% (7/25). Fatal outcome was significantly associated with a negative IgM test result ($p = 0.016$), longer PT ($p = 0.038$), and nausea ($p = 0.015$).

A previous study established that CCHF patients who die rarely mount a detectable IgM response, and laboratory diagnosis should therefore include reverse transcription PCR (*8*). A positive association of death with longer PT also has been previously described (*9*). A new finding from this study was the association between fatal outcome and nausea.

Our findings are important for persons in Afghanistan, especially in Herat Province, because the study identified demographic variables (age and occupation) that can be further investigated by a risk factor study. Our findings also are important for persons traveling to Herat Province. Only 1 CCHF case has thus far been reported in a tourist returning home from northwestern Afghanistan, where the disease was acquired (*10*). Our findings can also be used to refine the CCHF case definition for improved clinical awareness in Afghanistan.

Our study demonstrates that Herat Province remains the endemic focus of CCHF in Afghanistan, and the number of cases is increasing over time. Control and mitigation measures implemented for CCHF in Herat have not been successful in containing this fatal disease. Considering the major social and economic consequences and the health burden CCHF places on the community, alternative or enhanced public health measures, including improved surveillance and risk communication, are necessary to control CCHF in Herat and neighboring provinces. Our findings might serve as a template and reference for future CCHF surveillance activities in this region.

About the Author

Dr. Niazi is head of the Department of Public Health and Infectious Diseases in the Faculty of Medicine, Herat University. His primary research interests include public health and emerging infectious diseases, with a focus on vectorborne viral diseases.

References

1. Shayan S, Bokaean M, Shahrivar MR, Chinikar S. Crimean-Congo hemorrhagic fever. Lab Med. 2015;46:180–9. http://dx.doi.org/10.1309/LMN1P2FRZ7BKZSCO
2. Mertens M, Schmidt K, Ozkul A, Groschup MH. The impact of Crimean-Congo hemorrhagic fever virus on public health. Antiviral Res. 2013;98:248–60. http://dx.doi.org/10.1016/j.antiviral.2013.02.007
3. Mustafa ML, Ayazi E, Mohareb E, Yingst S, Zayed A, Rossi CA, et al. Crimean-Congo hemorrhagic fever, Afghanistan, 2009. Emerg Infect Dis. 2011;17:1940–1. http://dx.doi.org/10.3201/eid1710.110061
4. Niazi A-u-R. Clinical epidemiology of Crimean-Congo hemorrhagic fever in west region of Afghanistan. Herat (Afghanistan): Herat University Press; 2017.
5. World Health Organization. Communicable disease profile. Afghanistan and neighboring countries. January 2002 [cited 2012 Apr 17]. https://www.who.int/diseasecontrol_emergencies/toolkits/Afghanistan_profile.pdf
6. Hui P, Cook DJ, Lim W, Fraser GA, Arnold DM. The frequency and clinical significance of thrombocytopenia complicating critical illness: a systematic review. Chest. 2011;139:271–8. http://dx.doi.org/10.1378/chest.10-2243
7. Swanepoel R, Gill DE, Shepherd AJ, Leman PA, Mynhardt JH, Harvey S. The clinical pathology of Crimean-Congo hemorrhagic fever. Rev Infect Dis. 1989;11(Suppl 4):S794–800. http://dx.doi.org/10.1093/clinids/11.Supplement_4.S794
8. Tezer H, Polat M. Diagnosis of Crimean-Congo hemorrhagic fever. Expert Rev Anti Infect Ther. 2015;13:555–66. http://dx.doi.org/10.1586/14787210.2015.1021782
9. Bastug A, Kayaaslan B, Kazancioglu S, Aslaner H, But A, Akinci E, et al. Crimean-Congo hemorrhagic fever: prognostic factors and the association of leukocyte counts with mortality. Jpn J Infect Dis. 2016;69:51–5. http://dx.doi.org/10.7883/yoken.JJID.2014.566
10. Chamberlain J, Atkinson B, Logue CH, Latham J, Newman ENC, Hewson R. Genome sequence of ex-Afghanistan Crimean-Congo hemorrhagic fever virus SCT strain, from an imported United Kingdom case in October 2012. Genome Announc. 2013;1:e00161–13. http://dx.doi.org/10.1128/genomeA.00161-13

Address for correspondence: David T. Williams, CSIRO, Australian Animal Health Laboratory, 5 Portarlington Rd, Geelong, VIC 3220, Australia; email: d.williams@csiro.au

Prolonged Zika Virus RNA Detection in Semen of Immunosuppressed Patient

Christina Petridou, David Bonsall, Aleem Ahmed, Mark Roberts, Carolyn Bell, Mariateresa de Cesare, Rory Bowden, Victoria Graham, Daniel Bailey, Andrew Simpson, Emma Aarons

Author affiliations: Rare and Imported Pathogens Laboratory, Public Health England Porton, Salisbury, UK (C. Petridou, V. Graham, D. Bailey, A. Simpson, E. Aarons); University of Oxford, Oxford, UK (D. Bonsall, M. de Cesare, R. Bowden); Leicester Royal Infirmary, Leicester, UK (A. Ahmed); Worcestershire Royal Hospital, Worcester, UK (M. Roberts); South Warwickshire National Health System Foundation Trust, Warwick, UK (C. Bell)

DOI: https://doi.org/10.3201/eid2508.181543

Zika virus RNA has been detected in semen samples collected ≤370 days after symptom onset. We report unusual persistence of Zika virus RNA in semen, confirmed by sequencing at 515 days after symptom onset and detectable for >900 days, in a patient with immunosuppression.

Detection of Zika virus RNA in semen was described previously in an immunocompetent man 370 days after symptom onset; envelope and precursor of M protein gene sequencing indicated high genetic stability in semen 3–4 months after symptom onset (*1*). We report detection of Zika virus RNA in semen over a longer period in a 43-year-old immunosuppressed man in the United Kingdom.

The patient has multicentric reticulohistiocytosis (MRH), a rare rheumatologic condition, which was diagnosed in 2015. When MRH was diagnosed, the patient had multiple pruritic, firm papules and nodules on his face and neck. He also had lesions with a characteristic coral bead appearance at periungal sites. In addition, he had severe joint pain and stiffness affecting his hands and knees and drenching sweats. His MRH diagnosis was confirmed by testing of a punch biopsy of a lesion. He was HIV negative, and his immunoglobulin levels and immunoglobulin electrophoresis results were normal. He was initially treated with topical steroids and antihistamines, but he only had limited relief. He was prescribed oral steroids and required high doses to control his symptoms. Clinicians added methotrexate and hydroxychloroquine to his medications as steroid-sparing agents and to reduce the chance his MRH would progress to erosive disease.

Table. Serial Zika virus genome sequence and culture results from semen of a patient with immunosuppression, United Kingdom*

Sample no.	Days after symptom onset	RT-PCR C_t value†	Sequence coverage, %‡	Average read depth	Sequencing platform§	Mutations detected	Culture result
1	13	19	99.9 (min depth 2), 88.4 (min depth 40)	386.9	MinION	Reference	Frozen sample: unsuccessful
2	46	26	ND		NA	NA	Fresh sample: unsuccessful
3	167	Subthreshold	ND		NA	NA	ND
4	194	No RNA detected¶	ND		NA	NA	ND
5	241	31	Unsuccessful		NA	NA	ND
6	257	34	44 (min depth 2), 0 (min depth 40)	3.3	MinION	None	Frozen sample: unsuccessful
7	278	No RNA detected¶	ND		NA	NA	ND
8	326	26	76 (min depth 2), 6 (min depth 40)	13.2	MinION	None	Fresh sample: unsuccessful
9	396	29	ND		NA	NA	ND
10	515	24	98.1 (min depth 5)	33.3	MiSeq	K3272E, Syn2921	Fresh sample: unsuccessful
11	687	39	ND		NA	NA	ND
12	941	32	ND		NA	NA	ND

*C_t, cycle threshold; min, minimum; NA, not applicable; ND, not done; RT-PCR, reverse transcription PCR.
†Before PCR, nucleic acid was extracted from samples 1–7 using the EZ1 Virus Mini Kit (QIAGEN, https://www.qiagen.com). Samples 8–12 were extracted using the MagNA Pure 96 DNA and Viral NA Small Volume Kit (LifeScience-Roche Diagnostics Corporation, https://lifescience.roche.com). C_t values <40 with acceptable amplification curves are interpreted as positive, but results for samples with C_t values >35 are confirmed by reextraction and repeat PCR in triplicate, where possible.
‡Conservative read-depth thresholds were selected for comparative analyses of the day 13 (sample 1) and day 515 (sample 10) consensus genomes.
§MinION (Oxford Nanopore Technologies, https://nanoporetech.com); MiSeq (Illumina, https://www.illumina.com).
¶Confirmed on reextraction and repeat PCR testing.

In April 2016, seven months after starting his disease-modifying antirheumatic drugs, the patient experienced fever and a new widespread maculopapular rash. He had returned to the United Kingdom from Brazil 7 days before. We detected Zika virus RNA in plasma taken 1 day after symptom onset by using real-time reverse transcription PCR methods described by Pyke et al. (*2*), with modifications (Appendix, http://wwwnc.cdc.gov/EID/article/25/8/18-1543-App1.pdf). We did not detect Zika virus nonstructural protein 1–specific antibodies by ELISA (EUROIMMUN, https://www.euroimmun.com) in initial samples, but we noted seroconversion on day 13 (Appendix Figure). After diagnosing Zika virus infection, clinicians stopped the patient's methotrexate and hydroxychloroquine, but he remained on prednisolone to prevent a flare-up of his MRH (Appendix Figure). The patient's clinical course of Zika virus infection was unremarkable.

A previous study reported that Zika virus RNA was detected in several semen samples taken within 6 months of symptom onset (*3*). We tested subsequent semen samples from this patient and found Zika virus RNA persisted at a viral load sufficient for sequencing 515 days after symptom onset (Table; Appendix Figure). To date, Zika virus RNA remains detectable in further semen samples, although at higher cycle threshold values (Table). The patient remains asymptomatic for Zika virus infection despite persistent detection of Zika virus RNA in his semen.

We attempted viral culture on multiple semen samples, as previously described (*3*), but were unsuccessful (Table). We constructed sequencing libraries from total seminal plasma-extracted RNA enriched by using a panel of oligonucleotide probes, 120 nt in length, designed to capture all known Asian Zika virus strains, according to previously described methods (*4*). We prepared libraries for previously collected semen samples from before day 326 and sequenced these using MinION (Oxford Nanopore Technologies, https://nanoporetech.com). We did the same for the day 515 sample and sequenced it using MiSeq (Illumina, https://www.illumina.com). We used double indexing to prevent cross-contamination and index misassignment errors.

We also prepared 90 plasma samples from patients infected with hepatitis C, collected for a separate study, in parallel with the day 515 sample. We did this to exclude the possibility of cross-contamination from our patient's previous samples, particularly the day 13 sample, which were shipped, prepared, and sequenced 6 months earlier. We did not detect Zika virus in any of the hepatitis C samples. We found no evidence of cross-contamination with Zika virus sequences during processing that could explain the near-whole genomes detected in the day 515 sample. Consensus sequences were consistent with all samples having come from the same patient with only 2 mutations, 1 synonymous change at codon 2921 and a K3272E substitution, acquired during the 502 days between the first and last samples sequenced (Table). We deposited sequence data in GenBank (accession nos. MH763832–3).

Counotte et al. systematically reviewed all available evidence on the risk for sexual transmission of Zika virus (*5*). Data from case reports, case series, cohort studies, in vitro work, and animal studies indicate that the infectious period for sexual transmission of Zika virus is considerably shorter than the period during which viral RNA can be detected in semen. As a result, the World Health Organization now recommends male travelers with potential Zika virus exposure delay conception for ≥3 months rather than ≥6 months (*6*).

In our case, Zika virus RNA might have persisted in semen because of failed immune clearance secondary to the patient's MRH or his immunosuppressive drug treatment. However, when advising returning male travelers in couples planning pregnancy, clinicians should be aware that Zika virus RNA shedding in semen might be intermittent and persist for longer in patients with immunosuppression.

Acknowledgments

We thank Tim Brooks, Steve Pullen, Azim Ansari, Megan MacDiarmid, and Paul Klenerman for their valuable contributions.

About the Author

Dr. Petridou is an infectious diseases registrar working at the Rare and Imported Pathogens Laboratory at Porton Down, Salisbury, United Kingdom. Her research interest is in Zika virus infection and she previously worked as the Zika virus registrar at Porton Down.

References

1. Barzon L, Percivalle E, Pacenti M, Rovida F, Zavattoni M, Del Bravo P, et al. Virus and antibody dynamics in travelers with acute Zika virus infection. Clin Infect Dis. 2018;66:1173–80. http://dx.doi.org/10.1093/cid/cix967
2. Pyke AT, Daly MT, Cameron JN, Moore PR, Taylor CT, Hewitson GR, et al. Imported Zika virus infection from the Cook Islands into Australia, 2014. PLoS Curr. 2014;6:1–7. http://dx.doi.org/10.1371/currents.outbreaks.4635a54dbffba2156fb2fd76dc49f65e
3. Atkinson B, Thorburn F, Petridou C, Bailey D, Hewson R, Simpson AJ, et al. Presence and persistence of Zika virus RNA in semen, United Kingdom, 2016. Emerg Infect Dis. 2017;23:611–5. http://dx.doi.org/10.3201/eid2304.161692
4. Theze J, Li T, du Plessis L, Bouquet J, Kraemer MUG, Somasekar S et al. Genomic epidemiology reconstructs the introduction and spread of Zika virus in Central America and Mexico. Cell Host Microbe, 2018; 23:855–64. 1. 2. 3. 4. http://dx.doi.org/10.1016/j.chom.2018.04.017
5. Counotte MJ, Kim CR, Wang J, Bernstein K, Deal CD, Broutet NJN, et al. Sexual transmission of Zika virus and other flaviviruses: a living systematic review. PLoS Med. 2018; 15:e1002611. http://dx.doi.org/10.1371/journal.pmed.1002611
6. World Health Organization. WHO guidelines for the prevention of sexual transmission of Zika virus: executive summary. Geneva: The Organization; 2019. https://www.who.int/reproductivehealth/zika/en

Address for correspondence: Christina Petridou or Emma Aarons, Rare and Imported Pathogens Laboratory, Public Health England Porton, Salisbury, UK; email: christina.petridou@nhs.net or emma.aarons@phe.gov.uk

No Evidence for Role of Cutavirus in Malignant Melanoma

Ulrike Wieland, Steffi Silling, Martin Hufbauer, Cornelia Mauch, Paola Zigrino, Frank Oellig, Alexander Kreuter, Baki Akgül

Author affiliations: University of Cologne, Cologne, Germany (U. Wieland, S. Silling, M. Hufbauer, C. Mauch, P. Zigrino, B. Akgül); Institute of Pathology, Mülheim an der Ruhr, Germany (F. Oellig); Helios St. Elisabeth Hospital Oberhausen, University Witten/Herdecke, Witten, Germany (A. Kreuter)

DOI: https://doi.org/10.3201/eid2508.190096

Cutavirus was previously found in cutaneous melanoma. We detected cutavirus DNA in only 2/185 melanoma biopsies and in 0/52 melanoma metastases from patients in Germany. Viral DNA was localized in the upper epidermal layers. Swab specimens from healthy skin were cutavirus positive for 3.8% (9/237) of immunocompetent and 17.1% (35/205) of HIV-positive men.

Cutavirus, a novel human protoparvovirus with linear single-stranded DNA, has been detected in fecal samples from children with diarrhea and in cutaneous T-cell lymphomas (CTCL) (*1*,*2*). Recently, Mollerup et al. reported the identification of cutavirus in 1 of 10 cutaneous malignant melanomas using viral enrichment methods with high-throughput sequencing and real-time PCR (*3*). This discovery raised questions concerning tropism and pathogenicity of cutavirus in human skin. We performed a retrospective study to determine cutavirus DNA prevalence and viral load in a large collection of formalin-fixed paraffin-embedded tissue biopsy specimens of malignant melanomas and in forehead swabs of healthy skin of immunocompetent and HIV-positive persons in Germany.

We used 185 cutaneous malignant melanoma biopsy specimens from 179 patients and 52 melanoma metastases from 42 patients from Germany for analyses with cutavirus real-time PCR (Appendix, http://wwwnc.cdc.gov/EID/article/25/8/19-0096-App1.pdf). We detected cutavirus DNA only in 2 nodular malignant melanomas, located on the abdomen of a 64-year-old man (MM-A) and on the cheek of an 85-year-old woman (MM-B). Viral DNA loads in these biopsies were 0.3 (MM-A) and 2.8 (MM-B) cutavirus DNA copies per β-globin gene copy. None of the 52 analyzed metastases carried cutavirus DNA (Table). The cutavirus PCR results of the 2 melanomas could be confirmed by sequencing and by in situ hybridization. In both melanomas, the cutavirus DNA–specific signals could be

Table. Cutavirus DNA detection and DNA load in cutaneous malignant melanomas, melanoma metastases, and forehead swabs of healthy nonlesional skin from persons in Germany*

Sample type	No. samples analyzed	No. cutavirus DNA–positive samples† (%; 95% CI)	Median cutavirus DNA load (IQR)‡
Malignant melanoma tumor biopsies§¶	185	2 (1.1; 0.3–3.9)	0.30; 2.82#
Malignant melanoma metastases§**	52	0 (0; 0–6.9)	NA
Skin swabs of HIV-positive men§	205	35 (**17.1**; 12.5–22.8)	0.33 (0.66–3.81)
Skin swabs of healthy male controls§	237	9 (**3.8**; 2.0–7.1)	2.31 (0.19–11.72)

*Bold type indicates statistical significance. IQR, interquartile range; NA, not applicable.
†All samples were analyzed with CUTA-UPL5 real-time PCR as described in the Appendix (https://wwwnc.cdc.gov/EID/article/25/8/19-0096-App1.pdf). The formalin-fixed paraffin-embedded (FFPE) biopsies (melanomas and metastases) were also analyzed with 2 different real-time PCRs targeting the cutavirus nonstructural 1 gene (Appendix). These PCRs did not detect further cutavirus DNA–positive biopsies.
‡Cutavirus DNA load was determined in all cutavirus DNA–positive samples and was defined as cutavirus DNA copies per β-globin gene copy.
§Details of the biopsies and skin swab specimens are provided in the Appendix.
¶From 21 cutavirus DNA–negative malignant melanomas, fresh frozen tissue could be analyzed in addition to the FFPE tissue samples (CUTA-UPL5-PCR). Cutavirus DNA was not detected in any of the 21 fresh frozen tissue samples. The cellular input of the fresh frozen tissue samples ranged from 1,230 to 40,600 β-globin gene copies per 2 μL extracted DNA (median 8,330, mean 10,892), indicating a high cellular input.
#Shown here are the viral DNA loads found in the 2 cutavirus DNA–positive nodular malignant melanomas, MM-A and MM-B.
**For 6 of the melanoma metastases, the primary tumor was also analyzed and was cutavirus DNA negative. The 2 patients with cutavirus DNA–positive melanoma biopsies (MM-A and MM-B) did not have metastatic disease.

detected only in the superficial layers and on the surface of the skin but not in the tumor cells (Appendix Figure).

To analyze the prevalence of cutavirus on healthy nonlesional skin, we used 442 forehead swab specimens from 237 immunocompetent men and 205 HIV-positive men that were available from a previous study (*4*) (Appendix). We found cutavirus DNA significantly more frequently on the skin of HIV-positive men than on the skin of healthy controls (17.1% vs. 3.8%; $p<0.001$ by 2-sided χ^2 test; Table). Among HIV-positive men, we found a trend for a higher cutavirus prevalence in patients with AIDS compared with those without AIDS (14/59 [23.7%; 95% CI 14.7–36.0] vs. 19/140 [13.6%; 95% CI 8.9–20.2]; $p = 0.078$ by 2-sided χ^2 test). The range of viral DNA loads found in the 44 cutavirus-positive skin swabs was 0.004–268.75 (median 0.41; interquartile range [IQR] 0.0–3.57); there was no significant difference between HIV-negative and HIV-positive men ($p = 0.389$ by Mann-Whitney-U test; Table).

Mollerup et al. found cutavirus DNA in 1 of 10 melanomas from Denmark and suggested investigating the role of cutavirus in cutaneous cancer (*3*). We detected cutavirus DNA in only 2 of 185 melanoma biopsy specimens and in none of 52 metastases. In situ hybridization localized the viral DNA on the surface of the 2 cutavirus-positive melanomas and not within the malignant cells. Our data therefore argue against an oncogenic role of cutavirus in malignant melanoma.

Väisänen et al. found cutavirus DNA in 2.9% of 136 skin biopsy specimens from 123 organ transplant recipients and in none of 159 skin biopsy specimens of 98 healthy adults (*5*). In accordance with Väisänen et al., we also found cutavirus more frequently in immunosuppressed patients than in healthy (immunocompetent) adults. Their finding related to healthy adults is in contrast to our results; however, we analyzed not skin biopsy specimens but widespread skin swab specimens covering ≈10 cm^2 of forehead skin (*4*). Our cutavirus DNA prevalence data on normal skin of immunocompetent adults (3.8%) are in line with cutavirus IgG seroprevalence rates reported for adults in Finland, Iran, and Kenya (4.2%–5.6%). Lower cutavirus IgG seroprevalence rates have been found in the United States (0%) and Iraq (1%) (*6*).

A pathogenic role of cutavirus has been investigated in further malignancies. Concerning CTCL, conflicting results have been reported. Phan et al. have found cutavirus DNA in 23.5% (4/17) (*1*) and Väisänen et al. in 16% (4/25) of CTCL of the mycosis fungoides type (*5*). Our group recently analyzed 189 biopsies of various cutaneous B- and T-cell lymphoma types and detected cutavirus DNA only in 5.8% of 104 mycosis fungoides biopsy specimens (*7*). In contrast, Bergallo et al. could not detect cutavirus in 55 CTCL samples (*8*). The in situ hybridization results of a cutavirus-positive mycosis fungoides sample analyzed by Phan et al. pointed to a localization of the viral DNA in the superficial parts of the lesion (*1*), similar to the results we show. Therefore, it remains unclear whether cutavirus plays a role in the development of CTCL. Recently, Dickinson et al. could not detect cutavirus in oropharyngeal and oral cavity squamous cell carcinomas (*9*).

In summary, our data on cutavirus DNA prevalence and localization argue against an oncogenic role of cutavirus in malignant melanoma. However, oncolytic properties of this virus or viral hit-and-run oncogenesis cannot be excluded (*10*). Cutavirus seems to be more frequent on healthy skin of immunosuppressed patients than on the skin of immunocompetent persons and could be part of the human skin virome. It is possible that cutavirus is an apathogenic virus shed from human skin.

Acknowledgments

We thank Monika Junk for excellent technical assistance.

The study was supported by intramural funds of the Faculty of Medicine of the University of Cologne (Koeln Fortune no. 2680-9067-01 and 2680-9159-01) and by the Deutsche Forschungsgemeinschaft (DFG, German Research Foundation, project no. 73111208–SFB 829 [Z4 project to C.M.]).

About the Author

Dr. Wieland is a professor of virology at the Institute of Virology of the University of Cologne, Germany. Her research interests include diagnosis and epidemiology of viral diseases.

References

1. Phan TG, Dreno B, da Costa AC, Li L, Orlandi P, Deng X, et al. A new protoparvovirus in human fecal samples and cutaneous T cell lymphomas (mycosis fungoides). Virology. 2016;496:299–305. http://dx.doi.org/10.1016/j.virol.2016.06.013
2. Väisänen E, Fu Y, Hedman K, Söderlund-Venermo M. Human protoparvoviruses. Viruses. 2017;9:E354. http://dx.doi.org/10.3390/v9110354
3. Mollerup S, Fridholm H, Vinner L, Kjartansdóttir KR, Friis-Nielsen J, Asplund M, et al. Cutavirus in cutaneous malignant melanoma. Emerg Infect Dis. 2017;23:363–5. http://dx.doi.org/10.3201/eid2302.161564
4. Wieland U, Silling S, Scola N, Potthoff A, Gambichler T, Brockmeyer NH, et al. Merkel cell polyomavirus infection in HIV-positive men. Arch Dermatol. 2011;147:401–6. http://dx.doi.org/10.1001/archdermatol.2011.42
5. Väisänen E, Fu Y, Koskenmies S, Fyhrquist N, Wang Y, Keinonen A, et al. Cutavirus DNA in malignant and non-malignant skin of cutaneous T-cell lymphoma and organ transplant patients but not of healthy adults. Clin Infect Dis. 2019;68:1904–10. http://dx.doi.org/10.1093/cid/ciy806
6. Väisänen E, Mohanraj U, Kinnunen PM, Jokelainen P, Al-Hello H, Barakat AM, et al. Global distribution of human protoparvoviruses. Emerg Infect Dis. 2018;24:1292–9. http://dx.doi.org/10.3201/eid2407.172128
7. Kreuter A, Nasserani N, Tigges C, Oellig F, Silling S, Akgül B, et al. Cutavirus infection in primary cutaneous B- and T-cell lymphoma. JAMA Dermatol. 2018;154:965–7. http://dx.doi.org/10.1001/jamadermatol.2018.1628
8. Bergallo M, Daprà V, Fava P, Ponti R, Calvi C, Fierro MT, et al. Lack of detection of cutavirus DNA using PCR real time in cutaneous T-cell lymphomas (CTCL). G Ital Dermatol Venereol. 2018;•••. http://dx.doi.org/10.23736/S0392-0488.18.06161-8
9. Dickinson A, Xu M, Silén S, Wang Y, Fu Y, Sadeghi M, et al. Newly detected DNA viruses in juvenile nasopharyngeal angiofibroma (JNA) and oral and oropharyngeal squamous cell carcinoma (OSCC/OPSCC). Eur Arch Otorhinolaryngol. 2019;276:613–7. http://dx.doi.org/10.1007/s00405-018-5250-7
10. Hufbauer M, Akgül B. Molecular mechanisms of human papillomavirus induced skin carcinogenesis. Viruses. 2017;9:E187. http://dx.doi.org/10.3390/v9070187

Address for correspondence: Ulrike Wieland, University of Cologne Institute of Virology, Fuerst-Pueckler-Str. 56, 50935 Cologne, Germany; email: ulrike.wieland@uni-koeln.de

Intrafamily Transmission of Monkeypox Virus, Central African Republic, 2018

Camille Besombes, Ella Gonofio, Xavier Konamna, Benjamin Selekon, Antoine Gessain, Nicolas Berthet, Jean-Claude Manuguerra, Arnaud Fontanet, Emmanuel Nakouné

Author affiliations: Institut Pasteur, Paris, France (C. Besombes, A. Gessain, N. Berthet, J.-C. Manuguerra, A. Fontanet); Institut Pasteur de Bangui, Bangui, Central African Republic (E. Gonofio, X. Konamna, B. Selekon, E. Nakouné); Centre National de la Recherche Scientifique, Paris (A. Gessain, N. Berthet); Unité Pasteur-CNAM Risques Infectieux et Emergents, Conservatoire National des Arts et Métiers, Paris (A. Fontanet)

DOI: https://doi.org/10.3201/eid2508.190112

Monkeypox is a rare viral zoonotic disease; primary infections are reported from remote forest areas of Central and West Africa. We report an investigation of a monkeypox outbreak in Lobaye, southwest Central African Republic, in October 2018.

Monkeypox, a zoonotic disease caused by an *Orthopoxvirus*, has clinical signs and symptoms in humans similar to smallpox and a case-fatality rate of 10% (*1*). The specific reservoir species for monkeypox virus remains, to a large extent, unidentified (*2*). Spillover events of monkeypox have been reported in remote forest areas of Central and West Africa. After zoonotic infection, the virus can be transmitted from person to person (*1*).

To date, human monkeypox outbreaks in the Central African Republic (CAR) have been small: ≈10 cases, restricted to a family or village. Primary infection in these outbreaks occurred from contact with wild fauna, with secondary transmission among close contacts in the community (*3*,*4*) and limited nosocomial transmission (*5*). Since 2000, the Virology Laboratory of the Institut Pasteur de Bangui (IP Bangui), a regional reference center for monkeypox, has reported 20 monkeypox outbreaks across several regions of CAR, totaling ≈100 cases, particularly in the region of Lobaye (*3*,*4*). In 2018 alone, IP Bangui investigated 6 different outbreaks in CAR, indicating a possible increase in frequency of outbreaks *(6*,*7*).

On September 27, 2018, a healthcare worker from Zomea Kaka healthcare center in Lobaye reported to IP Bangui about 3 cases of suspected monkeypox in an Aka Pygmy family. A 25-year-old female sought care at the health center, 10 km from her village, for maculopapular rash and lesions. She was afebrile. Her signs and symptoms indicated

resolving late stage monkeypox infection. She was accompanied by her 2 daughters, 5 months and 4 years of age, both showing typical symptoms of active monkeypox infection, notably maculopapular rash on the palms of their hands and soles of their feet (Appendix Figure, http://wwwnc.cdc.gov/EID/article/25/8/19-0112-App1.pdf). Blood or pus samples taken from the 3 patients were confirmed positive for monkeypox infection by PCR on September 29 (*8*) (Appendix).

On October 5, IP Bangui carried out an investigation among contacts of the index case-patient, in collaboration with the Ministry of Health and the World Health Organization CAR Country Office. The index case-patient reported butchering 3 small mammals known in local Aka language as Yabo (African civet, *Civettictis civetta*), Gbè (Emin's pouched rat, *Cricetomys emini*), and Sende (African rope squirrel, *Funesciurus anerythrus*). She butchered 1 of each in a forested area 2 weeks before the onset of rash.

During October 6–10, two additional family contacts from the village, the index case-patient's 2 sisters, 7 and 16 years of age, reported symptoms consistent with monkeypox infection. Healthcare workers collected blood or pus samples from the patients, and IP Bangui confirmed monkeypox infection by PCR. On October 26, monkeypox infection was confirmed in another family contact, the index case-patient's 33-year-old sister-in-law. The dates of the onset of symptoms suggest 3 waves of intrafamilial transmission (Table) (*9*).

IP Bangui conducted further investigations by using *Orthopoxvirus* serologic assays (Appendix) on blood samples collected from 2 healthcare worker contacts on October 5 and from 31 village contacts on October 25. Results revealed evidence of *Orthopoxvirus* serologic response in the index case-patient's mother; 2 healthcare workers who had cared for the index case-patient; and the index case-patient's brother, who brought her the wild animals (Table).

Serologic evidence of possible monkeypox infection can indicate prior exposure to the virus or, among persons >38 years of age, immunization against smallpox, and might explain the restricted size of the outbreak in the village. However, smallpox vaccination campaigns with a live-attenuated vaccinia virus ended in 1979 in CAR. Consequently, an increasingly larger proportion of the population is immunologically naive to *Orthopoxvirus* infection.

This investigation identified 5 clinical cases of secondary monkeypox infection spread over 3 waves of intrafamilial infection, originating from an index case-patient with primary infection possibly attributable to contact with wild fauna. The prompt declaration and isolation of suspected cases, as well as possible naturally

Table. Molecular and serologic evidence of index case-patient and contacts with known and possible exposure to monkeypox virus, Central African Republic, 2018*

Patients	Age, y/sex	Symptom onset date	Signs/ symptoms	Animal contact	Collection date	Sample type		PCR‡		IgG§		Smallpox vaccine¶
						Blood	Pus†	MPXV	CPXV	MPXV	CPXV	
Index case-patient	25/F	2018 Sep 8	Rash, lesions	Y	2018 Sep 27	Y	N	+	–	–	–	N
Contacts												
Daughter	0.4/F	2018 Sep 20	Fever, rash, lesions	N	2018 Sep 27	N	Y	+	–	ND	ND	N
Daughter	4/F	2018 Sep 26	Fever, rash, lesions	N	2018 Sep 27	Y	N	+	–	–	–	N
Sister	16/F	2018 Oct 6	Rash, lesions	N	2018 Oct 8	N	Y	+	–	ND	ND	N
Sister	7/F	2018 Oct 9	Rash, lesions	N	2018 Oct 11	Y	N	+	–	–	–	N
SIL	33/F	2018 Oct 24	Rash, lesions	N	2018 Oct 25	Y	N	+	–	–	–	N
Mother	49/F	NA	None	N	2018 Oct 5	Y	N	ND	ND	+	+	Y
Son	13/M	NA	None	Y	2018 Oct 5	Y	N	ND	ND	–	–	N
Brother	49/M	NA	None	Y	2018 Oct 25	Y	N	ND	ND	+	–	Y
Brother of SIL	8/M	NA	None	NK	2018 Oct 25	Y	N	ND	ND	+	+	N
Nephew of SIL	13/M	NA	None	NK	2018 Oct 25	Y	N	ND	ND	–	–	N
HCW	34/M	NA	None	N	2018 Oct 5	Y	N	ND	ND	+	+	N
HCW	45/F	NA	None	N	2018 Oct 5	Y	N	ND	ND	+	+	Y
Social contact	22/F	NA	None	NK	2018 Oct 25	Y	N	ND	ND	+	–	N

*A total of 33 contacts were tested, 2 HCWs and 31 village contacts. CPXV, cowpox virus; HCW, healthcare worker; MPXV, monkeypox virus; NA, not applicable; ND, not done; NK, not known; SIL, sister-in-law; +, positive; –, negative.
†Samples obtained by HCWs after training on collecting swab samples.
‡Quantitative and conventional PCR were performed by using generic primers G2R-G and Congo Basin primers C3L (*8*).
§In-house tests were performed by using MPXV antigen isolated from local human cases and CPXV antigen related to Brighton Red strain.
¶History of smallpox vaccination was determined by verbal report and presence of scar.

acquired immunity or persistence of vaccine-derived immunity within the community, likely contributed to the restricted extent of secondary transmission. Further studies are needed to clarify risk factors for primary and secondary monkeypox transmission.

Positive serologic findings in healthcare workers during this investigation also highlight the limited infection prevention and control resources, such as isolation rooms, gowns, gloves, N95 respirators, and goggles, to protect healthcare workers responding to outbreaks in CAR. For communities located in remote forest areas in which zoonotic spillover and secondary transmission are thought to occur regularly, health center capacity and resources need to be strengthened. Health centers urgently need training on case recognition for healthcare workers, access to diagnostic capacities, and appropriate infection prevention and control measures to reduce the possibility of secondary transmission in these areas (*10*).

Acknowledgments

The authors thank Romain Duda for his assistance with identification of the animal species in Aka language. We also acknowledge Rebecca Grant for her relevant suggestions and her kind participation in the formatting of this research letter.

About the Author

Dr. Besombes is an infectious and tropical disease clinician who works as a researcher in the Emerging Diseases Epidemiology Unit at Institut Pasteur, Paris, France. Her primary research interests include tropical diseases, specifically zoonotic and vectorborne diseases, and hepatitis Delta virus infection.

References

1. Durski KN, McCollum AM, Nakazawa Y, Petersen BW, Reynolds MG, Briand S, et al. Emergence of monkeypox—West and Central Africa, 1970–2017. MMWR Morb Mortal Wkly Rep. 2018;67:306–10. http://dx.doi.org/10.15585/mmwr.mm6710a5
2. Sklenovská N, Van Ranst M. Emergence of monkeypox as the most important orthopoxvirus infection in humans. Front Public Health. 2018;6:241. http://dx.doi.org/10.3389/fpubh.2018.00241
3. Berthet N, Nakouné E, Whist E, Selekon B, Burguière AM, Manuguerra JC, et al. Maculopapular lesions in the Central African Republic. Lancet. 2011;378:1354. http://dx.doi.org/10.1016/S0140-6736(11)61142-2
4. Kalthan E, Tenguere J, Ndjapou SG, Koyazengbe TA, Mbomba J, Marada RM, et al. Investigation of an outbreak of monkeypox in an area occupied by armed groups, Central African Republic. Med Mal Infect. 2018;48:263–8. http://dx.doi.org/10.1016/j.medmal.2018.02.010
5. Nakoune E, Lampaert E, Ndjapou SG, Janssens C, Zuniga I, Van Herp M, et al. A nosocomial outbreak of human monkeypox in the Central African Republic. Open Forum Infect Dis. 2017;4:ofx168. http://dx.doi.org/10.1093/ofid/ofx168
6. ProMED-mail. Monkeypox—Africa (12): Central African Republic. 2018 Jul 30 [cited 2018 Oct 24]. https://www.promedmail.org, archive no. 20180730.5936829.
7. ProMED-mail. Monkeypox—Africa (05): Central African Republic (Haute-Kotto). 2018 Apr 4 [cited 2019 Jan 7]. https://www.promedmail.org, archive no. 20180403.5726159.
8. Li Y, Zhao H, Wilkins K, Hughes C, Damon IK. Real-time PCR assays for the specific detection of monkeypox virus West African and Congo Basin strain DNA. J Virol Methods. 2010;169:223–7. http://dx.doi.org/10.1016/j.jviromet.2010.07.012
9. Di Giulio DB, Eckburg PB. Human monkeypox: an emerging zoonosis. Lancet Infect Dis. 2004;4:15–25. http://dx.doi.org/10.1016/S1473-3099(03)00856-9
10. Munster VJ, Bausch DG, de Wit E, Fischer R, Kobinger G, Muñoz-Fontela C, et al. Outbreaks in a rapidly changing Central Africa—lessons from Ebola. N Engl J Med. 2018;379:1198–201. http://dx.doi.org/10.1056/NEJMp1807691

Address for correspondence: Emmanuel Nakouné, Arboviruses, Viral Haemorragic Viruses, Emerging Viruses and Zoonosis Unit, Institut Pasteur de Bangui, Bangui, Central African Republic; email: emmanuel.nakoune@pasteur-bangui.org

Intact *Mycobacterium leprae* Isolated from Placenta of a Pregnant Woman, China

Zhiming Chen,[1] Yanfei Kuang,[1] Haiqin Jiang, Wenyue Zhang, Ying Shi, Santosh Chokkakula, Huan Chen, Junhua Li, Hongsheng Wang

Author affiliations: Chinese Academy of Medical Sciences Institute of Dermatology, Nanjing, China (Z. Chen, H. Jiang, W. Zhang, Y. Shi, S. Chokkakula, H. Wang); Hunan Provincial Center for Disease Control and Prevention, Changsha, China (Y. Kuang, H. Chen, J. Li); Jiangsu Key Laboratory of Molecular Biology for Skin Diseases and STIs, Nanjing (H. Wang); Nanjing Medical University Center for Global Health, Nanjing (H. Wang)

DOI: https://doi.org/10.3201/eid2508.190114

Whether *Mycobacterium leprae* transmits from placenta to fetus remains unknown. We describe the case of a pregnant woman with untreated histoid leproma. Although her newborn was healthy, laboratory examination revealed intact *M. leprae* present in the placenta, suggesting that the placental barrier might prevent vertical dissemination of *M. leprae*.

[1]These authors contributed equally to and are co–first authors for this article.

Leprosy is an infectious disease caused by *Mycobacterium leprae* in susceptible persons. The disease affects the skin and peripheral nerves and, in later stages, can cause irreversible disability. Dissemination of *M. leprae* is thought to occur through nasal mucosa (*1*). However, in pregnant patients, whether *M. leprae* can transmit to the fetus remains unknown. We report the case of a pregnant woman who had histoid leproma and refused therapy until after birth. The Ethics Committee of the Chinese Academy of Medical Sciences' Institute of Dermatology approved this study, and all persons provided informed consent before sample collection.

In December 2017, a pregnant woman sought care at the Chinese Academy of Medical Sciences' Institute of

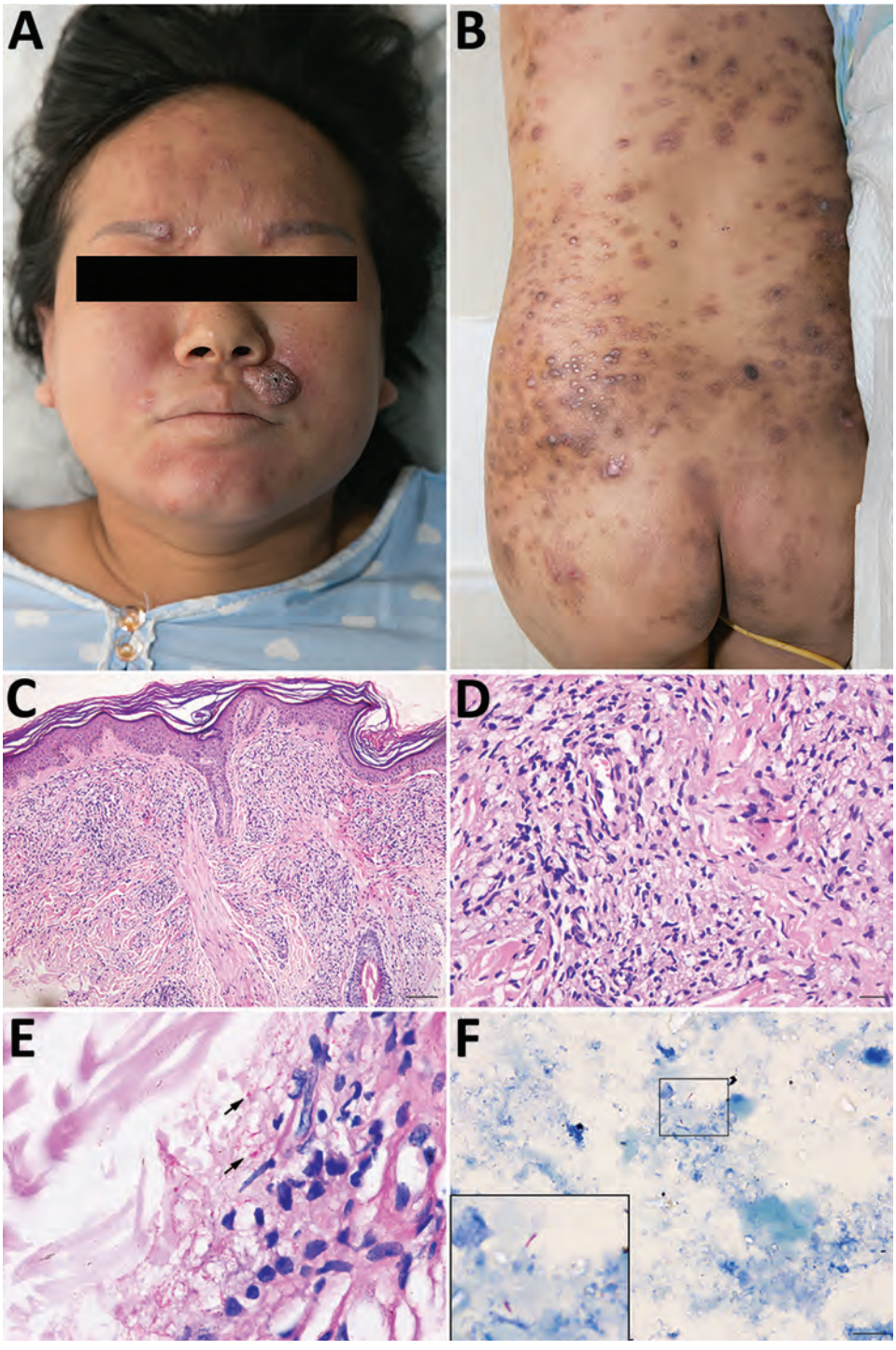

Figure. Clinical features of *Mycobacterium leprae* infection in pregnant woman and pathologic characteristics of a biopsy and placenta samples, China, December 2017. A, B) multiple brown papules and firm nodules on the woman's trunk and face and ichthyosis presentation on the anterior tibia. C, D) Testing of biopsy sample from the face demonstrates subepidermal clear zone, nodular proliferation of spindle-shaped histiocytes in the dermis. Hematoxylin and eosin stain; original magnification ×10 (C) and ×40 (D). E) Numerous acid-fast bacilli in dermis (arrows). Acid-fast stain; original magnification ×100. F) Intact rod-shaped *M. leprae* from placenta homogenate; inset shows larger view. Acid-fast stain, original magnification ×100.

Dermatology (Nanjing, China) with a 9-month history of asymptomatic multiple erythema and nodose lesions on her trunk. She had experienced dry skin and dysesthesia in both lower extremities for ≥10 years. In 2009, she had a sudden rash of erythema on her trunk and lower extremities, which was treated as eczema, without improvement. She began losing her eyebrows in 2015. Her pregnancy was discovered 3 months before admission. Since her illness onset, she had experienced no fevers or joint pain, and her family history was negative for leprosy.

Physical examination revealed multiple brown papules and firm nodules on her trunk and face (Figure, panels A, B). Superficial sensation was slightly impaired over the lower extremities. No peripheral nerve or superficial lymph node enlargement was observed. Her eyebrows were lost completely. A skin biopsy from her face revealed a subepidermal clear zone, numerous foamy histiocytes throughout the dermis, dense cellularity, and few perivascular lymphocytes. Prominent acid-fast bacilli were observed inside the dermis (Figure, panels C–E). PCR was performed to detect *M. leprae* DNA fragments of *RLEP* and *FolP1*. Samples from a facial lesion tested positive. Serologic examination of the patient's peripheral blood using ELISA was positive for antibodies of NDO-BSA (IgM), MMP-II (IgG), and LID-1 (IgG) (Appendix Table 1, https://wwwnc.cdc.gov/EID/article/25/8/19-0114-App1.pdf).

The patient refused treatment, citing concern about adverse effects on the fetus. Her condition was monitored with ultrasounds at serial intervals. At 37 weeks' gestation, her amniotic membranes ruptured. She was transferred to an isolated operating room and underwent a cesarean delivery. She delivered a healthy baby girl. At the patient's request, she was housed separately from her infant, and she decided not to breast-feed. After delivery, the patient was treated with dapsone, rifampin, and clofazimine, in accordance with World Health Organization recommendations (*2*).

After delivery, we collected fresh samples from the patient, including breast milk, umbilical cord, umbilical cord blood, and placenta, as well as nasal mucosa swab and serum specimens from the patient, her newborn, and her elder daughter for bacterial and serologic analysis. Intact acid-fast bacilli were found in placenta homogenates from the patient (Figure, panel F; Appendix Figure). Serologic testing for NDO, MMP-II, and LID antibodies by ELISA were all positive in the patient, whereas only MMP-II and LID antibodies were found in the newborn (Appendix Table 1). We also conducted PCR testing of various samples; some results were positive for the mother and her elder daughter, but none were positive for the newborn (Appendix Table 2). One month later, serologic test results for the infant were almost negative for *M. leprae* antibodies (Appendix Table 3). The patient's lesions resolved, and her family members were shown to be healthy during follow-ups.

Leprosy can be exacerbated during pregnancy and, without treatment, can cause permanent damage to the skin, nerves, and eyes because of suppression of cell-mediated immunity in pregnancy. Downgrading reactions can occur, especially in the third trimester (*3*). Therefore, treating leprosy during pregnancy is critical. For multibacillary leprosy patients, World Health Organization treatment guidelines recommend multidrug therapy using rifampin, dapsone, and clofazimine (*2*). These agents must never be used alone as monotherapy for leprosy nor be stopped during pregnancy (*4*).

Our patient refused treatment, citing concerns for adverse effects on the fetus; consequently, her condition dramatically worsened during the third trimester. Fortunately, no nerves or important organs were damaged. The patient's breast milk was negative for DNA, RNA, and antibodies of *M. leprae*. Serum samples from umbilical cord blood were positive for DNA and IgG of *M. leprae* but negative for RNA and IgM. Notably, a substantial number of *M. leprae* organisms were detected in the placenta (Figure, panel F; Appendix Figure).

Our findings support the assumption that the placental barrier can effectively stop vertical transmission of leprosy as well as the consensus that breast-feeding by women receiving multidrug therapy is safe for infants, given that no DNA or RNA of *M. leprae* were detected in breast milk (*5*,*6*). Although antileprosy drugs can be excreted into breast milk, no adverse effects have been reported except skin discoloration in the infant because of clofazimine (*7*). The patient's elder daughter's serum sample and nasal mucosa swab specimen were positive for *M. leprae* DNA and RNA by PCR, confirming that she was an *M. leprae* carrier. Households experiencing such a situation need to be screened with regular follow-ups (*8*).

Acknowledgments

We thank Lemuel Tsang for his invaluable suggestions during manuscript preparation.

This study was supported by the CAMS Innovation Fund for Medical Sciences (grant nos. 2016-I2M-1-005 and 2017-I2M-B&R-14) and Jiangsu Provincial Key Research and Development (grant no. BE2018619).

About the Author

Dr. Zhiming Chen works at the Chinese Academy of Medical Sciences' Institute of Dermatology and at Peking Union Medical College. His major research interests are cutaneous mycobacterial infection and genodermatosis.

References

1. Job CK, Jayakumar J, Kearney M, Gillis TP. Transmission of leprosy: a study of skin and nasal secretions of household contacts of leprosy patients using PCR. Am J Trop Med Hyg. 2008;78:518–21. http://dx.doi.org/10.4269/ajtmh.2008.78.518

2. World Health Organization. Chemotherapy of leprosy. World Health Organ Tech Rep Ser. 1994;847:1–24.
3. Duncan ME, Pearson JM, Ridley DS, Melsom R, Bjune G. Pregnancy and leprosy: the consequences of alterations of cell-mediated and humoral immunity during pregnancy and lactation. Int J Lepr Other Mycobact Dis. 1982;50:425–35.
4. World Health Organization. WHO model prescribing information: drugs used in leprosy [cited 2019 Jan 20]. https://apps.who.int/medicinedocs/en/d/Jh2988e
5. Gimovsky AC, Macri CJ. Leprosy in pregnant woman, United States. Emerg Infect Dis. 2013;19:1693–4. http://dx.doi.org/10.3201/eid1910.130463
6. Shale MJ. Women with leprosy. A woman with leprosy is in double jeopardy. Lepr Rev. 2000;71:5–17. http://dx.doi.org/10.5935/0305-7518.20000003
7. Ozturk Z, Tatliparmak A. Leprosy treatment during pregnancy and breastfeeding: a case report and brief review of literature. Dermatol Ther (Heidelb). 2017;30:e12414. http://dx.doi.org/ 10.1111/dth.12414
8. Listed N. The final push strategy to eliminate leprosy as a public health problem: questions and answers. Lepr Rev. 2002;73:279–81.

Address for correspondence: Hongsheng Wang, Institute of Dermatology, Chinese Academy of Medical Sciences, Department of Mycobacterium, St. 12 Jiangwangmiao, Nanjing, Jiangsu 210042, China; email: whs33@vip.sina.com; Junhua Li, Hunan Provincial Center for Disease Control and Prevention, Changsha, Hunan, China; email: hncdcbgs@126.com

Zoonotic Virus Seroprevalence among Bank Voles, Poland, 2002–2010

Maciej Grzybek, Tarja Sironen, Sanna Mäki, Katarzyna Tołkacz, Mohammed Alsarraf, Aneta Strachecka, Jerzy Paleolog, Beata Biernat, Klaudiusz Szczepaniak, Jolanta Behnke-Borowczyk, Antti Vaheri, Heikki Henttonen, Jerzy M. Behnke,[1] Anna Bajer[1]

Author affiliations: Medical University of Gdansk, Gdansk, Poland (M. Grzybek, B. Biernat); University of Helsinki, Helsinki, Finland (T. Sironen, S. Mäki, A. Vaheri); University of Warsaw, Warsaw, Poland (K. Tołkacz, M. Alsarraf, A. Bajer); University of Life Sciences in Lublin, Lublin, Poland (A. Strachecka, J. Paleolog, K. Szczepaniak); Poznan University of Life Sciences, Poznan, Poland (J. Behnke-Borowczyk); Natural Resources Institute Finland, Helsinki (H. Henttonen); University of Nottingham, Nottingham, UK (J.M. Behnke)

DOI: https://doi.org/10.3201/eid2508.190217

[1]These authors contributed equally to this article.

Bank voles in Poland are reservoirs of zoonotic viruses. To determine seroprevalence of hantavirus, arenavirus, and cowpox virus and factors affecting seroprevalence, we screened for antibodies against these viruses over 9 years. Cowpox virus was most prevalent and affected by extrinsic and intrinsic factors. Long-term and multisite surveillance is crucial.

The most prevalent rodentborne zoonotic viruses in Europe are hantaviruses, lymphocytic choriomeningitis virus (LCMV), cowpox virus (CPXV), and Puumala virus (PUUV) (*1*). In 2016, a total of 18 countries in Europe reported 2,190 cases of hantavirus disease, mainly caused by PUUV. The occurrence of rodentborne viruses in Poland is not well documented. The first outbreak of hantavirus infections among humans (9 cases) was reported in 2007. During 2012–2016, a total of 79 cases of hantavirus infections were reported in Poland, 55 of them in Podkarpackie Province in 2014 (*2*). In 2015, a case of human cowpox infection was reported in Poland (*3*).

We conducted a multisite, long-term study of hantavirus and arenavirus seroprevalence in northeastern Poland. Our objectives were to monitor seroprevalence of LCMV, CPVX, and PUUV in 3 populations of bank voles (*Myodes glareolus*) from ecologically similar but disparate sites in northeastern Poland and to analyze intrinsic (host sex, host age) and extrinsic (study year, study sites) factors that might affect seroprevalence among these rodent populations.

Study sites were located in the Mazury Lake District region in northeastern Poland (Appendix Figure 1, https://wwwnc.cdc.gov/EID/article/25/8/19-0217-App1.pdf). The sites and methods used for trapping rodents and sampling and processing trapped animals have been described (*4*). We analyzed serum samples by using an immunofluorescence assay (IFA) (Appendix Figure 2). We diluted serum samples 1:10 in phosphate-buffered saline and tested their reactivity to hantaviruses by using a PUUV IFA, to cowpox viruses by using a CPXV IFA, and to arenaviruses by using an LCMV IFA (*5*). IFAs were conducted as previously described (*6*,*7*). The statistical approach has been comprehensively documented (*4*).

We tested 652 bank voles and detected antibodies against all 3 viruses. Overall seroprevalence of combined viral infections was 25.9% (95% CI 23.0%–29.1%), but most infections were attributable to CPXV (seroprevalence 25% [95% CI 22.1%–28.2%]). Only 2 voles were LCMV seropositive (0.3% [95% CI 0.2%–0.9%]), and only 5 were PUUV seropositive (0.76% [95% CI 0.4%–1.6%]). We therefore confined further analyses to CPXV.

The effect of study year on CPXV seroprevalence (by χ^2/d.f.) was highly significant (χ^2_2 31.2; p<0.001); seroprevalence was 2.7 times higher among bank voles sampled in

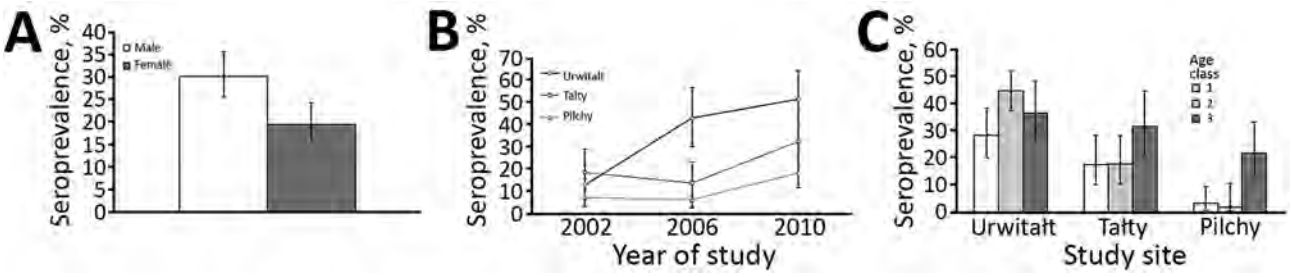

Figure. Seroprevalence of cowpoxvirus (CPXV) in bank voles in Poland, 2002–2010. A) By sex; B) by study site location and year of study; C) by study site location and vole age class (class 1—immature juvenile bank voles; class 2—mostly young adult bank voles; and class 3—breeding older animals). Error bars indicate 95% CI.

2010 (36.1% [95% CI 31.7%–40.7%]) than in 2002 (13.1% [7.4%–21.0%]). CPXV seroprevalence also varied markedly among voles from the 3 study sites (χ^2_2 46.84; p<0.001); seroprevalence was highest among voles from Urwitałt (38.4% [95% CI 33.9%–43.1%]) and lower among voles from Tałty (23.0% [19.3%–27.2%]) and Pilchy (10.3% [95% CI 5.7%–17.4%]). CPXV seroprevalence was also significantly affected by the sex of the host (χ^2_1 10.1; p = 0.001) and was 1.5 times higher for male than female voles (Figure, panel A). Seroprevalence increased with host age (χ^2_2 12.73; p = 0.002) and was lowest among voles from age class 1 (immature) (16.0% [95% CI 10.0%–24.1%]) and higher among those from age class 2 (mostly young adults) (27.2% [95% CI 23.2%–31.5%]) and age class 3 (breeding older adults) (30.1% [95% CI 25.9%–34.6%]).

The differences in seroprevalence between sites were also confounded by interaction with study year (year × site × presence/absence of antibodies against CPXV; χ^2_4 12.76; p = 0.012). Seroprevalence increased significantly at all 3 study sites from 2006 to 2010 and was highest in Urwitałt (0.83-fold). The largest seroprevalence increases from 2006 to 2010 were in Tałty (2.35-fold) and Pilchy (2.9-fold) (Figure, panel B).

The pattern of age-related changes in seroprevalence also differed between study sites (site × age × presence/absence of antibodies against CPXV; χ^2_4 = 17.45; p = 0.002) (Figure, panel C). In Urwitałt, the overall seroprevalence was highest among voles in age class 2 (44.5% [95% CI 37.5%–51.8%]), 1.57-fold lower among voles in age class 1, and 1.22-fold lower among voles in age class 3. In Tałty and Pilchy, seroprevalence was highest among voles from age class 3. In Tałty, seroprevalence was 1.8-fold higher among voles in age class 3 compared with voles in other age classes. In Pilchy, seroprevalence among voles in age class 3 was 10.8-fold higher than among voles in age class 2.

Our data show that CPXV was the dominant viral pathogen among bank voles in Poland during the study period, although PUUV and LCMV were also found. Our finding that the highest seroprevalence was among bank voles from Urwitałt complements our previous reports on other pathogens, reflects the importance of extrinsic effects on prevalence, and establishes that the sites from which host populations are sampled is the most influential factor affecting prevalence (*4*).

Our results provide additional information about the role of bank voles in Poland as infectious virus reservoirs. Although short-term cross-sectional studies are useful as a starting point (*8*), to obtain a comprehensive ecologic picture, long-term monitoring (several years and preferably a decade or longer) and a multisite approach are crucial. Identifying rodent species that can serve as reservoirs for zoonotic disease viruses and predicting regions where new outbreaks are most likely to happen are crucial steps for preventing and minimizing the extent of zoonotic disease among humans (*9*).

Acknowledgments

We thank the University of Nottingham, Warsaw University, and the Medical University of Gdansk for financial support. M.G. thanks Alicja Rost and Ewa Zieliniewicz for their assistance in the laboratory.

This research received support from Sigrid Jusélius Foundation, Helsinki, and the Natural Resources Institute Finland. J.M.B. received support from the Royal Society, the British Ecological Society, and the Grabowski Fund. A.B. received support from the Polish State Committee for Scientific Research and the British Council's Young Scientist Programme. M.G. received support from the Ministry of Science and Higher Education in Poland, Fellowship for Outstanding Scientists (428/STYP/11/2016).

About the Author

Dr. Grzybek is a parasitologist holding the position of assistant professor in the Department of Tropical Parasitology, Medical University of Gdansk, Poland. His research interests include epidemiology and ecology of macroparasites and microparasites in rodents, especially bank voles. He is also interested in host–parasite interactions and intrinsic and extrinsic factors that influence these relationships.

References

1. Kallio-Kokko H, Uzcategui N, Vapalahti O, Vaheri A. Viral zoonoses in Europe. FEMS Microbiol Rev. 2005;29:1051–77. http://dx.doi.org/10.1016/j.femsre.2005.04.012
2. European Centre for Disease Prevention and Control. Hantavirus infection. Annual epidemiological report for 2016 [cited 2019 June 20]. https://ecdc.europa.eu/sites/portal/files/documents/hantavirus-infection-annual-epidemiological-report-2016.pdf
3. Świtaj K, Kajfasz P, Kurth A, Nitsche A. Cowpox after a cat scratch–case report from Poland. Ann Agric Environ Med. 2015;22:456–8. http://dx.doi.org/10.5604/12321966.1167713
4. Grzybek M, Bajer A, Bednarska M, Al-Sarraf M, Behnke-Borowczyk J, Harris PD, et al. Long-term spatiotemporal stability and dynamic changes in helminth infracommunities of bank voles (*Myodes glareolus*) in NE Poland. Parasitology. 2015;142:1722–43. http://dx.doi.org/10.1017/S0031182015001225
5. Hedman K, Vaheri A, Brummer-Korvenkontio M. Rapid diagnosis of hantavirus disease with an IgG-avidity assay. Lancet. 1991;338:1353–6. http://dx.doi.org/10.1016/0140-6736(91)92235-T
6. Kallio-Kokko H, Laakkonen J, Rizzoli A, Tagliapietra V, Cattadori I, Perkins SE, et al. Hantavirus and arenavirus antibody prevalence in rodents and humans in Trentino, Northern Italy. Epidemiol Infect. 2006;134:830–6. http://dx.doi.org/10.1017/S0950268805005431
7. Pelkonen PM, Tarvainen K, Hynninen A, Kallio ERK, Henttonen K, Palva A, et al. Cowpox with severe generalized eruption, Finland. Emerg Infect Dis. 2003;9:1458–61. http://dx.doi.org/10.3201/eid0911.020814
8. Sadkowska-Todys M, Dudek-Godeau D, Kamińska S, Baumann-Popczyk A, Czerwiński M, Kucharczyk B, et al. Occurrence and maintenance of hantavirus infections among rodent populations in their natural habitat—results of a field study from Podkarpackie Province, Poland 2010–2012. Przegl Epidemiol.2015; 69:283–8, 395–9.
9. Han BA, Schmidt JP, Bowden SE, Drake JM. Rodent reservoirs of future zoonotic diseases. Proc Natl Acad Sci U S A. 2015; 112:7039–44. http://dx.doi.org/10.1073/pnas.1501598112

Address for correspondence: Maciej Grzybek, Medical University of Gdansk, Department of Tropical Parasitology, Powstania Styczniowego 9B, 81-519 Gdynia, Poland; email: maciej.grzybek@gumed.edu.pl

Polio-Like Manifestation of Powassan Virus Infection with Anterior Horn Cell Involvement, Canada

Christopher Picheca,[1] Vignan Yogendrakumar,[1] James I. Brooks, Carlos Torres, Elizabeth Pringle, Jocelyn Zwicker

Author affiliation: University of Ottawa, Ottawa, Ontario, Canada

DOI: https://doi.org/10.3201/eid2508.190399

[1]These first authors contributed equally to this article.

Evidence of spinal cord involvement in Powassan virus infection is largely limited to mouse models. We report a case of a polio-like illness caused by Powassan virus infection in a 62-year-old man in Canada. Magnetic resonance imaging showed T2 hyperintensities in the anterior horns of the cervical spinal cord.

Powassan virus (POWV) is a tickborne flavivirus, named after Powassan, Ontario, Canada, the location of the first documented human infection in 1958 (*1*). Since then, ≈150 cases of POWV infection have been reported globally, and incidence has increased over time. A total of 125 POWV cases have been identified since 2008, 33 (26%) in 2017 (*2*). In Canada, most reported POWV infections have been in the Great Lakes region. A small number of cases have been reported in the Maritime provinces (*3*).

POWV is transmitted by members of the *Ixodes* genus of ticks, including *I. cookei* and the more opportunistic and aggressive *I. scapularis*. POWV has 2 lineages; lineage 2 (deer tick virus) has emerged quickly in parts of North America, along with the expanding range of *I. scapularis* ticks.

POWV infection typically begins with prodromal symptoms including fever, nausea, headache, and myalgia. Central nervous system involvement includes an altered level of consciousness, paralysis, or ophthalmoplegia (*4*). POWV encephalitis has a 10% mortality rate, and ≤50% of survivors suffer residual deficits (*5*). Studies with mice have demonstrated that POWV can affect motor neurons in the anterior horns of the spinal cord (*6*). These same neurons are affected by poliovirus, West Nile virus, and enterovirus D68 (*7*). However, POWV infection with cord involvement in humans is not well documented; 1 human case demonstrated motor neuron pathology after POWV lineage 2 infection (*8*), and a second case with suspected motor neuronopathy was reported in 2018 (*9*).

We present the case of a 62-year-old man living in urban Ontario who experienced nausea, vomiting, and abdominal pain while vacationing in rural Newfoundland. He sought treatment at a hospital in Nova Scotia and experienced diplopia and ataxia. A computed tomography scan of the head did not show any acute intracranial event.

The patient became febrile and experienced dysarthria, weakness, and respiratory distress. Cerebrospinal fluid analysis showed pleocytosis (159×10^6 total nucleated cells: 42% neutrophils, 43% lymphocytes) and elevated protein levels (0.79 g/L). He was started on empiric treatment with ceftriaxone, ampicillin, acyclovir, and dexamethasone. Results of tests for *Cryptococcus*, HIV, syphilis, Lyme disease, herpes simplex viruses 1 and 2, varicella zoster virus, and acid-fast bacilli were negative. Initial arbovirus serology results were negative. The patient worsened, requiring intubation and transfer to an intensive care unit.

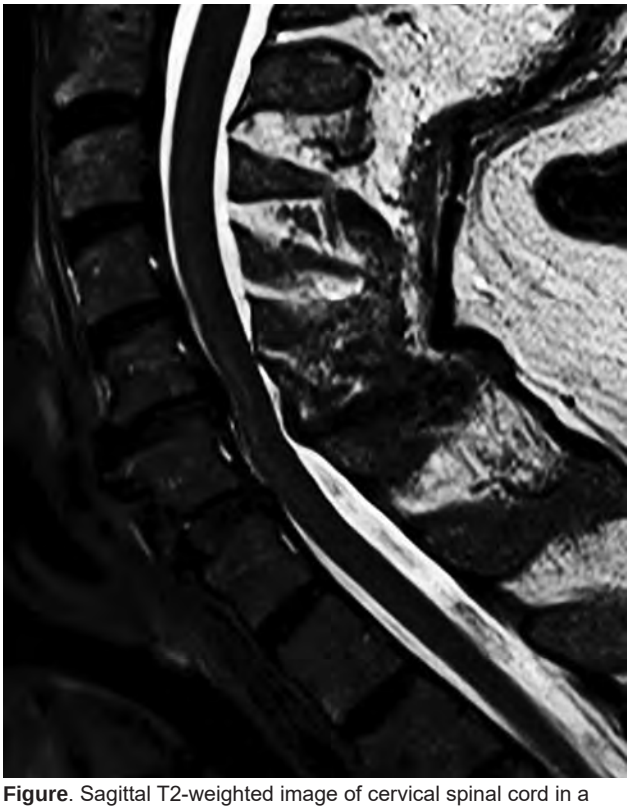

Figure. Sagittal T2-weighted image of cervical spinal cord in a patient with Powassan virus infection, Canada. A longitudinal hyperintensity of the anterior horn is visible from C3 to C6.

Seven days after arriving at the hospital, the patient was unable to lift his arms and was transferred to a tertiary center in Ottawa, Ontario (The Ottawa Hospital). Neurologic exam showed facial and extraocular muscle weakness. He had flaccid tone and absent power in his upper extremities and reduced strength in his lower extremities. Sensation was preserved. Nerve conduction studies demonstrated diffusely low motor amplitudes, normal sensory amplitudes, and normal conduction velocities suggestive of a motor neuronopathy. Electromyography in the acute phase was not possible due to poor patient cooperation.

Results of paired convalescent arbovirus serology collected 1 month after symptom onset were positive. Testing at the National Microbiology Laboratory confirmed POWV infection (hemagglutination inhibition titer 1:80, plaque-reduction neutralization titer 1:160). Magnetic resonance imaging (MRI) of the brain showed infratentorial and supratentorial leptomeningeal enhancement. An MRI of the cervical spine showed increased T2-weighted signal involving the anterior horns from C3 to C6 (Figure; Appendix Figure, https://wwwnc.cdc.gov/EID/article/25/8/19-0399-App1.pdf).

Follow-up MRI of the brain and spine 1 month later showed interval resolution of leptomeningeal abnormalities, but abnormal signal within the anterior horn of the cervical spine remained. Electrodiagnostic testing repeated 6 months after symptom onset again showed normal sensory nerve conduction studies and abnormal motor nerve conduction studies. There was diffuse denervation in all cervical myotomes including the paraspinal muscles, confirming a motor neuronopathy consistent with a poliomyelitis-like presentation of POWV. We suspect that initial arbovirus serology was performed too early in the disease course, because paired serology 4 weeks later demonstrated seroconversion and confirmed diagnosis.

Our case shares similarities with a recently published report of POWV infection (*9*). In that case, a patient vacationing in the Luskville region of Quebec, Canada, experienced cranial nerve pathologies and flaccid weakness of the upper extremities. Electrodiagnostic testing showed evidence of diffuse denervation and reinervation across multiple myotomes that was consistent with a motor neuronopathy. Imaging of the brain showed only mild hyperintensities that would not account for the patient's disproportionate weakness. A spinal MRI was not performed. As in our case, acute arbovirus serology results were initially negative but were positive in paired testing (*9*).

The incidence of POWV infection has increased since 2017 (*7*). *I. scapularis* ticks and deer tick virus may be becoming more widely disseminated in northern regions, potentially due to warming climates, whereas infection with prototypical POWV transmitted by *I. cookei* ticks remains rare and stable in distribution (*10*). It is possible that Canada will see an increasing number of cases similar to ours. Our findings emphasize the need to include POWV infection in the differential diagnosis for patients with polio-like symptoms in tick-endemic regions.

About the Author

Dr. Picheca and Dr. Yogendrakumar are resident physicians specializing in neurology at the University of Ottawa. Dr. Picheca has an interest in infectious diseases. Dr. Yogendrakumar's primary research interests are in stroke and intracerebral hemorrhage.

References

1. McLean DM, Donohue WL. Powassan virus: isolation of virus from a fatal case of encephalitis. Can Med Assoc J. 1959;80:708–11.
2. Centers for Disease Control and Prevention. Statistics & maps: Powassan virus. 2018 [cited 2019 Mar 13]. https://www.cdc.gov/powassan/statistics.html
3. Corrin T, Greig J, Harding S, Young I, Mascarenhas M, Waddell LA. Powassan virus, a scoping review of the global evidence. Zoonoses Public Health. 2018 [cited 2019 Mar 13]. http://dx.doi.org/10.1111/zph.12485
4. Sung S, Wurcel AG, Whittier S, Kulas K, Kramer LD, Flam R, et al. Powassan meningoencephalitis, New York, New York, USA. Emerg Infect Dis. 2013;19. http://dx.doi.org/10.3201/eid1909.121846

5. Ebel GD. Update on Powassan virus: emergence of a North American tick-borne flavivirus. Annu Rev Entomol. 2010;55: 95–110. http://dx.doi.org/10.1146/annurev-ento-112408-085446
6. Santos RI, Hermance ME, Gelman BB, Thangamani S. Spinal cord ventral horns and lymphoid organ involvement in Powassan virus infection in a mouse model. Viruses. 2016;8:220. http://dx.doi.org/10.3390/v8080220
7. Hermance ME, Thangamani S. Powassan virus: an emerging arbovirus of public health concern in North America. Vector Borne Zoonotic Dis. 2017;17:453–62. http://dx.doi.org/10.1089/vbz.2017.2110
8. Tavakoli NP, Wang H, Dupuis M, Hull R, Ebel GD, Gilmore EJ, et al. Fatal case of deer tick virus encephalitis. N Engl J Med. 2009;360:2099–107. http://dx.doi.org/10.1056/NEJMoa0806326
9. Sanderson M, Lindsay LR, Campbell TM, Morshed M. A case of Powassan encephalitis acquired in southern Quebec. CMAJ. 2018;190:E1478–80. http://dx.doi.org/10.1503/cmaj.180905
10. Fatmi SS, Zehra R, Carpenter DO. Powassan virus—a new reemerging tick-borne disease. Front Public Health. 2017;5:342. http://dx.doi.org/10.3389/fpubh.2017.00342

Address for correspondence: Vignan Yogendrakumar, The Ottawa Hospital, Civic Campus, 1053 Carling Ave, Ottawa, ON K1Y 4E9, Canada; email: vyogendrakumar@toh.ca

etymologia

Poliomyelitis [pō'-lē-ō-mī-ə-lī-'təs]

Ronnie Henry

From the Greek *polios* (“gray”) + *myelos* (“marrow”), poliomyelitis may have plagued humanity since antiquity. The funerary stele of the Egyptian priest Ruma (circa 1400 BCE) shows a shortened, withered leg, in what is believed to be one of the earliest depictions of polio. The first clinical description was in 1789 by Michael Underwood. Karl Landsteiner and Erwin Popper identified poliovirus in 1908, and 40 years later John Enders, Thomas Weller, and Frederick Robbins were able to grow poliovirus in tissue culture cells, work for which they received the Nobel Prize in Medicine or Physiology in 1954. This breakthrough facilitated vaccine research, and the first inactivated polio vaccine, developed by Jonas Salk and his team, was licensed in 1955. Six years later, Albert Sabin and his team developed a live, attenuated oral polio vaccine.

Because broad immunization campaigns made progress toward regional polio elimination in the Americas, in 1988 the World Health Assembly declared a goal of global polio eradication. Through a partnership between Rotary International, the World Health Organization, the United Nations Children’s Fund, the Centers for Disease Control and Prevention, and the Bill & Melinda Gates Foundation, the Global Polio Eradication Initiative has achieved a 99.9% decrease in the global incidence of polio. Today, wild poliovirus transmission occurs in only Afghanistan and Pakistan, and 4 of the 6 World Health Organization regions have formally declared the elimination of the indigenous wild poliovirus. Of the 3 types of poliovirus, type 2 wild poliovirus was declared eradicated globally in 2015, and type 3 wild poliovirus has not been detected since 2012. With only 33 cases globally from type 1 wild poliovirus in 2018, the task remains to eliminate polio in its last niches.

This historic 1975 photograph shows a laboratory technician preparing doses of polio vaccine by placing a liquid droplet of the vaccine on each of these sugar cubes, which would subsequently be ingested orally by each recipient. Photo: Public Health Image Library, Centers for Disease Control and Prevention, 1975.

Sources

1. Pearce JM. Poliomyelitis (Heine-Medin disease). J Neurol Neurosurg Psychiatry. 2005;76:128. https://doi.org/10.1136/jnnp.2003.028548
2. Global Polio Eradication Initiative. History of polio [cited 2019 Jun 21]. http://polioeradication.org/polio-today/history-of-polio
3. Global Polio Eradication Initiative. Our mission [cited 2019 Jun 21] http://polioeradication.org/who-we-are/our-mission

Address for correspondence: Ronnie Henry, Centers for Disease Control and Prevention, 1600 Clifton Rd NE, Mailstop E28, Atlanta, GA 30329-4027, USA; email: boq3@cdc.gov

DOI: https://doi.org/10.3201/eid2508.ET2508

Recombinant GII.Pe-GII.4 Norovirus, Thailand, 2017–2018

Watchaporn Chuchaona, Jira Chansaenroj, Nasamon Wanlapakorn, Sompong Vongpunsawad, Yong Poovorawan

Author affiliation: Chulalongkorn University, Bangkok, Thailand

DOI: https://doi.org/10.3201/eid2508.190365

During June 2017–December 2018, norovirus was responsible for 10.9% of acute gastroenteritis cases in Thailand. Genogroup I (GI) was found in 14% of samples, of which 12 were co-infected with genogroup II (GII). In 35.8% of samples, GII.Pe-GII.4 Sydney predominated. Diverse recombinant strains of GI and GII norovirus co-circulated year-round.

Norovirus is a major cause of nonbacterial acute gastroenteritis; sporadic cases and outbreaks occur among children and adults (*1*). Most strains infecting humans belong to genogroups I and II (GI and GII), of which GII.4 has been most predominant (*2*). Reemergence of norovirus infection is attributed to new variants resulting from frequent recombination between the end of open reading frame (ORF) 1, encoding the RNA-dependent RNA polymerase (RdRp), and ORF2, encoding the major capsid protein (VP1) of the norovirus genome. Lack of a robust cell culture system for human norovirus infection in humans and lack of long-lasting neutralizing antibodies in previously infected persons present challenges for vaccine development.

In recent years, a relative increase in global prevalence of norovirus has been attributed to GII.P16-GII.4, GII.17, and GII.P16-GII.2 (*3*–*5*). As in temperate regions, norovirus infection in Thailand occurs as sporadic cases and outbreaks year-round. After the recent increase of GII.P16-GII.2 in Thailand in late 2016 (*6*), we sought to identify the most frequently identified genotype(s).

During June 2017–December 2018, we tested 2,704 fecal/rectal swab samples from patients with acute gastroenteritis (watery diarrhea and sometimes vomiting) in hospitals in Bangkok (King Chulalongkorn Memorial Hospital and Bangpakok 9 International Hospital; n = 2,385 patients), Khon Kaen (n = 70), Phitsanulok (n = 199), and Saraburi (n = 50), Thailand. Mean patient age ± SD was 27.9 ± 25.1 years (range 1 month–103 years). These samples were collected for diagnostic tests routinely ordered by clinicians and served as convenient research samples; most (>95%) patients were inpatients. The institutional review board of Chulalongkorn University approved this study (IRB 634/59).

We extracted viral RNA from 10% (wt/vol) fecal suspension with phosphate-buffered saline by using Ribospin vRD II (GeneAll, http://www.geneall.com) and subjected it to TaqMan Fast Virus 1-Step real-time reverse transcription PCR (RT-PCR) (Thermo Fisher, https://www.thermofisher.com) (*7*). We dual typed norovirus-positive samples by using RT-PCR to amplify the partial RdRp and VP1 genes (*6*) (GenBank accession nos. MK589361–402, MK590421–687, and MK590696–962). For genotyping, we used the Norovirus Genotyping Tool (http://www.rivm.nl/mpf/norovirus/typingtool). We phylogenetically analyzed nucleotide sequences by using the maximum-likelihood method with 1,000 bootstrap replicates in MEGA7 (http://www.megasoftware.net).

A total of 296 (10.9%) of 2,704 samples were positive for norovirus (patient mean age ± SD 14.8 ± 19.9 years, range 3 months–88 years). A minority of strains (42/296) were genotype GI (GI.3 15/42, GI.5 14/42, GI.1 6/42, GI.7 6/42, GI.4 1/42) (Appendix Figure 1, https://wwwnc.cdc.gov/EID/article/25/8/19-0365-App1.pdf). Most positive samples (266/296) were GII strains, of which 12 were co-infected with GI/GII. The 3 most common RdRp genotypes were GII.Pe (40.6%, 108/266), GII.P16 (28.6%, 76/266), and GII.P17 (16.2%, 43/266) (Figure, panel A). Among samples for which VP1 genotyping was successful, most were GII.4 Sydney (56.8%, 151/266), followed by GII.17 (16.2%, 43/266), GII.6 (5.3%, 14/266), GII.3 (5.3%, 14/266), GII.13 (4.9%, 13/266), GII.2 (4.1%, 11/266), and others (7.5%, 20/266) (Figure, panel B). The most prevalent strains were recombinant GII.Pe-GII.4 Sydney (39.9%, 106/266), GII.P16-GII.4 Sydney (17%, 45/266), and GII.P17-GII.17 (15%, 39/266). Although RdRp genotype GII.Pe is usually associated with VP1 genotype GII.4 Sydney, we identified 1 strain each of GII.Pe-GII.3 and GII.Pe-GII.13.

In this study, norovirus infections were frequently detected in children ≤5 years of age (60.1%, 178/296, mean age ± SD 2.2 ± 1.3 years). Using cycle threshold (C_t) as a surrogate for viral load, we age stratified norovirus-positive patients (GII.Pe-GII.4 Sydney) into 3 age groups, <2, 2–5, and >5 years (Appendix Figure 2). Mean viral load was higher among children ≤5 years of age (C_t = 19.0) than among those >5 years of age (C_t = 25.1) ($p<0.01$).

In Thailand, the most frequently identified norovirus genotype throughout 2018 was GII.Pe-GII.4 Sydney. In the United States, GII.Pe-GII.4 Sydney first emerged in 2012 and was prevalent until mid-2015 (*3*,*8*); however, it represented minor variants elsewhere and has not been previously associated with increased norovirus activity in Thailand (*9*). Although GII.P16-GII.4 Sydney subsequently emerged in many industrialized countries, both GII.Pe-GII.4 Sydney and GII.P16-GII.4 Sydney circulated concurrently in Thailand after the upsurge of GII.17 in 2015–2016 and GII.P16-

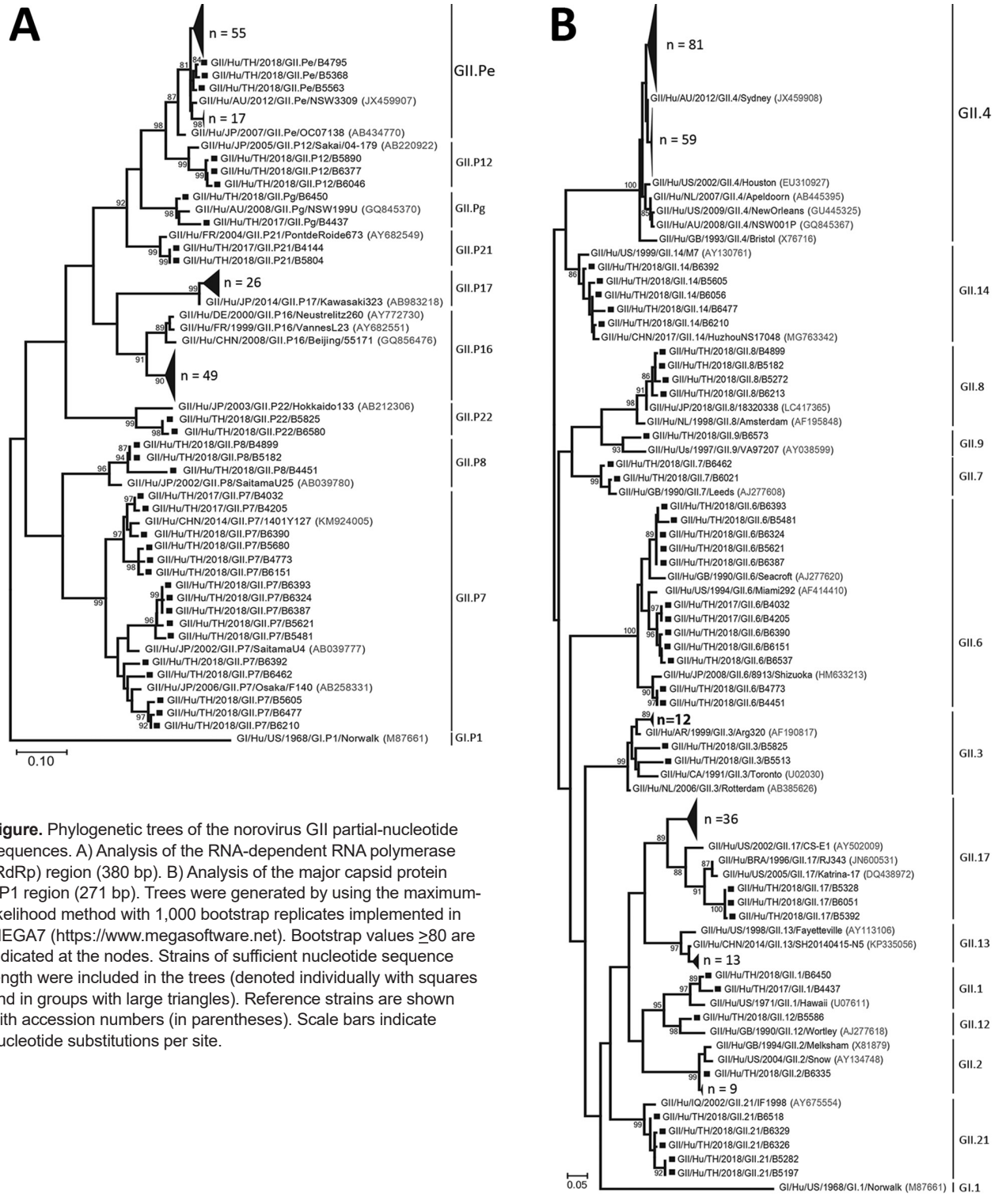

Figure. Phylogenetic trees of the norovirus GII partial-nucleotide sequences. A) Analysis of the RNA-dependent RNA polymerase (RdRp) region (380 bp). B) Analysis of the major capsid protein VP1 region (271 bp). Trees were generated by using the maximum-likelihood method with 1,000 bootstrap replicates implemented in MEGA7 (https://www.megasoftware.net). Bootstrap values ≥80 are indicated at the nodes. Strains of sufficient nucleotide sequence length were included in the trees (denoted individually with squares and in groups with large triangles). Reference strains are shown with accession numbers (in parentheses). Scale bars indicate nucleotide substitutions per site.

GII.2 in 2016–2017 in Thailand (*6*). Three years later, GII.17 continued to be detected sporadically, albeit at low levels. Therefore, norovirus circulation in Thailand at times differed from the global trend, which cannot be explained by factors such as geographic location and warm climate alone.

The significance of GI/GII co-infection in some samples is unclear but is probably not the result of laboratory contamination because as many as 7 combinations were identified (4 samples of GI.5/GII.17; 2 each of GI.3/GII.P16-GII.4 Sydney and GI.5/GII.P16-GII.21; and 1 each of GI.1/GII.P8-

GII.6, GI.3/GII.17, GI.7/GII.17, and GI.7/GII.P7-GII.6). We did not perform dual typing on GI strains because they were less predominant than GII strains. However, future analysis of their recombination patterns will be useful for better characterizing these rare but potentially significant genotypes. This study was somewhat limited by lack of detailed clinical information accompanying the submitted samples and absence of surveillance from southern Thailand (≈14% of the country's population). Molecular epidemiology and continued surveillance of norovirus strain diversity will increase awareness among clinicians and help epidemiologists determine global transmission patterns.

This work was supported by the Research Chair Grant from the National Science and Technology Development Agency (P-15-50004) and the Center of Excellence in Clinical Virology of Chulalongkorn University and Hospital (GCE 59-009-30-005). Support for W.C. was provided by the Tuition/Fee and Stipend Scholarship for Graduate Students (Faculty of Medicine of Chulalongkorn University) and a scholarship from Chulalongkorn University Graduate School to commemorate the Celebrations on the Auspicious Occasion of Her Royal Highness Princess Maha Chakri Sirindhorn's 60th Birthday.

About the Author

Ms. Chuchaona is a doctoral graduate student at Chulalongkorn University. Her primary research interests include viral gastroenteritis caused by norovirus and rotavirus.

References

1. Ahmed SM, Hall AJ, Robinson AE, Verhoef L, Premkumar P, Parashar UD, et al. Global prevalence of norovirus in cases of gastroenteritis: a systematic review and meta-analysis. Lancet Infect Dis. 2014;14:725–30. http://dx.doi.org/10.1016/S1473-3099(14)70767-4
2. Vinjé J. Advances in laboratory methods for detection and typing of norovirus. J Clin Microbiol. 2015;53:373–81. http://dx.doi.org/10.1128/JCM.01535-14
3. Chan MCW, Hu Y, Chen H, Podkolzin AT, Zaytseva EV, Komano J, et al. Global spread of norovirus GII.17 Kawasaki 308, 2014–2016. Emerg Infect Dis. 2017;23:1359–1354. http://dx.doi.org/10.3201/eid2308.161138
4. Niendorf S, Jacobsen S, Faber M, Eis-Hübinger AM, Hofmann J, Zimmermann O, et al. Steep rise in norovirus cases and emergence of a new recombinant strain GII.P16-GII.2, Germany, winter 2016. Euro Surveill. 2017;22:30447. http://dx.doi.org/10.2807/1560-7917.ES.2017.22.4.30447
5. van Beek J, de Graaf M, Al-Hello H, Allen DJ, Ambert-Balay K, Botteldoorn N, et al.; NoroNet. Molecular surveillance of norovirus, 2005-16: an epidemiological analysis of data collected from the NoroNet network. Lancet Infect Dis. 2018;18:545–53. http://dx.doi.org/10.1016/S1473-3099(18)30059-8
6. Thanusuwannasak T, Puenpa J, Chuchaona W, Vongpunsawad S, Poovorawan Y. Emergence of multiple norovirus strains in Thailand, 2015-2017. Infect Genet Evol. 2018;61:108–12. http://dx.doi.org/10.1016/j.meegid.2018.03.021
7. Debbink K, Costantini V, Swanstrom J, Agnihothram S, Vinjé J, Baric R, et al. Human norovirus detection and production, quantification, and storage of virus-like particles. Curr Protoc Microbiol. 2013;31:15K.1.1–15K.1.45.
8. Yang Z, Vinjé J, Kulka M. Complete genome sequence of human norovirus GII.Pe-GII.4 Sydney from the United States. Genome Announc. 2017;5:e00159–17. http://dx.doi.org/10.1128/genomeA.00159-17
9. Botha JC, Taylor MB, Mans J. Comparative analysis of South African norovirus GII.4 strains identifies minor recombinant variants. Infect Genet Evol. 2017;47:26–34. http://dx.doi.org/10.1016/j.meegid.2016.11.004

Address for correspondence: Yong Poovorawan, Center of Excellence in Clinical Virology, Faculty of Medicine, Chulalongkorn University, 1873 Rama 4 Rd, Pathumwan, Bangkok 10330, Thailand; email: yong.p@chula.ac.th

Sneathia amnii and Maternal Chorioamnionitis and Stillbirth, Mozambique

Pio Vitorino,[1] Rosauro Varo,[1] Paola Castillo, Juan Carlos Hurtado, Fabiola Fernandes, Ana Marta Valente, Rita Mabunda, Sibone Mocumbi, Joy M. Gary, Tiffany G. Jenkinson, Inacio Mandomando, Dianna M. Blau, Robert F. Breiman, Quique Bassat

Author affiliations: Centro de Investigação em Saúde de Manhiça, Maputo, Mozambique (P. Vitorino, R. Varo, A.M. Valente, R. Mabunda, I. Mandomando, Q. Bassat); ISGlobal Hospital Clinic–Universitat de Barcelona, Barcelona, Spain (R. Varo, P. Castillo, J.C. Hurtado, A.M. Valente, Q. Bassat); Hospital Clínic, Barcelona (P. Castillo, J.C. Hurtado); Hospital Central de Maputo, Maputo (F. Fernandes, S. Mocumbi); Universidade Eduardo Mondlane, Maputo (F. Fernandes, S. Mocumbi); Centers for Disease Control and Prevention, Atlanta, Georgia, USA (J.M. Gary, T.G. Jenkinson, D.M. Blau); Emory Global Health Institute, Atlanta (R.F. Breiman); Institució Catalana de Recerca i Estudis Avançats (ICREA), Barcelona (Q. Bassat); Hospital Sant Joan de Déu, Barcelona (Q. Bassat); Consorcio de Investigación Biomédica en Red de Epidemiología y Salud Pública (CIBERESP), Madrid, Spain (Q. Bassat)

DOI: https://doi.org/10.3201/eid2508.190526

[1]These authors contributed equally to this article.

We report a case of *Sneathia amnii* as the causative agent of maternal chorioamnionitis and congenital pneumonia resulting in a late fetal death in Mozambique, with strong supportive postmortem molecular and histopathologic confirmation. This rare, fastidious gram-negative coccobacillus has been reported to infrequently cause abortions, stillbirths, and neonatal infections.

Sneathia amnii, formerly designated *Leptotrichia amnionii*, is a rare, fastidious, gram-negative coccobacillus, first described in the amniotic fluid of a woman with a fetal demise (*1*). The inherent difficulties in conventionally culturing this pathogen led to its initial identification through analyzing the 16S rRNA gene; its genome was recently sequenced (*1*,*2*). *S. amnii* is an opportunistic agent of the female urogenital tract (*3*,*4*) associated with cases of spontaneous abortion (miscarriage) and neonatal meningitis (*1*,*5*,*6*). We describe a perinatal case of *S. amnii* infection in a mother–fetus dyad, which we documented and investigated with the minimally invasive tissue sampling (MITS) postmortem procedure (*7*).

An otherwise healthy multigravida 37-year-old woman, at an estimated gestational age of 39 weeks, was admitted to Manhiça District Hospital, southern Mozambique, in labor. During pregnancy, she had attended 2 antenatal consultations and received the standard of care for pregnant women in Mozambique; mild anemia was treated with ferrous sulfate and folic acid supplements. Serologic tests for syphilis and HIV were both negative. Upon arrival at the hospital, the mother was afebrile and hemodynamically stable; she had a fully effaced uterine cervix, thin and elastic, 2 cm dilation; intact amniotic membranes; and cephalic fetal presentation with heartbeat present. Physical examination did not provide additional information. Labor progressed with spontaneous rupture of membranes. No additional documentation of the fetal heartbeat was available before delivery. Two hours after arrival, a fresh stillborn female weighing 3.5 kg was born by spontaneous vaginal delivery. Size was normal, and no macroscopic congenital abnormalities were observed. The mother was discharged next day without complications.

As part of Mozambique's Child Health and Mortality Prevention Surveillance (CHAMPS), after obtaining written, informed consent, we conducted MITS by biopsy needle of tissues and body fluids, in addition to placenta, to ascertain the cause of the stillbirth (*7*). Samples are subject to thorough histopathologic, molecular, and microbiological investigation, including universal screening for HIV-1, *Mycobacterium tuberculosis*, and malaria parasites. We performed conventional microbiological cultures of blood and cerebrospinal fluid (CSF); we inoculated ≈3 mL of blood into aerobic blood culture bottle (BACTEC system; Becton Dickinson, https://www.bd.com) and cultured CSF samples into blood, chocolate, and MacConkey agar plates. We performed multipathogen molecular screening using TaqMan Array Card (Applied Biosystems, https://www.thermofisher.com) in whole blood, CSF, lung, and rectal swab samples (*8*). We prepared and examined tissue samples using conventional pathologic methods and targeted immunohistochemical staining (*9*).

We isolated no microorganisms in CSF or blood, nor did we detect a likely pathogen in any of the unfixed

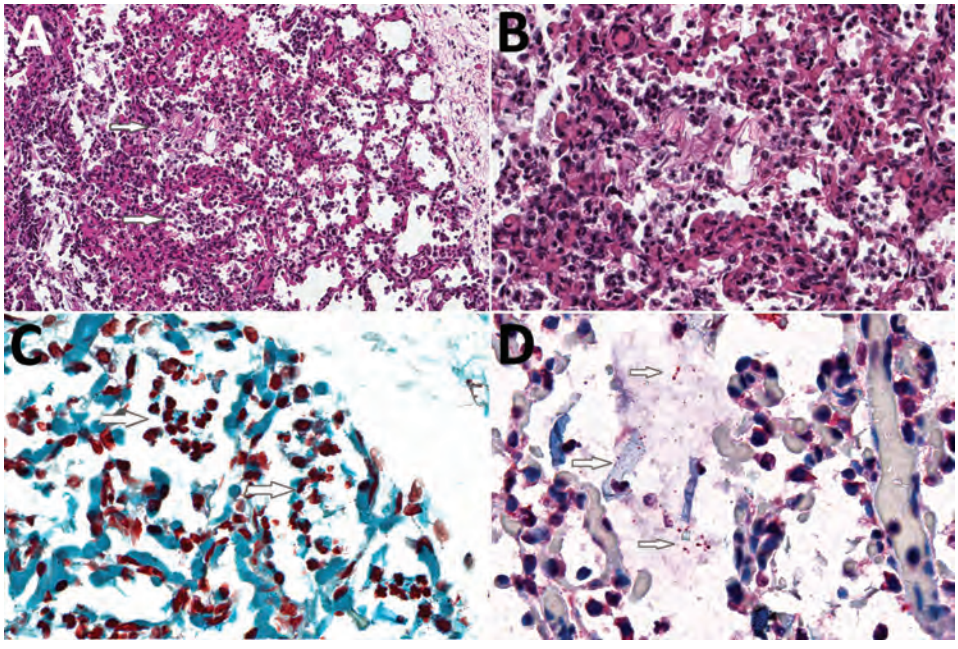

Figure. Histologic evidence of amniotic fluid aspiration, bronchopneumonia, and intraalveolar gram-negative coccobacilli in the lung of a stillborn infant, Mozambique. A) Hematoxylin and eosin stain of lung tissue showing acute inflammation within alveoli (bronchopneumonia, upper arrow) and moderate numbers of aspirated squames (lower arrow), consistent with intrauterine fetal distress and associated aspiration of amniotic fluid. Original magnification ×20. B) Higher magnification of panel A tissue showing acute inflammation within alveoli (bronchopneumonia) and a clump of aspirated squames. Original magnification ×40. C) Gram stain of lung showing multiple small, gram-negative coccobacilli mixed with acute inflammation within alveoli (arrows indicate regions with bacteria). Original magnification ×63. D) Polybacterial immunohistochemical assay of lung tissue targeting multiple bacteria highlights the coccobacilli within alveoli (top and bottom arrows). Aspirated squames are also present (middle arrow). Original magnification ×63.

postmortem tissues. At CHAMPS reference pathology laboratories, examination of tissue samples showed similar morphological findings in placental and miscellaneous tissues that suggested infection, including an acute inflammatory infiltrate in the lungs compatible with bronchopneumonia. We also found moderate numbers of aspirated squames and increased alveolar macrophages, indicating intrauterine fetal distress and associated aspiration of amniotic fluid. No aspirated meconium was apparent. Gram stain revealed gram-negative coccobacilli in alveoli and adjacent bronchioles. We conducted a cross-reactive immunohistochemical assay targeting multiple bacteria in the lung samples using paneubacteria and gram type–specific PCR assays targeting the 16S rRNA gene; we identified *S. amnii* by sequence analysis of positive amplicons (Figure, panels A–C). We observed no remarkable histopathologic findings in the liver or brain, and the cross-reactive polybacterial immunohistochemical assay was negative in brain tissue. Placental tissue and umbilical cord showed an acute chorioamnionitis with maternal response (inflammation in the membranes, stage 2) and fetal response (inflammation in the umbilical cord, stage 2) showing umbilical arteritis with rare gram-negative coccobacilli. There was no immunohistochemical evidence of bacteria in this tissue (Figure 1, panel D). We obtained an amplicon from placental tissue by paneubacteria PCR; however, we could not confirm the presence of *S. amnii* sequences.

CHAMPS procedures include the review of all clinical, microbiological, molecular, and histopathological data, along with the verbal autopsy, by a multidisciplinary panel of local experts (D.M. Blau et al., unpub. data). The panel concluded that the immediate cause of this stillbirth could be attributed to a congenital pneumonia, caused by *S. amnii*, that could have originated in the mother's placenta; we determined that chorioamnionitis was the main maternal condition associated with the child's death. The presence of *Sneathia* sp. bacteria in amniotic fluid can lead to inflammation and histologic chorioamnionitis, amnionitis, or both (*10*).

S. amnii has been identified in different settings as a pathologic agent in women and children (*1*,*3*–*6*). In this case in a rural setting in Africa, *S. amnii* was the causative agent in a stillbirth with congenital pneumonia, a diagnosis supported by strong postmortem molecular and histopathologic confirmation. As CHAMPS evaluation continues in Mozambique, as well as at sites in 6 additional countries in sub-Saharan Africa and south Asia, we expect the importance of this pathogen to become clearer.

The Spanish Agency of Cooperation and International Development (AECID) funds the core activities of Centro de Investigação em Saúde de Manhiça. R.V. had a fellowship from the Rio Hortega program of the Instituto de Salud Carlos III (ISCIII) grant no. CD16/00024.

J.M.G. received grants from the Gates Foundation during the study period. The other authors declare that they have no competing interests.

About the Authors

Dr. Vitorino is a clinical researcher at Centro de Investigação em Saúde de Manhiça, Maputo, Mozambique. Her research interests are in pediatric infectious diseases and key determinants of pediatric causes of death in resource-constrained settings. Dr. Varo is a medical research fellow with ISGlobal whose interests include malaria clinical trials and key determinants of pediatric causes of death in resource-constrained settings.

References

1. Shukla SK, Meier PR, Mitchell PD, Frank DN, Reed KD. *Leptotrichia amnionii* sp. nov., a novel bacterium isolated from the amniotic fluid of a woman after intrauterine fetal demise. J Clin Microbiol. 2002;40:3346–9. https://doi.org/10.1128/JCM.40.9.3346-3349.2002
2. Harwich MD Jr, Serrano MG, Fettweis JM, Alves JM, Reimers MA, Buck GA, et al.; Vaginal Microbiome Consortium (additional members). Genomic sequence analysis and characterization of *Sneathia amnii* sp. nov. BMC Genomics. 2012;13(Suppl 8):S4. https://doi.org/10.1186/1471-2164-13-S8-S4
3. Gundi VA, Desbriere R, La Scola B. *Leptotrichia amnionii* and the female reproductive tract. Emerg Infect Dis. 2004;10:2056–7. https://doi.org/10.3201/eid1011.031019
4. Thilesen CM, Nicolaidis M, Lökebö JE, Falsen E, Jorde AT, Müller F. *Leptotrichia amnionii*, an emerging pathogen of the female urogenital tract. J Clin Microbiol. 2007;45:2344–7. https://doi.org/10.1128/JCM.00167-07
5. Boennelycke M, Christensen J, Arpi M, Krause S. *Leptotrichia amnionii* found in septic abortion in Denmark. Scand J Infect Dis. 2007;39:382–3. https://doi.org/10.1080/00365540601053022
6. Decroix V, Goudjil S, Kongolo G, Mammeri H. *'Leptotrichia amnionii'*, a newly reported cause of early onset neonatal meningitis. J Med Microbiol. 2013;62:785–8. https://doi.org/10.1099/jmm.0.051870-0
7. Menendez C, Castillo P, Martínez MJ, Jordao D, Lovane L, Ismail MR, et al. Validity of a minimally invasive autopsy for cause of death determination in stillborn babies and neonates in Mozambique: an observational study. PLoS Med. 2017;14:e1002318. https://doi.org/10.1371/journal.pmed.1002318
8. Diaz MH, Waller JL, Theodore MJ, Patel N, Wolff BJ, Benitez AJ, et al. Development and implementation of multiplex TaqMan array cards for specimen testing at Child Health and Mortality Prevention Surveillance (CHAMPS) site laboratories. Clin Infect Dis. In press 2019.
9. Martines RB, Ritter JM, Gary J, Shieh W-J, Ordi J, Hale M, et al. Pathology and telepathology methods in the Child Health and Mortality Prevention Surveillance Network (CHAMPS). Clin Infect Dis. In press 2019.
10. Han YW, Shen T, Chung P, Buhimschi IA, Buhimschi CS. Uncultivated bacteria as etiologic agents of intra-amniotic inflammation leading to preterm birth. J Clin Microbiol. 2009;47:38–47. https://doi.org/10.1128/JCM.01206-08

Address for correspondence: Rosauro Varo, Centro de Investigação em Saúde de Manhiça, Clinical Department, Rua 12 Cambeve, Manhica, Maputo 1919, Mozambique; email: rosauro.varo@manhica.net

In Memoriam: Myron Gilbert Schultz (1935–2016)

David M. Morens, Rohit A. Chitale

In 1954, a freshman veterinary student became "engaged in an inner struggle" (*1*). A wise mentor took him to hear a minister speak about the missionary physician Albert Schweitzer (1875–1965), who had devoted his entire life to serving others. "I was astonished that such a man could exist," the student remembered (*1*). Each morning the student repeated an 18th century prayer reflecting the teachings of physician-philosopher-rabbi Moses ben Maimon, or Maimonides (1135–1204): "Grant that I may be filled with love for my art and for my fellow man. May the thirst for gain and the desire for fame be far from my heart" (*2*). With renewed purpose, the young scholar finished his Doctor of Veterinary Medicine degree (1958), then his Medical Doctor degree (1962). Thus began the remarkable, humanistic career of Myron Gilbert ("Mike") Schultz (Figure). Sixty years later, that career still flourished in humanistic faith.

Myron Gilbert Schultz, DVM, MD, DCMT, FACP, was born to middle-class parents in the Bronx, New York City, New York, USA, on January 6, 1935. After graduation from the Bronx High School of Science, he spent 2 years (1952–1954) at the New York State College of Agriculture, 4 more at the New York State College of Veterinary Medicine, Cornell (1954–1958), and another 4 at Albany Medical College (1958–1962), during which time he supported himself by practicing veterinary medicine at the Saratoga Raceway and, as he would later relate, repeatedly abandoning the horses to rush back and deliver babies.

With DVM and MD degrees in hand, Mike interned at the US Public Health Service Hospital (Boston, MA, USA). This internship led to his recruitment by Alexander D. Langmuir (1910–1993) and a transformative 2-year stint in Langmuir's Atlanta-based Epidemic Intelligence Service (EIS) training program at the (then-named) Center for Disease Control (CDC). Mike's EIS experiences included a 1964 deployment to Vietnam to investigate infectious disease threats in the war and an important friendship with James Harlan Steele, DVM (1913–2013), the renowned veterinary epidemiologist/epizootiologist whose leadership helped to formulate their shared concept of "One Health"—the idea that humans, animals, and the environment are all part of an intertwined ecosystem with respect to disease occurrence and microbial evolution—and to shape the conceptualization of emerging infectious diseases (*3*). At the end of those 2 years in EIS, Mike was held in such regard that he was sent off on 2 successive career development assignments: an infectious diseases fellowship at New York City's Bellevue Hospital (1965–1966) and another year at the London School of Hygiene and Tropical Medicine (1966–1967).

At just 32 years of age, Mike returned to CDC to become chief of the newly created Parasitic Diseases Branch (1967–1973), and when the branch was elevated to a division, he was named its director (1973–1982). These were years of extraordinary productivity. Almost immediately after becoming branch chief, Mike began studying the national epidemiology of *Pneumocystis carinii* (now named *P. jirovecii*) pneumonia (*4*,*5*), which, 14 years later, would provide the first evidence of the AIDS epidemic (*6*). He established human giardiasis as an important endemic and travel-associated disease (*7*); contributed significantly to the new field of travel medicine (*8*,*9*), initiating the "Yellow Book" of health information for travelers; co-developed the Field Epidemiology Training Program to teach epidemiology around the world; created CDC's Parasitic Diseases Drug Service, bringing to patients worldwide important drugs, such as pentamidine to treat African trypanosomiasis; studied parasitic disease outbreaks in Micronesia, in Native Americans, and in US mental institutions; chaired the first international symposium on dracunculiasis (Guinea worm disease), now close to eradication; and dealt with a host of other

Image not available

Figure. Myron Gilbert "Mike" Schultz (1935–2016). His career in global public health and zoonotic disease control spanned 53 years, almost entirely at the Centers for Disease Control and Prevention (CDC).

Author affiliations: National Institutes of Health, Bethesda, Maryland, USA (D.M. Morens); Associate Editor, Emerging Infectious Diseases, Atlanta, Georgia, USA (D.M. Morens); PATH, Seattle, Washington, USA (R.A. Chitale)

DOI: https://doi.org/10.3201/eid2508.190356

parasitic diseases directly and through leadership of a talented cadre of CDC scientists and EIS officers (*10–13*).

During this same time, Mike also displayed great talent as a medical historian, evidenced by a rigorously researched special article in the New England Journal of Medicine about Daniel Carrión's 1885 elucidation of bartonellosis (*14*); medical detective work on Robert Louis Stevenson's creation of Dr. Jekyll and Mr. Hyde (*15*); and, most memorably, lectures and publications about US Public Health Service epidemiologist József (known as Joseph) Goldberger (1874–1929) (*16*), who discovered the mode of acquisition of pellagra. (D.M.M. remembers Mike's utter delight when, in 1976, he learned that an incoming member of that year's EIS class, Mark Goldberger, MD, was none other than the great-great nephew of Joseph Goldberger). Mike wrote with reverence about 2 additional giants of US epidemiology who pioneered the concepts of emerging infectious diseases, Theobald Smith (1859–1934) and Calvin Schwabe (1927–2006); his later series of Photo Quiz essays published in Emerging Infectious Diseases—each essay based on identifying a photograph of a scientist who had made important contributions—taught a new generation about the field's history (Appendix Table, https://wwwnc.cdc.gov/EID/article/25/8/19-0356-App1.pdf). Mike displayed yet another talent: writing elegant memoriams upon the deaths of admired scientists, such as malariologist Meir Yoelli (1912–1975) (*17*).

Within Mike's first decade at CDC, the pattern of his work and ethical approach had been set: hard work, a high level of accomplishment, a humanistic outlook, concern for less fortunate persons, and a desire to improve lives through medicine and public health. He gave to others without seeking reward or recognition. He respected heroism and sacrifice—not only the sacrifices of men like Schweitzer but also men like Carrión, who died after inoculating himself to discover the cause of bartonellosis (*14*); like Goldberger, the Eastern European immigrant who overcame oppressive anti-semitism (*16*); and even like Stevenson, who abandoned his world of comfort to die of tuberculosis on a remote Pacific island among beloved native Samoans (*18*). Mike cared greatly about migrants and refugees; his essay on forgotten diseases, an early formulation of what are now called neglected tropical diseases, was as much about forgotten people as about forgotten diseases (*19*).

Some said Mike was shy, but those who knew him well would disagree. D.M.M. recalls a co-authored biographical sketch about microbiologist-epidemiologist Charles Nicolle (1866–1936) (*20*). In an exchange of manuscript drafts, D.M.M.'s intended upgrade of a paragraph on Nicolle's probable isolation of the 1918 influenza pandemic virus was firmly rebuffed: Nicolle's elegant work elucidating the cause of typhus made him great, Mike insisted; Nicolle's other accomplishments were subordinate and needed to stay that way—and they did.

Mike was still restlessly productive and engaged when in 2008 he joined CDC's Global Disease Detection program, in what would be his last professional position. Mike was attracted to new challenges, which the young program provided. Work in the event-based surveillance unit, located inside CDC's Emergency Operations Center, was fast-paced and often frenetic, and it should have been too much for a man of advancing years. But Mike embraced the work and even thrived in its stressful team environment. He still saw the world with an almost childlike wonder; he was fascinated by the new public health approaches and technologies. R.A.C. recalls Mike's delight that, through CDC's disease detection systems, 1 dead cow could be identified in the middle of Saudi Arabia—a harbinger of a potential zoonosis. Voicing the apocryphal "Chinese curse" (actually a mid-20th-century saying of disputed English language origin), Mike would comment that "We live in interesting times!," a wry observation he repeated over many years and through many different challenges.

And so it seemed like the end of a noble era when Mike Schultz died, at age 81, on February 19, 2016. Those who mourned his passing spanned 3 generations, from each continent, across many disciplines, including a large loving family and a host of cherished friends and colleagues. The remembrances that poured forth, written independently by many different people, were strikingly alike in describing Mike as "selfless," "dedicated," and possessing "passion, wisdom, and patience." The New York Times described Mike's identification of the AIDS epidemic (*21*), but Mike unselfishly credited colleague Sandy Ford (1950–2015) as having noticed, in 1981, increased pentamidine requests for desperately ill men (*6*), representing a first important clue to uncovering AIDS. Nor did Mike mention his many prestigious awards, including 2 Public Health Service Meritorious Service Awards, CDC's William C. Watson, Jr., Medal of Excellence, or the Bailey K. Ashford Medal from the American Society of Tropical Medicine and Hygiene, for which he credited his mentors and his wife, Selma, for having inspired him to work to "end the suffering… that ruins the lives of hundreds of millions of people…" (*22*).

The London School of Hygiene and Tropical Medicine remembers Mike's Frederick Murgatroyd Award as best student and for the renowned mentors who became lifelong friends, including Ben Kean (1912–1993) and Leonard Bruce-Chwatt (1907–1989), head of the (Sir Ronald) Ross Institute (*23*). The American Veterinary Medical Association noted Mike's leadership in parasitology, his co-founding of CDC's Field Epidemiology Training Program, and his leadership in developing the clinical specialty of travel medicine (*24*). Mike's life work bound together the fabric of global public health over >5 decades.

However, the legacy of Mike Schultz is not only one of awards, publications, and accomplishments but also of thousands of acts of generosity, given freely to all, in the capacity of mentor, friend, humanitarian, philosopher, and lover of knowledge. Whatever was going on at CDC, indeed in global public health, Mike was likely to be there, comfortably in the shadows, helping, teaching, encouraging and praising others, leading quietly and by example, showing how the rigor of science and the humanism of the healing arts could be brought to those who most needed help.

What more can be said about Mike? He was a devoted family man and an imaginative artist: his award-winning sculpture, Galatea, once on display at the Atlanta Memorial Art Center, not only moved but also emitted the recorded notes of the Bachianas Brasileiras No. 5 of composer Heitor Villa-Lobos (1887–1959). He was quietly proud of his scientific and artistic work but embarrassed by adulation, uncomfortable with attention to his virtues. We share 2 unrelated observations that describe Mike well. After his death, a colleague wrote in the West African language Yoruba that Mike was "an omolubi, a person of honor who believes in hard work, respects the rights of others, and gives to the community in action and deeds, a person of integrity… a man of character." In 1997, Mike himself wrote the following words upon the death of his close friend, Meir Yoelli: "In his company, ordinary things were transfigured; they became romantic and acquired great import… I watched him bring a moment of joy to a shoeshine man…. In his presence… the world was no longer prosaic... He was, without exception, the finest man I have ever known" (*17*).

In aspiring to live up to the humanitarian ideals of men like Yoelli, Goldberger, and Schweitzer, Mike Schultz lived a life of richness and meaning; he touched countless others with his gentle spirit, his faith, and his belief in their inherent worthiness, inspiring them to find their own best selves. He now sits quietly in the company of his great heroes, and we remember him as one of them.

Acknowledgments

We thank Selma Schultz, Joseph Schultz, Naomi Mass, Karl A. Western, and Frederic Shaw for research assistance and helpful comments.

References

1. Schultz MG. The challenge of Albert Schweitzer. New Physician. 1960;9:43–7.
2. Herz M. Tägliches gebet eines arztes bevor er seine kranken besucht. Aus der Hebräischen handschrift eines berühmten Jüdischen arztes in Egypten aus dem zwölften jahrhundert. Deutsches Museum. 1793;1:43–5.
3. Schultz MG. Emerging zoonoses. N Engl J Med. 1983;308:1285–6. http://dx.doi.org/10.1056/NEJM198305263082109
4. Western KA, Perera DR, Schultz MG. Pentamidine isethionate in the treatment of *Pneumocystis carinii* pneumonia. Ann Intern Med. 1970;73:695–702. http://dx.doi.org/10.7326/0003-4819-73-5-695
5. Walzer PD, Perl DP, Krogstad DJ, Rawson PG, Schultz MG. *Pneumocystis carinii* pneumonia in the United States. Epidemiologic, diagnostic, and clinical features. Ann Intern Med. 1974;80:83–93. http://dx.doi.org/10.7326/0003-4819-80-1-83
6. Schultz MG, Bloch AB. In memoriam: Sandy Ford (1950–2015). Emerg Infect Dis. 2016;22:764–5. http://dx.doi.org/10.3201/eid2204.151336
7. Schultz MG. Editorial: Giardiasis. JAMA. 1975;233:1383–4. http://dx.doi.org/10.1001/jama.233.13.13833
8. Schultz MG. Unde venis? (Where have you been?). JAMA. 1984; 251:512–3. http://dx.doi.org/10.1001/jama.1984.03340280062033
9. Schultz MG. Emporiatrics—travellers' health. Br Med J (Clin Res Ed). 1982;285:582–3. http://dx.doi.org/10.1136/bmj.285.6342.582
10. Schultz MG. Entero-Vioform for preventing travelers' diarrhea. JAMA. 1972;220:273–4. http://dx.doi.org/10.1001/jama.1972.03200020081018
11. Walzer PD, Judson FN, Murphy KB, Healy GR, English DK, Schultz MG. Balantidiasis outbreak in Truk. Am J Trop Med Hyg. 1973;22:33–41. http://dx.doi.org/10.4269/ajtmh.1973.22.33
12. Schultz MG. Malaria in migrants and travellers. Trans R Soc Trop Med Hyg. 1989;83(Suppl):31–4. http://dx.doi.org/10.1016/0035-9203(89)90600-7
13. Western KA, Benson GD, Gleason NN, Healy GR, Schultz MG. Babesiosis in a Massachusetts resident. N Engl J Med. 1970; 283:854–6. http://dx.doi.org/10.1056/NEJM197010152831607
14. Schultz MG. Daniel Carrión's experiment. N Engl J Med. 1968; 278:1323–6. http://dx.doi.org/10.1056/NEJM196806132782405
15. Schultz MG. The "strange case" of Robert Louis Stevenson. JAMA.1971; 216:90–4. http://dx.doi.org/10.1001/jama.1971.03180270056010
16 Schultz MG. Joseph Goldberger and pellagra. Am J Trop Med Hyg. 1977;26(Suppl):1088–92. http://dx.doi.org/10.4269/ajtmh.1977.26.1088
17. Schultz MG. Dr. Meir Yoelli (1912–1975). Trop Med Hyg News. 1976;25:14–7.
18. Morens DM. At the deathbed of consumptive art. Emerg Infect Dis. 2002;8:1353–8. http://dx.doi.org/10.3201/eid0811.020549
19. Schultz MG. The forgotten problems of forgotten people. In: Wood C, Rue Y, eds. Health policies in developing countries. Royal Society of Medicine. International Congress and Symposium Series no. 24. London (UK): The Royal Society of Medicine; 1980. p. 57–62.
20. Schultz MG, Morens DM. Charles-Jules-Henri Nicolle. Emerg Infect Dis. 2009;15:1519–22. http://dx.doi.org/10.3201/eid1509.090891
21. Roberts S. Dr. Myron G. Schultz, who helped identify AIDS crisis, dies at 81. The New York Times. 2016 Mar 5 [cited 2019 Jun 15]. https://www.nytimes.com/2016/03/06/health/dr-myron-g-schultz-who-helped-identify-aids-crisis-dies-at-81.html
22. Schultz MG. Remarks of Dr. Myron G. Schultz upon accepting the 1980 Bailey K. Ashford Award. Trop Med Hyg News. 1980;29:18–9.
23. Rodney N. Obituary: Dr. Myron G. Schultz. LSTMH Alumni Blog, 2 August 2016 [cited 2019 Jun 15]. https://blogs.lshtm.ac.uk/alumni/2016/08/02/obituary-dr-myron-g-schultz
24. Obituaries. Myron G. Schultz. JAVMA News, 2 May 2016 cited 2019 Jun 15]. https://www.avma.org/News/JAVMANews/Pages/160515y.aspx

Address for correspondence: David M. Morens, National Institute of Allergy and Infectious Diseases, National Institutes of Health, Bldg 31, Rm 7A-03, 31 Center Dr, MSC 2520, Bethesda, MD 20892-2520, USA; email: dm270q@nih.gov

Vincent van Gogh (1853–1890). *First Steps, after Millet* (1890) (detail)**.** Oil on canvas; 28 1/2 in x 35 7/8 in/72.4 cm x 91.1 cm. Gift of George N. and Helen M. Richard, 1964. Image © The Metropolitan Museum of Art. Image source: Art Resource, NY.

The Power of First Steps

Byron Breedlove, Kathleen Gensheimer

A number of paintings by the Dutch artist Vincent van Gogh feature children. One such painting, *First Steps, after Millet*, on this month's cover, depicts a milestone moment for many parents and children. Father and daughter face each other with outstretched arms as the young child totters from her mother's steadying hands.

At the time van Gogh completed this work focusing on a child's first steps, he was a voluntary resident of the Saint-Paul asylum in Saint-Rémy-de-Provence, France, where he lived and worked from May 1889 until June 1890. He sought care there after suffering a mental breakdown on December 23, 1888, and continuing to experience hallucinations and delusions.

Despite several relapses of mental illness, van Gogh completed about 150 paintings during his time at the asylum. As noted by the Metropolitan Museum of Art, "His initial confinement to the grounds of the hospital is reflected in his imagery, from his depictions of its corridors to the irises and lilacs of its walled garden, visible from the window of the spare room he was allotted to use as a studio." Later during his stay, he ventured outside the grounds, where he painted olive groves and cypresses.

Author affiliation: Centers for Disease Control and Prevention, Atlanta, Georgia, USA (B. Breedlove); Food and Drug Administration, Silver Spring, Maryland, USA; Editorial Board, *Emerging Infectious Diseases* (K. Gensheimer)

Van Gogh received black and white prints or photographs of works created by other artists from his younger brother Theo and used their content as his subjects. The Metropolitan Museum of Art explains that van Gogh considered his copies of other artists' works to be "interpretations" or "translations," and he compared "his role as an artist to that of a musician playing music written by another composer." Working in his improvised studio in a barred cell, he would select a black-and-white image as his subject and "improvise color on it."

Prominent among those sources were works by the French painter Jean-François Millet, an artist who had influenced van Gogh's decision to paint scenes from rural life. In all, van Gogh completed 21 paintings copied from works by Millet, including *First Steps, after Millet*. Millet's *First Steps* is a pre-Impressionist black crayon sketch on tan paper.

In the painting, van Gogh remained largely faithful to Millet's drawing—the clothes drying on the fence; the spade laying across the furrows in the soil; and the posture and gestures of the man, woman, and child. He changed the perspective somewhat, revealing the sky, adding a gate, increasing the distance between the figures. In conveying the universal emotion of a tender moment, van Gogh does not focus on facial details. He painted his translation with characteristic brisk, hooked, curved strokes and relied on

muted shades of browns, blues, and greens and wisps of white, in contrast to Millet's lines that are more flowing and use only a monochromatic pallet.

First Steps, after Millet reminds us of the stakes in protecting the health of mothers and children from infectious diseases, many of which are preventable and have receded because of public health efforts and medical breakthroughs. *Achievements in Public Health, 1900–1999: Healthier Mothers and Babies* reported that, at the beginning of the 20th century in the United States—a decade after van Gogh completed his painting—for every 1,000 live births, approximately 100 infants died before 1 year of age and 6 to 9 women died of pregnancy-related complications. During 1915–1997, the infant mortality rate dropped more than 90%, from 100 to 7.2 per 1,000 live births; during 1900–1997, the maternal mortality rate declined almost 99%, to less than 0.1 reported deaths.

Despite such progress, mothers and children continue to be at risk for emerging and reemerging infectious diseases globally and within the United States. Four diseases provide examples. In 2015–2016, the unanticipated and abrupt occurrence of Zika infections was linked to an increase in severe birth defects in affected regions. The full effect of the teratogenic potential for this vectorborne disease is still not fully understood. Malaria**,** another vectorborne disease**,** disproportionally affects infants and children under 5 years of age and pregnant women. Pregnant women who have malaria experience higher rates of miscarriage, intrauterine demise, premature delivery, low-birth-weight neonates, and neonatal death. Another example is Ebola virus infection. Although no evidence suggests that pregnant women are more susceptible to infection from Ebola virus than the general population, limited evidence does suggest that pregnant women are more likely to be at increased risk than the general population for severe illness and death when infected. *Listeria monocytogenes*, an important foodborne pathogen in the United States, provides the fourth example. Pregnant women, fetuses, and newborns are more likely than others to acquire invasive listeriosis, which can result in stillbirth, preterm labor, newborn sepsis, and meningitis.

Other diseases also illustrate the continuing threat emerging and reemerging infectious diseases pose to mothers and children. Annual influenza seasons, including the 2009 H1N1 influenza pandemic, highlight the risks to pregnant and puerperal women, who may disproportionately become ill and die. Sometimes the rise in a noninfectious condition causes infectious diseases to reemerge and threaten maternal and child health. For instance, the US opioid epidemic has resulted in mothers becoming infected with hepatitis C, HIV, syphilis, and other sexually transmitted diseases. When those infections occur in mothers, they can also be transmitted to newborns.

Death rates for mothers and children are generally higher in developing countries than in developed nations. Each step we take helps create a stronger global culture promoting the health of mothers and their young children. Even steps as small as those metaphorically depicted by van Gogh are vital for supporting public health efforts to promote maternal and child health.

Disclosure

K.G. reports no relevant financial disclosures.

Disclaimer

The opinions and conclusions expressed in this article are solely the views of the authors and do not necessarily reflect those of the US Centers for Disease Control and Prevention and US Food and Drug Administration.

Bibliography

1. Beigi RH. Emerging infectious diseases in pregnancy. Obstet Gynecol. 2017;129:896–906. https://doi.org/10.1097/AOG.0000000000001978
2. Callow P. Vincent van Gogh: a life. Chicago: Ivan R Dee; 1990. p. 246.
3. Centers for Disease Control and Prevention. Achievements in public health, 1900–1999: healthier mothers and babies. MMWR Morb Mortal Wkly Rep. 1999;48:849–58 [cited 2019 Jun 28]
4. Centers for Disease Control and Prevention. *Listeria* (listeriosis): people at risk—pregnant women and newborns, 2016 [cited 2019 Jun 14]. https://www.cdc.gov/listeria/risk-groups/pregnant-women.html
5. Centers for Disease Control and Prevention. Guidance for screening and caring for pregnant women with Ebola virus disease for healthcare providers in US hospitals [cited 2019 Jul 3] https://www.cdc.gov/vhf/ebola/clinicians/evd/pregnant-women.html
6. Delaney A, Mai C, Smoots A, Cragan J, Ellington S, Langlois P, et al. Population-based surveillance of birth defects potentially related to Zika virus infection—15 states and U.S. territories, 2016. MMWR Morb Mortal Wkly Rep. 2018;67:91–6. https://doi.org/10.15585/mmwr.mm6703a2
7. Jacob JA. US infant mortality rate declines but still exceeds other developed countries. JAMA. 2016;315:451–2. https://doi.org/10.1001/jama.2015.18886
8. Mace KE, Arguin PM, Lucchi NW, Tan KR. Malaria surveillance—United States, 2016. MMWR Surveill Summ. 2019;68:1–35. PubMed https://doi.org/10.15585/mmwr.ss6805a1
9. Metropolitan Museum of Art. First steps, after Millet [cited 2019 Jun 8] https://www.metmuseum.org/toah/works-of-art/64.165.2/
10. Metropolitan Museum of Art. Vincent van Gogh (1853–1890) [cited 2019 Jun 8] https://www.metmuseum.org/toah/hd/gogh/hd_gogh.htm
11. Riding A. Arts abroad; first, van Gogh's Millet, then van Gogh's van Gogh. Oct. 28, 1998. New York Times [cited 2019 Jun 9]. https://www.nytimes.com./1998/10/28/arts/arts-abroad-first-van-gogh-s-millet-then-van-gogh-s-van-gogh.html
12. Van Gogh Museum. Brotherly love: Vincent and Theo [cited 2019 Jun 9] https://www.vangoghmuseum.nl/en/stories/nature-and-the-artist#14

Address for correspondence: Byron Breedlove, EID Journal, Centers for Disease Control and Prevention, 1600 Clifton Rd NE, Mailstop H16-2, Atlanta, GA 30329-4027, USA; email: wbb1@cdc.gov

EMERGING INFECTIOUS DISEASES®

Upcoming Issue

- Clinical Characteristics and Treatment Outcomes for Patients Infected with *Mycobacterium haemophilum*
- Genotyping Method for Potential Common Source of *Enterocytozoon bieneusi* Microsporidia Infection in Hematology Unit
- Epidemiology of Carbapenemase-Producing *Klebsiella pneumoniae* in a Hospital, Portugal
- *Theileria orientalis* Ikeda Genotype in Cattle, Virginia, USA
- Impact of Pneumococcal Conjugate Vaccines on Pneumococcal Meningitis in England and Wales, 2000–2016
- Epidemiologic Shift in Candidemia Driven by *Candida auris*, South Africa, 2016–2017
- Delays in Coccidioidomycosis Diagnosis and Relationship to Healthcare Utilization, Arizona, USA
- Cluster of Nasal Rhinosporidiosis, Eastern Province, Rwanda
- Rodent Host Abundance and Climate Variability as Predictors of Tickborne Disease Risk 1 Year in Advance
- *Rickettsia japonica* Infections in Humans, China, 2014–2017
- Control and Elimination of Extensively Drug-Resistant *Acinetobacter baumanii* in an Intensive Care Unit
- *Candida auris* in Germany and Previous Exposure to Foreign Healthcare
- Disseminated Emergomycosis in a Person with HIV Infection from Uganda: Molecular Identification of *Emergomyces pasteurianus* or a Close Relative from a Pathology Block
- Fatal Cases of Invasive Fungal Disease after Isavuconazole Treatment Failure, France

Complete list of articles in the September issue at http://www.cdc.gov/eid/upcoming.htm

Upcoming Infectious Disease Activities

October 2–6, 2019
ID Week
Washington, DC, USA
https://idweek.org/

November 20–24, 2019
ASTMH
American Society of Tropical Medicine and Hygiene
68th Annual Meeting
National Harbor, MD, USA
https://www.astmh.org/

February 20–23, 2020
International Society for Infectious Diseases
Kuala Lumpur, Malaysia
https://www.isid.org/

March 8–11, 2020
Conference on Retroviruses and Opportunistic Infections
Boston, MA, USA
https://www.croiconference.org/

June 18–22, 2020
American Society for Microbiology
Chicago, IL, USA
https://www.asm.org/

Announcements

Email announcements to EIDEditor (eideditor@cdc.gov). Include the event's date, location, sponsoring organization, and a website. Some events may appear only on EID's website, depending on their dates.

Correction: Vol. 18, No. 1

An odds ratio and 95% CI were incorrect in Identifying Risk Factors for Shiga Toxin–producing *Escherichia coli* by Payment Information (H. Wilking et al.). The correct data for salad bar purchases were odds ratio 5.83, 95% CI 1.42–23.88. The article has been corrected online (https://wwwnc.cdc.gov/eid/article/18/1/11-1044_article).

Correction: Vol. 25, No. 6

Author Olga Ivanov should have also been listed as affiliated with Sechenov University, Moscow, Russia, in Multirecombinant Enterovirus A71 Subgenogroup C1 Isolates Associated with Neurologic Disease, France, 2016–2017 (S. Tomba Ngangas et al.). The article has been corrected online (https://wwwnc.cdc.gov/eid/article/25/6/18-1460_article).

Earning CME Credit

To obtain credit, you should first read the journal article. After reading the article, you should be able to answer the following, related, multiple-choice questions. To complete the questions (with a minimum 75% passing score) and earn continuing medical education (CME) credit, please go to http://www.medscape.org/journal/eid. Credit cannot be obtained for tests completed on paper, although you may use the worksheet below to keep a record of your answers.

You must be a registered user on http://www.medscape.org. If you are not registered on http://www.medscape.org, please click on the "Register" link on the right hand side of the website.

Only one answer is correct for each question. Once you successfully answer all post-test questions, you will be able to view and/or print your certificate. For questions regarding this activity, contact the accredited provider, CME@medscape.net. For technical assistance, contact CME@medscape.net. American Medical Association's Physician's Recognition Award (AMA PRA) credits are accepted in the US as evidence of participation in CME activities. For further information on this award, please go to https://www.ama-assn.org. The AMA has determined that physicians not licensed in the US who participate in this CME activity are eligible for AMA PRA Category 1 Credits™. Through agreements that the AMA has made with agencies in some countries, AMA PRA credit may be acceptable as evidence of participation in CME activities. If you are not licensed in the US, please complete the questions online, print the AMA PRA CME credit certificate, and present it to your national medical association for review.

Article Title

Zika Virus Infection in Pregnant Women, Yucatan, Mexico

CME Questions

1. Your patient is a 26-year-old pregnant woman in Merida, Yucatán, Mexico, who may have been exposed to Zika virus (ZIKV) infection during her second trimester. According to the prospective cohort study by Romer and colleagues, which of the following statements about demographic and epidemiological findings of pregnant women during the initial phase of ZIKV introduction into Yucatán, Mexico, is correct?

A. Among 115 pregnant women monitored for signs of active or recent ZIKV infection, estimated ZIKV cumulative incidence was 0.12 and symptomatic-to-asymptomatic ratio was 3.2
B. Risk for ZIKV infection was consistent throughout 2016 and 2017
C. Older age, socioeconomic status, and rural vs urban residence predicted ZIKV positivity
D. The cohort detected ZIKV cases 3 weeks before Yucatán State's passive surveillance system, but shape and temporality of the epidemiologic curve was similar in both

2. According to the prospective cohort study by Romer and colleagues, which of the following statements about the laboratory findings of pregnant women with recent or acute ZIKV infection during the initial phase of ZIKV introduction into Yucatán, Mexico, is correct?

A. There is known to be high concordance in ZIKV detection from concurrent blood and urine samples
B. Prolonged viremia in this study and others is unusual for other arboviruses, and its role in pathogenesis of congenital diseases or on dissemination of infection is unclear
C. Of 22 paired blood and urine samples at baseline, 10 were positive for ZIKV infection in both samples
D. Urine samples alone were sufficient to detect nearly all cases

3. According to the prospective cohort study by Romer and colleagues, which of the following statements about clinical findings of pregnant women with recent or acute ZIKV infection during the initial phase of ZIKV introduction into Yucatán, Mexico, is correct?

A. Exanthema was the most specific clinical sign, and clinical features were highly predictive of ZIKV infection
B. The combination of signs with highest specificity was fever, retro-orbital pain, and joint edema, but sensitivity was low
C. Congenital ZIKV disease was detected in 3 newborns
D. Physicians should suspect ZIKV infection in pregnant women with exanthema and without fever, with or without other signs and symptoms

Earning CME Credit

To obtain credit, you should first read the journal article. After reading the article, you should be able to answer the following, related, multiple-choice questions. To complete the questions (with a minimum 75% passing score) and earn continuing medical education (CME) credit, please go to http://www.medscape.org/journal/eid. Credit cannot be obtained for tests completed on paper, although you may use the worksheet below to keep a record of your answers.

You must be a registered user on http://www.medscape.org. If you are not registered on http://www.medscape.org, please click on the "Register" link on the right hand side of the website.

Only one answer is correct for each question. Once you successfully answer all post-test questions, you will be able to view and/or print your certificate. For questions regarding this activity, contact the accredited provider, CME@medscape.net. For technical assistance, contact CME@medscape.net. American Medical Association's Physician's Recognition Award (AMA PRA) credits are accepted in the US as evidence of participation in CME activities. For further information on this award, please go to https://www.ama-assn.org. The AMA has determined that physicians not licensed in the US who participate in this CME activity are eligible for AMA PRA Category 1 Credits™. Through agreements that the AMA has made with agencies in some countries, AMA PRA credit may be acceptable as evidence of participation in CME activities. If you are not licensed in the US, please complete the questions online, print the AMA PRA CME credit certificate, and present it to your national medical association for review.

Article Title

Retrospective Cohort Study of Lassa Fever in Pregnancy, Southern Nigeria

CME Questions

1. You are advising an obstetric center in Nigeria regarding management of pregnant women with Lassa fever (LF). According to the retrospective study of 30 cases seen in Nigeria between January 2009 and March 2018 by Okogbenin and colleagues, which of the following statements about maternal and fetal outcomes for 2 broad patterns of clinical presentation in 30 pregnant patients with LF—patients with complications (n = 16) vs. patients with milder, nonspecific symptoms (n = 14)—is correct?

A. All 16 women with complications (coma, convulsions, irrational behavior, extravaginal bleeding, or oliguria) also had intrauterine fetal death or an abortive process
B. Of 16 women with complications, 5 died within 1 week
C. Of 14 women with milder symptoms (fever, malaise, cough, or sore throat), 9 had a live fetus on ultrasound, and 3 women died
D. Of the 30 women, 15 presented with fever

2. According to the retrospective study of 30 cases seen in Nigeria between January 2009 and March 2018 by Okogbenin and colleagues, which of the following statements about predictors of maternal and fetal outcomes in 30 pregnant patients with LF is correct?

A. Presentation in the third trimester and breast pain or engorgement were each independently associated with maternal and fetal or perinatal death
B. Extravaginal bleeding, convulsions, and oliguria were each independently associated with maternal and fetal or perinatal death
C. Mortality rates remained constant throughout the study
D. Changes in Nigeria and at ISTH were unlikely to affect mortality during the study

3. According to the retrospective study of 30 pregnant patients with LF by Okogbenin and colleagues, which of the following statements about clinical implications of maternal and fetal outcomes is correct?

A. LF in pregnancy is a relatively rare cause of maternal mortality in Nigeria
B. Evacuation is recommended for most patients
C. Most patients first seen at other facilities before coming to ISTH had already been diagnosed with LF
D. For women presenting with a live fetus, good outcomes contrast with previous reports and support a conservative approach to obstetric management of LF in Nigeria

Emerging Infectious Diseases is a peer-reviewed journal established expressly to promote the recognition of new and reemerging infectious diseases around the world and improve the understanding of factors involved in disease emergence, prevention, and elimination.

The journal is intended for professionals in infectious diseases and related sciences. We welcome contributions from infectious disease specialists in academia, industry, clinical practice, and public health, as well as from specialists in economics, social sciences, and other disciplines. Manuscripts in all categories should explain the contents in public health terms. For information on manuscript categories and suitability of proposed articles, see below and visit http://wwwnc.cdc.gov/eid/pages/author-resource-center.htm.

Summary of Authors' Instructions

Authors' Instructions. For a complete list of EID's manuscript guidelines, see the author resource page: http://wwwnc.cdc.gov/eid/page/author-resource-center.

Manuscript Submission. To submit a manuscript, access Manuscript Central from the Emerging Infectious Diseases web page (www.cdc.gov/eid). Include a cover letter indicating the proposed category of the article (e.g., Research, Dispatch), verifying the word and reference counts, and confirming that the final manuscript has been seen and approved by all authors. Complete provided Authors Checklist.

Manuscript Preparation. For word processing, use MS Word. Set the document to show continuous line numbers. List the following information in this order: title page, article summary line, keywords, abstract, text, acknowledgments, biographical sketch, references, tables, and figure legends. Appendix materials and figures should be in separate files.

Title Page. Give complete information about each author (i.e., full name, graduate degree(s), affiliation, and the name of the institution in which the work was done). Clearly identify the corresponding author and provide that author's mailing address (include phone number, fax number, and email address). Include separate word counts for abstract and text.

Keywords. Use terms as listed in the National Library of Medicine Medical Subject Headings index (www.ncbi.nlm.nih.gov/mesh).

Text. Double-space everything, including the title page, abstract, references, tables, and figure legends. Indent paragraphs; leave no extra space between paragraphs. After a period, leave only one space before beginning the next sentence. Use 12-point Times New Roman font and format with ragged right margins (left align). Italicize (rather than underline) scientific names when needed.

Biographical Sketch. Include a short biographical sketch of the first author—both authors if only two. Include affiliations and the author's primary research interests.

References. Follow Uniform Requirements (www.icmje.org/index.html). Do not use endnotes for references. Place reference numbers in parentheses, not superscripts. Number citations in order of appearance (including in text, figures, and tables). Cite personal communications, unpublished data, and manuscripts in preparation or submitted for publication in parentheses in text. Consult List of Journals Indexed in Index Medicus for accepted journal abbreviations; if a journal is not listed, spell out the journal title. List the first six authors followed by "et al." Do not cite references in the abstract.

Tables. Provide tables within the manuscript file, not as separate files. Use the MS Word table tool, no columns, tabs, spaces, or other programs. Footnote any use of boldface. Tables should be no wider than 17 cm. Condense or divide larger tables. Extensive tables may be made available online only.

Figures. Submit editable figures as separate files (e.g., Microsoft Excel, PowerPoint). Photographs should be submitted as high-resolution (600 dpi) .tif or .jpg files. Do not embed figures in the manuscript file. Use Arial 10 pt. or 12 pt. font for lettering so that figures, symbols, lettering, and numbering can remain legible when reduced to print size. Place figure keys within the figure. Figure legends should be placed at the end of the manuscript file.

Videos. Submit as AVI, MOV, MPG, MPEG, or WMV. Videos should not exceed 5 minutes and should include an audio description and complete captioning. If audio is not available, provide a description of the action in the video as a separate Word file. Published or copyrighted material (e.g., music) is discouraged and must be accompanied by written release. If video is part of a manuscript, files must be uploaded with manuscript submission. When uploading, choose "Video" file. Include a brief video legend in the manuscript file.

Types of Articles

Perspectives. Articles should not exceed 3,500 words and 50 references. Use of subheadings in the main body of the text is recommended. Photographs and illustrations are encouraged. Provide a short abstract (150 words), 1-sentence summary, and biographical sketch. Articles should provide insightful analysis and commentary about new and reemerging infectious diseases and related issues. Perspectives may address factors known to influence the emergence of diseases, including microbial adaptation and change, human demographics and behavior, technology and industry, economic development and land use, international travel and commerce, and the breakdown of public health measures.

Synopses. Articles should not exceed 3,500 words in the main body of the text or include more than 50 references. Use of subheadings in the main body of the text is recommended. Photographs and illustrations are encouraged. Provide a short abstract (not to exceed 150 words), a 1-line summary of the conclusions, and a brief biographical sketch of first author or of both authors if only 2 authors. This section comprises case series papers and concise reviews of infectious diseases or closely related topics. Preference is given to reviews of new and emerging diseases; however, timely updates of other diseases or topics are also welcome. If detailed methods are included, a separate section on experimental procedures should immediately follow the body of the text.

Research. Articles should not exceed 3,500 words and 50 references. Use of subheadings in the main body of the text is recommended. Photographs and illustrations are encouraged. Provide a short abstract (150 words), 1-sentence summary, and biographical sketch. Report laboratory and epidemiologic results within a public health perspective. Explain the value of the research in public health terms and place the findings in a larger perspective (i.e., "Here is what we found, and here is what the findings mean").

Policy and Historical Reviews. Articles should not exceed 3,500 words and 50 references. Use of subheadings in the main body of the text is recommended. Photographs and illustrations are encouraged. Provide a short abstract (150 words), 1-sentence summary, and biographical sketch. Articles in this section include public health policy or historical reports that are based on research and analysis of emerging disease issues.

Dispatches. Articles should be no more than 1,200 words and need not be divided into sections. If subheadings are used, they should be general, e.g., "The Study" and "Conclusions." Provide a brief abstract (50 words); references (not to exceed 15); figures or illustrations (not to exceed 2); tables (not to exceed 2); and biographical sketch. Dispatches are updates on infectious disease trends and research that include descriptions of new methods for detecting, characterizing, or subtyping new or reemerging pathogens. Developments in antimicrobial drugs, vaccines, or infectious disease prevention or elimination programs are appropriate. Case reports are also welcome.

Research Letters Reporting Cases, Outbreaks, or Original Research. EID publishes letters that report cases, outbreaks, or original research as Research Letters. Authors should provide a short abstract (50-word maximum), references (not to exceed 10), and a short biographical sketch. These letters should not exceed 800 words in the main body of the text and may include either 1 figure or 1 table. Do not divide Research Letters into sections.

Letters Commenting on Articles. Letters commenting on articles should contain a maximum of 300 words and 5 references; they are more likely to be published if submitted within 4 weeks of the original article's publication.

Commentaries. Thoughtful discussions (500–1,000 words) of current topics. Commentaries may contain references (not to exceed 15) but no abstract, figures, or tables. Include biographical sketch.

Another Dimension. Thoughtful essays, short stories, or poems on philosophical issues related to science, medical practice, and human health. Topics may include science and the human condition, the unanticipated side of epidemic investigations, or how people perceive and cope with infection and illness. This section is intended to evoke compassion for human suffering and to expand the science reader's literary scope. Manuscripts are selected for publication as much for their content (the experiences they describe) as for their literary merit. Include biographical sketch.

Books, Other Media. Reviews (250–500 words) of new books or other media on emerging disease issues are welcome. Title, author(s), publisher, number of pages, and other pertinent details should be included.

Conference Summaries. Summaries of emerging infectious disease conference activities (500–1,000 words) are published online only. They should be submitted no later than 6 months after the conference and focus on content rather than process. Provide illustrations, references, and links to full reports of conference activities.

Online Reports. Reports on consensus group meetings, workshops, and other activities in which suggestions for diagnostic, treatment, or reporting methods related to infectious disease topics are formulated may be published online only. These should not exceed 3,500 words and should be authored by the group. We do not publish official guidelines or policy recommendations.

Photo Quiz. The photo quiz (1,200 words) highlights a person who made notable contributions to public health and medicine. Provide a photo of the subject, a brief clue to the person's identity, and five possible answers, followed by an essay describing the person's life and his or her significance to public health, science, and infectious disease.

Etymologia. Etymologia (100 words, 5 references). We welcome thoroughly researched derivations of emerging disease terms. Historical and other context could be included.

Announcements. We welcome brief announcements of timely events of interest to our readers. Announcements may be posted online only, depending on the event date. Email to eideditor@cdc.gov.

Vol 25, No 8, August 2019

EMERGING INFECTIOUS DISEASES

Pages 1445–1624

Vincent van Gogh (1853–1890), *First Steps, after Millet* (1890). Oil on canvas; 28 1/2 in x 35 7/8 in./72.4 cm x 91.1 cm. Gift of George N. and Helen M. Richard, 1964. Image © The Metropolitan Museum of Art. Image source: Art Resource, NY

DEPARTMENT OF
HEALTH & HUMAN SERVICES
Public Health Service
Centers for Disease Control and Prevention (CDC)
Mailstop D61, Atlanta, GA 30329-4027

ISSN 1080-6040